

Special Issue Reprint

Organophosphorus Chemistry

A New Perspective

Edited by
Jakub Adamek

www.mdpi.com/journal/molecules

Organophosphorus Chemistry: A New Perspective

Organophosphorus Chemistry: A New Perspective

Editor

Jakub Adamek

MDPI • Basel • Beijing • Wuhan • Barcelona • Belgrade • Manchester • Tokyo • Cluj • Tianjin



Editor

Jakub Adamek
Department of Organic
Chemistry, Bioorganic
Chemistry and Biotechnology
Silesian University of Technology
Gliwice
Poland

Editorial Office

MDPI
St. Alban-Anlage 66
4052 Basel, Switzerland

This is a reprint of articles from the Special Issue published online in the open access journal *Molecules* (ISSN 1420-3049) (available at: www.mdpi.com/journal/molecules/special_issues/organophosphorus_chemistry_perspective).

For citation purposes, cite each article independently as indicated on the article page online and as indicated below:

| |
|--|
| LastName, A.A.; LastName, B.B.; LastName, C.C. Article Title. <i>Journal Name</i> Year , <i>Volume Number</i> , Page Range. |
|--|

ISBN 978-3-0365-8037-1 (Hbk)

ISBN 978-3-0365-8036-4 (PDF)

© 2023 by the authors. Articles in this book are Open Access and distributed under the Creative Commons Attribution (CC BY) license, which allows users to download, copy and build upon published articles, as long as the author and publisher are properly credited, which ensures maximum dissemination and a wider impact of our publications.

The book as a whole is distributed by MDPI under the terms and conditions of the Creative Commons license CC BY-NC-ND.

Contents

About the Editor vii

Jakub Adamek

Special Issue "Organophosphorus Chemistry: A New Perspective"

Reprinted from: *Molecules* **2023**, *28*, 4752, doi:10.3390/molecules28124752 1

Jakub Adamek, Mirosława Grymel, Anna Kuźnik and Agnieszka Październiak-Holewa

1-Aminoalkylphosphonium Derivatives: Smart Synthetic Equivalents of *N*-Acyliminium-Type Cations, and Maybe Something More: A Review †

Reprinted from: *Molecules* **2022**, *27*, 1562, doi:10.3390/molecules27051562 5

Mirosława Grymel, Anna Lalik, Alicja Kazek-Kęsik, Marietta Szewczyk, Patrycja Grabiec and Karol Erfurt

Design, Synthesis and Preliminary Evaluation of the Cytotoxicity and Antibacterial Activity of Novel Triphenylphosphonium Derivatives of Betulin

Reprinted from: *Molecules* **2022**, *27*, 5156, doi:10.3390/molecules27165156 37

Anna Kuźnik, Dominika Kozicka, Wioleta Hawranek, Karolina Socha and Karol Erfurt

One-Pot and Catalyst-Free Transformation of *N*-Protected 1-Amino-1-Ethoxyalkylphosphonates into Bisphosphonic Analogs of Protein and Non-Protein α -Amino Acids

Reprinted from: *Molecules* **2022**, *27*, 3571, doi:10.3390/molecules27113571 57

Maria Vassaki, Savvina Lazarou, Petri Turhanen, Duane Choquesillo-Lazarte and Konstantinos D. Demadis

Drug-Inclusive Inorganic–Organic Hybrid Systems for the Controlled Release of the Osteoporosis Drug Zoledronate

Reprinted from: *Molecules* **2022**, *27*, 6212, doi:10.3390/molecules27196212 81

Esa Kukkonen, Emilia Josefina Virtanen and Jani Olavi Moilanen

α -Aminophosphonates, -Phosphinates, and -Phosphine Oxides as Extraction and Precipitation Agents for Rare Earth Metals, Thorium, and Uranium: A Review

Reprinted from: *Molecules* **2022**, *27*, 3465, doi:10.3390/molecules27113465 95

Anna Brol and Tomasz K. Olszewski

Deamination of 1-Aminoalkylphosphonic Acids: Reaction Intermediates and Selectivity

Reprinted from: *Molecules* **2022**, *27*, 8849, doi:10.3390/molecules27248849 123

Xabier del Corte, Aitor Maestro, Adrián López-Francés, Francisco Palacios and Javier Vicario

Synthesis of Tetrasubstituted Phosphorus Analogs of Aspartic Acid as Antiproliferative Agents

Reprinted from: *Molecules* **2022**, *27*, 8024, doi:10.3390/molecules27228024 139

Ewa Chmielewska, Natalia Miodowska, Błażej Dziuk, Mateusz Psurski and Paweł Kafarski

One-Pot Phosphonylation of Heteroaromatic Lithium Reagents: The Scope and Limitations of Its Use for the Synthesis of Heteroaromatic Phosphonates

Reprinted from: *Molecules* **2023**, *28*, 3135, doi:10.3390/molecules28073135 161

Ignacy Janicki and Piotr Kielbasiński

Highly *Z*-Selective Horner–Wadsworth–Emmons Olefination Using Modified Still–Gennari-Type Reagents

Reprinted from: *Molecules* **2022**, *27*, 7138, doi:10.3390/molecules27207138 179

Marek Koprowski, Krzysztof Owsianik, Łucja Knopik, Vivek Vivek, Adrian Romaniuk and Ewa Różycka-Sokołowska et al.
Comprehensive Review on Synthesis, Properties, and Applications of Phosphorus (P^{III}, P^{IV}, P^V)
Substituted Acenes with More Than Two Fused Benzene Rings
Reprinted from: *Molecules* **2022**, *27*, 6611, doi:10.3390/molecules27196611 **189**

About the Editor

Jakub Adamek

Jakub Adamek graduated from the Faculty of Chemistry of the Silesian University of Technology in 2008. Four years later, he completed his Ph.D. thesis entitled “Studies on the transformation of α -amino acids in their phosphorus analogs via 1-(N-acylamino)alkylphosphonium salts” and he won the Sigma-Aldrich and Polish Chemical Society Award for the best Ph.D. thesis in organic chemistry (2013). In 2023, he completed his habilitation entitled “Structure/reactivity correlation for phosphonium precursors in reactions via iminium cation/imine-type systems”. Currently, he is an Assistant Professor at the Department of Organic Chemistry, Bioorganic Chemistry, and Biotechnology of the Silesian University of Technology in Gliwice. His main research interests are focused on organic chemistry with a special emphasis on modern synthetic methodologies (electroorganic synthesis, microwave- and ultrasound-assisted synthesis), reaction mechanisms, and structure elucidation of novel organic compounds using spectroscopy. These topics are mainly associated with organophosphorus compounds. As part of the research activity, he published three chapters in monographs and more than 30 scientific papers. He is also a co-author of nine patents and over 55 oral and poster communications at national and international scientific conferences. He has participated in five national and one international research projects.

Editorial

Special Issue “Organophosphorus Chemistry: A New Perspective”

Jakub Adamek ^{1,2} 

¹ Department of Organic Chemistry, Bioorganic Chemistry and Biotechnology, Silesian University of Technology, B. Krzywoustego 4, 44-100 Gliwice, Poland; jakub.adamek@polsl.pl; Tel.: +48-032-237-1724; Fax: +48-032-237-2094

² Biotechnology Center, Silesian University of Technology, B. Krzywoustego 8, 44-100 Gliwice, Poland

The European Chemical Society (EuChemS) and the European Parliament (Science and Policy Workshop, 25 May 2023) recognize phosphorus as one of the key chemical elements in daily life. It is not only a component of the human body but also a foundation of the agrochemical industry. Today, it is often said that we are living in “the golden age of phosphorus chemistry”. In this context, organophosphorus chemistry is also gaining importance as one of the fastest-growing branches of organic chemistry. In the laboratory, phosphorus-containing compounds (also called P-compounds) are widely used as reagents (starting materials, precursors of active intermediates such as ylides or iminium-type cations, etc.), catalysts (PTC, organocatalysis), and solvents (PILs) [1–4]. Due to the interesting properties of P-compounds (especially their biological activity), they are used on a large scale in medicine (e.g., bone disorder drugs, anticancer and antiviral agents, and antihelminthics in veterinary applications), agriculture (e.g., pesticides), and industry (e.g., production of lubricants or plastic materials) [5–7]. However, in the age of much-needed care for the natural environment, we face new challenges. Innovative approaches to the synthesis and isolation of P-compounds (taking into account the aspects of green chemistry and sustainability), followed by their responsible use and disposal (neutralization), may prove crucial in the near future.

In this Special Issue, seven original research articles and three reviews covering aspects of recent advances in the synthesis, transformation, and properties of organophosphorus compounds were published.

The first two articles concern phosphonium salts and the properties of the phosphonium moiety [8,9]. In a review article, Adamek et al. collected information on the synthesis and reactivity of 1-aminoalkylphosphonium derivatives [8]. As shown, these types of compounds can be considered not only as smart synthetic equivalents of *N*-acyliminium-type cations in the α -amidoalkylation reaction but also as convenient reagents in cyclizations or effective precursors of ylides in the Wittig reaction. In turn, Grymel et al. described the synthesis and, subsequently, the cytotoxicity and antibacterial activity of triphenylphosphonium derivatives of betulin [9]. In total, nine new molecular hybrids of betulin with covalent linkage of the alkyltriphenylphosphonium moiety to the parent skeleton were obtained, with good to excellent yields. They showed high cytotoxicity (greater than natural betulin) toward the cell lines tested (HCT 116 and MCF-7), as well as antimicrobial properties against the Gram-positive reference *Staphylococcus aureus* ATCC 25923 and *Staphylococcus epidermidis* ATCC 12228 bacteria.

The next two articles address bisphosphoric systems, together with their synthesis and application [10,11]. Kuźnik et al. disclosed a simple and effective strategy for the synthesis of *N*-protected bisphosphoric analogs of protein and non-protein α -amino acids [10]. Indeed, the method based on the three-component reaction of 1-(*N*-acylamino)-1-ethoxyphosphonates with triphenylphosphonium tetrafluoroborate and triethyl phosphite allowed for the acquisition of 14 compounds with yields in the range of 40–96%. The

Citation: Adamek, J. Special Issue “Organophosphorus Chemistry: A New Perspective”. *Molecules* **2023**, *28*, 4752. <https://doi.org/10.3390/molecules28124752>

Received: 9 June 2023

Accepted: 12 June 2023

Published: 14 June 2023



Copyright: © 2023 by the author. Licensee MDPI, Basel, Switzerland. This article is an open access article distributed under the terms and conditions of the Creative Commons Attribution (CC BY) license (<https://creativecommons.org/licenses/by/4.0/>).

proposed methodology can also be used in the synthesis of unsymmetric bisphosphoric compounds via the sequential formation of C-P bonds with different phosphorus nucleophiles. The importance of research on bisphosphonates was also emphasized by Demadis et al. in their manuscript on drug-inclusive, inorganic–organic hybrid systems for the controlled release of zoledronate [11]. Two coordination polymers containing alkaline earth metal ions (Sr^{2+} and Ba^{2+}) and zoledronate (ZOL, the anti-osteoporotic drug) were synthesized and characterized. On the basis of the conducted studies, the influences of the type of cation on both the initial rate of drug release and the final value of the plateau release were determined.

The other articles are related to phosphonate compounds, their synthesis, reactivity, and biological properties [12–16]. Moilanen et al. prepared an interesting review article about the applications of α -aminophosphonates, -phosphinates, and -phosphine oxides as extraction and precipitation agents for rare earth metals, thorium, and uranium [12]. The authors described the most important methods for the synthesis of the abovementioned organophosphorus compounds and characterized their ability as extractants and precipitation agents. Some future perspectives related to the tunability of the solubility and coordination affinity of the α -amino-functionalized organophosphorus compounds were also discussed. Olszewski et al. described the deamination of 1-aminoalkylphosphonic acids in reaction with HNO_2 [13]. Mechanistic research and analysis of the obtained products allowed the authors to propose a plausible mechanism reaction with the formation of 1-phosphonoalkylium ions as reactive intermediates. Vicario et al. presented a general strategy for the synthesis of a wide family of α -aminophosphonate analogs of aspartic acid with tetrasubstituted carbons via the aza-Reformatsky reaction of α -iminophosphonates, generated from α -aminophosphonates [14]. In total, more than 20 such compounds were synthesized. Their cytotoxicity was also evaluated, and the structure–activity profile was determined. A one-pot lithiation–phosphonylation protocol to prepare heteroaromatic phosphonic acids was reported by Chmielewska et al. [15]. The scope of application and limitations of the proposed method were explored. The antiproliferative activity of the compounds obtained was also tested. Kielbasiński and Janicki described the application of alkyl di-(1,1,1,3,3,3-hexafluoroisopropyl)phosphonoacetates in the highly Z-selective Horner–Wadsworth–Emmons olefination as modified Still–Gennari-type reagents [16]. Excellent results, with an up to a 98:2 Z:E product ratio and up to quantitative yield, were achieved using the abovementioned reagents in the olefination of aromatic aldehydes.

Finally, the review article prepared by Balczewski et al. introduces readers to the chemistry of linearly fused aromatics, called acenes [17]. This study is not only a retrospective investigation but also a presentation of the current state of knowledge on the synthesis, properties, and applications of phosphorus (P^{III} , P^{IV} , P^{V})-substituted acenes.

In conclusion, organophosphorus chemistry continues to attract the unwavering interest of many research groups. The level of the research presented is high, and its subject matter attracts great attention, as evidenced by increasing metrics (citations, views). Therefore, I would like to thank all the authors who chose to report their results in this Special Issue and acknowledge the contributions of the Academic Editors: Gabriele Micheletti, Constantina Papatriantafyllopoulou, Erika Bálint, and György Keglevich; all the peer reviewers; and the members of the Editorial Team, especially Marlene Zhang. Your support has been invaluable.

Conflicts of Interest: The author declares no conflict of interest.

References

1. He, R.; Ding, C.; Marouka, K. Phosphonium Salts as Chiral Phase-Transfer Catalysts: Asymmetric Michael and Mannich Reactions of 3-Aryloxindoles. *Angew. Chem.* **2009**, *48*, 4559–4561. [CrossRef] [PubMed]
2. Bradaric, C.J.; Downard, A.; Kennedy, C.; Robertson, A.J.; Zhou, Y. Industrial preparation of phosphonium ionic liquids. *Green Chem.* **2003**, *5*, 143–152. [CrossRef]
3. Allen, D.W.; Loakes, D.; Tebby, J. *Organophosphorus Chemistry*; The Royal Society of Chemistry: London, UK, 2016; Volume 45. [CrossRef]

4. Maryanoff, B.E.; Reitz, A.B. The Wittig olefination reaction and modifications involving phosphoryl-stabilized carbanions. Stereochemistry, mechanism, and selected synthetic aspects. *Chem. Rev.* **1989**, *89*, 863–927. [CrossRef]
5. Kolodiaznyy, O.I. Phosphorus Compounds of Natural Origin: Prebiotic, Stereochemistry, Application. *Symmetry* **2021**, *13*, 889. [CrossRef]
6. Russell, R.G.G. Bisphosphonates: The first 40 years. *Bone* **2011**, *49*, 2. [CrossRef]
7. Caminade, A.-M. Phosphorus Dendrimers as Nanotools against Cancers. *Molecules* **2020**, *25*, 3333. [CrossRef]
8. Adamek, J.; Grymel, M.; Kuźnik, A.; Październiak-Holewa, A. 1-Aminoalkylphosphonium Derivatives: Smart Synthetic Equivalents of *N*-Acyliminium-Type Cations, and Maybe Something More: A Review. *Molecules* **2022**, *27*, 1562. [CrossRef]
9. Grymel, M.; Lalik, A.; Kazek-Kęsik, A.; Szewczyk, M.; Grabiec, P.; Erfurt, K. Design, Synthesis and Preliminary Evaluation of the Cytotoxicity and Antibacterial Activity of Novel Triphenylphosphonium Derivatives of Betulin. *Molecules* **2022**, *27*, 5156. [CrossRef] [PubMed]
10. Kuźnik, A.; Kozicka, D.; Hawranek, W.; Socha, K.; Erfurt, K. One-Pot and Catalyst-Free Transformation of *N*-Protected 1-Amino-1-Ethoxyalkylphosphonates into Bisphosphonic Analogs of Protein and Non-Protein α -Amino Acids. *Molecules* **2022**, *27*, 3571. [CrossRef] [PubMed]
11. Vassaki, M.; Lazarou, S.; Turhanen, P.; Choquesillo-Lazarte, D.; Demadis, K.D. Drug-Inclusive Inorganic–Organic Hybrid Systems for the Controlled Release of the Osteoporosis Drug Zoledronate. *Molecules* **2022**, *27*, 6212. [CrossRef]
12. Kukkonen, E.; Virtanen, E.J.; Moilanen, J.O. α -Aminophosphonates, -Phosphinates, and -Phosphine Oxides as Extraction and Precipitation Agents for Rare Earth Metals, Thorium, and Uranium: A Review. *Molecules* **2022**, *27*, 3465. [CrossRef] [PubMed]
13. Brol, A.; Olszewski, T.K. Deamination of 1-Aminoalkylphosphonic Acids: Reaction Intermediates and Selectivity. *Molecules* **2022**, *27*, 8849. [CrossRef] [PubMed]
14. del Corte, X.; Maestro, A.; López-Francés, A.; Palacios, F.; Vicario, J. Synthesis of Tetrasubstituted Phosphorus Analogs of Aspartic Acid as Antiproliferative Agents. *Molecules* **2022**, *27*, 8024. [CrossRef] [PubMed]
15. Chmielewska, E.; Miodowska, N.; Dziuk, B.; Psurski, M.; Kafarski, P. One-Pot Phosphonylation of Heteroaromatic Lithium Reagents: The Scope and Limitations of Its Use for the Synthesis of Heteroaromatic Phosphonates. *Molecules* **2023**, *28*, 3135. [CrossRef] [PubMed]
16. Janicki, I.; Kiełbasiński, P. Highly *Z*-Selective Horner–Wadsworth–Emmons Olefination Using Modified Still–Gennari-Type Reagents. *Molecules* **2022**, *27*, 7138. [CrossRef] [PubMed]
17. Koprowski, M.; Owsianik, K.; Knopik, Ł.; Vivek, V.; Romaniuk, A.; Różycka-Sokołowska, E.; Balczewski, P. Comprehensive Review on Synthesis, Properties, and Applications of Phosphorus (P^{III} , P^{IV} , P^V) Substituted Acenes with More Than Two Fused Benzene Rings. *Molecules* **2022**, *27*, 6611. [CrossRef] [PubMed]

Disclaimer/Publisher’s Note: The statements, opinions and data contained in all publications are solely those of the individual author(s) and contributor(s) and not of MDPI and/or the editor(s). MDPI and/or the editor(s) disclaim responsibility for any injury to people or property resulting from any ideas, methods, instructions or products referred to in the content.

Review

1-Aminoalkylphosphonium Derivatives: Smart Synthetic Equivalents of *N*-Acyliminium-Type Cations, and Maybe Something More: A Review †

Jakub Adamek ^{1,2,*} , Mirosława Grymel ^{1,2,3} , Anna Kuźnik ^{1,2}  and Agnieszka Październiak-Holewa ^{1,2} 

¹ Department of Organic Chemistry, Bioorganic Chemistry and Biotechnology, Silesian University of Technology, B. Krzywoustego 4, 44-100 Gliwice, Poland; mirosława.grymel@polsl.pl (M.G.); anna.kuznik@polsl.pl (A.K.); agnieszka.pazdzierniak-holewa@polsl.pl (A.P.-H.)

² Biotechnology Center, Silesian University of Technology, B. Krzywoustego 8, 44-100 Gliwice, Poland

³ Department of Chemical Organic Technology and Petrochemistry, Faculty of Chemistry, Silesian University of Technology, B. Krzywoustego 4, 44-100 Gliwice, Poland

* Correspondence: jakub.adamek@polsl.pl; Tel.: +48-032-237-1724; Fax: +48-032-237-2094

† With a special dedication to Roman Mazurkiewicz in honor of the achievements within his career along with thanks from his scientific pupils.

Abstract: *N*-acyliminium-type cations are examples of highly reactive intermediates that are willingly used in organic synthesis in intra- or intermolecular α -amidoalkylation reactions. They are usually generated in situ from their corresponding precursors in the presence of acidic catalysts (Brønsted or Lewis acids). In this context, 1-aminoalkyltriarylphosphonium derivatives deserve particular attention. The positively charged phosphonium moiety located in the immediate vicinity of the *N*-acyl group significantly facilitates C_{α} - P^+ bond breaking, even without the use of catalyst. Moreover, minor structural modifications of 1-aminoalkyltriarylphosphonium derivatives make it possible to modulate their reactivity in a simple way. Therefore, these types of compounds can be considered as smart synthetic equivalents of *N*-acyliminium-type cations. This review intends to familiarize a wide audience with the unique properties of 1-aminoalkyltriarylphosphonium derivatives and encourage their wider use in organic synthesis. Hence, the most important methods for the preparation of 1-aminoalkyltriarylphosphonium salts, as well as the area of their potential synthetic utilization, are demonstrated. In particular, the structure–reactivity correlations for the phosphonium salts are discussed. It was shown that 1-aminoalkyltriarylphosphonium salts are not only an interesting alternative to other α -amidoalkylating agents but also can be used in such important transformations as the Wittig reaction or heterocyclizations. Finally, the prospects and limitations of their further applications in synthesis and medicinal chemistry were considered.

Keywords: phosphonium salts; *N*-acyliminium cations; α -amidoalkylation; α -amidoalkylating agents; ylides; Wittig reaction

Citation: Adamek, J.; Grymel, M.; Kuźnik, A.; Październiak-Holewa, A. 1-Aminoalkylphosphonium Derivatives: Smart Synthetic Equivalents of *N*-Acyliminium-Type Cations, and Maybe Something More: A Review. *Molecules* **2022**, *27*, 1562. <https://doi.org/10.3390/molecules27051562>

Academic Editor: György Keglevich

Received: 26 January 2022

Accepted: 24 February 2022

Published: 26 February 2022

Publisher's Note: MDPI stays neutral with regard to jurisdictional claims in published maps and institutional affiliations.



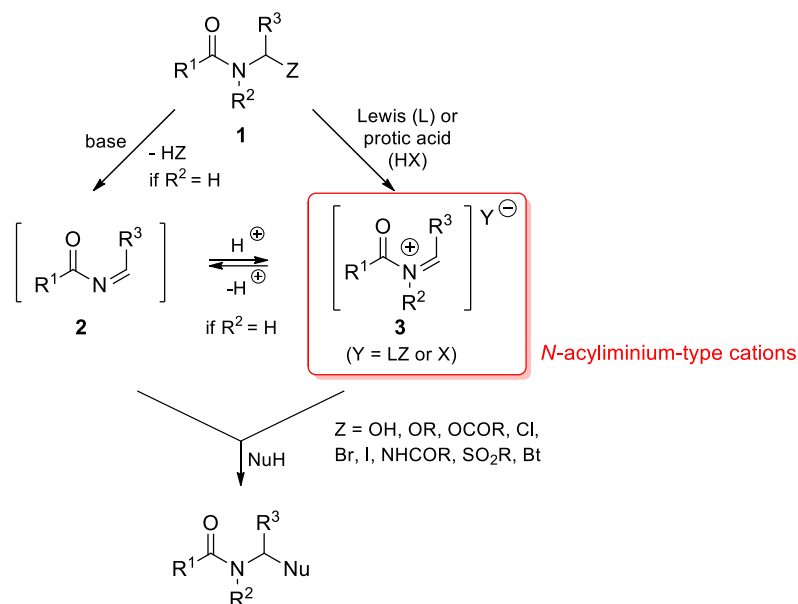
Copyright: © 2022 by the authors. Licensee MDPI, Basel, Switzerland. This article is an open access article distributed under the terms and conditions of the Creative Commons Attribution (CC BY) license (<https://creativecommons.org/licenses/by/4.0/>).

1. Introduction

α -Amidoalkylation reactions play an increasingly important role in organic synthesis as convenient and effective methods for the formation of C-C and C-heteroatom bonds, particularly of the intramolecular type, allowing the synthesis of carbo- or heterocyclic systems. In most cases, *N*-acylimine **2** or *N*-acyliminium cations **3** are the correct α -amidoalkylating agents and they are generated from precursors with the relevant structure **1** (Scheme 1) [1–23].

Many examples of α -amidoalkylating agent precursors and their applications in α -amidoalkylations have been reported in the literature. A brief summary is given in Table 1. Compared to the precursors described therein, 1-aminoalkylphosphonium derivatives are relatively unknown compounds. However, they have unique structural features

which promote the generation of *N*-acyliminium-type cations. One of the most important is the presence of a positively charged phosphonium moiety (which easily departs as triarylphosphine PAr_3) in the immediate vicinity of the acyl group.



Scheme 1. The α -amidoalkylation reaction.

Moreover, the reactivity of 1-aminoalkylphosphonium derivatives can be modulated by simple structural modifications, e.g., by changing the amino protecting group or by the introduction of electron-withdrawing substituents to the phosphonium moiety (replacing Ph_3P by $(3\text{-C}_6\text{H}_4\text{Cl})_3\text{P}$ or $(4\text{-C}_6\text{H}_4\text{CF}_3)_3\text{P}$; see Figure 1). Depending on the structure of the phosphonium salt used, the α -amidoalkylations may require a basic or acidic catalyst. However, the introduction of the abovementioned activating structural modifications allows one, in many cases, to conduct the reactions under milder and even catalyst-free conditions. Furthermore, such modifications not only affect the reactivity but also the course of the reaction (for example, to reduce side reactions), or even make it possible to change the type of reaction taking place (the α -amidoalkylation reaction vs the Wittig reaction).

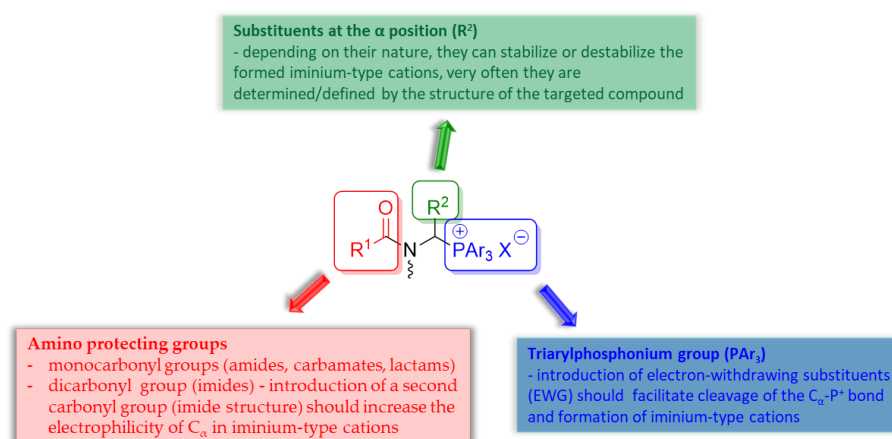
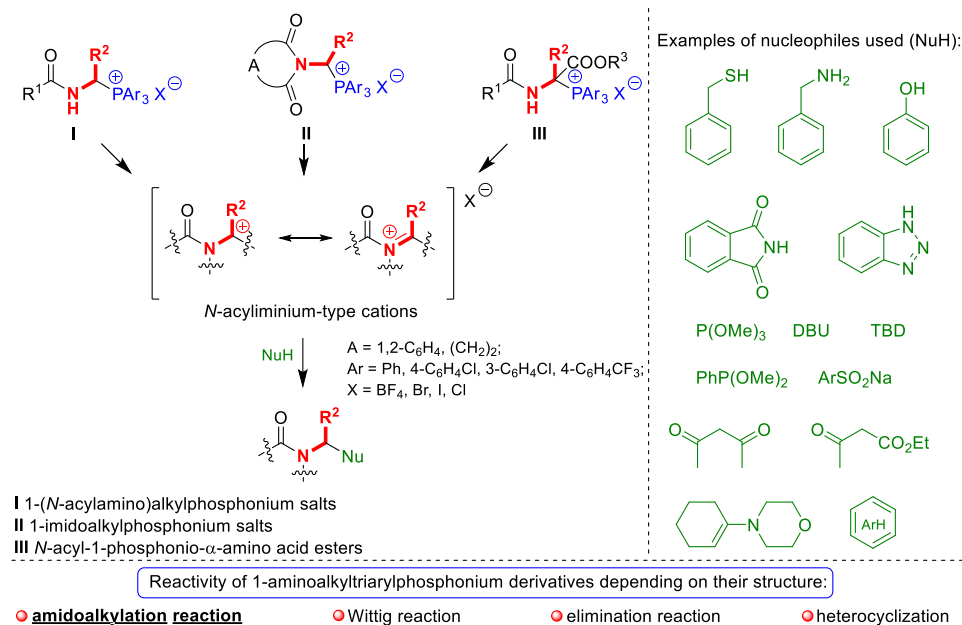


Figure 1. Areas of potential structural modifications within phosphonium precursors of α -amid oalkylating agents.

The main purpose of this review paper is to organize and disseminate current knowledge about 1-aminoalkylphosphonium derivatives. To help understand the presented issues, three classes of these P-compounds have been distinguished. Three separate chapters

are dedicated to them, where general properties, the most important methods for preparation as well as synthetic applications are described. Particularly, the correlation between the structure and the reactivity of phosphonium derivatives I-III is discussed. Scheme 2 provides a classification and a brief summary of the chemistry of 1-aminoalkylphosphonium derivatives.

1-Aminoalkyltriarylphosphonium derivatives as synthetic equivalents of *N*-acyliminium-type cations:

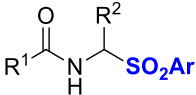


Scheme 2. Classification and reactivity of 1-aminoalkylphosphonium derivatives.

Table 1. Summary of characteristics for the most important precursors of α -amidoalkylating agents 1.

| Structure of Precursor | Summary of Characteristics | Examples of Use in α -Amidoalkylation (Selected Research or Review Literature) ^a |
|------------------------|--|--|
| | limited structural diversity, limited reactivity, parent compounds for the other α -amidoalkylating agents, activation with acidic catalysts, synthesis from amides (or imides) and aldehydes (mostly in situ)—only <i>N</i> -hydroxymethylamides (or -imides) can be easily isolated | [3,4,6–12] |
| | limited reactivity, high structural diversity, activation with acidic catalysts, main synthesis methods based on electrochemical alkoxylation | [5–9,12–14] |
| | high reactivity, rather low yields in α -amidoalkylation reactions (lots of by-products), difficulties in the preparation, purification and storage | [6–9,12] |
| | high reactivity (good leaving group), high structural diversity, activation with acidic catalysts, easy to use and storage, diverse methods of synthesis, broad scope of application | [8,9,12,16–19] |

Table 1. Cont.

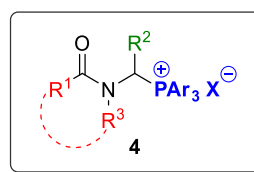
| Structure of Precursor | Summary of Characteristics | Examples of Use in α -Amidoalkylation (Selected Research or Review Literature) ^a |
|---|---|--|
|  | high reactivity (good leaving group), high structural diversity, activation with acidic catalysts, easy to use and storage, diverse methods of synthesis, broad scope of application, currently the most popular and convenient | [8,9,12,20–23] |

^a Selected examples aimed at showing the most recent interest in α -amidoalkylation reactions.

2. 1-Aminoalkyltriarylphosphonium Derivatives

2.1. 1-(*N*-acylamino)alkylphosphonium Salts

Compounds with general formula **4** (Figure 2) are often called 1-(*N*-acylamino)alkylphosphonium salts, because a lot of the described models are amide derivatives (e.g., $R^1 = \text{H}$, Me, Et, *t*-Bu, Ph, Bn, etc.; $R^3 = \text{H}$). It is not an exact name because this group also includes lactams (e.g., $R^1, R^3 = (\text{CH}_2)_3$), carbamates ($R^1 = t\text{-BuO}$, BnO; $R^3 = \text{H}$) or urea derivatives (e.g., $R^1 = \text{NMe}_2$, $R^3 = \text{H}$). In the α -position, there may be hydrogen ($R^2 = \text{H}$), alkyl ($R^2 = \text{Me}$, Et, *i*-Bu, etc.), aryl ($R^2 = \text{Ph}$, 2-thienyl, 1-naphtyl, etc.) or more complex substituents (e.g., $\text{CH}_2\text{CO}_2-t\text{-Bu}$, $\text{CH}_2\text{C}_6\text{H}_4\text{OBn}$, $\text{PO}(\text{OEt})_2$ etc.). The positively charged triarylphosphonium group PAR_3 (Ar = Ph, 3- $\text{C}_6\text{H}_4\text{Cl}$, 4- $\text{C}_6\text{H}_4\text{CF}_3$) is also directly bonded to C_α .



$R^1 = \text{Me}, t\text{-Bu}, \text{Ph}, \text{Bn}, \text{MeO}, t\text{-BuO}, \text{BnO}, \text{NMe}_2$; $R^3 = \text{H}$; $R^1, R^3 = (\text{CH}_2)_3$;
 $R^2 = \text{H}, \text{Me}, \text{Et}, i\text{-Pr}, i\text{-Bu}, \text{CH}_2\text{OMe}, \text{CH}_2\text{O}t\text{-Bu}, \text{CH}_2\text{CO}_2\text{Me}, \text{CH}_2\text{CH}=\text{CH}_2, \text{Bn}, \text{CH}_2\text{C}_6\text{H}_4\text{OBn}, \text{PO}(\text{OEt})_2$ etc.;
 Ar = Ph, 3- $\text{C}_6\text{H}_4\text{Cl}$, 4- $\text{C}_6\text{H}_4\text{CF}_3$, 4- $\text{C}_6\text{H}_4\text{OMe}$; X = BF_4 , Br, Cl, ClO_4 , I.

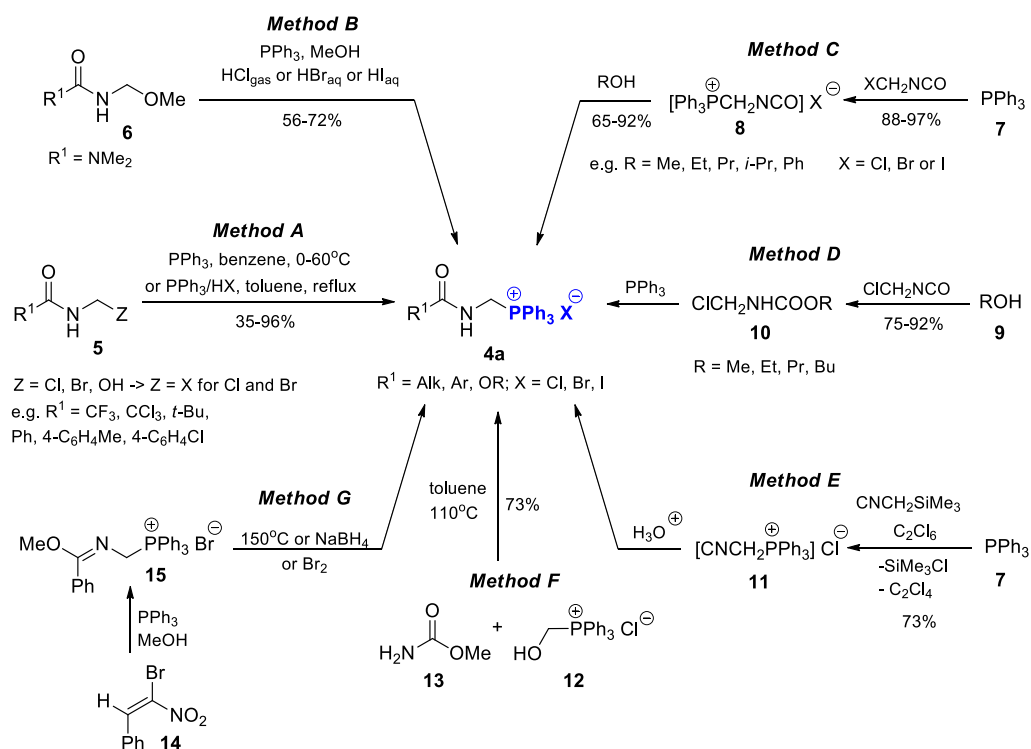
Figure 2. General structure of 1-(*N*-acylamino)alkylphosphonium salts **4**.

1-(*N*-acylamino)alkyltriphenylphosphonium salts **4** (Ar = Ph) are crystalline, stable at room temperature compounds that can be stored under laboratory conditions for a long time. They are well soluble in DCM and MeCN, but insoluble in diethyl ether. The most effective method of their purification is crystallization from DCM/ Et_2O or MeCN/ Et_2O systems. 1-(*N*-acylamino)alkyltriarylphosphonium salts **4** which are derivatives of triarylphosphines with electron-withdrawing substituents (Ar = 3- $\text{C}_6\text{H}_4\text{Cl}$ or 4- $\text{C}_6\text{H}_4\text{CF}_3$) are less stable. They are usually synthesized just before the reaction and used without purification. The type of phosphonium group used has a huge impact on the reactivity of the whole molecule, which will be discussed later in this review.

2.1.1. Preparation

In the last century, most of the methods for the synthesis of 1-(*N*-acylamino)alkyltriaryl phosphonium salts **4** concerned 1-(*N*-acylamino)methyltriphenylphosphonium salts (**4a**, $R^2 = \text{H}$, Scheme 3). Between 1972 and 1991, Drach, Brovarets and co-workers [24–27] showed that 1-(*N*-acylamino)methylphosphonium chlorides (**4a**, X = Cl) can be obtained, in a simple reactions, by alkylation of triphenylphosphine (but also tributylphosphine PBu_3 or hexaethylphosphorus triamide $\text{P}(\text{NEt}_2)_3$) with *N*-(chloromethyl)amides (**5**, Z = Cl) (Scheme 3, Method A). They also used *N*-(hydroxymethyl)amides (**5**, Z = OH) as alkylating agents, that were *N*-(chloromethyl)amides precursors (Scheme 3, Method A) [27]. In 1974, Devlin and Walker reported similar reactions, which were carried out at room temperature, using AcOEt as a solvent. They obtained 1-(*N*-benzoylamino)methyltriphenylphosphonium bromide or chloride (**4a**, X = Br or Cl) from *N*-(bromomethyl)benzamide or *N*-(chloromethyl)

benzamide, respectively, in 54% and 69% yield (Scheme 3, Method A) [28]. Triphenylphosphine was also alkylated with *N*-(methoxymethyl)urea derivative **6** (Scheme 3, Method B). Reactions were carried out in methanol by bubbling HCl gas through the substrate solution or by treating it with aqueous HBr or HI [29]. 1-(*N*-alkoxycarbonyl)methyltriphenylphosphonium chlorides or bromides (**4a**, R¹ = OR, X = Cl or Br) were obtained by Kozhushko et al. in the reaction of triphenylphosphine with chloromethylisocyanate or bromomethylisocyanate and further hydrolysis of the isocyanate group (Scheme 3, Method C) [30,31]. In analogous reactions, the corresponding triphenylphosphonium iodides (**4a**, R¹ = OR, X = I) were also obtained by adding methyl iodide in the first step of the synthesis [32]. The same authors also described reactions in which phosphonium salts **4a** (R¹ = OR, X = Cl) were obtained by alkylation of triphenylphosphine with *N*-(chloromethyl)carbamates **10**, that were previously generated from alcohol and methyl isocyanide (Scheme 3, Method D) [33]. In turn, Zinner and Fehlhammer described the two-stage method for the synthesis of 1-(*N*-formylamino)methyltriphenylphosphonium chloride **4a** (R¹ = H, X = Cl). Initially, they conducted the alkylation of triphenylphosphine using trimethylsilyl isocyanide in the presence of hexachloroethane in THF. The acidic hydrolysis of indirectly formed isocyanomethyltriphenylphosphonium chloride **11** finally yielded the expected phosphonium salt **4a** (Scheme 3, Method E) [34]. However, the authors did not report the yield of the hydrolysis step.

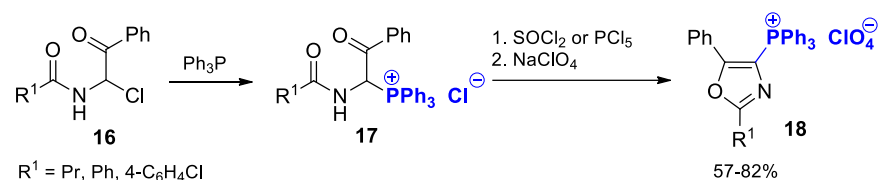


Scheme 3. Methods for the synthesis of 1-(*N*-acylamino)methyltriphenylphosphonium salts **4a**.

Only a few of the described methods for synthesizing 1-(*N*-acylamino)methyltriphenyl phosphonium salts **4a** were based on other approaches than the alkylation of triphenylphosphine by *N*-(halomethyl)amides, their precursors or related compounds. One of these methods involved the alkylation of methyl carbamate with hydroxymethyltriphenylphosphonium chloride **12**, which resulted in the production of 1-(*N*-methoxycarbonyl)aminomethyltriphenylphosphonium chloride **4a** (R¹ = OMe, X = Cl) in 73% yield (Scheme 3, Method F) [35]. Devlin and Walker demonstrated that the treatment of 2-bromo-2-nitrostyrene **14** with triphenylphosphine in methanol gave the phosphonium salt **15** in 47% yield. The vacuum pyrolysis of salt **15** at 150 °C, reduction with NaHBF₄ in methanol or refluxing in chloroform with addition of bromine led to a mixture containing 1-(*N*-benzoylamino)methyltriphenyl

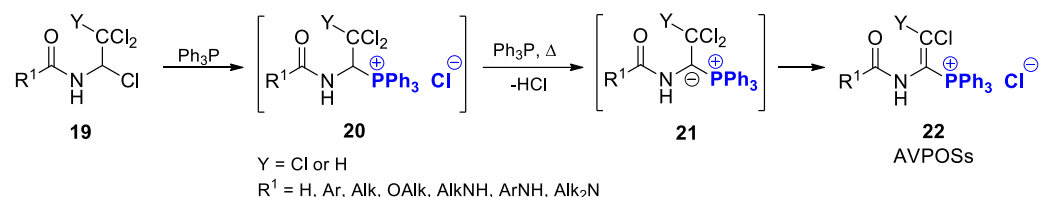
enylphosphonium bromide **4a** ($R^1 = \text{Ph}$, $X = \text{Br}$) as the main product (Scheme 3, Method G) [28,36].

There are few data available in the literature on the synthesis of 1-substituted phosphonium salts **4**. In 1975, Drach et al. demonstrated that the reaction of triphenylphosphine with *N*-(1-benzoyl-1-chloromethyl)amides **16** led to triphenylphosphonium salts **17** with a benzoyl group at the 1-position. However, salts **17** turned out to be hygroscopic and unstable. Thus, the authors decided to transform them into more stable oxazolones **18** (Scheme 4) [37].



Scheme 4. Synthesis of 1-(*N*-acylamino)benzoylmethyltriphenylphosphonium chlorides **17**.

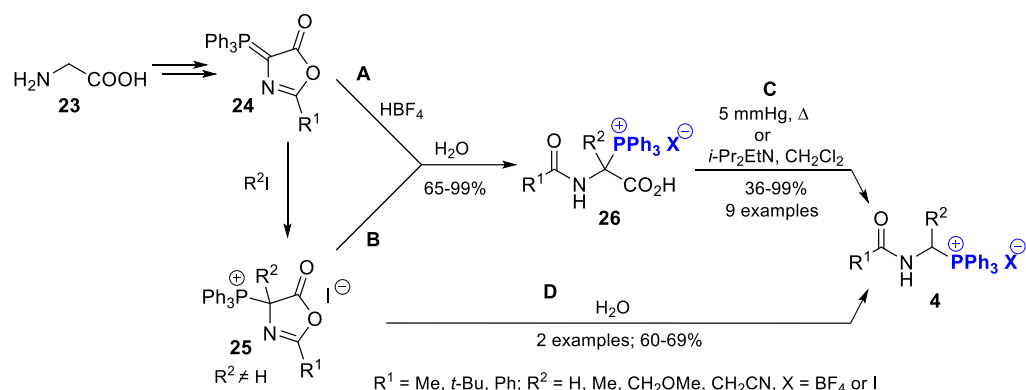
Next, Drach et al. described the route for the synthesis of various 1-(*N*-acylamino)-substituted vinylphosphonium salts **22**, which was based on the condensation of triphenylphosphine with *N*-polychloroalkylamides **19** [38,39]. As reported by the authors, in the first step, the salts **20** were probably formed, which further split off hydrogen chloride, resulting in the formation of the corresponding vinylphosphonium salts **22**, typically in yields above 90% (Scheme 5). 1-(*N*-acylamino)vinylphosphonium salts (AVPOSs) **22** are unique reagents for various types of heterocyclization, which was comprehensively discussed by Drach, Brovarets, and co-workers in 2002 [39].



Scheme 5. Synthesis of 1-(*N*-acylamino)vinylphosphonium salts (AVPOSs) **22**.

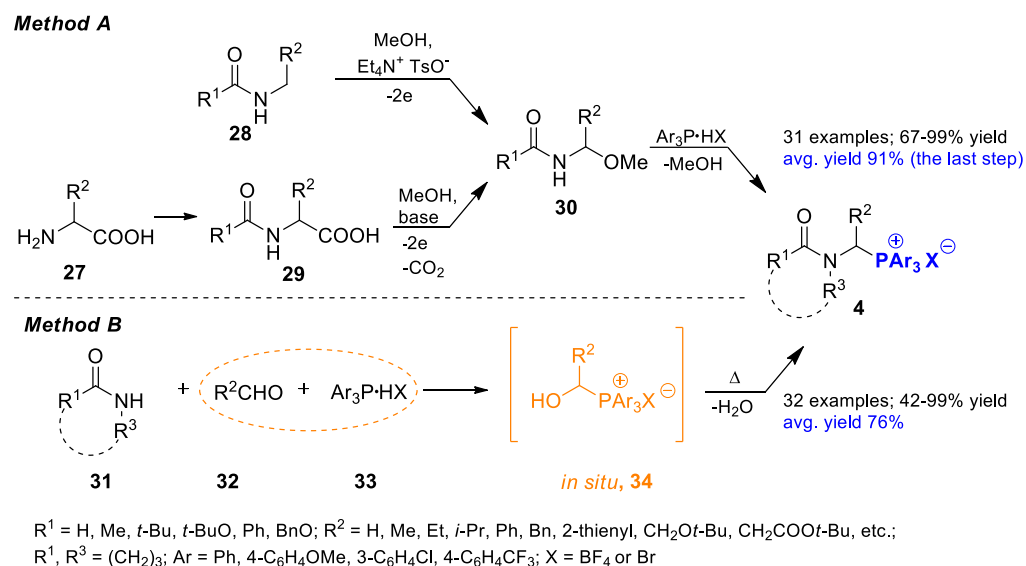
At about the same time, Mazurkiewicz et al. started more extensive research on the synthesis of structurally diverse 1-(*N*-acylamino)alkyltriarylphosphonium salts **4**. Wherein, the common feature of these methods was the raw materials, which was *N*-protected α -amino acids. The use of α -amino acids or their derivatives as substrates was greatly advantageous, due to almost unlimited availability and structural diversity of such compounds.

The first approach was based on using 4-triphenylphosphoranylidene-5(4*H*)-oxazolones **24** or 4-alkyl-4-triphenylphosphonio-5(4*H*)-oxazolones **25**, obtained from glycine (Scheme 6) [40]. Phosphoranylidene-5(4*H*)-oxazolones **24**, were hydrolyzed at room temperature in the presence of HBF_4 to *N*-acyl- α -triphenylphosphonioglycines **26** ($R^2 = \text{H}$, Scheme 6/A). Similarly, phosphonium iodides **25** were exposed to water in the mixture of THF/DCM, but without any acidic catalyst. Under these conditions, compounds **25** were transformed, in a few days, into *N*-acyl-1-triphenylphosphonio- α -amino acids **26** ($R^2 = \text{Me}$, Scheme 6/B). In the next stage, 1-triphenylphosphonio- α -amino acids **26** were heated at 105–115 °C under reduced pressure (5 mmHg) or treated with diisopropylethylamine in DCM at 20 °C, which resulted in their decarboxylation to corresponding 1-(*N*-acylamino)alkyltriphenylphosphonium salts **4**, usually in good yields (Scheme 6/C). The authors also showed, that in the case of hydrolysis of 4-alkyl-4-triphenylphosphonio-5(4*H*)-oxazolones **25** with a bulky substituent in the 4-position, the reaction proceeded with simultaneous decarboxylation and gave the expected 1-(*N*-acylamino)alkyltriphenylphosphonium salts **4** in one reaction step (Scheme 6/D) [41,42].



Scheme 6. Synthesis of 1-(*N*-acylamino)alkylphosphonium salts **4** from oxazolones.

However, the two most important and general methods for the synthesis of 1-(*N*-acylamino)alkylphosphonium salts **4** were developed by Mazurkiewicz and Adamek in the last 10 years (Scheme 7) [43,44].



Scheme 7. Modern strategy in the synthesis of 1-(*N*-acylamino)alkylphosphonium salts **4**; Method A—Synthesis based on the electrochemical alkoxylation; Method B—Non-electrochemical synthesis based on the one-pot, three components coupling.

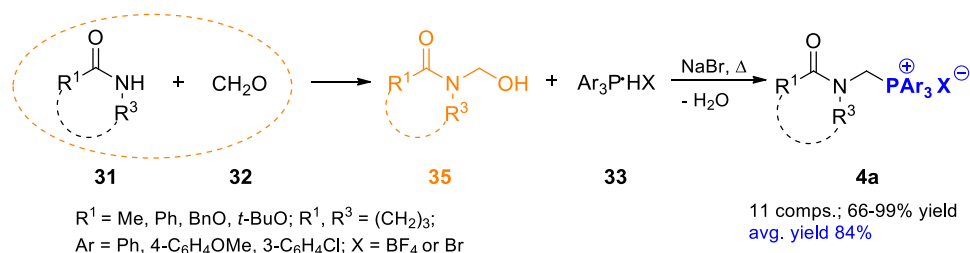
The first, three-stage method begins with the appropriate protection of α -amino acid functional groups (the NH_2 group and other groups susceptible to electrochemical oxidation). Next, electrochemical decarboxylative α -methoxylation (or more generally, alkoxylation) takes place. As the authors noted, the electrochemical oxidations could be carried out in methanol with the addition of sodium methoxide as a base or in the presence of a solid-supported base ($\text{SiO}_2\text{-Pip}$); wherein the latter process (based on a solid-supported base) proceeded in excellent yields and had a less complicated work-up. Recently, a simpler and even more efficient, standardized method for preparation of *N,O*-acetals **30** using the commercially available ElectraSyn 2.0 setup (graphite electrodes, Et_3N as a base, room temp.) was described [45].

The last step is the substitution of the methoxy group in the reaction of *N,O*-acetals **30** with various types of phosphonium salts ($\text{Ar}_3\text{P}\cdot\text{HX}$, Scheme 7; Method A). The proposed method allows high yields (up to 99%) to be obtained not only for the simplest 1-(*N*-acylamino)alkylphosphonium salts **4** (e.g., $R^2 = \text{H}$), but also for much more complex structure, including derivatives of phosphine with various substituents ($\text{Ar} = \text{Ph}, 3\text{-C}_6\text{H}_4\text{Cl}, 4\text{-C}_6\text{H}_4\text{CF}_3$) [43,46]. Moreover, the raw material base can be expanded, since

N-methoxyalkyl derivatives can be obtained by electrochemical oxidation of amides, carbamates or lactams. However, this is a less efficient process and an aqueous work-up of the reaction mixture is necessary [47].

In 2021, a procedure for the preparation of *N*-protected aminoalkylphosphonium salts (including 1-(*N*-acylamino)alkylphosphonium ones) in one reaction step from aldehydes and either amides, carbamates, lactams, or urea in the presence of phosphonium salts **33** -Ar₃P·HX (Scheme 7; Method B) was described [44]. Using a one-pot methodology, the simple work-up of the reaction mixture (no chromatography) makes 1-(*N*-acylamino)alkylphosphonium salts obtainable in high yields under relatively mild conditions (even at room temperature, but usually at 50 °C for 1 h). So far, it is the only general method of obtaining *N*-protected aminoalkylphosphonium salts without the use of electrochemical techniques [44]. Mechanistic studies showed that in the first step of the transformation, aldehydes and phosphonium salts (Ar₃P·HX) form 1-hydroxyalkylphosphonium salts **34**, which then react with amide-type substrates **31** to give the desired 1-(*N*-acylamino)alkylphosphonium salts **4** in good to excellent yields [44].

Next, it was shown that by conducting the reaction step-by-step and changing the order of the reacting compounds, 1-(*N*-acylamino)alkylphosphonium salts **4** could also be obtained. However, the procedure is effective only for formaldehyde (or paraformaldehyde). Hydroxymethylamides **35**, already mentioned in the introduction (see also Table 1), are generated during such a transformation (Scheme 8). This method works well for the synthesis of *N*-protected aminomethyltriarylphosphonium salts **4a**, but requires a catalyst (NaBr) and elevated temperatures (70–135 °C) [48].



Scheme 8. Step-by-step procedure for the synthesis of *N*-protected aminomethylphosphonium salts **4a**.

The presented methods (Schemes 7 and 8) are based on a wide and diverse base of raw materials (α -amino acids, amide-type compounds, aldehydes), and provide easy access to structurally diverse 1-(*N*-acylamino)alkylphosphonium salts **4** also in the synthesis on a larger gram-scale [44,48].

2.1.2. Synthetic Utilization

Synthetic applications of 1-(*N*-acylamino)alkylphosphonium salts **4** are summarized in Figure 3. The high reactivity of such compounds is mainly related to the possibility of easy cleaving of the C $_{\alpha}$ -P⁺ bond (Scheme 9).

The strength of the C $_{\alpha}$ -P⁺ bond can be further reduced by introducing electron-withdrawing substituents to the phosphonium moiety (Scheme 10, Ar = 3-C₆H₄Cl and 4-C₆H₄CF₃). The equilibrium in such systems was examined and described in 2018 [46]. As can be seen, it is shifted toward more stable and less reactive 1-(*N*-acylamino)alkylphosphonium salts (reactivity: PS-CF₃ > PS-Cl > PS-H; stability: PS-CF₃ < PS-Cl < PS-H).

The ease of formation of iminium-type cations **3** from phosphonium salts **4** was essential in the α -amidoalkylation reactions of various types of nucleophiles (C-nucleophiles and heteronucleophiles). In many cases, the generation of such reactive intermediates can proceed without the use of any catalysts, which is an amazing advantage compared to other α -amidoalkylating agents described in the literature (e.g., *N*-(1-methoxyalkyl)amides, α -amido sulfones, or *N*-(benzotriazolylalkyl)amides) [12,20].

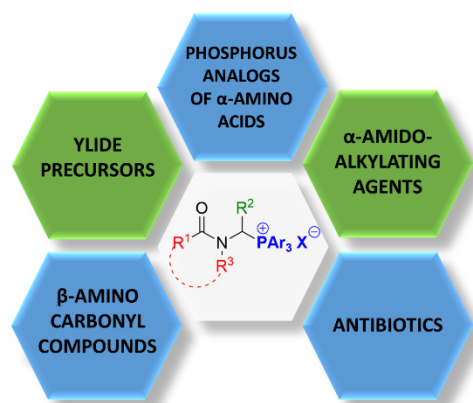
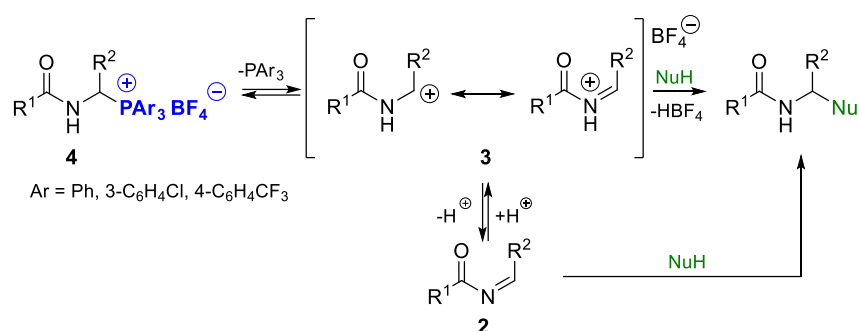
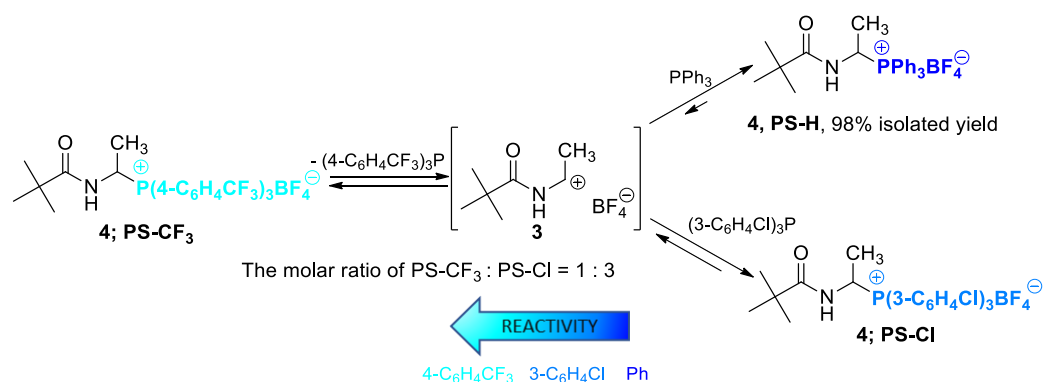


Figure 3. Applications of 1-(*N*-acylamino)alkylphosphonium salts **4**.



Scheme 9. 1-(*N*-acylamino)alkyltriarylphosphonium salts **4** as precursors of *N*-acylimines **2** and *N*-acyliminium-type cations **3**.

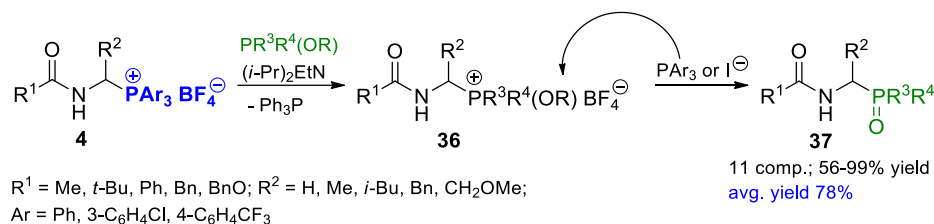


Scheme 10. Generation of *N*-acyliminium-type cations from 1-(*N*-acylamino)alkyltriarylphosphonium salts **4**.

One of the most widely described α -amidoalkylation reactions involving 1-(*N*-acylamino)alkylphosphonium salts is the reaction with *P*-nucleophiles: phosphites, phosphonites, or phosphinites. The products of these transformations are called phosphorus analogs of α -amino acids **37** (more precisely: 1-aminoalkanephosphonic acid derivatives, 1-aminoalkanephosphinic acid derivatives, or 1-aminoalkylphosphine oxide derivatives), and they are extremely interesting in terms of their biological activity [49].

Initially, the Michaelis–Arbuzov-type reaction with a double catalytic system was used for the synthesis of such compounds. A base (e.g., the Hünig's base-(*i*-Pr)₂EtN) facilitates the cleavage of the C _{α} -P⁺ bond and the formation of corresponding *N*-acylimine. In turn, the iodide anion (introduced as methyltriphenylphosphonium iodide) enables dealkylation of the intermediate alkoxyphosphonium salt **36** (Scheme 11) [50–52]. Further studies showed that the reaction could be carried out also under a catalytic-free conditions [46,52].

It was also possible, for the first time, to isolate and characterize one of the intermediates **36** ($R^1 = t\text{-Bu}$; $R^2 = \text{Me}$; $R^3, R^4 = \text{OR} = \text{OEt}$, Scheme 11), thus proving the reaction mechanism [46].



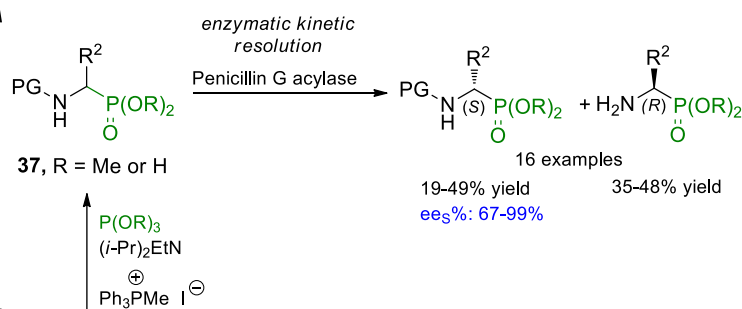
P-nucleophiles - $\text{PR}^3\text{R}^4(\text{OR})$:

$\text{P}(\text{OMe})_3, \text{P}(\text{OEt})_3, \text{EtP}(\text{OEt})_2, \text{PhP}(\text{OMe})_2, \text{PhP}(\text{OEt})_2, \text{Ph}_2\text{P}(\text{OMe})$

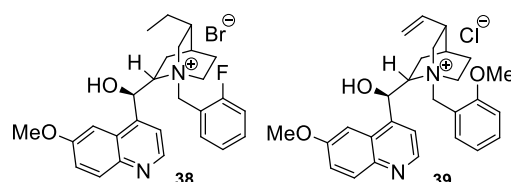
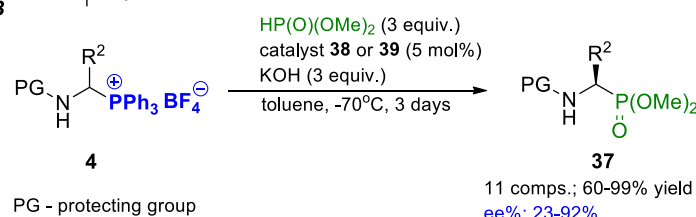
Scheme 11. Michaelis–Arbuzov-type reaction of 1-(*N*-acylamino)alkylphosphonium salts **4** with *P*-nucleophiles.

Unfortunately, the major disadvantage of these reactions is the complete racemization of the products. However, two solutions were proposed to overcome this drawback. The first was enzymatic kinetic resolution of products using Penicillin G acylase from *Escherichia coli* (Scheme 12, Method A) [53,54]. The second was changing the synthetic approach and to conduct organocatalytic α -amidoalkylation of *P*-nucleophiles (e.g., dimethyl phosphite; Michaelis–Becker-type reaction) by 1-(*N*-acylamino)alkyltriphenylphosphonium salts in PTC systems using Cinchona alkaloid derivatives **38** and **39** as catalysts (Scheme 12, Method B) [55].

Method A

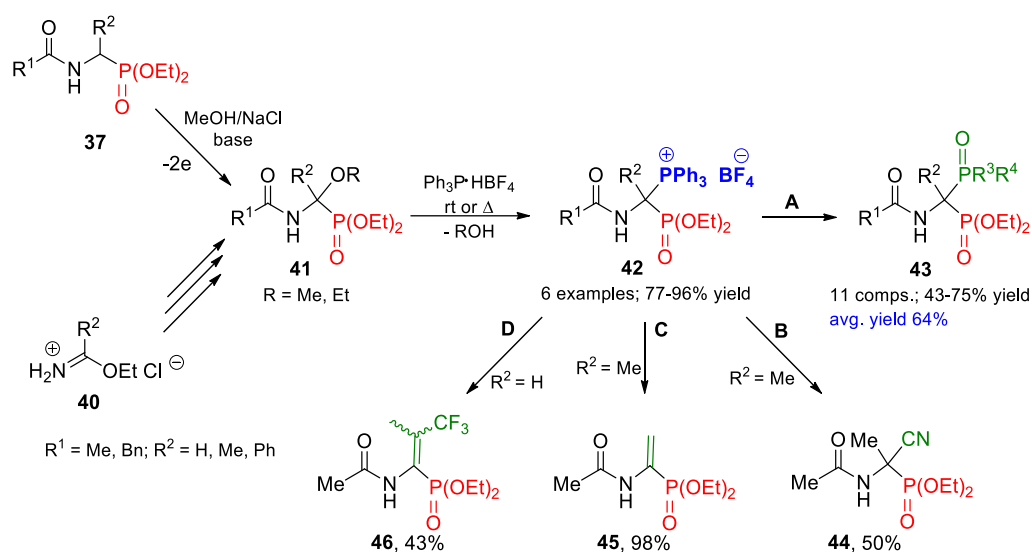


Method B



Scheme 12. Methods for the obtaining of enantiomerically enriched phosphorus analogs of α -amino acids **37** via 1-(*N*-acylamino)alkyltriphenylphosphonium salts **4** based on enzymatic kinetic resolution (Method A) or organocatalytic α -amidoalkylation of *P*-nucleophiles in PTC systems (Method B).

Further research on phosphorus analogs of α -amino acids **37** revealed the possibility of transforming them into bisphosphoric acid esters **43**, which also exhibit important biological activity (Scheme 13) [56,57].



Scheme 13. Synthesis and applications of 1-(*N*-acylamino)-1-triphenylphosphoniumalkylphosphonates **42**. Reagents and conditions: (A) R^3R^4POR (e.g., $P(OEt)_3$, $MeP(OEt)_2$, $Ph_2P(OMe)$, etc.), (*i*-Pr) $_2EtN$, $Ph_3P^+Me I^-$, 20–60 °C, 0.3–6 h; (B) KCN, 18-crown-6, 20 °C, 24 h; (C) (*i*-Pr) $_2EtN$, 20 °C, 5 h; (D) $MeC(O)CF_3$, K_2CO_3 , 18-crown-6, 50 °C, 4 h.

Electrochemical alkoxylation of compounds **37** followed by substitution of the alkoxy group leads to 1-(*N*-acylamino)-1-triphenylphosphoniumalkylphosphonates **42**. They can be also synthesized in a multi-stage procedure from imidate hydrochlorides **40** (Scheme 13).

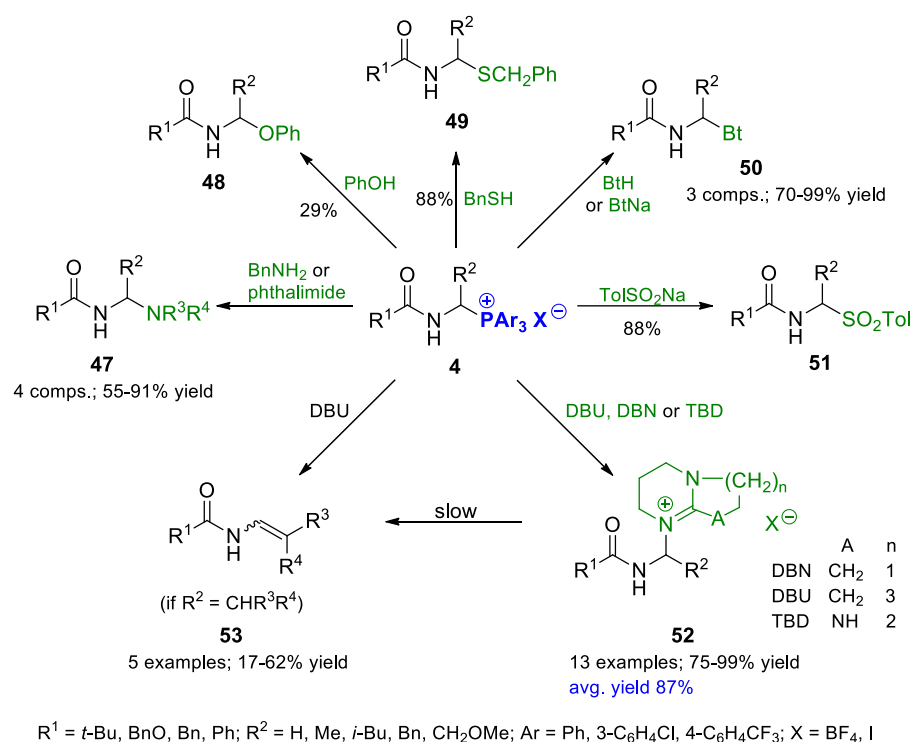
As shown, the high reactivity of the phosphonium salts **42** can be used not only in the α -amidoalkylation reactions of phosphorus or carbon nucleophiles (Scheme 13, route A and B) but also in the elimination (Scheme 13; route C) or Wittig reaction (Scheme 13, route D) [57].

In the years between 2012 and 2021, Mazurkiewicz (triphenylphosphonium derivatives) and then Adamek (phosphonium salts with weakened $C_{\alpha}-P^+$ bond) explored the possibility of α -amidoalkylation of various other heteronucleophiles (Scheme 14) [46,51,58]. They demonstrated that, under appropriate conditions, *N*-protected 1-aminoalkyltriarylphosphonium salts **4** react with a wide variety of nucleophiles including mercaptans ($PhCH_2SH$), phenol ($PhOH$), amines ($PhCH_2NH_2$), phthalimide, benzotriazole (BtH) or its salts (BtNa), and sodium aryl sulfinates (Ar^2SO_2Na) [46,51].

Initially, reactions were carried out at an elevated temperature (60 °C) in the presence of Hünig's base (for 1-(*N*-acylamino)alkyltriphenylphosphonium salts **4**, $Ar = Ph$, Scheme 14) [51]. The use of 1-(*N*-acylamino)alkyltriarylphosphonium salts **4** with a weakened $C_{\alpha}-P^+$ bond strength ($Ar = 3-C_6H_4Cl$, $4-C_6H_4CF_3$, Scheme 14) made it possible to conduct these reactions at room temperature without the use of catalysts [46].

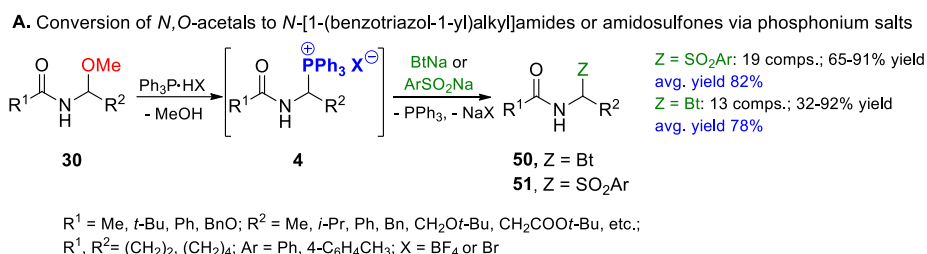
The extraordinary α -amidoalkylating properties of 1-(*N*-acylamino)alkylphosphonium salts **4** also allow the α -amidoalkylation of "non-nucleophilic" bases, such as DBU (1,8-diazabicyclo(5.4.0)undec-7-ene), DBN (1,5-diazabicyclo(4.3.0)non-5-ene) or TBD (1,5,7-triazabicyclo(4.4.0)dec-5-ene; Scheme 14). The corresponding 1-(*N*-acylamino)alkylamidinium or guanidinium salts **52** are products in these reactions. They can be isolated but show limited stability; for example, salts **52** with a hydrogen at the β -position underwent transformation to enamides **53**. As shown, enamides **53** can also be obtained directly from phosphonium salts **4** with an appropriate structure (hydrogen at the β -position) by an elimination reaction (Scheme 14) [58].

Interestingly, the 1-(*N*-acylamino)alkylphosphonium salts **4** can be converted to other α -amidoalkylating agents such as *N*-[1-(benzotriazol-1-yl)alkyl]amides **50** or α -amido sulfones **51**. So far, they have been synthesized mainly in a three-component condensation of aldehyde with an amide-type substrate (amides, lactams, urea derivatives, etc.) in the presence of benzotriazole (BtH) or aryl sulfinates, respectively [12,20].

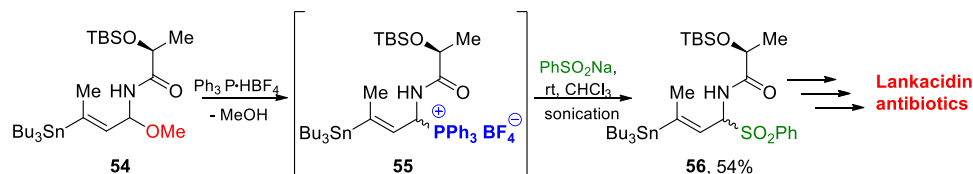


Scheme 14. Reactivity of 1-(*N*-acylamino)alkyltriarylphosphonium salts **4** with nucleophiles.

The proposed methodology extended the base of raw materials with *N,O*-acetals **30** obtained from α -amino acids or amide-type substrates in electrochemical oxidation (alkoxylation). As shown, 1-(*N*-acylamino)alkylphosphonium salts **4** do not have to be isolated in this type of transformation (Scheme 15A, see also Section 2.1.1, Scheme 7) [47,59].



B. Practical use of the transformation OMe \rightarrow PPh₃ \rightarrow SO₂Ph in the synthesis of Lankacidin antibiotics

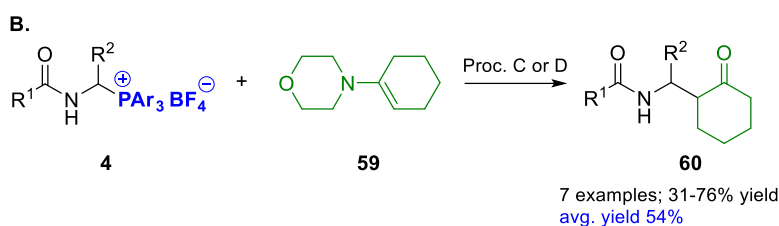
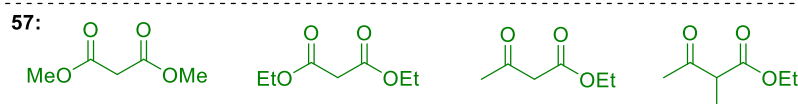
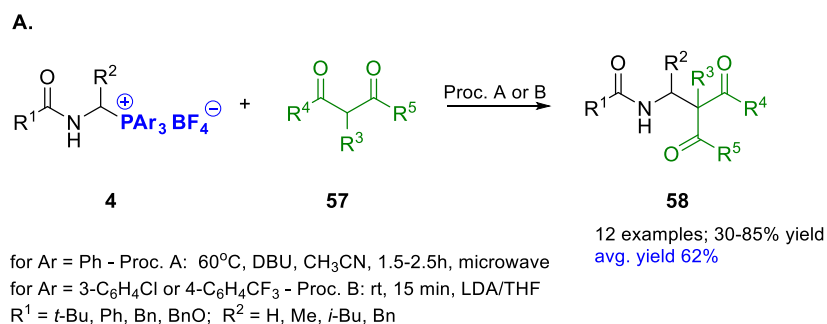


Scheme 15. The synthetic use of the transformation of *N,O*-acetals to *N*-[1-(benzotriazol-1-yl)alkyl]amides **50** or α -amido sulfones **51**, **56** via phosphonium salts.

Such transformations gained attention and were used for the preparation of substrates for α -amido sulfone-based intermolecular Mannich addition in the stereodivergent synthesis of lankacyclinol (Lankacidin antibiotics; Scheme 15/B) [60–62].

High reactivity of 1-(*N*-acylamino)alkylphosphonium salts **4** is also revealed in reactions with *C*-nucleophiles leading to the formation of β -aminocarbonyl systems **58** and **60**. In the case of 1,3-dicarbonyl compounds **57** (dimethyl or diethyl malonate, ethyl acetoacetate, and ethyl 2-methylacetoacetate), it was necessary to use bases (DBU or LDA-lithium diisopropylamide) as catalysts to produce enolate anions [46,51]. However, the use of

1-(*N*-acylamino)alkyltriarylphosphonium salts **4** with a weakened C $_{\alpha}$ -P $^{+}$ bond made it possible to conduct the reaction under slightly milder conditions (Scheme 16/A). This was similar in the reaction with 1-morpholinocyclohexene **59**; replacing the triphenylphosphonium residue (Ar = Ph) with a triarylphosphonium group (Ar = 3-C $_6$ H $_4$ Cl or 4-C $_6$ H $_4$ CF $_3$) facilitates the transformation (Scheme 16B) [46,51].

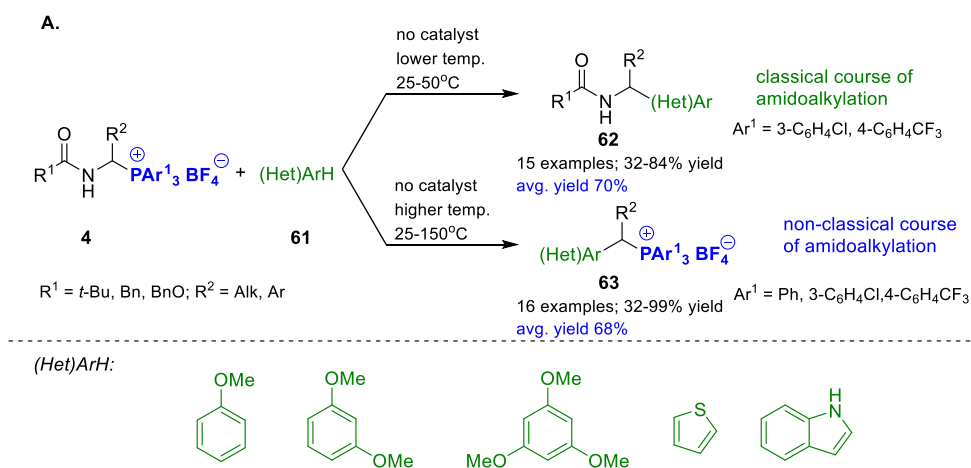
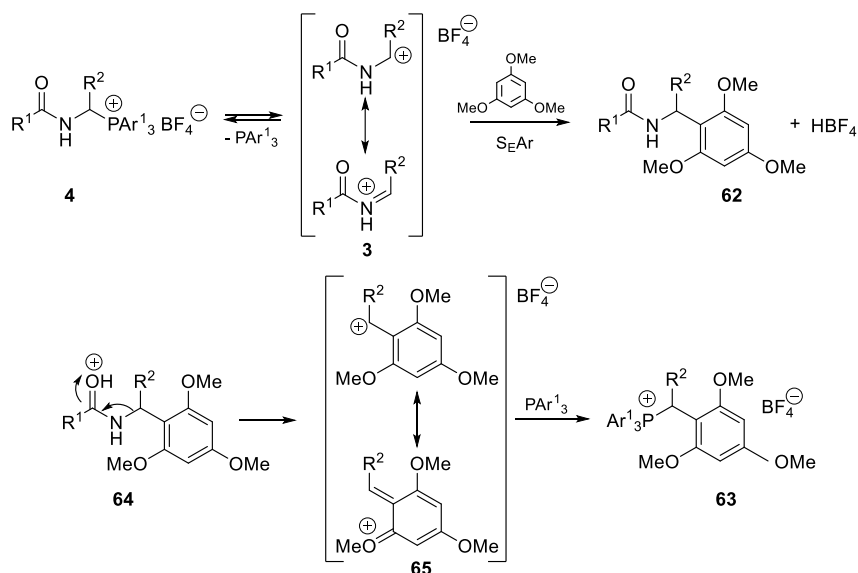


for Ar = Ph - Proc. C: 1. 60°C, (*i*-Pr) $_2$ EtN, 1h, molar ratio of 1:2:1.2, microwave; 2. citric acid (20%); 3. KHCO $_3$
for Ar = 3-C $_6$ H $_4$ Cl or 4-C $_6$ H $_4$ CF $_3$ - Proc. D: 1. rt, 1h, molar ratio of 1:2; 2. citric acid (20%); 3. KHCO $_3$
R 1 = *t*-Bu, Ph, Bn, BnO; R 2 = H, Me, *i*-Bu, Bn, CH $_2$ O*t*-Bu

Scheme 16. Conditions and yields for reactions of 1-(*N*-acylamino)alkyltriarylphosphonium salts **4** with 1,3-dicarbonyl compounds (**A**) or 1-morpholinocyclohexene (**B**).

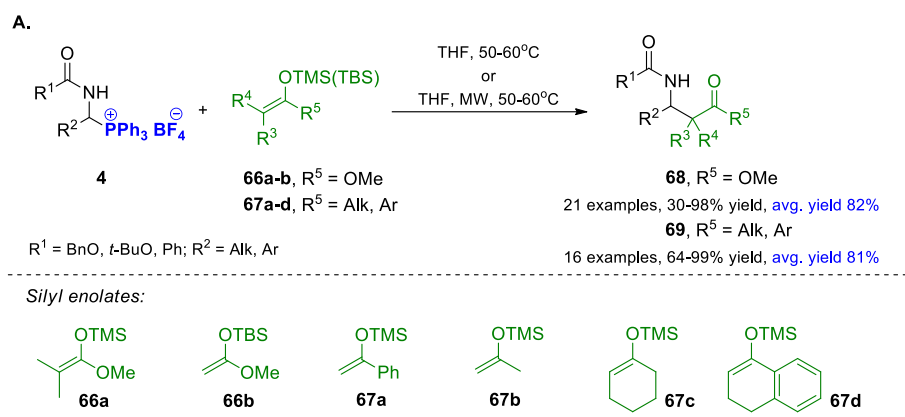
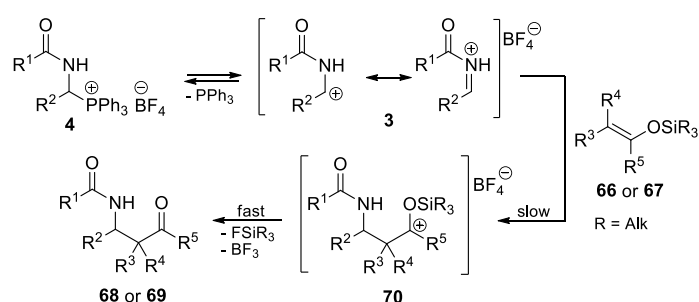
In 2018, Adamek et al. examined the reactivity of 1-(*N*-acylamino)alkyltriarylphosphonium salts **4** towards various aromatic systems (Scheme 17/A). It was demonstrated that phosphonium salts **4** react with arenes or heteroarenes under non-catalytic conditions. Reactions of triphenylphosphonium salts **4** (Ar = Ph, Scheme 17) required an elevated temperature and led to the formation of 1-arylalkylphosphonium salts **63** (non-classical α -amidoalkylation products). In turn, the use of 1-(*N*-acylamino)alkyltriarylphosphonium salts **4** with a weakened C $_{\alpha}$ -P $^{+}$ bond made it possible to carry out the transformations to the expected classical products-*N*-(1-arylalkyl)amides **62** at room temperature. Moreover, it was found that 1-arylalkylphosphonium salts **63** are formed from *N*-(1-arylalkyl)amides **62** in the consecutive-type reaction what is included in the plausible mechanism proposed by the authors (Scheme 17/B) [63].

The spontaneous generation of reactive *N*-acyliminium cations from 1-(*N*-acylamino)alkyltriarylphosphonium salts **4** (under catalyst-free conditions) was also used in reactions with silyl enolates **66** or **67**, to provide *N*-protected β -amino esters **68**, as well as *N*-protected β -amino ketones **69** in good to excellent yields (Scheme 18/A). As Październiok-Holewa et al. demonstrated, the process can be carried out in THF at 50 °C or 60 °C using conventional heating or microwave irradiation. The proposed mechanism of the transformation included, in the first stage, the formation of the reactive *N*-acyliminium cation **3**, which further reacts with the silyl enolate to give silyloxy-substituted carbenium ion **70**, which fast undergoes a desilylation reaction to give β -amino carbonyl compounds **68** or **69** (Scheme 18/B) [64].

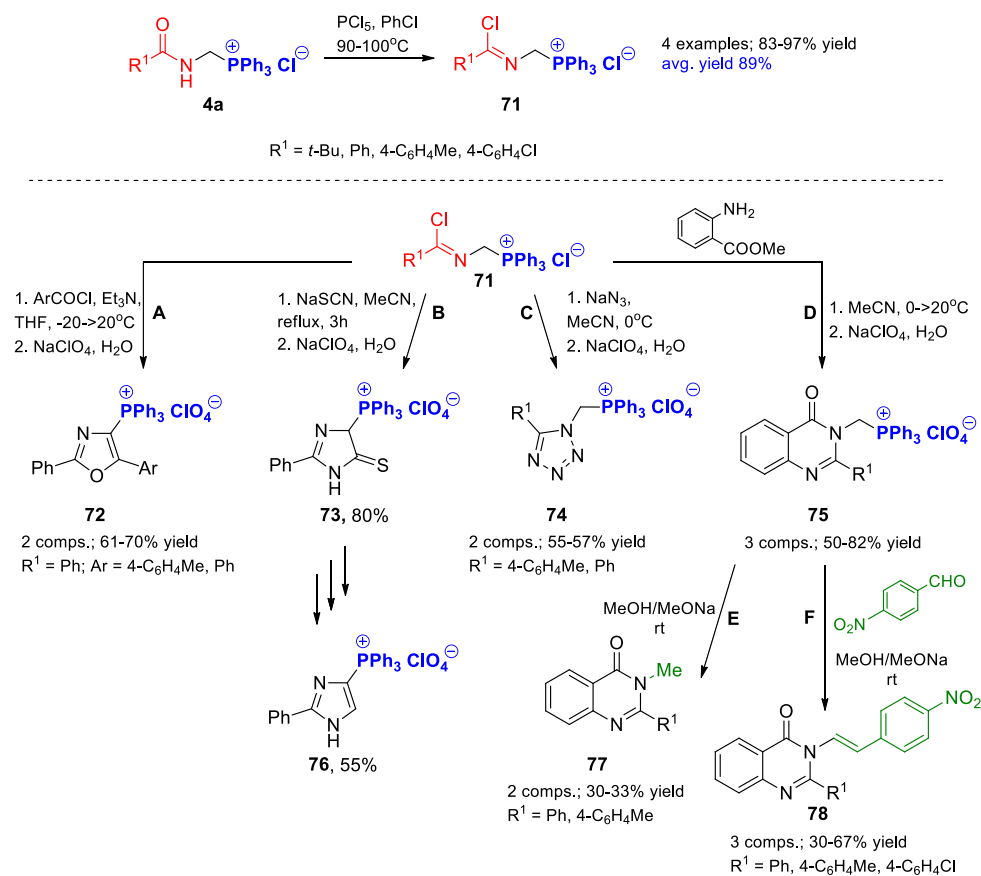
**B. Plausible mechanism**

Scheme 17. Reaction of 1-(*N*-acylamino)alkyltriarylposphonium salts **4** with aromatic compounds: (A) synthetic routes, (B) plausible mechanism.

1-(*N*-acylamino)alkyltriarylposphonium salts **4** are bifunctional compounds and their reactivity is not related only to the phosphonium moiety. Already in the 1980s, the transformation of *N*-acylaminoethyltriphenylphosphonium salts **4a** into imidoyl chlorides **71** was described [26]. They turned out to be valuable reagents in cyclization reactions, in which heterocyclic systems such as oxazole, imidazole, tetrazole, or quinoxalinone derivatives **72–76** can be obtained (Scheme 19/A–D) [26,65,66]. The presence of a triphenylphosphonium group enables further modification of the synthesized heterocycles, which was demonstrated in the example of the quinoxalinones **75** (a structural motif of *N*-acylaminoalkylphosphonium salt can also be indicated here). These compounds undergo a reduction under mild conditions (Scheme 19/E). They can also be used as ylide precursors in the Wittig reaction with 4-nitrobenzaldehyde (Scheme 19/F) [26,65,66].

**B. Plausible mechanism**

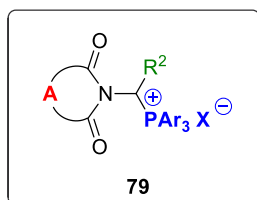
Scheme 18. Reaction of 1-(*N*-acylamino)alkyltriarylyphosphonium salts **4** with silyl enolates—(A) conditions and yields, (B) plausible mechanism.



Scheme 19. Synthesis of imidoyl chlorides **71** and their further transformations.

2.2. 1-Imidoalkyltriarylphosphonium Salts

Structures of the 1-imidoalkylphosphonium salts **79** described in the literature are based on a phthalimide ($A = 1,2\text{-C}_6\text{H}_4$) or succinimide ($A = (\text{CH}_2)_2$) ring (Figure 4). Two electron-withdrawing carbonyl groups connected to the nitrogen atom reduce the electron density at C_α , thus increasing its electrophilicity. In the α -position there may be hydrogen ($R^2 = \text{H}$), alkyl ($R^2 = \text{Me, Et, } i\text{-Bu}$) or aryl ($R^2 = \text{Ph}$) substituent. C_α is also directly bonded to the triarylphosphonium group PAr_3 ($\text{Ar} = \text{Ph, } 4\text{-C}_6\text{H}_4\text{Cl, } 3\text{-C}_6\text{H}_4\text{Cl, } 4\text{-C}_6\text{H}_4\text{CF}_3$), which is positively charged and can act as a nucleofugal group.



$A = (\text{CH}_2)_2, 1,2\text{-C}_6\text{H}_4, 1,8\text{-C}_{10}\text{H}_6$;

$R^2 = \text{H, Me, Et, } i\text{-Bu, Ph}$;

$\text{Ar} = \text{Ph, } 3\text{-C}_6\text{H}_4\text{Cl, } 4\text{-C}_6\text{H}_4\text{Cl, } 4\text{-C}_6\text{H}_4\text{CF}_3, 4\text{-C}_6\text{H}_4\text{OMe}$; $X = \text{BF}_4, \text{Br, Cl, I}$.

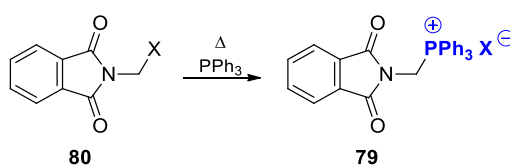
Figure 4. General structure of 1-imidoalkylphosphonium salts **79**.

In most cases, the 1-imidoalkylphosphonium salts are stable solids that can be stored under laboratory conditions for a long time. Interestingly, some of them also show biological activities such as cytotoxic or antimicrobial properties [67–69].

2.2.1. Preparation

In general, there is not much information in the literature on the methods for synthesis of 1-imidoalkylphosphonium salts **79**, and most of them concern the simplest ones—imidomethylphosphonium salts ($R^2 = \text{H}$). To the best of our knowledge, the first attempt to prepare imidomethylphosphonium salts was reported in 1961 by Hellmann and Schumacher [70]. It consisted in the reaction of phthalimidomethyltrimethylammonium iodide with triphenylphosphine in methanol. Such a reaction was later used several times; however, the structure of the substrate and conditions were slightly modified (mainly the solvent, temperature, and reaction time, Table 2).

Table 2. Conditions and yields for the synthesis of phthalimidomethylphosphonium salts **79**.

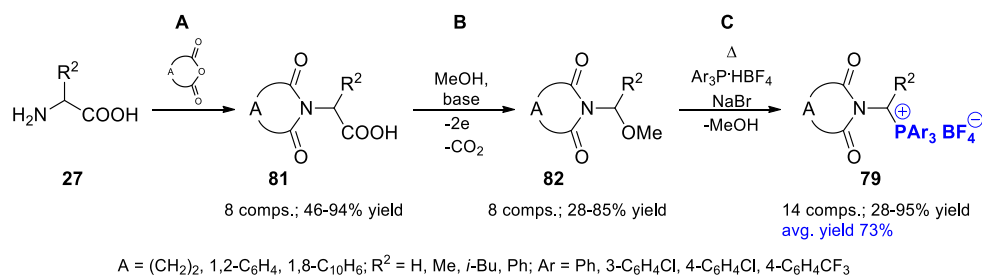


| Entry | Substrate 80 | Solvent | Conditions | Yield of 79 , % | Refs. |
|-------|--------------------------------------|----------|---------------|------------------------|----------------------|
| | X | | | | |
| 1 | $(\text{Me}_3\text{N})^+ \text{I}^-$ | methanol | reflux, 4 h | 58 | [70] |
| 2 | Cl | benzene | reflux, 2 h | - | [70] |
| 3 | Br | acetone | reflux, 3 min | 80 | [24] |
| 4 | Br | benzene | reflux, 22 h | 68 | [67,71] ^a |
| 5 | Br | toluene | reflux, 24 h | - | [72] |

^a Compound **79** ($X = \text{Br}$) is also formed as a by-product in the reaction with $\text{Pd}(\text{PPh}_3)_4$ (rt, benzene).

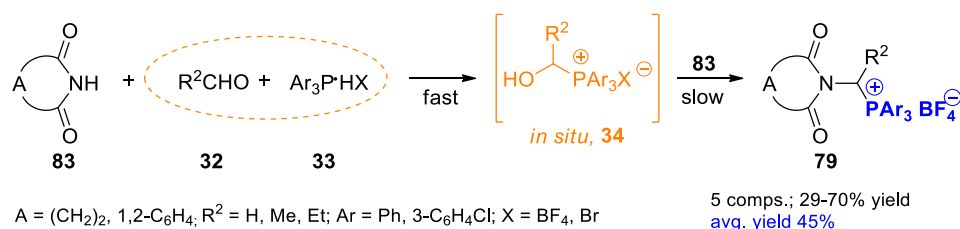
After several decades, general methods for the synthesis of imidoalkylphosphonium salts appeared. The first one consisted of three stages: (A) the protection of amino group (from amino acids) by smelting phthalic, succinic or 1,8-naphthalic anhydride with the corresponding amino acid at 140–170 °C; (B) electrochemical decarboxylative α -methoxylation

of 1-imidoalkancarboxylic acids **81**; (C) the displacement of the methoxy group by the triarylphosphine by smelting of the *N*-(1-methoxyalkyl)imides **82** with triarylphosphonium tetrafluoroborates in the presence of NaBr as catalyst (Scheme 20) [73].



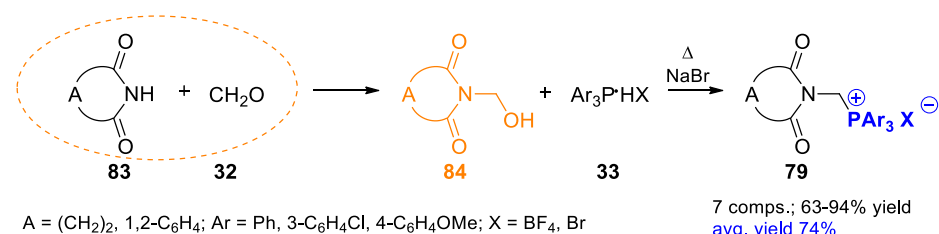
Scheme 20. Three-step synthesis of 1-imidoalkylphosphonium salts **79** from amino acids.

Next, 1-imidoalkylphosphonium salts **79** were prepared in the three-component coupling of aldehydes and imides in the presence of triarylphosphonium salts Ar₃P·HX (Scheme 21). An interesting fact is the formation of an intermediate hydroxyalkylphosphonium salt **34** in situ from aldehyde and triarylphosphonium salt (Ar₃P·HX) during the reaction (see also Section 2.1.1, Scheme 7) [44].



Scheme 21. Three-component coupling of aldehydes, imides, and triarylphosphonium salts in the synthesis of 1-imidoalkylphosphonium salts **79**.

As it was demonstrated, 1-imidomethylphosphonium salts **79** can also be obtained in the step-by-step procedure. This time, at first, formaldehyde (reactions with other aldehydes are ineffective) and imides form hydroxymethylimides **84** which, after isolation and purification, are reacted with triarylphosphonium salts **33** (Ar₃P·HX) in the last stage (Scheme 22). The use of NaBr as a catalyst had a positive effect on the reaction (both on reaction time and yield) when Ar₃P·HBF₄ was used (for Ar₃P·HBr no catalyst is needed) [48].



Scheme 22. Step-by-step method for the synthesis of 1-imidoalkylphosphonium salts **79** from imides.

The last two methods allow for the fast synthesis of 1-imidoalkylphosphonium salts **79** (especially 1-imidomethylphosphonium salts) from readily available substrates, even on a larger scale (5–20 g). Besides, the advantage of both strategies is that they rely on non-electrochemical procedures, thus they are an interesting complement to previously described method.

2.2.2. Synthetic Utilization

The most important synthetic applications of 1-imidoalkylphosphonium salts **79** are summarized in Figure 5. Due to certain structural features (dicarbonyl protecting group and thus no NH proton), 1-imidoalkylphosphonium salts **79** can be considered as potential precursors of ylides in the Wittig reaction. These properties of phthalimidomethyltriphenylphosphonium bromide **79** were used by Tan and co-workers in the first stage of multi-step synthesis of compounds **85** and **86**, which are known to modulate the activity of the TAAR₁ receptor (the trace amine-associated receptor 1, see Table 3) [72].

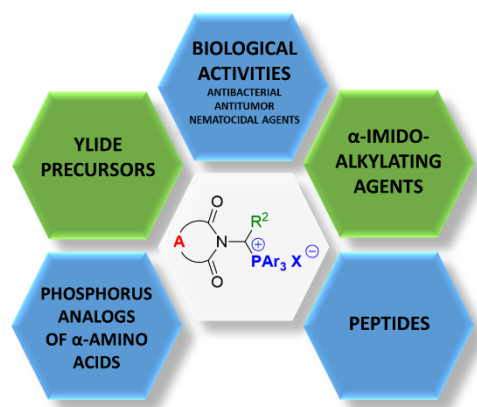


Figure 5. Applications of 1-imidoalkylphosphonium salts **79**.

Table 3. Application of phthalimidomethyltriphenylphosphonium bromide as ylide precursors.

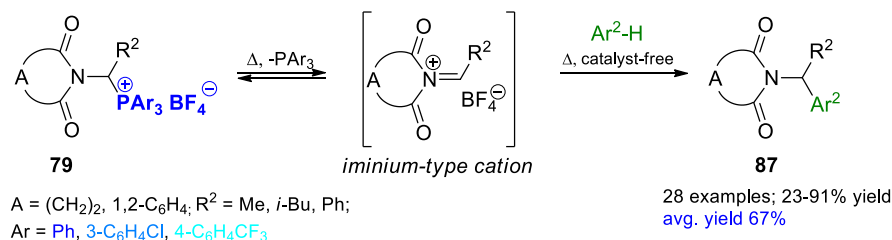
| Phosphonium Salt 79 | Carbonyl Components | Conditions | Intermediate Compound | Targeted Compound |
|----------------------------|---------------------|----------------------------|-----------------------|-------------------|
| | 85 | | 86 | |
| | | KHMDS, THF, 0 °C → RT, 86% | 85 | |
| | | KHMDS, THF, 0 °C → RT, 77% | 86 | |

Recently, the possibilities of using 1-imidoalkylphosphonium salts in imidoalkylation reactions with carbon- or heteronucleophiles have been explored.

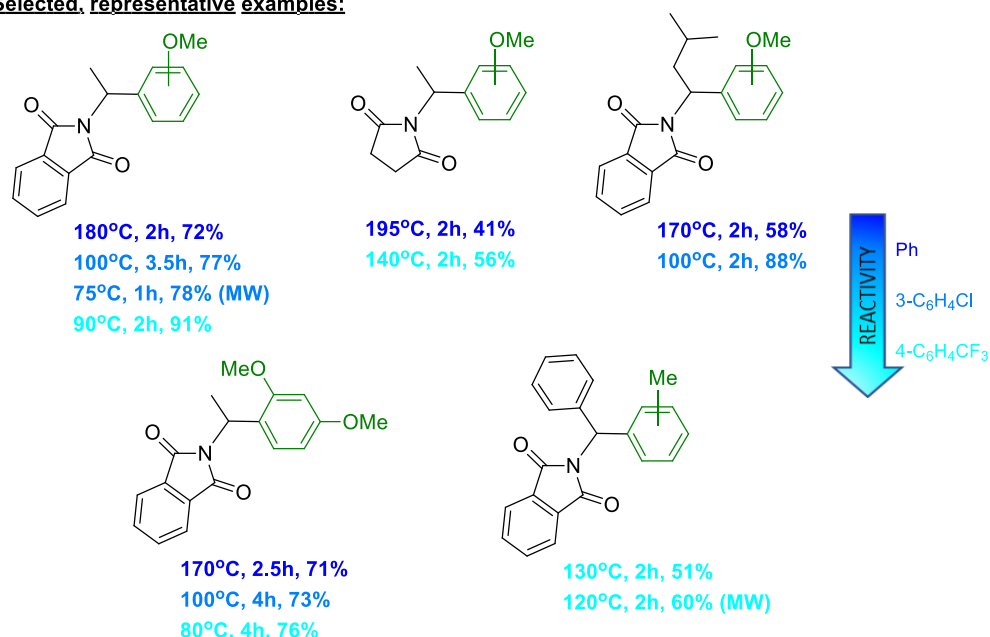
In 2017, the Friedel–Crafts-type reaction of 1-imidoalkylphosphonium salts with various aromatic compounds was described. *N*-(1-arylalkyl)imides **87** were the main products of these transformations (Scheme 23) [73].

The presence of the dicarbonyl protection increases the electrophilicity of the C_α. In addition, the use of phosphonium salts which were derivatives of triarylphosphines with electron-withdrawing substituents make it easier to cleave the C_α-P⁺ bond (first step of the reaction, Scheme 23). Such structural modifications facilitated reactions with aromatic systems, also with weakly activated anisole and toluene (see Scheme 23 and compare the relation between the required reaction temperature and the type of phosphonium moiety).

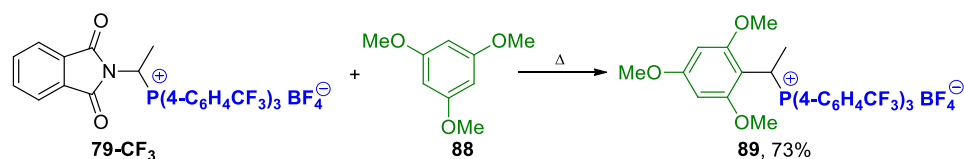
It is worth noting that, contrary to the reaction of the 1-(*N*-acylamino)alkylphosphonium salts **4** with arenes described in this review (Section 2.1.2), no consecutive reaction leading to the so-called non-classical α -amidoalkylation products (1-arylalkylphosphonium salts **63**, see also Scheme 17) was observed. The only exception was the reaction of phosphonium salts **79**-CF₃ with 1,3,5-trimethoxybenzene (Scheme 24).



Selected, representative examples:



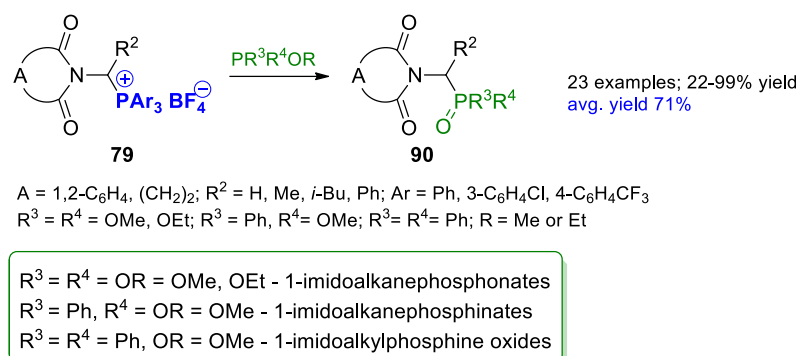
Scheme 23. Friedel–Crafts-type reaction of 1-imidoalkylphosphonium salts **79** with various aromatic compounds—conditions and yields (MW—microvawe assisted reaction).



Scheme 24. Unusual course of the reaction of 1-imidoalkylphosphonium salt **79**-CF₃ with a highly activated aromatic system—1,3,5-trimethoxybenzene.

1-Imidoalkylphosphonium salts have also been used in the synthesis of imidoalkane phosphonates, imidoalkane phosphinates, and imidoalkylphosphine oxides. Generally, these compounds exhibit interesting biological properties, including antibacterial and antifungal activities or can be used in the synthesis of many bioactive compounds such as phosphopeptides (acting as enzyme inhibitors), oligonucleotides, cytotoxic agents (for example Cryptophycin **52**) or 2,4,5-imidazolidinetriones (herbicides and plant growth regulators) [74,75].

The strategy for preparation of P-compounds **90** from phosphonium salts **79** was based on the Michaelis–Arbuzov-type reaction with the appropriate phosphorus nucleophiles (Scheme 25) [76].

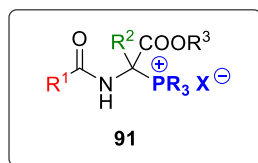


Scheme 25. Michaelis–Arbuzov-type reaction of 1-imidoalkylphosphonium salts **79** with selected phosphorus nucleophiles.

It was observed that the reactivity of phosphonium salts **79** strongly depends on their structure. Good yields were obtained only from 1-(*N*-phthalimido)alkylphosphonium salt derivatives of tris(3-chlorophenyl)phosphine and tris(4-trifluoromethylphenyl)phosphine. However, a relatively large excess of phosphorus nucleophile and the addition of methyltriphenylphosphonium iodide ($\text{MePPh}_3^+\text{I}^-$) as a catalyst that can facilitate the reaction were required (the most preferred molar ratio of reagents is 1:10:0.25 of phosphonium salt:*P*-nucleophile:catalyst).

2.3. *N*-acyl-1-phosphonio- α -amino Acid Esters

The general structural formula of *N*-acyl-1-phosphonio- α -amino acid esters **91** is shown in Figure 6. In most cases, structures of this kind of phosphonium salts described in the literature are based on a glycinate skeleton ($R^2 = \text{H}$), although derivatives of other proteinogenic and non-proteinogenic α -amino acids, containing in the α position alkyl ($R^2 = \text{Me, CH}_2\text{OMe, CH}_2\text{CN, CH}_2\text{CH}=\text{CH}_2$) or alkyl-aryl substituent ($R^2 = \text{CH}_2\text{Ph, CH}_2\text{Bt}$) are also known. C_α is most often directly bonded to the positively charged triphenylphosphonium group ($R = \text{Ph}$), and less often tributylphosphonium group ($R = \text{Bu}$). In the structure of the phosphonium salts in question, the carboxyl group is protected as an ethyl or methyl ester ($R^3 = \text{Me, Et}$), while the protected amino group is present as an amide ($R^1 = \text{Me, } t\text{-Bu, Ph}$) or carbamate ($R^1 = \text{MeO, } t\text{-BuO, PhCH}_2\text{O}$) moiety. The most common counterion to the positively charged phosphonium group is the tetrafluoroborate, bromide or iodide anion ($X = \text{BF}_4, \text{Br, I}$).

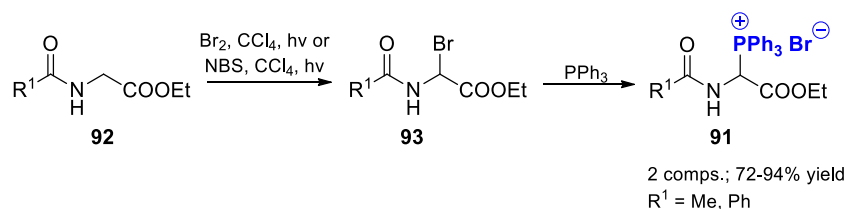


$R^1 = \text{Me, } t\text{-Bu, Ph, MeO, } t\text{-BuO, BnO};$
 $R^2 = \text{H, Me, CH}_2\text{OMe, CH}_2\text{CN, CH}_2\text{CH}=\text{CH}_2, \text{Bn, CH}_2\text{Bt};$
 $R^3 = \text{Me, Et};$
 $R = \text{Ph, Bu}; X = \text{BF}_4, \text{Br, I}.$

Figure 6. General structure of *N*-acyl-1-phosphonio- α -amino acid esters **91**.

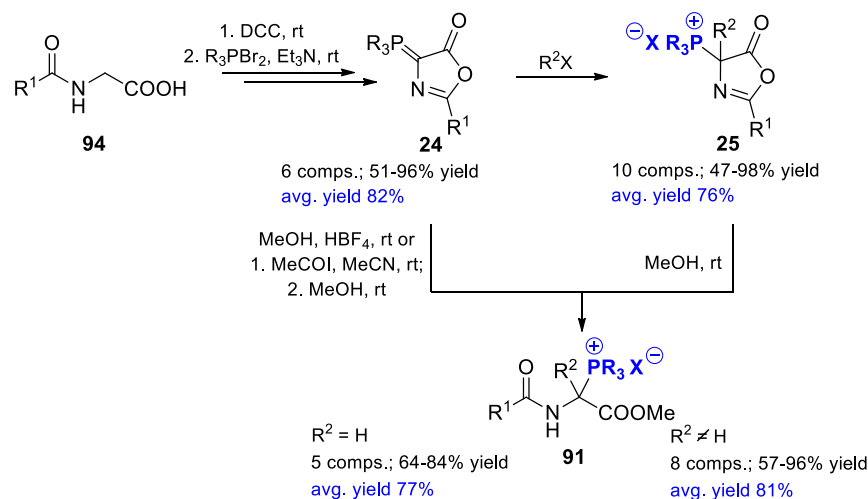
2.3.1. Preparation

For a wide group of compounds belonging to *N*-acyl-1-triphenylphosphonio- α -amino acid esters **91**, *N*-acyl-1-triphenylphosphonioglycinates ($R^2 = \text{H}$) are the best known ones. They were prepared for the first time in 1983 by Kober and Steglich from ethyl *N*-acyl-1-bromoglycinates **93** by their reaction with triphenylphosphine. The starting 1-bromoglycine derivatives **93** were previously obtained in situ in the reaction of photochemical bromination of *N*-acylglycine ethyl esters **92** with bromine or *N*-bromosuccinimide carried out in tetrachloromethane (Scheme 26) [77].



Scheme 26. Method for the synthesis of *N*-acyl-1-triphenylphosphonioglycinate bromides **91** from glycine derivatives **92** via 1-bromoglycinates **93**.

In 1996, Mazurkiewicz and Pierwocha developed a simple route for the transformation of *N*-acylated glycine **94** into the 4-phosphoranylidene-5(4*H*)-oxazolones **24** [40]. The corresponding 5(4*H*)-oxazolone, obtained here as an intermediate in the reaction of the starting compound with DCC (*N,N'*-dicyclohexylcarbodiimide), is phosphorylated in situ with dibromotriphenylphosphorane (R₃PBr₂) in the presence of triethylamine. The resulting phosphoranylidene-5(4*H*)-oxazolones **24** can be further effectively converted into *N*-acyl-1-triphenylphosphonioglycinates (R² = H), as well as esters of other *N*-acyl-1-triphenylphosphonio- α -amino acids **91** (Scheme 27).



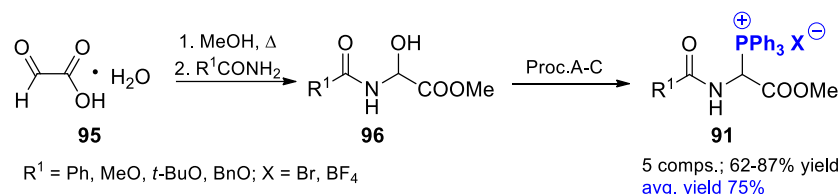
R¹ = Me, *t*-Bu, Ph, *i*-Pr; R² = H, Me, CH₂OMe, CH₂CN, CH₂CH=CH₂, Bn, CH₂Bt; R = Ph, Bu; X = BF₄, Br, I.

Scheme 27. Synthesis of *N*-acyl-1-triphenylphosphonio- α -amino acid esters **91** via phosphoranylidene-5(4*H*)-oxazolones **24**.

However, the most convenient procedure for the synthesis of *N*-acyl-1-triphenylphosphonioglycinate tetrafluoroborates (**91**, X = BF₄) is to treat a solution of phosphoranylidene-5(4*H*)-oxazolones **24** in methanol with an ethereal solution of tetrafluoroboric acid [78]. An alternative method for the synthesis of *N*-acyl-1-triphenylphosphonioglycinates with an iodide counterion (**91**, X = I) is a two-stage procedure that consists in the reaction of phosphoranylideneoxazolone **24** with acetyl iodide performed in acetonitrile, followed by the subsequent reaction of the acylation product with methanol [78,79]. Similarly, the synthesis of *N*-acyl-1-triphenylphosphonio- α -amino acids **91** with an alkyl substituent at the α -position (R² ≠ H) by alkylation of 4-phosphoranylidene-5(4*H*)-oxazolones **24** with alkyl halides [80], and the next opening of the oxazolone ring under the treatment with methanol or methanol in the presence of an acidic catalyst was also described (Scheme 27) [81].

In 2004, three methods for the transformation of *N*-alkoxycarbonyl-1-hydroxyglycinates **96** into especially interesting *N*-alkoxycarbonyl-1-triphenylphosphonioglycinates **91** (R¹ = MeO, *t*-BuO, BnO) were developed by Mazurkiewicz et al. The proposed synthetic routes included the following transformations: phosphorylation of *N*-alkoxycarbonyl-1-hydroxyglycinates **96** with Ph₃P·Br₂ in the presence of Et₃N (Procedure A), the reaction of *N*-alkoxycarbonyl-1-hydroxyglycinates **96** with DCC and Ph₃P·HBF₄ in the presence

of Ph_3P as a catalyst (Procedure B), and a new kind of the Mitsunobu reaction using $\text{Ph}_3\text{P}\cdot\text{HBF}_4$ as a nucleophile conjugated acid (Procedure C, Scheme 28) [82].



Scheme 28. Methodology for the synthesis of *N*-acyl-1-triphenylphosphonioglycinates **91** via α -hydroxyglycinates. Reagents and conditions: Procedure A: $\text{Ph}_3\text{P}\cdot\text{Br}_2$, Et_3N , Ph_3P , DCM, rt; Procedure B: DCC, $\text{Ph}_3\text{P}\cdot\text{HBF}_4$, Ph_3P , DCM, rt; Procedure C: DEAD (diethyl azodicarboxylate), $\text{Ph}_3\text{P}\cdot\text{HBF}_4$, Ph_3P , THF, rt.

2.3.2. Synthetic Utilization

N-Acyl-1-triphenylphosphonio- α -amino acid esters **91** are, in most cases, crystalline compounds, stable at room temperature, moderately sensitive to moisture, and well soluble in DCM and MeCN, but insoluble in diethyl ether. They can be easily purified by crystallization consisting of dissolution in DCM or MeCN at room temperature and precipitation with diethyl ether [78–82]. It is worth emphasizing that they are easily accessible from *N*-acylglycine even at kilogram scale (Schemes 26 and 27). All of these features of *N*-acyl-1-triphenylphosphonio- α -amino acid esters, as well as their diverse reactivity make these compounds interesting reagents in organic syntheses (Figure 7).

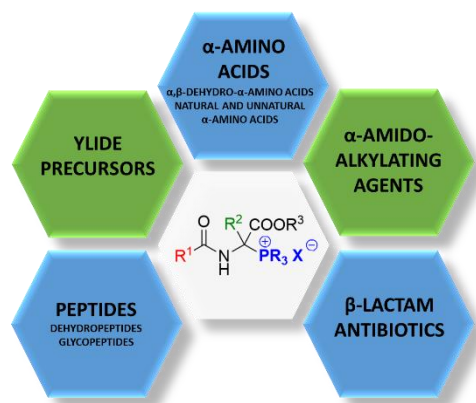
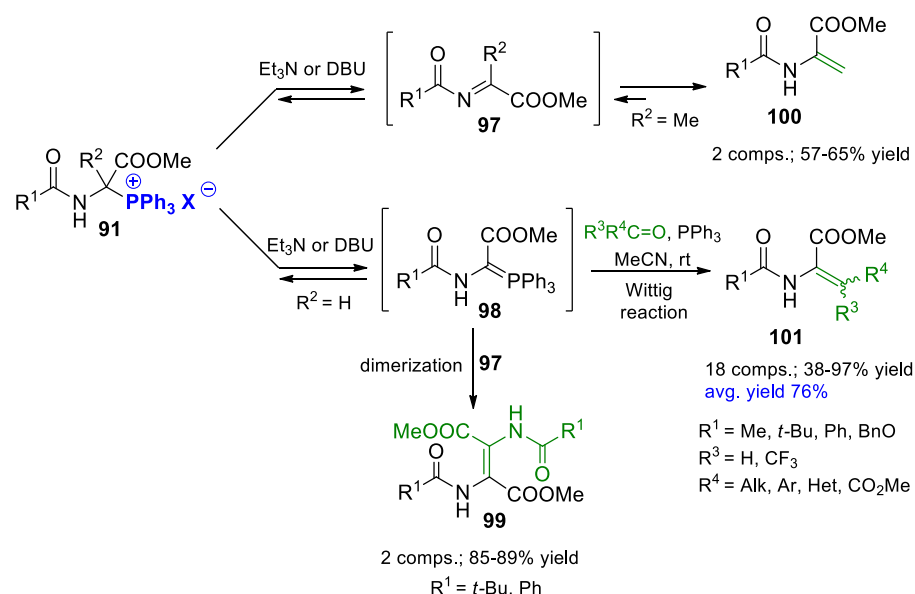


Figure 7. Applications of *N*-acyl-1-phosphonio- α -amino acid esters **91**.

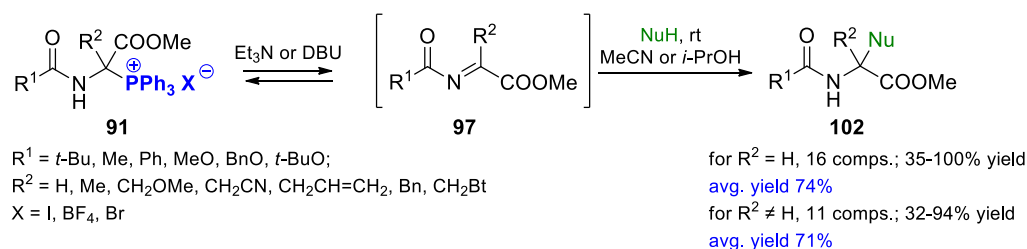
The directions of *N*-acyl-1-triphenylphosphonio- α -amino acid esters reactivity, and thus, the possibility of their further applications, were recognized during comprehensive research on their behavior in the presence of organic bases [83]. Reactions of *N*-acyl-1-triphenylphosphonio- α -amino acid methyl esters **91** with DBU and triethylamine were investigated then as the crucial step of the base catalysed displacement of the triphenylphosphonium group by various nucleophiles. Initially, this was observed by Kober, and Steglich, and later confirmed by Mazurkiewicz and Grymel, that *N*-acyl-1-triphenylphosphonioglycinates **91**, upon treatment with bases, were converted into a mixture of the corresponding *N*-acyliminoacetate **97** and *N*-acyl-1-triphenylphosphoranylidene-glycinate **98**. Both the iminoacetate **97** and the ylide **98** turned out to be highly reactive, instable compounds that remained in an equilibrium and reacted slowly with each other providing the fumaric acid derivative **99**. In the case of *N*-acyl-1-triphenylphosphonio- α -amino acid esters **91** with the quaternary α -carbon, the α -substituted homologues of *N*-acyliminoacetate **97** can undergo further tautomerization into the corresponding enamine **100** (Scheme 29) [83].



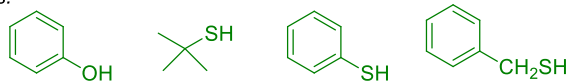
Scheme 29. Various pathways for synthetic applications of *N*-acyl-1-triphenylphosphonio- α -amino acid esters **91** in the presence of a base (Et₃N or DBU).

The application of *N*-acyl-1-triphenylphosphonioglycinates **91** as the precursors of phosphonium ylides **98** in the Wittig reaction with aliphatic or aromatic aldehydes in the presence of Et₃N allowed the development of a simple and efficient procedure for the synthesis of α,β -dehydro- α -amino acid derivatives **101** (Scheme 29) [84].

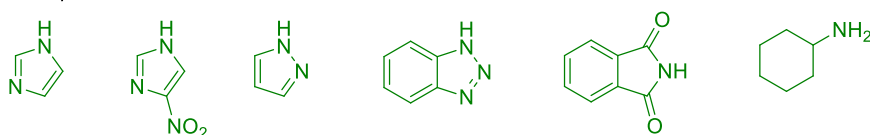
On the other hand, methods for the displacement of the triphenylphosphonium group with a variety oxygen, sulfur, nitrogen and carbon nucleophilic agents, consisting in the addition of a nucleophile to the activated C=N double bond of the *N*-acylimino intermediate **97**, opened up new routes for the synthesis of biologically important natural and unnatural non-proteinogenic α -amino acids by double functionalization of the glycine α -position with electrophilic and nucleophilic reagent (Scheme 30) [78,79,81].



O- and *S*-nucleophiles:



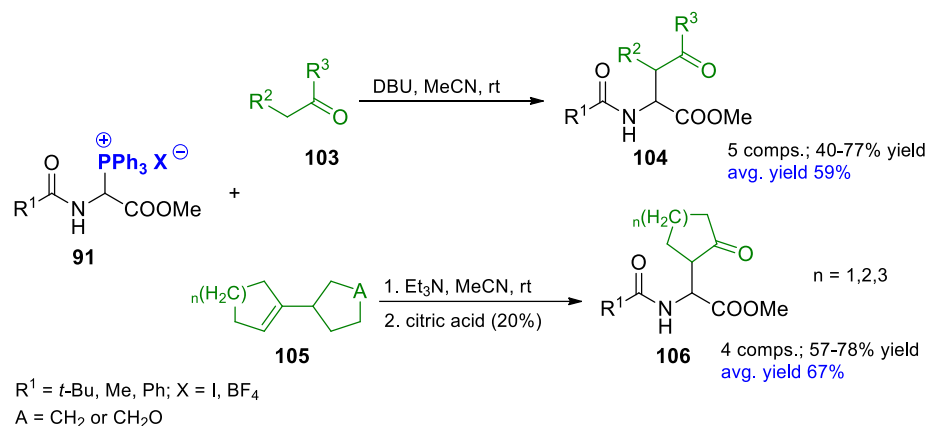
N-nucleophiles:



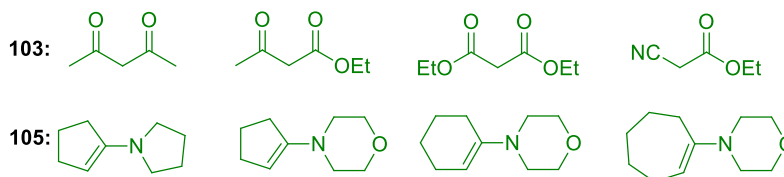
Scheme 30. Synthetic applications of *N*-acyl-1-triphenylphosphonio- α -amino acid esters **91** in reactions with heteronucleophiles.

N-acyl-1-triphenylphosphonio- α -amino acid esters **91** react easily with a wide variety of oxygen, sulphur and nitrogen nucleophiles including phenol (PhOH), mercaptans (*t*-BuSH, PhSH, PhCH₂SH), imidazole, 4-nitroimidazole, pyrazole, benzotriazole,

phthalimide, cyclohexylamine (Scheme 30) [78,81] and two kinds of carbon nucleophiles: enolates **103** of activated carbonyl compounds or enamines **105** (Scheme 31) [79]. Reactions were conducted in acetonitrile or methanol at room temperature in the presence of DBU or triethylamine, and the corresponding α -amino acid derivatives **102**, **104**, and **106** (including α,α -difunctionalized derivatives) were usually obtained in good to excellent yields [78,79,81].



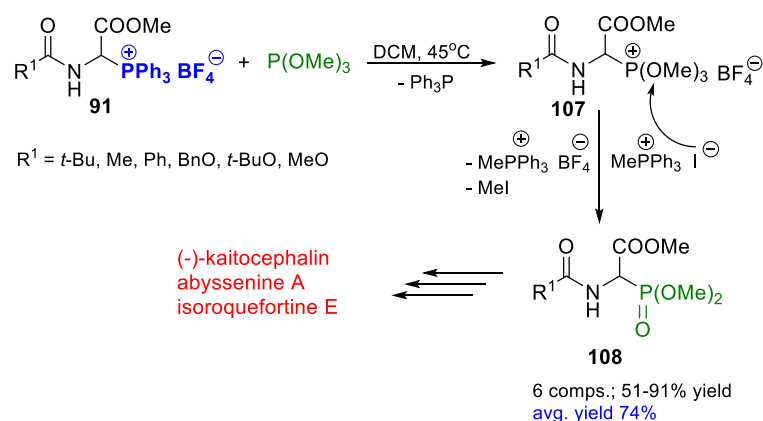
C-nucleophiles:



Scheme 31. Synthetic applications of *N*-acyl-1-triphenylphosphonio- α -amino acid esters **91** in reactions with C-nucleophiles.

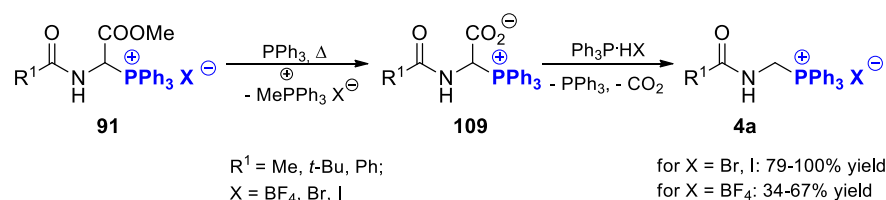
This great interest in natural non-proteinogenic α -amino acids results from their diverse biological activities as antibiotics, pharmaceuticals, natural pesticides, and growth regulators, as well as their use in the synthesis of enzymes, hormones, new chemotherapeutics, synthetic immunostimulants, and other protein structured compounds [85,86]. The importance of α,α -disubstituted α -amino acids has been comprehensively discussed by many authors [87,88].

As demonstrated by Mazurkiewicz and Kuźnik, *N*-acyl-1-triphenylphosphonioglycinate tetrafluoroborates **91** are also convenient starting compounds for the transformation into *N*-acyl- α -(dialkoxyphosphoryl)glycinates **108** by the Michaelis–Arbuzow-type reaction with trimethylphosphite in the presence of methyltriphenylphosphonium iodide as a catalyst (Scheme 32) [89]. Among others, α -(dialkoxyphosphoryl)glycinates became the crucial synthetic tool commonly used for the synthesis of many natural products (including β -lactam antibiotics) or α,β -dehydro- α -amino acids by the Wadsworth–Emmons reaction [90–96]. As is known, hydrogenation of the latter compounds using chiral catalysts is considered to be one of the most general methods for the enantioselective synthesis of α -amino acids, including non-proteinogenic α -amino acids of diverse biological activities [97–100].



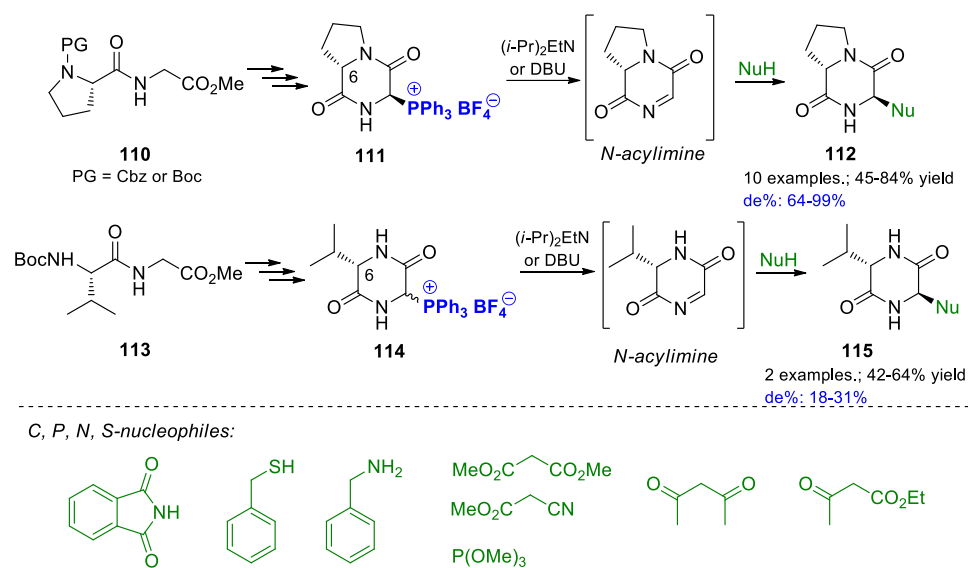
Scheme 32. Transformation of *N*-acyl-1-triphenylphosphonioglycinate tetrafluoroborates **91** into *N*-acyl- α -(dimethoxyphosphoryl)glycinates **108** and selected examples of their further use in the synthesis of biologically active compounds.

Although *N*-acyl-1-triphenylphosphonioglycinates **91** are relatively stable, they undergo interesting transformations at high temperatures. Thermogravimetric investigations revealed that during the process of the melting of salts **91**, they underwent demethoxycarbonylation, providing *N*-acylaminomethyltriphenylphosphonium salts **4a** (18–50%), along with methyltriphenylphosphonium salts (22–68%). When this reaction was performed in the presence of Ph_3P and $\text{Ph}_3\text{P}\cdot\text{HX}$ ($\text{X} = \text{Br}, \text{BF}_4, \text{I}$) the process of demethoxycarbonylation for *N*-acyl-1-triphenylphosphonioglycinate bromides and iodides ($\text{X} = \text{Br}, \text{I}$) occurred at 95–130 °C in good to excellent yields (79–100%); whereas for *N*-acyl-1-triphenylphosphonioglycinate tetrafluoroborates **91** ($\text{X} = \text{BF}_4$) as starting compounds, the analogous transformation occurred at about 170–175 °C, giving the corresponding phosphonium tetrafluoroborates **4a** in much lower yields (34–67%; Scheme 33) [101]. The practical significance of this process is due to the fact that the obtained 1-(*N*-acylamino)alkyltriphenyl phosphonium salts **4a** can be used as valuable α -amidoalkylating agents (see also Section 2.1.2).



Scheme 33. Thermal stability of *N*-acyl-1-triphenylphosphonio- α -amino acid esters **91**.

The crucial structural motif for *N*-acyl-1-triphenylphosphonio- α -amino acid esters (amino, phosphonium and carbonyl groups bonded to the same carbon atom) can be a part of more complex systems. In this regard, 3-triphenylphosphonio-2,5-piperazinedione **111**, **114** can be considered as structurally similar compounds to the phosphonium salts **91**. They can be obtained from dipeptides in multistep procedure described by Mazurkiewicz and Gorewoda in 2011 [102]. The retention of configuration (position 6) results in the formation of chiral glycine cation equivalents **111**, **114** which can be used for a diastereoselective nucleophilic substitution of the triphenylphosphonium group with *S*-, *N*-, *P*-, and *C*-nucleophiles (Scheme 34). Reactions were conducted at 0 or 25 °C in the presence of a base (*i*-Pr₂EtN or DBU) and were particularly effective (high yields and high de%) for the proline derivative **111** [102].



Scheme 34. Synthetic use of 3-triphenylphosphonio-2,5-piperazinedione **111**, **114**-chiral glycine cation equivalents.

3. Conclusions

1-Aminoalkylphosphonium derivatives are, in most cases, crystalline compounds, stable at room temperature and well soluble in chloroform, dichloromethane or acetonitrile, which makes them easy to store (even for a long time) and convenient to use reagents. On the other hand, they show remarkable reactivity especially towards various kinds of nucleophiles (both carbon- and heteronucleophiles). Moreover, the structure of such phosphonium salts is easy to modify by changing the *N*-protecting group or introducing electron-withdrawing or electron-donating substituents to the phosphonium moiety by using appropriately modified phosphines in the key stage of the synthesis. It allows for the control and, more interestingly, the targeting of the reactivity of these phosphonium compounds (α -amidoalkylation reaction vs. Wittig reaction).

All these factors make the 1-aminoalkylphosphonium derivatives an interesting group of “smart-reagents” with great potential as precursors of reactive intermediates such as *N*-acyliminium-type cations (generated without the need for any catalysts), or ylides. This was used in the synthesis of such compounds as phosphorus analogs of α -amino acids, β -aminocarbonyl systems, 1-arylalkylphosphonium salts or α,β -dehydro- α -amino acids, which are very important because of their valuable biological and chemical properties. However, most of the described reactions were intermolecular (did not lead to cyclization) and were not conducted in a stereocontrolled manner. These two aspects require further research because such transformations are of great importance in the synthesis of natural, biologically active compounds. It seems that, especially in this field, the easy ability to control the $\text{C}_\alpha\text{-P}^+$ bond strength and introduce structural modifications within phosphonium salts may be crucial (Figure 8—new challenges/asymmetric synthesis/cyclization). Studies on cyclization and stereocontrol of reactions involving 1-aminoalkylphosphonium salts are in progress.

It is worth adding that, not only many of the described compounds obtained from 1-aminoalkylphosphonium salts derivatives, but also some phosphonium salts themselves show interesting biological properties. However, in this case, the area of potential application should also be much more explored. 1-Aminoalkylphosphonium salts derivatives can be an ideal tool for the modification of already known structures with proven biological activity. Furthermore, recent reports on mitochondria-targeted phosphonium salts inspire the design and synthesis of molecular hybrids or conjugates that will use the targeting properties of the triphenylphosphonium (TPP) group, its biological properties, or both (Figure 8—new challenges/biological activity).

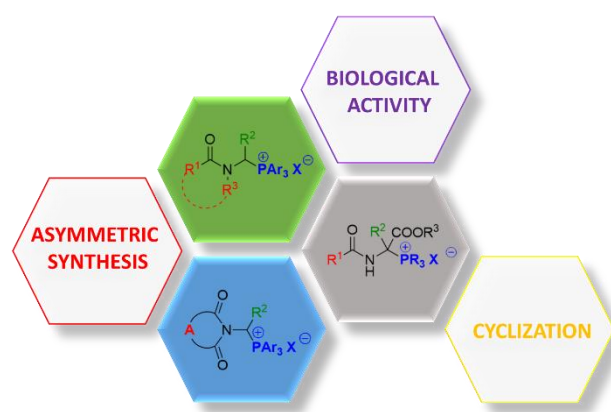


Figure 8. 1-Aminoalkylphosphonium derivatives—new challenges.

We hope that the presented data will encourage further research on 1-aminoalkylphosphonium salt derivatives and will contribute to discovering their full potential.

Author Contributions: Conceptualization, J.A.; data curation, J.A., M.G., A.K. and A.P.-H.; writing—original draft preparation, J.A., M.G., A.K. and A.P.-H.; writing—review and editing, J.A., M.G., A.K. and A.P.-H.; supervision, J.A. All authors have read and agreed to the published version of the manuscript.

Funding: This work was supported under the Rector’s Habilitation Grant, Silesian University of Technology (Poland), No. 04/020/RGH20/1006. This research was also supported by Silesian University of Technology (Poland) Grant BK No. 04/050/BK_21/0116.

Institutional Review Board Statement: Not applicable.

Informed Consent Statement: Not applicable.

Data Availability Statement: Not applicable.

Conflicts of Interest: The authors declare no conflict of interest.

References

- Neto, B.A.D.; Rocha, R.O.; Rodrigues, M.O. Catalytic Approaches to Multicomponent Reactions: A Critical Review and Perspectives on the Roles of Catalysis. *Molecules* **2022**, *27*, 132. [CrossRef]
- Kokkala, P.; Rajeshkumar, T.; Mpakali, A.; Stratikos, E.; Vogiatzis, K.D.; Georgiadis, D. A Carbodiimide-Mediated P–C Bond-Forming Reaction: Mild Amidoalkylation of *P*-Nucleophiles by Boc-Aminals. *Org. Lett.* **2021**, *23*, 1726–1730. [CrossRef]
- Heravi, M.M.; Zadsirjan, V.; Heydari, M.; Masoumi, B. Organocatalyzed Asymmetric Friedel-Crafts Reactions: An Update. *Chem. Rec.* **2019**, *19*, 2236–2340. [CrossRef]
- Aranzamendi, E.; Sotomayor, N.; Lete, E. Phenolic Activation in Chiral Brønsted Acid-Catalyzed Intramolecular α -Amidoalkylation Reactions for the Synthesis of Fused Isoquinolines. *ACS Omega* **2017**, *2*, 2706–2718. [CrossRef]
- Huang, Y.-Y.; Cai, C.; Yang, X.; Lv, Z.-C.; Schneider, U. Catalytic Asymmetric Reactions with *N,O*-Aminals. *ACS Catal.* **2016**, *6*, 5747–5763. [CrossRef]
- Kataja, A.O.; Masson, G. Imine and iminium precursors as versatile intermediates in enantioselective organocatalysis. *Tetrahedron* **2014**, *70*, 8783–8815. [CrossRef]
- Maryanoff, B.E.; Zhang, H.C.; Cohen, J.H.; Turchi, I.J.; Maryanoff, C.A. Cyclizations of *N*-acyliminium ions. *Chem. Rev.* **2004**, *104*, 1431–1628. [CrossRef]
- Yazici, A.; Pyne, S.G. Intermolecular addition reactions of *N*-acyliminium ions (Part I). *Synthesis* **2009**, 339–368. [CrossRef]
- Yazici, A.; Pyne, S.G. Intermolecular addition reactions of *N*-acyliminium ions (Part II). *Synthesis* **2009**, 513–541. [CrossRef]
- Aranzamendi, E.; Arrasate, S.; Sotomayor, N.; González-Díaz, H.; Lete, E. Chiral Brønsted Acid Catalyzed Enantioselective α -Amidoalkylation Reactions: A Joint Experimental and Predictive Study. *ChemistryOpen* **2016**, *5*, 540–549. [CrossRef]
- Zhang, S.; Shi, X.; Li, J.; Hou, Z.; Song, Z.; Su, X.; Peng, D.; Wang, F.; Yu, Y.; Zhao, G. Nickel-Catalyzed Amidoalkylation Reaction of γ -Hydroxy Lactams: An Access to 3-Substituted Isoindolinones. *ACS Omega* **2019**, *4*, 19420–19436. [CrossRef]
- Mazurkiewicz, R.; Październiak-Holewa, A.; Adamek, J.; Zielińska, K. α -Amidoalkylating agents: Structure, synthesis, reactivity and application. *Adv. Heterocycl. Chem.* **2014**, *111*, 43–94. [CrossRef]

13. Touati, B.; El Bouakher, A.; Taillier, C.; Othman, R.B.; Trabelsi-Ayadi, M.; Antoniotti, S.; DuÇach, E.; Dalla, V. Enolizable Carbonyls and *N,O*-Acetals: A Rational Approach for Room-Temperature Lewis Superacid-Catalyzed Direct- α -Amidoalkylation of Ketones and Aldehydes. *Chem. Eur. J.* **2016**, *22*, 6012–6022. [CrossRef] [PubMed]
14. Schneider, A.E.; Manolikakes, G. Bi(OTf)₃-Catalyzed Multicomponent α -Amidoalkylation Reactions. *J. Org. Chem.* **2015**, *80*, 6193–6212. [CrossRef] [PubMed]
15. Vinogradov, M.G.; Olga, V.; Turova, O.V.; Zlotin, S.G. The progress in the chemistry of *N*-acyliminium ions and their use in stereoselective organic synthesis. *Russ. Chem. Rev.* **2017**, *86*, 1–17. [CrossRef]
16. Katritzky, A.R.; Abdel-Fattah, A.A.A.; Celik, I. Benzotriazole-mediated amidoalkylations of nitroalkanes, nitriles, alkynes and esters. *ARKIVOC* **2007**, *11*, 96–113. [CrossRef]
17. Katritzky, A.R.; Manju, K.; Singh, S.K.; Meher, N.K. Benzotriazole mediated amino-, amido-, alkoxy- and alkylthioalkylation. *Tetrahedron* **2005**, *61*, 2555–2581. [CrossRef]
18. Katritzky, A.R.; Mehta, S.; He, H.Y. Syntheses of Pyrrolo- and Indoloisoquinolinones by Intramolecular Cyclizations of 1-(2-Arylethyl)-5-benzotriazolylpyrrolidin-2-ones and 3-Benzotriazolyl-2-(2-arylethyl)-1-isoindolinones. *J. Org. Chem.* **2001**, *66*, 148–152. [CrossRef] [PubMed]
19. Katritzky, A.R.; Kirichenko, K.; Elsayed, A.M.; Ji, Y.; Fang, Y. Convenient Preparation of tert-Butyl β -(Protected amino)esters. *J. Org. Chem.* **2002**, *67*, 4957–4959. [CrossRef]
20. Petrini, M. α -Amido Sulfones as Stable Precursors of Reactive *N*-Acylimino Derivatives. *Chem. Rev.* **2005**, *105*, 3949–3977. [CrossRef]
21. Ballini, R.; Palmieri, A.; Petrini, M.; Torregiani, E. Solventless Clay-Promoted Friedel–Crafts Reaction of Indoles with α -Amido Sulfones: Unexpected Synthesis of 3-(1-Arylsulfonylalkyl) Indoles. *Org. Lett.* **2006**, *8*, 4093–4096. [CrossRef]
22. Das, B.; Damodar, K.; Bhunia, N. A Simple and Efficient Access to α -Amino Phosphonates from *N*-Benzyloxycarbonylamino Sulfones Using Indium(III) Chloride. *J. Org. Chem.* **2009**, *74*, 5607–5609. [CrossRef] [PubMed]
23. Marcantoni, E.; Palmieri, A.; Petrini, M. Recent synthetic applications of α -amido sulfones as precursors of *N*-acylimino derivatives. *Org. Chem. Front.* **2019**, *6*, 2142–2182. [CrossRef]
24. Drach, B.; Kirsanov, A.; Sviridov, E. Reaction of *N*-chloromethyl amides of acids with triphenylphosphine. *Zh. Obshch. Khim.* **1972**, *42*, 953–954.
25. Smolii, O.B.; Brovarets, V.S.; Drach, B.S. Substituted Methylphosphonium Salts with an Imidoyl Chloride Group. *Zh. Obshch. Khim.* **1986**, *56*, 2802–2803.
26. Smolii, O.B.; Brovarets, V.S.; Pirozhenko, V.V.; Drach, B.S. Cyclocondensation of *N*-Substituted Imidoyl Chlorides Containing a Phosphonium Group. *Zh. Obshch. Khim.* **1988**, *58*, 2465–2471.
27. Kasukhin, L.F.; Brovarets, V.S.; Smolii, O.B.; Kurg, V.V.; Budnik, L.V.; Drach, B.S. *N*-Acylaminomethyl and Substituted 1-Acylaminoethenylphosphonium Salts As Inhibitors of Acetylcholinesterase. *Zh. Obshch. Khim.* **1991**, *61*, 2679–2684.
28. Devlin, C.J.; Walker, B.J. Reactions of bromonitroalkenes with trivalent phosphorus. Part II. Reaction in methanol. *J. Chem. Soc. Perkin Trans.* **1974**, *1*, 453–460. [CrossRef]
29. Petersen, H.; Reuther, W. α -Ureidoalkylierung von Phosphor (III)-Verbindungen. *Justus Liebigs Ann. Chem.* **1972**, *766*, 58–72. [CrossRef]
30. Kozhushko, B.N.; Gumenyuk, A.V.; Palichuk, Y.A.; Shokol, V.A. Trialkyl- et Triaryl-(Isocyanatomethyl) Chlorophosphoranes. *Zh. Obshch. Khim.* **1977**, *47*, 333–339.
31. Shokol, V.A.; Silina, E.B.; Kozhushko, B.N.; Golik, G.A. Bromomethyl Isocyanate and Its Phosphorylated Derivatives. *Zh. Obshch. Khim.* **1979**, *49*, 312–316.
32. Kozhushko, B.N.; Silina, E.B.; Gumenyuk, A.V.; Turov, A.V.; Shokol, V.A. Triaryl(Isocyanatomethyl)Phosphonium Iodides. *Zh. Obshch. Khim.* **1980**, *50*, 2210–2215.
33. Shokol, V.A.; Kozhushko, B.N.; Gumenyuk, A.V. Trialkyl- And Aryldialkyl(Isocyanatomethyl)Ammonium Chlorides. *Zh. Obshch. Khim.* **1977**, *47*, 1110–1118.
34. Zinner, G.; Fehlhammer, W.P. Isocyanomethylenetriphenylphosphorane. *Angew. Chem. Int. Ed. Engl.* **1985**, *24*, 979–980. [CrossRef]
35. Frank, A.W.; Drake, G.L. Synthesis and properties of carbamate derivatives of tetrakis(hydroxymethyl)phosphonium chloride. *J. Org. Chem.* **1977**, *42*, 4040–4045. [CrossRef]
36. Devlin, C.J.; Walker, B.J. A possible azirine intermediate in the reaction of bromonitroalkenes with triphenylphosphine. *J. Chem. Soc. D Chem. Comm.* **1970**, 917–918. [CrossRef]
37. Drach, B.S.; Dolgushina, I.Y.; Sinita, A.D. Application of Omega-Chloro-Omega-Acylamidoacetophenones for Synthesis of Phosphorylated Oxazoles. *Zh. Obshch. Khim.* **1975**, *45*, 1251–1255.
38. Brovarets, V.S.; Lobanov, O.P.; Vinogradova, T.K.; Drach, B.S. Preparation and Properties of 2-Chloro-1-Acylaminovinyltriphenylphosphonium Chlorides. *Zh. Obshch. Khim.* **1984**, *54*, 288–301.
39. Drach, B.S.; Brovarets, V.S.; Smolii, O.B. Acylamino-Substituted Vinylphosphonium Salts in Syntheses of Derivatives of Nitrogen Heterocycles. *Russ. J. Gen. Chem.* **2002**, *72*, 1661–1687. [CrossRef]
40. Mazurkiewicz, R.; Pierwocha, A.W. Phosphoranylidene-5(4*H*)-oxazolones—A novel synthesis and properties. *Monatsh. Chem.* **1996**, *127*, 219–225. [CrossRef]

41. Mazurkiewicz, R.; Październiak-Holewa, A.; Grymel, M. Synthesis and decarboxylation of *N*-acyl- α -triphenylphosphonio- α -amino acids: A new synthesis of α -(*N*-acylamino)alkyltriphenylphosphonium salts. *Tetrahedron Lett.* **2008**, *49*, 1801–1803. [CrossRef]
42. Mazurkiewicz, R.; Październiak-Holewa, A.; Grymel, M. *N*-Acyl- α -triphenylphosphonio- α -amino Acids: Synthesis and Decarboxylation to α -(*N*-Acylamino)alkyltriphenylphosphonium Salts. *Phosphorus Sulfur Silicon Relat. Elem.* **2009**, *184*, 1017–1027. [CrossRef]
43. Mazurkiewicz, R.; Adamek, J.; Październiak-Holewa, A.; Zielińska, K.; Simka, W.; Gajos, A.; Szymura, K. α -Amidoalkylating Agents from *N*-Acyl- α -amino Acids: 1-(*N*-Acylamino)alkyltriphenylphosphonium Salts. *J. Org. Chem.* **2012**, *77*, 1952–1960. [CrossRef] [PubMed]
44. Adamek, J.; Zieleźny, P.; Erfurt, K. *N*-protected 1-aminoalkylphosphonium salts from amides, carbamates, lactams, or imides. *J. Org. Chem.* **2021**, *86*, 5852–5862. [CrossRef]
45. Wałęcka-Kurczyk, A.; Adamek, J.; Walczak, K.; Michalak, M.; Październiak-Holewa, A. Non-Kolbe electrolysis of *N*-protected- α -amino acids: A standardized method for the synthesis of *N*-protected (1-methoxyalkyl)amines. *RSC Adv.* **2022**, *12*, 2107–2114. [CrossRef]
46. Adamek, J.; Węgrzyk, A.; Kończewicz, J.; Walczak, K.; Erfurt, K. 1-(*N*-Acylamino)alkyltriarylphosphonium Salts with Weakened C_{α} - P^{+} Bond Strength—Synthetic Applications. *Molecules* **2018**, *23*, 2453. [CrossRef] [PubMed]
47. Adamek, J.; Mazurkiewicz, R.; Październiak-Holewa, A.; Grymel, M.; Kuźnik, A.; Zielińska, K. 1-(*N*-Acylamino)alkyl Sulfones from *N*-Acyl- α -amino Acids or *N*-Alkylamides. *J. Org. Chem.* **2014**, *79*, 2765–2770. [CrossRef]
48. Kozicka, D.; Zieleźny, P.; Erfurt, K.; Adamek, J. Amide-type substrates in the synthesis of *N*-protected 1-aminomethylphosphonium salts. *Catalysts* **2021**, *11*, 552. [CrossRef]
49. Mucha, A.; Kafarski, P.; Berlicki, L. Remarkable Potential of the α -Aminophosphonate/Phosphinate Structural Motif in Medicinal Chemistry. *J. Med. Chem.* **2011**, *54*, 5955–5980. [CrossRef] [PubMed]
50. Mazurkiewicz, R.; Październiak-Holewa, A.; Kononienko, A. A Novel Synthesis of 1-Aminoalkanephosphonic Acid Derivatives from 1-(*N*-Acylamino)alkyltriphenylphosphonium Salts. *Phosphorus Sulfur Silicon* **2010**, *185*, 1986–1992. [CrossRef]
51. Październiak-Holewa, A.; Adamek, J.; Mazurkiewicz, R.; Zielińska, K. Amidoalkylating Properties of 1-(*N*-Acylamino)Alkyltriphenylphosphonium Salts. *Phosphorus Sulfur Silicon Relat. Elem.* **2013**, *188*, 205–212. [CrossRef]
52. Adamek, J.; Październiak-Holewa, A.; Zielińska, K.; Mazurkiewicz, R. Comparative Studies on the Amidoalkylating Properties of *N*-(1-Methoxyalkyl)Amides and 1-(*N*-Acylamino)Alkyltriphenylphosphonium Salts in the Michaelis–Arbuzov-Like Reaction: A New One-Pot Transformation of *N*-(1-Methoxyalkyl)Amides into Phosphonic or Phosphinic Analogs of *N*-Acyl- α -Amino Acids. *Phosphorus Sulfur Silicon Relat. Elem.* **2013**, *188*, 967–980. [CrossRef]
53. Zielińska, K.; Mazurkiewicz, R.; Szymańska, K.; Jarzębski, A.; Magiera, S.; Erfurt, K. Penicillin G Acylase-Mediated Kinetic Resolution of Racemic 1-(*N*-Acylamino)alkylphosphonic and 1-(*N*-Acylamino)alkylphosphinic Acids and Their Esters. *J. Mol. Catal. B Enzym.* **2016**, *132*, 31–40. [CrossRef]
54. Zielińska, K.; Mazurkiewicz, R.; Szymańska, K.; Jarzębski, A. Batch and in-flow kinetic resolution of racemic 1-(*N*-acylamino)alkylphosphonic and 1-(*N*-acylamino)alkylphosphinic acids and their esters using immobilized penicillin G acylase. *Tetrahedron Asymmetry* **2017**, *28*, 146–152. [CrossRef]
55. Wałęcka-Kurczyk, A.; Walczak, K.; Kuźnik, A.; Stecko, S.; Październiak-Holewa, A. The Synthesis of α -Aminophosphonates via Enantioselective Organocatalytic Reaction of 1-(*N*-Acylamino)alkylphosphonium Salts with Dimethyl Phosphite. *Molecules* **2020**, *25*, 405. [CrossRef]
56. Kuźnik, A.; Mazurkiewicz, R.; Grymel, M.; Zielińska, K.; Adamek, J.; Chmielewska, E.; Bochno, M.; Kubica, S. New method for the synthesis of α -aminoalkylenebisphosphonates and their asymmetric phosphonyl-phosphinyl and phosphonyl-phosphinoyl analogues. *Beilstein J. Org. Chem.* **2015**, *11*, 1418–1424. [CrossRef]
57. Kuźnik, A.; Mazurkiewicz, R.; Zięba, M.; Erfurt, K. 1-(*N*-Acylamino)-1-triphenylphosphoniumalkylphosphonates: General synthesis and prospects for further synthetic applications. *Tetrahedron Lett.* **2018**, *59*, 3307–3310. [CrossRef]
58. Październiak-Holewa, A.; Adamek, J.; Zielińska, K.; Piernikarczyk, K.; Mazurkiewicz, R. *N*-(1-acyloaminoalkyl)amidinium salts derived from DBU or related bases as reactive intermediates in α -amidoalkylation reactions. *Arkivoc* **2012**, *4*, 314–329. [CrossRef]
59. Adamek, J.; Mazurkiewicz, R.; Październiak-Holewa, A.; Kuźnik, A.; Grymel, M.; Zielińska, K.; Simka, W. *N*-[1-(Benzotriazol-1-yl)alkyl]amides from *N*-acyl- α -amino acids or *N*-alkylamides. *Tetrahedron* **2014**, *70*, 5725–5729. [CrossRef]
60. Zheng, K.; Shen, D.; Zhang, B.; Hong, R. Stereodivergent Synthesis of Lankacyclinol and Its C2/C18-Congeners Enabled by a Bioinspired Mannich Reaction. *J. Org. Chem.* **2021**, *86*, 10991–11005. [CrossRef]
61. Zheng, K.; Shen, D.; Zhang, B.; Hong, R. Landscape of Lankacidin Biomimetic Synthesis: Structural Revisions and Biogenetic Implications. *J. Org. Chem.* **2020**, *85*, 13818–13836. [CrossRef]
62. Zheng, K.; Hong, R. The Fruit of Gold: Biomimicry in the Syntheses of Lankacidins. *Acc. Chem. Res.* **2021**, *54*, 3438–3451. [CrossRef]
63. Adamek, J.; Węgrzyk, A.; Krawczyk, M.; Erfurt, K. Catalyst-free Friedel-Crafts reaction of 1-(*N*-acylamino)alkyltriarylphosphonium salts with electron-rich arenes. *Tetrahedron* **2018**, *74*, 2575–2583. [CrossRef]
64. Październiak-Holewa, A.; Wałęcka-Kurczyk, A.; Musioł, S.; Stecko, S. Catalyst-free Mannich-type reaction of 1-(*N*-acylamino)alkyltriphenylphosphonium salts with silyl enolates. *Tetrahedron* **2019**, *75*, 732–742. [CrossRef]

65. Smolii, O.B.; Brovarets, V.S.; Drach, B.S. Reaction of the Chloride of *N*-(Triphenylphosphoniomethyl)benzimidoyl chloride with Sodium Rhodanide. *Zh. Obshch. Khim.* **1987**, *57*, 2145–2146.
66. Smolii, O.B.; Brovarets, V.S.; Drach, B.S. Reaction of the Chloride of *N*-(Triphenylphosphoniomethyl)benzimidoyl chloride with Carboxylic Acid Chlorides. *Zh. Obshch. Khim.* **1988**, *58*, 1670–1671.
67. Dubois, R.J.; Lin, C.-C.; Beisler, J.A. Synthesis and antitumor properties of some isoindolylalkylphosphonium salts. *J. Med. Chem.* **1978**, *21*, 303–306. [CrossRef]
68. Tessier, D.; Filteau, M.; Radu, I. New Antimicrobial Compositions and Uses Thereof. U.S. Patent US 2015/0201622 A1, 23 July 2015.
69. Tessier, D.; Filteau, M.; Radu, I. Antimicrobial Solution Comprising a Metallic Salt and a Surfactant. International Patent WO 2006105669 A1, 12 October 2006.
70. Hellmann, H.; Schumacher, O. Quartäre Phosphoniumsalze aus tertiären Phosphinen und quartären Ammoniumsalzen. *Justus Liebigs Ann. Chem.* **1961**, *640*, 79–84. [CrossRef]
71. Enzmann, A.; Eckert, M.; Ponikwar, W.; Polborn, K.; Schneiderbauer, S.; Beller, M.; Beck, W. Aminomethyl and Aminoacetyl Complexes of Palladium(II), Platinum(II), Iron(II) and Rhenium(I) with *N*-Phthaloyl as Amino Protecting Group and Mechanistic Studies on the Palladium-Catalyzed Amidocarbonylation. *Eur. J. Inorg. Chem.* **2004**, *6*, 1330–1340. [CrossRef]
72. Tan, E.S.; Naylor, J.C.; Groban, E.S.; Bunzow, J.R.; Jacobson, M.P.; Grandy, D.K.; Scanlan, T.S. The Molecular Basis of Species-Specific Ligand Activation of Trace Amine-Associated Receptor 1 (TAAR1). *ACS Chem. Biol.* **2009**, *4*, 209–220. [CrossRef]
73. Adamek, J.; Mazurkiewicz, R.; Węgrzyk, A.; Erfurt, K. 1-Imidoalkylphosphonium salts with modulated C α -P $^+$ bond strength: Synthesis and application as new active α -imidoalkylating agents. *Beilstein J. Org. Chem.* **2017**, *13*, 1446–1455. [CrossRef] [PubMed]
74. Clavé, G.; Reverte, M.; Vasseur, J.-J.; Smietana, M. Modified internucleoside linkages for nuclease-resistant oligonucleotides. *RSC Chem. Biol.* **2021**, *2*, 94–150. [CrossRef]
75. Nahrwold, M.; Bogner, T.; Eissler, S.; Verma, S.; Sewald, N. “Clicktophycin-52”: A Bioactive Cryptophycin-52 Triazole Analogue. *Org. Lett.* **2010**, *12*, 1064–1067. [CrossRef] [PubMed]
76. Adamek, J.; Węgrzyk-Schlieter, A.; Steć, K.; Walczak, K.; Erfurt, K. Michaelis-Arbuzov-Type Reaction of 1-Imidoalkyltriarylphosphonium Salts with Selected Phosphorus Nucleophiles. *Molecules* **2019**, *24*, 3405. [CrossRef]
77. Kober, R.; Steglich, W. Untersuchungen zur Reaktion von Acylaminobrommalonestern und Acylaminobromessigestern mit Trialkylphosphiteneine einfache Synthese von 2-Amino-2-(diethoxyphosphoryl) Essigsäure Ethylester. *Liebigs Ann. Chem.* **1983**, *4*, 599–609. [CrossRef]
78. Mazurkiewicz, R.; Grymel, M. *N*-Acyl- α -triphenylphosphonioglycinates: A Novel Cationic Glycine Equivalent and its Reactions with Heteroatom Nucleophiles. *Monatsh. Chem.* **1999**, *130*, 597–604. [CrossRef]
79. Mazurkiewicz, R.; Grymel, M. A new synthesis of α -amino acid derivatives by reaction of *N*-acyl- α -triphenylphosphonioglycinates with carbon nucleophiles. *Phosphorus Sulfur Silicon* **2000**, *164*, 33–43. [CrossRef]
80. Mazurkiewicz, R.; Pierwocha, A.W. 4-Phosphoranylidene-5(4*H*)-oxazolones II. Reactions with alkylating agents. *Monatsh. Chem.* **1997**, *128*, 893–900. [CrossRef]
81. Grymel, M.; Kuźnik, A.; Mazurkiewicz, R. *N*-Acyl- α -triphenylphosphonio- α -amino acid esters as synthetic equivalents of α -amino acid α -cations. *Phosphorus Sulfur Silicon* **2015**, *190*, 429–439. [CrossRef]
82. Mazurkiewicz, R.; Grymel, M.; Kuźnik, A. Three New in situ Syntheses of *N*-Acyl- α -triphenylphosphonioglycinates. *Monatsh. Chem.* **2004**, *135*, 799–806. [CrossRef]
83. Mazurkiewicz, R.; Grymel, M. Reaction of *N*-Acyl- α -triphenylphosphonio- α -amino Acid Esters with Organic Bases: Mechanism of the Base-Catalyzed Nucleophilic Substitution of the Triphenylphosphonium Group. *Monatsh. Chem.* **2002**, *133*, 1197–1204. [CrossRef]
84. Mazurkiewicz, R.; Kuźnik, A.; Grymel, M.; Kuźnik, N. *N*-Acyl- α -triphenylphosphonioglycinates in the Synthesis of α,β -Dehydro- α -amino Acid Derivatives. *Monatsh. Chem.* **2004**, *135*, 807–815. [CrossRef]
85. Gentilucci, L.; De Marco, R.; Cerisoli, L. Chemical Modifications Designed to Improve Peptide Stability: Incorporation of Non-Natural Amino Acids, Pseudo-Peptide Bonds, and Cyclization. *Curr. Pharm. Des.* **2010**, *16*, 3185–3203. [CrossRef]
86. Meester, W.J.N.; van Maarseveen, J.H.; Schoemaker, H.E.; Hiemstra, H.; Rutjes, F.P.J.T. Glyoxylates as Versatile Building Blocks for the Synthesis of α -Amino Acid and α -Alkoxy Acid Derivatives via Cationic Intermediates. *Eur. J. Org. Chem.* **2003**, *2003*, 2519–2529. [CrossRef]
87. Heimgartner, H.; Braun, K.; Linden, A. Synthesis and conformational analysis of pentapeptides containing enantiomerically pure 2,2-disubstituted glycines. *Helv. Chim. Acta* **2008**, *91*, 526–558. [CrossRef]
88. Ohfuné, Y.; Shinada, T. Enantio- and Diastereoselective Construction of α,α -Disubstituted α -Amino Acids for the Synthesis of Biologically Active Compounds. *Eur. J. Org. Chem.* **2005**, *2005*, 5127–5143. [CrossRef]
89. Mazurkiewicz, R.; Kuźnik, A. A new convenient synthesis of *N*-acyl-2-(dimethoxyphosphoryl)glycinates. *Tetrahedron Lett.* **2006**, *47*, 3439–3442. [CrossRef]
90. Kobayashi, K.; Tanaka, K.; Kogen, H. Recent topics of the natural product synthesis by Horner–Wadsworth–Emmons reaction. *Tetrahedron Lett.* **2018**, *59*, 568–582. [CrossRef]
91. Mazurkiewicz, R.; Kuźnik, A.; Grymel, M.; Październiak-Holewa, A. α -Amino acid derivatives with a C α -P bond in organic synthesis. *Arkivoc* **2007**, *6*, 193–216. [CrossRef]

92. Pfefferkorn, J.A.; Nugent, R.A.; Gross, R.J.; Greene, M.L.; Mitchell, M.A.; Reding, M.T.; Funk, L.A.; Anderson, R.; Wells, P.A.; Shelly, J.A.; et al. Inhibitors of HCV NS5B polymerase. Part 2: Evaluation of the northern region of (2Z)-2-benzoylamino-3-(4-phenoxy-phenyl)-acrylic acid. *Bioorg. Med. Chem. Lett.* **2005**, *15*, 2812–2818. [CrossRef] [PubMed]
93. Shangguan, N.; Joullié, M.M. Total synthesis of isoroquefortine E and phenylahistin. *Tetrahedron Lett.* **2009**, *50*, 6755–6757. [CrossRef] [PubMed]
94. Wang, W.; Xiong, C.; Zhang, J.; Hruby, V.J. Practical, asymmetric synthesis of aromatic-substituted bulky and hydrophobic tryptophan and phenylalanine derivatives. *Tetrahedron* **2002**, *58*, 3101–3110. [CrossRef]
95. Cativiela, C.; Diaz de Villegas, M.D.; Gálvez, J.A.; Su, G. Horner-Wadsworth-Emmons reaction for the synthesis of unusual alpha,beta-didehydroamino acids with a chiral axis. *Arkivoc* **2004**, *4*, 59–66. [CrossRef]
96. Aguado, G.P.; Moglioni, A.G.; Ortuño, R.M. Enantiodivergent synthesis of cyclobutyl-(Z)- α,β -dehydro- α -amino acid derivatives from (–)-cis-pinonic acid. *Tetrahedron Asymmetry* **2003**, *14*, 217–223. [CrossRef]
97. Etayo, P.; Vidal-Ferran, A. Rhodium-catalysed asymmetric hydrogenation as a valuable synthetic tool for the preparation of chiral drugs. *Chem. Soc. Rev.* **2013**, *42*, 728–754. [CrossRef] [PubMed]
98. Adamczyk, M.; Akireddy, S.R.; Reddy, R.E. Nonproteinogenic amino acids: An efficient asymmetric synthesis of (S)-(–)-acromelobic acid and (S)-(–)-acromelobinic acid. *Tetrahedron* **2002**, *58*, 6951–6963. [CrossRef]
99. Blaskovich, M.A. *Handbook on Syntheses of Amino Acids, General Routes to Amino Acids*; American Chemical Society & Oxford University Press: New York, NY, USA, 2010.
100. Yasuno, Y.; Mizutani, I.; Sueuchi, Y.; Wakabayashi, Y.; Yasuo, N.; Shimamoto, K.; Shinada, T. Catalytic Asymmetric Hydrogenation of Dehydroamino Acid Esters with Biscarbamate Protection and Its Application to the Synthesis of xCT Inhibitors. *Chem. Eur. J.* **2019**, *25*, 5145–5148. [CrossRef]
101. Adamek, J.; Mrowiec-Białon, J.; Październiak-Holewa, A.; Mazurkiewicz, R. Thermogravimetric investigations of the dealkoxy-carbonylation of *N*-acyl- α -triphenylphosphonioglycinates. *Thermochim. Acta* **2011**, *512*, 22–27. [CrossRef]
102. Gorewoda, T.; Mazurkiewicz, R.; Simka, W.; Mlostoń, G.; Schroeder, G.; Kubicki, M.; Kuźnik, N. 3-Triphenylphosphonio-2,5-piperazinediones as new chiral glycine cation equivalents. *Tetrahedron Asymmetry* **2011**, *22*, 823–833. [CrossRef]

Article

Design, Synthesis and Preliminary Evaluation of the Cytotoxicity and Antibacterial Activity of Novel Triphenylphosphonium Derivatives of Betulin

Mirosława Grymel^{1,2,3,*} , Anna Lalik^{3,4}, Alicja Kazek-Kęsik⁵ , Marietta Szewczyk¹, Patrycja Grabiec¹ and Karol Erfurt² 

¹ Department of Organic Chemistry, Bioorganic Chemistry and Biotechnology, Silesian University of Technology, B. Krzywoustego 4, 44-100 Gliwice, Poland

² Department of Chemical Organic Technology and Petrochemistry, Silesian University of Technology, B. Krzywoustego 4, 44-100 Gliwice, Poland

³ Biotechnology Center, Silesian University of Technology, B. Krzywoustego 8, 44-100 Gliwice, Poland

⁴ Department of Systems Biology and Engineering, Silesian University of Technology, Akademicka 16, 44-100 Gliwice, Poland

⁵ Department of Inorganic, Analytical Chemistry and Electrochemistry, Silesian University of Technology, B. Krzywoustego 6, 44-100 Gliwice, Poland

* Correspondence: mirosława.grymel@polsl.pl; Tel.: +48-032-237-1873; Fax: +48-032-237-2094

Abstract: For several decades, natural products have been widely researched and their native scaffolds are the basis for the design and synthesis of new potential therapeutic agents. Betulin is an interesting biologically attractive natural parent molecule with a high safety profile and can easily undergo a variety of structural modifications. Herein, we describe the synthesis of new molecular hybrids of betulin via covalent linkage with an alkyltriphenylphosphonium moiety. The proposed strategy enables the preparation of semi-synthetic derivatives (28-TPP⁺ BN and 3,28-bisTPP⁺ BN) from betulin through simple transformations in high yields. The obtained results showed that the presence of a lipophilic cation improved the solubility of the tested analogs compared to betulin, and increased their cytotoxicity. Among the triphenylphosphonium derivatives tested, analogs **7a** (IC₅₀ of 5.56 μM) and **7b** (IC₅₀ of 5.77 μM) demonstrated the highest cytotoxicity against the colorectal carcinoma cell line (HCT 116). TPP⁺-conjugates with betulin showed antimicrobial properties against Gram-positive reference *Staphylococcus aureus* ATCC 25923 and *Staphylococcus epidermidis* ATCC 12228 bacteria, at a 200 μM concentration in water. Hence, the conjugation of betulin's parent backbone with a triphenylphosphonium moiety promotes transport through the hydrophobic barriers of the mitochondrial membrane, making it a promising strategy to improve the bioavailability of natural substances.

Keywords: betulin; triphenylphosphonium cation; anticancer; antibacterial activity

Citation: Grymel, M.; Lalik, A.; Kazek-Kęsik, A.; Szewczyk, M.; Grabiec, P.; Erfurt, K. Design, Synthesis and Preliminary Evaluation of the Cytotoxicity and Antibacterial Activity of Novel Triphenylphosphonium Derivatives of Betulin. *Molecules* **2022**, *27*, 5156. <https://doi.org/10.3390/molecules27165156>

Academic Editor: Gabriele Micheletti

Received: 21 July 2022

Accepted: 10 August 2022

Published: 12 August 2022

Publisher's Note: MDPI stays neutral with regard to jurisdictional claims in published maps and institutional affiliations.



Copyright: © 2022 by the authors. Licensee MDPI, Basel, Switzerland. This article is an open access article distributed under the terms and conditions of the Creative Commons Attribution (CC BY) license (<https://creativecommons.org/licenses/by/4.0/>).

1. Introduction

Advancements in medical science have allowed for the treatment of a wide range of diseases, however, many disorders lack necessary pharmaceuticals. The high systemic toxicity of medicinal preparations and increasing resistance of tumor cells to a significant number of drugs often limits anticancer therapy success. According to World Health Organization (WHO) reports, cancerous diseases are one of the biggest problems of modern medicine and are one of the main causes of death in the world in the 21st century [1]. Therefore, drug design is an important issue in modern medicinal chemistry. Despite many innovative tools that allow for the development of extremely advanced methods of treatment, many therapies are still based on active substances of natural origin. These substances act as basic structures that can be subjected to various chemical modifications in order to improve their physicochemical and pharmacokinetic properties.

For several decades, natural products (NPs) have been widely researched in terms of searching for new drugs. It is NPs that are an invaluable source of native scaffolds, which are the basis for the design and development of new potential therapeutic agents. Naturally occurring pentacyclic lupane-type triterpenoids have attracted a lot of attention including betulin (BN, 3-lup-20(29)-ene-3,28-diol), which is one of the most available terpenoids in the plant kingdom. BN is a cheap, easily accessible natural active substance that can be readily extracted from the bark of several species of trees, especially white birch (*Betula pubescens*) [2,3]. Due to the presence of simply transformable functional groups in its skeleton (including C³-OH, C²⁸-OH), BN has high synthetic potential for numerous semi-synthetic derivatives. BN is an interesting example of a biologically attractive natural parent molecule with a high safety profile and the possibility of making a variety of structural modifications (Figure 1) [3–5].

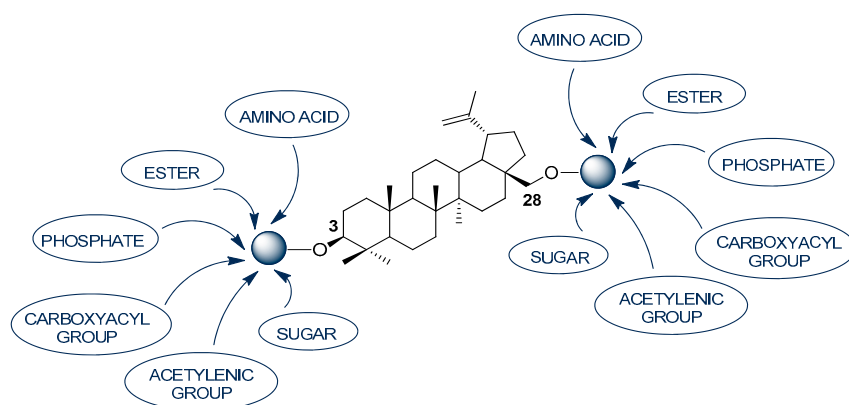


Figure 1. The selected modifications of the BN skeleton at positions C-3 and C-28 [3–5].

The multidirectional biological activity of natural BN has been confirmed by numerous research articles. Additionally, the reported derivatives of BN have shown a broad spectrum of bio-activity in terms of anticancer [4,6–10], antimalarial activity [11], antibacterial [12–14], antiviral [4,15–17], anti-inflammatory [18,19], or hepatoprotective properties [3]. Moreover, BN has a positive effect on the treatment of atopic dermatitis [20]. However, despite the abundance of BN, well-developed isolation methods from plant material as well as many studies confirming its very good biological properties, its use as a potential therapeutic agent is limited due to its low bioavailability, high hydrophobicity, and insufficient intracellular accumulation. The pentacyclic molecule and hydrophobic nature of the skeleton of BN hinders its ability to reach the target in vivo and obtain the desired therapeutic effect in acceptable therapeutic doses [21].

One of the most promising strategies for the design and synthesis of effective therapeutic agents is the conjugation of a native skeleton (e.g., BN) with triphenylphosphonium cation (TPP[⊕]) of low molecular weight, which promotes accumulation inside the cell's mitochondria. Furthermore, the presence of the TPP[⊕] group in a molecular hybrid improves the pharmacokinetic properties including solubility, bioavailability, and intermembrane transport as well as selectivity in targeting drugs for a specific purpose. The high lipophilicity and large ionic radius of TPP[⊕] effectively reduce the activation energy required for membrane passage. The presence of a delocalized lipophilic cation can accelerate the transport of biologically active molecules across the mitochondrial membrane [22]. Studies have shown that, in contrast to other cellular organelles, mitochondria have a high negative transmembrane potential ($\Delta\psi_m$). This potential is much higher for tumor cells, providing an opportunity for the selective delivery and accumulation of anticancer agents in mitochondria-targeted therapies [21–24].

Thus, the TPP[⊕] moiety not only affects the physical properties, but also the mechanism of action of a potential drug. In addition, it increases the selectivity, which often reduces the drug dose, and in turn diminishes the harmful side effects [24,25]. Therefore, research

into mitochondria-targeted anticancer drugs is an attractive prospect [24–28]. The strategy of modification of the native skeleton via conjugating with the TPP⁺ group has been used successfully for anticancer drugs such as doxorubicin [29], cisplatin [26], chlorambucil [30], metformin [31], and tamoxifen [32] because it facilitates their transport and selective accumulation in cancer cells (Figure 2).

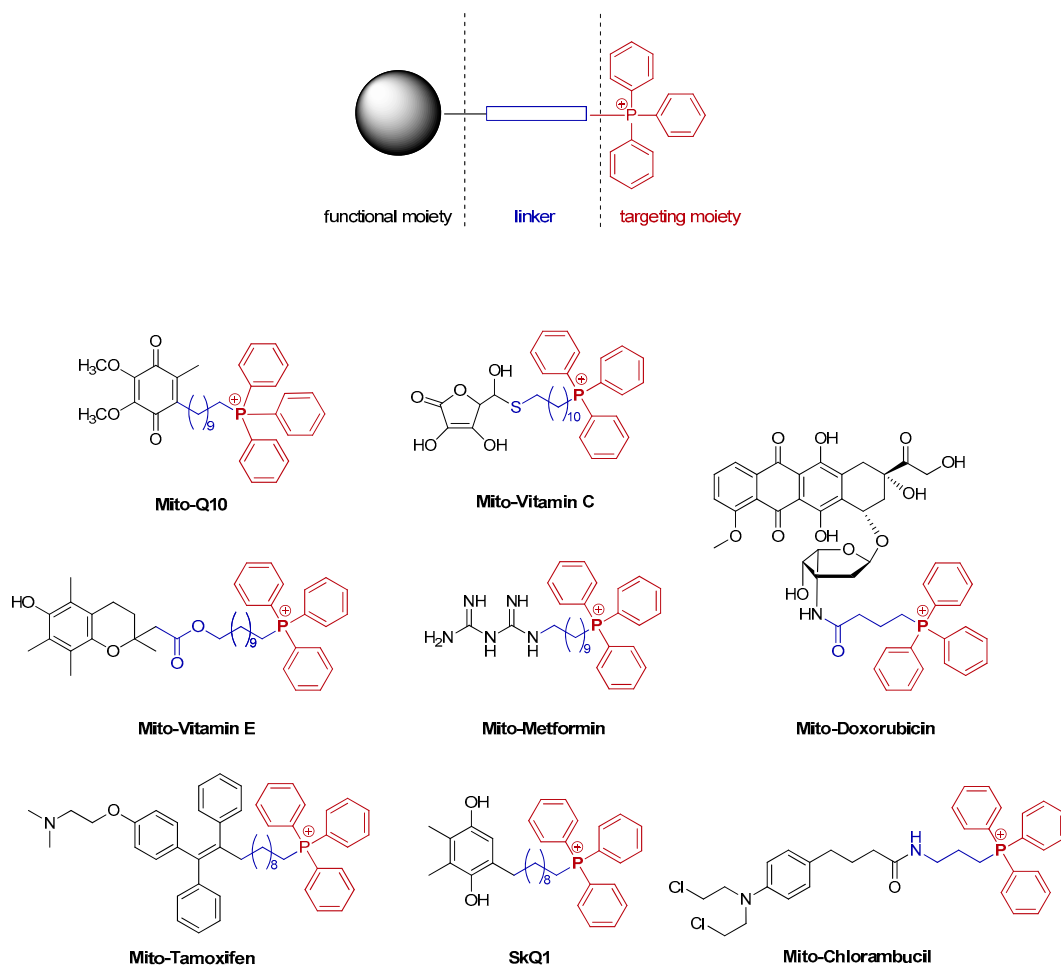


Figure 2. Examples of the TPP⁺-conjugated compounds [24,26,29–35].

Mitochondria play a vital role in a wide range of physiological and pathological processes. They are the main source of reactive oxygen species, and at the same time, are particularly susceptible to oxidative damage, contributing to the development of many diseases. Due to their functions, mitochondria may be an important molecular target for anticancer drugs as well as in the treatment of cardiovascular diseases or neurodegenerative diseases (e.g., Alzheimer’s disease or Parkinson’s disease) [36]. Non-targeted antioxidant therapeutics show low effectiveness, therefore, attempts have been made to modify them to increase the drug accumulation in the mitochondrial matrix. For example, Mito-Q10, (coenzyme Q10) has been described as a potential agent for the treatment of sepsis or Parkinson’s disease (Figure 2) [24,36].

A relatively novel group of potential *mitocans* (acronym derived from the terms mitochondria and cancer) is conjugates of pentacyclic lupane-type triterpenoids including *BN* or betulinic acid (*BA*) with the lipophilic cation TPP⁺ [28]. Spivak et al. [21,28,37–39], Tsepaveva et al. [23,40,41], Ye et al. [42], and Xu et al. [43] reported the preparation of *BA* or *BN* conjugates, in which one or two TPP⁺ moieties were linked to the triterpenoid skeleton at positions C-2, C-3, C-28, or C-30 by the carbon–carbon or ester bonds, as shown in Figures 3 and 4. The cytotoxic effect of these TPP⁺-analogs against various types of tumor cells toward *Schistosoma Mansoni* and antibacterial activity was analyzed [21,23,28,37–44].

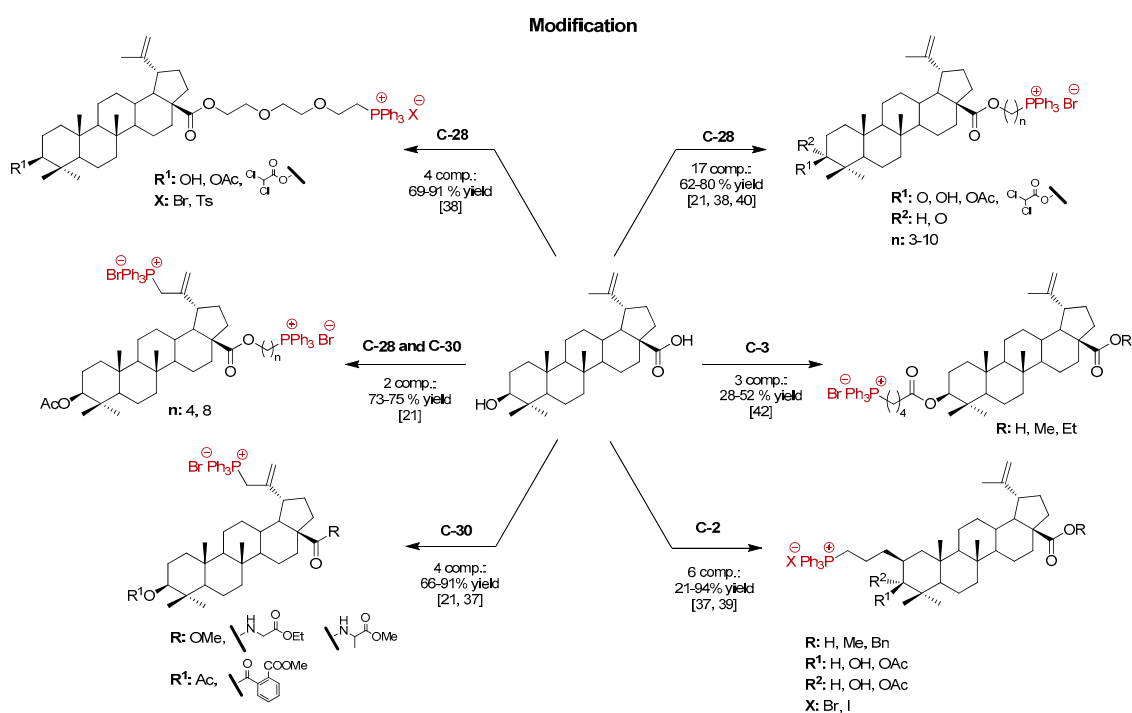


Figure 3. The chemical structures of the TPP⁺-conjugated with BA.

In the library of known triphenylphosphonium derivatives of pentacyclic lupane-type triterpenoids, betulinic acid derivatives definitely dominate (TPP⁺-conjugated with BA, about 30 compounds, Figure 3). Both BN and BA are common in the plant kingdom, especially in the outer layer of the birch bark (*Betulaceae*, *Betula*, *Betula pendula*). However, BN is considerably more available (BN content was up to 34%, and BA was only 0.3% of dry weight [6]), which may be an advantage in terms of the economic analysis of methods in obtaining potential therapeutic agents.

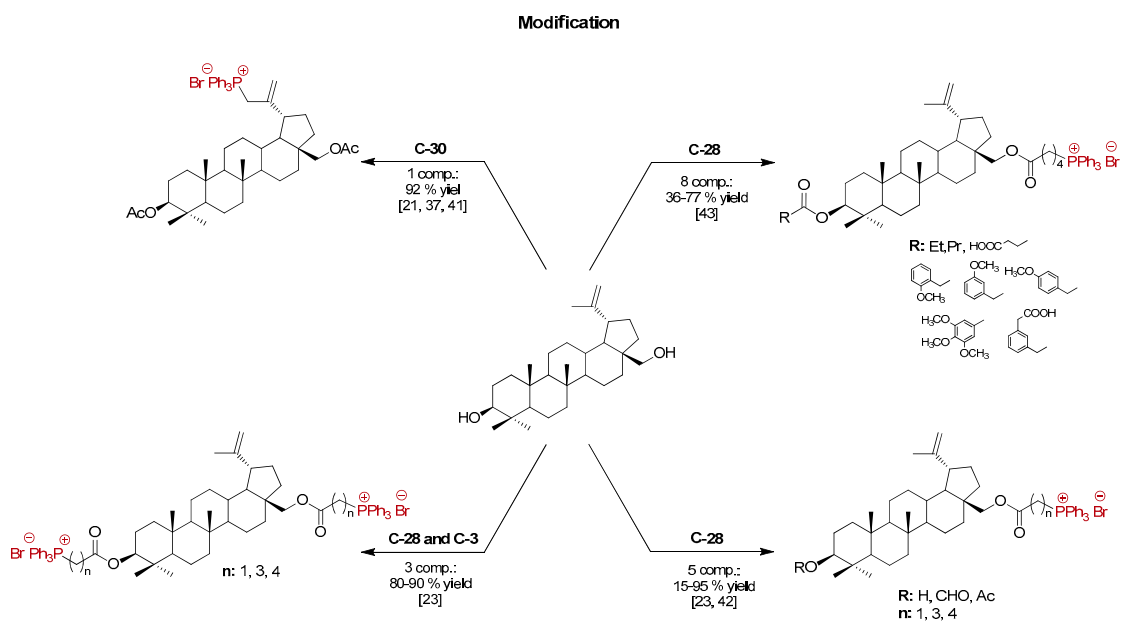
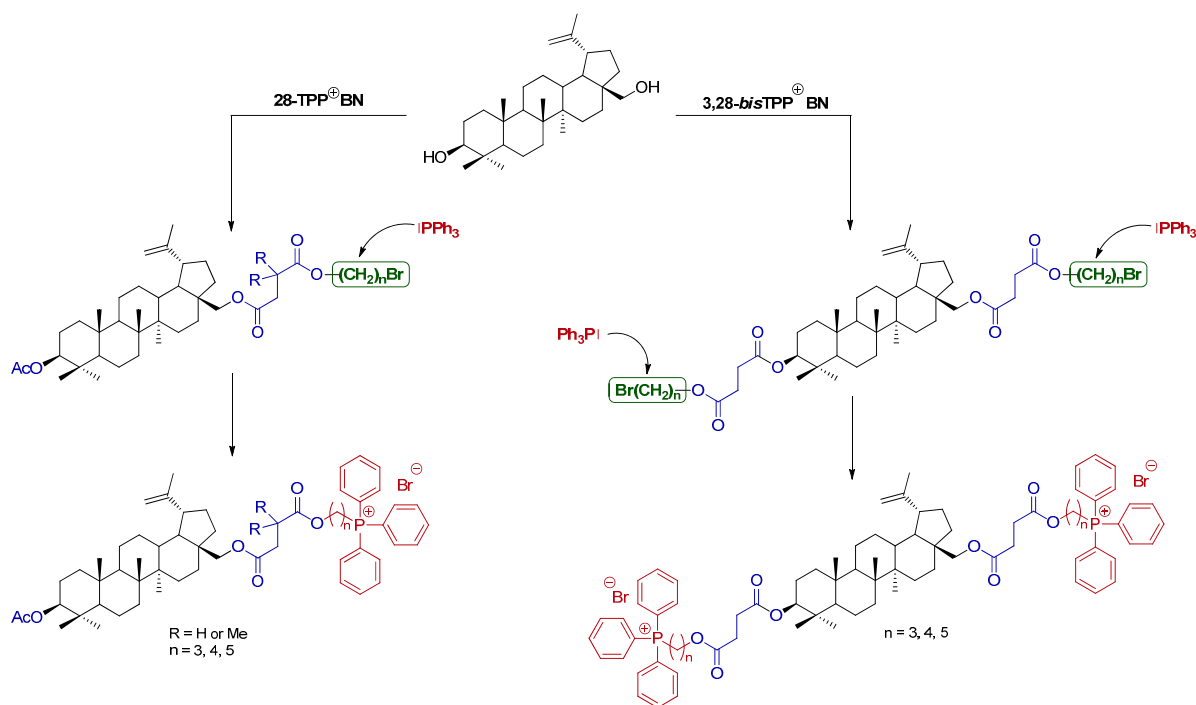


Figure 4. The chemical structures of the TPP⁺-conjugated with BN.

Although BN derivatives have been extensively explored, to date, no structures have demonstrated the desired biological properties at a satisfactory dosage that would allow them to be used as drugs. The aim of the presented study was to evaluate the relationships

between the biological effects and the structure of the new triphenylphosphonium derivatives of *BN*. Hence, we designed and synthesized molecular hybrids of *BN* by covalently linking a lipophilic alkyltriphenylphosphonium moiety (shown in dark red, Scheme 1) to the parent skeleton of *BN* through a linker (shown in blue, Scheme 1). In addition, in order to obtain a library of compounds intended for the initial assessment of biological activity (e.g., cytotoxicity, antibacterial activity), structural modifications of the *BN* skeleton were conducted via the introduction of one or two TPP[⊕] moieties at the C-28 or C-3 and C-28 positions. We prepared a series of the *mono*- and *bis*TPP[⊕] derivatives of *BN* through the multi-step synthesis (3 or 5 step) and their bio-activity was analyzed.



Scheme 1. The synthetic route for the preparation of 28-TPP[⊕] *BN* and 3,28-*bis*TPP[⊕] *BN*.

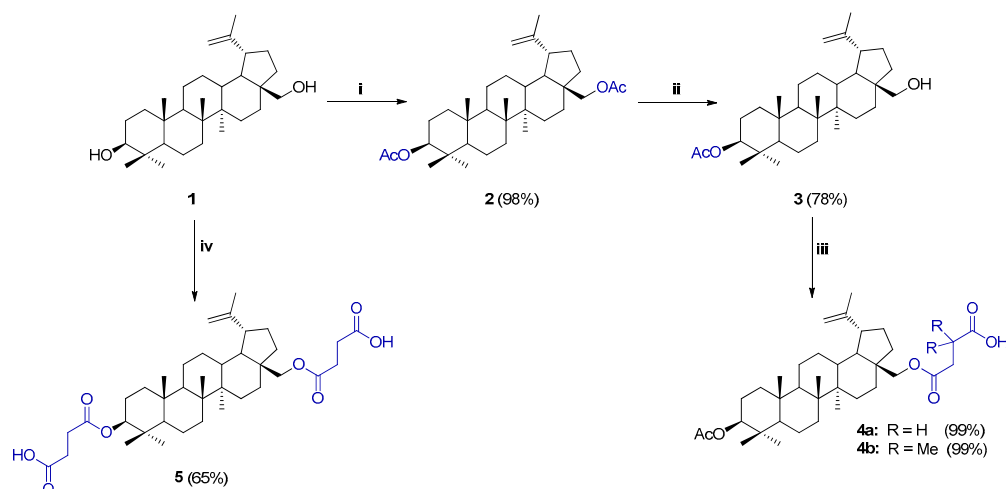
2. Results and Discussion

2.1. Synthesis of *BN* Analogs (2–5)

Starting materials 3,28-*O,O'*-diacetylbetulin **2** and 3-*O*-acetylbetulin **3** were synthesized according to the protocol described by Thibeault et al. (Scheme 2) [45]. In the first step, betulin was esterified with an excess of acetic anhydride in pyridine (Py) in the presence of 4-(dimethylamino)pyridine (DMAP) to give ester **2** in 98% yield. Then, the C-28 position of the *BN* backbone was selectively deprotected by treating crystalline ester **2** with aluminum isopropoxide (*i*-PrO)₃Al in *i*-PrOH. After 2 h at 80 °C, followed by column chromatography purification, analog **3** was obtained in 78% yield.

The next step involved the introduction of a linker terminated with a carboxyl group (O(CO)CH₂CR₂COOH, R = H or Me) at position C-28 (*mono*-substituted *BN* analog **4**) or C-3 and C-28 (*disubstituted BN* analog **5**) of *BN*. The carboxyacyl moiety seemed to be an ideal linker component as it allowed for further structural modifications. In addition, numerous literature reports have suggested that the combination of the triterpene skeleton with this type of moiety improved the biological properties including anti-HIV, antibacterial, or antifungal activity [46,47]. In accordance with the published procedures [48,49] with some modifications, analog **3** was reacted with succinic anhydride (SA) or 2,2-dimethylsuccinic anhydride (DMSA) in dry pyridine in the presence of DMAP at reflux for 18–20 h. The synthesis of 3,28-*O,O'*-*bis*(3-carboxypropanoyl)betulin **5** was performed in a similar manner, but the reagents were used in a molar ratio of *BN*:SA (1:10) at reflux for 9 h. The crude products were purified by chloroform extraction and washed with the water and HCl

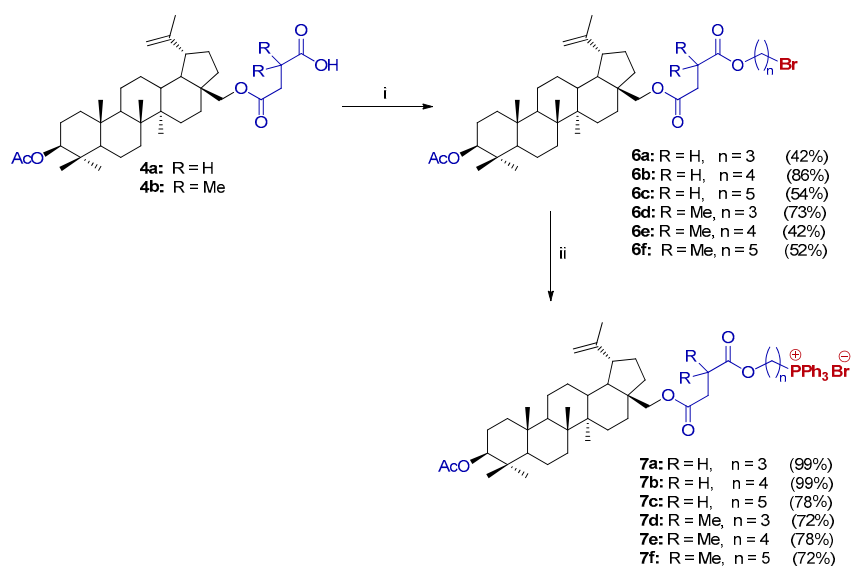
solution. The BN analogs were obtained in excellent yields (**4a**: 99%, **4b**: 99%, **5**: 65%, Scheme 2).



Scheme 2. The synthesis of the BN analogs (**2–5**). Reagents and conditions: (i) Ac_2O , DMAP, Py, r.t., 24 h; (ii) $(i\text{-PrO})_3\text{Al}$, $i\text{-PrOH}$, 80 °C, 2 h; (iii) SA or DMSA, DMAP, Py, reflux, 18–20 h; (iv) SA, Py, reflux, 9 h.

2.2. Synthesis of 28-TPP[⊕]-Conjugates Derivatives of BN

The synthesis method of new molecular BN hybrids (28-TPP[⊕] BN) with one TPP moiety attached via the linker $\text{C}^{28}\text{-O}(\text{CO})\text{CH}_2\text{CR}_2\text{COO}(\text{CH}_2)_n$ developed by our group consists of a few steps, as shown in Scheme 3. The desired analogs were synthesized via alkylation of the carboxyl group of (carboxyacyl)betulin **4** with dibromoalkanes in a molar ratio of **4**: $\text{Br}(\text{CH}_2)_n\text{Br}$ (1:3) in a DMF/MeCN system in the presence of K_2CO_3 at 50 °C for 18–20 h. 1,3-Dibromopropane, 1,4-dibromobutane, and 1,5-dibromopentane were employed to examine the influence of the chain length on bio-activity. 3-*O*-Acetyl-28-*O'*-(3',3'-dimethyl-3'-(bromoalkoxycarbonyl)propanoyl)betulin (**6a–6c**) and 3-*O*-acetyl-28-*O'*-(3',3'-dimethyl-3'-(bromoalkoxycarbonyl)propanoyl)betulin (**6d–6f**) were isolated by extraction with ethyl acetate and subsequent purification by column chromatography to produce the products in satisfactory yields (42–86%).

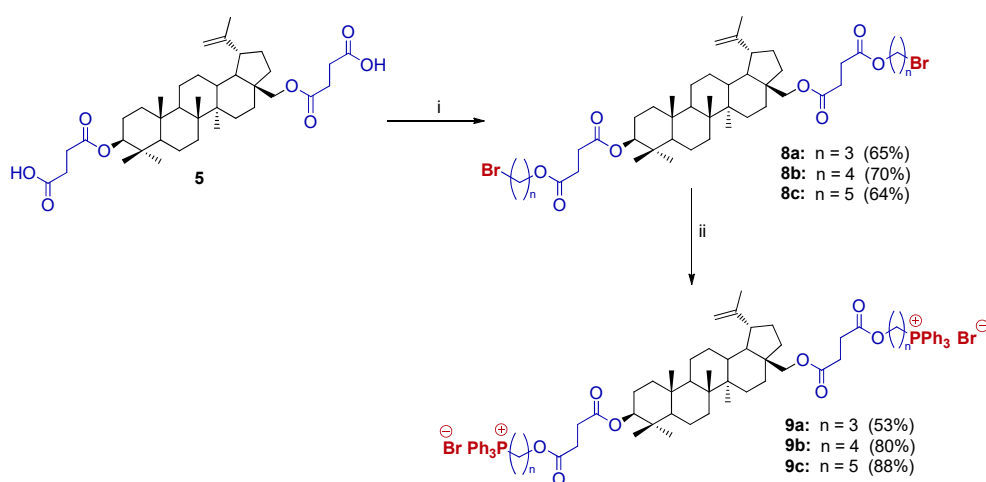


Scheme 3. The synthesis of the 28-TPP[⊕] BN derivative **7**. Reagents and conditions: (i) $\text{Br}(\text{CH}_2)_n\text{Br}$, DMF/MeCN (10/1, v/v), K_2CO_3 , 50 °C, 18–20 h; (ii) Ph_3P , argon, 120 °C, 6–12 h.

The final step of the 28-TPP[⊕] BN synthesis was the substitution of the bromide anion of analog **6** with the TPP group by heating a homogenous mixture of 28-(bromoalkoxycarbonyl)propanoyl)betulin **6** and triphenylphosphine without a solvent under an Ar atmosphere. Optimization of the procedure consisted of examining the proportions of reagents, the temperature and reaction time, where at a molar ratio of analog **6**/triphenylphosphine (1:2) at 120 °C for 6–12 h, the highest yields were obtained. Additionally, column chromatography was not necessary for all analogs, but all required extraction with diethyl ether and then crystallization from the diethyl ether/ethyl acetate (1:4, *v/v*), resulting in a high yield (72–99%, Scheme 3).

2.3. Synthesis of 3,28-bisTPP[⊕]-Conjugates Derivatives of BN

We also investigated the influence of two TPP[⊕] groups in the molecular hybrids of BN toward their pharmacokinetic properties. The synthetic route of 3,28-bisTPP[⊕] BN is depicted in Scheme 4.



Scheme 4. The synthesis of 3,28-bisTPP[⊕] BN **9**. Reagents and conditions: (i) Br(CH₂)_nBr, DMF/MeCN (10/1, *v/v*), K₂CO₃, 50 °C, 18–20 h; (ii) triphenylphosphine, Ar, 120 °C, 12–24 h.

In the first step, 3,28-*O,O'*-bis(3-carboxypropanoyl)betulin **5** was reacted with 1,3-dibromopropane, 1,4-dibromobutane or 1,5-dibromopentane at a molar ratio of **5**/Br(CH₂)_nBr (1:6) in a DMF/MeCN system with K₂CO₃ at 50 °C for 20 h. The analog **8** was obtained in satisfactory yields (64–70%) according to the procedure described above. Then, the homogeneous mixture (**8** and triphenylphosphine) was heated at 120 °C without solvent under an Ar atmosphere. The final product **9** was isolated by extraction (diethyl ether, and diethyl ether/ethyl acetate) at elevated temperature in good yields (80–88%, Scheme 4). Only analog **9a** required column chromatography (53% yield).

The structures of all of the synthesized compounds (**2–9**) were confirmed by spectroscopic methods (¹H, ¹³C, ³¹P NMR, FTIR, and HRMS, Supplementary Materials). The ³¹P NMR spectra of analogs **7** and **9** showed signals confirming the presence of TPP[⊕] in the range of 19.4–24.8 ppm. A characteristic feature in the ¹³C NMR spectra of the organophosphorus compounds was the splitting of specific signals into doublets caused by coupling the phosphorus atom with selected carbon atoms. Chemical shifts and J_{C-P} coupling constants of great diagnostic value observed for the TPP[⊕] group are summarized in Table 1.

Table 1. The chemical shifts and coupling constants characteristic of TPP[⊕] moiety in the synthesized triphenylphosphonium analogs of BN (7 and 9).

| | ¹³ C NMR (CDCl ₃ , TMS, δ (ppm)/J _{C-P} (Hz)) | | | | |
|-----------------------|--|--------------------------|--------------------------|---------------------------|--------------------------|
| | TPP [⊕] | | | | |
| | <u>CH</u> ₂ P [⊕] | <i>C</i> _{ipso} | <i>C</i> _{meta} | <i>C</i> _{ortho} | <i>C</i> _{para} |
| 7a | 19.8/52.3 | 118.1/85.7 | 130.5/12.1 | 133.8/9.8 | 135.0/3.0 |
| 7b | 22.2/50.6 | 118.3/84.9 | 130.4/12.1 | 133.8/9.9 | 134.9/3.0 |
| 7c | 22.7/49.4 | 118.4/85.0 | 130.5/12.1 | 133.7/9.8 | 134.9/3.0 |
| 7d | 19.4/51.8 | 118.3/86.3 | 130.4/12.6 | 133.8/10.4 | 134.9/0.5 |
| 7e | 22.1/49.3 | 118.3/88.1 | 130.4/12.6 | 133.7/10.4 | 134.9/0.5 |
| 7f | 22.7/50.1 | 118.4/85.8 | 130.4/12.4 | 133.7/9.9 | 134.9/3.0 |
| 9a | 19.7/51.8 | 118.1/86.3 | 130.5/12.8 | 133.8/9.2 | 135.1/0.5 |
| 9b | 22.2/50.0 | 118.2/88.8 | 130.4/12.9 | 133.7/9.9 | 135.0/3.0 |
| 9c | 22.8/49.3 | 118.4/85.0 | 130.5/12.2 | 133.8/9.8 | 135.0/3.0 |
| δ, ppm | 19.4–22.8 | 118.1–118.4 | 130.4–130.5 | 133.7–133.8 | 134.9–135.0 |
| J _{C-P} , Hz | 49.3–52.3 | 84.9–88.1 | 12.1–12.9 | 9.2–10.4 | 0.5–3.0 |

2.4. Cytotoxicity Studies

The obtained new molecular hybrids of BN were screened in order to initially investigate their cytotoxicity as well as examine the relationships between the structure and biological effect. The common element of all of the tested compounds was the presence of a lipophilic moiety (CH₂)_nTPP[⊕] (n = 3, 4, 5). The research was conducted on two groups of compounds: 28-TPP[⊕] BN and 3,28-*bis*TPP[⊕] BN. Their cytotoxicity was investigated on two cancer cell lines: HCT 116 (colorectal carcinoma cell line) and MCF-7 (human breast adenocarcinoma cell line). The proliferation of tumor cells treated with the tested compounds (7 and 9) at 12.5–3.125 μM concentrations were determined after 24 h of incubation. Additionally, all compounds were tested against the NHDF cell line (Normal Human Dermal Fibroblast cells) to assess their safety. The effect of these compounds was compared with that of BN doses, as shown in Figure 5. Half-maximal inhibitory concentrations (IC₅₀) of triphenylphosphonium analogs of BN were determined using a CCK-8 assay and are summarized in Table 2.

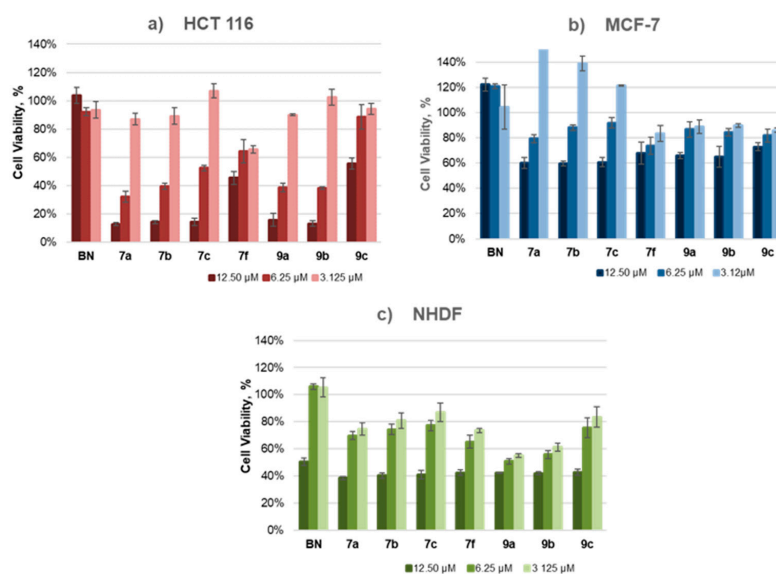
**Figure 5.** The dependence of cell viability on the concentration of BN and 28-TPP[⊕] BN (7) and the 3,28-*bis*TPP[⊕] BN analog (9) after 24 h of incubation.

Table 2. A summary of the cytotoxic effects of *BN*, 28-TPP[⊕] *BN* (**7**), and 3,28-*bis*TPP[⊕] *BN* (**9**) on the HCT 116 and MCF-7 cancer cell lines and NHDF.

| No. | R | n | Activity IC ₅₀ , μM ^{a,b} | | |
|-----------|----|---|---|--------------|--------------|
| | | | HCT 116 | MCF-7 | NHDF |
| <i>BN</i> | — | — | neg | neg | neg |
| 7a | H | 3 | 5.56 ± 0.28 | 13.71 ± 0.54 | 9.68 ± 0.27 |
| 7b | H | 4 | 5.77 ± 0.27 | 14.35 ± 0.38 | 10.71 ± 0.25 |
| 7c | H | 5 | 6.48 ± 0.04 | 15.52 ± 0.92 | 11.29 ± 0.53 |
| 7f | Me | 5 | 12.71 ± 0.89 | 50.47 ± 3.92 | 10.03 ± 0.48 |
| 9a | H | 3 | 6.32 ± 0.27 | 31.30 ± 3.02 | 5.91 ± 0.33 |
| 9b | H | 4 | 7.97 ± 0.51 | 23.60 ± 0.33 | 8.02 ± 0.35 |
| 9c | H | 5 | 18.99 ± 0.51 | 53.30 ± 5.41 | 10.60 ± 0.34 |

^a Cytotoxicity was evaluated using the CCK-8 assay; ^b Incubation time 24 h; Data are presented as the mean ± standard deviation (n = 3); neg: no activity in the concentration range used.

As expected, triphenylphosphonium derivatives of *BN* showed greater cytotoxicity than the parent *BN* toward all of the cell lines tested. The level of inhibition of cell viability depended on the concentration of the tested substances and cell type. The tested analogs of *BN* had the greatest effect on the viability of the HCT 116 cells (Figure 5a) and the lowest on the viability of the MCF-7 cells (Figure 5b).

When comparing the biological effect of the *mono*-TPP[⊕] *BN* derivatives (**7a–7c**, linker without an additional Me group), it seemed that the length of the linker did not influence their activity in the in vitro tests. The 28-TPP[⊕] *BN* conjugates (**7a–7c**) with a variable length, and an alkyl linker (n = 3, 4, 5) similarly inhibited the viability in both tumor cells (HCT 116: IC₅₀ = 5.56–6.48, MCF-7: IC₅₀ = 13.71–15.52). The exception was analog **9c**, with two TPP[⊕] cations and a pentyl chain, which, compared to compounds with a shorter linker (propyl or butyl chain), showed lower cytotoxicity against the HCT 116 cells (IC₅₀: **9a** < **9b** < **9c**; Table 2). Importantly, compounds **7a–7c** were almost twice less toxic toward the healthy cells (NHDF), with IC₅₀ values ranging from 9.68 to 11.29 μM, which demonstrated their selectivity.

Unfortunately, in the course of further studies, it was revealed that the introduction of an additional Me group into the linker **7f** reduced this bio-activity compared to compound **7c** against the HCT 116 and MCF-7 tumor cells whereas no significant effect of the Me groups attached to the linker was observed on the bio-activity of compound **7f** in normal NHDF cells.

We observed that the presence of both one and two lipophilic cations improved the solubility of the tested analogs compared to *BN*, which slightly increased their cytotoxicity, especially against the colorectal carcinoma cell line (HCT 116). Among the triphenylphosphonium derivatives of *BN* tested, analogs **7a** (IC₅₀ of 5.56 μM) and **7b** (IC₅₀ of 5.77 μM) demonstrated the highest cytotoxicity against this cell line at low micromolar concentrations. This supported the hypothesis that the conjugation of the *BN* native backbone with the TPP[⊕] moiety allowed for its transport through the hydrophobic barriers of the mitochondrial membrane, making it a promising strategy to improve the bioavailability of natural substances.

2.5. Antibacterial Studies

Investigations were carried out using different concentrations of solutions from 25 to 250 μM. A 25 μM concentration of the tested derivatives was not enough to inhibit the growth of both Gram-positive *S. aureus* ATCC 25923 bacteria. When the concentration of analogs **7d–7f** and **9a–9c** increased to 200 μM, the growth of *S. aureus* ATCC 25923 and *S. epidermidis* ATCC 12228 was inhibited. Furthermore, the optical density of all compounds remained unchanged after 18 h of bacteria culture. In the case of analogs **7a–7c**, the optical density values were between 0.9 and 2.2 when they were cultured with *S. aureus* ATCC 25923. The bacterial growth was slower compared to the control sample (TSB-

culture medium). However, the studied TPP[⊕]-BN derivatives did not inhibit the growth of *S. epidermidis* ATCC 12228 bacteria. However, at a 250 μM concentration, analogs **7a** and **7b** greatly inhibited the growth of *S. aureus* ATCC 25923 and *S. epidermidis* ATCC 12228. In the case of analog **7c**, the optical density increased up to 0.7 after 18 h of the sample culture with both kinds of Gram-positive bacteria. In contrast, the reference sample's (TSB) optical density increased to 7.5 for *S. aureus* ATCC 25923, and 4.9 for *S. epidermidis* ATCC 12228 after 18 h of bacteria culture. All of the investigated compounds did not inhibit the growth of Gram-negative *Escherichia coli* ATCC 25922 bacteria. All of the analog values of the measured optical density were similar to that of the reference sample (5.0–5.1, Table 3).

Table 3. The results of the antimicrobial analysis using Gram-positive and Gram-negative bacteria cultured with the investigated compounds at 37 °C for 18 h. The results are presented as the differences between the optical density measurements of the samples before and after culture (McFarland's scale (CFU/mL)).

| No. | <i>S. aureus</i> ATCC 25923 | | <i>S. epidermidis</i> ATCC 12228 | | <i>Escherichia coli</i> ATCC 25922 | |
|---------|--------------------------------|--------|-------------------------------------|--------|---------------------------------------|--------|
| | 200 μM | 250 μM | 200 μM | 250 μM | 200 μM | 250 μM |
| BN | 5.1 | 5.6 | neg | 4.7 | neg | neg |
| 7a | 0.9 | 0 | neg | 0 | neg | neg |
| 7b | 2.2 | 0 | neg | 0 | neg | neg |
| 7c | 1.0 | 0.1 | neg | 0.7 | neg | neg |
| 7d | 0 | 0 | 0 | 0 | neg | neg |
| 7e | 0 | 0 | 0 | 0 | neg | neg |
| 7f | 0 | 0 | 0 | 0 | neg | neg |
| 9a | 0 | 0 | 0 | 0 | neg | neg |
| 9b | 0 | 0 | 0 | 0 | neg | neg |
| 9c | 0 | 0 | 0 | 0 | neg | neg |
| Control | 7.5 | 7.5 | 4.1 | 4.9 | 5.1 | 5.0 |

0: no difference between samples after 18 h of bacteria culture (bacteria grow was inhibited); neg: negative results (analog BN did not inhibit bacteria growing).

The obtained results showed that 28-TPP[⊕] BN (**7d–7f**) and 3,28-*bis*TPP[⊕] BN (**9a–9c**) could be employed as agents for the inhibition of Gram-positive bacteria (*S. aureus* ATCC 25923 and *S. epidermidis* ATCC 12228) growth at a concentration of 200 μM in an aqueous solution.

3. Materials and Methods

3.1. General Information

NMR spectra (¹H and ¹³C) were recorded on a Varian spectrometer at operating frequencies of 600 or 400 MHz and 150 or 100 MHz, respectively, using TMS as the resonance shift standard. CDCl₃ was used as the solvent, which was purchased from ACROS Organics (Geel, Belgium). The ³¹P NMR spectra were acquired using a Varian 400 spectrometer at 161.9 MHz, where the resonance shift of H₃PO₄ was determined as 0 ppm. All chemical shifts (δ) were reported in ppm and coupling constants (*J*) in Hz. The following abbreviations were used to explain the observed multiplicities: s—singlet; d—doublet; dd—double doublet; ddd—doublet of double doublet; t—triplet, dd~t—overlapping double doublet that resembles a triplet (with similar values of coupling constants); m—multiplet; br—broad. IR-spectra were measured on a Nicolet 6700 FT-IR spectrophotometer, Thermo Scientific (Waltham, MA, USA) (attenuated total reflectance method; ATR). High resolution mass spectrometry analyses were performed using a Waters Xevo G2 Q-TOF mass spectrometer (Waters Corporation, Milford, MA, USA) equipped with an ESI source operating in positive-ion mode. The accurate mass and composition for the molecular ion adducts were calculated using MassLynx software (Waters) incorporated in the instrument.

Reactions were monitored by TLC analysis on precoated plates of silica gel 60 F₂₅₄ (Merck Millipore, Burlington, MA, USA). The TLC plates were inspected under UV light (λ = 254 nm) or charring after spraying with 10% solution of sulfuric acid in ethanol.

Crude products were purified using column chromatography performed on silica gel 60 (70–230 mesh, Fluka).

3,28-*O,O'*-Diacylbetulin **2**; 3-*O*-acetylbetulin **3** [45], 3-*O*-acetyl-28-*O'*-(3'-carboxypropanoyl)betulin **4a**; 3-*O*-acetyl-28-*O'*-(3',3'-dimethyl-3'-carboxypropanoyl)betulin **4b** [48], and 3,28-*O,O'*-bis(3'-carboxypropanoyl)betulin **5** [49] were prepared according to the respective published procedures.

All chemicals used in the study were purchased from Sigma-Aldrich (St. Louis, MO, USA), Fluka, Avantor (Radnor Township, PA, USA) and ACROS Organics, and used without further purification.

3.2. Chemistry

3.2.1. General Procedure for the Synthesis of 3-*O*-Acetyl-28-*O'*-(carboxyacyl)betulin (**4**)

3-*O*-Acetylbetulin (**3**, 2.50 mmol, 1.21 g, 1 eq.), SA (7.50 mmol, 0.75 g, 3 eq.) or DMSA (7.50 mmol, 0.96 g, 3 eq.) and DMAP (7.50 mmol, 0.92 g, 3 eq.) were dissolved in dry pyridine (19 mL). The reaction mixture was stirred under reflux for 18–20 h. After cooling to rt, 10% hydrochloric acid solution (20 mL) and water (35 mL) were added. The product was extracted with CHCl₃ (4 × 70 mL). The combined organic extracts were washed with water (70 mL), 5% hydrochloric acid solution (140 mL), brine (70 mL), water (70 mL), dried over MgSO₄, and filtered. The solvent was evaporated under reduced pressure producing analog **4a**, which was used in the next step without further purification. Analog **4b** was purified using column chromatography (DCM/MeOH, gradient: 100:1 to 50:1).

3-*O*-Acetyl-28-*O'*-(3'-carboxypropanoyl)betulin (**4a**) was obtained as a resin (1.45 g, 99% yield); $R_f = 0.78$ (DCM/MeOH, 10:1, *v/v*). ¹H NMR (600 MHz, CDCl₃): δ_H 0.75, 0.76, 0.88, 0.94, 1.31 (all s, 3H each, H-23–H-27), 1.60 (s, 3H $J_1 = 5.9$ Hz, H-30), 0.62–2.06 (m, 24H, CH, CH₂ BN scaffold), 1.96 (s, 3H, CH₃CO), 2.34 (td, 1H, $J_2 = 11.0$ Hz, H-19), 2.54–2.63 (m, 4H, O(CO)CH₂CH₂), 3.80 (d, 1H, $J = 10.8$ Hz, H-28b), 4.22 (d, 1H, $J = 13.2$ Hz, H-28a), 4.38 (dd, 1H, $J_1 = 5.4$ Hz, $J_2 = 10.8$ Hz, H-3), 4.50 (s, 1H, H-29b), 4.60 (s, 1H, H-29a) ppm; ¹³C NMR (150 MHz, CDCl₃): δ_C 14.7, 16.0, 16.2, 16.5, 18.2, 19.1, 20.8, 21.3, 23.7, 25.1, 27.0, 27.9, 28.8, 29.1, 29.5, 29.7, 34.1, 34.5, 37.1, 37.6, 37.8, 38.4, 40.9, 42.7, 46.4, 47.7, 48.8, 50.3, 55.4, 63.2, 80.9, 109.9, 150.1, 171.1, 172.4, 176.9 ppm; IR (ATR) ν: 2938, 1729, 1714, 1244, 1158 cm⁻¹.

3-*O*-Acetyl-28-*O'*-(3',3'-dimethyl-3'-carboxypropanoyl)betulin (**4b**) was obtained as a resin (1.52 g, 99% yield); $R_f = 0.64$ (DCM/MeOH, 10:1, *v/v*). ¹H NMR (600 MHz, CDCl₃): δ_H 0.83, 0.84, 0.96, 1.02, 1.31 (all s, 3H each, H-23–H-27), 1.39 (s, 6H, CMe₂), 1.68 (s, 3H, H-30), 0.70–2.00 (m, 24H, CH, CH₂ BN scaffold), 2.04 (s, 3H, CH₃CO), 2.41 (td, 1H, $J_1 = 5.8$ Hz, $J_2 = 11.1$ Hz, H-19), 2.64 (s, 2H, O(CO)CH₂), 3.87 (d, 1H, $J = 10.9$ Hz, H-28b), 4.26 (d, 1H, $J = 9.2$ Hz, H-28a), 4.47 (dd, 1H, $J_1 = 5.6$ Hz, $J_2 = 10.7$ Hz, H-3), 4.58 (s, 1H, H-29b), 4.68 (s, 1H, H-29a) ppm; ¹³C NMR (150 MHz, CDCl₃): δ_C 14.7, 16.0, 16.1, 16.4, 18.1, 19.1, 20.7, 21.2, 23.6, 25.1, 25.2, 25.3, 26.9, 27.9, 29.5, 29.7, 34.0, 34.5, 37.0, 37.5, 37.7, 38.3, 40.4, 40.8, 42.6, 44.3, 46.2, 47.6, 48.7, 50.2, 55.3, 63.0, 81.9, 109.8, 150.0, 171.06, 171.4, 183.0 ppm; IR (ATR) ν: 2940, 1728, 1703, 1242, 1193 cm⁻¹.

3.2.2. Synthesis of 3,28-*O,O'*-Bis(3'-carboxypropanoyl)betulin (**5**)

BN (2.50 mmol, 1.11 g, 1 eq.) and SA (25.00 mmol, 2.50 g, 10 eq.) were dissolved in dry pyridine (26 mL) and stirred under reflux for 9 h. After cooling to r.t., 10% hydrochloric acid solution (26 mL) and water (48 mL) were added. The product was extracted with CHCl₃ (6 × 120 mL). The combined organic layers were concentrated to a 200 mL volume, washed with water (200 mL), 5% hydrochloric acid solution (2 × 90 mL), brine (200 mL), H₂O (200 mL), dried over MgSO₄, and filtered. Then, the solvent was evaporated under reduced pressure.

3,28-*O,O'*-Bis(3'-carboxypropanoyl)betulin (**5**) was obtained as a resin (1.04 g, 65% yield); $R_f = 0.23$ (DCM:MeOH, 100:1). ¹H NMR (600 MHz, CDCl₃): δ_H 0.83, 0.84, 0.85, 0.98, 1.03 (all s, 3H each, H-23–H-27), 1.69 (s, 3H, H-30), 0.70–2.00 (m, 24H, CH, CH₂ BN scaffold), 2.43 (td, 1H, $J_1 = 5.8$ Hz, $J_2 = 11.1$ Hz, H-19), 2.60–2.70 (m, 8H, 2 × O(CO)CH₂CH₂), 3.88 (d, 1H, $J = 10.9$ Hz, H-28b), 4.31 (d, 1H, $J = 11.0$ Hz, H-28a), 4.50 (dd, 1H, $J_1 = 5.6$ Hz, $J_2 = 10.8$

Hz, H-3), 4.59 (dd, 1H, $J_1 = 1.4$ Hz, $J_2 = 2.3$ Hz, H-29b), 4.68 (d, 1H, $J = 2.0$ Hz, H-29a) ppm; ^{13}C NMR (150 MHz, CDCl_3): δ_{C} 14.8, 16.0, 16.1, 16.5, 18.2, 19.1, 20.8, 23.6, 25.2, 27.0, 27.9, 29.0, 29.1, 29.3, 29.6, 29.7, 34.1, 34.4, 37.1, 37.6, 37.8, 38.3, 40.9, 42.7, 46.5, 47.7, 48.8, 50.3, 55.4, 63.2, 81.6, 109.9, 150.1, 171.7, 172.3, 177.9, 178.0 ppm; IR (ATR) ν : 2944, 1709, 1160, cm^{-1} .

3.2.3. General Procedure for the Synthesis of Bromides of BN (6)

To a solution of BN derivative (**4**, 0.25 mmol, 1 eq.) and K_2CO_3 (0.25 mmol, 34.6 mg, 1 eq.) in DMF (1 mL/100 mg **4**) and MeCN (0.1 mL/100 mg **4**), the appropriate dibromoalkane ($\text{Br}(\text{CH}_2)_n\text{Br}$, $n = 3, 4, 5$; 0.75 mmol, 3 eq.) was added. The reaction was carried out at 50 °C for 18–21 h. After the reaction was completed, the obtained mixture was diluted with cold water and extracted with ethyl acetate (5×19 mL). The combined organic layers were washed with brine (2×65 mL), dried over MgSO_4 , and the solvent was evaporated under reduced pressure. Then, crude product **6** was washed with methanol (2×0.5 mL) and purified using column chromatography (DCM/MeOH, gradient: 100:1 to 50:1).

3-*O*-Acetyl-28-*O'*-(3'-(3''-bromopropoxyoxycarbonyl)propanoyl)betulin (**6a**) was obtained as a resin (74.1 mg, 42% yield); $R_f = 0.18$ (DCM:MeOH, 100:1). HRMS (ESI^+) m/z : calcd for $\text{C}_{39}\text{H}_{61}\text{BrO}_6\text{Na}$ ($[\text{M}+\text{Na}]^+$) 727.3549; found 727.3546; ^1H NMR (600 MHz, CDCl_3): δ_{H} 0.83, 0.84, 0.85, 0.97, 1.03 (all s, 3H each, H-23–H-27), 1.68 (s, 3H, H-30), 0.70–2.00 (m, 24H, CH, CH_2 BN scaffold), 2.04 (s, 3H, CH_3CO), 2.16–2.20 (m, 2H, CH_2 fragment of linker), 2.43 (td, 1H, $J_1 = 5.8$ Hz, $J_2 = 11.1$ Hz, H-19), 2.64–2.66 (m, 4H, $\text{O}(\text{CO})\text{CH}_2\text{CH}_2$), 3.46 (t, 2H, $J = 6.5$ Hz, CH_2Br), 3.87 (d, 1H, $J = 11.1$ Hz, H-28b), 4.24 (t, 2H, $J = 6.1$ Hz, $(\text{CO})\text{OCH}_2$), 4.29 (dd, 1H, $J_1 = 1.9$ Hz, $J_2 = 11.1$ Hz, H-28a), 4.46 (dd, 1H, $J_1 = 5.9$ Hz, $J_2 = 10.5$ Hz, H-3), 4.59 (s, br, 1H, H-29b), 4.68 (s, br, 1H, H-29a) ppm; ^{13}C NMR (150 MHz, CDCl_3): δ_{C} 14.7, 16.0, 16.1, 16.4, 18.1, 19.1, 21.3, 20.7, 23.6, 25.1, 27.0, 27.9, 29.1, 29.2, 29.3, 29.5, 29.7, 31.6, 34.1, 34.5, 37.0, 37.5, 37.7, 38.3, 40.8, 42.6, 46.4, 47.7, 48.7, 50.2, 55.3, 62.4, 63.1, 80.8, 109.9, 150.0, 170.9, 172.1, 172.5 ppm; IR (ATR) ν : 2943, 1731, 1244, 1155, 732 cm^{-1} .

3-*O*-Acetyl-28-*O'*-(3'-(4''-bromobutyloxyoxycarbonyl)propanoyl)betulin (**6b**) was obtained as a resin (154.8 mg, 86% yield); $R_f = 0.28$ (DCM:MeOH, 100:1). HRMS (ESI^+) m/z : calcd for $\text{C}_{40}\text{H}_{64}\text{BrO}_6$ ($[\text{M}+\text{H}]^+$) 719.3886, found 719.3885; ^1H NMR (400 MHz, CDCl_3): δ_{H} 0.83, 0.84, 0.85, 0.97, 1.03 (all s, 3H each, H-23–H-27), 1.68 (s, 3H, H-30), 0.75–2.00 (m, 28H, CH, CH_2 BN scaffold and $(\text{CH}_2)_2$ fragment of linker), 2.04 (s, 3H, CH_3CO), 2.43 (td, 1H, $J_1 = 5.8$ Hz, $J_2 = 11.1$ Hz, H-19), 2.61–2.68 (m, 4H, $\text{O}(\text{CO})\text{CH}_2\text{CH}_2$), 3.44 (t, 2H, $J = 6.0$ Hz, CH_2Br), 3.88 (d, 1H, $J = 11.1$ Hz, H-28b), 4.13 (t, 2H, $J = 6.0$ Hz, $(\text{CO})\text{OCH}_2$), 4.29 (d, 1H, $J = 11.1$ Hz, H-28a), 4.45–4.49 (m, 1H, H-3), 4.59 (s, br, 1H, H-29b), 4.68 (s, br, H-29a) ppm; ^{13}C NMR (100 MHz, CDCl_3): δ_{C} 14.7, 16.0, 16.1, 16.4, 18.1, 19.1, 20.7, 21.3, 23.6, 25.1, 27.0, 27.2, 27.9, 29.1, 29.2, 29.3, 29.5, 29.7, 33.0, 34.1, 34.5, 37.0, 37.5, 37.7, 38.3, 40.8, 42.6, 46.4, 47.7, 48.7, 50.2, 55.3, 63.0, 63.7, 80.9, 109.8, 150.0, 170.9, 172.2, 172.5 ppm; IR (ATR) ν : 2946, 1732, 1246, 1156, 734 cm^{-1} .

3-*O*-Acetyl-28-*O'*-(3'-(5''-bromopentyloxyoxycarbonyl)propanoyl)betulin (**6c**) was obtained as a resin (99.1 mg, 54% yield); $R_f = 0.31$ (DCM:MeOH, 100:1). HRMS (ESI^+) m/z : calcd for $\text{C}_{41}\text{H}_{65}\text{BrO}_6\text{Na}$ ($[\text{M}+\text{Na}]^+$) 755.3862, found 755.3870; ^1H NMR (600 MHz, CDCl_3): δ_{H} 0.83, 0.84, 0.85, 0.97, 1.03 (all s, 3H each, H-23–H-27), 1.68 (s, 3H, H-30), 0.70–2.00 (m, 30H, CH, CH_2 BN scaffold and $(\text{CH}_2)_3$ fragment of linker), 2.04 (s, 3H, CH_3CO), 2.43 (td, 1H, $J_1 = 5.8$ Hz, $J_2 = 11.1$ Hz, H-19), 2.62–2.66 (m, 4H, $\text{O}(\text{CO})\text{CH}_2\text{CH}_2$), 3.42 (t, 2H, $J = 6.1$ Hz, CH_2Br), 3.87 (d, 1H, $J = 10.8$ Hz, H-28b), 4.10 (t, 2H, $J = 6.6$ Hz, $(\text{CO})\text{OCH}_2$), 4.29 (d, 1H, 11.1 Hz, H-28a), 4.46 (dd, 1H, $J_1 = 5.6$ Hz, $J_2 = 10.8$ Hz, H-3), 4.59 (s, br, 1H, H-29b), 4.68 (d, 1H, $J = 2.3$ Hz, H-29a) ppm; ^{13}C NMR (150 MHz, CDCl_3): δ_{C} 14.7, 16.0, 16.1, 16.4, 18.1, 19.1, 20.7, 21.2, 23.6, 24.5, 25.1, 27.0, 27.7, 27.9, 29.1, 29.2, 29.5, 29.7, 32.2, 33.3, 34.1, 34.5, 37.0, 37.5, 37.7, 38.3, 40.8, 42.6, 46.4, 47.7, 48.7, 50.2, 55.3, 63.0, 64.3, 80.8, 109.8, 150.0, 170.9, 172.2, 172.5 ppm; IR (ATR) ν : 2942, 1730, 1244, 1155, 731 cm^{-1} .

3-*O*-Acetyl-28-*O'*-(3',3'-dimethyl-3'-(3''-bromopropoxyoxycarbonyl)propanoyl)betulin (**6d**) was obtained as a resin (133.9 mg, 73% yield); $R_f = 0.28$ (DCM:MeOH, 100:1); HRMS (ESI^+) m/z : calcd for $\text{C}_{41}\text{H}_{66}\text{BrO}_6$ ($[\text{M}+\text{H}]^+$) 733.4043, found 733.4045; ^1H NMR (400 MHz, CDCl_3): δ_{H} 0.76, 0.77, 0.89, 0.95, 1.32 (all s, 3H each, H-23–H-27), 1.21 (s, 6H, CMe_2), 1.61 (s, 3H, H-30), 0.65–1.93 (m, 24H, CH, CH_2 BN scaffold), 1.97 (s, 3H, CH_3CO), 2.12 (d, 2H, $J = 6.3$ Hz, CH_2

fragment of linker), 2.35 (td, 1H, $J_1 = 5.7$ Hz, $J_2 = 11.1$ Hz, H-19), 2.56 (s, 2H, O(CO)CH₂), 3.39 (t, 2H, $J = 6.6$ Hz, CH₂Br), 3.78 (d, 1H, $J = 11.0$ Hz, H-28b), 4.14–4.21 (m, 3H, H-28a and (CO)OCH₂), 4.40 (dd, 1H, $J_1 = 5.6$ Hz, $J_2 = 10.8$ Hz, H-3), 4.52 (s, br, 1H, H-29b), 4.61 (s, br, 1H, H-29a) ppm; ¹³C NMR (100 MHz, CDCl₃): δ_C 14.7, 16.0, 16.1, 16.5, 18.1, 19.1, 20.8, 21.3, 23.7, 25.1, 25.5, 25.6, 27.0, 27.9, 29.5, 29.7, 31.7, 34.1, 34.5, 37.0, 37.6, 37.8, 38.4, 40.6, 40.9, 42.7, 44.5, 46.3, 47.7, 48.8, 50.3, 55.4, 62.5, 62.9, 80.9, 109.9, 150.0, 171.0, 172.0, 176.4 ppm; IR (ATR) ν : 2931, 1732, 1245, 1177 cm⁻¹.

3-*O*-Acetyl-28-*O'*-(3',3'-dimethyl-3'-(4''-bromobutyloxycarbonyl)propanoyl)betulin (**6e**) was obtained as a resin (78.5 mg, 42% yield); $R_f = 0.29$ (DCM:MeOH, 100:1); HRMS (ESI⁺) m/z : calcd for C₄₂H₆₈BrO₆ ([M+H]⁺) 747.4199, found 747.4194; ¹H NMR (400 MHz, CDCl₃): δ_H 0.77, 0.78, 0.89, 0.95, 1.32 (all s, 3H each, H-23–H-27), 1.20 (s, 6H, CMe₂), 1.61 (s, 3H, H-30), 0.70–1.93 (m, 28H, CH, CH₂ BN scaffold and (CH₂)₂ fragment of linker), 1.97 (s, 3H, CH₃CO), 2.35 (td, 1H, $J_1 = 5.7$ Hz, $J_2 = 10.9$ Hz, H-19), 2.56 (s, 2H, O(CO)CH₂), 3.37 (t, 2H, $J = 6.6$ Hz, CH₂Br), 3.78 (d, 1H, $J = 11.0$ Hz, H-28b), 4.05 (t, 2H, $J = 6.3$ Hz, (CO)OCH₂), 4.17 (d, 1H, $J = 11.1$ Hz H-28a), 4.39–4.42 (m, 1H, H-3), 4.52 (s, br, 1H, H-29b), 4.61 (s, br, H-29a) ppm; ¹³C NMR (100 MHz, CDCl₃): δ_C 14.7, 16.0, 16.1, 16.5, 18.1, 19.1, 20.8, 21.3, 23.7, 25.1, 25.46, 25.48, 27.0, 27.2, 27.9, 29.3, 29.5, 29.7, 33.1, 34.1, 34.5, 37.0, 37.6, 37.8, 38.4, 40.9, 40.6, 42.7, 44.5, 46.3, 47.7, 48.8, 50.3, 55.4, 62.8, 63.7, 80.9, 109.9, 150.0, 171.0, 172.0, 176.6 ppm; IR (ATR) ν : 2942, 1731, 1246, 1178 cm⁻¹.

3-*O*-Acetyl-28-*O'*-(3',3'-dimethyl-3'-(5''-bromopentyloxycarbonyl)propanoyl)betulin (**6f**) was obtained as a resin (99.0 mg, 52% yield); $R_f = 0.23$ (DCM:MeOH, 100:1); HRMS (ESI⁺) m/z : calcd for C₄₃H₇₀BrO₆ ([M+H]⁺) 761.4356, found 761.4353; ¹H NMR (600 MHz, CDCl₃): δ_H 0.76, 0.77, 0.89, 0.95, 1.32 (all s, 3H each, H-23–H-27), 1.20 (s, 6H, CMe₂), 1.61 (s, 3H, H-30), 0.65–1.92 (m, 30H, CH, CH₂ BN scaffold and (CH₂)₃ fragment of linker), 1.97 (s, 3H, CH₃CO), 2.35 (td, 1H, $J_1 = 5.8$ Hz, $J_2 = 11.1$ Hz, H-19), 2.56 (s, 2H, O(CO)CH₂), 3.35 (t, 2H, $J = 6.7$ Hz, CH₂Br), 3.78 (dd, 1H, $J_1 = 1.3$ Hz, $J_2 = 11.1$ Hz, H-28b), 4.02 (t, 2H, $J = 6.5$ Hz, (CO)OCH₂), 4.17 (dd, 1H, $J_1 = 2.2$ Hz, $J_2 = 11.0$ Hz, H-28a), 4.39 (dd, 1H, $J_1 = 5.6$ Hz, $J_2 = 10.8$ Hz, H-3), 4.51 (s, br, 1H, H-29b), 4.61 (d, 1H, $J = 2.3$ Hz, H-29a) ppm; ¹³C NMR (150 MHz, CDCl₃): δ_C 14.7, 16.0, 16.1, 16.5, 18.1, 19.1, 20.8, 21.3, 23.7, 24.6, 25.1, 25.5, 27.0, 27.7, 27.9, 29.5, 29.7, 32.2, 33.4, 34.1, 34.5, 37.0, 37.6, 37.8, 38.4, 40.6, 40.9, 42.7, 44.5, 46.3, 47.7, 48.8, 50.3, 55.4, 62.8, 64.3, 80.8, 109.9, 150.1, 171.0, 171.6, 176.6 ppm; IR (ATR) ν : 2941, 1730, 1245, 1105 cm⁻¹.

3.2.4. General Procedure for the Synthesis of Triphenylphosphonium Derivatives of BN (7, 28-TPP[⊕] BN)

The bromide derivative of BN (**6**, 0.1 mmol, 1 eq.) and triphenylphosphine (0.2 mmol, 52.5 mg, 2 eq.) were dissolved in dry DCM (1.0–1.5 mL) and stirred at room temperature for 10–15 min until homogenization was reached. The solvent was evaporated under reduced pressure and the residue was heated in an oil bath at 120 °C under an Ar atmosphere for 6–12 h. The obtained mixture was washed with diethyl ether (**7a–7c**: 3 × 4 mL; **7d–7f**: 5 × 3 mL) at 50 °C. Then, the crude product was crystallized from ethyl acetate/diethyl ether (1:4, *v/v*) and dried under reduced pressure at 50 °C for 4 h.

3-*O*-Acetyl-28-*O'*-(3'-(3''-triphenylphosphoniopropoxy)carbonyl)propanoyl)betulin bromide (**7a**) was obtained as a resin (95.8 mg, 99% yield); HRMS (ESI⁺) m/z : calcd for C₅₇H₇₆O₆P⁺ ([M]⁺) 887.5380, found 887.5383; ¹H NMR (600 MHz, CDCl₃): δ_H 0.83, 0.84, 0.85, 0.95, 0.96 (all s, 3H each, H-23–H-27), 1.67 (s, 3H, H-30), 0.70–1.95 (m, 26H, CH, CH₂ BN scaffold and CH₂ fragment of linker), 2.04 (s, 3H, CH₃CO), 2.38 (td, 1H, $J_1 = 5.7$ Hz, $J_2 = 0.8$ Hz, H-19), 2.60–2.66 (m, 4H, O(CO)CH₂CH₂), 3.84 (d, 1H, $J = 11.0$ Hz, H-28b), 4.09–3.99 (m, 2H, CH₂P), 4.22 (d, 1H, $J = 11.0$ Hz, H-28a), 4.39–4.45 (m, 2H, (CO)OCH₂), 4.46 (dd, 1H, $J_1 = 5.1$ Hz, $J_2 = 11.1$ Hz, H-3), 4.59 (s, br, H-29b), 4.67 (s, br, H-29a), 7.71–7.90 (m, 15H, PPh₃), ppm; ¹³C NMR (100 MHz, CDCl₃): δ_C 14.7, 16.0, 16.1, 16.5, 18.1, 19.1, 19.5, 19.8 (d, $J_{C,P}$ 52.3 Hz), 20.8, 21.3, 22.3, 22.4, 23.6, 25.1, 27.0, 27.9, 29.1, 29.2, 29.5, 29.6, 34.0, 34.5, 37.0, 37.6, 37.8, 38.3, 40.8, 42.6, 46.4, 47.8, 48.7, 50.2, 55.3, 62.9, 63.4 (d, $J_{C,P} = 17.4$ Hz), 80.8, 109.9, 118.1 (d, $J_{C,P} = 85.7$ Hz), 130.5 (d, $J_{C,P} = 12.1$ Hz), 133.8 (d, $J_{C,P} = 9.8$ Hz), 135.0 (d, $J_{C,P} = 3.0$ Hz), 150.0,

171.0, 172.0, 172.8 ppm; ^{31}P NMR (162 MHz, CDCl_3): δ_{P} 24.75 ppm; IR (ATR) ν : 2942, 1729, 1246, 1156, 691 cm^{-1} .

3-*O*-Acetyl-28-*O'*-(3'-(4''-triphenylphosphoniobutyloxycarbonyl)propanoyl)betulin bromide (**7b**) was obtained as a resin (97.2 mg, 99% yield); HRMS (ESI^+) m/z : calcd for $\text{C}_{58}\text{H}_{78}\text{O}_6\text{P}^+$ ($[\text{M}]^+$) 901.5536, found 901.5550; ^1H NMR (600 MHz, CDCl_3): δ_{H} 0.83, 0.84, 0.85, 0.96, 1.00 (all s, 3H each, H-23–H-27), 1.68 (s, 3H, H-30), 0.72–1.97 (m, 26H, CH, CH_2 BN scaffold and CH_2 fragment of linker), 2.04 (s, 3H, CH_3CO), 2.12 (q, 2H, $J = 7.1$ Hz, CH_2 fragment of linker), 2.40 (td, 1H, $J_1 = 5.8$ Hz, $J_2 = 11.0$ Hz, H-19), 2.48–2.59 (m, 4H, $\text{O}(\text{CO})\text{CH}_2\text{CH}_2$), 3.85 (d, 1H, $J = 11.0$ Hz, H-28b), 3.97–4.06 (m, 2H, CH_2P), 4.14 (t, 2H, $J = 5.8$ Hz, $(\text{CO})\text{OCH}_2$), 4.24 (d, 1H, $J = 11.1$ Hz, H-28a), 4.47 (dd, 1H, $J_1 = 5.3$ Hz, $J_2 = 11.0$ Hz, H-3), 4.59 (s, br, 1H, H-29b) 4.67 (s, br, H-29a), 7.66–7.92 (m, 15H, PPh_3) ppm; ^{13}C NMR (100 MHz, CDCl_3): δ_{C} 14.7, 16.0, 16.1, 16.5, 18.1, 19.1, 19.26, 19.33, 20.7, 20.8, 21.3, 22.2 (d, $J_{\text{C,P}} = 50.6$ Hz), 23.7, 25.1, 27.0, 27.9, 29.1, 29.2, 29.5, 29.7, 34.1, 34.5, 37.0, 37.6, 37.8, 38.3, 40.9, 42.7, 46.4, 47.7, 48.7, 50.2, 55.3, 63.0, 63.6, 80.9, 109.9, 118.3 (d, $J_{\text{C,P}} = 84.9$ Hz), 130.4 (d, $J_{\text{C,P}} = 12.1$ Hz), 133.8 (d, $J_{\text{C,P}} = 9.9$ Hz), 134.9 (d, $J_{\text{C,P}} = 3.0$ Hz), 150.0, 171.0, 172.2, 172.6 ppm; ^{31}P NMR (162 MHz, CDCl_3): δ_{P} 24.61 ppm; IR (ATR) ν : 2945, 1731, 1246, 1156, 691 cm^{-1} .

3-*O*-Acetyl-28-*O'*-(3'-(5''-triphenylphosphoniopentyloxycarbonyl)propanoyl)betulin bromide (**7c**) was obtained as a resin (77.7 mg, 78% yield); HRMS (ESI^+): calcd for $\text{C}_{59}\text{H}_{80}\text{O}_6\text{P}^+$ ($[\text{M}]^+$) m/z : 915.5693, found 915.5715; ^1H NMR (600 MHz, CDCl_3): δ_{H} 0.83, 0.84, 0.85, 0.96, 1.01 (all s, 3H each, H-23–H-27), 1.67 (s, 3H, H-30), 0.70–1.97 (m, 30H, CH, CH_2 BN scaffold and $(\text{CH}_2)_3$ fragment of linker), 2.04 (s, 3H, CH_3CO), 2.41 (td, 1H, $J_1 = 5.8$ Hz, $J_2 = 11.1$ Hz, H-19), 2.55–2.65 (m, 4H, $\text{O}(\text{CO})\text{CH}_2\text{CH}_2$), 3.86 (d, 1H, $J = 11.0$ Hz, H-28b), 3.91–3.98 (m, 2H, CH_2P), 4.03 (t, 2H, $J = 6.4$ Hz, $(\text{CO})\text{OCH}_2$), 4.25 (d, 1H, $J = 11.1$ Hz, H-28a), 4.47 (dd, 1H, $J_1 = 5.4$ Hz, $J_2 = 11.0$ Hz, H-3), 4.58 (s, br, H-29b), 4.67 (s, br, H-29a), 7.67–7.91 (m, 15H, PPh_3) ppm; ^{13}C NMR (100 MHz, CDCl_3): δ_{C} 14.7, 16.0, 16.1, 16.5, 18.1, 19.1, 20.7, 21.3, 22.2, 22.3, 22.7 (d, $J_{\text{C,P}} = 49.4$ Hz), 23.7, 25.1, 26.5, 26.7, 27.0, 27.9, 28.1, 29.1, 29.2, 29.5, 29.7, 34.1, 34.5, 37.0, 37.5, 37.8, 38.3, 40.8, 42.6, 46.4, 47.7, 48.7, 50.2, 55.3, 62.9, 65.8, 80.9, 109.8, 118.4 (d, $J_{\text{C,P}} = 85.0$ Hz), 130.5 (d, $J_{\text{C,P}} = 12.1$ Hz), 133.7 (d, $J_{\text{C,P}} = 9.8$ Hz), 134.9 (d, $J_{\text{C,P}} = 3.0$ Hz), 150.1, 171.0, 172.3, 172.7 ppm; ^{31}P NMR (161.9 MHz, CDCl_3): δ_{P} 24.37 ppm; IR (ATR) ν : 2946, 1731, 1246, 1157, 692 cm^{-1} .

3-*O*-Acetyl-28-*O'*-(3',3'-dimethyl-3'-(3''-triphenylphosphoniopropylloxycarbonyl)propanoyl)betulin bromide (**7d**) was obtained as a resin (71.7 mg, 72% yield); HRMS (ESI^+) m/z : calcd for $\text{C}_{59}\text{H}_{80}\text{O}_6\text{P}^+$ ($[\text{M}]^+$) 915.5693, found 915.5717; ^1H NMR (600 MHz, CDCl_3): δ_{H} 0.80, 0.83, 0.84, 0.87, 0.94 (all s, 3H each, H-23–H-27), 1.21 (s, 3H, CMe), 1.22 (s, 3H, CMe), 1.66 (s, 3H, H-30), 0.68–2.08 (m, 26H, CH, CH_2 BN scaffold and CH_2 fragment of linker), 2.04 (s, 3H, CH_3CO), 2.29 (td, 1H, $J_1 = 5.8$ Hz, $J_2 = 10.8$ Hz, H-19), 2.63–2.66 (m, 2H, $2 \times \text{O}(\text{CO})\text{CH}_2$), 3.76 (d, 1H, $J = 11.0$ Hz, H-28a), 4.01–4.10 (m, 3H, CH_2P and H-28b), 4.45–4.48 (m, 3H, H-3 and $(\text{CO})\text{OCH}_2$), 4.58 (s, br, 1H, H-29b), 4.63 (s, br, 1H, H-29a), 7.69–7.91 (m, 15H, PPh_3) ppm; ^{13}C NMR (150 MHz, CDCl_3): δ_{C} 14.7, 15.9, 16.1, 16.5, 18.1, 19.0, 19.4 (d, $J_{\text{C,P}} = 51.8$ Hz), 20.8, 21.3, 22.4, 23.6, 25.1, 25.4, 25.5, 26.9, 27.9, 29.5, 29.7, 34.0, 34.5, 37.0, 37.6, 37.8, 38.3, 40.6, 40.8, 42.6, 44.3, 46.3, 47.8, 48.6, 50.2, 55.3, 62.6, 63.9 (d, $J_{\text{C,P}} = 18.4$ Hz), 80.8, 109.9, 118.3 (d, $J_{\text{C,P}} = 86.3$ Hz), 130.4 (d, $J_{\text{C,P}} = 12.6$ Hz), 133.8 (d, $J_{\text{C,P}} = 10.4$ Hz), 134.9 (d, $J_{\text{C,P}} = 0.5$ Hz), 150.0, 171.0, 172.0, 176.7 ppm; ^{31}P NMR (161.9 MHz, CDCl_3): δ_{P} 19.38 ppm; IR (ATR) ν : 2946, 1727, 1248, 1177, 725, 690 cm^{-1} .

3-*O*-Acetyl-28-*O'*-(3',3'-dimethyl-3'-(4''-triphenylphosphoniobutyloxycarbonyl)propanoyl)betulin bromide (**7e**) was obtained as a resin (78.8 mg, 78% yield); HRMS (ESI^+) m/z : calcd for $\text{C}_{60}\text{H}_{82}\text{O}_6\text{P}^+$ ($[\text{M}]^+$) 929.5849, found 929.5861; ^1H NMR (600 MHz, CDCl_3): δ_{H} 0.75, 0.76, 0.77, 0.88, 0.89 (all s, 3H each, H-23–H-27), 1.051 (s, 3H, CMe), 1.054 (s, 3H, CMe), 1.60 (s, 3H, H-30), 0.68–1.90 (m, 26H, CH, CH_2 BN scaffold, and CH_2 fragment of linker), 1.97 (s, 3H, CH_3CO), 2.08 (q 2H, $J = 6.7$ Hz CH_2 fragment of linker), 2.30 (td, 1H, $J_1 = 5.7$ Hz, $J_2 = 10.8$ Hz, H-19), 2.45 (s, 2H, $\text{O}(\text{CO})\text{CH}_2$), 3.72 (d, 1H, $J = 11.0$ Hz, H-28b), 3.87–3.92 (m, 2H, CH_2P), 4.07–4.10 (m, 3H, H-28a and $(\text{CO})\text{OCH}_2$), 4.39 (dd, 1H, $J_1 = 5.3$ Hz, $J_2 = 11.0$ Hz, H-3), 4.51 (s, br, 1H, H-29b), 4.58 (d, 1H, $J = 2.3$ Hz, H-29a), 7.61–7.87 (m, 15H, PPh_3) ppm; ^{13}C NMR (150 MHz, CDCl_3): δ_{C} 14.6, 16.0, 16.1, 16.4, 18.1, 19.0, 19.1, 20.7, 21.2, 22.1 (d, $J_{\text{C,P}}$

= 49.3 Hz), 23.6, 25.1, 25.3, 26.9, 27.9, 29.1, 29.2, 29.5, 29.6, 34.0, 34.4, 36.9, 37.5, 37.7, 38.3, 40.5, 40.8, 42.6, 44.2, 46.2, 47.6, 48.6, 50.2, 55.3, 62.7, 63.2, 80.8, 109.8, 118.3 (d, $J_{C,P}$ = 88.1 Hz), 130.4 (d, $J_{C,P}$ = 12.6 Hz), 133.7 (d, J_{P} = 10.4 Hz), 134.9 (d, $J_{C,P}$ = 0.5 Hz), 149.9, 171.0, 171.5, 176.5 ppm; ^{31}P NMR (162 MHz, CDCl_3): δ_{P} 24.52 ppm; IR (ATR) ν : 2948, 1725, 1248, 1179, 723, 690 cm^{-1} .

3-*O*-Acetyl-28-*O'*-(3',3'-dimethyl-3'-(5''-triphenylphosphoniopentylloxycarbonyl)propanoyl)betulin bromide (**7f**) was obtained as a resin (73.7 mg, 72% yield); HRMS (ESI⁺) m/z : calcd for $\text{C}_{61}\text{H}_{84}\text{O}_6\text{P}^+$ ($[\text{M}]^+$) 943.6006, found 943.6042; ^1H NMR (600 MHz, CDCl_3): δ_{H} 0.82, 0.83, 0.84, 0.94, 0.97 (all s, 3H each, H-23–H-27), 1.20 (s, 3H, CMe), 1.21 (s, 3H, CMe), 1.66 (s, 3H, H-30), 0.67–1.96 (m, 30H, CH, CH_2 BN scaffold and $(\text{CH}_2)_3$ fragment of linker), 2.03 (s, 3H, CH_3CO), 2.38 (td, 1H, J_1 = 5.8 Hz, J_2 = 10.9 Hz, H-19), 2.57 (s, 2H, $\text{O}(\text{CO})\text{CH}_2$), 3.83 (d, 1H, J = 11.0 Hz, H-28b), 3.88–3.95 (m, 2H, CH_2P), 4.01 (t, 2H, J = 6.7 Hz, $(\text{CO})\text{OCH}_2$), 4.17 (d, 1H, J = 11.0 Hz, H-28a), 4.46 (dd, 1H, J_1 = 5.5 Hz, J_2 = 10.5 Hz, H-3), 4.57 (s, br, 1H, H-29b), 4.64 (s, br, 1H, H-29a), 7.65–7.91 (m, 15H, PPh_3) ppm; ^{13}C NMR (100 MHz, CDCl_3): δ_{C} 14.7, 16.0, 16.1, 16.5, 18.1, 19.1, 20.8, 21.3, 22.21, 22.25, 22.7 (d, $J_{C,P}$ = 50.1 Hz), 23.6, 25.1, 25.4, 25.5, 26.4, 26.6, 26.9, 27.9, 28.0, 29.5, 29.7, 34.1, 34.5, 37.0, 37.5, 37.8, 38.3, 40.5, 40.8, 42.6, 44.4, 46.2, 47.7, 48.7, 50.2, 55.3, 62.7, 63.9, 80.9, 109.8, 118.4 (d, $J_{C,P}$ = 85.8 Hz), 130.4 (d, $J_{C,P}$ = 12.4 Hz), 133.7 (d, $J_{C,P}$ = 9.9 Hz), 134.9 (d, $J_{C,P}$ = 3.0 Hz), 150.0, 171.0, 171.7, 176.6 ppm; ^{31}P NMR (161.9 MHz, CDCl_3): δ_{P} 24.35 ppm; IR (ATR) ν : 2948, 1727, 1247, 1181, 725, 690 cm^{-1} .

3.2.5. General Procedure for the Synthesis of 3,28-Bis(bromoalkoxycarbonyl)propanoyl)betulin (**8**)

3,28-*O,O'*-Bis(3'-carboxypropanoyl)betulin (**5**, 0.25 mmol, 160.6 mg, 1 eq.), DMF (2 mL/100 mg **5**) and MeCN (0.2 mL/100 mg **5**), the appropriate dibromoalkane ($\text{Br}(\text{CH}_2)_n\text{Br}$, n = 3, 4, 5; 1.5 mmol, 6 eq.) and K_2CO_3 (0.50 mmol, 69.1 mg, 2 eq.) were stirred at 50 °C for 18–20 h. The obtained mixture was diluted with cold water (10 × volume) and extracted with ethyl acetate (6 × 19 mL). The combined organic layers were washed with brine (2 × 90 mL), dried over MgSO_4 , and the solvent was evaporated under reduced pressure. Then, crude product **8** was washed with methanol (2 × 1.0 mL) and was further purified by column chromatography (DCM/MeOH, gradient: 100:1 to 50:1).

3,28-*O,O'*-Bis(3'-(3''-bromopropylloxycarbonyl)propanoyl)betulin (**8a**) was obtained as a resin (143.8 mg, 65% yield); R_f = 0.23 (DCM:MeOH, 100:1); HRMS (ESI⁺) m/z : calcd for $\text{C}_{44}\text{H}_{69}\text{Br}_2\text{O}_8$ ($[\text{M}+\text{H}]^+$) 833.3359, found 833.3360; ^1H NMR (600 MHz, CDCl_3): δ_{H} 0.83, 0.84, 0.85, 0.97, 1.02 (all s, 3H each, H-23–H-27), 1.68 (s, 3H, H-30), 0.74–2.03 (m, 24H, CH, CH_2 BN scaffold), 2.15–2.21 (m, 4H, 2 × CH_2 fragment of linker), 2.43 (td, 1H, J_1 = 5.8 Hz, J_2 = 11.1 Hz, H-19), 2.61–2.68 (m, 8H, 2 × $\text{O}(\text{CO})\text{CH}_2\text{CH}_2$), 3.45–3.47 (m, 4H, 2 × CH_2Br), 3.87 (d, 1H, J = 10.3 Hz, H-28b), 4.22–4.26 (m, 4H, 2 × $(\text{CO})\text{OCH}_2$), 4.29 (dd, 1H, J_1 = 1.9 Hz, J_2 = 11.0 Hz, H-28a), 4.46–4.51 (m, 1H, H-3), 4.59 (s, br, 1H, H-29b), 4.68 (d, 1H, J = 2.1 Hz, H-29a) ppm; ^{13}C NMR (150 MHz, CDCl_3): δ_{C} 14.7, 16.0, 16.1, 16.5, 18.1, 19.1, 20.8, 23.6, 25.1, 27.0, 27.9, 29.10, 29.16, 29.2, 29.3, 29.5, 29.6, 29.7, 31.6, 31.7, 34.1, 34.5, 37.0, 37.6, 37.8, 38.3, 40.9, 42.7, 46.4, 47.7, 48.8, 50.3, 55.4, 62.39, 62.43, 63.1, 81.4, 109.9, 150.1, 171.9, 172.1, 172.2, 172.5 ppm; IR (ATR) ν : 2943, 1732, 1157 cm^{-1} .

3,28-*O,O'*-Bis(3'-(4''-bromobutylloxycarbonyl)propanoyl)betulin (**8b**) was obtained as a resin (159.8 mg, 70% yield); R_f = 0.26 (DCM:MeOH, 100:1); HRMS (ESI⁺) m/z : calcd for $\text{C}_{46}\text{H}_{72}\text{Br}_2\text{O}_8\text{Na}$ ($[\text{M}+\text{Na}]^+$) 933.3492, found 933.3525; ^1H NMR (600 MHz, CDCl_3): δ_{H} 0.83, 0.84, 0.85, 0.97, 1.02 (all s, 3H each, H-23–H-27), 1.68 (s, 3H, H-30), 0.70–2.06 (m, 32H, CH, CH_2 BN scaffold and 2 × $(\text{CH}_2)_2$ fragment of linker), 2.43 (td, 1H, J_1 = 5.7 Hz, J_2 = 11.1 Hz, H-19), 2.60–2.68 (m, 8H, 2 × $\text{O}(\text{CO})\text{CH}_2\text{CH}_2$), 3.43–3.45 (m, 4H, 2 × CH_2Br), 3.87 (d, 1H, J = 11.0 Hz, H-28b), 4.11–4.13 (m, 4H, 2 × $(\text{CO})\text{OCH}_2$), 4.29 (d, 1H, J = 11.0 Hz, H-28a), 4.48 (dd, 1H, J_1 = 5.8 Hz, J_2 = 10.5 Hz, H-3), 4.58 (s, br, 1H, H-29b), 4.68 (s, br, 1H, H-29a) ppm; ^{13}C NMR (150 MHz, CDCl_3): δ_{C} 14.6, 15.9, 16.0, 16.4, 18.0, 19.0, 20.7, 23.5, 25.0, 25.1, 26.9, 27.1, 27.8, 29.1, 29.0, 29.41, 29.44, 29.6, 32.9, 34.0, 34.4, 36.9, 37.4, 37.7, 38.2, 40.8, 42.6, 46.3, 47.6, 48.7, 50.1, 55.3, 62.9, 63.5, 63.6, 81.2, 109.8, 149.9, 171.8, 172.09, 172.14, 172.4 ppm; IR (ATR) ν : 2944, 1730, 1157 cm^{-1} .

3,28-*O,O'*-Bis(3'-(5''-bromopentylloxycarbonyl)propanoyl)betulin (**8c**) was obtained as a resin (150.5 mg, 64% yield); $R_f = 0.32$ (DCM:MeOH, 100:1); HRMS (ESI⁺) m/z : calcd for C₄₈H₇₆Br₂O₈Na ([M+Na]⁺) 961.3805, found 961.3886; ¹H NMR (600 MHz, CDCl₃): δ_H 0.83, 0.84, 0.85, 0.97, 1.02 (all s, 3H each, H-23–H-27), 1.68 (s, 3H, H-30), 0.72–2.00 (m, 36H, CH, CH₂ BN scaffold and 2 × (CH₂)₃ fragment of linker), 2.43 (td, 1H, $J_1 = 5.8$ Hz, $J_2 = 11.1$ Hz, H-19), 2.60–2.68 (m, 8H, 2 × O(CO)CH₂CH₂), 3.40–3.42 (m, 4H, 2 × CH₂Br), 3.87 (d, 1H, $J = 12.2$ Hz, H-28b), 4.08–4.11 (m, 4H, 2 × (CO)OCH₂), 4.29 (dd, 1H, $J_1 = 2.0$ Hz, $J_2 = 11.2$ Hz, H-28a), 4.49 (dd, 1H, $J_1 = 5.5$ Hz, $J_2 = 10.9$ Hz, H-3), 4.59 (s, br, 1H, H-29b), 4.68 (d, 1H, $J = 2.2$ Hz, H-29a) ppm; ¹³C NMR (150 MHz, CDCl₃): δ_C 14.7, 16.0, 16.1, 16.5, 18.1, 19.1, 20.8, 23.6, 24.6, 25.1, 27.0, 27.7, 27.9, 28.1, 28.2, 29.2, 29.5, 29.3, 29.7, 32.3, 33.4, 34.1, 34.5, 37.0, 37.6, 37.8, 38.3, 40.9, 42.7, 46.4, 47.7, 48.8, 50.2, 55.4, 63.0, 64.3, 64.4, 81.3, 109.9, 150.1, 171.9, 172.25, 172.32, 172.6 ppm; IR (ATR) ν: 2943, 1731, 1157 cm⁻¹.

3.2.6. General Procedure for the Synthesis of Bis(triphenylphosphonium) Derivatives of BN (9, 3,28-bisTPP[⊕] BN)

3,28-*O,O'*-Bis(3'-(3''-bromoalkoxycarbonyl)propanoyl)betulin (**8a–8c**) (0.1 mmol, 1 eq.) and triphenylphosphine (0.3 mmol, 78.7 mg, 3 eq.) were dissolved in dry DCM (1–2 mL) and stirred at room temperature for 10–15 min until homogenization was reached. The solvent was evaporated under reduced pressure, and the residue was heated in an oil bath at 120 °C under an Ar atmosphere. The obtained mixture was washed with diethyl ether (5 × 4 mL) at 50 °C. Then, the crude product was crystalized from ethyl acetate/diethyl ether (1:4, *v/v*) and dried under reduced pressure at 50 °C for 6 h or purified using column chromatography (DCM:MeOH, 10:1, *v/v*).

3,28-*O,O'*-Bis(3'-(3''-triphenylphosphoniopropylloxycarbonyl)propanoyl)betulin bromide (**9a**) was obtained as a resin (74.7 mg, 53% yield); $R_f = 0.13$ (DCM:MeOH, 10:1); HRMS (ESI⁺) m/z : calcd for C₄₀H₄₉O₄P²⁺ ([M]²⁺) 624.3368, found 624.3379; ¹H NMR (600 MHz, CDCl₃): δ_H 0.70, 0.72, 0.73, 0.88, 0.89 (all s, 3H each, H-23–H-27), 1.60 (s, 3H, H-30), 0.60–1.90 (m, 24H, CH, CH₂ BN scaffold), 1.92–2.00 (m, 4H, 2 × CH₂ fragment of linker), 2.31 (td, 1H, $J_1 = 5.7$ Hz, $J_2 = 10.9$ Hz, H-19), 2.51–2.60 (m, 8H, 2 × O(CO)CH₂CH₂), 3.75 (d, 1H, $J = 10.8$ Hz, H-28b), 3.92–3.99 (m, 4H, 2 × CH₂P), 4.17 (dd, 1H, $J_1 = 1.9$ Hz, $J_2 = 11.0$ Hz, H-28a), 4.31 (dd, 1H, $J_1 = 5.7$ Hz, $J_2 = 10.4$ Hz, H-3), 4.34–4.38 (m, 4H, 2 × (CO)OCH₂), 4.52 (s, br, 1H, H-29b), 4.60 (d, 1H, $J = 2.2$ Hz, H-29a), 7.63–7.83 (m, 30H, 2 × PPh₃) ppm; ¹³C NMR (150 MHz, CDCl₃): δ_C 14.7, 16.0, 16.1, 16.5, 18.1, 19.1, 19.7 (d, $J_{C,P} = 51.8$ Hz), 20.8, 22.3, 23.6, 25.1, 27.0, 28.0, 29.1, 29.5, 29.4, 29.7, 34.1, 34.5, 37.0, 37.6, 37.8, 38.3, 40.9, 42.7, 46.4, 47.8, 48.7, 50.3, 55.4, 62.9, 63.5 (d, $J_{C,P} = 18.4$ Hz), 81.3, 109.9, 118.1 (d, $J_{C,P} = 86.3$ Hz), 130.5 (d, $J_{C,P} = 12.8$ Hz), 133.8 (d, $J_{C,P} = 9.2$ Hz), 135.1 (d, $J_{C,P} = 0.5$ Hz), 150.0, 171.99, 172.0, 172.1, 172.7 ppm; ³¹P NMR (162 MHz, CDCl₃): δ_P 24.61, 24.54 ppm; IR (ATR) ν: 2946, 1730, 1438, 1158, 724, 691 cm⁻¹.

3,28-*O,O'*-Bis(3'-(4''-triphenylphosphoniobutylloxycarbonyl)propanoyl)betulin bromide (**9b**) was obtained as a resin (115.0 mg, 80% yield); $R_f = 0.19$ (DCM:MeOH, 10:1); HRMS (ESI⁺) m/z : calcd for C₄₁H₅₁O₄P²⁺ ([M]²⁺) 638.3525, found 638.3536; ¹H NMR (600 MHz, CDCl₃): δ_H 0.73, 0.75, 0.89, 0.93, 1.18 (all s, 3H each, H-23–H-27), 1.61 (s, 3H, H-30), 0.60–2.05 (m, 32H, CH, CH₂ BN scaffold and 2 × (CH₂)₂ fragment of linker), 2.38 (td, 1H, $J_1 = 5.6$ Hz, $J_2 = 10.9$ Hz, H-19), 2.41–2.52 (m, 8H, 2 × O(CO)CH₂CH₂), 3.77 (d, 1H, $J = 10.1$ Hz, H-28b), 3.89–3.97 (m, 4H, 2 × CH₂P), 4.05–4.08 (m, 4H, 2 × (CO)OCH₂), 4.22 (d, 1H, $J_1 = 11.4$ Hz, H-28a), 4.35 (m, 1H, H-3), 4.52 (s, br, 1H, H-29b), 4.61 (d, 1H, $J = 3.1$ Hz, H-29a), 7.58–7.87 (m, 30H, 2 × PPh₃) ppm; ¹³C NMR (100 MHz, CDCl₃): δ_C 14.7, 16.0, 16.1, 16.5, 18.1, 19.1, 19.2, 19.3, 20.8, 22.2, (d, $J_{C,P} = 50.0$ Hz), 23.6, 25.1, 25.3, 27.0, 27.9, 28.9, 29.0, 29.1, 29.5, 29.6, 34.0, 34.5, 37.0, 37.5, 37.8, 38.3, 40.8, 42.7, 46.4, 47.7, 48.7, 50.2, 55.4, 63.0, 63.4, 81.3, 109.9, 118.2 (d, $J_{C,P} = 88.8$ Hz), 130.4 (d, $J_{C,P} = 12.9$ Hz), 133.7 (d, $J_{C,P} = 9.9$ Hz), 135.0 (d, $J_{C,P} = 3.0$ Hz), 150.0, 171.9, 172.16, 172.18, 172.6 ppm; ³¹P NMR (162 MHz, CDCl₃): δ_P 24.51 ppm; IR (ATR) ν: 2936, 1728, 1438, 1160, 725, 691 cm⁻¹.

3,28-*O,O'*-Bis(3'-(5''-triphenylphosphoniopentylloxycarbonyl)propanoyl)betulin bromide (**9c**) was obtained as a resin (129.0 mg, 88% yield); $R_f = 0.11$ (DCM:MeOH, 10:1); HRMS (ESI⁺)

m/z : calcd for $C_{42}H_{53}O_4P^{2+}$ ($[M]^{2+}$) 652.3681, found 652.3667; 1H NMR (400 MHz, $CDCl_3$): δ_H 0.73, 0.74, 0.87, 0.92, 1.17 (all s, 3H each, H-23–H-27), 1.59 (s, 3H, H-30), 0.60–1.97 (m, 36H, CH, CH_2 BN scaffold and $2 \times (CH_2)_3$ fragment of linker), 2.33 (td, 1H, $J_1 = 5.7$ Hz, $J_2 = 10.8$ Hz, H-19), 2.44–2.57 (m, 8H, $2 \times O(CO)CH_2CH_2$), 3.77 (d, 1H, $J = 11.4$ Hz, H-28b), 3.78–3.88 (m, 4H, $2 \times CH_2P$), 3.89–3.98 (m, 4H, $2 \times (CO)OCH_2$), 4.18 (d, 1H, $J = 11.3$ Hz, H-28a), 4.37 (dd, 1H, $J = 8.0$ Hz, H-3), 4.50 (s, br, 1H, H-29b), 4.59 (s, br, 1H, H-29a), 7.60–7.82 (m, 30H, $2 \times PPh_3$) ppm; ^{13}C NMR (100 MHz, $CDCl_3$): δ_C 14.7, 16.0, 16.1, 18.5, 18.1, 19.1, 20.8, 22.2, 22.3, 22.8 (d, $J_{C,P} = 49.3$ Hz), 23.6, 25.1, 26.7, 27.9, 28.1, 29.1, 29.2, 29.5, 29.7, 34.1, 34.5, 37.0, 37.6, 37.8, 38.3, 40.9, 42.7, 46.4, 47.7, 48.8, 50.2, 55.4, 63.0, 64.00, 64.04, 81.2, 109.9, 118.4 (d, $J_{C,P} = 85.0$ Hz), 130.5 (d, $J_{C,P} = 12.2$ Hz), 133.8 (d, $J_{C,P} = 9.8$ Hz), 135.0 (d, $J_{C,P} = 3.0$ Hz), 150.1, 172.0, 172.28, 172.30, 172.6 ppm; ^{31}P NMR (162 MHz, $CDCl_3$): δ_P 24.36 ppm.

3.3. Biological Evaluation

3.3.1. Cytotoxicity Assay

Cell Lines

The human colorectal carcinoma cell line (HCT 116) and the human breast adenocarcinoma cell line (MCF-7) cells were purchased from the American Type Culture Collection (ATCC, Manassas, VA, USA). The Normal Human Dermal Fibroblast (NHDF) cells were purchased from Lonza (Dermal Fibroblasts, Lonza, Poland). All cells were cultured under standard conditions at 37 °C in a humidified atmosphere at 5% CO_2 in DMEM/F12 medium (PAA) supplemented with 10% of heat-inactivated fetal bovine serum (FBS, EURx, Gdansk, Poland) and antibiotics (penicillin/streptomycin).

Cell Viability Assay

Cells were seeded at 7500 (HCT 116) or 10,000 (MCF-7, NHDF) cells/well in 96-well plates. After 24 h, the culture medium was removed and 100 μ L of fresh medium containing the test compounds at 0–12.5 μ M concentrations was added to the culture wells. The test compounds were dissolved in DMSO to obtain a stock solution with a concentration of 5 mM (betulin) or 10 mM (other test compounds). The stock solution was diluted with the fresh culture medium to the desired concentration. Controls were cells grown in medium without the addition of test compounds. After 24 h of incubation with the test compounds, 10 μ L of CCK-8 reagent (Bimake, Houston, TX, USA) was added to each well. After 2 h, the absorbance of the samples was measured at a wavelength of 450 nm using a microplate reader (Epoch, BioTek Instruments, Winooski, VT, USA). The determinations were conducted in at least three biological replications (each biological replication contained 3 technical replications). The cell viability rate was calculated using CalcuSyn software (version 2.0, Biosoft, Cambridge, UK).

3.3.2. Antibacterial Assay

Antibacterial analysis was performed using the *S. aureus* ATCC 25923, *S. epidermidis* ATCC 12228, and *Escherichia coli* ATCC 25922 bacteria strains. The test compounds were dissolved in DMSO to obtain a stock solution with a concentration of 5 mM (betulin) or 10 mM (other test compounds). The stock solution was diluted with water to the desired concentration (25–250 μ M). Then, 1 mL of the investigated solutions was mixed with 1 mL of culture medium (TSB, Biomaxima, Lublin, Poland) in a sterile glass tube. The initial concentration of bacteria was around 5×10^6 CFU/mL. The concentration of bacteria was measured using an optical densitometer before and after 18 h of bacteria culture in glass tubes at 37 °C (incubator POL-EKO, Wodzislaw Slaski, Poland). The investigations were repeated for three independent samples. The control sample was the culture medium without any supplementation.

4. Conclusions

In conclusion, we designed and synthesized nine new molecular hybrids of BN by covalent linkage of the alkyltriphenylphosphonium moiety to the parent skeleton via

the linker $O(CO)CH_2CR_2COO$. We developed a few-stage methodology that enabled the preparation of both *mono*- and *bis*(TPP^{\oplus}) derivatives from easily available, cheap, natural active substance (*BN*) by simple transformations in high yields. The advantage of this protocol are the simple synthetic procedures and easy purification of the final products.

As expected, the triphenylphosphonium derivatives of *BN* showed a greater cytotoxicity than natural *BN* toward the cell lines tested (HCT 116 and MCF-7). Importantly, analogs (**7a–7c**) with one triphenylphosphonium cation were almost twice less toxic against healthy cells (NHDF), which demonstrated their selectivity. TPP^{\oplus} -conjugates with *BN* showed antimicrobial properties against the Gram-positive reference *S. aureus* ATCC 25923 and *S. epidermidis* ATCC 12228 bacteria when their concentration in the water solution was 200 μ M.

The obtained results show that the bioavailability of natural *BN* can be improved by combining its backbone via linkers with a mitochondria-targeted TPP^{\oplus} moiety. Additionally, our study provides important data about the properties of *BN* conjugates with TPP^{\oplus} and encourages further research on the structural modifications of the parent *BN* skeleton.

Supplementary Materials: The following can be downloaded at: <https://www.mdpi.com/xxx/s1>. Supporting information includes the 1H , ^{13}C , ^{31}P NMR spectra of betulin and all of the synthesized compounds (1–9) as well as the gHSQC and FTIR for the selected compounds.

Author Contributions: Conceptualization and methodology, M.G.; Synthesis and characterization of chemical compounds, M.S. and P.G.; Cytotoxicity tests, A.L.; Antibacterial tests, A.K.-K.; Mass spectra, K.E.; Supervision, M.G.; Analysis and interpretation of the results, M.G., A.L., A.K.-K., M.S. and P.G.; Writing—original draft preparation, M.G., A.L., A.K.-K., M.S. and P.G.; Writing—review and editing, M.G.; Supervision, M.G. All authors have read and agreed to the published version of the manuscript.

Funding: This research was supported by the Silesian University of Technology (Poland) Grant BK No. 04/020/BK_22/1035 and Grant BK No. 04/050/BK_22/0139.

Institutional Review Board Statement: Not applicable.

Informed Consent Statement: Not applicable.

Data Availability Statement: Not applicable.

Conflicts of Interest: The authors declare no conflict of interest.

Sample Availability: Samples of compounds **7** and **9** are available from the authors.

References

- Sung, H.; Ferlay, J.; Siegel, R.L.; Laversanne, M.; Soerjomataram, I.; Jemal, A.; Bray, F. Global Cancer Statistics 2020: GLOBOCAN Estimates of Incidence and Mortality Worldwide for 36 Cancers in 185 Countries. *CA Cancer J. Clin.* **2021**, *71*, 209–249. [CrossRef] [PubMed]
- Krasutsky, P.A. Birch Bark Research and Development. *Nat. Prod. Rep.* **2006**, *23*, 919–942. [CrossRef]
- Amiri, S.; Dastghaib, S.; Ahmadi, M.; Mehrbod, P.; Khadem, F.; Behrouj, H.; Aghanoori, M.-R.; Machaj, F.; Ghamsari, M.; Rosik, J.; et al. Betulin and Its Derivatives as Novel Compounds with Different Pharmacological Effects. *Biotechnol. Adv.* **2020**, *38*, 107409–107448. [CrossRef] [PubMed]
- Jonnalagadda, S.C.; Suman, P.; Morgan, D.C.; Seay, J.N. Recent Developments on the Synthesis and Applications of Betulin and Betulinic Acid Derivatives as Therapeutic Agents. *Stud. Nat. Prod. Chem.* **2017**, *53*, 45–84. [CrossRef]
- Grymel, M.; Pastuch-Gawołek, G.; Lalik, A.; Zawojak, M.; Boczek, S.; Krawczyk, M.; Erfurt, K. Glycoconjugation of Betulin Derivatives Using Copper-Catalyzed 1,3-Dipolar Azido-Alkyne Cycloaddition Reaction and a Preliminary Assay of Cytotoxicity of the Obtained Compounds. *Molecules* **2020**, *25*, 6019. [CrossRef] [PubMed]
- Hordyjewska, A.; Ostapiuk, A.; Horecka, A. Betulin and Betulinic Acid in Cancer Research. *J. Pre-Clin. Clin. Res.* **2018**, *12*, 72–75. [CrossRef]
- Drag-Zalesińska, M.; Drag, M.; Poręba, M.; Borska, S.; Kulbacka, J.; Saczko, J. Anticancer Properties of Ester Derivatives of Betulin in Human Metastatic Melanoma Cells (Me-45). *Cancer Cell Int.* **2017**, *17*, 4–14. [CrossRef] [PubMed]
- So, H.M.; Eom, H.J.; Lee, D.; Kim, S.; Kang, K.S.; Lee, I.K.; Baek, K.-H.; Park, J.Y.; Kim, K.H. Bioactivity Evaluations of Betulin Identified from the Bark of *Betula Platyphylla* Var. *Japonica* for Cancer Therapy. *Arch. Pharm. Res.* **2018**, *41*, 815–822. [CrossRef] [PubMed]

9. Chrobak, E.; Jastrzębska, M.; Bębenek, E.; Kadela-Tomanek, M.; Marciniak, K.; Latocha, M.; Wrzalik, R.; Kusz, J.; Boryczka, S. Molecular Structure, In Vitro Anticancer Study and Molecular Docking of New Phosphate Derivatives of Betulin. *Molecules* **2021**, *26*, 737. [CrossRef] [PubMed]
10. Orchel, A.; Chodurek, E.; Jaworska-Kik, M.; Padaszyński, P.; Kaps, A.; Chrobak, E.; Bębenek, E.; Boryczka, S.; Borkowska, P.; Kasperczyk, J. Anticancer Activity of the Acetylenic Derivative of Betulin Phosphate Involves Induction of Necrotic-Like Death in Breast Cancer Cells In Vitro. *Molecules* **2021**, *26*, 615. [CrossRef]
11. Karagöz, A.Ç.; Leidenberger, M.; Hahn, F.; Hampel, F.; Friedrich, O.; Marschall, M.; Kappes, B.; Tsogoeva, S.B. Synthesis of New Betulinic Acid/Betulin-Derived Dimers and Hybrids with Potent Antimalarial and Antiviral Activities. *Bioorg. Med. Chem.* **2019**, *27*, 110–115. [CrossRef] [PubMed]
12. Viszwapriya, D.; Subramenium, G.A.; Radhika, S.; Pandian, S.K. Betulin Inhibits Cariogenic Properties of Streptococcus Mutans by Targeting VicRK and Gtf Genes. *Antonie Van Leeuwenhoek* **2017**, *110*, 153–165. [CrossRef] [PubMed]
13. Salin, O.; Alakurtti, S.; Pohjala, L.; Siiskonen, A.; Maass, V.; Maass, M.; Yli-Kauhaluoma, J.; Vuorela, P. Inhibitory Effect of the Natural Product Betulin and Its Derivatives against the Intracellular Bacterium Chlamydia Pneumoniae. *Biochem. Pharmacol.* **2010**, *80*, 1141–1151. [CrossRef]
14. Alakurtti, S.; Heiska, T.; Kiriazis, A.; Sacerdoti-Sierra, N.; Jaffe, C.L.; Yli-Kauhaluoma, J. Synthesis and Anti-Leishmanial Activity of Heterocyclic Betulin Derivatives. *Bioorg. Med. Chem.* **2010**, *18*, 1573–1582. [CrossRef] [PubMed]
15. Peçak, P.; Orzechowska, B.; Chrobak, E.; Boryczka, S. Novel Betulin Dicarboxylic Acid Ester Derivatives as Potent Antiviral Agents: Design, Synthesis, Biological Evaluation, Structure–Activity Relationship and in-Silico Study. *Eur. J. Med. Chem.* **2021**, *225*, 113738. [CrossRef] [PubMed]
16. Zhao, H.; Liu, Z.; Liu, W.; Han, X.; Zhao, M. Betulin Attenuates Lung and Liver Injuries in Sepsis. *Int. Immunopharmacol.* **2016**, *30*, 50–56. [CrossRef]
17. Wu, H.; Morris-Natschke, S.L.; Xu, X.; Yang, M.; Cheng, Y.; Yu, S.; Lee, K. Recent Advances in Natural Anti HIV Triterpenoids and Analogs. *Med. Res. Rev.* **2020**, *40*, 2339–2385. [CrossRef] [PubMed]
18. Ren, C.; Jin, J.; Hu, W.; Chen, Q.; Yang, J.; Wu, Y.; Zhou, Y.; Sun, L.; Gao, W.; Zhang, X.; et al. Betulin Alleviates the Inflammatory Response in Mouse Chondrocytes and Ameliorates Osteoarthritis via AKT/Nrf2/HO-1/NF-KB Axis. *Front. Pharmacol.* **2021**, *12*, 754038. [CrossRef] [PubMed]
19. Laavola, M.; Haavikko, R.; Hämäläinen, M.; Leppänen, T.; Nieminen, R.; Alakurtti, S.; Moreira, V.M.; Yli-Kauhaluoma, J.; Moilanen, E. Betulin Derivatives Effectively Suppress Inflammation in Vitro and in Vivo. *J. Nat. Prod.* **2016**, *79*, 274–280. [CrossRef] [PubMed]
20. De Benedetto, A.; Agnihothri, R.; McGirt, L.Y.; Bankova, L.G.; Beck, L.A. Atopic Dermatitis: A Disease Caused by Innate Immune Defects? *J. Invest. Dermatol.* **2009**, *129*, 14–30. [CrossRef]
21. Spivak, A.Y.; Nedopekina, D.A.; Khalitova, R.R.; Gubaidullin, R.R.; Odinokov, V.N.; Bel’skii, Y.P.; Bel’skaya, N.V.; Khazanov, V.A. Triphenylphosphonium Cations of Betulinic Acid Derivatives: Synthesis and Antitumor Activity. *Med. Chem. Res.* **2017**, *26*, 518–531. [CrossRef]
22. Honig, B.H.; Hubbell, W.L.; Flewelling, R.F. Electrostatic Interactions in Membranes and Proteins. *Annu. Rev. Biophys. Biophys. Chem.* **1986**, *15*, 163–193. [CrossRef] [PubMed]
23. Tsepaveva, O.V.; Nemtarev, A.V.; Abdullin, T.I.; Grigor’eva, L.R.; Kuznetsova, E.V.; Akhmadishina, R.A.; Ziganshina, L.E.; Cong, H.H.; Mironov, V.F. Design, Synthesis, and Cancer Cell Growth Inhibitory Activity of Triphenylphosphonium Derivatives of the Triterpenoid Betulin. *J. Nat. Prod.* **2017**, *80*, 2232–2239. [CrossRef] [PubMed]
24. Zielonka, J.; Joseph, J.; Sikora, A.; Hardy, M.; Ouari, O.; Vasquez-Vivar, J.; Cheng, G.; Lopez, M.; Kalyanaraman, B. Mitochondria-Targeted Triphenylphosphonium-Based Compounds: Syntheses, Mechanisms of Action, and Therapeutic and Diagnostic Applications. *Chem. Rev.* **2017**, *117*, 10043–10120. [CrossRef] [PubMed]
25. Kalyanaraman, B.; Cheng, G.; Hardy, M.; Ouari, O.; Lopez, M.; Joseph, J.; Zielonka, J.; Dwinell, M.B. A Review of the Basics of Mitochondrial Bioenergetics, Metabolism, and Related Signaling Pathways in Cancer Cells: Therapeutic Targeting of Tumor Mitochondria with Lipophilic Cationic Compounds. *Redox Biol.* **2018**, *14*, 316–327. [CrossRef] [PubMed]
26. Marrache, S.; Pathak, R.K.; Dhar, S. Detouring of Cisplatin to Access Mitochondrial Genome for Overcoming Resistance. *Proc. Natl. Acad. Sci. USA* **2014**, *111*, 10444–10449. [CrossRef] [PubMed]
27. Smith, R.A.J.; Hartley, R.C.; Murphy, M.P. Mitochondria-Targeted Small Molecule Therapeutics and Probes. *Antioxid. Redox Signal.* **2011**, *15*, 3021–3038. [CrossRef]
28. Spivak, A.Y.; Nedopekina, D.A.; Gubaidullin, R.R.; Dubinin, M.V.; Belosludtsev, K.N. Conjugation of Natural Triterpenic Acids with Delocalized Lipophilic Cations: Selective Targeting Cancer Cell Mitochondria. *J. Pers. Med.* **2021**, *11*, 470. [CrossRef]
29. Han, M.; Vakili, M.R.; Soleymani Abyaneh, H.; Molavi, O.; Lai, R.; Lavasanifar, A. Mitochondrial Delivery of Doxorubicin via Triphenylphosphine Modification for Overcoming Drug Resistance in MDA-MB-435/DOX Cells. *Mol. Pharm.* **2014**, *11*, 2640–2649. [CrossRef] [PubMed]
30. Millard, M.; Gallagher, J.D.; Olenyuk, B.Z.; Neamati, N. A Selective Mitochondrial-Targeted Chlorambucil with Remarkable Cytotoxicity in Breast and Pancreatic Cancers. *J. Med. Chem.* **2013**, *56*, 9170–9179. [CrossRef] [PubMed]
31. Boukalova, S.; Stursa, J.; Werner, L.; Ezrova, Z.; Cerny, J.; Bezawork-Geleta, A.; Pecinova, A.; Dong, L.; Drahotka, Z.; Neuzil, J. Mitochondrial Targeting of Metformin Enhances Its Activity against Pancreatic Cancer. *Mol. Cancer Ther.* **2016**, *15*, 2875–2886. [CrossRef] [PubMed]

32. Rohlenova, K.; Sachaphibulkij, K.; Stursa, J.; Bezawork-Geleta, A.; Blecha, J.; Endaya, B.; Werner, L.; Cerny, J.; Zobalova, R.; Goodwin, J.; et al. Selective Disruption of Respiratory Supercomplexes as a New Strategy to Suppress Her2 high Breast Cancer. *Antioxid. Redox Signal.* **2017**, *26*, 84–103. [CrossRef]
33. Skulachev, V.P. A Biochemical Approach to the Problem of Aging: “Megaproject” on Membrane-Penetrating Ions. The First Results and Prospects. *Biochem. Mosc.* **2007**, *72*, 1385–1396. [CrossRef] [PubMed]
34. Antonenko, Y.N.; Avetisyan, A.V.; Bakeeva, L.E.; Chernyak, B.V.; Chertkov, V.A.; Domnina, L.V.; Ivanova, O.Y.; Izyumov, D.S.; Khailova, L.S.; Klishin, S.S.; et al. Mitochondria-Targeted Plastoquinone Derivatives as Tools to Interrupt Execution of the Aging Program. *Biochemistry* **2008**, *73*, 1273–1287. [PubMed]
35. Severin, F.F.; Severina, I.I.; Antonenko, Y.N.; Rokitskaya, T.I.; Cherepanov, D.A.; Mokhova, E.N.; Vyssokikh, M.Y.; Pustovidko, A.V.; Markova, O.V.; Yaguzhinsky, L.S.; et al. Penetrating cation/fatty acid anion pair as a mitochondria-targeted protonophore. *Proc. Natl. Acad. Sci. USA* **2010**, *107*, 663–668. [CrossRef]
36. Smith, R.A.J.; Hartley, R.C.; Cochemé, H.M.; Murphy, M.P. Mitochondrial Pharmacology. *Trends Pharmacol. Sci.* **2012**, *33*, 341–352. [CrossRef]
37. Spivak, A.Y.; Keiser, J.; Vargas, M.; Gubaidullin, R.R.; Nedopekina, D.A.; Shakurova, E.R.; Khalitova, R.R.; Odinkov, V.N. Synthesis and Activity of New Triphenylphosphonium Derivatives of Betulin and Betulinic Acid against *Schistosoma Mansoni* in Vitro and in Vivo. *Bioorg. Med. Chem.* **2014**, *22*, 6297–6304. [CrossRef] [PubMed]
38. Nedopekina, D.A.; Gubaidullin, R.R.; Odinkov, V.N.; Maximchik, P.V.; Zhivotovsky, B.; Bel’skii, Y.P.; Khazanov, V.A.; Manuylova, A.V.; Gogvadze, V.; Spivak, A.Y. Mitochondria-Targeted Betulinic and Ursolic Acid Derivatives: Synthesis and Anticancer Activity. *MedChemComm* **2017**, *8*, 1934–1945. [CrossRef]
39. Spivak, A.Y.; Nedopekina, D.A.; Shakurova, E.R.; Khalitova, R.R.; Gubaidullin, V.N.; Odinkov, V.N.; Dzhemilev, U.M.; Bel’skii, Y.P.; Bel’skaya, N.V.; Stankevic, S.A.; et al. Synthesis of lupane triterpenoids with triphenylphosphonium substituents and studies of their antitumor activity. *Russ. Chem. Bull. Int. Ed.* **2013**, *62*, 188–198. [CrossRef]
40. Tsepaveva, O.V.; Nemtarev, A.V.; Salikhova, T.I.; Abdullin, T.I.; Grigor’eva, L.R.; Khozyainova, S.A.; Mironov, V.F. Synthesis, Anticancer, and Antibacterial Activity of Betulinic and Betulonic Acid C-28-Triphenylphosphonium Conjugates with Variable Alkyl Linker Length. *Anticancer Agents Med. Chem.* **2020**, *20*, 286–300. [CrossRef]
41. Tsepaveva, O.V.; Mironov, V.F.; Khairutdinov, B.I.; Zue, Y.F. Reaction of 30-Bromolup-20(29)-ene-3 β ,28-diyl Diacetate with Triphenylphosphine. *Russ. J. Org. Chem.* **2014**, *50*, 919–920. [CrossRef]
42. Ye, Y.; Zhang, T.; Yuan, H.; Li, D.; Lou, H.; Fan, P. Mitochondria-Targeted Lupane Triterpenoid Derivatives and Their Selective Apoptosis-Inducing Anticancer Mechanisms. *J. Med. Chem.* **2017**, *60*, 6353–6363. [CrossRef] [PubMed]
43. Xu, G.; Xu, X.; Liu, J.; Jia, Q.; Ke, C.; Zhang, H.; Xu, C.; Ou, E.; Tan, W. Mitochondria-Targeted Triphenylphosphonium Conjugated C-3 Modified Betulin: Synthesis, Antitumor Properties and Mechanism of Action. *ChemMedChem* **2022**, *17*, e202100659. [CrossRef] [PubMed]
44. Grymel, M.; Zawojak, M.; Adamek, J. Triphenylphosphonium Analogues of Betulin and Betulinic Acid with Biological Activity: A Comprehensive Review. *J. Nat. Prod.* **2019**, *82*, 1719–1730. [CrossRef]
45. Thibeault, D.; Gauthier, C.; Legault, J.; Bouchard, J.; Dufour, P.; Pichette, A. Synthesis and Structure–Activity Relationship Study of Cytotoxic Germanicane- and Lupane-Type 3 β -O-Monodesmosidic Saponins Starting from Betulin. *Bioorg. Med. Chem.* **2007**, *15*, 6144–6157. [CrossRef] [PubMed]
46. Kazakova, O.B.; Giniyatullina, G.V.; Yamansarov, E.Y.; Tolstikov, G.A. Betulin and Ursolic Acid Synthetic Derivatives as Inhibitors of Papilloma Virus. *Bioorg. Med. Chem. Lett.* **2010**, *20*, 4088–4090. [CrossRef]
47. Kashiwada, Y.; Chiyo, J.; Ikeshiro, Y.; Nagao, T.; Okabe, H.; Cosentino, L.M.; Fowke, K.; Lee, K.H. 3,28-Di-O-(Dimethylsuccinyl)-Betulin Isomers as Anti-HIV Agents. *Bioorg. Med. Chem. Lett.* **2001**, *11*, 183–185. [CrossRef]
48. Komissarova, N.G.; Dubovitskii, S.N.; Orlov, A.V.; Shitikova, O.V. New Conjugates of Betulin with 2-Aminoethanesulfonic Acid. *Chem. Nat. Compd.* **2019**, *55*, 300–304. [CrossRef]
49. Krukiewicz, K.; Bednarczyk-Cwynar, B.; Turczyn, R.; Zak, J.K. EQCM Verification of the Concept of Drug Immobilization and Release from Conducting Polymer Matrix. *Electrochim. Acta* **2016**, *212*, 694–700. [CrossRef]

Article

One-Pot and Catalyst-Free Transformation of *N*-Protected 1-Amino-1-Ethoxyalkylphosphonates into Bisphosphonic Analogs of Protein and Non-Protein α -Amino Acids

 Anna Kuźnik ^{1,2,*} , Dominika Kozicka ^{1,2}, Wioleta Hawranek ¹, Karolina Socha ¹ and Karol Erfurt ³ 

¹ Department of Organic Chemistry, Bioorganic Chemistry and Biotechnology, Silesian University of Technology, B. Krzywoustego 4, 44-100 Gliwice, Poland; dominika.kozicka@polsl.pl (D.K.); wiolhaw@gmail.com (W.H.); karosoc504@student.polsl.pl (K.S.)

² Biotechnology Center, Silesian University of Technology, B. Krzywoustego 8, 44-100 Gliwice, Poland

³ Department of Chemical Organic Technology and Petrochemistry, Silesian University of Technology, B. Krzywoustego 4, 44-100 Gliwice, Poland; karol.erfurt@polsl.pl

* Correspondence: anna.kuznik@polsl.pl; Tel.: +48-032-237-1613; Fax: +48-032-237-2094

Abstract: Herein, we describe the development of one-pot transformation of α -ethoxy derivatives of phosphorus analogs of protein and non-protein α -amino acids into biologically important *N*-protected 1-aminobisphosphonates. The proposed strategy, based on the three-component reaction of 1-(*N*-acylamino)-1-ethoxyphosphonates with triphenylphosphonium tetrafluoroborate and triethyl phosphite, facilitates good to excellent yields under mild reaction conditions. The course of the reaction was monitored by ³¹P NMR spectroscopy, allowing the identification of probable intermediate species, thus making it possible to propose a reaction mechanism. In most cases, there is no need to use a catalyst to provide transformation efficiency, which increases its attractiveness both in economic and ecological terms. Furthermore, we demonstrate that the one-pot procedure can be successfully applied for the synthesis of structurally diverse *N*-protected bisphosphonic analogs of α -amino acids. As shown, the indirect formation of the corresponding phosphonium salt as a reactive intermediate during the conversion of 1-(*N*-acylamino)-1-ethoxyphosphonate into a 1-aminobisphosphonate derivative is a crucial component of the developed methodology.

Keywords: α -aminobisphosphonates; α -ethoxyphosphonates; phosphonium salts; *N*-acylimidates; Michaelis–Becker reaction; Michaelis–Arbuzov reaction

Citation: Kuźnik, A.; Kozicka, D.; Hawranek, W.; Socha, K.; Erfurt, K. One-Pot and Catalyst-Free Transformation of *N*-Protected 1-Amino-1-Ethoxyalkylphosphonates into Bisphosphonic Analogs of Protein and Non-Protein α -Amino Acids. *Molecules* **2022**, *27*, 3571. <https://doi.org/10.3390/molecules27113571>

Academic Editor: Erika Bálint

Received: 19 May 2022

Accepted: 30 May 2022

Published: 2 June 2022

Publisher's Note: MDPI stays neutral with regard to jurisdictional claims in published maps and institutional affiliations.



Copyright: © 2022 by the authors. Licensee MDPI, Basel, Switzerland. This article is an open access article distributed under the terms and conditions of the Creative Commons Attribution (CC BY) license (<https://creativecommons.org/licenses/by/4.0/>).

1. Introduction

1-(*N*-Acylamino)alkylene-1,1-bisphosphonates belong to the group of geminal 1-amino-1,1-bisphosphonates (ABPs), and they are characterized by the presence of the P-C(N)-P skeleton. In addition to being synthetic analogs of inorganic pyrophosphate, which is a regulator of calcium metabolism in living organisms, these compounds are considered as structural analogs of α -aminophosphonic acids, which are phosphorus equivalents of α -amino acids [1]. It is known that α -aminophosphonic acids exhibit significant biological activity, including anti-viral, anti-bacterial, anti-inflammatory, and anti-tumor, are potent enzyme inhibitors, and act as herbicides and regulators of plant growth [2–5]. Their functionalization with an additional phosphoryl group results in the formation of 1 amino-1,1-bisphosphonates (Figure 1a), the activity of which is even stronger, due to the presence of a P-C-P backbone, which has a documented affinity for hydroxyapatite and is resistant to enzymatic hydrolysis [6]. The above factors determine the biological properties of ABPs and the wide range of applications associated therewith.

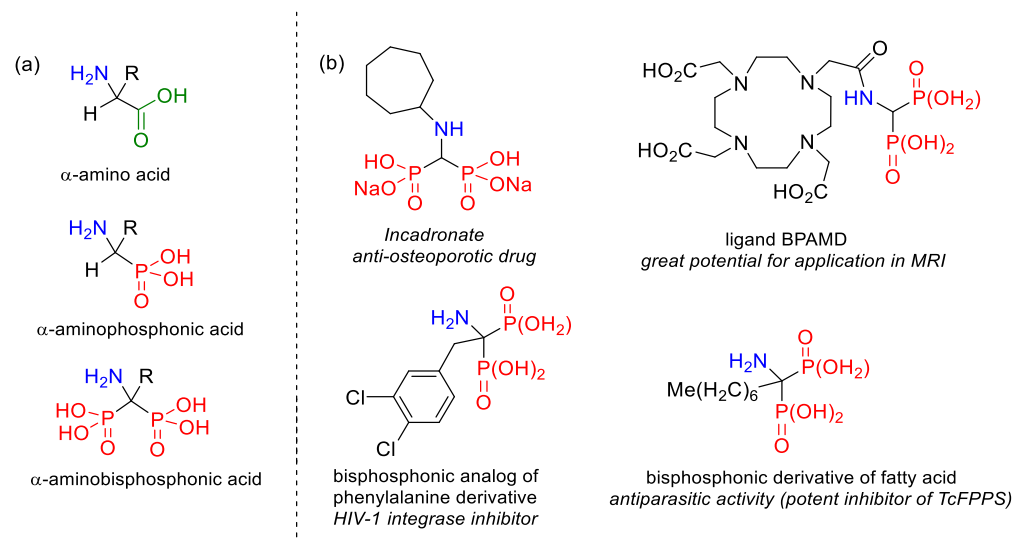


Figure 1. (a) Comparison of the structures of α -amino acid, α -aminophosphonic acid and α -aminobisphosphonic acid. (b) Representative examples of α -aminobisphosphonates with medical applications.

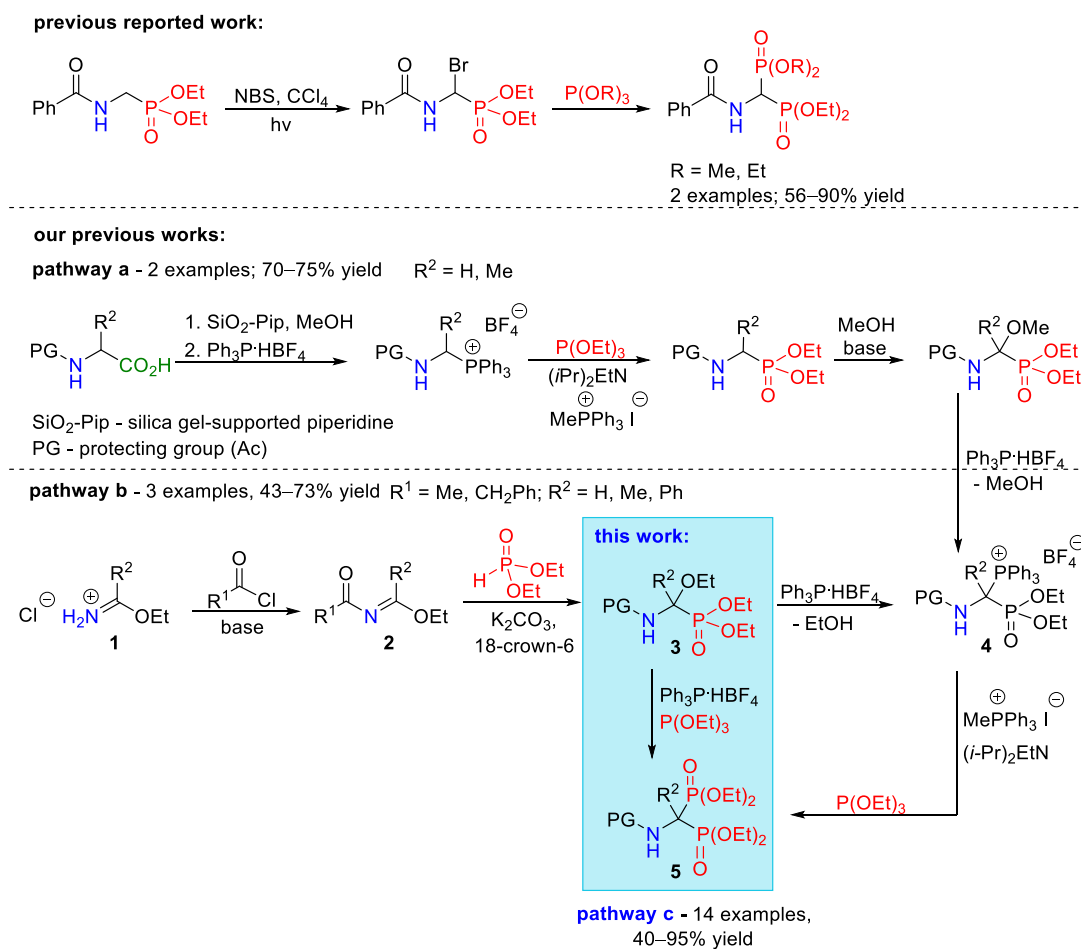
Along with 1-hydroxy-1,1-bisphosphonates, ABPs are a potent inhibitors of bone resorption used in clinical practice in the treatment of diseases such as osteoporosis, Paget's disease, or hypercalcemia [7,8]. An example of this is cycloheptylaminoethylene-1,1-bisphosphonate, which is a representative of the latest generation of anti-osteoporotic drugs, commercialized as Incadronate [9]. In addition to anti-resorptive activity, ABPs also show other useful properties, including anti-bacterial [10], anti-viral [11], anti-parasitic [12,13], and herbicidal [14], which provides evidence of their continued development as therapeutics and plant protection agents (Figure 1b). Clinical trials have been conducted on the use of ABPs in oncological therapy, especially immunotherapy [15]. Moreover, thanks to their high affinity for hydroxyapatite and the presence of the amino group in the α position, which enables their further structural modification, they have also become of interest for new drug delivery systems to bone tissue. This is achieved by the formation of conjugates with pharmacological agents, such as radioisotopes, anti-inflammatory drugs, proteins, and agents intended for augmentation of systemic bone mass or antibiotics. The conjugates of ABPs with cytostatics appear to be particularly promising, and they are being tested for their potential use in targeted anti-cancer therapies [16,17]. The high affinity for mineralized tissues is also utilized in the synthesis of new diagnostic agents that enable the imaging of bone tissue by MRI or PET, which is an interesting alternative to the currently used scintigraphy [18]. Great potential for application as a contrast agent in MRI imaging is demonstrated by the complex of the BPAMD ligand with gadolinium, containing a fragment of ABP as a "bone-seeking" moiety (Figure 1b) [19]. The chelating properties of some ABPs are also used to remove radioactive metallic toxins from water or blood [20], as well as for the functionalization of the surface of supermagnetic iron oxide nanoparticles (SPION) used in MRI [18].

Due to the important applications of ABPs, the development of a general and efficient method for their synthesis, or the improvement of previous synthetic methods, still attracts much attention. Currently, there is a range of different methods for the preparation of ABPs. However, they are often utilized for the simplest representatives of this group of compounds, i.e., derivatives of ABPs containing only hydrogen and a variously substituted amino group at the central carbon atom. Among the known methods for the synthesis of ABPs, the following should be mentioned: three-component condensation of amines with dialkyl phosphites in the presence of ethyl orthoformate [21–23], Beckmann rearrangement of oximes in the presence of phosphites by using POCl_3 as a promoter [24], prolonged heating of nitriles with excess phosphoric acid in the presence of phosphorus trichloride and anhydrous benzenesulfonic acid [12], bisphosphonylation of amides

using diethyl phosphite in the Tf_2O -activated reaction in the presence of 2,6-lutidine a base [25], double hydrophosphonylation of nitriles with dialkyl phosphites mediated by titanocene/propylene oxide [26], or $\text{ZnCl}_2/\text{Et}_3\text{N}$ system [20], as well as nickel-catalyzed double hydrophosphonylation of aromatic nitriles with trialkyl phosphites assisted by Et_3B as a reaction promoter [27]. Most of these synthetic strategies, especially those using unreactive nitriles, are carried out under harsh reaction conditions and in the presence of catalytic systems or mediators (often hazardous agents). What is more, as the side chains attached to the α carbon have a significant influence on the biological activities [8,28], it seems that the purposeful synthesis of functionalized α -aminobisphosphonate derivatives is of big importance in the search for compounds with a desirable biomedical profile. This is especially true of such models with the substituents at the α -position identical with those characteristic for natural α -amino acids, both protein and non-protein. The development of a general method for the synthesis of ABPs, providing structural diversity of the product and performed under mild, preferably catalyst-free reaction conditions, is thus highly sought after.

Recently, we have focused our efforts on developing a new synthetic procedure that allows access to not only α -aminobisphosphonic acids derivatives but also to their asymmetrical analogs. This allows the scope of applicability to be extended and thus the universality of the proposed method for synthesis of bisphosphorus organic compounds. Because each of the phosphorus groups is introduced separately into the final molecule, it has been found that phosphorus analogs of α -amino acids functionalized with a nucleofugal group at the α position are convenient substrates for this type of transformation. To the best of our knowledge, there are only a few reports on the preparation of tetraethyl 1-(*N*-acylamino)alkylene-1,1-bisphosphonates in the Michaelis–Arbuzov-type reaction of triethyl phosphite with diethyl 1-(*N*-acylamino)alkylphosphonates containing a nucleofugal group at the α -position. Despite the presence of the *N*-acylamino group and the dialkoxyphosphoryl group with an electron-withdrawing inductive effect, this type of functionalization of 1-(*N*-acylamino)alkylphosphonates is necessary to display the electrophilicity of their α -carbon required for further reaction. Thus, only one example of this type of transformation has been reported in the literature involving diethyl 1-(*N*-benzoylamino)bromomethylphosphonate synthesized by photochemical bromination of the starting 1-(*N*-benzoylamino)methylphosphonate with NBS [29]. The subsequent Michaelis–Arbuzov-type reaction of diethyl 1-(*N*-benzoylamino)bromomethylphosphonate with trimethyl and triethyl phosphites provided the expected 1-(*N*-benzoylamino)methylene-1,1-bisphosphonates in a yield of 56–90% (Scheme 1).

Other substrates that have been used in this reaction in the presence of Hünig's base and methyltriphenylphosphonium iodide as catalysts are diethyl 1-(*N*-acetylamino)-1-triphenylphosphoniumalkylphosphonate tetrafluoroborates **4**, which can be considered as α -functionalized triphenylphosphonium derivatives of 1-(*N*-acylamino)alkylphosphonates [30]. The starting phosphonium salts **4** were synthesized here from diethyl 1-aminoalkylphosphonates readily available from *N*-acyl- α -amino acids [31,32] by initially subjecting them to electrochemical oxidation to introduce the nucleofugal methoxy group into the α -position, which was followed by nucleophilic substitution of the obtained diethyl 1-(*N*-acetylamino)-1-methoxyalkylphosphonates with triphenylphosphonium tetrafluoroborate (Scheme 1, pathway a). The biggest limitation of this transformation is the electrochemical oxidation step, which was efficiently performed for only two of the simplest models of phosphorus analogs of α -amino acids, namely for the derivative of glycine and alanine, having at the α -position a hydrogen atom or a methyl group, respectively. Attempts to perform this process for the phosphorus analogs of valine and phenylalanine have failed, possibly due to a steric hindrance of the bulky substituent at the α -position.



Scheme 1. Synthetic routes for the synthesis of tetraethyl 1-(*N*-acylamino)alkylene-1,1-bisphosphonates from α -functionalized derivatives of phosphorus analogs of α -amino acids, such as diethyl 1-(*N*-benzoylamino)bromomethylphosphonate [29] and diethyl 1-(*N*-acetylamino)-1-triphenylphosphoniumalkylphosphonate tetrafluoroborates **4** obtained from α -methoxyphosphonates (pathway a) [30] or α -ethoxyphosphonates (pathway b) [33].

To overcome this problem, we looked for a different method of obtaining α -alkoxy derivatives of diethyl α -aminophosphonates with the result of the development of another procedure for the preparation of diethyl 1-(*N*-acylamino)-1-ethoxyalkylphosphonates **3** obtained in a Michaelis–Becker-type reaction of ethyl *N*-acylimidates **2** with diethyl phosphite (Scheme 1, pathway b) [33]. This opened up the wider applicability of this method, since the electrochemical oxidation step required in the previous transformation is omitted in this case, while the starting *N*-acylimidates **2** are readily available from the well-known class of chemical compounds, i.e., ethyl imidate hydrochlorides **1** [34,35]. We then converted 1-(*N*-acylamino)-1-ethoxyalkylphosphonates **3** into diethyl 1-(*N*-acylamino)-1-triphenylphosphoniumalkylphosphonate tetrafluoroborates **4**, whose utility in the synthesis of tetraethyl 1-(*N*-acylamino)alkylene-1,1-bisphosphonates **5** has so far been described for only three models of α -ethoxy derivatives of diethyl alkylphosphonates **3**, such as phosphorus analogs of glycine, alanine and phenylglycine, which have the amino group protected with selected acyl groups (acetyl or phenylacetyl). The target tetraethyl 1-(*N*-acylamino)alkylene-1,1-bisphosphonates **5** were synthesized here in the Michaelis–Arbuzov-type α -amidoalkylation reaction of triethyl phosphite with the previously obtained phosphonium salts **4** in a double catalytic system in the presence of methyltriphenylphosphonium iodide and Hünig’s base.

In a continuation of our efforts to improve the recently developed procedure for the preparation of organobisphosphorus compounds, and hoping that it has the potential

to become a general method for the synthesis of ABPs, we report an efficient, catalyst-free one-pot transformation of α -ethoxyaminophosphonate derivatives into tetraethyl 1-(*N*-acylamino)alkylene-1,1-bisphosphonates possessing at the α position a side chain identical with those characteristic for natural α -amino acids, both protein and non-protein (Scheme 1, pathway c).

2. Results and Discussion

2.1. Optimization of Conditions for the Synthesis of α -Ethoxy Derivatives of Phosphorus Analogs of α -Amino Acids

The starting diethyl 1-(*N*-acylamino)-1-ethoxyalkylphosphonates (Table 1, **3a–n**) were synthesized according to a previously described two-step protocol with some modifications (Scheme 2) [33]. The general procedure consists of acylation of the imidate hydrochloride **1** with an acyl chloride (Step 1) and the Michaelis–Becker-like addition of diethyl phosphite to ethyl *N*-acylimidate **2** (Step 2).

Table 1. Yields of the Michaelis–Becker-like nucleophilic addition of diethyl phosphite to ethyl *N*-acylimidates ¹.

| Entry | Comp. 3 | PG | R ² | Nu (eq.) | Time [days] | Temperature [°C] | Yield ² |
|-------|-----------|-----|--|----------|-------------|------------------|--------------------|
| 1 | 3a | Cbz | Me | 1.2 | 2 | rt | 94 |
| 2 | 3b | Piv | Me | 1.2 | 3 | rt | 74 |
| 3 | 3c | Cbz | H | 1.2 | 2 | −10 | 93 |
| 4 | 3d | Cbz | CH ₂ Ph | 2 | 4 | −20 | 88 |
| 5 | 3e | Ac | CH ₂ Ph | 1.2 | 4 | rt | 53 |
| 6 | 3f | Cbz | Et | 1.2 | 3 | −5 | 82 |
| 7 | 3g | Cbz | Pr | 2 | 4 | −10 | 68 |
| 8 | 3h | Cbz | <i>i</i> -Pr | 2 | 7 | −40 | 53 |
| 9 | 3i | Cbz | Bu | 2 | 4 | −10 | 54 |
| 10 | 3j | Cbz | <i>i</i> -Bu | 3 | 7 | −40 | 32 |
| 11 | 3k | Ac | <i>i</i> -Bu | 2 | 7 | −40 | 65 |
| 12 | 3l | Cbz | CH ₂ OMe | 1.2 | 4 | −10 | 91 |
| 13 | 3m | Cbz | Ph | 1.2 | 3 | rt | 82 |
| 14 | 3n | Cbz | 1,4-CH ₂ -C ₆ H ₄ OMe | 3 | 3 | −25 | 70 |

¹ Reaction conditions: diethyl *N*-acylimidate **2** (1 eq.), diethyl phosphite (1.2–3.0 eq.), 18-crown-6 (0.12 eq.), K₂CO₃ (1.35 eq.), hexane. ² Isolated yield.

These modifications in the acylation step of ethyl imidate hydrochlorides **1**, most often with benzyl chloroformate, require a different base for this reaction (hitherto, Et₃N has been used in the acylation reaction with acetyl chloride). This change was introduced following optimization studies to select an appropriate base to improve the efficiency of acylation, and sometimes even allow it to be carried out, taking into account the key role of the base environment in this reaction. Since the use of Et₃N in the acylation reaction of ethyl acetimidate hydrochloride **1a** with benzyl chloroformate was unsuccessful (Scheme 2, entry 1), 2,4,6-collidine and (*i*-Pr)₂EtN (Hünig's base) were used as bases for this reaction. When the weaker aromatic base such as 2,4,6-collidine was used, the expected reaction took place with the product being isolated in a moderate yield of 55% (entry 2). Therefore, we tried to perform the same reaction using Hünig's base with comparable strength to Et₃N but non-nucleophilic in nature to prevent side reactions. This facilitated a higher yield of 90% for the acylation product (entry 3). The lack of nucleophilic character of Hünig's base can be explained by the presence of two sterically extended isopropyl groups. Based on this successful result, the acylation reactions for all the remaining ethyl imidate hydrochlorides with benzyl chloroformate were carried out with the use of this base (Scheme 2), except for the 2-methoxyacetimidate hydrochloride **1l** which, in the case of 2,4,6-collidine, proved to be much more effective (entry 15).

| Entry | Imidate 2 | R ¹ | R ² | Base | Yield ² [%] |
|-------|-----------------|---------------------|--|----------------------------------|------------------------|
| 1 | 2a | OCH ₂ Ph | Me | Et ₃ N | – |
| 2 | 2a | OCH ₂ Ph | Me | 2,4,6-collidine | 55 |
| 3 | 2a | OCH ₂ Ph | Me | (<i>i</i> -Pr) ₂ EtN | 90 |
| 4 | 2b | <i>t</i> -Bu | Me | Et ₃ N | 80 |
| 5 | 2c | OCH ₂ Ph | H | (<i>i</i> -Pr) ₂ EtN | 34 |
| 6 | 2d ³ | OCH ₂ Ph | CH ₂ Ph | (<i>i</i> -Pr) ₂ EtN | 88 |
| 7 | 2e | Me | CH ₂ Ph | Et ₃ N | 85 |
| 8 | 2f | OCH ₂ Ph | Et | (<i>i</i> -Pr) ₂ EtN | 80 |
| 9 | 2g | OCH ₂ Ph | Pr | (<i>i</i> -Pr) ₂ EtN | 95 |
| 10 | 2h | OCH ₂ Ph | <i>i</i> -Pr | (<i>i</i> -Pr) ₂ EtN | 79 |
| 11 | 2i | OCH ₂ Ph | Bu | (<i>i</i> -Pr) ₂ EtN | 91 |
| 12 | 2j | OCH ₂ Ph | <i>i</i> -Bu | (<i>i</i> -Pr) ₂ EtN | 99 |
| 13 | 2k | Me | <i>i</i> -Bu | 2,4,6-collidine | 63 |
| 14 | 2k | Me | <i>i</i> -Bu | (<i>i</i> -Pr) ₂ EtN | 99 |
| 15 | 2l | OCH ₂ Ph | CH ₂ OMe | 2,4,6-collidine | 74 |
| 16 | 2m ⁴ | OCH ₂ Ph | Ph | (<i>i</i> -Pr) ₂ EtN | 58 |
| 17 | 2n | OCH ₂ Ph | 1,4-CH ₂ -C ₆ H ₄ OMe | (<i>i</i> -Pr) ₂ EtN | 98 |

¹ Reaction conditions: imidate hydrochloride **1** (1 eq.), base (2.2 eq.), acyl chloride (1 eq.), CH₂Cl₂, Ar atmosphere, rt. ² Isolated yield. ³ Hünig's base (2.1 eq.) was dosed in two equal portions, before and after the addition of benzyl chloroformate (1.25 eq.). ⁴ Toluene was used as a solvent.

Scheme 2. Two-step synthesis of 1-(*N*-acylamino)-1-ethoxyalkylphosphonates from ethyl imidate hydrochlorides and yields of acylation of ethyl imidate hydrochlorides **1** with acid chlorides in a presence of selected bases.

As for the second step of the synthesis of 1-(*N*-acylamino)-1-ethoxyalkylphosphonates **3**, i.e., the nucleophilic addition of diethyl phosphite to ethyl *N*-acylimidates **2** in the Michaelis–Becker-like reaction, the modification was required to improve its efficiency. For most of the synthesized models, especially those with an amine group protected with a Cbz group, it consisted of reducing the reaction temperature under PTC conditions up to -40 °C and using a two-fold molar excess of the nucleophile in some cases. Therefore, it was possible to obtain the expected products, which were isolated by extraction initially with hexane and then with dichloromethane and subsequent purification of the extracts by column chromatography in satisfactory yields (Table 1).

2.2. Development of an Optimized One-Pot Procedure for the Synthesis of Bisphosphonate Analogs of α -Amino Acids

The electrophilicity of the α -carbon atom of the synthesized α -ethoxyphosphonate derivative **3** is too low to allow its direct transformation into the target bisphosphonate **5** using the Michaelis–Arbuzov-type reaction with triethyl phosphite [30]. Therefore, to increase the electrophilicity of this position, it was necessary to convert α -ethoxyphosphonate **3** to the corresponding phosphonium salt **4**, which is much more reactive and thus susceptible to subsequent reaction with the nucleophilic triethyl phosphite. To better understand the reaction mechanism for the preparation of diethyl 1-(*N*-acylamino)-1-triphenylphosphoniumalkylphosphonate tetrafluoroborates **4** from 1-(*N*-acylamino)-1-ethoxyalkylphosphonates **3**, we attempted the synthesis of another model phosphonium salt from the α -ethoxy derivative of the

phosphorus analog of phenylalanine **3d** with the intention of isolating and purifying it. For this purpose, triphenylphosphonium tetrafluoroborate was added to α -ethoxyphosphonate in a slight molar deficiency (0.9 eq. to 1 eq. **3d**). To our surprise, the ^{31}P NMR analysis of the reaction mixture taken after 10 and 30 min at room temperature did not confirm the presence of the expected phosphonium salt **4d**. Therefore, this synthesis was repeated according to the same procedure, but modifying the reaction conditions by lowering the temperature to -15°C . Again, no characteristic signals belonging to the corresponding phosphonium salt were found. Due to the predicted instability of the synthesized diethyl 1-(*N*-benzyloxycarbonylamino)-1-triphenylphosphonium-2-phenylethylphosphonate tetrafluoroborate, it was decided to conduct another experiment at -40°C , which was analogous to the described procedure above but with a slight molar excess of triphenylphosphonium tetrafluoroborate (5%). After 40 min of reaction, NMR analysis was performed, which provided very promising results with two clearly visible doublets at 13.9 and 39.8 ppm of the same coupling constant ($J = 12.9\text{ Hz}$), confirming the presence of the desired phosphonium salt **4d** (Figure 2b).

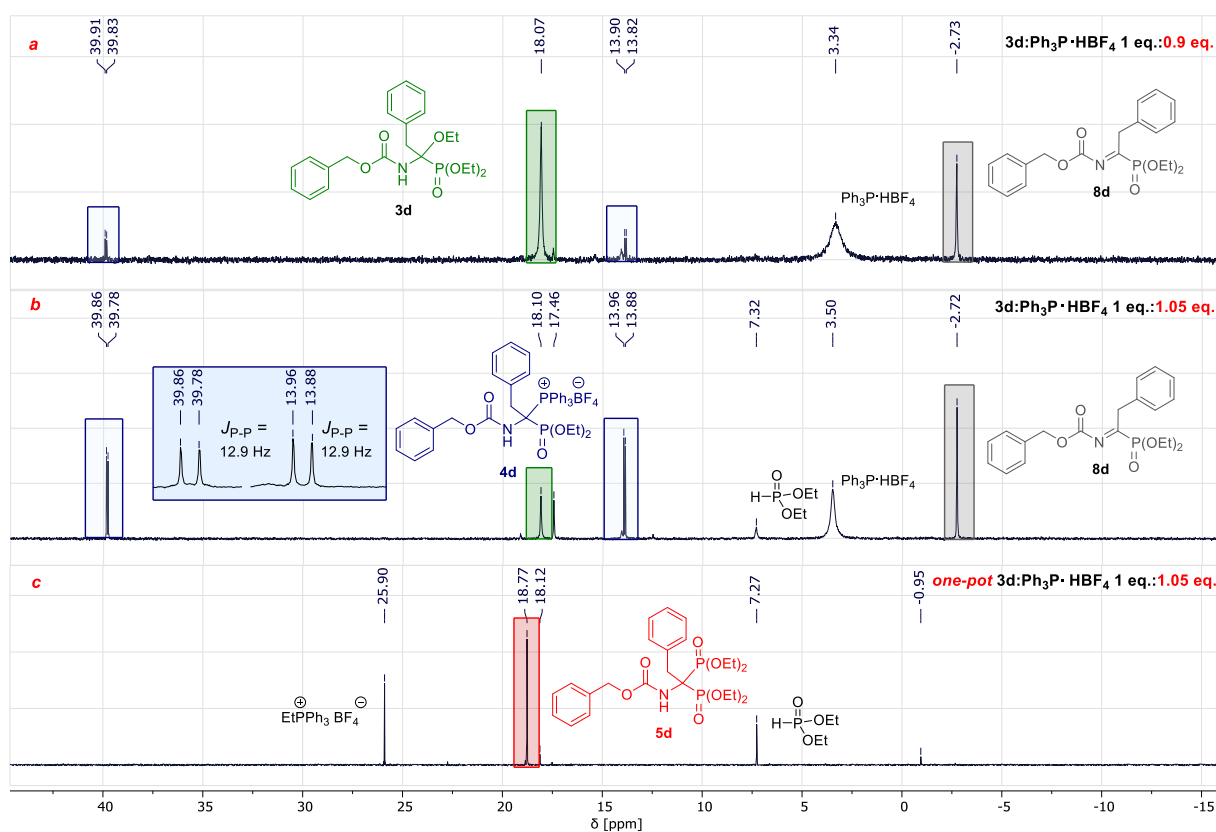
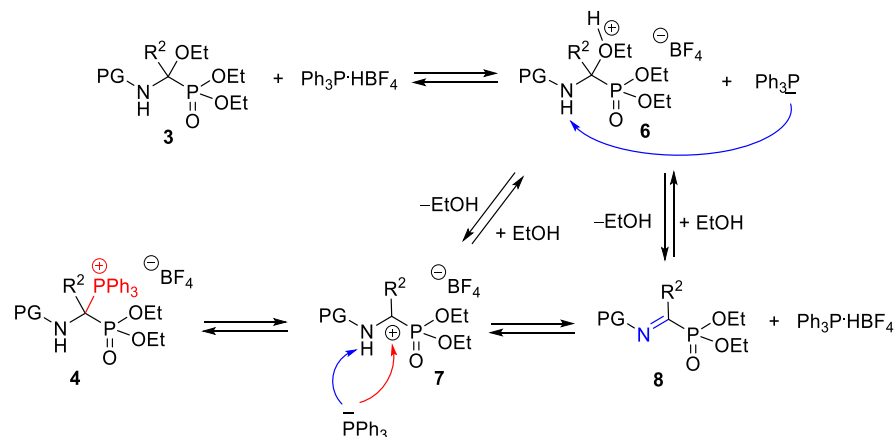


Figure 2. (a) ^{31}P NMR spectrum of the reaction mixture obtained in the synthesis of phosphonium salt **4d** carried out with a slight molar deficiency of $\text{Ph}_3\text{P}\cdot\text{HBF}_4$ at -40°C . (b) ^{31}P NMR spectrum of the reaction mixture obtained in the synthesis of a phosphonium salt **4d** conducted with a slight molar excess of $\text{Ph}_3\text{P}\cdot\text{HBF}_4$ at -40°C . (c) ^{31}P NMR spectrum of the reaction mixture obtained in the one-pot synthesis of bisphosphonic derivative **5d** performed with the use of $\text{Ph}_3\text{P}\cdot\text{HBF}_4$ in a molar excess at room temperature.

In subsequent experiments, the conditions for the synthesis of **4d** were modified in order to assess their impact on the reaction course (Figure 2). Initially, it was assumed that in the synthesis of phosphonium salt, the temperature was a determining factor having an influence on the reaction course. This was based on the results of the first experiments, in which two expected doublets at 13.9 and 39.8 ppm were observed only for the reaction carried out at -40°C . However, subsequent experiments showed that it is not the temperature but the molar ratio of triphenylphosphonium tetrafluoroborate to

substrate **3** that is of key importance for obtaining phosphonium salt **4**. During a detailed analysis of reaction mixture ^{31}P NMR spectra, it was observed that in those syntheses in which a slight molar deficiency of $\text{Ph}_3\text{P}\cdot\text{HBF}_4$ was used, the following signals were present in the spectrum, at approximately 18.1 ppm of high intensity together with a weaker signal at -2.8 ppm and broad intense signal at 3.3 ppm corresponding to $\text{Ph}_3\text{P}\cdot\text{HBF}_4$ in the equilibrium (Figure 2a). In contrast, there was a lack of the signal at 18.1 ppm when excess $\text{Ph}_3\text{P}\cdot\text{HBF}_4$ was used, and the equilibrium of the reaction shifted toward an intermediate with the signal at about -2.8 ppm, and phosphonium salt **4d**, appearing in the form of two doublets (Figure 2b).

An explanation is presented in Scheme 3, which illustrates the proposed mechanism for the formation of phosphonium salt **4** in an equilibrium reaction via intermediates **6–8**. In the first step, α -ethoxyphosphonate **3** reacts with triphenylphosphonium tetrafluoroborate to give salt **6** with a protonated ethoxy group in the α position and liberated triphenylphosphine. When there is a shortage of triphenylphosphonium tetrafluoroborate in relation to reaction substrate, it becomes partially blocked at this stage. Ethanol is cleaved from the resulting salt **6**, the iminophosphonate **8** (which is in equilibrium with iminium type-cation **7**) is formed and $\text{Ph}_3\text{P}\cdot\text{HBF}_4$ is regenerated. This results in an intense ^{31}P NMR spectrum signal at approximately 18.1 ppm, belonging to the starting compound **3d**, along with the broad signal of $\text{Ph}_3\text{P}\cdot\text{HBF}_4$ (3.3 ppm) and intermediate iminophosphonate **8** at about -2.8 ppm (which is consistent with the literature data for this type of imines [36]). Conversely, in the case of an excess of triphenylphosphonium tetrafluoroborate (higher acidity of the reaction mixture), iminium-type cation **7** is formed more readily. Finally, the active electrophilic center of iminium-type cation **7** is attacked by triphenylphosphine and the desired phosphonium salt **4** is formed (Scheme 3).



Scheme 3. A plausible mechanism for the formation of diethyl 1-(*N*-acylamino)-1-triphenylphosphoniumalkylphosphonate tetrafluoroborate **4** proposed based on the analysis of ^{31}P NMR spectra (161.9 MHz/ CDCl_3 ; ppm) of reaction mixtures obtained in reactions of substrate **3** and $\text{Ph}_3\text{P}\cdot\text{HBF}_4$ used in various molar ratios.

The confirmation of the proposed phosphonium salt **4** formation mechanism is illustrated in the ^{31}P NMR spectra of the reaction mixture (Figure 2a,b), with signals belonging to α -ethoxyphosphonate **3d** at approximately 18.1 ppm, $\text{Ph}_3\text{P}\cdot\text{HBF}_4$ at 3.3 ppm, intermediate iminophosphonate **8d** at about -2.8 ppm and expected phosphonium salt **4d** with the corresponding two doublets at 13.9 and 39.8 ppm. The presence of all these signals on the spectra of the reaction mixtures is evidence that this is an equilibrium reaction, in the course of which the acidity of the environment is of critical importance. On the other hand, reducing the temperature allows an unstable reaction intermediate to be observed in the ^{31}P NMR spectrum as two intense doublets belonging to the expected phosphonium salt **4d**.

On the basis of the postulated mechanism, it was concluded that diethyl 1-(*N*-benzyloxycarbonylamino) -1-triphenylphosphonium-2-phenylethylphosphonate tetraflu-

oroborate **4d**, which is a reactive intermediate in this synthetic route, has to be used *in situ* in the subsequent transformation into α -aminobisphosphonate derivative **5d**. Hence, we attempted to transform diethyl 1-(*N*-acylamino)-1-ethoxyalkylphosphonates **3** into 1-(*N*-acylamino)alkylene-1,1-bisphosphonates **5** via the corresponding phosphonium salts using a one-pot method (Figure 2c). Our screening tests, described above with the use of the model **3d** as substrate, showed that during the synthesis of phosphonium salt **4d**, iminophosphonate **8d** is spontaneously formed in the equilibrium mixture. From this, we concluded that the addition of Hünig's base as a catalyst in the synthesis of the bisphosphonates is redundant. Indeed, carrying out the one-pot synthesis of tetraethyl 1-(*N*-benzyloxycarbonylamino)-2-phenylethylene-1,1-bisphosphonate **5d** by dissolving all the reactants, namely substrate **3d**, $\text{Ph}_3\text{P}\cdot\text{HBF}_4$ and triethylphosphite, used in a molar ratio of 1:1.05:1.5, in dichloromethane at 0–5 °C in the presence of methyltriphenylphosphonium iodide as a catalyst (0.25 eq.) and left at this temperature for 45 min, then at room temperature overnight, resulted in the expected product **5d** with an estimated yield of 52% (Table 2, entry 1). This success inspired further optimization of the transformation conditions. This included the question of whether the presence of methyltriphenylphosphonium iodide is necessary here, since the function of the dealkylating agent for triethoxyphosphonium salt, obtained as an intermediate in the Michaelis–Arbuzov reaction, could potentially be performed by triphenylphosphine that is present in the reaction mixture [37,38]. The next experiment was therefore carried out in an analogous manner but without the addition of any catalysts, providing an estimate yield of bisphosphonate **5d** of 73% (Table 2, entry 2). This result provided unequivocal evidence that the catalyst methyltriphenylphosphonium iodide is not required for this reaction to proceed efficiently, and thus, the reaction takes place in an autocatalytic system. It was also considered whether the dosing of the reactants at a reduced temperature is required and what molar ratio of $\text{Ph}_3\text{P}\cdot\text{HBF}_4$ to α -ethoxyphosphonate **3d** will be the most favorable. Table 2 shows the molar ratios of these reagents used together with the bisphosphonate yields afforded in the given experiments when performed at room temperature. It was found that it is sufficient to use a slight molar excess of $\text{Ph}_3\text{P}\cdot\text{HBF}_4$ at the level of 5–8% in the synthesis of α -aminobisphosphonate, and that room temperature is optimal for this transformation (entries 3 and 4). The progress of the reaction was monitored by NMR spectroscopy, and finally, it was concluded that 6 h was sufficient time for the substrate to completely react (entry 5). The product was isolated from the reaction mixture by extraction with toluene and subsequent purification of the extract by column chromatography to afford the target bisphosphonate in a yield of 86%.

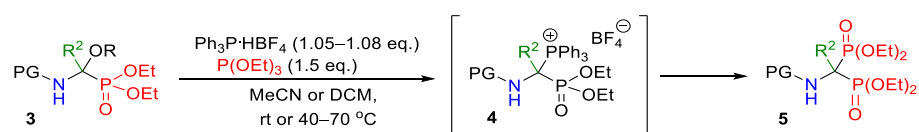
Table 2. Screening of reaction conditions in the synthesis of bisphosphonate model **5d** from α -ethoxyphosphonate **3d** by the one-pot method.

| Entry | Molar Ratios | | $\text{MePh}_3\text{P}^+ \text{I}^-$ | Temperature [°C] | Time [h] | Yield [%] ¹ |
|-------|--------------|--|--------------------------------------|----------------------------|----------|------------------------|
| | 3d | $\text{Ph}_3\text{P}\cdot\text{HBF}_4$ | | | | |
| 1 | 1 | 1.06 | + | 0–5 for 45 min. then rt | 24 | 52 |
| 2 | 1 | 1.08 | – | 0–5 for 45 min. then rt | 24 | 73 |
| 3 | 1 | 1.05 | – | rt | 24 | 77 |
| 4 | 1 | 1.27 | – | rt | 24 | 75 |
| 5 | 1 | 1.06 | – | rt | 6 | 86 ² |

¹ Yield estimated from the ¹H NMR spectrum of the reaction mixture relative to the known mass of the internal standard (diphenyldimethylsilane). ² Isolated yield. + Denotes the addition of $\text{MePh}_3\text{P}^+ \text{I}^-$ as a catalyst. – Denotes that the experiment was performed without the addition of $\text{MePh}_3\text{P}^+ \text{I}^-$.

2.3. Scope of the Reaction

We then studied the scope of the one-pot reaction for the synthesis of various models of bisphosphonic analogs of protein and non-protein α -amino acids **5** according to the previous optimal conditions (Scheme 4).



| Entry | ABP 5 | PG | R ² | Solvent | Time [h] | Temperature [°C] | Yield ¹ |
|-------|-----------------|-----|--|---------------------------------|----------|------------------|--------------------|
| 1 | 5a | Cbz | Me | MeCN | 6.5 | 40 | 95 |
| 2 | 5a | Cbz | Me | CH ₂ Cl ₂ | 6.5 | 40 | 72 |
| 3 | 5b | Piv | Me | MeCN | 6 | 60 | 62 |
| 4 | 5c ² | Cbz | H | MeCN | 8 | 70 | 82 |
| 5 | 5d | Cbz | CH ₂ Ph | MeCN | 6 | rt | 73 |
| 6 | 5d | Cbz | CH ₂ Ph | CH ₂ Cl ₂ | 6 | rt | 86 |
| 7 | 5e | Ac | CH ₂ Ph | MeCN | 24 | rt | 59 |
| 8 | 5e | Ac | CH ₂ Ph | CH ₂ Cl ₂ | 24 | rt | 54 |
| 9 | 5f | Cbz | Et | MeCN | 5 | rt | 90 |
| 10 | 5f | Cbz | Et | CH ₂ Cl ₂ | 5 | rt | 79 |
| 11 | 5g | Cbz | Pr | MeCN | 6 | rt | 95 |
| 12 | 5g | Cbz | Pr | CH ₂ Cl ₂ | 6 | rt | 77 |
| 13 | 5h | Cbz | <i>i</i> -Pr | CH ₂ Cl ₂ | 5 | rt | 72 |
| 14 | 5i | Cbz | Bu | MeCN | 24 | rt | 90 |
| 15 | 5j | Cbz | <i>i</i> -Bu | MeCN | 24 | rt | 74 |
| 16 | 5j ³ | Cbz | <i>i</i> -Bu | MeCN | 24 | rt | 62 |
| 17 | 5k | Ac | <i>i</i> -Bu | MeCN | 24 | rt | 69 |
| 18 | 5l ⁴ | Cbz | CH ₂ OMe | MeCN | 5 | 70 | 52 |
| 19 | 5m | Cbz | Ph | MeCN | 8 | 60 | 40 |
| 20 | 5n | Cbz | 1,4-CH ₂ -C ₆ H ₄ OMe | MeCN | 24 | rt | 74 |
| 21 | 5n | Cbz | 1,4-CH ₂ -C ₆ H ₄ OMe | CH ₂ Cl ₂ | 24 | rt | 84 |

¹ Isolated yield. ² It was impossible to perform a one-pot synthesis of this derivative; therefore, a corresponding phosphonium salt **4c** was first obtained using Ph₃P·HBF₄ in a molar ratio of 1.12 to 1 relative to substrate **3c**, which was further transformed in situ into the bisphosphonate **5c** in the presence of a catalytic amount of Hünig's base (0.42 eq.). ³ The synthesis was performed using 1.2 eq. of P(OEt)₃. ⁴ In the synthesis of the model **5l** by the one-pot method, the most advantageous was the use of Ph₃P·HBF₄ in a molar ratio of 1.2 to 1 relative to the substrate **3l** and the addition of Hünig's base (0.2 eq. to neutralize the excess of Ph₃P·HBF₄ + 0.3 eq. as a catalytic amount).

Scheme 4. Conditions and yields for the synthesis of tetraethyl 1-(*N*-acylamino)alkylene-1,1-bisphosphonates in the Michaelis–Arbuzov-like reaction.

These optimized conditions were tested on other α -ethoxyphosphonates **3** containing either aromatic or aliphatic substituents at the α position with straight or branched chains, e.g., for valine and nor-valine or leucine and nor-leucine analogs. For most models, these conditions were well matched, and it was enough to combine all reagents without any catalyst in a chosen solvent and leave it for 5 to 24 h at room temperature to successfully perform the reaction. Subsequent isolation of the obtained product initially by extraction with toluene and then column chromatography provided target compounds **5** with good to excellent yields (72–95%; Cbz-protected amino group). However, in some cases, the use of elevated temperature (40–70 °C) was required to conduct the reaction under catalyst-free conditions (Scheme 4, entries 1–3, 19).

For the majority of the synthesized bisphosphonic derivatives of α -amino acids, the amino group was protected with an easily removable benzyloxycarbonyl group. However, the tested procedure also worked well for models with the amino group protected with other acyl groups, such as acetyl or pivaloyl, leading to expected product yields in a moderate range of 54–62% (entries 3, 7, 8, 17).

We also tested the influence of the solvent on the yield of ABPs during synthesis, finding a general relationship that acetonitrile is a better solvent for this transformation. How-

ever, for some bisphosphonates, a higher reaction yield was noted with dichloromethane (cf. entries 5, 6 and 20, 21).

For one model, namely the *N*-Cbz-protected α -ethoxy derivative of phosphorus analog of leucine, the impact of the excess of triethyl phosphite on the efficiency of the synthesis of the corresponding bisphosphonate **5j** was also evaluated. We noted that the reaction yield was higher with the use of 1.5 eq. of $P(OEt)_3$ (74%) than for 1.2 eq. of the nucleophile used (62%) (entries 15, 16).

It should be noted that in the case of the bisphosphonic derivative of serine **5l**, the final one-pot reaction was successfully carried out only when the Hünig's base was also used as a catalyst and when the reaction temperature was raised to 70 °C. The selection of such parameters undoubtedly facilitated the transformation of the indirectly formed phosphonium salt **4l** into the target product **5l** (Figure 3b), which was obtained with a yield of 52% (Scheme 4, entry 18). The course of the reaction at a lower temperature or without the use of a catalyst ended at the stage of phosphonium salt generation, which can be seen in the ^{31}P NMR spectrum of the reaction mixture in the form of two doublets with the same coupling constant, which was accompanied by the very small signal of the desired product **5l** ($\delta = 17.9$ ppm) (Figure 3a).

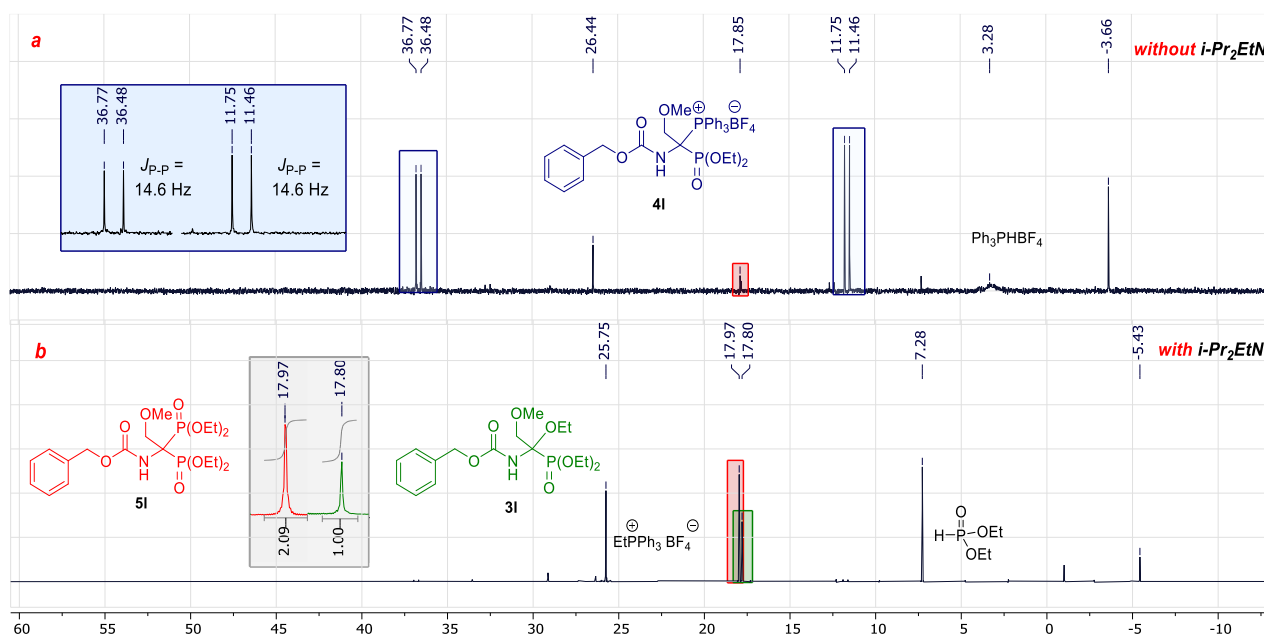
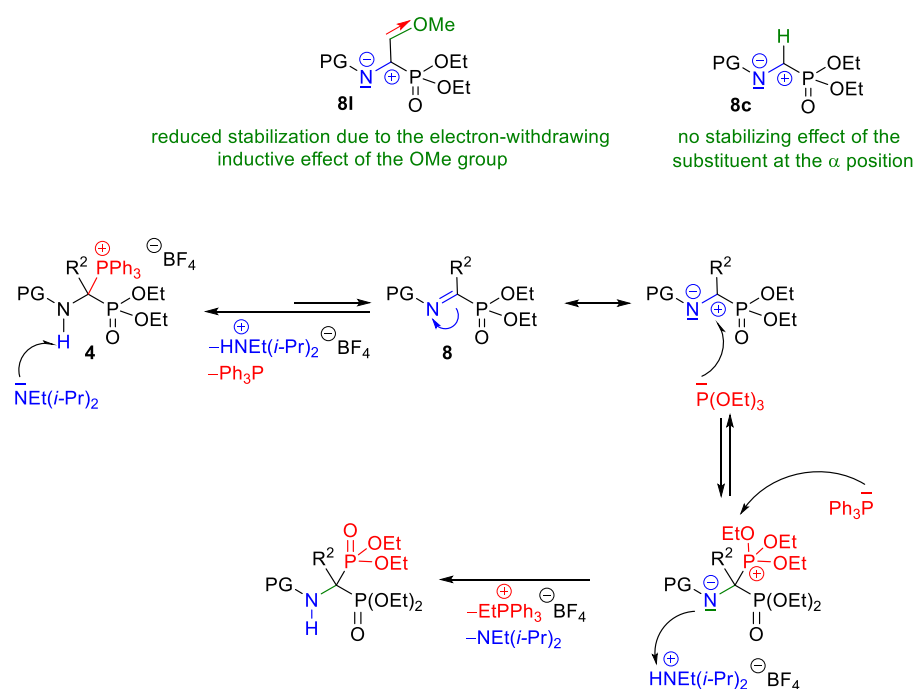


Figure 3. (a) ^{31}P NMR spectrum of the reaction mixture obtained from the synthesis of the bisphosphonic derivative of serine **5l** without the use of Hünig's base catalyst at 70 °C. (b) ^{31}P NMR spectrum of the reaction mixture obtained in the synthesis of bisphosphonic derivative of serine **5l** performed in the presence of catalytic Hünig's base at 70 °C.

The functional role of Hünig's base as a catalyst in the synthesis of a bisphosphonic serine derivative relies on assisting the generation of the corresponding *N*-acyliminophosphonate **8l** from the resulting phosphonium salt **4l** during the final Michaelis–Arbuzov-type reaction. This is the rate-determining step of the transformation. For the serine model, due to the presence of an electron-withdrawing methoxymethyl group at the α position, the stabilization of the iminophosphonate **8l** is reduced (Scheme 5), so that the reaction equilibrium is strongly shifted toward the phosphonium salt **4l**. Hence, the addition of Hünig's base is necessary to allow the Michaelis–Arbuzov-type reaction to be performed, as it is shown in the postulated mechanism for this transformation (Scheme 5).



Scheme 5. The role of Hünig's base as a catalyst for the Michaelis–Arbuzow-type reaction in the synthesis of bisphosphonic derivatives of serine **5b** ($\text{R}^2 = \text{CH}_2\text{OMe}$) and glycine **5c** ($\text{R}^2 = \text{H}$) models.

Moreover, in the case of the bisphosphonic derivative of glycine **5c**, not only was the Hünig's base catalyst and an increased temperature (70°C) required, but the intended one-pot transformation was not achieved. This is likely due to the reversible nature of the transformation being carried out, during which the recovery of the starting α -ethoxyphosphonate **3c** in the equilibrium reaction was privileged (Scheme 3), due to the presence of ethanol in the reaction mixture. To overcome this problem, the synthesis of the bisphosphonic derivative **5c** was carried out according to a two-step procedure. First, the phosphonium salt **4c** was obtained by heating the residue after evaporation of the solvent from a homogeneous mixture, which was prepared by dissolving α -ethoxyphosphonate **3c** and triphenylphosphonium tetrafluoroborate at 85°C under reduced pressure for 5 h. Next, the crude phosphonium salt **4c** was subjected to the Michaelis–Arbuzow-type reaction after dissolving in acetonitrile by treatment with triethylphosphite in the presence of Hünig's base, resulting in a very good yield of the target product **5c** (82%) (Scheme 4, entry 4).

Regarding the prospects for the further use of synthesized bisphosphonate models **5**, we will carry out structural modifications to increase their application potential in medical chemistry. One future research direction involves the synthesis of conjugates by combining compounds with proven biological activity (e.g., anti-cancer) with α -aminobisphosphonates that can be used as drug carriers. Their functional role in these complexes includes not only the targeted delivery of pharmaceuticals to the bone tissue but also synergistic action with anti-cancer drugs. Minor modifications to the structure of α -aminobisphosphonates will also be of interest. The acylation of α -aminobisphosphonates with the use of appropriate chloroacyl chlorides will allow the production of building blocks that are useful in the synthesis of a ligands, which can be used as potential contrast agents for imaging of bone mineral by MRI after complexing with paramagnetic ions.

3. Materials and Methods

3.1. General Information

Melting points were determined in capillaries in a Stuart Scientific SMP3 melting point apparatus and were uncorrected. $^1\text{H-NMR}$ spectra were acquired on a Varian 400 spectrometer at an operating frequency of 400 MHz using tetramethylsilane (TMS) as the resonance shift standard. $^{13}\text{C-NMR}$ spectra were recorded on a Varian 400 at 100 MHz, us-

ing solvent resonance as the internal standard. ^{31}P -NMR spectra were recorded on a Varian 400 at 161.9 MHz without the resonance shift standard, with respect to H_3PO_4 as 0 ppm. All chemical shifts (δ) are reported in ppm and coupling constants (J) in Hz. IR-spectra were measured on a Nicolet 6700 FT-IR spectrophotometer, Thermo Scientific (attenuated total reflectance method; ATR). The high-resolution mass spectra (HRMS) were obtained by electrospray ionization (ESI) using a Waters Corporation Xevo G2 QTOF instrument. The reactions of Michaelis–Becker-like addition of diethyl phosphite to ethyl *N*-acylimidates were performed at reduced temperatures using Julabo ultra-low refrigerated-circulator F81-ME. For TLC analysis, Merck TLC silica gel 60 F₂₅₄ plates were used. The plates were visualized by UV light (254 nm) and/or dipped in a solution of cerium sulfate and tetrahydrate of ammonium heptamolybdate in $\text{H}_2\text{SO}_{4\text{aq}}$ and heated. Kieselgel 60 (Merck, 0.040–0.063 mm) was used for column chromatography.

Materials. All solvents and common reagents were obtained from commercial suppliers. Diethyl phosphite and triethyl phosphite were purchased from Acros Organics.

^1H , ^{13}C , ^{31}P NMR spectrum of all new compounds **3**, **4c** and **5** are available in Supplementary Materials.

3.2. Substrate Synthesis

Commercially available ethyl acetimidate and ethyl benzimidate hydrochlorides (**1a** and **1m**) were used. Ethyl formimidate hydrochloride **1c** was synthesized according to the procedure described by Schmitz and Ohme [39]. The rest of ethyl imidate hydrochlorides **1** were obtained according to the protocol given by Yadav and Babu [40].

General procedure for the synthesis of diethyl 1-(*N*-acylamino)-1-ethoxyalkylphosphonates **3**.

Step 1: *N*-Acylation reactions of ethyl imidate hydrochlorides **1** were carried out according to the modified procedure described by Kuźnik et al. [33]. The appropriate base (17.6 mmol, 2.2 eq.) (Scheme 2) was added to a solution of ethyl imidate hydrochloride **1** (8.0 mmol, 1.0 eq.) in dry CH_2Cl_2 (25 mL) and cooled in an ice bath. Then, acid chloride (8.0 mmol, 1.0 eq.) was added to the reaction mixture dropwise. The ice bath was removed, and the mixture was stirred under argon atmosphere, at room temperature, for 24 h, and the solvent was evaporated under reduced pressure. To separate the product from base hydrochloride, hexane (15 mL) was added to the residue. The precipitate was filtered over celite, and the filtrate was concentrated to give ethyl *N*-acylimidate **2**.

Due to the instability of the ethyl *N*-(benzyloxycarbonyl)formimidate **2c**, *N*-acylation of ethyl formimidate hydrochloride **1c** was carried out in an ice bath, and the reaction time was reduced to 2 h. The obtained compound was immediately used in the next step.

Synthesis of ethyl *N*-(benzyloxycarbonyl)phenylacetimidate **2d** was performed using Hünig's base (2.1 eq.), added in two equal portions, before and after the addition of benzyl chloroformate (1.25 eq.). *N*-Acylation of ethyl benzimidate hydrochloride **1m** was carried out using toluene as a solvent.

Ethyl N-(benzyloxycarbonyl)acetimidate (**2a**). Pale yellow oil; 90% yield (1.592 g). ^1H -NMR (400 MHz, CDCl_3): δ 7.40–7.32 (m, 5H), 5.19 (s, 2H), 4.16 (q, $J = 7.2$ Hz, 2H), 2.05 (s, 3H) 1.28 (t, $J = 7.2$ Hz, 3H). ^{13}C -NMR (100 MHz, CDCl_3): δ 167.9, 161.5, 135.9, 128.5, 128.4, 128.3, 68.1, 63.2, 18.4, 13.8. HRMS (ESI) m/z : calcd for $\text{C}_{12}\text{H}_{15}\text{NO}_3\text{Na}$ [$\text{M} + \text{Na}$] $^+$ 244.0950, found 244.0951.

Ethyl N-(pivaloyl)acetimidate (**2b**) [41]. Pale yellow oil; 80% yield (1.095 g). ^1H -NMR (400 MHz, CDCl_3): δ 4.12 (q, $J = 7.0$ Hz, 2H), 1.98 (s, 3H), 1.29 (t, $J = 7.2$ Hz, 3H), 1.18 (s, 9H). ^{13}C -NMR (100 MHz, CDCl_3): δ 191.7, 161.3, 62.5, 41.4, 27.1, 18.0, 14.0. HMRS (ESI) m/z : calcd for $\text{C}_9\text{H}_{18}\text{NO}_2$ [$\text{M} + \text{H}$] $^+$ 172.1338, found 172.1343.

Ethyl N-(benzyloxycarbonyl)formimidate (**2c**). Pale yellow oil; 34% yield (565 mg). ^1H -NMR (400 MHz, CDCl_3): δ 8.45 (s, 1H), 7.54–7.28 (m, 5H), 5.12 (s, 2H), 4.34 (q, $J = 7.0$ Hz, 2H), 1.34 (t, $J = 7.0$ Hz, 3H). ^{13}C -NMR (100 MHz, CDCl_3): δ 167.1, 161.9, 135.6, 128.53, 128.51, 128.3, 68.4, 64.5, 13.8. HRMS (ESI) m/z : calcd for $\text{C}_{11}\text{H}_{14}\text{NO}_3$ [$\text{M} + \text{H}$] $^+$ 208.0974, found 208.0977.

Ethyl N-(benzyloxycarbonyl)-2-phenylacetimidate (**2d**). Pale yellow oil; 88% yield (2.095 g). ^1H -NMR (400 MHz, CDCl_3): δ 7.35–7.19 (m, 10H), 5.13 (s, 2H), 4.16 (q, $J = 7.2$ Hz, 2H), 3.68

(s, 2H), 1.25 (t, $J = 7.2$ Hz, 3H). ^{13}C -NMR (100 MHz, CDCl_3): δ 167.9, 161.1, 135.7, 134.2, 129.2, 128.6, 128.5, 128.3, 127.0, 68.2, 63.5, 38.8, 13.8. HRMS (ESI) m/z : calcd for $\text{C}_{18}\text{H}_{20}\text{NO}_3$ $[\text{M} + \text{H}]^+$ 298.1443, found 298.1443.

Ethyl N-(acetyl)-2-phenylacetimidate (2e) [42]. Pale yellow oil; 85% yield (1.389 g). ^1H -NMR (400 MHz, CDCl_3): δ 7.26–7.53 (m, 5H), 4.10 (q, $J = 7.0$ Hz, 2H), 3.66 (s, 2H), 1.96 (s, 3H), 1.17 (t, $J = 7.2$ Hz, 3H). ^{13}C -NMR (100 MHz, CDCl_3): δ 183.4, 161.1, 134.5, 129.3, 128.6, 127.1, 62.9, 38.3, 26.3, 13.8. HRMS (ESI) m/z : calcd for $\text{C}_{12}\text{H}_{16}\text{NO}_2$ $[\text{M} + \text{H}]^+$ 206.1181, found 206.1184.

Ethyl N-(benzyloxycarbonyl)propanimidate (2f). Pale yellow oil; 80% yield (1.507 g). ^1H -NMR (400 MHz, CDCl_3): δ 7.42–7.30 (m, 5H), 5.19 (s, 2H), 4.15 (q, $J = 7.2$ Hz, 2H), 2.36 (q, $J = 7.6$ Hz, 2H), 1.28 (t, $J = 7.2$ Hz, 3H), 1.12 (t, $J = 7.6$ Hz, 3H). ^{13}C -NMR (100 MHz, CDCl_3): δ 170.7, 161.4, 135.9, 128.5, 128.4, 128.3, 68.1, 63.0, 26.1, 13.8, 10.5. HRMS (ESI) m/z : calcd for $\text{C}_{13}\text{H}_{17}\text{NO}_3\text{Na}$ $[\text{M} + \text{Na}]^+$ 258.1106, found 258.1108.

Ethyl N-(benzyloxycarbonyl)butanimidate (2g) [43]. Pale yellow oil; 95% yield (1.899 g). ^1H -NMR: (400 MHz, CDCl_3): δ 7.42–7.28 (m, 5H), 5.19 (s, 2H), 4.15 (q, $J = 7.2$ Hz, 2H), 2.30 (t, $J = 7.6$ Hz, 2H), 1.57 (sext, $J = 7.6$ Hz, 2H), 1.28 (t, $J = 7.2$ Hz, 3H), 0.86 (t, $J = 7.4$ Hz, 3H). ^{13}C -NMR: (100 MHz, CDCl_3): δ 169.8, 161.3, 135.9, 128.5, 128.3, 68.0, 62.9, 34.4, 19.5, 13.8, 13.6. HMRS (ESI) m/z : calcd for $\text{C}_{14}\text{H}_{19}\text{NO}_3\text{Na}$ $[\text{M} + \text{Na}]^+$ 272.1263, found 272.1264.

Ethyl N-(benzyloxycarbonyl)-2-methylpropanimidate (2h). Pale yellow oil; 79% yield (1.580 g). ^1H -NMR (400 MHz, CDCl_3): δ 7.41–7.30 (m, 5H), 5.18 (s, 2H), 4.12 (q, $J = 7.2$ Hz, 2H), 2.72 (sept, $J = 7.0$ Hz, 1H), 1.27 (t, $J = 7.2$ Hz, 3H), 1.12 (d, $J = 6.8$ Hz, 6H). ^{13}C -NMR (100 MHz, CDCl_3): δ 172.2, 161.2, 136.0, 128.5, 128.4, 128.2, 68.1, 62.9, 32.8, 19.5, 13.7. HMRS (ESI) m/z : calcd for $\text{C}_{14}\text{H}_{20}\text{NO}_3$ $[\text{M} + \text{H}]^+$ 250.1443 found 250.1445.

Ethyl N-(benzyloxycarbonyl)pentanimidate (2i) [43]. Yellow oil; 91% yield (1.912 g). ^1H -NMR (400 MHz, CDCl_3): δ 7.42–7.29 (m, 5H), 5.18 (s, 2H), 4.14 (q, $J = 7.2$ Hz, 2H), 2.32 (t, $J = 7.8$ Hz, 2H), 1.53 (qu, $J = 7.6$ Hz, 2H), 1.28 (t, $J = 7.2$ Hz, 3H), 1.25 (sext, $J = 7.2$ Hz, 2H) 0.85 (t, $J = 7.2$ Hz, 3H) ^{13}C -NMR (100 MHz, CDCl_3): δ 170.0, 161.4, 135.9, 128.5, 128.3, 68.1, 63.0, 32.4, 28.2, 22.3, 13.9, 13.6. HMRS (ESI) m/z : calcd for $\text{C}_{15}\text{H}_{21}\text{NO}_3\text{Na}$ $[\text{M} + \text{Na}]^+$ 286.1419, found 286.1417.

Ethyl N-(benzyloxycarbonyl)-3-methylbutanimidate (2j). Yellow oil; 99% yield (2.083 g). ^1H -NMR (400 MHz, CDCl_3): δ 7.42–7.26 (m, 5H), 5.18 (s, 2H), 4.15 (q, $J = 7.0$ Hz, 2H), 2.02 (d, $J = 7.2$ Hz, 2H), 1.97 (sept, $J = 6.8$ Hz, 1H), 1.28 (t, $J = 7.2$ Hz, 3H), 0.85 (d, $J = 6.8$ Hz, 6H). ^{13}C -NMR (100 MHz, CDCl_3): δ 169.1, 161.3, 135.9, 128.6, 128.5, 128.4, 68.0, 62.9, 41.1, 26.3, 22.2, 13.9. HMRS (ESI) m/z : calcd for $\text{C}_{15}\text{H}_{22}\text{NO}_3$ $[\text{M} + \text{H}]^+$ 264.1600, found 264.1599.

Ethyl N-(acetyl)-3-methylbutanimidate (2k). Pale yellow oil; 99% yield (1.358 g). ^1H -NMR (400 MHz, CDCl_3): δ 4.09 (q, $J = 7.1$ Hz, 2H), 2.20 (d, $J = 7.2$ Hz, 2H), 2.16 (s, 3H) 2.05 (m, 1H), 1.28 (t, $J = 7.0$ Hz, 3H), 0.95 (d, $J = 6.8$ Hz, 6H). ^{13}C -NMR (100 MHz, CDCl_3): δ 183.4, 162.2, 62.4, 41.0, 26.7, 26.1, 22.3, 13.9. HRMS (ESI) m/z : calcd for $\text{C}_9\text{H}_{18}\text{NO}_2$ $[\text{M} + \text{H}]^+$ 172.1338, found 172.1343.

Ethyl N-(benzyloxycarbonyl)-2-methoxyacetimidate (2l). Pale yellow oil; 74% yield (1.481 g). ^1H -NMR (400 MHz, CDCl_3): δ 7.42–7.30 (m, 5H), 5.17 (s, 2H), 4.20 (q, $J = 7.2$ Hz, 2H), 4.10 (s, 2H), 3.24 (s, 3H), 1.30 (t, $J = 7.2$ Hz, 3H). ^{13}C -NMR (100 MHz, CDCl_3): δ 164.4, 160.6, 135.9, 128.7, 128.4, 128.2, 69.7, 68.0, 63.5, 59.6, 13.8. HMRS (ESI) m/z : calcd for $\text{C}_{13}\text{H}_{17}\text{NO}_4\text{Na}$ $[\text{M} + \text{Na}]^+$ 274.1055, found 274.1057.

Ethyl N-(benzyloxycarbonyl)benzimidate (2m). Pale yellow oil; 58% yield (1.316 g). ^1H -NMR (400 MHz, CDCl_3): δ 7.55–7.50 (m, 5H), 5.12 (s, 2H), 4.34 (q, $J = 7.0$ Hz, 2H), 1.34 (t, $J = 7.0$ Hz, 3H). ^{13}C -NMR (100 MHz, CDCl_3): δ 167.1, 161.9, 135.6, 128.53, 128.51, 128.3, 68.4, 64.5, 13.8. HRMS (ESI) m/z : calcd for $\text{C}_{17}\text{H}_{18}\text{NO}_3$ $[\text{M} + \text{H}]^+$ 284.1287, found 284.1290.

Ethyl N-(benzyloxycarbonyl)-2-(4-methoxyphenyl)acetimidate (2n). Yellow oil; 96% yield (2.519 g). ^1H -NMR (400 MHz, CDCl_3): δ 7.36–7.32 (m, 5H), 7.11–7.09 (m, 2H), 6.80–6.76 (m, 2H), 5.13 (s, 2H), 4.15 (q, $J = 7.2$ Hz, 2H), 3.77 (s, 3H), 3.61 (s, 2H), 1.25 (t, $J = 7.2$ Hz, 3H). ^{13}C -NMR (100 MHz, CDCl_3): δ 168.06, 161.19, 158.62, 135.76, 130.26, 128.57, 128.51, 128.31, 113.90, 68.17, 63.42, 55.20, 37.96, 13.79. HMRS (ESI) m/z : calcd for $\text{C}_{19}\text{H}_{22}\text{NO}_4$ $[\text{M} + \text{H}]^+$ 328.1549, found 328.1546.

Step 2: Transformation of ethyl *N*-acylimidates **2** into diethyl 1-(*N*-acylamino)-1-ethoxyalkylphosphonates **3** was carried out according to the modified protocol given by Kuźnik et al. [33]. Potassium carbonate (4 wt % H₂O) (2.7 mmol, 373 mg, 1.35 eq.) and 18-crown-6 (0.24 mmol, 63 mg, 0.12 eq.) were added to the solution of ethyl *N*-acylimidate **2** (2 mmol, 1 eq.) in hexane (6.4 mL). Then, diethyl phosphite (2.4 mmol, 331 mg, 0.31 mL, 1.2 eq. or 4.0 mmol, 552 mg, 0.51 mL, 2 eq. or 6.0 mmol, 829 mg, 0.77 mL, 3 eq.) was added dropwise. The reaction mixture was stirred vigorously at room or reduced temperature for the appropriate time period (Table 1). Then, K₂CO₃ was filtered off, and crude product was isolated by washing first with hexane and then with CH₂Cl₂. The crude product was further purified by column chromatography on silica gel using the mixture of CH₂Cl₂/MeOH/Et₃N (100:1:1) as the eluent.

Diethyl 1-(N-benzyloxycarbonylamino)-1-ethoxyethylphosphonate (3a). White solid; 94% yield (338 mg); mp 69.4 to 71.0 °C. ¹H-NMR (400 MHz, CDCl₃): δ 7.39–7.30 (m, 5H), 5.71 (br d, *J* = 7.9 Hz, 1H), 5.09 (ABq, *J* = 12.2 Hz, 2H), 4.24–4.12 (m, 4H)^a, 3.67–3.60 (m, 2H), 1.90 (d, *J* = 15.0 Hz, 3H), 1.34 (t, *J* = 7.2 Hz, 3H) and 1.32 (t, *J* = 7.2 Hz, 3H)^b, 1.17 (t, *J* = 7.0, 3H). ¹³C-NMR (100 MHz, CDCl₃): δ 154.6 (d, *J* = 16.4 Hz), 136.2, 128.5, 128.2, 128.1, 84.4 (d, *J* = 196.8 Hz), 66.7, 63.8 (d, *J* = 6.9 Hz), 63.4 (d, *J* = 6.9 Hz), 58.5 (d, *J* = 8.0 Hz), 18.9, 16.4 (d, *J* = 5.3 Hz), 15.4. ³¹P-NMR (162 MHz, CDCl₃): δ 18.5. IR (ATR): 3203, 1717, 1541, 1224, 1047, 960, 750 cm⁻¹. HMRS (ESI) *m/z*: calcd for C₁₆H₂₇NO₆P [M + H]⁺ 360.1576, found 360.1578. ^aOverlapping signals of P(O)(OCH₂CH₃)₂ groups. ^bOverlapping signals of P(O)(OCH₂CH₃)₂ groups.

Diethyl 1-(N-pivaloylamino)-1-ethoxyethylphosphonate (3b). Colorless oil; 74% yield (230 mg). ¹H-NMR (400 MHz, CDCl₃): δ 6.41 (br d, *J* = 7.5 Hz, 1H), 4.26–4.14 (m, 4H)^a, 3.67–3.59 (m, 2H), 1.95 (d, *J* = 15.4 Hz, 3H), 1.35 (t, *J* = 7.0 Hz, 3H) and 1.34 (t, *J* = 7.0 Hz, 3H)^b, 1.22 (s, 9H), 1.19 (t, *J* = 7.0 Hz, 3H). ¹³C-NMR (100 MHz, CDCl₃): δ 178.8 (d, *J* = 9.9 Hz), 84.9 (d, *J* = 194.5 Hz), 63.9 (d, *J* = 6.9 Hz), 63.1 (d, *J* = 6.9 Hz), 58.6 (d, *J* = 9.5 Hz), 39.9, 27.5, 18.7, 16.5 (d, *J* = 5.3 Hz), 16.4 (d, *J* = 5.4 Hz), 15.5. ³¹P-NMR (162 MHz, CDCl₃): δ 19.1. IR (ATR): 3283, 1676, 1519, 1244, 1021, 958 cm⁻¹. HMRS (ESI) *m/z*: calcd for C₁₃H₂₉NO₅P [M + H]⁺ 310.1783, found 310.1790. ^aOverlapping signals of P(O)(OCH₂CH₃)₂ groups. ^bOverlapping signals of P(O)(OCH₂CH₃)₂ groups.

Diethyl 1-(N-benzyloxycarbonylamino)-1-ethoxymethylphosphonate (3c). Colorless oil; 93% yield (321 mg). ¹H-NMR (400 MHz, CDCl₃): δ 7.39–7.32 (m, 5H), 5.65 (dd, *J*₁ = 10.8, 4.3 Hz, 1H), 5.24 (dd, *J*₁ = 10.8 Hz, *J*₂ = 9.3 Hz, 1H), 5.15 (ABq, *J* = 12.2 Hz, 2H), 4.24–4.11 (m, 4H)^a, 3.81–3.74 (m, 1H), 3.65–3.57 (m, 1H), 1.33 (t, *J* = 7.2 Hz, 3H) and 1.29 (t, *J* = 7.0 Hz, 3H)^b, 1.22 (t, *J* = 7.2 Hz, 3H). ¹³C-NMR (100 MHz, CDCl₃): δ 156.0 (d, *J* = 12.2 Hz), 135.9, 128.6, 128.3, 128.1, 77.4 (d, *J* = 201.1 Hz), 67.4, 65.4 (d, *J* = 12.9 Hz), 63.7 (d, *J* = 6.5 Hz), 63.2 (d, *J* = 6.9 Hz), 16.38 (d, *J* = 5.3 Hz) and 16.36 (d, *J* = 5.3 Hz)^a, 14.9. ³¹P-NMR (162 MHz, CDCl₃): δ 15.9. IR (ATR): 3221, 1720, 1526, 1229, 1026, 977, 752 cm⁻¹. HMRS (ESI) *m/z*: calcd for C₁₅H₂₅NO₆P [M + H]⁺ 346.1419, found 346.1426. ^aOverlapping signals of P(O)(OCH₂CH₃)₂ groups. ^bOverlapping signals of P(O)(OCH₂CH₃)₂ groups.

Diethyl 1-(N-benzyloxycarbonylamino)-1-ethoxy-2-phenylethylphosphonate (3d). White solid; 88% yield (383 mg); mp 78.2 to 79.5 °C. ¹H-NMR (400 MHz, CDCl₃): δ 7.38–7.17 (m, 10H), 5.81 (br d, *J* = 10.6 Hz, 1H), 5.14 (ABq, *J* = 12 Hz, 2H), 4.09–3.68 (m, 7H)^a, 3.41 (dd, *J*₁ = 14.4 Hz, *J*₂ = 11.1 Hz, 2H), 1.23 (t, *J* = 7.2 Hz, 3H) and 1.21 (t, *J* = 7.2 Hz, 3H)^b, 1.05 (t, *J* = 7.0 Hz, 3H). ¹³C-NMR (100 MHz, CDCl₃): δ 154.6 (d, *J* = 16.4 Hz), 136.1, 135.6 (d, *J* = 3.6 Hz), 131.2, 128.5, 128.24, 128.19, 127.6, 126.5, 87.1 (d, *J* = 186.5 Hz), 66.8, 63.2 (d, *J* = 7.2 Hz), 62.9 (d, *J* = 7.2 Hz), 59.4 (d, *J* = 4.6 Hz), 39.1 (d, *J* = 2.9 Hz), 16.3 (d, *J* = 5.8 Hz), 16.0 (d, *J* = 6.1 Hz), 15.2. ³¹P-NMR (162 MHz, CDCl₃): δ 17.5. IR (ATR): 3204, 1726, 1548, 1245, 1019, 959, 754, 701 cm⁻¹. HMRS (ESI) *m/z*: calcd for C₂₂H₃₀NO₆NaP [M + Na]⁺ 458.1708, found 458.1704. ^aOverlapping signals of C_αCH₂C₆H₅ and P(O)(OCH₂CH₃)₂ groups. ^bOverlapping signals of P(O)(OCH₂CH₃)₂ groups.

Diethyl 1-(N-acetylamino)-1-ethoxy-2-phenylethylphosphonate (3e). White solid; 53% yield (183 mg); mp 92.8 to 94.3 °C. ¹H-NMR (400 MHz, CDCl₃): δ 7.33–7.20 (m, 5H), 6.12 (br d, *J* = 11.4 Hz, 1H), 4.12–3.92 (m, 5H)^a, 3.87–3.71 (m, 2H), 3.39 (dd, *J*₁ = 14.5 Hz, *J*₂ = 9.1 Hz,

1H), 2.04 (s, 3H), 1.29 (t, $J = 7.0$ Hz, 3H), 1.23 (t, $J = 7.0$ Hz, 3H), 1.10 (t, $J = 7.0$ Hz, 3H). ^{13}C -NMR (100 MHz, CDCl_3): δ 170.3 (d, $J = 9.2$ Hz), 135.6 (d, $J = 4.0$ Hz), 131.1, 127.7, 126.6, 87.6 (d, $J = 185.9$ Hz), 63.4 (d, $J = 7.2$ Hz), 62.8 (d, $J = 7.2$ Hz), 59.9 (d, $J = 5.3$ Hz), 38.9, 24.5, 16.4 (d, $J = 6.1$ Hz), 16.1 (d, $J = 6.1$ Hz), 15.2. ^{31}P -NMR (162 MHz, CDCl_3): δ 17.9. IR (ATR): 3185, 1670, 1548, 1218, 1029, 962, 749, 696 cm^{-1} . HMRS (ESI) m/z : calcd for $\text{C}_{16}\text{H}_{27}\text{NO}_5\text{P}$ [$\text{M} + \text{H}$] $^+$ 344.1627, found 344.1627. ^aOverlapping signals of $\text{C}_\alpha\text{CH}_2\text{C}_6\text{H}_5$ and $\text{P}(\text{O})(\text{OCH}_2\text{CH}_3)_2$ groups.

Diethyl 1-(N-benzyloxycarbonylamino)-1-ethoxypropylphosphonate (3f). White solid; 82% yield (306 mg); mp 59.4 to 60.8 °C. ^1H -NMR (400 MHz, CDCl_3): δ 7.38–7.30 (m, 5H), 5.77 (d, $J = 8.0$ Hz, 1H), 5.09 (ABq, $J = 10.0$ Hz, 2H), 4.24–4.11 (m, 4H)^a, 3.68–3.56 (m, 2H), 2.61 (ddq, $J_1 = 23.4$ Hz, $J_2 = 15.0$ Hz, $J_3 = 7.5$ Hz, 1H), 2.25 (tq, $J_1 = 14.9$ Hz, $J_2 = 7.5$ Hz, 1H), 1.33 (t, $J = 7.0$ Hz, 3H) and 1.32 (t, $J = 7.0$ Hz, 3H)^b, 1.17 (t, $J = 7.0$ Hz, 3H), 1.02 (t, $J = 7.6$ Hz, 3H). ^{13}C -NMR (100 MHz, CDCl_3): δ 154.4 (d, $J = 16.2$), 136.2, 128.5, 128.3, 128.1, 87.7 (d, $J = 189.5$ Hz), 66.7, 63.6 (d, $J = 7.2$ Hz), 63.1 (d, $J = 7.1$ Hz), 58.4 (d, $J = 7.2$ Hz), 25.2, 16.4 (d, $J = 5.7$ Hz), 15.3, 8.5 (d, $J = 2.1$ Hz). ^{31}P -NMR (162 MHz, CDCl_3): δ 19.0. IR (ATR): 3253, 1231, 1024, 773 cm^{-1} . HMRS (ESI) m/z : calcd for $\text{C}_{17}\text{H}_{28}\text{NO}_6\text{NaP}$ [$\text{M} + \text{Na}$] $^+$ 396.1552, found 396.1545. ^aOverlapping signals of $\text{P}(\text{O})(\text{OCH}_2\text{CH}_3)_2$ groups. ^bOverlapping signals of $\text{P}(\text{O})(\text{OCH}_2\text{CH}_3)_2$ groups.

Diethyl 1-(N-benzyloxycarbonylamino)-1-ethoxybutylphosphonate (3g). Colorless oil; 68% yield (263 mg). ^1H -NMR (400 MHz, CDCl_3): δ 7.39–7.31 (m, 5H), 5.78 (br d, $J = 8.0$ Hz, 1H), 5.08 (ABq, $J = 12.2$ Hz, 2H), 4.23–4.11 (m, 4H)^a, 3.68–3.55 (m, 2H), 2.61–2.47 (m, 1H), 2.23–2.11 (m, 1H), 1.54–1.44 (m, 2H), 1.33 (t, $J = 7.0$ Hz, 3H) and 1.32 (t, $J_1 = 7.0$ Hz, 3H)^b, 1.16 (t, $J = 7.0$ Hz, 3H), 0.93 (t, $J = 7.4$ Hz, 3H). ^{13}C -NMR (100 MHz, CDCl_3): δ 154.4 (d, $J = 16.1$ Hz), 136.2, 128.5, 128.1, 128.0, 87.3 (d, $J = 189.7$ Hz), 66.6, 63.6 (d, $J = 7.1$ Hz), 63.1 (d, $J = 7.0$ Hz), 58.4 (d, $J = 7.4$ Hz), 34.4, 17.2 (d, $J = 2.0$ Hz), 16.4 (d, $J = 5.5$ Hz), 15.3, 14.4. ^{31}P -NMR (162 MHz, CDCl_3): δ 19.0. IR (ATR): 2976, 1737, 1499, 1240, 1019, 969, 742 cm^{-1} . HMRS (ESI) m/z : calcd for $\text{C}_{18}\text{H}_{30}\text{NO}_6\text{NaP}$ [$\text{M} + \text{Na}$] $^+$ 410.1708, found 410.1706. ^aOverlapping signals of $\text{P}(\text{O})(\text{OCH}_2\text{CH}_3)_2$ groups. ^bOverlapping signals of $\text{P}(\text{O})(\text{OCH}_2\text{CH}_3)_2$ groups.

Diethyl 1-(N-benzyloxycarbonylamino)-1-ethoxy-2-methylpropylphosphonate (3h). White solid; 53% yield (205 mg); mp 54.2 to 55.5 °C. ^1H -NMR (400 MHz, CDCl_3): δ 7.37–7.31 (m, 5H), 5.91 (br d, $J = 10.8$ Hz, 1H), 5.09 (ABq, $J = 12.2$ Hz, 2H), 4.21–4.12 (m, 4H)^a, 3.68–3.56 (m, 2H), 3.19 (dsept, $J_1 = 32.6$ Hz, $J_2 = 7.0$ Hz, 1H), 1.33 (t, $J = 7.0$ Hz, 3H), 1.15 (t, $J = 7.0$ Hz, 3H), 1.12 (d, $J = 6.8$ Hz, 3H), 1.06 (d, $J = 6.8$ Hz, 3H). ^{13}C -NMR (100 MHz, CDCl_3): δ 154.6 (d, $J = 18.2$ Hz), 136.3, 128.5, 128.2, 128.1, 90.2 (d, $J = 185.8$ Hz), 66.7, 63.4 (d, $J = 7.2$ Hz), 62.9 (d, $J = 7.6$ Hz), 58.6 (d, $J = 6.5$ Hz), 31.4, 17.7 (d, $J = 3.1$ Hz), 17.5, 16.4 (d, $J = 5.3$ Hz), 15.3. ^{31}P -NMR (162 MHz, CDCl_3): δ 19.7. IR (ATR): 3218, 1723, 1544, 1239, 1023, 976, 745 cm^{-1} . HMRS (ESI) m/z : calcd for $\text{C}_{18}\text{H}_{31}\text{NO}_6\text{P}$ [$\text{M} + \text{H}$] $^+$ 388.1889, found 388.1890. ^aOverlapping signals of $\text{P}(\text{O})(\text{OCH}_2\text{CH}_3)_2$ groups.

Diethyl 1-(N-benzyloxycarbonylamino)-1-ethoxypentylphosphonate (3i). White solid; 54% yield (217 mg); mp 53.1 to 54.7 °C. ^1H -NMR (400 MHz, CDCl_3): δ 7.36–7.28 (m, 5H), 5.78 (br d, $J = 8.4$ Hz, 1H), 5.08 (ABq, $J = 12.2$ Hz, 2H), 4.23–4.11 (m, 4H)^a, 3.68–3.56 (m, 2H), 2.61–2.47 (m, 1H), 2.26–2.14 (m, 1H), 1.49–1.41 (m, 2H), 1.35–1.26 (m, 2H), 1.33 (t, $J = 7.0$ Hz, 3H), 1.32 (t, $J = 7.0$ Hz, 3H), 1.16 (t, $J = 7.0$ Hz, 3H), 0.91 (t, $J = 7.2$ Hz, 3H). ^{13}C -NMR (100 MHz, CDCl_3): δ 154.3 (d, $J = 16.1$ Hz), 136.2, 128.4, 128.1, 128.0, 87.3 (d, $J = 189.5$ Hz), 66.6, 63.5 (d, $J = 7.2$ Hz) and 63.1 (d, $J = 7.2$ Hz), 58.3 (d, $J = 7.2$ Hz), 31.9, 25.8 (d, $J = 1.9$ Hz), 22.9, 16.3 (d, $J = 5.6$ Hz), 15.2, 13.9. ^{31}P -NMR (162 MHz, CDCl_3): δ 19.0. IR (ATR): 2973, 1722, 1545, 1240, 1022, 985, 754 cm^{-1} . HMRS (ESI) m/z : calcd for $\text{C}_{19}\text{H}_{32}\text{NO}_6\text{NaP}$ [$\text{M} + \text{Na}$] $^+$ 424.1865, found 424.1863. ^aOverlapping signals of $\text{C}_\alpha\text{CH}_2\text{CH}_2\text{CH}_2\text{CH}_3$ and $\text{P}(\text{O})(\text{OCH}_2\text{CH}_3)_2$ groups.

Diethyl 1-(N-benzyloxycarbonylamino)-1-ethoxy-3-methylbutylphosphonate (3j). Colorless oil; 32% yield (135.7 mg). ^1H -NMR (400 MHz, CDCl_3): δ 7.36–7.31 (m, 5H), 5.88 (br d, $J = 8.8$ Hz, 1H), 5.08 (ABq, $J = 12.2$ Hz, 2H), 4.25–4.11 (m, 4H)^a, 3.61 (qd, $J = 7.0, 1.0$ Hz, 2H), 2.62 (ddd, $J_1 = 26.3$ Hz, $J_2 = 15.0$ Hz, $J_3 = 7.9$ Hz, 1H), 2.09–2.03 (m, 1H), 1.96 (ddd, $J_1 = 15.0$ Hz, $J_2 = 9.1$ Hz, $J_3 = 4.3$ Hz, 1H), 1.34 (t, $J = 7.2$ Hz, 3H) and 1.32 (t, $J = 7.2$ Hz, 3H)^b, 1.16 (t, $J = 7.0$ MHz, 3H), 1.00 (d, $J = 6.8$ Hz, 3H), 0.94 (d, $J = 6.8$ Hz, 3H). ^{13}C -NMR (100 MHz, CDCl_3): δ 154.4 (d,

$J = 16.7$ Hz), 136.2, 128.5, 128.14, 128.06, 87.9 (d, $J = 188.2$ Hz), 66.6, 63.8 (d, $J = 7.2$ Hz), 62.9 (d, $J = 7.2$ Hz), 58.5 (d, $J = 7.2$ Hz), 40.3, 24.5 (d, $J = 4.6$ Hz), 23.2, 16.40 (d, $J = 5.7$ Hz) and 16.38 (d, $J = 5.7$ Hz)^b, 15.1. ³¹P-NMR (162 MHz, CDCl₃): δ 19.2. IR (ATR): 3248, 1739, 1499, 1242, 1021, 967, 749 cm⁻¹. HMRS (ESI) m/z : calcd for C₁₉H₃₂NO₆NaP [M + Na]⁺ 424.1865, found 424.1862. ^aOverlapping signals of P(O)(OCH₂CH₃)₂ groups. ^aOverlapping signals of P(O)(OCH₂CH₃)₂ groups. ^bOverlapping signals of P(O)(OCH₂CH₃)₂ groups.

Diethyl 1-(N-acetylamino)-1-ethoxy-3-methylbutylphosphonate (3k). White solid; 64% yield (198 mg); mp 58.6 to 59.7 °C. ¹H-NMR (400 MHz, CDCl₃): δ 6.30 (br d, $J = 7.6$ Hz, 1H), 4.28–4.13 (m, 4H)^a, 3.70–3.58 (m, 2H), 2.81–2.70 (m, 1H), 1.98–1.92 (m, 2H), 2.02 (s, 3H), 1.35 (t, $J = 7.0$ Hz, 3H) and 1.34 (t, $J = 7.0$ Hz, 3H)^b, 1.18 (t, $J = 7.2$ Hz, 3H), 1.00 (d, $J = 6.7$ Hz, 3H), 0.95 (d, $J = 6.7$ Hz, 3H). ¹³C-NMR (100 MHz, CDCl₃): δ 170.1 (d, $J = 12.9$ Hz), 88.8 (d, $J = 187.3$ Hz), 64.1 (d, $J = 7.2$ Hz), 62.7 (d, $J = 7.2$ Hz), 59.0 (d, $J = 8.0$ Hz), 39.7, 24.9, 24.7 (d, $J = 3.0$ Hz), 24.5, 23.1, 16.43 (d, $J = 6.1$ Hz) and 16.40 (d, $J = 5.3$ Hz)^b, 15.1. ³¹P-NMR (162 MHz, CDCl₃): δ 19.6. IR (ATR): 3197, 1670, 1541, 1224, 1070, 956, 759 cm⁻¹. HMRS (ESI) m/z : calcd for C₁₃H₂₉NO₅P [M + H]⁺ 310.1783, found 310.1776. ^aOverlapping signals of P(O)(OCH₂CH₃)₂ groups. ^aOverlapping signals of P(O)(OCH₂CH₃)₂ groups. ^bOverlapping signals of P(O)(OCH₂CH₃)₂ groups.

Diethyl 1-(N-benzyloxycarbonylamino)-1-ethoxy-2-methoxyethylphosphonate (3l). White solid; 91% yield (354 mg); mp 60.1 to 62.1 °C. ¹H-NMR (400 MHz, CDCl₃): δ 7.37–7.30 (m, 5H), 5.97 (br d, $J = 11.0$ Hz, 1H), 5.10 (ABq, $J = 12.0$ Hz, 2H), 4.26–4.15 (m, 5H)^a, 3.92 (dd, $J_1 = 10.6$ Hz, $J_2 = 9.3$ Hz, 2H), 3.75–3.61 (m, 2H), 3.41 (s, 3H), 1.34 (td, $J_1 = 7.2$ Hz, $J_2 = 0.4$ Hz, 3H) and 1.33 (td, $J_1 = 7.2$ Hz, $J_2 = 0.4$ Hz, 3H)^b, 1.18 (t, $J = 7.2$ Hz, 3H). ¹³C-NMR (100 MHz, CDCl₃): δ 154.4 (d, $J = 14.3$ Hz), 136.1, 128.5, 128.2, 128.1, 86.0 (d, $J = 188.8$ Hz), 72.5, 67.0, 63.6 (d, $J = 7.2$ Hz), 63.5 (d, $J = 6.9$ Hz), 59.4, 59.3 (d, $J = 6.0$ Hz), 16.4 (d, $J = 5.7$ Hz), 15.4. ³¹P-NMR (162 MHz, CDCl₃): δ 17.9. IR (ATR): 3227, 2985, 1733, 1528, 1245, 1027, 987, 758 cm⁻¹. HMRS (ESI) m/z : calcd for C₁₇H₂₈NO₇NaP [M + Na]⁺ 412.1501, found 412.1494. ^aOverlapping signals of C_αCH₂OMe and P(O)(OCH₂CH₃)₂ groups.

Diethyl 1-(N-benzyloxycarbonylamino)-1-ethoxy-1-phenylmethylphosphonate (3m). White solid; 82% yield (345 mg); mp 96.6 to 97.6 °C. ¹H-NMR (400 MHz, CDCl₃): δ 7.55–7.52 (m, 2H) and 7.35–7.28 (m, 8H)^a, 6.23 (d, $J = 10$ Hz, 1H), 5.04 (ABq, $J = 12.4$ Hz, 2H), 4.14–3.67 (m, 6H)^b, 1.26 (t, $J = 7.0$ Hz, 3H) and 1.25 (td, $J_1 = 7.0$ Hz, $J_2 = 0.8$ Hz, 3H)^c, 1.17 (t, $J = 7.2$ Hz, 3H). ¹³C-NMR (100 MHz, CDCl₃): δ 154.4 (d, $J = 20.9$ Hz), 136.0, 128.4, 128.14, 128.11, 127.75, 127.72, 127.41, 127.37, 87.3 (d, $J = 185.8$ Hz), 67.0, 64.5 (d, $J = 7.2$ Hz), 63.8 (d, $J = 7.7$ Hz), 59.8 (d, $J = 6.1$ Hz), 16.3 (d, $J = 5.7$ Hz), 16.2 (d, $J = 5.6$ Hz), 15.3. ³¹P-NMR (162 MHz, CDCl₃): δ 15.4. IR (ATR): 3195, 1729, 1541, 1234, 1027, 957, 737 cm⁻¹. HMRS (ESI) m/z : calcd for C₂₁H₂₈NO₆NaP [M + Na]⁺ 445.1552, found 444.1546. ^aOverlapping signals of PhCH₂O and C_αPh groups. ^aOverlapping signals of PhCH₂O and P(O)(OCH₂CH₃)₂ groups. ^cOverlapping signals of P(O)(OCH₂CH₃)₂ groups.

Diethyl 1-(N-benzyloxycarbonylamino)-1-ethoxy-2-(4-methoxyphenyl)ethylphosphonate (3n). White solid; 70% yield (326 mg); mp 80.1 to 81.6 °C. ¹H-NMR (400 MHz, CD₃CN): δ 7.40–7.33 (m, 5H), 7.20–7.16 (m, 2H), 6.79–6.75 (m, 2H), 5.91 (br d, $J = 10.0$ Hz, 1H), 5.11 (s, 2H), 4.05–3.87 (m, 4H)^a, 3.80–3.72 (m, 1H)^b, 3.74 (s, 3H)^b, 3.67–3.57 (m, 2H), 1.17 (td, $J_1 = 7.0$, $J_2 = 0.5$ Hz, 3H), 1.13 (t, $J = 7.0$ Hz, 3H), 1.10 (td, $J_1 = 7.0$ Hz, $J_2 = 0.5$ Hz, 3H). ¹³C-NMR (100 MHz, CDCl₃): δ 159.5, 155.4 (d, $J = 14.1$ Hz), 138.0, 133.1, 129.5, 129.1, 129.0, 128.5 (d, $J = 3.8$ Hz), 114.0, 88.3 (d, $J = 187.3$ Hz), 67.2, 63.78 (d, $J = 7.2$ Hz) and 62.73 (d, $J = 7.2$ Hz)^a, 60.1 (d, $J = 4.2$ Hz), 55.8, 39.1 (d, $J = 5.0$ Hz), 15.7 (d, $J = 5.7$ Hz) and 15.6 (d, $J = 5.7$ Hz), 14.6. ³¹P-NMR (162 MHz, CD₃CN): δ 17.29. IR (ATR): 3197, 2973, 1720, 1514, 1255, 1019, 972, 738, 697 cm⁻¹. HMRS (ESI) m/z : calcd for C₂₃H₃₂NO₇NaP [M + Na]⁺ 488.1814, found 488.1812. ^aOverlapping signals of P(O)(OCH₂CH₃)₂ groups. ^bOverlapping signals of C₆H₄OCH₃ and C_αCH₂C₆H₄CH₃ groups.

Synthesis of diethyl 1-(N-benzyloxycarbonylamino)-1-triphenylphosphonium-methylphosphonate tetrafluoroborate **4c**.

Diethyl 1-(N-benzyloxycarbonylamino)-1-triphenylphosphoniummethylphosphonate tetrafluoroborate **4c** was synthesized as previously described by Kuźnik et al. [33]. In

brief, triphenylphosphonium tetrafluoroborate (1.12 mmol, 392 mg, 1.12 eq.) and diethyl 1-(*N*-benzyloxycarbonylamino)-1-ethoxymethylphosphonate **3c** (1.0 mmol, 345 mg, 1 eq.) were dissolved in dry CH₂Cl₂ (5 mL) for homogenization. The solvent was evaporated, and the residue was heated in an oil bath at 85 °C under reduced pressure for 5 h. The resulting phosphonium salt **4c** was used in the next step without further purification.

Diethyl 1-(N-benzyloxycarbonylamino)-1-triphenylphosphoniummethylphosphonate (4c) Colorless crystals; 95% yield (615 mg), mp 163.7 to 164.9 °C. ¹H-NMR (400 MHz, CDCl₃): δ 7.85–7.58 (m, 16H)^a 7.33–7.25 (m, 5H), 5.96 (ddd, *J* = 22.7, 16.6, 9.9 Hz, 1H), 4.96 (ABq, *J* = 12.6 Hz, 2H), 4.17–4.07 (m, 2H), 3.95–3.84 (m, 2H), 1.23 (t, *J* = 7.1 Hz, 3H), 1.15 (t, *J* = 7.1 Hz, 3H). ¹³C-NMR (100 MHz, CDCl₃): δ 156.3, 135.7, 135.1 (d, *J* = 3.1 Hz), 134.8 (d, *J* = 10.3 Hz), 130.1 (d, *J* = 13.0 Hz), 128.4, 128.1, 128.0, 116.9 (d, *J* = 84.7 Hz), 67.9, 65.1 (d, *J* = 7.6 Hz), 64.9 (d, *J* = 6.9 Hz), 48.1 (dd, *J* = 152.8, 48.5 Hz), 16.1 (d, *J* = 6.1 Hz), 16.0 (d, *J* = 5.0 Hz). ³¹P-NMR (162 MHz, CDCl₃): 27.5 (d, *J* = 37.5 Hz), 11.2 (d, *J* = 37.5 Hz). IR (ATR) 3213, 1712, 1522, 1273, 1008, 747, 688. HRMS (ESI) *m/z*: calcd for C₃₁H₃₄NO₅P₂ [M + H]⁺ 562.1912, found 562.1912. ^aOverlapping signals of ⁺PPh₃ and NH groups.

3.3. General Procedure for the One-Pot Synthesis of Tetraethyl 1-(*N*-acylamino)alkylene-1,1-bisphosphonates **5**

Triethyl phosphite (1.5 mmol, 249 mg, 0.26 mL, 1.5 eq.) was added to a solution of diethyl 1-(*N*-acylamino)-1-ethoxyalkylphosphonate **3** (1.0 mmol) and triphenylphosphonium tetrafluoroborate (1.05–1.08 mmol, 368 mg–378 mg, 1.05–1.08 eq.) in dry MeCN or CH₂Cl₂ (4 mL). The reaction mixture was heated or left at room temperature for the appropriate time period (Scheme 4). Then, the solvent was evaporated under reduced pressure, and the residue was extracted with toluene (3 to 5 times). After evaporation of the toluene, the crude product **5** was purified by column chromatography on silica gel using the mixture of CH₂Cl₂/MeOH (20:1) as the eluent.

The synthesis of compound **5l** was carried out in an analogous manner but with larger excess of triphenylphosphonium tetrafluoroborate (1.2 mmol, 420 mg, 1.2 eq.) and the addition of Hünig's base (0.5 mmol, 65 mg, 87 μL, 0.5 eq.).

Synthesis of tetraethyl 1-(*N*-benzyloxycarbonylamino)methylene-1,1-bisphosphonate **5c**.

Triethyl phosphite (1.5 mmol, 249 mg, 258 μL, 1.5 eq.) and Hünig's base (0.42 mmol, 54 mg, 73 μL, 0.42 eq.) were added to a solution of crude diethyl 1-(*N*-benzyloxycarbonylamino)-1-triphenylphosphoniummethylphosphonate tetrafluoroborate **4c** (1.0 mmol, 649 mg, 1 eq.) in dry MeCN (4 mL). The mixture was heated at 70 °C for 8 h. The product **5c** was isolated and purified in an analogous manner as described in the procedure above.

Tetraethyl 1-(N-benzyloxycarbonylamino)ethylene-1,1-bisphosphonate (5a). Colorless crystals; 95% yield (430 mg), mp 47.1 to 48.7 °C. ¹H-NMR (400 MHz, CDCl₃): δ 7.36–7.31 (m, 5H), 5.40 (br t, *J* = 3.4 Hz, 1H), 5.07 (s, 2H), 4.25–4.12 (m, 8H)^a, 1.98 (t, *J* = 17.0 Hz, 3H), 1.33 (t, *J* = 7.2 Hz, 6H) and 1.31 (t, *J* = 7.2 Hz, 6H)^b. ¹³C-NMR (100 MHz, CDCl₃): 154.3, 136.3, 128.4, 128.11, 128.09, 66.7, 63.83 (d, *J* = 3.4 Hz) and 63.80 (d, *J* = 3.4 Hz) and 63.75 (d, *J* = 3.4 Hz) and 63.72 (d, *J* = 3.4 Hz)^a, 55.8 (t, *J* = 146.9 Hz), 16.5–16.3 (m)^b, 16.2 (br t, *J* = 4.1 Hz). ³¹P-NMR (162 MHz, CDCl₃): 19.6. IR (ATR) 3218, 1714, 1537, 1229, 1016, 958, 750. HRMS (ESI) *m/z*: calcd for C₁₈H₃₂NO₈P₂ [M + H]⁺ 452.1603, found 452.1610. ^aOverlapping signals of P(O)(OCH₂CH₃)₂ groups. ^bOverlapping signals of P(O)(OCH₂CH₃)₂ groups.

Tetraethyl 1-(N-pivaloylamino)ethylene-1,1-bisphosphonate (5b). Colorless crystals; 62% yield (247 mg), mp 50.8 to 52.3 °C. ¹H-NMR (400 MHz, CDCl₃): δ 6.19 (br t, *J* = 4.6 Hz, 1H), 4.28–4.19 (m, 8H)^a, 2.01 (t, *J* = 17.0 Hz, 3H), 1.35 (t, *J* = 7.0 Hz, 12H), 1.20 (s, 9H). ¹³C-NMR (100 MHz, CDCl₃): δ 177.7 (t, *J* = 5.1 Hz), 63.76 (d, *J* = 3.4 Hz) and 63.73 (d, *J* = 3.4 Hz) and 63.67 (d, *J* = 3.4 Hz) and 63.64 (d, *J* = 3.4 Hz)^a, 56.7 (t, *J* = 144.9 Hz), 39.8, 27.4, 16.7 (t, *J* = 4.5 Hz), 16.5–16.4 (m)^b. ³¹P-NMR (162 MHz, CDCl₃): 20.0. IR (ATR) 3276, 1677, 1515, 1233, 1016, 945. HRMS (ESI) *m/z*: calcd for C₁₅H₃₄NO₇P₂ [M + H]⁺ 402.1811, found 402.1813. ^aOverlapping signals of P(O)(OCH₂CH₃)₂ groups. ^bOverlapping signals of P(O)(OCaH₂CH₃)₂ groups.

Tetraethyl 1-(N-benzyloxycarbonylamino)methylene-1,1-bisphosphonate (5c). Colorless crystals; 82% yield (357 mg), mp 59.8 to 60.7 °C. ¹H-NMR (400 MHz, CDCl₃): δ 7.36–7.31 (m, 5H), 5.32 (br d, *J* = 10.4 Hz, 1H), 5.15 (s, 2H), 4.59 (td *J*₁ = 21.9, *J*₂ = 10.4 Hz), 4.25–4.12 (m, 8H)^a, 1.32 (t, *J* = 7.0 Hz, 6H) and 1.29 (t, *J* = 7.0 Hz, 6H)^b. ¹³C-NMR (100 MHz, CDCl₃): δ 155.5 (t, *J* = 4.9 Hz), 135.9, 128.5, 128.3, 128.1, 67.6, 63.5, 46.0 (t, *J* = 146.8 Hz), 16.3–16.2 (m)^b. ³¹P-NMR (162 MHz, CDCl₃): 16.3. IR (ATR) 3354, 1717, 1528, 1266, 1019, 977, 736. HRMS (ESI) *m/z*: calcd for C₁₇H₂₉NO₈NaP₂ [M + Na]⁺ 460.1266, found 460.1261. ^aOverlapping signals of P(O)(OCH₂CH₃)₂ groups. ^bOverlapping signals of P(O)(OCH₂CH₃)₂ groups.

Tetraethyl 1-(N-benzyloxycarbonylamino)-2-phenylethylene-1,1-bisphosphonate (5d). Colorless crystals; 86% yield (455 mg), mp 60.2 to 61.5 °C. ¹H-NMR (400 MHz, CDCl₃) δ 7.44–7.34 (m, 5H), 7.26–7.16 (m, 5H), 5.44 (t, *J* = 12.7 Hz, 1H), 5.18 (s, 2H), 4.30–4.15 (m, 4H)^a, 4.13–4.03 (m, 2H), 3.98–3.88 (m, 2H), 3.58 (dd, *J* = 15.3, 11.7 Hz, 2H), 1.30 (t, *J* = 7.2 Hz, 6H), 1.19 (t, *J* = 7.2 Hz, 6H). ¹³C-NMR (100 MHz, CDCl₃) δ 154.9 (t, *J* = 8.8 Hz), 136.4, 135.3 (t, *J* = 8.6 Hz), 131.2, 128.49, 128.45, 128.2, 127.7, 126.7, 67.1, 63.9 (d, *J* = 7.5 Hz), 63.0 (d, *J* = 7.4 Hz), 61.2 (t, *J* = 143.1 Hz), 35.5, 16.3 (d, *J* = 6.3 Hz), 16.2 (d, *J* = 6.2 Hz). ³¹P-NMR (162 MHz, CDCl₃): 18.8. IR (ATR) 3224, 1711, 1534, 1266, 1022, 963, 752. HRMS (ESI) *m/z*: calcd for C₂₄H₃₅NO₈NaP₂ [M + Na]⁺ 550.1736, found 550.1732. ^aOverlapping signals of P(O)(OCH₂CH₃)₂ groups.

Tetraethyl 1-(N-acetylamino)-2-phenylethylene-1,1-bisphosphonate (5e). Colorless crystals; 59% yield (255 mg); mp 91.0 to 92.3 °C. ¹H-NMR (400 MHz, CDCl₃): δ 7.28–7.19 (m, 5H), 6.04 (br t, *J* = 13.3 Hz, 1H), 4.33–4.25 (m, 4H)^a, 4.16–4.06 (m, 2H), 4.04–3.94 (m, 2H), 3.57 (dd, *J* = 15.3, 12.0 Hz, 2H), 2.05 (s, 3H), 1.35 (t, *J* = 7.1 Hz, 6H), 1.23 (t, *J* = 7.1 Hz, 6H). ¹³C-NMR (100 MHz, CDCl₃): δ 169.9 (t, *J* = 7.3 Hz), 135.5 (t, *J* = 8.2 Hz), 131.1, 127.7, 126.9, 64.1 (d, *J* = 7.3 Hz), 62.9 (d, *J* = 7.6 Hz), 61.4 (t, *J* = 143.1 Hz), 35.2, 23.9, 16.4 (d, *J* = 6.2 Hz), 16.1 (d, *J* = 6.5 Hz). ³¹P-NMR (162 MHz, CDCl₃): 19.2. IR (ATR) 3305, 2989, 1684, 1537, 1245, 1065, 1008, 962. HRMS (ESI) *m/z*: calcd for C₁₈H₃₁NO₇NaP₂ [M + Na]⁺ 458.1473, found 458.1467. ^aOverlapping signals of P(O)(OCH₂CH₃)₂ groups.

Tetraethyl 1-(N-benzyloxycarbonylamino)propylene-1,1-bisphosphonate (5f). Colorless crystals; 90% yield (417 mg), mp 61.6 to 62.8 °C. ¹H-NMR (400 MHz, CDCl₃) δ 7.37–7.31 (m, 5H), 5.47 (br t, *J* = 8.3 Hz, 1H), 5.08 (s, 2H), 4.27–4.15 (m, 8H)^a, 2.42 (tq, *J*₁ = 16.0 Hz, *J*₂ = 7.7 Hz, 2H), 1.34 (t, *J* = 7.0 Hz, 6H) and 1.32 (t, *J* = 7.0 Hz, 6H)^b, 1.11 (t, *J* = 7.4 Hz, 3H). ¹³C-NMR (100 MHz, CDCl₃) δ 154.3 (t, *J* = 8.0 Hz), 136.4, 128.4, 128.1, 66.8, 63.67 (d, *J* = 3.5 Hz) and 63.64 (d, *J* = 3.5 Hz)^b, 63.42 (d, *J* = 3.5 Hz) and 63.38 (d, *J* = 3.5 Hz)^a, 60.4 (t, *J* = 144.4 Hz), 23.8 (t, *J* = 3.0 Hz), 16.5–16.3 (m)^b, 9.1 (t, *J* = 6.5 Hz). ³¹P-NMR (162 MHz, CDCl₃): 20.0. IR (ATR) 3422, 1737, 1503, 1248, 1022, 968, 770. HRMS (ESI) *m/z*: calcd for C₁₉H₃₃NO₈NaP₂ [M + Na]⁺ 488.1579, found 488.1577. ^aOverlapping signals of P(O)(OCH₂CH₃)₂ groups. ^bOverlapping signals of P(O)(OCH₂CH₃)₂ groups.

Tetraethyl 1-(N-benzyloxycarbonylamino)butylene-1,1-bisphosphonate (5g). Colorless crystals; 95% yield (457 mg), mp 66.7 to 68.5 °C. ¹H-NMR (400 MHz, CDCl₃) δ 7.37–7.30 (m, 5H), 5.46 (br t, *J* = 8.2 Hz, 1H), 5.08 (s, 2H), 4.26–4.14 (m, 8H)^a, 2.36–2.24 (m, 2H), 1.61–1.55 (m, 2H), 1.33 (t, *J* = 7.0 Hz, 6H) and 1.32 (t, *J* = 7.0 Hz, 6H)^b, 0.93 (t, *J* = 7.3 Hz, 3H). ¹³C-NMR (100 MHz, CDCl₃): δ 154.3 (t, *J* = 7.6 Hz), 136.4, 128.4, 128.1, 66.8, 63.66 (d, *J* = 3.5 Hz) and 63.63 (d, *J* = 3.5 Hz)^a, 63.43 (d, *J* = 3.5 Hz) and 63.40 (d, *J* = 3.5 Hz)^a, 60.1 (t, *J* = 143.5 Hz), 32.7 (t, *J* = 3.0 Hz), 17.7 (t, *J* = 6.2 Hz), 16.45 (d, *J* = 2.9 Hz) and 16.43 (d, *J* = 2.6 Hz) and 16.40 (d, *J* = 2.7 Hz) and 16.37 (d, *J* = 2.9 Hz)^b, 14.5. ³¹P-NMR (162 MHz, CDCl₃): 20.1. IR (ATR) 1735, 1499, 1243, 1017, 958, 740. HRMS (ESI) *m/z*: calcd for C₂₀H₃₅NO₈NaP₂ [M + Na]⁺ 502.1736, found 502.1731. ^aOverlapping signals of P(O)(OCH₂CH₃)₂ groups. ^bOverlapping signals of P(O)(OCH₂CH₃)₂ groups.

Tetraethyl 1-(N-benzyloxycarbonylamino)-2-methylpropylene-1,1-bisphosphonate (5h). Colorless oil; 72% yield (344 mg). ¹H-NMR (400 MHz, CDCl₃): δ 7.37–7.28 (m, 5H), 5.71 (t, *J* = 10.1 Hz, 1H), 5.09 (s, 2H), 4.28–4.13 (m, 8H)^a, 3.06 (tsept, *J*₁ = 23.6, *J*₂ = 7.0 Hz 1H), 1.33 (t, *J* = 7.0 Hz, 6H) and 1.32 (t, *J* = 7.0 Hz, 6H)^b, 1.22 (d, *J* = 6.9 Hz, 6H). ¹³C-NMR (100 MHz, CDCl₃): δ 154.3 (t, *J* = 8.2 Hz), 136.4, 128.4, 128.0, 66.8, 64.6 (t, *J* = 139.2 Hz), 63.40 (d, *J* = 3.6 Hz) and 63.36 (d, *J* = 3.6 Hz)^a, 63.11 (d, *J* = 3.5 Hz) and 63.08 (d, *J* = 3.6 Hz)^a, 30.7, 18.8 (t, *J* = 4.3 Hz),

16.40 (d, $J = 3.0$ Hz) and 16.37 (d, $J = 2.9$ Hz) and 16.34 (d, $J = 2.9$ Hz) and 16.31 (d, $J = 3.0$ Hz)^b. ³¹P-NMR (162 MHz, CDCl₃): 20.7. IR (ATR) 3433, 1743, 1500, 1244, 1019, 966, 741. HRMS (ESI) m/z : calcd for C₂₀H₃₆NO₈P₂ [M + H]⁺ 480.1916, found 480.1917. ^aOverlapping signals of P(O)(OCH₂CH₃)₂ groups. ^bOverlapping signals of P(O)(OCH₂CH₃)₂ groups.

Tetraethyl 1-(N-benzyloxycarbonylamino)pentylene-1,1-bisphosphonate (5i). Colorless crystals; 90% yield (444 mg), mp 56.0 to 57.2 °C. ¹H-NMR (400 MHz, CDCl₃) δ 7.37–7.29 (m, 5H), 5.47 (br t, $J = 8.5$ Hz, 1H), 5.08 (s, 2H), 4.26–4.14 (m, 8H)^a, 2.38–2.26 (m, 2H), 1.57–1.49 (m, 2H), 1.37–1.25 (m, 2H) and 1.33 (t, $J = 7.0$ Hz, 6H) and 1.32 (t, $J = 7.0$ Hz, 6H)^b, 0.90 (t, $J = 7.3$ Hz, 3H). ¹³C-NMR (100 MHz, CDCl₃) δ 154.3 (t, $J = 7.3$ Hz), 136.4, 128.4, 128.0, 66.7, 63.59 (d, $J = 3.5$ Hz) and 63.55 (d, $J = 3.5$ Hz)^b, 63.38 (d, $J = 3.4$ Hz) and 63.34 (d, $J = 3.5$ Hz)^b, 60.0 (t, $J = 144.4$ Hz), 30.4 (t, $J = 3.0$ Hz), 26.2 (t, $J = 6.0$ Hz), 23.0, 16.39 (d, $J = 2.7$ Hz) and 16.36 (d, $J = 2.6$ Hz) and 16.33 (d, $J = 2.6$ Hz) and 16.31 (d, $J = 2.7$ Hz)^a, 13.9. ³¹P-NMR (162 MHz, CDCl₃): 20.1. IR (ATR) 3224, 1736, 1498, 1233, 1019, 953, 772. HRMS (ESI) m/z : calcd for C₂₁H₃₇NO₈NaP₂ [M + Na]⁺ 516.1892, found 516.1889. ^aOverlapping signals of P(O)(OCH₂CH₃)₂ groups. ^bOverlapping signals of C_αCH₂CH₂CH₂CH₃ and P(O)(OCH₂CH₃)₂ groups. ^cOverlapping signals of P(O)(OCH₂CH₃)₂ groups.

Tetraethyl 1-(N-benzyloxycarbonylamino)-3-methylbutylene-1,1-bisphosphonate (5j). Colorless crystals; 74% yield (367 mg), mp 54.9 to 55.5 °C. ¹H-NMR (400 MHz, CDCl₃) δ 7.35–7.30 (m, 5H), 5.55 (br t, $J = 12.0$ Hz, 1H), 5.09 (s, 2H), 4.28–4.16 (m, 8H)^a, 2.19–2.11 (m, 3H), 1.33 (t, $J = 7.1$ Hz, 12H), 0.95 (d, $J = 6.2$ Hz, 6H). ¹³C-NMR (100 MHz, CDCl₃): 154.4 (t, $J = 8.0$ Hz), 136.4, 128.4, 128.14, 128.06, 66.9, 63.56 (d, $J = 3.5$ Hz) and 63.52 (d, $J = 3.5$ Hz)^a, 63.34 (d, $J = 3.5$ Hz) and 63.30 (d, $J = 3.5$ Hz)^a, 60.7 (t, $J = 142.9$ Hz), 38.6 (t, $J = 2.2$ Hz), 25.2 (t, $J = 7.8$ Hz), 24.2, 16.44–16.26 (m)^b. ³¹P-NMR (162 MHz, CDCl₃): 20.4. IR (ATR) 3231, 1716, 1528, 1250, 1026, 967, 749. HRMS (ESI) m/z : calcd for C₂₁H₃₇NO₈NaP₂ [M + Na]⁺ 516.1892, found 516.1891. ^aOverlapping signals of P(O)(OCH₂CH₃)₂ groups. ^bOverlapping signals of P(O)(OCH₂CH₃)₂ groups.

Tetraethyl 1-(N-acetylamino)-3-methylbutylene-1,1-bisphosphonate (5k). Colorless crystals; 69% yield (278 mg), mp 108.8 to 110.3 °C. ¹H-NMR (400 MHz, CDCl₃) δ 6.25 (br t, $J = 13.0$ Hz, 1H), 4.28–4.17 (m, 8H)^a, 2.18–2.07 (m, 3H), 2.02 (s, 3H), 1.349 (t, $J = 7.0$ Hz, 6H) and 1.345 (t, $J = 7.0$ Hz, 6H)^b, 0.96 (d, $J = 6.3$ Hz, 6H). ¹³C-NMR (100 MHz, CDCl₃): δ 169.2 (t, $J = 6.9$ Hz), 63.6 (d, $J = 7.3$ Hz), 63.1 (d, $J = 7.2$ Hz), 60.9 (t, $J = 143.2$ Hz), 38.4 (t, $J = 2.6$ Hz), 25.4 (t, $J = 8.0$ Hz), 24.2, 23.9, 16.4 (d, $J = 6.0$ Hz) and 16.3 (d, $J = 6.3$ Hz)^b. ³¹P-NMR (162 MHz, CDCl₃): 20.9. IR (ATR) 3441, 1682, 1541, 1234, 1023, 971. HRMS (ESI) m/z : calcd for C₁₅H₃₄NO₇P₂ [M + H]⁺ 402.1811, found 402.1811. ^aOverlapping signals of P(O)(OCH₂CH₃)₂ groups. ^bOverlapping signals of P(O)(OCH₂CH₃)₂ groups.

Tetraethyl 1-(N-benzyloxycarbonylamino)-2-methoxyethylene-1,1-bisphosphonate (5l). Colorless oil; 52% yield (248 mg), ¹H-NMR (400 MHz, CDCl₃) δ 7.36–7.28 (m, 5H), 5.56 (br t, $J = 8.0$ Hz, 1H), 5.09 (s, 2H), 4.26–4.12 (m, 10H)^a, 3.39 (s, 3H), 1.32 (t, $J = 7.0$ Hz, 12H). ¹³C-NMR (100 MHz, CDCl₃): δ 154.4 (t, $J = 6.2$ Hz), 136.3, 128.4, 128.1, 128.0, 70.1, 66.9, 63.59 (d, $J = 3.5$ Hz) and 63.55 (d, $J = 3.6$ Hz) and 63.52 (d, $J = 3.6$ Hz)^b, 60.5 (t, $J = 142.7$ Hz), 59.1, 16.4–16.3 (m)^c. ³¹P-NMR (162 MHz, CDCl₃): 18.0. IR (ATR) 1741, 1498, 1254, 1023, 973, 733. HRMS (ESI) m/z : calcd for C₁₉H₃₃NO₉NaP₂ [M + Na]⁺ 504.1528, found 504.1526. ^aOverlapping signals of and C_αCH₂OCH₃ and P(O)(OCH₂CH₃)₂ groups. ^bOverlapping signals of P(O)(OCH₂CH₃)₂ groups. ^cOverlapping signals of P(O)(OCH₂CH₃)₂ groups.

Tetraethyl 1-(N-benzyloxycarbonylamino)phenylmethylene-1,1-bisphosphonate (5m). Colorless crystals; 40% yield (204 mg); mp 66.1 to 68.0 °C. ¹H-NMR (400 MHz, CDCl₃) δ 7.70–7.66 (m, 2H) and 7.38–7.25 (m, 8H)^a, 5.93 (br s, 1H), 5.12 (s, 2H), 4.16–3.94 (m, 8H)^b, 1.21 (t, $J = 7.0$ Hz, 12H). ¹³C-NMR (100 MHz, CDCl₃) δ 154.4 (br s), 136.3, 132.0, 128.4, 128.1 (t, $J = 5.0$ Hz), 127.6 (t, $J = 2.6$ Hz), 127.5 (t, $J = 2.3$ Hz), 67.1, 64.25 (d, $J = 3.7$ Hz) and 64.21 (d, $J = 3.6$ Hz) and 64.08 (d, $J = 3.6$ Hz) and 64.05 (d, $J = 3.8$ Hz)^b, 64.15 (t, $J = 140.4$ Hz), 16.26 (d, $J = 3.1$ Hz) and 16.23 (d, $J = 3.0$ Hz)^c. ³¹P-NMR (162 MHz, CDCl₃): 17.1. IR (ATR) 3218, 1723, 1530, 1014, 949, 750, 697. HRMS (ESI) m/z : calcd for C₂₃H₃₃NO₈NaP₂ [M + Na]⁺ 536.1579, found 536.1570. ^aOverlapping signals of PhCH₂O and C_αPh groups. ^bOverlapping signals of P(O)(OCH₂CH₃)₂ groups. ^cOverlapping signals of P(O)(OCH₂CH₃)₂ groups.

Tetraethyl 1-(N-benzyloxycarbonylamino)-2-(4-methoxyphenyl)ethylene-1,1-bisphosphonate (5n). Colorless crystals; 74% yield (412 mg), mp 71.7 to 73.5 °C. ¹H-NMR (400 MHz, CDCl₃) δ 7.44–7.34 (m, 5H), 7.14–7.09 (m, 2H), 6.71–6.69 (m, 2H), 5.43 (br t, *J* = 12.8 Hz), 5.17 (s, 2H), 4.29–4.17 (m, 4H), 4.13–4.08 (m, 2H), 4.05–3.91 (m, 2H), 3.75 (s, 3H), 3.52 (dd, *J*₁ = 15.3, *J*₂ = 11.8 Hz, 2H), 1.31 (t, *J* = 7.1 Hz, 6H), 1.21 (t, *J* = 7.1 Hz, 6H). ¹³C-NMR (100 MHz, CDCl₃) δ 158.5, 154.9 (t, *J* = 8.8 Hz), 136.3, 132.1, 128.46, 128.45, 128.2, 127.2 (t, *J* = 8.6 Hz), 113.1, 67.0, 63.9 (d, *J* = 7.4 Hz), 63.0 (d, *J* = 7.6 Hz), 61.1 (t, *J* = 143.0 Hz), 55.2, 34.7, 16.3 (d, *J* = 6.3 Hz), 16.2 (d, *J* = 6.2 Hz). ³¹P-NMR (162 MHz, CDCl₃): 19.0. IR (ATR) 3251, 1715, 1513, 1247, 1028, 953, 774. HRMS (ESI) *m/z*: calcd for C₂₅H₃₇NO₉NaP₂ [M + Na]⁺ 580.1841, found 580.1839.

4. Conclusions

In conclusion, we developed a simple and efficient methodology for the preparation of *N*-protected bisphosphonic analogs of protein and non-protein α-amino acids. The optimization of our procedure, consisting of the reaction of 1-(*N*-acylamino)-1-ethoxyphosphonates **3** with triphenylphosphonium tetrafluoroborate and triethyl phosphite, highlights the one-pot synthesis conducted in mild conditions. In most cases, there is no need to use any catalyst as it is autocatalytic in nature. Relatively easy access to the starting α-ethoxyphosphonates **3**, obtained from ethyl *N*-acylimidates **2**, simple work-up of the reaction mixture and good to excellent yields of the target products **5** are additional advantages of the proposed protocol. The methodology provided constitutes a convenient approach for the synthesis of structurally diverse *N*-protected 1-aminobisphosphonate derivatives **5** and can be considered a new universal strategy for the construction of bisphosphorus organic compounds containing the P-C(N)-P skeleton.

It is worth emphasizing that the one-pot method reported here proceeds through the indirect transformation of α-ethoxyphosphonates, non-reactive in the Michaelis–Arbuzow-type reaction, into the corresponding phosphonium salts **4** of high reactivity and thus susceptibility to further reaction with phosphorus nucleophiles. This is another confirmation of the synthetic potential of phosphonium salts, which are increasingly gaining in importance. As reactive intermediates, they often enable transformations that are difficult to perform with other methods.

Supplementary Materials: The following can be downloaded at: <https://www.mdpi.com/article/10.3390/molecules27113571/s1>. Supporting information includes ¹H, ¹³C, ³¹P NMR of all new compounds **3**, **4c** and **5**, as well as a tabulated summary of the characteristic ¹³C NMR data of these compounds.

Author Contributions: Conceptualization, A.K.; methodology, A.K. and D.K.; formal analysis, A.K., D.K., W.H., K.S. and K.E.; investigation, A.K., D.K., W.H., K.S. and K.E.; writing—original draft preparation, A.K.; writing—review and editing, A.K. and D.K.; visualization, A.K. and D.K.; supervision, A.K. All authors have read and agreed to the published version of the manuscript.

Funding: This research received no external funding.

Institutional Review Board Statement: Not applicable.

Informed Consent Statement: Not applicable.

Data Availability Statement: Not applicable.

Conflicts of Interest: The authors declare no conflict of interest.

Sample Availability: Samples of all described compounds are available from the authors.

References

- Romanenko, V.D.; Kukhar, V.P. 1-Amino-1,1-Bisphosphonates. Fundamental Syntheses and New Developments. *Arkivoc* **2012**, *4*, 127–166. [CrossRef]
- Kafarski, P.; Lejczak, B. Aminophosphonic Acids of Potential Medical Importance. *Curr. Med. Chem.-Anti-Cancer Agents* **2001**, *1*, 301–312. [CrossRef] [PubMed]

3. Mucha, A.; Kafarski, P.; Berlicki, L. Remarkable Potential of the α -Aminophosphonate/Phosphinate Structural Motif in Medicinal Chemistry. *J. Med. Chem.* **2011**, *54*, 5955–5980. [CrossRef]
4. Orsini, F.; Sello, G.; Sisti, M. Aminophosphonic Acids and Derivatives. Synthesis and Biological Applications. *Curr. Med. Chem.* **2010**, *17*, 264–289. [CrossRef]
5. Kukhar, V.P.; Hudson, H.R. *Aminophosphonic and Aminophosphinic Acids: Chemistry and Biological Activity*; Kukhar, V.P., Hudson, H.R., Eds.; John Wiley & Sons Ltd.: New York, NY, USA, 2000; ISBN 978-0-471-89149-9.
6. Russell, R.G.G. Bisphosphonates: The First 40 years. *Bone* **2011**, *49*, 2–19. [CrossRef]
7. Widler, L.; Jaeggi, K.A.; Glatt, M.; Müller, K.; Bachmann, R.; Bisping, M.; Born, A.-R.; Cortesi, R.; Guiglia, G.; Jeker, H.; et al. Highly Potent Geminal Bisphosphonates. From Pamidronate Disodium (Aredia) to Zoledronic Acid (Zometa). *J. Med. Chem.* **2002**, *45*, 3721–3738. [CrossRef]
8. Zhang, S.; Gangal, G.; Uludağ, H. ‘Magic Bullets’ for Bone Diseases: Progress in Rational Design of Bone-Seeking Medicinal Agents. *Chem. Soc. Rev.* **2007**, *36*, 507–531. [CrossRef]
9. Hiraga, T.; Tanaka, S.; Yamamoto, M.; Nakajima, T.; Ozawa, H. Inhibitory Effects of Bisphosphonate (YM175) on Bone Resorption Induced by a Metastatic Bone Tumor. *Bone* **1996**, *18*, 1–7. [CrossRef]
10. Wang, L.; Kamath, A.; Das, H.; Li, L.; Bukowski, J.F. Antibacterial Effect of Human $\gamma\delta$ T Cells In Vivo. *J. Clin. Investig.* **2001**, *108*, 1349–1357. [CrossRef]
11. Chmielewska, E.; Kafarski, P. Physiologic Activity of Bisphosphonates—Recent Advances. *Open Pharm. Sci. J.* **2016**, *3*, 56–78. [CrossRef]
12. Szajnman, S.H.; Ravaschino, E.L.; Docampo, R.; Rodriguez, J.B. Synthesis and Biological Evaluation of 1-Amino-1,1-Bisphosphonates Derived from Fatty Acids against Trypanosoma Cruzi Targeting Farnesyl Pyrophosphate Synthase. *Bioorg. Med. Chem. Lett.* **2005**, *15*, 4685–4690. [CrossRef] [PubMed]
13. Yajima, S.; Hara, K.; Sanders, J.M.; Yin, F.; Ohsawa, K.; Wiesner, J.; Jomaa, H.; Oldfield, E. Crystallographic Structures of Two Bisphosphonate:1-Deoxyxylulose-5-Phosphate Reductoisomerase Complexes. *J. Am. Chem. Soc.* **2004**, *126*, 10824–10825. [CrossRef] [PubMed]
14. Occhipinti, A.; Berlicki, L.; Giberti, S.; Dziędziola, G.; Kafarski, P.; Forlani, G. Effectiveness and Mode of Action of Phosphonate Inhibitors of Plant Glutamine Synthetase: Phosphonate Inhibitors of Plant Glutamine Synthetase. *Pest. Manag. Sci.* **2010**, *66*, 51–58. [CrossRef] [PubMed]
15. Ferlazzo, V.; Sferrazza, C.; Caccamo, N.; Di Fede, G.; Di Lorenzo, G.; D’Asaro, M.; Meraviglia, S.; Dieli, F.; Rini, G.; Salerno, A. In Vitro Effects of Aminobisphosphonates on $\gamma\delta$ T Cell Activation and Differentiation. *Int. J. Immunopathol. Pharmacol.* **2006**, *19*, 309–317. [CrossRef] [PubMed]
16. Farrell, K.B.; Karpeisky, A.; Thamm, D.H.; Zinnen, S. Bisphosphonate Conjugation for Bone Specific Drug Targeting. *Bone Rep.* **2018**, *9*, 47–60. [CrossRef] [PubMed]
17. Uludag, H. Bisphosphonates as a Foundation of Drug Delivery to Bone. *Curr. Pharm. Des.* **2002**, *8*, 1929–1944. [CrossRef] [PubMed]
18. Kuźnik, A.; Październiak-Holewa, A.; Jewula, P.; Kuźnik, N. Bisphosphonates—Much More than Only Drugs for Bone Diseases. *Eur. J. Pharm.* **2020**, *866*, 172773. [CrossRef]
19. Kubiček, V.; Rudovský, J.; Kotek, J.; Hermann, P.; Vander Elst, L.; Muller, R.N.; Kolar, Z.L.; Wolterbeek, H.T.; Peters, J.A.; Lukeš, I. A Bisphosphonate Monoamide Analogue of DOTA: A Potential Agent for Bone Targeting. *J. Am. Chem. Soc.* **2005**, *127*, 16477–16485. [CrossRef]
20. Kaboudin, B.; Esfandiari, H.; Moradi, A.; Kazemi, F.; Aoyama, H. ZnCl_2 -Mediated Double Addition of Dialkylphosphite to Nitriles for the Synthesis of 1-Aminobisphosphonates. *J. Org. Chem.* **2019**, *84*, 14943–14948. [CrossRef]
21. Kaboudin, B.; Alipour, S. A Microwave-Assisted Solvent- and Catalyst-Free Synthesis of Aminomethylene Bisphosphonates. *Tetrahedron Lett.* **2009**, *50*, 4243–4245. [CrossRef]
22. Balakrishna, A.; Narayana Reddy, M.V.; Rao, P.V.; Kumar, M.A.; Kumar, B.S.; Nayak, S.K.; Reddy, C.S. Synthesis and Bio-Activity Evaluation of Tetraphenyl(Phenylamino) Methylene Bisphosphonates as Antioxidant Agents and as Potent Inhibitors of Osteoclasts In Vitro. *Eur. J. Med. Chem.* **2011**, *46*, 1798–1802. [CrossRef] [PubMed]
23. Lin, Y.-S.; Park, J.; De Schutter, J.W.; Huang, X.F.; Berghuis, A.M.; Sebag, M.; Tsantrizos, Y.S. Design and Synthesis of Active Site Inhibitors of the Human Farnesyl Pyrophosphate Synthase: Apoptosis and Inhibition of ERK Phosphorylation in Multiple Myeloma Cells. *J. Med. Chem.* **2012**, *55*, 3201–3215. [CrossRef] [PubMed]
24. Yokomatsu, T.; Yoshida, Y.; Nakabayashi, N.; Shibuya, S. Simple and Efficient Method for Preparation of Conformationally Constrained Aminomethylene Gem-Diphosphonate Derivatives via Beckmann Rearrangement. *J. Org. Chem.* **1994**, *59*, 7562–7564. [CrossRef]
25. Wang, A.-E.; Chang, Z.; Sun, W.-T.; Huang, P.-Q. General and Chemoselective Bisphosphonylation of Secondary and Tertiary Amides. *Org. Lett.* **2015**, *17*, 732–735. [CrossRef] [PubMed]
26. Midrier, C.; Lantsoght, M.; Volle, J.-N.; Pirat, J.-L.; Virieux, D.; Stevens, C.V. Hydrophosphonylation of Alkenes or Nitriles by Double Radical Transfer Mediated by Titanocene/Propylene Oxide. *Tetrahedron Lett.* **2011**, *52*, 6693–6696. [CrossRef]
27. Islas, R.E.; García, J.J. Nickel-Catalyzed Hydrophosphonylation and Hydrogenation of Aromatic Nitriles Assisted by Lewis Acid. *ChemCatChem* **2019**, *11*, 1337–1345. [CrossRef]

28. Abdou, W.M.; Shaddy, A.A. The Development of Bisphosphonates for Therapeutic Uses, and Bisphosphonate Structure-Activity Consideration. *Arxivoc* **2008**, *9*, 143–182. [CrossRef]
29. Schrader, T.; Steglich, W.; Kober, R. Synthese von 1-Aminophosphonsäure-Derivaten Über Acyliminophosphonsäure-Ester. *Synthesis* **1986**, *5*, 372–375. [CrossRef]
30. Kuźnik, A.; Mazurkiewicz, R.; Grymel, M.; Zielińska, K.; Adamek, J.; Chmielewska, E.; Bochno, M.; Kubica, S. A New Method for the Synthesis of α -Aminoalkylidenebisphosphonates and Their Asymmetric Phosphonyl-Phosphinyl and Phosphonyl-Phosphinoyl Analogues. *Beilstein J. Org. Chem.* **2015**, *11*, 1418–1424. [CrossRef]
31. Mazurkiewicz, R.; Adamek, J.; Październiak-Holewa, A.; Zielińska, K.; Simka, W.; Gajos, A.; Szymura, K. α -Amidoalkylating Agents from *N*-Acyl- α -Amino Acids: 1-(*N*-Acylamino)Alkyltriphenylphosphonium Salts. *J. Org. Chem.* **2012**, *77*, 1952–1960. [CrossRef]
32. Mazurkiewicz, R.; Październiak-Holewa, A.; Kononienko, A. A Novel Synthesis of 1-Aminoalkanephosphonic Acid Derivatives from 1-(*N*-Acylamino)-Alkyltriphenylphosphonium Salts. *Phosphorus Sulfur Silicon Relat. Elem.* **2010**, *185*, 1986–1992. [CrossRef]
33. Kuźnik, A.; Mazurkiewicz, R.; Zięba, M.; Erfurt, K. 1-(*N*-Acylamino)-1-Triphenylphosphoniumalkylphosphonates: General Synthesis and Prospects for Further Synthetic Applications. *Tetrahedron Lett.* **2018**, *59*, 3307–3310. [CrossRef]
34. Neilson, D.G. *The Chemistry of Amidines and Imidates*; Patai, S., Ed.; John Wiley & Sons Ltd.: New York, NY, USA, 1975; pp. 385–489. [CrossRef]
35. Roger, R.; Neilson, D.G. The Chemistry of Imidates. *Chem. Rev.* **1961**, *61*, 179–211. [CrossRef]
36. Rassukana, Y.; Kolotylo, M.; Sinitza, O.; Pirozhenko, V.; Onys'ko, P. α -Iminotrifluoroethylphosphonates: The First Representatives of N-H Imidoyl Phosphonates. *Synthesis* **2007**, *17*, 2627–2630. [CrossRef]
37. Adamek, J.; Październiak-Holewa, A.; Zielińska, K.; Mazurkiewicz, R. Comparative Studies on the Amidoalkylating Properties of *N*-(1-Methoxyalkyl)Amides and 1-(*N*-Acylamino)Alkyltriphenylphosphonium Salts in the Michaelis–Arbuzov-Like Reaction: A New One-Pot Transformation of *N*-(1-Methoxyalkyl)Amides into Phosphonic or Phosphinic Analogs of *N*-Acyl- α -Amino Acids. *Phosphorus Sulfur Silicon Relat. Elem.* **2013**, *188*, 967–980. [CrossRef]
38. Adamek, J.; Węgrzyk, A.; Kończewicz, J.; Walczak, K.; Erfurt, K. 1-(*N*-Acylamino)Alkyltriarylphosphonium Salts with Weakened C α -P+ Bond Strength—Synthetic Applications. *Molecules* **2018**, *23*, 2453. [CrossRef]
39. Ohme, R.; Schmitz, E. A Simple Synthesis of Alkyl Formimidates. *Angew. Chem. Int. Ed. Engl.* **1967**, *6*, 566. [CrossRef]
40. Yadav, V.K.; Babu, K.G. A Remarkably Efficient Markovnikov Hydrochlorination of Olefins and Transformation of Nitriles into Imidates by Use of AcCl and an Alcohol. *Eur. J. Org. Chem.* **2005**, *2005*, 452–456. [CrossRef]
41. Yamamoto, Y.; Morita, Y.; Minami, K. 1,3-Oxazines and related compounds. XII. Facile synthesis of 2,4-disubstituted 6H-1,3-oxazin-6-ones. *Chem. Pharm. Bull.* **1986**, *34*, 1980–1986. [CrossRef]
42. Harizi, A. Synthese Originale de 5-Aryl (ou 5-benzyl)-2-[(1-Diethoxyphosphonyl)methyl]-1,3,4-oxadiazoles par Action du Phosphonomethylhydrazide sur les Imidates *N*-Acyles. *Phosphorus Sulfur Silicon Relat. Elem.* **2006**, *181*, 2377–2385. [CrossRef]
43. Emura, T.; Kimura, N.; Nagafuji, T. Preparation of Benzene Derivatives Having NOS Inhibitory Activity. Patent WO 9746515, 11 December 1997.

Article

Drug-Inclusive Inorganic–Organic Hybrid Systems for the Controlled Release of the Osteoporosis Drug Zoledronate

Maria Vassaki ¹, Savvina Lazarou ¹, Petri Turhanen ², Duane Choquesillo-Lazarte ³
and Konstantinos D. Demadis ^{1,*}

¹ Crystal Engineering, Growth and Design Laboratory, Department of Chemistry, University of Crete, 71003 Heraklion, Greece

² School of Pharmacy, University of Eastern Finland, Biocenter Kuopio, P.O. Box 1627, 70211 Kuopio, Finland

³ Laboratorio de Estudios Cristalográficos, IACT, CSIC-Universidad de Granada, 18100 Granada, Spain

* Correspondence: demadis@uoc.gr

Abstract: Bisphosphonates (BPs) are common pharmaceutical treatments used for calcium- and bone-related disorders, the principal one being osteoporosis. Their antiresorptive action is related to their high affinity for hydroxyapatite, the main inorganic substituent of bone. On the other hand, the phosphonate groups on their backbone make them excellent ligands for metal ions. The combination of these properties finds potential application in the utilization of such systems as controlled drug release systems (CRSs). In this work, the third generation BP drug zoledronate (ZOL) was combined with alkaline earth metal ions (e.g., Sr²⁺ and Ba²⁺) in an effort to synthesize new materials. These metal–ZOL compounds can operate as CRSs when exposed to appropriate experimental conditions, such as the low pH of the human stomach, thus releasing the active drug ZOL. CRS networks containing Sr²⁺ or Ba²⁺ and ZOL were physicochemically and structurally characterized and were evaluated for their ability to release the free ZOL drug during an acid-driven hydrolysis process. Various release and kinetic parameters were determined, such as initial rates and release plateau values. Based on the drug release results of this study, there was an attempt to correlate the ZOL release efficiency with the structural features of these CRSs.

Keywords: osteoporosis; bisphosphonates; zoledronate; metal phosphonates; hybrid materials; controlled release; MOFs; strontium; barium

Citation: Vassaki, M.; Lazarou, S.; Turhanen, P.; Choquesillo-Lazarte, D.; Demadis, K.D. Drug-Inclusive Inorganic–Organic Hybrid Systems for the Controlled Release of the Osteoporosis Drug Zoledronate. *Molecules* **2022**, *27*, 6212. <https://doi.org/10.3390/molecules27196212>

Academic Editor: Constantina Papatriantafyllopoulou

Received: 12 August 2022

Accepted: 16 September 2022

Published: 21 September 2022

Publisher's Note: MDPI stays neutral with regard to jurisdictional claims in published maps and institutional affiliations.



Copyright: © 2022 by the authors. Licensee MDPI, Basel, Switzerland. This article is an open access article distributed under the terms and conditions of the Creative Commons Attribution (CC BY) license (<https://creativecommons.org/licenses/by/4.0/>).

1. Introduction

Bisphosphonates (BPs) have been introduced to the pharmaceutical market since the late 1970s as drugs for disorders of calcium metabolism [1]. BPs are chemically stable structural analogs of inorganic pyrophosphate. They possess a carbon in the place of the bridging O of pyrophosphate. This endows them with resistance to hydrolysis and high affinity for hydroxyapatite (HAP), the principal natural mineral component of bone and teeth [2].

Zoledronate (ZOL, Figure 1) is a third generation N-containing BP drug, 5000 times more potent than etidronate, a 1st generation drug. It is administered as a solution or in tablet form (as zoledronic acid) under several commercial names (e.g., Zometa[®]). It exhibits an affinity constant $K_{app} = 34.7 \pm 1.8 \times 10^5 \text{ M}^{-1}$ for hydroxyapatite [3]. The binding affinity determines drug absorption and retention by the bone. These features affect its osteoclast inhibition potency. ZOL was approved in 2001 (by the FDA) for the treatment of several bone-related disorders (e.g., osteoporosis, high blood calcium due to cancer, bone breakdown due to cancer, Paget's disease of bone and Duchenne muscular dystrophy).

In general, BPs are administered orally and in some cases via injection. Their bioavailability is very low (depending on the individual BP) and only a small portion of the drug is absorbed by the intestine, distributed via blood in the body and finally reaching bone. Hence, the therapeutic dosage is usually increased in order to achieve effective patient

treatment, resulting in several side effects, such as hypocalcemia, osteomyelitis, osteonecrosis of the lower jaw, “flu”-like symptoms, bone pain, and gastro-intestinal, ocular and renal side effects [4].

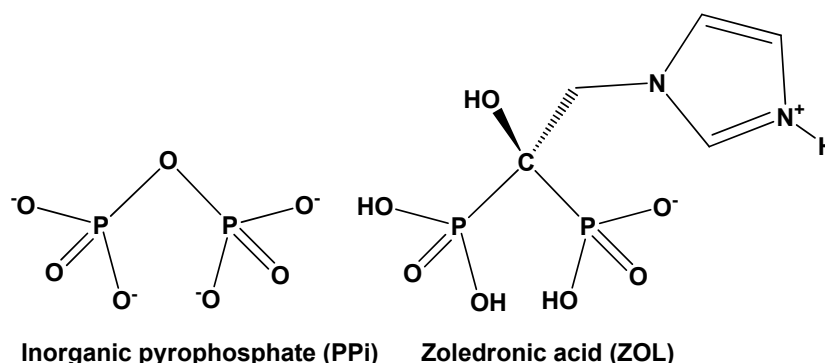


Figure 1. Schematic structures of inorganic pyrophosphate (PPI, left, in its fully deprotonated form) and zoledronic acid (right, in its zwitterionic form).

One strategy to reduce side effects is the fabrication of controlled release systems (CRSs) that could demonstrate release of the active BP drug in a predictable and controlled way. One approach is to view BPs as organic ligands for metal ions. The presence of the anionic phosphonate groups on the BP backbone endows them with strong affinity for metal ions in aqueous solutions [5]. Hence, metal-containing hybrid materials were constructed by combining BPs with biologically acceptable metal ions such as Mg^{2+} and Ca^{2+} , or their surrogates Sr^{2+} and Ba^{2+} . Some biological applications of coordination compounds and metal organic frameworks (MOFs) included their evaluation as CRSs under different conditions that mimic the conditions in human body (e.g., the gastrointestinal tract) [6].

Recently, we initiated a systematic study of metal-containing coordination polymers in which the linker is an actual BP drug. The scope of this study includes the synthesis of such metal–BP systems, their full structural elucidation, and the evaluation of their ability to act as sources of the BP drug when exposed to appropriate conditions. For example, Mg^{2+} – and Ca^{2+} –containing complexes and coordination polymers of various structural motifs were synthesized with four BP drugs (etidronate, pamidronate, alendronate and neridronate) and were studied as CRSs [7]. Their metal–O(phosphonate) coordination bonds can undergo hydrolysis (at low pH), leading to the controlled release of the active BP drug. These were coined “self-sacrificial MOFs” because their decomposition must precede drug release. The coordination of the BP drug by the metal ions resulted in substantially reduced initial release rates and lower final % release compared to the respective control system (with “free” drug and no metals). Recently, the 3rd generation anti-osteoporotic drug risedronate (RIS) was used for the synthesis of two new coordination polymers, namely $[Ca(RIS)(H_2O)]_n$ (Ca–RIS) and $[Sr(RIS)(H_2O)]_n$ (Sr–RIS) [8]. These two novel compounds were physicochemically and structurally characterized and were also evaluated for their RIS release features under acidic conditions (pH = 1.3) that mimic the human stomach. It was found that the drug release profiles Ca- and Sr–RIS (in the presence of linear polyethyleneimine polymer as drug solubility enhancer) were 4–5 times faster than the “free” RIS system.

In this paper, the synthesis and characterization of two CRSs for the drug ZOL are presented, namely Sr–ZOL and Ba–ZOL. In addition, the controlled release of ZOL is studied in these systems and compared to the “free” ZOL system (no metals). To the best of our knowledge, this is the first systematic controlled release study of the ZOL drug.

2. Results

2.1. Synthesis and Characterization of (Sr/Ba)–ZOL Compounds

The new (Sr/Ba)–ZOL compounds were synthesized under ambient conditions in mildly acidic pH (3.5), by reacting ZOL acid monohydrate with strontium or barium chloride, respectively, Figure 2 (upper). The solution pH is crucial for isolating tractable

products. Excessively low pH will cause crystallization of unreacted ZOL, whereas high pH will result in fast product precipitation that is usually amorphous, or with low crystallinity. Inevitably, extensive experimentation with various solution pH values must be carried out. It was found that the pH of 3.5 is optimal for the isolation of pure, monophasic products. These syntheses yielded single crystals suitable for X-ray diffraction studies. The crystals were isolated and studied by scanning electron microscopy as well. The morphology and the size of the crystals of the two compounds are shown in Figure 2.

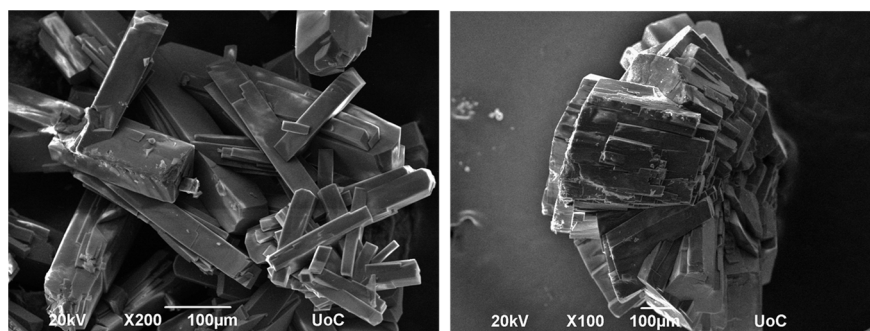
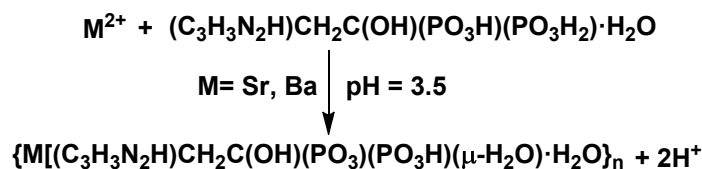


Figure 2. Reaction scheme for the synthesis of (Sr/Ba)–ZOL (upper) and SEM images of single crystals of Sr–ZOL (lower left) and Ba–ZOL (lower right).

The (Sr/Ba)–ZOL compounds were studied by ATR-IR spectroscopy (see Figure S1, Supplementary Materials). The vibrational frequencies between $2600\text{--}3200\text{ cm}^{-1}$ are attributed to N–H stretching vibration and C–H symmetric and antisymmetric stretching vibrations of the heteroaromatic ring of imidazole [9]. The spectral region $900\text{--}1200\text{ cm}^{-1}$ is complex and includes several characteristic vibrations related to the $-\text{PO}_3$ moieties of ZOL [10]. The other frequencies between $1440\text{--}1650\text{ cm}^{-1}$ are assigned to the C=C and C=N stretching vibrations of the heterocyclic aromatic ring [9]. The range $700\text{--}850\text{ cm}^{-1}$ is associated with out of plane bending of C–H of imidazole [10].

2.2. Powder and Single Crystal X-ray Diffraction Studies of (Sr/Ba)–ZOL Compounds

Bulk solid products of the (Sr/Ba)–ZOL compounds were studied by powder X-ray diffraction to ensure that they were pure and monophasic. Comparison of the calculated (from the crystal structure determination, see below) and measured X-ray diffraction diagrams ensured that the samples were single phases (Figures S2–S4, Supplementary Materials).

Suitable crystals for single crystal X-ray diffraction and structure determination were obtained by syntheses at ambient conditions (see Materials and Methods). The crystallographic data of the compounds Sr–ZOL and Ba–ZOL are summarized in Table 1 and their cif files are provided as Supplementary Materials.

The starting material, ZOL acid, exists as a zwitterion, because the “external” N atom is protonated, while one phosphonate group is singly deprotonated [11]. However, in the structures of Sr–ZOL and Ba–ZOL it exhibits a total charge of “−2” to counterbalance the “+2” charge of the metal cation. This means that one of the phosphonate groups (P1) is mono-deprotonated, whereas the other (P2) is bis-deprotonated. Hence, ZOL behaves as a zwitterion in the Metal-ZOL structures. Sr–ZOL and Ba–ZOL are principally isostructural, with only minor differences in the hydrogen-bonding scheme. Hence, structural details of the Ba-ZOL compound will be discussed. A representation of the basic structure of Sr/Ba-ZOL is shown in Figure 3. Each ZOL ligand coordinates to three metals, and hence, Sr/Ba-ZOL are 2D coordination polymers. The mono-deprotonated phosphonate (P1)

bridges two neighboring metal centers by using two O atoms (O1 and O2), while the third O atom (O3) remains non-coordinated. Interestingly, O1 is the protonated oxygen with the longest P-O bond length 1.534 Å. The fully deprotonated phosphonate (P2) also bridges two metal centers, but in a very different fashion. Two of the O atoms (O4 and O5) chelate a metal center (forming a 4-membered ring), while the third O atom (O6) binds a neighboring metal. The -OH group and the imidazole ring (both connected to the central C) are non-coordinating.

Table 1. Crystal data for compounds Sr-ZOL and Ba-ZOL.

| | Sr-ZOL | Ba-ZOL |
|--------------------------|---|---|
| Empirical Formula | C ₅ H ₁₂ SrN ₂ O ₉ P ₂ | C ₅ H ₁₂ BaN ₂ O ₉ P ₂ |
| <i>M_r</i> | 393.73 | 443.43 |
| Crystal System | triclinic | triclinic |
| Space Group | P $\bar{1}$ | P $\bar{1}$ |
| a (Å) | 6.3648(2) | 6.479(2) |
| b (Å) | 6.6900(2) | 6.837(2) |
| c (Å) | 13.9296(5) | 14.173(5) |
| α (°) | 102.5690(10) | 77.532(12) |
| β (°) | 91.4870(10) | 88.748(11) |
| γ (°) | 90.1080(10) | 89.021(10) |
| V (Å³) | 578.703 | 612.819 |
| Z | 2 | 2 |
| R factor (%) | 2.98 | 3.80 |
| CCDC code | 2195677 | 2195679 |

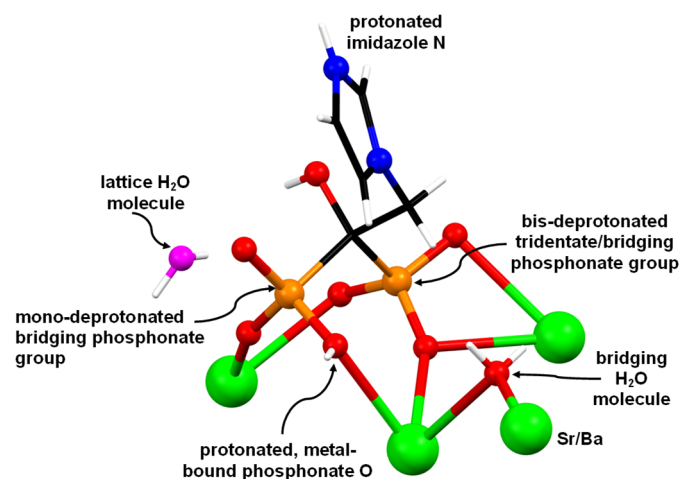


Figure 3. Depiction of the environment of the ZOL ligand in the structure of compounds Sr-ZOL and Ba-ZOL. Color codes: metal centers, green; P, orange; O, red; C, black; N, blue; H, white; lattice H₂O, magenta.

The P-O bond lengths are influenced by the protonation state of ZOL, but also by the coordination to a metal center. For example, in the structure of free ZOL (anhydrous) there are two “long” P-O bonds (1.548 Å and 1.554 Å) that correspond to the fully protonated -P-O-H moieties and a “short” P-O bond for the P=O moiety (1.498 Å) [12]. In the same structure, there is a mono-deprotonated phosphonate group (-PO₃H⁻) that has been generated by internal protonation of one of the N atoms in the imidazole ring. There are also two kinds of P-O bonds for the -PO₃H⁻ group, a “short” P=O bond (1.505 Å)

and two “long” P–O bonds (1.555 Å and 1.527 Å). The former is the P–O(H) bond, and the latter is the P–O[−] bond. Hence, it appears that the P–O bond is somewhat shortened upon deprotonation. The case of the Sr/Ba–ZOL structures is more complicated because there is metal coordination involved. We will examine the Sr–ZOL case as the example and discuss the two crystallographically and chemically different phosphonate groups (P1 and P2). The phosphonate group P2 is fully deprotonated and coordinated asymmetrically to three Sr centers (with monodentate, chelating and bridging modes). P2 displays two “short” P–O bonds (P2–O4 1.505 Å and P2–O5 1.516 Å) and one “long” bond P2–O6 1.555 Å. Hence, the “short” P–O bonds are reminiscent of the P=O and P–O[−] moieties. We assign the presence of the “long” bond to the particular coordination mode of the ZOL ligand. The phosphonate group P1 is mono-deprotonated and coordinated asymmetrically to two Sr centers (with monodentate modes, but the entire phosphonate bridges two Sr centers). P1 displays two “short” P–O bonds (P1–O2 1.505 Å and P1–O3 1.510 Å) and one “long” bond P1–O1 1.559 Å. The two “short” P–O bonds, of almost equal length, must be the result of delocalization of the negative charge (−1) over the P=O and P–O[−] moieties. The O atom of the “long” P–O bond is protonated (and coordinated to the Sr), consistent with the length of the bond.

In both compounds Sr/Ba–ZOL, the coordination sphere of the M²⁺ center can be described as a biaugmented trigonal prism (C_{2v}, based on SHAPE analysis), while they form six coordination bonds with oxygen atoms of three different ZOL ligands and two bonds with water molecules; see Figure 4. A list of all types of interactions in the structures of ZOL acid monohydrate, Sr–ZOL and Ba–ZOL, can be found in Table 2. Both these metal-bound H₂O molecules are positioned *cis* to each other and bridge neighboring metals. The Ba²⁺ cation chains are arranged in such a way that they lie parallel to the b-axis (Figure 4). The Ba–O bond distances (Figure 4) are between 2.621 Å and 3.049 Å. There are two types of interactions between the chains, hydrogen bonds and π – π stacking interactions. The latter are shown in Figure 4 together with those in the structure of ZOL acid monohydrate. They occur between the imidazole rings that are positioned in the interlayer space.

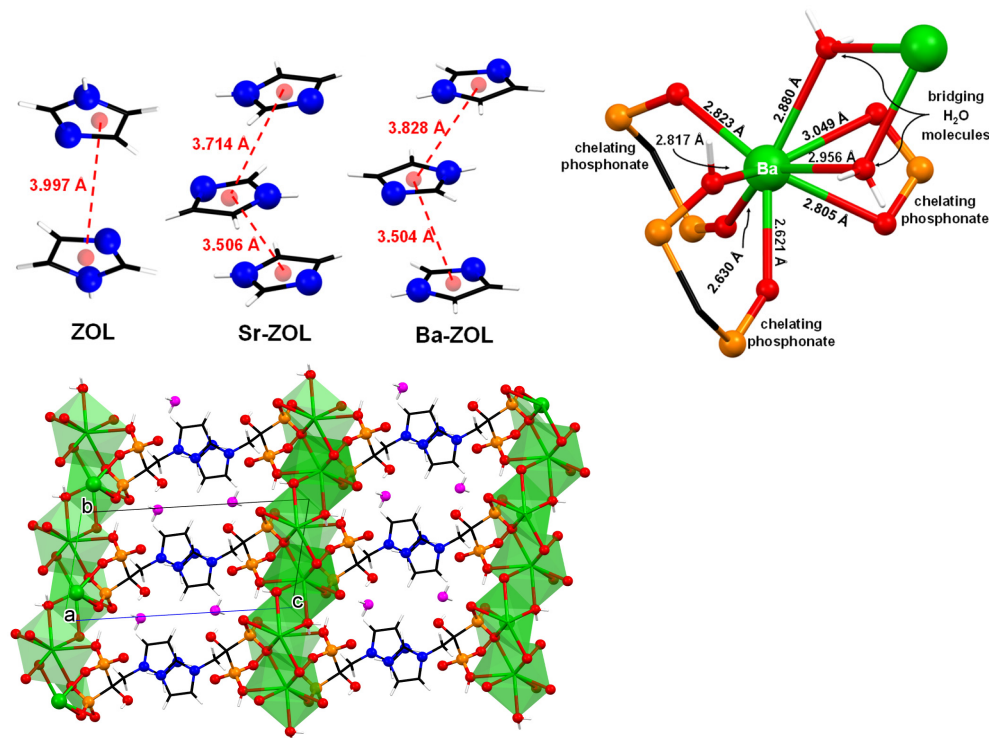


Figure 4. Various views of the crystal structures of Sr/Ba–ZOL: comparative π – π stacking interactions (**upper left**). The coordination sphere of the of Ba²⁺ center with Ba–O bond distances (**upper right**). Packing of three 2D layers along the b-axis (**lower**). Color codes: Ba, green; P, orange; O, red; C, black; N, blue; H, white, lattice H₂O, magenta.

Table 2. All types of interactions present in the structure of ZOL acid monohydrate, Sr-ZOL and Ba-ZOL.

| Compound. | P _A | P _B | N | OH | Total H-Bonds ¹ | π - π Interactions | M-O Bonds (PO ₃ /H ₂ O/OH) ² | Total Interactions | Lattice H ₂ O | M ²⁺ Cations |
|----------------|----------------|----------------|---|----|----------------------------|----------------------------|---|--------------------|--------------------------|-------------------------|
| ZOL Molecule 1 | 5 | 4 | 1 | 1 | 11 | 1 | 0 | 12 | 1 | 0 |
| ZOL Molecule 2 | 3 | 6 | 1 | 1 | | | | | | |
| Sr-ZOL | 5 | 4 | 1 | 1 | 11 | 2 | 6/2/0 | 21 | 1 | 1 |
| Ba-ZOL | 4 | 3 | 1 | 1 | 9 | 2 | 6/2/0 | 19 | 1 | 1 |

¹ Only the intermolecular H-bonds are considered. ² The OH is the substituent on the central C of ZOL.

There is one lattice water molecule (O9) per asymmetric unit in the structure of the M-ZOL compounds. It is situated in the interlayer space, but close to the metal-phosphonate layer. It forms three hydrogen bonds, two with phosphonate O atoms from neighboring units (O9...O5 2.761 Å and O9...O3 2.698 Å) and one with the C-OH group (O9...O6 2.644 Å). The protonated N of the imidazole ring forms a hydrogen bond with an uncoordinated O of the phosphonate P1 (O3...N2 2.625 Å).

2.3. Controlled Release Study of “Free” ZOL, Sr-ZOL and Ba-ZOL

Three controlled release systems (CRSs) were evaluated in the form of tablets: (a) the “free” drug ZOL acid monohydrate, (b) Sr-ZOL, and (c) Ba-ZOL. In each case, the active agent (the “free” ZOL drug and its metal-ZOL coordination compounds) was mixed and ground with the appropriate excipients in the solid form, and these powders were pressed into tablets. These tablets were immersed into acidic solutions and aliquots were withdrawn at specific time intervals. The detailed protocols for tablet preparation, sampling and drug quantification are described in detail in Sections 4.4 and 4.5. Under the acidic conditions of the drug release experiments, hydrolysis of the metal-O bonds occurs that leads to the degradation of the crystal lattice and the release of ZOL into the acidic medium. The drug release was quantified by ¹H NMR spectroscopy and the results were plotted in graphs as “% ZOL released” vs. time (in hours). The release curves for all systems are shown in Figure 5 and some kinetic parameters are collected in Table 3.

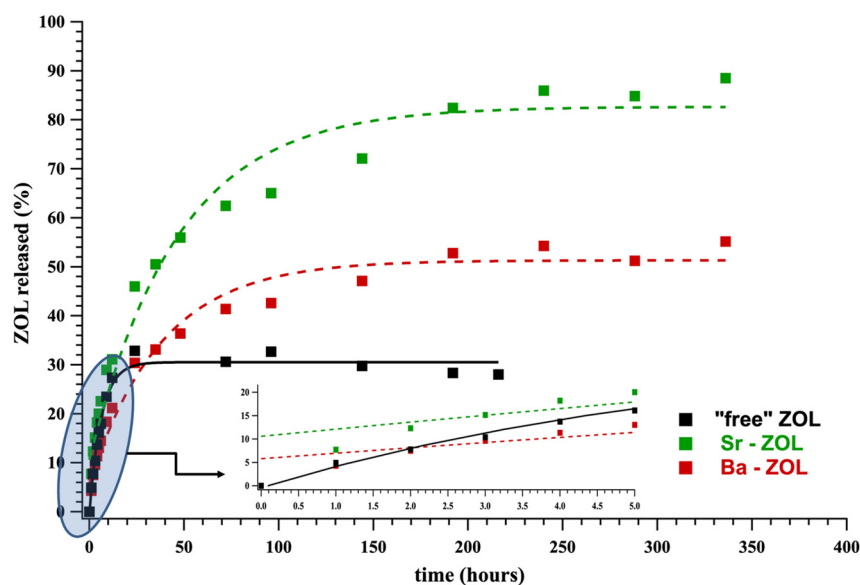
**Figure 5.** ZOL release curves from Sr- and Ba-ZOL containing tablets and comparison with the “free” ZOL system.

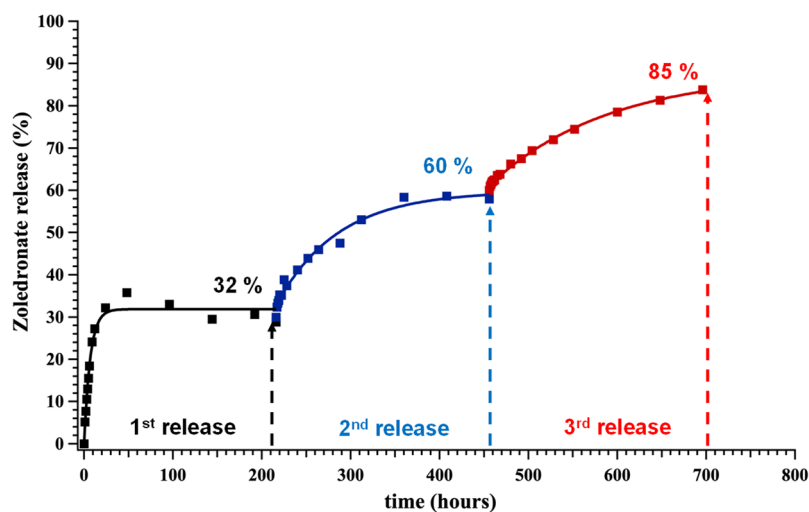
Table 3. Kinetic data for the drug release from tablets with “free” ZOL, Sr-ZOL and Ba-ZOL.

| | Initial Rate ($\mu\text{mol}/\text{min}$) ¹ | Plateau BP (%) | t_p (h) ² | $t_{1/2}$ (h) ³ |
|------------|--|----------------|------------------------|----------------------------|
| “free” ZOL | 0.39 | 30 | 25.5 | 4.3 |
| Sr-ZOL | 0.50 | 80 | 153.2 | 24.4 |
| Ba-ZOL | 0.33 | 50 | 134.1 | 20.8 |

¹ Calculated based on the initial linear portion of the curve (see inset, Figure 5). ² t_p is defined as the time required for the plateau value to be reached. ³ $t_{1/2}$ is defined as the time required for half of the plateau value to be reached.

The Ba-ZOL system exhibits an initial rate of 0.33 $\mu\text{mol}/\text{min}$, slightly lower than the “free” ZOL system, 0.39 $\mu\text{mol}/\text{min}$. Furthermore, 134.1 hours are needed for the Ba-ZOL system to reach an equilibrium (plateau) of 50%, while the t_p is only 25.5 h for the “free” ZOL to reach its plateau value of 30%. We assigned the slower release kinetics of ZOL from the Ba-ZOL system to the hydrolysis of the Ba-O bonds, a requirement for the detachment of ZOL molecules from the coordination network and their subsequent dissolution into the aqueous phase. The Sr-ZOL system displays an enigmatic behavior. First, its initial rate (0.50 $\mu\text{mol}/\text{min}$) is higher than the “free” ZOL system (0.39 $\mu\text{mol}/\text{min}$) and the Ba-ZOL system (0.33 $\mu\text{mol}/\text{min}$). Secondly, its plateau value of 80% is higher than that of the Ba-ZOL system, and it needs an even longer time (153.2 h) to reach it. Interpretation of these results is presented in the Discussion section.

Furthermore, we wanted to investigate whether a tablet, after reaching the plateau value is still active in release of the active drug. For this purpose, a series of consecutive release steps were set up in the following way. The “free” ZOL tablet was selected for this study. After the first plateau of 32% was established (25.5 h), the release experiment was allowed to proceed for up to ~210 h to ensure equilibrium. At that point, the aqueous phase was replaced with a “fresh” one (pre-acidified at pH 1.3), thus signifying the onset of a second release (second step). The second release was allowed to proceed up to the 450th hour, reaching a cumulative plateau value of 60%. By following the same methodology, a third step was initiated immediately after, reaching a cumulative plateau value of 85%. The results are shown in Figure 6. A fourth step was also done (results shown in Figure S5, Supplementary Materials), allowing the system to release the ZOL quantitatively. These results prove that the ZOL-containing tablet, if placed under the appropriate conditions, can release 100% of the active ingredient and the entire quantity of ZOL is solvent-accessible. Such a step-wise behavior has been noted in the controlled release of etidronate and pamidronate from silica-based hydrogels [13].

**Figure 6.** Cumulative, step-wise release of ZOL from the “free” ZOL system.

3. Discussion

One of the main advantages of using crystalline metal–bisphosphonate materials as controlled release systems is the knowledge of the precise identity of the drug-releasing compound. There are two basic requirements for this: (a) the synthetic protocols must yield monophasic products, and (b) the crystal structure of the product must be known. A successful synthesis outcome involves extensive experimentation with variables such as solution pH, reactant concentrations and molar ratios and temperature (and pressure, in the case of hydrothermal synthesis). For these Sr/Ba–ZOL systems, the optimum synthesis pH was 3.5, which yielded crystalline solids with Sr/Ba–ZOL molar ratio 1:1.

The published crystal structures containing the BP zoledronate include its “free” forms, its organic salt forms and its metal-containing forms. The “free” forms include two polymorphs (monoclinic and triclinic) of anhydrous zoledronic acid [12], zoledronic acid monohydrate [14], and zoledronic acid trihydrate [15,16]. The organic salt forms of zoledronate include the cytosinium zoledronate trihydrate [17], the dicyclohexylammonium zoledronate [18] and the bis(ammonium) zoledronate [19]. The metal-containing forms of zoledronate include structures with metal centers, such as K^+ [20], Zn^{2+} [21], Mn^{2+} [22], Fe^{3+} [22], Co^{2+} [23], Ni^{2+} [23], and Cu^{2+} [24].

ZOL release experiments were carried out at pH 1.3. This value was selected to mimic the pH of the human stomach. We are aware of the fact that the stomach fluid is a much more complicated system, which cannot be fully simulated in the laboratory. However, based on the fact that metal phosphonate compounds are unstable at such low pH, it was decided that pH is the principal factor for the acid-driven hydrolysis of the M–O(phosphonate) bonds and this approach is sufficient for a “proof-of-concept”. 1H NMR spectroscopy was used for the quantification of ZOL in the supernatant phase. It was preferred over ^{31}P NMR, which is time consuming and impractical for this particular application. We have successfully used ^{31}P NMR for quantification of drugs without any hydrogens, for example clodronate (unpublished results). The controlled release curves of all systems studied here are shown in Figures 5 and 6. The results obtained here show that the metal-containing ZOL systems exhibit similar (Ba–ZOL) or higher (Sr–ZOL) initial release rates than the “free” ZOL system (no metals). This observation is in contrast to what was noted in our previous work [7] for other BP drugs, in which the “free” drug was released much faster than the metal-containing drugs. The results obtained herein appear to be counterintuitive because the hydrolysis of the M–O bonds in the Sr–ZOL and Ba–ZOL systems does not appear to slow down the release kinetics of the active ZOL.

The release features of the “free” ZOL system may be related to the stability of the crystal lattice of the compound. The water solvent must overcome several stabilizing interactions. There are medium-strength π – π interactions between the imidazole rings (centroid-to-centroid distance 3.997 Å). The presence of one lattice water further stabilizes the crystal structure because hydrogen bonds are formed with the phosphonate groups. Each ZOL molecule forms 11 hydrogen bonds in total (phosphonate groups and imidazole ring), Table 2. As mentioned above, ZOL exists as a zwitterion in its crystal lattice, so, effectively it may behave as a “dipole”. Hence, its crystal packing is not only a result of hydrogen bonding interactions, but also of ionic interactions, the latter acting to further stabilize the crystal lattice.

Both metal–ZOL compounds can be described as 2D coordination polymers, propagated by various phosphonate bridging modes. There are π – π interactions (Figure 4) between the ZOL imidazole rings and the centroid-to-centroid distances range from 3.504 Å to 3.828 Å. There are 11 H-bonding interactions (per molecular unit) in Sr–ZOL and 9 in Ba–ZOL. The coordination geometry of the metal centers is the same in the two compounds. The Sr–ZOL displays the fastest initial rate. Careful examination of its crystal structure reveals that the layers are not stabilized by H-bonding, and for that reason, they can be readily exfoliated by the water solvent. Thus, the Sr–O bonds are exposed to the acidic medium and could be easily hydrolyzed.

Both Sr–ZOL and Ba–ZOL compounds are isostructural, with only minor differences in the hydrogen-bonding scheme. According to the argument that Sr–O(phosphonate) bonds are stronger (and harder to hydrolyze) than the corresponding Ba–O(phosphonate) bonds, the Sr–ZOL system should demonstrate slower release kinetics than the Ba–ZOL system. However, this is not the case, as evidenced by the parameters in Table 3. The only viable explanation for this phenomenon lies with the morphology and size of the metal–ZOL particles. The Sr–ZOL particles are needle-like, in contrast to crystal aggregates in Ba–ZOL, therefore exposing a much larger surface to the solvent. Since the dissolution process is surface-dependent, it is reasonable to expect that Sr–ZOL should undergo dissolution much more effectively (and rapidly) than Ba–ZOL. Furthermore, the particle size of Sr–ZOL is much smaller than that of Ba–ZOL.

4. Materials and Methods

4.1. Materials

All reagents that were utilized as sources of metal ions were from commercial sources. Strontium chloride hexahydrate ($\text{SrCl}_2 \cdot 6\text{H}_2\text{O}$) and barium chloride dihydrate, ($\text{BaCl}_2 \cdot 2\text{H}_2\text{O}$) were purchased from Sigma-Aldrich (St. Louis, MO, USA). The tablet excipients lactose (Serva), cellulose (Merck) and silica (Alfa-Aesar) were from commercial sources. Deionized (DI) water was used in all experiments and was produced from a laboratory ion exchange column.

4.2. Instrumentation

Scanning electron microscopy. Elemental analyses and SEM images of the morphology of the metal–BPs collected with a JOEL JSM-6390LV electron microscope.

Single crystal X-ray diffraction. Measured crystals were prepared under inert conditions immersed in perfluoropolyether as protecting oil for manipulation. Suitable crystals were mounted on MiTeGen Micromounts™, and these samples were used for data collection. Data were collected with a Bruker D8 Venture diffractometer with graphite monochromated $\text{CuK}\alpha$ radiation ($\lambda = 1.54178 \text{ \AA}$). The data were processed with APEX3 suite [25]. The structures were solved by intrinsic phasing using the ShelXT program [26], which revealed the position of all non-hydrogen atoms. These atoms were refined on F^2 by a full-matrix least-squares procedure, using the anisotropic displacement parameter [27]. All hydrogen atoms were located in different Fourier maps and were included as fixed contributions riding on attached atoms with isotropic thermal displacement parameters 1.2- or 1.5-times those of the respective atom. The Olex2 software was used as a graphical interface [28]. Molecular graphics were generated using mercury [29]. The crystallographic data for the reported structures were deposited with the Cambridge Crystallographic Data Center as supplementary publication nos. CCDC 2195677 and 2195679. Copies of the data can be obtained free of charge at <http://www.ccdc.cam.ac.uk/products/csd/request>.

Powder X-ray diffraction. The powder X-ray diffraction (XRD) patterns were performed on PANalytical X'Pert Pro diffractometer, a configuration of the Bragg–Brentano, equipped with monochromator Ge(111) ($\text{Cu K}\alpha_1$) and detector X'Celerator.

4.3. Synthetic Protocols

Synthesis of (1-hydroxy-2-(1H-imidazol-1-yl)ethane-1,1-diyl)bis(phosphonic acid), zoledronic acid monohydrate (ZOL). ZOL was synthesized by following a previously reported method with some modifications [30]. A mixture of 1-imidazoleacetic acid (10 g, 0.079 mol), phosphorous acid (6.5 g, 0.079 mol), and methanesulfonic acid (25 mL) was heated to 65–70 °C followed by addition of PCl_3 (13.8 mL, 21.7 g, 2.0 eq) for over 0.5 h under nitrogen atmosphere. After the PCl_3 addition, the mixture was stirred at 65–70 °C overnight and cold distilled water (70 mL) was added to a cooled solution with vigorous stirring. After refluxing overnight, the reaction mixture was allowed to cool to room temperature and EtOH (140 mL) was added by stirring and the mixture was left at room temperature for a couple days. The formed solids were collected by filtration, washed with EtOH and

finally with acetone and dried under reduced pressure. The final product was obtained as a white solid (11.9 g, 52% yield). ^1H NMR (D_2O): δ 7.70 (s, 1H), 7.21 (s, 1H), 6.84 (s, 1H), 4.44 (t, 2H, $^3J_{\text{HP}} = 9.7$). ^{13}C NMR (D_2O , CD_3OD as ref.) δ 141.1, 126.8, 123.9, 76.2 (t, $^1J_{\text{CP}} = 131.5$, P-C-P), 53.2 (t, $^2J_{\text{CP}} = 3.4$). ^{31}P NMR (D_2O) δ 16.4. Peak assignments can be found in the Supplementary Materials. NMR data were consistent to those reported in the literature [30].

Synthesis of M-ZOL, $\{\{\text{M}[(\text{C}_3\text{H}_4\text{N}_2)\text{CH}_2\text{C}(\text{OH})(\text{PO}_3\text{H})(\text{PO}_3)(\text{H}_2\text{O})]\cdot\text{H}_2\text{O}\}_n$ (M = Sr, Ba). ZOL acid monohydrate (27 mg, 0.1 mmol) and either $\text{SrCl}_2\cdot 6\text{H}_2\text{O}$ (13 mg, 0.05 mmol) or $\text{BaCl}_2\cdot 2\text{H}_2\text{O}$ (12 mg, 0.05 mmol) were dissolved in ~ 10 mL DI H_2O under stirring until fully dissolved. The solution pH was adjusted to 3.5 (using stock solutions of NaOH and HCl, as needed). The final mixture was left under quiescent conditions for solvent evaporation. After 7–10 days (depending on ambient temperature) a colorless crystalline product formed, it was isolated by filtration, rinsed with DI water and left to dry under air. Bulk product purity was confirmed by powder X-ray diffraction (comparison of the calculated and experimental powder patterns) and elemental analysis. Yield: For Sr-ZOL 17 mg (43%), for Ba-ZOL 20 mg (45%). Elemental analysis (%): For Sr-ZOL, calcd. for $\{\{\text{Sr}[(\text{C}_3\text{H}_4\text{N}_2)\text{CH}_2\text{C}(\text{OH})(\text{PO}_3\text{H})(\text{PO}_3)(\text{H}_2\text{O})]\cdot\text{H}_2\text{O}\}_n$, M.W. 393.73: C 15.24; H 3.05; N 7.11. Found: C 14.94; H 3.26; N 7.09. For Ba-ZOL, calcd. for $\{\{\text{Ba}[(\text{C}_3\text{H}_4\text{N}_2)\text{CH}_2\text{C}(\text{OH})(\text{PO}_3\text{H})(\text{PO}_3)(\text{H}_2\text{O})]\cdot\text{H}_2\text{O}\}_n$, M.W. 443.43: C 13.53; H 2.71; N 6.31. Found: C 13.31; H 2.83; N 6.37.

4.4. Preparation of Tablets for ZOL Release

Tablets were prepared by mechanical mixing of ground powders (with a mortar-and-pestle) of the drug component (850 μmol of ZOL content) and three commonly used excipients, i.e., lactose, cellulose and silica. Subsequently, a tablet was prepared by applying 10 tons of pressure in a hydraulic press. The tablet total weight was 1.000 g. Identical tablets that contained equimolar amounts of the metal-BPs (Sr-ZOL and Ba-ZOL) and the three excipients were fabricated. The quantities used in the tablets are shown in Table 4.

Table 4. Quantities of active agents (free ZOL or metal-ZOL) and excipients utilized for tablet preparation.

| Tablet | ZOL acid·H ₂ O | Sr-ZOL * | Ba-ZOL * |
|-----------------|---------------------------|----------|----------|
| MW (g/mol) | 290.11 | 393.73 | 443.43 |
| Drug system (g) | 0.247 | 0.335 | 0.377 |
| Lactose (g) | 0.251 | 0.222 | 0.208 |
| Cellulose (g) | 0.251 | 0.222 | 0.208 |
| Silica (g) | 0.251 | 0.222 | 0.208 |

* Multiple syntheses of Sr- and Ba-ZOL were necessary to collect the required quantity (see Section 4.3).

4.5. Quantification of ZOL

Each tablet described above was immersed in a glass beaker containing 50 mL of deionized water whose pH was adjusted to 1.3, using hydrochloric acid. The ZOL-containing tablet (as prepared above) was placed in a plastic net and was immersed into the solution (50 mL of deionized water whose pH was adjusted to 1.3 using hydrochloric acid) just above the stirring bar. Mild stirring was applied to ensure solution homogeneity. Aliquots of the solution were withdrawn (sample volume 350 μL) every hour for the first 6 hours, then every 3 h until the 12th hour, and then every 12 h until the 48th h of the release experiment. After the 48th h, samples were withdrawn every 24 h or every 48 h or longer, if necessary. Each sample was placed in an NMR tube, and then the D_2O standard solution (150 μL) was added. The concentration of the D_2O TSP standard solution was 4.337 μmol . Quantification of ZOL concentration in each sample was achieved by peak integration (singlet at 8.75 ppm, which is the H on the C between the two N atoms of the imidazole ring) in the ^1H NMR spectrum and its comparison to the peak of the TSP standard solution peak [$-\text{Si}(\text{CH}_3)_3$]. For representative ^1H NMR spectra, see Figures S6 and S7, Supplementary

Materials. Initial rates were calculated based on the initial linear portion of the curve (see Figure S8, Supplementary Materials).

5. Conclusions

The main findings of the present study are as follows:

- (1) Two novel coordination polymers containing the alkaline-earth metal ions Sr²⁺ and Ba²⁺ and the anti-osteoporotic drug ZOL were synthesized and structurally characterized.
- (2) Sr-ZOL and Ba-ZOL are isostructural 2D coordination polymers.
- (3) Both Sr-ZOL and Ba-ZOL were utilized as controlled release systems (excipient-containing tablets) of the active drug ZOL in conditions that mimic the human stomach (pH = 1.3).
- (4) The drug release profiles of Sr-ZOL and Ba-ZOL were compared to that of “free” ZOL (absence of metals). Contrary to the working hypothesis, it was found that the release of ZOL is not delayed compared to the “free” ZOL system. In fact, in the case of Sr-ZOL, it is accelerated.
- (5) This behavior was rationalized based on the structural idiosyncrasies of each system. The overall drug release profile for each system was the result of several structural factors, such as presence or absence of π - π interactions between the ZOL imidazole rings, H-bonding interactions and strength of the metal-O(phosphonate) bonds. However, it seems that the governing factor for Sr-ZOL releasing the active drug more rapidly than Ba-ZOL is the particle size and morphology.

Based on these results, the role of the metal cation in such coordination polymers apparently influences both the initial drug release rates and the final plateau release value. Hence, with proper selection of the metal ion, these features can be controlled (increased or decreased, at will). Further research efforts along these lines are underway in our group that build upon results obtained and knowledge built [7,8,13,31–34].

Supplementary Materials: The following supporting information can be downloaded at: <https://www.mdpi.com/article/10.3390/molecules27196212/s1>: Figure S1. ATR-IR spectra of zoledronic acid, Ba-ZOL, and Sr-ZOL. Figure S2. Comparison of the calculated and measured X-ray diffraction diagrams of zoledronic acid monohydrate. Figure S3. Comparison of the calculated and measured X-ray diffraction diagrams of Ba-ZOL. Figure S4. Comparison of the calculated and measured X-ray diffraction diagrams of Sr-ZOL. Figure S5. Cumulative, step-wise release of ZOL from the “free” ZOL system. Figure S6. ¹H, ¹³C and ³¹P NMR spectra of zoledronic acid monohydrate. Figure S7. ¹H NMR spectra of released zoledronic acid from the Ba-ZOL and Sr-ZOL systems. Figure S8. Initial rates of drug release from “free” ZOL, Sr-ZOL and Ba-ZOL.

Author Contributions: Conceptualization, K.D.D.; methodology, M.V. and P.T.; investigation, M.V., S.L., P.T. and D.C.-L.; data curation, M.V. and D.C.-L.; writing—original draft preparation, M.V. and K.D.D.; writing—review and editing, K.D.D., M.V., S.L., P.T. and D.C.-L.; supervision, K.D.D., project administration, K.D.D., funding acquisition, M.V. and K.D.D. All authors have read and agreed to the published version of the manuscript.

Funding: The research work was supported by the Hellenic Foundation for Research and Innovation (HFRI) under the HFRI PhD Fellowship grant (Fellowship Number: 258) to M.V. D.C.-L. acknowledges funding by project no. PGC2018-102047-B-I00 (MCIU/AEI/FEDER, UE).

Data Availability Statement: Data presented in this paper are available from the authors.

Conflicts of Interest: The authors declare no conflict of interest.

Sample Availability: Samples of the compounds described herein are available from the authors.

References

1. Xu, X.-L.; Gou, W.-L.; Wang, A.-Y.; Wang, Y.; Guo, Q.-Y.; Lu, Q.; Lu, S.-B.; Peng, J. Basic research and clinical applications of bisphosphonates in bone disease: What have we learned over the last 40 years? *J. Transl. Med.* **2013**, *11*, 303. [CrossRef]
2. Russell, R.G. Bisphosphonates: From bench to bedside. *Ann. N. Y. Acad. Sci.* **2006**, *1068*, 367–401. [CrossRef] [PubMed]

3. Nancollas, G.H.; Tang, R.; Phipps, R.J.; Henneman, Z.; Gulde, S.; Wu, W.; Mangood, A.; Russell, R.G.G.; Ebetino, F.H. Novel insights into actions of bisphosphonates on bone: Differences in interactions with hydroxyapatite. *Bone* **2006**, *38*, 617–627. [CrossRef] [PubMed]
4. Watts, N.B.; Diab, D.L. Long-Term Use of Bisphosphonates in Osteoporosis. *J. Clin. Endocrinol. Metab.* **2021**, *95*, 1555–1565. [CrossRef] [PubMed]
5. Spinthaki, A.; Matheis, J.; Hater, W.; Demadis, K.D. Antiscalant-driven inhibition and stabilization of “magnesium silicate” under geothermal stresses: The role of magnesium-phosphonate coordination chemistry. *Energy Fuels* **2018**, *32*, 11749–11760. [CrossRef]
6. Barbosa, J.S.; Pinto, M.; Barreiro, S.; Fernandes, C.; Mendes, R.F.; Lavrador, P.; Gaspar, V.M.; Mano, J.F.; Borges, F.; Remião, F.; et al. Coordination Compounds As Multi-Delivery Systems for Osteoporosis. *ACS Appl. Mater. Interfaces* **2021**, *13*, 35469–35483. [CrossRef] [PubMed]
7. Vassaki, M.; Papathanasiou, K.E.; Hadjicharalambous, C.; Chandrinou, D.; Turhanen, P.; Choquesillo-Lazarte, D.; Demadis, K.D. Self-Sacrificial MOFs for Ultra-Long Controlled Release of Bisphosphonate Anti-Osteoporotic Drugs. *Chem. Commun.* **2020**, *56*, 5166–5169. [CrossRef] [PubMed]
8. Vassaki, M.; Kotoula, C.; Turhanen, P.; Choquesillo-Lazarte, D.; Demadis, K.D. Calcium and Strontium Coordination Polymers as Controlled Delivery Systems of the Anti-Osteoporosis Drug Risedronate and the Augmenting Effect of Solubilizers. *Appl. Sci.* **2021**, *11*, 11383. [CrossRef]
9. Abood, N.A.; AL-Askari, M.; Saeed, B.A. Structures and Vibrational Frequencies of Imidazole, Benzimidazole and its 2-Alkyl Derivatives Determined by DFT Calculations. *Basrah J. Sci.* **2012**, *30*, 119–131.
10. Zenobi, M.C.; Luengo, C.V.; Avena, M.J.; Rueda, E.H. An ATR-FTIR Study of Different Phosphonic Acids in Aqueous Solution. *Spectrochim. Acta Part A* **2008**, *70*, 270–276. [CrossRef]
11. Povoroznyuk, V.V.; Grygorieva, V.N.; Pekhnyo, V.I.; Kozachkova, O.M.; Tsaryk, N.V. Zoledronic Acid and Its Calcium-contain Complexes in Treatment of Experimental Osteoporosis in Wistar Female Rats. *Biochem. Anal. Biochem.* **2017**, *6*, 340.
12. Chernyshev, V.V.; Shkavrov, S.V.; Paseshnichenko, K.A.; Puryaeva, T.P.; Velikodny, Y.A. Zoledronic acid: Monoclinic and triclinic polymorphs from powder diffraction data. *Acta Cryst.* **2013**, *C69*, 263–266. [CrossRef]
13. Papathanasiou, K.E.; Turhanen, P.; Brückner, S.I.; Brunner, E.; Demadis, K.D. Smart, programmable and responsive injectable hydrogels for controlled release of cargo osteoporosis drugs. *Sci. Rep.* **2017**, *7*, 4743. [CrossRef]
14. Fronczek CCDC 1562048: Experimental Crystal Structure Determination. Available online: <https://doi.org/10.5517/ccdc.csd.cc1pffn6>. (accessed on 19 September 2022).
15. Fronczek, F.R. CCDC 1562049: Experimental Crystal Structure Determination. Available online: <https://doi.org/10.5517/ccdc.csd.cc1pffp7> (accessed on 19 September 2022).
16. Ruscika, R.; Bianchi, M.; Quintero, M.; Martinez, A.; Vega, D.R. Solid-State Forms of Zoledronic Acid: Polymorphism in Hydrates. *J. Pharm. Sci.* **2010**, *99*, 4962–4972. [CrossRef]
17. Sridhar, B.; Ravikumar, K. Multiple hydrogen bonds in cytosinium zoledronate trihydrate. *Acta Cryst.* **2011**, *C67*, o115–o119. [CrossRef]
18. Sarkar, A.; Cukrowski, I. Tris(dicyclohexylammonium) hydrogen [1-hydroxy-2-(1H-imidazol-1-yl)-1-phosphonatoethane]phosphonate ethanol monosolvate monohydrate. *Acta Cryst.* **2011**, *E67*, o2980. [CrossRef]
19. Sikorska, M.; Chojnacki, J. Bis(ammonium) Zoledronate Dihydrate. *J. Crystallogr.* **2013**, *2013*, 741483. [CrossRef]
20. Freire, E.; Vega, D.R.; Baggio, R. Zoledronate complexes. I. Poly[[μ_2 -aqua[μ_3 -1-hydroxy-2-(1H,3H-imidazol-3-ium-1-yl)ethylidenediphosphonato]potassium(I)] monohydrate]. *Acta Cryst.* **2010**, *C66*, m13–m16. [CrossRef]
21. Freire, E.; Vega, D.R. Aquabis[1-hydroxy-2-(imidazol-3-ium-1-yl)-1,10-ethylidenediphosphonato- k^2O,O']-zinc(II) dehydrate. *Acta Cryst.* **2009**, *E65*, m1430–m1431.
22. Freire, E.; Quintero, M.; Vega, D.R.; Baggio, R. Crystal structure and magnetic properties of two new zoledronate complexes: A Mn dimer [Mn(II)(H₃Zol)₂·(H₂O)₂] and a Fe₁₅ molecular cluster [Fe(III)₁₅(HZol)₁₀(H₂Zol)₂(H₂O)₁₂(Cl₄·(H₂O)₂)·Cl₇·(H₂O)₆₅] (where H₄Zol: C₅H₁₀N₂O₇P₂ is zoledronic acid). *Inorg. Chim. Acta* **2013**, *394*, 229–236. [CrossRef]
23. Cao, D.-K.; Li, Y.-Z.; Zheng, L.-M. Layered Cobalt(II) and Nickel(II) Diphosphonates Showing Canted Antiferromagnetism and Slow Relaxation Behavior. *Inorg. Chem.* **2007**, *46*, 7571–7578. [CrossRef]
24. Qiu, L.; Lv, G.; Guo, L.; Chen, L.; Luo, S.; Zou, M.; Lin, J. Synthesis, crystal structure and antitumor effect of a novel copper(II) complex bearing zoledronic acid derivative. *Eur. J. Med. Chem.* **2015**, *89*, 42–50. [CrossRef]
25. Bruker APEX3. *APEX3 V2019.1*; Bruker-AXS: Madison, WI, USA, 2019.
26. Sheldrick, G.M. SHELXT—Integrated Space-Group and Crystal-Structure Determination. *Acta Crystallogr. Sect. A Found. Crystallogr.* **2015**, *71*, 3–8. [CrossRef]
27. Sheldrick, G.M. Crystal Structure Refinement with SHELXL. *Acta Crystallogr. Sect. C Struct. Chem.* **2015**, *71*, 3–8. [CrossRef]
28. Dolomanov, O.V.; Bourhis, L.J.; Gildea, R.J.; Howard, J.A.K.; Puschmann, H. OLEX2: A Complete Structure Solution, Refinement and Analysis Program. *J. Appl. Crystallogr.* **2009**, *42*, 339–341. [CrossRef]
29. Macrae, C.F.; Bruno, I.J.; Chisholm, J.A.; Edgington, P.R.; McCabe, P.; Pidcock, E.; Rodriguez-Monge, L.; Taylor, R.; van de Streek, J.; Wood, P.A. Mercury CSD 2.0—New Features for the Visualization and Investigation of Crystal Structures. *J. Appl. Crystallogr.* **2008**, *41*, 466–470. [CrossRef]

30. Martin, M.B.; Grimley, J.S.; Lewis, J.C.; Heath, H.T.; Bailey, B.N.; Kendrick, H.; Yardley, V.; Caldera, A.; Lira, R.; Urbina, S.J.A.; et al. Bisphosphonates Inhibit the Growth of *Trypanosoma brucei*, *Trypanosoma cruzi*, *Leishmania donovani*, *Toxoplasma gondii*, and *Plasmodium falciparum*: A Potential Route to Chemotherapy. *J. Med. Chem.* **2001**, *44*, 909–916. [CrossRef]
31. Papathanasiou, K.E.; Vassaki, M.; Spinthaki, A.; Alatzoglou, F.-E.G.; Tripodianos, E.; Turhanen, P.; Demadis, K.D. Phosphorus chemistry: From small molecules to polymers to pharmaceutical and industrial applications. *Pure Appl. Chem.* **2019**, *91*, 421–441. [CrossRef]
32. Papathanasiou, K.E.; Demadis, K.D. Polymeric Matrices for the Controlled Release of Phosphonate Active Agents for Medicinal Applications. In *Handbook of Polymers for Pharmaceutical Technologies, Bioactive and Compatible Synthetic/Hybrid Polymers*; Thakur, V.K., Thakur, M.K., Eds.; Wiley-Scrivener Publishing LLC: Salem, MA, USA, 2015; Chapter 4; Volume 4, pp. 87–122.
33. Papathanasiou, K.E.; Moschona, A.; Spinthaki, A.; Vassaki, M.; Demadis, K.D. Silica-Based Polymeric Gels as Platforms for Delivery of Phosphonate Pharmaceuticals. In *Polymer Gels: Synthesis and Characterization*; Thakur, V.K., Thakur, M.K., Eds.; Springer: Berlin/Heidelberg, Germany, 2018; Chapter 5; pp. 127–140.
34. Shearan, S.; Stock, N.; Emmerling, F.; Demel, J.; Wright, P.A.; Demadis, K.D.; Vassaki, M.; Costantino, F.; Vivani, R.; Sallard, S.; et al. New Directions in Metal Phosphonate and Phosphinate Chemistry. *Crystals* **2019**, *9*, 270. [CrossRef]

Review

α -Aminophosphonates, -Phosphinates, and -Phosphine Oxides as Extraction and Precipitation Agents for Rare Earth Metals, Thorium, and Uranium: A Review

Esa Kukkonen , Emilia Josefina Virtanen  and Jani Olavi Moilanen * 

Department of Chemistry, Nanoscience Centre, University of Jyväskylä, P.O. Box 35, FI-40014 Jyväskylä, Finland; esa.p.kukkonen@jyu.fi (E.K.); emilia.j.virtanen@jyu.fi (E.J.V.)

* Correspondence: jani.o.moilanen@jyu.fi; Tel.: +358-408-054-849

Abstract: α -Aminophosphonates, -phosphinates, and -phosphine oxides are a group of organophosphorus compounds that were investigated as extraction agents for rare earth (RE) metals and actinoids for the first time in the 1960s. However, more systematic investigations of their extraction properties towards REs and actinoids were not started until the 2010s. Indeed, recent studies have shown that these α -amino-functionalized compounds can outperform the commercial organophosphorus extraction agents in RE separations. They have also proven to be very efficient extraction and precipitation agents for recovering Th and U from RE concentrates. These actinoids coexist with REs in some of the commercially important RE-containing minerals. The efficient separation and purification of REs is becoming more and more important every year as these elements have a pivotal role in many existing technologies. If one also considers the facile synthesis of α -amino-functionalized organophosphorus extractants and precipitation agents, it is expected that they will be increasingly utilized in the extraction chemistry of REs and actinoids in the future. This review collates α -aminophosphonates, -phosphinates, and -phosphine oxides that have been utilized in the separation chemistry of REs and actinoids, including their most relevant synthetic routes and molecular properties. Their extraction and precipitation properties towards REs and actinoids are also discussed.

Keywords: α -aminophosphonates; α -aminophosphinates; α -aminophosphine oxides; rare earth elements; actinoids; separation; recovery; extraction; precipitation

Citation: Kukkonen, E.; Virtanen, E.J.; Moilanen, J.O. α -Aminophosphonates, -Phosphinates, and -Phosphine Oxides as Extraction and Precipitation Agents for Rare Earth Metals, Thorium, and Uranium: A Review. *Molecules* **2022**, *27*, 3465. <https://doi.org/10.3390/molecules27113465>

Academic Editor: Jakub Adamek

Received: 5 May 2022

Accepted: 25 May 2022

Published: 27 May 2022

Publisher's Note: MDPI stays neutral with regard to jurisdictional claims in published maps and institutional affiliations.



Copyright: © 2022 by the authors. Licensee MDPI, Basel, Switzerland. This article is an open access article distributed under the terms and conditions of the Creative Commons Attribution (CC BY) license (<https://creativecommons.org/licenses/by/4.0/>).

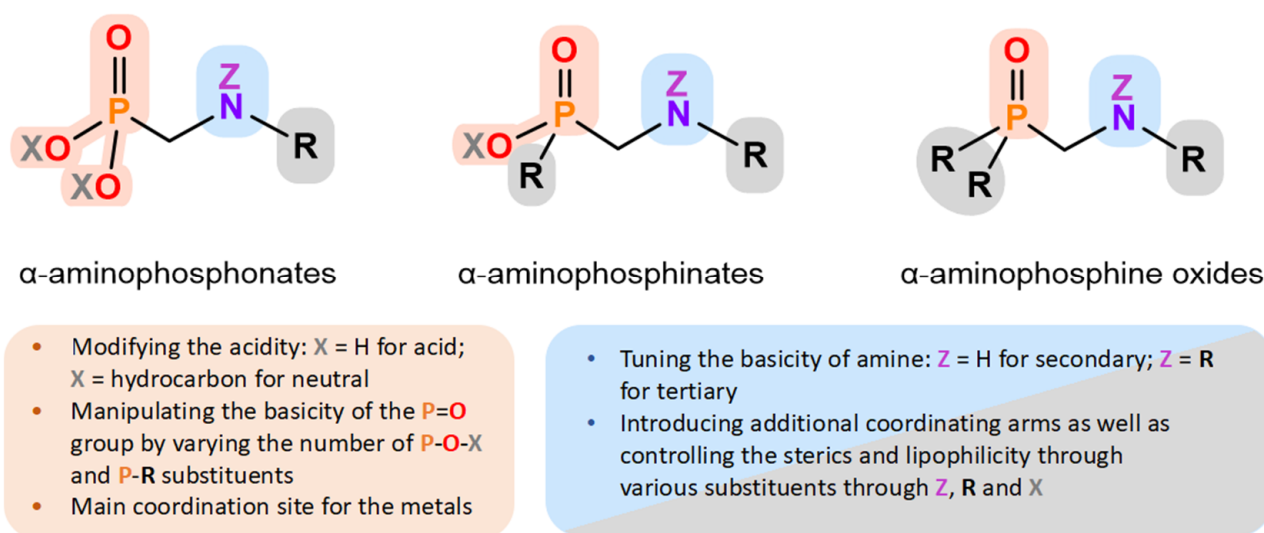
1. Introduction

Organophosphorus compounds are one of the main commercial extractants used to separate rare earth elements (RE; lanthanoids, Sc, and Y) in solvent extraction on an industrial scale [1]. The solvent extraction is based on two immiscible liquid phases, one of which is the (acidic) aqueous phase containing REs to be separated, and the other is an organic phase including extractants. Many factors, such as the selectivity and loading capacity of extractants, number of extraction, scrubbing, and stripping cycles, and back-extraction of the extracted metal, affect the efficiency of the extraction process, but in a simplified picture, it is the coordination affinity of the extractant towards metal ions that determines the extraction degree and separation of metal ions into different fractions [2,3]. Because the coordination affinity is dictated by the molecular structure of the extractant, a plethora of different organophosphorus extractants have been developed and investigated for the separation of REs by now [1,4,5]. Apart from solvent extraction, organophosphorus compounds have also been utilized in other separation methods to recover and separate REs. Illustrative examples of such methods are fractional precipitation and solid-phase extraction [6–9].

Organophosphorus extractants are usually classified into neutral and acidic compounds, the latter of which contains at least one acidic proton. They can also be divided into four different subgroups, which are phosphates ((RO)₃P(O)), phosphonates ((RO)₂P(O)R',

phosphinates ((RO)P(O)R'₂), and phosphine oxides (P(O)R'₃), according to their functional groups (R=H, organic substituent; R' = organic substituent) [3,10]. The basicity of organophosphorus extractants containing P=O and P-O-R bonds varies with the number of O atoms connected to the P atom; phosphine oxides are the most basic with one substituted oxygen atom, followed by phosphinates, phosphonates, and phosphates. An increase in the basicity is accompanied by an increase in the coordination strength of the extractant. Thus, phosphine oxides are usually the most efficient extractants for REs, but the separation of REs may be weaker with phosphine oxides as they may extract REs too effectively without significant separation compared to phosphinates, phosphonates, and phosphates.

The introduction of an amino group into organophosphorus compounds opens further synthetic strategies to modify their molecular structures, coordination affinity, and extraction properties [5]. For example, substituting H atoms of the amino group with new coordinating arms or long alkyl chains can increase the extractant's affinity towards REs or its lipophilicity, respectively [5,11]. Illustrative examples of organophosphorus extractants containing the amino group are α -aminophosphonates consisting of amino and phosphonate moieties with the general formula of (RO)₂P(O)CR'₂NR''₂. The R-R'' substituents can vary from H atoms to substituted hydrocarbons containing additional functional groups, making α -aminophosphonates versatile and modifiable chemical species. Replacing one of the -OR moieties of α -aminophosphonates with hydrocarbon gives α -aminophosphinates ((RO)P(O)(R')CR''₂NR'''₂), whereas the replacement of two of the -OR moieties leads to α -aminophosphine oxides ((RO)₂P(O)CR'₂NR''₂). As a group, these three families of α -amino-functionalized organophosphorus compounds can be classified as a subclass of organophosphorus extraction and precipitation agents that not only bear similar functional groups (P=O and amino moiety in the α position), but also have their distinct features (P-O-R vs. P-R bonds) that contribute to their complexation, extraction, and precipitation properties towards REs and actinoids (Scheme 1) [5]. Importantly, some of the α -amino-functionalized organophosphorus compounds have been proven to be better extractants for REs and actinoids than commercial extractants.



Scheme 1. Versatile frameworks of α -amino-functionalized organophosphorus extractants and precipitation agents that can be tailored for the extraction chemistry of REs and actinoids.

REs play a pivotal role in several applications utilized today. Illustrative examples of such applications are ceramics [12], alloys [13], photonics [14], catalysis [15], and permanent magnets [16]. Importantly, the latter are used in electric vehicles and wind turbines, which are key players in the green technology revolution contributing to fossil-fuel-free traffic and energy production, respectively [17]. Due to the suitability of REs for a wide range of applications, it has been predicted that the demand and price of REs will significantly increase in the future. As a matter of fact, the average price of Nd, the most crucial element

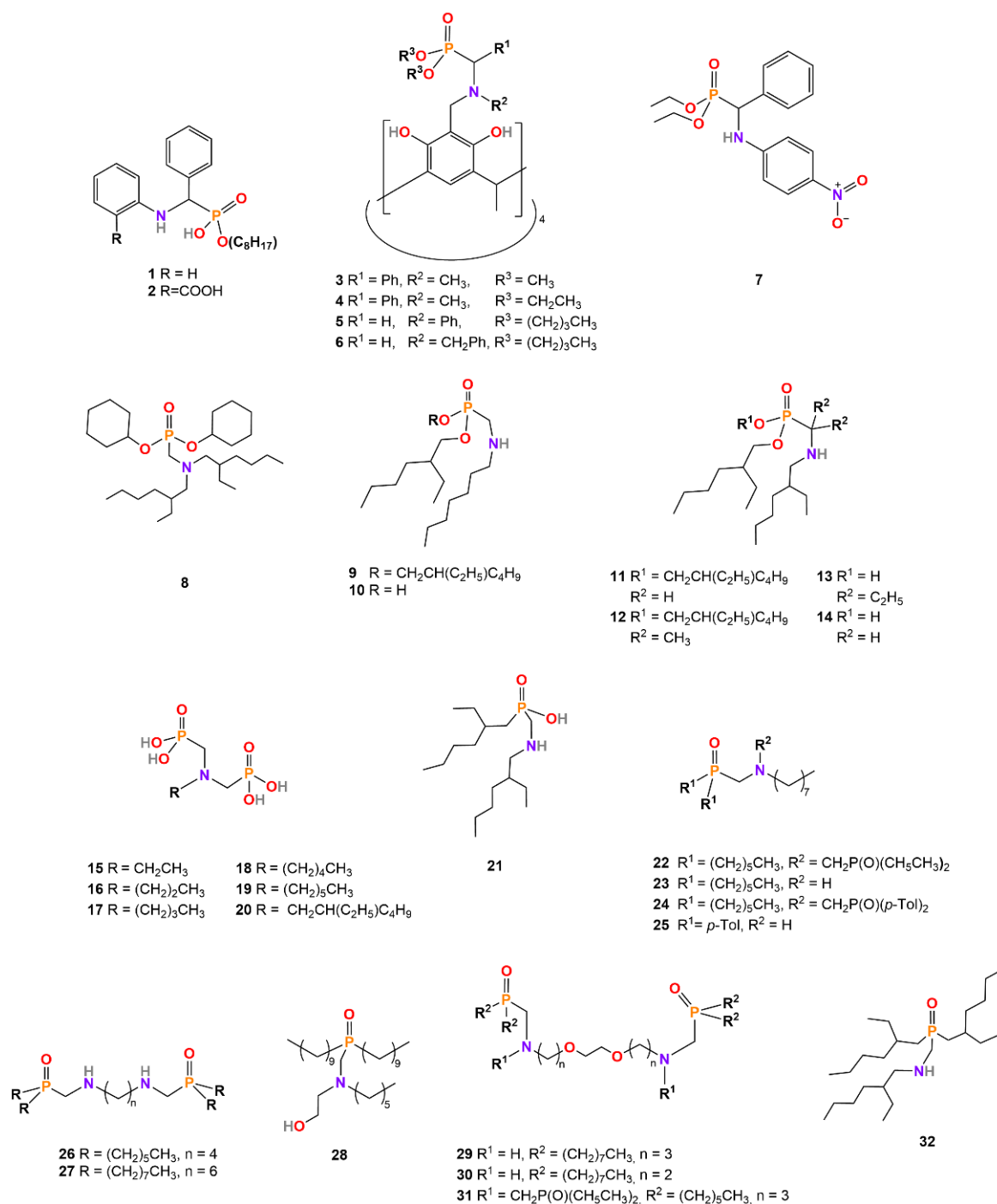
in Nd-based permanent magnets, has already increased from ~50 EUR/kg to a peak value of ~200 EUR/kg during the years 2018–2022 [18]. The increased demand and rise in prices of REs along with the environmental issues have considerably driven the development of separation methods, including solvent extraction, fractional precipitation and crystallization, electrolysis, and solid-phase extraction for recovering and separating REs from ores, raffinates, waste streams, and from each other during the last decade [1,19–21]. Despite the numerous efforts to utilize various waste streams as sources for REs, the main sources of REs are still ores, such as bastnäsite, monazite, and xenotime, as well as RE-bearing clay. The main ores of REs can also contain actinoids, such as U and Th. In particular, the content of Th can be up to 0.3 wt% and 20.0 wt% in bastnäsite and monazite, respectively, whereas U is typically found from bastnäsite (0.09 wt%) and xenotime (0.0–5.0 wt%), and sometimes from monazite, in which its content can be as high as 16 wt% [22,23]. Th has been proposed as a valuable alternative to the conventional uranium-based nuclear fuel for future nuclear reactors because it is more abundant than U, and overcomes many problems related to uranium-based nuclear fuel [24,25]. Therefore, the selective separation of actinoids from REs not only secures RE concentrates free of radioactive elements but also aims for the full valorization of RE ore by recovering every element from it.

Scope of the Review

Taking into account all the above-mentioned, α -aminophosphonate-, α -aminophosphinate-, and α -aminophosphine oxide-based extractants and precipitation agents have strong potential to develop the extraction chemistry of REs and actinoids that are critical elements for modern society. Thus, this review aims to illustrate the essential aspects of the chemistry of α -amino-functionalized organophosphorus compounds used for recovering REs and actinoids, as well as to discuss their extraction, precipitation, and separation properties towards the aforementioned elements. Liao et al. have reviewed the subject before [5], but with a strong focus on their own work and the separation of Ce(IV) and Th(IV) from other REs. Moreover, Chistyakov et al. briefly mentioned α -aminophosphonates in their review revolving around organophosphorus extractants [4]. Compared to the previously published reviews, we will take a strong molecular approach. The review is divided into seven sections, which are: an introduction (Section 1), the history (Section 2), synthesis (Section 3), and characterization (Section 4) of α -amino-functionalized organophosphorus compounds and their complexes by IR, compositions of extracted and precipitated complexes in solution phase (Section 5), extraction and precipitation properties of α -amino-functionalized organophosphorus compounds towards REs and actinoids (Section 6), and conclusions and future perspectives (Section 7). The review covers the relevant literature on the subject published from the 1960s to March 2022, but all α -amino-functionalized organophosphorus compounds used as sorption materials in the solid-phase extraction of REs and actinoids are excluded from this review [26–29].

2. The Short History of α -Aminophosphonates, -Phosphinates, and -Phosphine Oxides as Extraction and Precipitation Agents

Scheme 2 shows all α -aminophosphonates, -phosphinates, and -phosphine oxides studied in the extraction chemistry of REs, Th, and U from the 1960s to March 2022. Among these compounds, α -aminophosphonates **1–20** have dominated the field since the 1960s and, in particular, during the last ten years. In sharp contrast, there is only one acidic α -aminophosphinate **21** investigated so far, and the studies performed for α -aminophosphine oxides **22–32** were mainly done at the beginning of the 2010s, with the exception of one study that was published in 2020.



Scheme 2. Structures of the α -aminophosphonates (1–20), -phosphinate (21), and -phosphine oxides (22–32) studied for RE and actinoid separation.

The first extraction studies of REs and actinoids with α -aminophosphonates can be traced back to the 1960s and 1970s when Jagodic et al. investigated the extraction of REs and actinoids from the aqueous phase to the organic phase with mono-octyl ester of α -anilinobenzylphosphonic acid (1, MOABP) [30]. Later on, Jagodic et al. shifted their focus to the carboxylic derivative of MOABP, namely α -(2-carboxyanilino)benzylphosphonic acid (2, MOCABP), which was designed to extract divalent metals in addition to tri- and tetravalent metals. During the studies, Jagodic et al. not only proved the good extraction ability of MOCABP towards divalent metals from acidic solutions, but they also showed that MOCABP was a slightly better extractant for trivalent REs compared to MOABP [30–33].

After the pioneering work of Jagodic et al., interest in α -aminophosphonate-, α -aminophosphinate- and α -aminophosphine oxide-based extractants remained rather low, and it was not until the beginning of the 2000s that Fedorenko et al. published two papers focusing on calix[4]resorcinarenes, whose upper rims were functionalized with four α -aminophosphonate arms (**3–6**) [34,35]. The studies demonstrated that the four α -aminophosphonate arms facilitated the polydentate coordination of REs, leading to more efficient extraction of La(III) and Lu(III) compared to the extraction properties of O,O-diethyl[(4-nitrophenyl)aminobenzyl] phosphonate **7**. The synthesized calix[4]resorcinarenes functioned as neutral extractants because the deprotonation reaction of the phenolic protons of calix[4]resorcinarenes did not occur under the extraction conditions as proven by NMR studies. Additionally, by changing the length of the alkyl chain in the phosphonate moiety and the number of counterions (sodium picrate) in the extraction process, Jagodic et al. were able to vary the metal–ligand ratio of the extracted complexes from 1:1 to 1:2. In 2009, Cherkasov et al. synthesized a family of new α -aminophosphine oxides (**22–28**) with one or two phosphine oxide groups and one new α -aminophosphonate (**8**) and investigated their extraction properties towards Sc(III). They showed that the two-armed phosphine oxides were more selective compared to one-armed ones, albeit the degree of extraction of Sc(III) was rather similar for all investigated compounds. In summary, these three studies indicated that the polydentate extractants can outperform the monodentate ones bearing similar coordinating groups, not only in selectivity but also in efficiency, by a variable margin [11].

The 2010s, particularly the late 2010s, were a renaissance in the chemistry of α -amino-functionalized organophosphorus compounds targeted for extracting REs and actinoids. In 2012, Cherkasov et al. published three different α -aminophosphine oxides **22**, **29**, and **31** and investigated their efficiency to extract Nd(III), Sm(III), Dy(III), Yb(III), and Lu(III) from different acidic solutions (hydrochloric, nitric, or perchloric acid) to different organic phases (toluene, chloroform, or methylene chloride). Because the syntheses of **29** and **31** were challenging, their extraction studies were only carried out in perchloric acid containing Lu(III). Cherkasov et al. found out that the extraction efficiency of the synthesized extractants strongly depended on the nature of the acidic solution [36]. The extraction efficiencies of **29** and **31** were comparable with **22** in perchloric acid. In 2013, Cherkasov et al. performed extraction studies for Sc(III), Y(III), La(III), Ce(III), Nd(III), Sm(III), Gd(III), Lu(III), and U(IV) using bisphosphorylated azapodand **30** as an extractant without and with bis(pentadecyl)phosphoric acid to investigate the synergistic effect of two extractants [37].

These two studies were followed by the discovery of Cextrant 230 (**11**), which was patented in 2017 by Liao et al. [38]. Cextrant 230 turned out to be an efficient extractant to recover +4 oxidation state ions, such as Ce(IV) and Th(IV), from the RE mixtures containing La(III), Gd(III), and Yb(III) in sulfate media [39]. To explain the superior affinity of Cextrant 230 towards Ce(IV), Liao et al. compared the extraction ability between Cextrant 230 and di-(2-ethylhexyl) 2-ethylhexyl phosphonate (DEHEHP). Cextrant 230 and DEHEHP are very similar phosphonates containing one P-C, one P=O, and two P-O-C bonds, but the latter does not have an amino group. Based on the studies, they proposed that the better extraction ability of Cextrant 230 originates from its additional nitrogen atom, which can coordinate to the metal ion. However, the role of the nitrogen as a coordinating atom during the complexation has remained controversial to some extent (see below).

In the late 2010s and early 2020s, Liao et al. synthesized derivatives of Cextrant 230 by varying substituents in the amino group (**9**) [40] or methyl bridge (**12**) [41], or by converting the derivatives to acidic extractants (**10**, **13**, **14**) [42–44]. In the similar extraction conditions used for Cextrant 230, the derivatives **12** and **9** showed similar extraction properties to Cextrant 230 towards REs and actinoids, as the extraction efficiency of metal ions decreased in the following order Ce(IV) > Th(IV) > Sc(III) > other RE(III). Interestingly, among **9**, **11**, and **12**, the last one was much more selective towards Ce(IV) than Sc(III) and Th(IV) [39–41,45]. Liao et al. concluded that the bigger ionic radius of Th(IV) hinders the simultaneous coordination of the P=O group and the nitrogen atom [41].

The extraction efficiency of an acidic extractant can show strong pH dependency, as was observed for **10**, **13**, and **14** [42–44]. These three acidic extractants were mainly developed to separate heavier lanthanoids, which has been a challenge for commercial organophosphorus extractants such as 2-ethylhexylphosphoric acid mono-2-ethylhexyl ester (HEHEHP) and di-(2-ethylhexyl)phosphoric acid (D2EHPA). Indeed, the three aforementioned α -aminophosphonate extractants performed better on the separation of adjacent heavier lanthanoids than the commercial ones. The synergistic extraction properties of **10**, **13**, and **14** were also investigated with di-(2,4,4'-trimethylpentyl) phosphinic acid (Cyanex272), D2EHPA, and HEHEHP, respectively [46–48]. Compared to the solvent extraction containing only one extractant, the synergistic system can have several advantages, including better extraction efficiency, selectivity, and rate, improved solubility and stability of extracted complexes, a lower tendency to emulsification, and the formation of a third layer [46–49]. The synergistic studies were carried out for **10**, **13**, and **14** because Liao et al. aimed to enhance the challenging separation of heavier lanthanoids. In all three studies, they proved that the synergistic systems outperform the extraction efficiencies of single extractants, but the results for RE separation varied.

To the best of our knowledge, only one acidic α -aminophosphinate-based extractant (**21**) has been published so far in 2022 [50]. The development of this new extractant was driven by the findings from the previous studies carried out for the α -amino-functionalized organophosphorus extractants, which showed that most of the time, the α -amino-functionalized counterparts outperform traditional commercial extractants. Liao et al. compared the extraction performance of **21** to its structural analogue di-(2-ethylhexyl)phosphinic acid (P227). Although **21** did not separate the studied heavier REs as well as P227, **21** reached the extraction equilibrium in less than 5 min, and heavy REs loaded in the organic phase with **21** were easy to strip with inorganic acids within the pH range of 0 to 2 depending on the ionic radius of the REs. Prior to this study, in 2020, Liao et al. developed α -aminophosphine oxide **32** using the same reasoning as for **21**, but they also aimed for a higher extraction performance with **32** due to the strong basicity of the P=O group. Just like Cextractant 230, **32** extracted Ce(IV) effectively from the sulfate medium, but it was also easy to strip from the organic phase [51].

α -Aminophosphonates have also been used as precipitation agents for REs and actinoids [9]. In 2021, Moilanen et al. published a study focusing on the double-armed α -aminophosphonates (**15**–**20**) with short alkyl chains to increase their water solubility. The good water solubility of the investigated compounds enabled the precipitation of actinoids and REs directly from the acidic water phase, resulting in the very good separation of Sc(III), U(VI), and Th(IV) from REs, although the separation of the adjacent REs was minor.

It is evident from the above text that the extraction chemistry of REs and actinoids with α -amino-functionalized organophosphorus compounds that function either as extractants or precipitation agents evolved slowly at first, but during the last ten years, considerable progress has been made. In particular, the studies have shown that the extraction properties of α -amino-functionalized organophosphorus compounds can readily be changed by modifying their molecular frameworks with the well-established synthetic methods developed for the organophosphorus compounds.

3. Synthesis of α -Aminophosphonates, -Phosphinates, and -Phosphine Oxides

So far, three different synthetic approaches—Kabachnik–Fields, Pudovik, and Mannich—have been used to synthesize the α -aminophosphonates, α -aminophosphinates, and α -aminophosphine oxides studied in the extraction and separation chemistry of REs, Th, and U (Scheme 2 and Table 1). Among the utilized methods, the Kabachnik–Fields method has been the most used one.

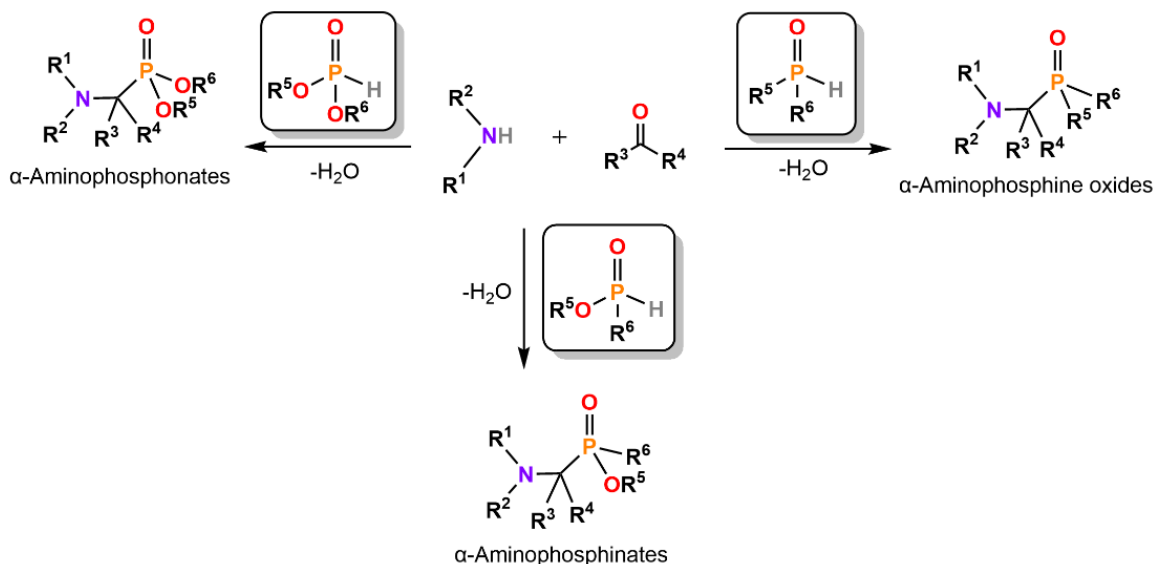
Table 1. Synthesis strategies, separation methods, and studied metals for the α -aminophosphonate, -phosphinate, and -phosphine oxide extractants.

| Extractant | Synthesis Strategy | Separation Method | Studied REs and Actinoids | Ref. |
|--------------------|----------------------|---|--|---------------|
| 1 MOABP | Pudovik | Solvent extraction | Y(III), La(III), Ce(III), Eu(III), Pr(III), Tb(III), Th(IV), U(IV), U(VI) | [31–33,52–55] |
| 2 MOCABP | Pudovik | Solvent extraction | La(III), Ce(III), Eu(III), Pr(III) | [30–33] |
| 3–5 | Mannich ^a | Solvent extraction | La(III), Lu(III) | [34,35] |
| 6 | Mannich ^a | Solvent extraction | La(III) | [34] |
| 7 | Pudovik | Solvent extraction | La(III) | [35] |
| 8 | Kabachnik–Fields | Solvent extraction | Sc(III) | [11] |
| 9 DEHAMP | Kabachnik–Fields | Solvent extraction | Sc(III), La(III), Ce(IV), Gd(III), Yb(III), Th(IV) | [40] |
| 10 HEHHAP | Kabachnik–Fields | Solvent extraction, synergistic solvent extraction with Cyanex272 | La(III), Ce(III), Pr(III), Nd(III), Sm(III), Eu(III), Gd(III), Tb(III), Dy(III), Ho(III), Y(III), Er(III), Tm(III), Yb(III), Lu(III) | [44,48] |
| 11 Cextrant 230 | Kabachnik–Fields | Solvent extraction | Sc(III), La(III), Ce(IV), Gd(III), Yb(III), Th(IV), U(VI) | [39,45,56] |
| 12 DEHAPP | Kabachnik–Fields | Solvent extraction | Sc(III), La(III), Ce(III), Ce(IV), Gd(III), Y(III), Yb(III), Th(IV) | [41] |
| 13 HEHAPP | Kabachnik–Fields | Solvent extraction, synergistic solvent extraction with D2EHPA | La(III), Ce(III), Pr(III), Nd(III), Sm(III), Eu(III), Gd(III), Tb(III), Dy(III), Ho(III), Y(III), Er(III), Tm(III), Yb(III), Lu(III) | [42,46] |
| 14 HEHAMP | Kabachnik–Fields | Solvent extraction, synergistic solvent extraction with HEHEHP | Sc(III), La(III), Pr(III), Nd(III), Sm(III), Eu(III), Gd(III), Tb(III), Dy(III), Ho(III), Y(III), Er(III), Tm(III), Yb(III), Lu(III) | [43,47] |
| 15–20 | Kabachnik–Fields | Precipitation | Sc(III), La(III), Ce(III), Pr(III), Nd(III), Sm(III), Eu(III), Gd(III), Tb(III), Dy(III), Ho(III), Y(III), Er(III), Tm(III), Yb(III), Lu(III), Th(IV), U(VI) | [9] |
| 21 EEAMPA | Kabachnik–Fields | Solvent extraction | La(III), Ce(III), Pr(III), Nd(III), Sm(III), Eu(III), Gd(III), Tb(III), Dy(III), Ho(III), Y(III), Er(III), Tm(III), Yb(III), Lu(III) | [50] |
| 22 | Kabachnik–Fields | Solvent extraction | Sc(III), Nd(III), Sm(III), Dy(III), Yb(III), Lu(III) | [11,36] |
| 23–28 | Kabachnik–Fields | Solvent extraction | Sc(III) | [11] |
| 29, 31 | Kabachnik–Fields | Solvent extraction | Lu(III) | [36] |
| 30 | Kabachnik–Fields | Solvent extraction | Sc(III), La(III), Ce(III), Nd(III), Sm(III), Gd(III), Y(III), Lu(III), U(VI) | [37] |
| 32 DEHAPO | Kabachnik–Fields | Solvent extraction | La(III), Ce(IV), Gd(III), Yb(III), Th(IV) | [51] |

^a The aminophosphonate moiety was synthesized with Kabachnik–Fields reaction.

The Kabachnik–Fields reaction includes a condensation reaction between primary or secondary amine, aldehyde or ketone, and either phosphite, phosphinate, or phosphine oxide resulting in α -aminophosphonates, -phosphinates, or -phosphine oxides, respectively (Scheme 3) [57,58]. This acid-catalyzed condensation reaction is advantageous to the synthesis of the aforementioned compounds for five reasons. (1) It is a simple one-pot reaction. (2) A variety of reagents with different substituents can be used in the reaction.

(3) The basicity of the synthesized compound can be modified by varying the nature of amine and phosphorus groups; tertiary amines are more basic than secondary amines, and the number of P-O-R groups influences the basicity of the P=O group. (4) Lipophilicity and steric bulk of the compound can be altered via the substituents R¹–R⁶. (5) More than one coordinating phosphonate, phosphinate, or phosphine oxide group can be attached to the compound by changing the stoichiometry of reagents [59].



Scheme 3. The general route for Kabachnik–Fields reaction for α -aminophosphonates, -phosphinates, and -phosphine oxides. Substituents R¹–R⁶ can be either H, alkyl, or aryl substituents.

α -Aminophosphonates **8–14** together with α -aminophosphinate **21** and α -aminophosphine oxides **22–32** were synthesized using the same procedure, by refluxing the reagents either in benzene, toluene, or acetonitrile and using *p*-toluenesulfonic acid as the acid catalyst [11,36,37,39–44,50,51]. The progress of the reaction was monitored by measuring the amount of water formed into the Dean–Stark trap. The reaction was complete when the formation of water was no longer observed. Unreacted catalytic *p*-toluenesulfonic acid was removed from the solution by reacting it with K₂CO₃ under reflux conditions. Finally, the solution was washed with water to separate the formed potassium tosylate and other impurities and dried with MgSO₄, yielding oily compounds [60,61].

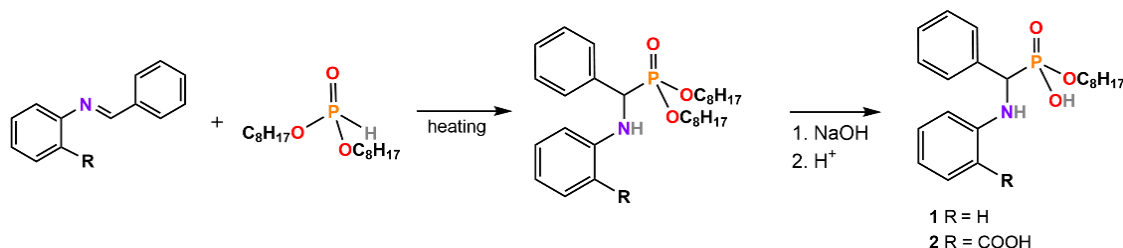
For 2-ethylhexyl ((2-ethylhexylamino) methyl) phosphonic acid (EEAMPA) **21** and bis(2-ethylhexyl) ((2-ethylhexylamino)methyl) phosphine oxide (DEHAPO) **32**, the phosphorous moieties were synthesized first by forming a Grignard reagent from 2-ethylhexyl bromide by mixing it with magnesium powder in THF and refluxing for 2 h, yielding (2-ethylhexyl)magnesium bromide. For compound **21**, the synthesized (2-ethylhexyl)magnesium bromide was reacted with triethylphosphite, yielding diethyl 2-ethylhexylphosphonite, which was then converted into ethyl 2-ethylhexylphosphinate by treating it with 6 M HCl [50]. In the case of **32**, (2-ethylhexyl)magnesium bromide was reacted with diethylphosphite, yielding bis(2-ethylhexyl)phosphine oxide. After the phosphorous moieties were synthesized, the reaction proceeded through the pathway described above, by refluxing the amine, phosphine, and aldehyde reagents in toluene. To obtain the hydroxyl group, the ethyl group in **21** was hydrolyzed with KOH in ethanol using KI as a catalyst [51].

Heptylaminomethyl phosphonic acid 2-ethylhexyl ester (HEHHAP) **10** was synthesized by hydrolyzing di(2-ethylhexyl)-N-heptylaminomethyl phosphonate (DEHAMP) **9** with NaOH in boiling ethanol for 6 h [44]. After removing the solvent, dissolving the sodium salt into toluene, and treating the solution with an acid, an oily product (**10**) was obtained. By using the same hydrolysis procedure, 2-ethylhexyl-3-(2-ethylhexylamino)pentan-3-yl phosphonic acid (HEHAPP) **13** and (2-ethylhexylamino)methyl phosphonic acid mono-

2-ethylhexyl ester (HEHAMP) **14** were obtained from di(2-ethylhexyl) (2-((2-ethylhexyl) amino) propan-2-yl) phosphonate (DEHAPP) **12** and di(2-ethylhexyl) (2-((2-ethylhexyl) amino)methyl) phosphonate (Cextrant 230) **11**, respectively [42,43].

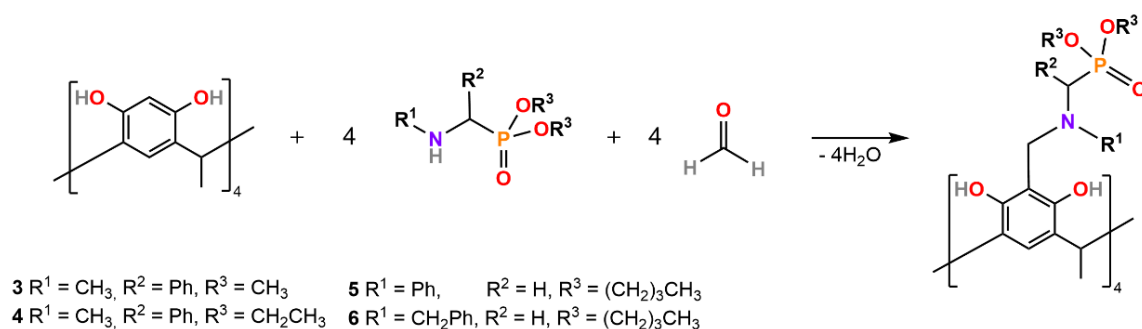
α -Aminobisphosphonates **15–20** were synthesized using water as a solvent and HCl as a catalyst instead of organic solvents and *p*-toluenesulfonic acid [9]. To obtain compounds with two phosphonic acid groups, two equivalents of phosphorous acid with respect to amine, as well as excess formaldehyde, were used in the reaction. The compounds were obtained by refluxing the reagents for 2–12 h in the acidic aqueous solution, followed by the precipitation of the products formed by adding ethanol or concentrating the reaction solution. The final products **15–20** were purified by recrystallizing them from hot ethanol or ethanol–water mixture.

α -Aminophosphonates mono-octyl α -anilinobenzylphosphonate (MOABP) **1**, mono-octyl α -(2-carboxyanilino)benzylphosphonic acid (MOCABP) **2**, and O,O-diethyl((4-nitrophenyl)aminobenzyl) phosphonate **7** were synthesized by Pudovik reaction, in which dialkylphosphite is reacted with an imine, typically under basic conditions, resulting in α -aminomethylphosphonates (Scheme 4) [62]. α -Aminophosphonates **1** and **2** were synthesized in solvent-free conditions by heating the imine and dioctylphosphite, either in a water or steam bath, for 8 h [30,63]. To obtain the mono-octyl derivatives of **1** and **2**, the dioctylphosphonate precursors were hydrolyzed by refluxing them in ethanol in the presence of NaOH for 20 h. The sodium salt of **2** precipitated out from the solution and was separated by filtration, whereas the sodium salt of **1** was obtained by removing the solvent and octanol formed in the reaction under vacuum. The sodium salts were then converted into phosphonate compounds by treating them with acid. Although the Pudovik reaction is among one of the three main approaches—Kabachnik–Fields, Mannich, and Pudovik—for synthesizing α -aminophosphonates, it has barely been utilized for the synthesis of α -aminophosphonate, -phosphinate, and -phosphine oxide extractants.



Scheme 4. The synthetic route for α -aminophosphonates **1** and **2** through the Pudovik reaction.

The Mannich reaction has been utilized for the synthesis of α -aminophosphonates **3–6** containing a calix[4]resorcinarene moiety that provides a framework to incorporate more than one coordinating arm into a single compound (Scheme 5). Indeed, the functionalization of the resorcinarene moiety with four aminophosphonate groups enhanced the coordination ability of **3–6** significantly, as it was reported that the unsubstituted compound does not form complexes with La(III) [34,35]. The Mannich reaction involves a condensation reaction between a carbonyl compound, formaldehyde, and either primary or secondary amine or ammonia under acidic conditions [64]. Typically, the aminophosphonate moieties for the ligands **3–6** were synthesized first with the Kabachnik–Fields reaction, by refluxing the secondary amine and phosphite reagent in the presence of an aldehyde for 2 h [34]. The obtained α -aminophosphonates were then heated with formaldehyde, while tetramethyl-calix[4]resorcinarene was slowly added to the solution. After the addition, the reaction mixtures were refluxed for 12 h to yield the targeted products.



Scheme 5. The synthesis of α -aminophosphonates 3–6 with the Mannich reaction.

Dimerization of the Synthesized α -Amino-Functionalized Organophosphorus Compounds

α -Aminophosphonates, -phosphinates, and -phosphine oxides that contain the terminal P=O functionality, along with N–H or P–OH functionalities, can form dimers through P=O - - H–N or P=O - - HO–P hydrogen bonds, respectively [30,53,65]. Dimerization for acidic α -aminophosphonates **1** and **2** was studied by performing molecular weight experiments in chloroform [30,53]. In solvents with a low dielectric constant, **1** likely forms the dimer through the P=O - - HO–P moieties of two molecules, resulting in an eight-membered ring structure. Additionally, it was shown that increasing the amount of **1** in the organic phase increased the formation of the dimer [32]. However, for **2**, it was observed that the compound forms dimers in concentrations between 0.001–0.01 M, but in higher concentrations, **2** starts to polymerize through the COOH and P(O)OH moieties [53]. Unfortunately, no dimerization studies for the other studied ligands containing the P=O, NH, and POH functionalities have been performed, but some of the recorded IR spectra of the investigated ligands indicate the formation of a dimer (see below).

4. Characterization of the Extracted Metal Complexes by IR

IR spectroscopy is a powerful and practical tool to characterize the synthesized α -amino-functionalized organophosphorus compounds and provide insight into their coordination modes with the extracted metals. The IR sample of an extracted complex can be taken directly from the organic phase onto a KBr crystal and heated with infrared light to evaporate the solvent [43,44]. This procedure results in a dry product from which the IR can be measured. So far, IR spectroscopy has been utilized to study the α -aminophosphonate and -phosphine oxide complexes of Sc(III), Ce(III), Ce(IV), Pr(III), Yb(III), Lu(III), Th(IV), and U(VI). Distinctive absorption bands for α -aminophosphonates and -phosphine oxides arise from the stretching (ν) and bending (δ) vibrations of the N–H, P=O, P–OH, and P–O–C functionalities. When an extractant coordinates to a metal ion, the absorption bands can shift if the changes in the electron density distribution and bond lengths are strong enough to alter the dipole moment of the compound [66]. For secondary amines, the distinctive vibration band appears in the region between 3500 cm^{-1} and 3100 cm^{-1} due to the stretching of the N–H bond. Additionally, in some cases, the bending vibration of the C–N–H bonds can be identified around 1510 cm^{-1} [67,68]. The P=O functionality exhibits only stretching vibrations, which can be observed between 1320 cm^{-1} and 1140 cm^{-1} depending on the substituents attached to the phosphorus atom. More electronegative substituents can shift the absorption band to near 1400 cm^{-1} , whereas substituents that can form hydrogen bonds, such as OH, shift the absorption band closer to 1100 cm^{-1} . Broad absorption bands that arise from P–OH functionality due to OH stretching vibrations typically range from 2800 to 2100 cm^{-1} . Absorption bands for P–OH bending vibrations can be observed around 1230 and 900 cm^{-1} , although these bands are typically weak and overshadowed by P=O and P–O–C vibration bands, respectively. Strong P–O–C stretching vibrations can be found between 1088 and 920 cm^{-1} . Additionally, C–H and C–C stretching and bending vibrations from the alkyl chains can be observed around 2900 cm^{-1} and throughout the fingerprint area of the IR spectrum. The shifting of these distinctive IR peaks upon a

complex formation gives information about the possible coordination sites of metal ions in the studied compounds.

4.1. Acidic α -Aminophosphonates

Acidic α -aminophosphonates are derivatives of aminophosphonic acids, for which the most distinctive absorption bands arise from the stretching and bending vibrations of the P–OH group. Complex formation for compounds **1** and **2** was investigated with Ce(III) and Pr(III), for compounds **10** and **13** with Yb(III) and Lu(III), and for **14** with Yb(III) [30,33,42–44]. Additionally, the metal complexes formed in the synergistic extractions with common extraction agents Cyanex272, D2EHPA, and HEHEHP were characterized by IR for ligands **10**, **13**, and **14**, respectively [46–48].

Compound **1** shows broad absorption bands for P–OH stretching vibrations at 2750–2600 cm^{-1} and 2400–2100 cm^{-1} and bending vibrations at 1750–1650 cm^{-1} , whereas only stretching vibrations at 3200–2600 cm^{-1} and 2400–2100 cm^{-1} were observed for **2**. The broadness of the absorption bands most likely originates from the dimerized compounds interacting through hydrogen bonds [30]. In their corresponding Ce(III) and Pr(III) complexes, these absorption bands are weaker [33]. Dimeric absorption bands were also observed for **10**+Cyanex272 and both **14** and its synergistic **14**+HEHEHP system [43,47,48]. For **10**, the dimeric absorption band was observed at 1688 cm^{-1} and for Cyanex272 at 1707 cm^{-1} . However, for their synergistic system, the band occurred at 1688 cm^{-1} and was not observed to disappear after the complex formation, which may indicate that **10** remains dimerized in the complex. For the sole **14** and **14**+HEHEHP synergistic system, the dimeric absorption bands were observed to occur at 1655 cm^{-1} and 1686 cm^{-1} , respectively. Both absorptions were observed to disappear after the metal complex formed, indicating that the dimers break upon complex formation. For **10**, **13**, and **14**, the P–OH stretching vibrations were observed at 2438 cm^{-1} , 2398 cm^{-1} , and 2314 cm^{-1} , respectively [42–44]. Additionally, an absorption band at 1643 cm^{-1} was observed for **13** and a P–OH bending band at 981 cm^{-1} for **14**. In the synergistic mixtures, the P–OH stretching vibrations were shifted to 2319 cm^{-1} , 2402 cm^{-1} , and 2317 cm^{-1} for **10**+Cyanex272, **13**+D2EHPA, and **14**+HEHEHP mixtures, respectively [46–48]. However, the absorption bands at 1643 cm^{-1} and 981 cm^{-1} remained unchanged. The P–OH stretching and bending vibrations observed for free compounds weakened or completely disappeared after the formation of the complexes, indicating that the extracted metals go through a cation exchange process with compounds **1**, **2**, **10**, **13**, and **14**, resulting in the deprotonation of the P–OH group.

Shifting of the P=O absorption bands was also observed in each complex. For **1** and **2**, absorption bands for the P=O stretching vibrations were observed at 1208 cm^{-1} and 1240 cm^{-1} , respectively. In the complexes, several absorption bands were seen between 1225–1155 cm^{-1} and 1215–1160 cm^{-1} for **1** and **2**, respectively, and a new absorption band formed at 1075 cm^{-1} . Compound **10** exhibits a P=O absorption band at 1216 cm^{-1} for the pure compound and at 1200 cm^{-1} for the synergistic mixture [44,48]. These absorption bands shifted to 1207 cm^{-1} and 1203 cm^{-1} , respectively, upon the complex formation with Yb(III). Interestingly, even stronger shifting of P=O absorption bands was observed for **13**, **13**+D2EHPA, **14**, and **14**+HEHEHP when they coordinated to REs. For example, the P=O absorption band for **13** was observed at 1225 cm^{-1} and for the synergistic mixture at 1231 cm^{-1} , which shifted to 1175 cm^{-1} and 1176 cm^{-1} , respectively, after the complex formation [42,46]. Similar shifting in the P=O absorption band occurred for **14**, although the shift was towards a higher wavenumber from 1159 cm^{-1} (pure compound) to 1204 cm^{-1} (complex) [43]. For the synergistic mixture of **14**+HEHEHP, the absorption band changed again towards a lower wavenumber, from 1206 cm^{-1} to 1145 cm^{-1} [47]. The relatively large shifts observed for the P=O absorption bands of **10**, **13**, and **14** and their synergistic systems indicated that the P=O moiety contributes to the complexation of REs. Additionally, the strong shifting of the P=O absorption bands could also originate from the breaking of the hydrogen-bonded dimer associated with the complex formation.

Unlike the P=O and P–OH absorption bands that had clearly shifted, only a small shift or no shift at all was observed for the P–O–C absorption bands of **1**, **2**, **10**, **10**+Cyanex272, **13**, **13**+D2EHPA, **14**, and **14**+HEHEHP upon complexation (Table 2) [30,33,42–44,46–48]. The strongest shift, from 1026 cm⁻¹ to 1041 cm⁻¹, was observed when **14** coordinated to Yb(III), but for all other systems, the shifts were within a few wavenumbers. Thus, it was assumed that the direct contribution of the P–O–C moiety to the coordination of metal ions is negligible.

Table 2. α -Amino-functionalized organophosphorus extractant systems and their metal complexes characterized by IR spectroscopy. Hyphen (-) denotes that no value was reported, slash (/) that the absorption band disappears, and n/a that the ligand lacks the functional group. Vibration modes are separated into stretching (ν) and bending (δ) as assigned in the original article, and the superscripts of the former denote whether the vibration is symmetric (s) or asymmetric (as).

| Extractant | Metal | P-OH (cm ⁻¹) | | ν P=O (cm ⁻¹) | | P-O-C (cm ⁻¹) | | N-H (cm ⁻¹) | | Ref. |
|--------------------------|--------------------|-------------------------------|---------|-------------------------------|---|---|---|-----------------------------|-----------------------------|---------|
| | | Ligand | Complex | Ligand | Complex | Ligand | Complex | Ligand | Complex | |
| 1 | Ce(III) Pr(III) | 1050– 1000 | weak | 1208 | 1225– 1155 | 1050– 1000 | weak | ν 3330 | ν 3330 | [30,33] |
| 2 | Ce(III) Pr(III) | 1050– 1000 | weak | 1240 | 1215– 1160 | 1050– 1000 | weak | ν 3300 | ν 3300 | [30,33] |
| 9 | Ce(IV) Th(IV) | n/a | n/a | 1250 | $\frac{1244_{\text{Ce}}}{1247_{\text{Th}}}$ | $\nu^{\text{as}}1014$ | $\nu^{\text{as}}1014$ | - | - | [40] |
| 10 | Yb(III) Lu(III) | $\nu^{\text{as}}2438$ | / | 1216 | $\frac{1206_{\text{Yb}}}{1207_{\text{Lu}}}$ | $\nu^{\text{as}}1040$ $\nu^{\text{s}}973$ | $\nu^{\text{as}}1040$ $\nu^{\text{s}}975$ | - | - | [44] |
| 10 + Cyanex272 | Yb(III) | $\nu^{\text{as}}2319$ | / | 1200 | 1203 | ν 1041 ν 957 | ν 1041 ν 954 | ν 3373 δ 1624 | ν 3381 δ 1615 | [48] |
| 11 | Ce(IV) Th(IV) | n/a | n/a | 1250 | $\frac{1200_{\text{Ce}}}{1238_{\text{Th}}}$ | $\nu^{\text{as}}1014$ | $\nu^{\text{as}}1014$ | ν 3451 | ν 3451 | [39] |
| | Sc(III) | n/a | n/a | 1230 | 1250 | $\nu^{\text{as}}1046$ $\nu^{\text{s}}1014$ | $\nu^{\text{as}}1046$ $\nu^{\text{s}}1014$ | δ 1650 | δ 1612 | [45] |
| | U(VI) | n/a | n/a | 1235 | 1256 | $\nu^{\text{as}}1016$ | $\nu^{\text{as}}1016$ | ν 3446 | ν 3446 | [56] |
| 12 | Ce(IV) | n/a | n/a | 1239 | 1126 | $\nu^{\text{as}}1043$ $\nu^{\text{s}}1010$ | $\nu^{\text{as}}1043$ $\nu^{\text{s}}1010$ | δ 1650 | δ 1600 | [41] |
| 13 | Yb(III) Lu(III) | $\nu^{\text{as}}2398$ 1643 | / | 1225 | 1175 | $\nu^{\text{as}}1050$ $\nu^{\text{s}}998$ | $\nu^{\text{as}}1050$ $\nu^{\text{s}}998$ | ν 3300 ^a | ν 3300 ^a | [42,46] |
| 13 + D2EHPA | Lu(III) | ν 2402 1643 | / | 1231 | 1176 | ν 1031 | ν 1031 | - | - | [46] |
| 14 | Yb(III) | ν 2314 δ 981 | / | 1159 | 1204 | ν 1026 | ν 1041 | - | - | [43] |
| 14 + HEHEHP | Yb(III) | ν 2317 δ 981 | / | 1206 | 1145 | $\nu^{\text{as}}1039$ | $\nu^{\text{as}}1041$ | δ 1620 | δ 1615 | [47] |
| 21 | Lu(III) | $\nu^{\text{as}}2318$ | / | 1146 | 1162 | n/a | n/a | δ 1614 | δ 1644 | [50] |
| 32 | Ce(IV) | n/a | n/a | 1054 | 1040 | n/a | n/a | 3311 1675 | 3396, 1666, 1614 | [51] |

^a Assigned as OH vibrations in the original article.

In the case of the investigated acidic α -aminophosphonates, no significant shifts or weakening in the absorption bands of the N-H functionality were observed. Therefore, it was concluded that the coordination occurs mainly through the P=O and P–O⁻ moieties of the aminophosphonic group, with no or only minor contribution from the NH group [33,42–44]. This is supported by the reported crystal structures of the RE complexes

of the aminophosphonic acids, with varying coordination numbers from six to nine, in most of which no N-RE bond has been detected [69–73]. There are few crystal structures where nitrogen is coordinated to RE, but typically, these α -aminophosphonates had either multiple nitrogen atoms coordinate to RE [74–76] or the coordination was dictated by carboxylic acid groups due to the oxophilic nature of REs [77,78].

4.2. Neutral α -Aminophosphonates

In contrast to the acidic α -aminophosphonates above, α -aminophosphonates **9**, **11**, and **12** are neutral extractants. Therefore, their most characteristic absorption bands arise only from the P=O, P-O-C, and NH functionalities. IR studies were carried out for **9**, **11**, and **12** and their corresponding metal complexes (Table 2). The studied RE metal ions were Ce(IV) and Th(IV) for **9**, Ce(IV), Th(IV), Sc(III), and U(VI) for **11**, and Ce(IV) for **12** [39–41,45,56]. All the solvent extraction studies were performed in sulfate medium, and therefore, absorption bands originating from SO_4^{2-} and HSO_4^- anions were also observed in the measured IR spectra.

Similar to the acidic α -aminophosphonates, a shift in the P=O stretching absorption band was observed for each α -aminophosphonate complex compared to the free extractants (Table 2). The shifts varied between 3 cm^{-1} and 113 cm^{-1} depending on the extractant and extracted metal [39–41,45,56]. The strongest shift, from 1239 cm^{-1} to 1126 cm^{-1} , was observed for **12** upon the complex formation with Ce(IV), whereas the smallest shift (3 cm^{-1}) was observed for **9** when it coordinated to Ce(IV). Based on the observed shifts in the IR spectra of **9**, **11**, and **12** upon complexation with metal ions, it was concluded that the P=O group participates in the complexation during the extraction process.

The absorption bands arising from the P–O–C moiety of **9**, **11**, and **12** were much less informative because they did not shift during the complexation, indicating no coordination affinity of the P-O-C moiety towards the investigated metal ions.

In contrast to the acidic α -aminophosphonates, where no shifting was observed for the NH absorption bands when they coordinated to metals, shifts were observed for **11** and **12** when they coordinated to Sc(III) and Ce(IV), respectively. However, in the case of **12**, the shift in the NH bending vibration can be attributed to the sulfate ions forming a complex with **12**. In the Sc(III) complex of **11**, the absorption band for the bending vibration of NH shifted from 1650 cm^{-1} to 1612 cm^{-1} . However, the NH stretching vibration remained the same in the free extractants and all investigated complexes. The shifts in NH bending vibrations could indicate the formation of a nitrogen–metal bond, but they can also originate from the interactions of the NH group with coordinating counteranions HSO_4^- and SO_4^{2-} [39,41,45,56].

As mentioned above, the coordinating SO_4^{2-} and HSO_4^- anions also give characteristic absorption bands in the IR spectrum. For the Ce(IV) and Th(IV) complexes of **9**, the bending vibration bands from SO_4^{2-} ions were observed to appear at 1118 cm^{-1} and 637 cm^{-1} and 1121 cm^{-1} and 640 cm^{-1} , respectively [40]. The SO_4^{2-} bending absorption bands appeared at similar regions for the Ce(IV) and Th(IV) complexes of **11**; however, only one bending absorption band could be determined for the Ce(IV) complex at 639 cm^{-1} [39]. For the Th(IV) complex of **11**, new absorption bands were observed at 1164 cm^{-1} and 641 cm^{-1} , whereas the U(VI) complex of **11** exhibited one new absorption band at 640 cm^{-1} [56]. The Sc(III) complex of **11**, in turn, exhibited one additional absorption band besides the absorption bands at 1119 cm^{-1} and 600 cm^{-1} assigned to the SO_4^{2-} bending vibration [45]. The new absorption band appeared at 650 cm^{-1} and was assigned to the stretching vibration of the HSO_4^- anion. The absorption band of HSO_4^- stretching can also be observed in the Ce(IV) complex of **12** at 641 cm^{-1} , in addition to the SO_4^{2-} bending absorption bands at 1122 cm^{-1} and 588 cm^{-1} [41]. All these characteristic absorption bands proved that the sulfate ions, along with α -aminophosphonates, participate in the extraction process of REs and actinoids.

4.3. α -Aminophosphine Oxides and Acidic α -Aminophosphinates

Because the α -aminophosphine oxides lack both the P–OH and P–O–C functionalities, only P=O and NH absorptions are relevant for the complex formation studies, but in the case of acidic α -aminophosphinates, derivatives of the α -aminophosphinic acid, P–OH absorption bands can also be investigated. The coordination affinities of α -aminophosphinic acid **21** and α -aminophosphine oxide **32** were investigated towards Lu(III) and Ce(IV), respectively, by IR [50,51].

Similarly to the acidic α -aminophosphonates above, **21** exhibited an absorption band for P–OH stretching at 2318 cm^{-1} that disappeared after the Lu(III) complex was formed, indicating deprotonation of the P–OH group due to the metal coordination [50]. Shifting of the P=O group was also observed during the coordination for both **21** and **32**, as the free ligands showed a stretching absorption band at 1146 cm^{-1} and 1054 cm^{-1} , which then shifted to 1162 cm^{-1} and 1040 cm^{-1} in the metal complexes, respectively [50,51]. The NH absorption bands were observed to shift from 1614 cm^{-1} to 1644 cm^{-1} for **21**, and from 3311 cm^{-1} and 1675 cm^{-1} to 3396 cm^{-1} and 1666 cm^{-1} for **32**, indicating coordination of the NH functionality to either the metals or sulfate ions. Additionally, in the IR spectra of **32**, a new absorption band formed at 1614 cm^{-1} , which was assigned to arise from NH absorption.

The extraction of Lu(III) with **21** was performed in nitrate medium, and therefore, new absorption bands from the NO_3^- stretching vibrations at 1510 cm^{-1} and 1350 cm^{-1} were observed for the metal complex [50]. For **32**, which was studied in sulfate media, new absorption bands appeared at 630 cm^{-1} , 584 cm^{-1} , and 439 cm^{-1} , which were assigned to the stretching vibrations of HSO_4^- anions, whereas a new absorption band at 960 cm^{-1} was assigned to the stretching vibration of the SO_4^{2-} [51]. These new absorption bands indicated that the NO_3^- anions for **21** and HSO_4^- and SO_4^{2-} anions for **32** were included in the respective complex formations.

5. Composition of Extracted and Precipitated Complexes

To rationalize the extraction properties of α -amino-functionalized organophosphorus compounds at the molecular level, understanding the compositions of the metal complexes formed in the extraction process is necessary. The most popular method for this purpose has been the utilization of bilogarithmic concentration isotherms. In these graphs, the logarithm of the distribution ratio D of the studied metal is plotted against the logarithm of the concentration of the studied component (e.g., extractant or anion) while all other environmental conditions are kept constant. The slopes of the resulting graphs will indicate the stoichiometry of molecules involved in the complexation. However, care should be taken in interpreting the results, as the method is not without its shortcomings [79].

Another method that has been used to examine the complex formation with other organophosphorus extractants, such as carbamoylmethylphosphine oxides (CMPOs), is ^{31}P NMR titration [80]. The method is based on changes in the ^{31}P shift(s) when metal is titrated with a ligand or vice versa. By plotting the chemical shift of ^{31}P against the concentration of RE and fitting the obtained graphs to theoretical models, the most likely metal–ligand ratios of the RE complexes are obtained.

The very first extraction study with the diaromatic α -aminophosphonate **1** did not focus on investigating the complex formation but nonetheless suggested the structures for the two uranium complexes of the extractant based on spectrophotometric and elemental analysis data. However, the data were inconsistent to some degree; the former and latter method indicated the coordination of two and four ligands to uranium, respectively [52]. In the follow-up study focusing on Eu(III) and Tb(III), the bilogarithmic concentration isotherms were used. The investigation revealed that both Eu(III) and Tb(III) form $\text{ML}_3\cdot\text{HL}$ complexes regardless of the acidic media used. The ligand HL on the second coordination sphere was found to have a substantial impact on the solubility of the complex, as pure EuL_3 , obtained via repeated ether washes of the isolated initial complex, was found to be insoluble in water and organic solvents [53]. The same extraction complex composition

$ML_3 \cdot HL$ for **1** and its COOH-containing analogue **2** was also obtained for Eu(III) and Ln(III) in several organic solvents in the later study (Table 3) [31].

Table 3. Reported chemical compositions of RE complexes of α -aminophosphonate, -phosphinate, and -phosphine oxide extractants and precipitation agents in solution. For compounds with acidic protons, HL and L denote the protonated and deprotonated versions of compounds, respectively.

| | Complex | Acid | Diluent | Ref. |
|---------------------------|---|--------------------------------|--|------|
| 1 | $U(VI)O_2L_2$ $U(IV)L_4$ | H_2SO_4 | Ligroin Recryst. from ethanol | [52] |
| 1 | $ML_3 \cdot HL / ML_2 \cdot HL_2$ (M=Eu, Tb) | HCl, HNO_3 , and $HClO_4$ | Ligroin | [53] |
| 1 | ML_3HL (M=Ln, Eu) | HCl, $HClO_4$ | Petroleum ether, $CHCl_3$, CCl_4 | [31] |
| 1 | $Ce(III)L_3 \cdot 2HL$ | HCl | $CHCl_3$, benzene | [33] |
| 1 | $Ce(III)L_3 \cdot HL$ | HCl | CCl_4 , cyclohexane | [33] |
| 1 | $PrL_3 \cdot HL$ | HCl | $CHCl_3$, benzene, CCl_4 | [33] |
| 1 | PrL_3 | HCl | cyclohexane | [33] |
| 2 | $ML_3 \cdot HL$ (M=Ln, Eu) | HCl | $CHCl_3$ | [31] |
| 2 | $Ce(III)L_3 \cdot 2HL$ | HCl | $CHCl_3$ | [33] |
| 2 | PrL_3 | HCl | $CHCl_3$ | [33] |
| 3 | LaX_3 | - | $CHCl_3$ | [35] |
| 3 | LuL_2X_3 or $LuLX_3$ * | - | $CHCl_3$ | [35] |
| 4 | LaL_2X_3 or $LaLX_3$ * | - | $CHCl_3$ | [35] |
| 4 | LuL_2X_3 or $LuLX_3$ * | - | $CHCl_3$ | [35] |
| 5 | LaL_2X_3 or $LaLX_3$ * | - | $CHCl_3$ | [35] |
| 5 | LuL_2X_3 | - | $CHCl_3$ | [35] |
| 6 | LaL_2Pic_3 | - | $CHCl_3$ | [34] |
| 7 | LaX_3 | - | $CHCl_3$ | [35] |
| 9 | $Ce(IV)(SO_4)_2 \cdot 2L$ | H_2SO_4 | heptane | [40] |
| 9 | $Th(HSO_4)_2SO_4 \cdot L$ | H_2SO_4 | heptane | [40] |
| 10 | $MClH_2L_4$ (M=Lu, Yb) | HCl | heptane | [44] |
| 10 + Cyanex272 | $MH_2Cl_2A_2B$ (A=10, M=Yb, Lu) | HCl | heptane | [48] |
| 11 | $Ce(IV)(HSO_4)_2SO_4 \cdot 2L$ | H_2SO_4 | heptane | [39] |
| 11 | $Th(HSO_4)_2SO_4 \cdot L$ | H_2SO_4 | heptane | [39] |
| 11 | $Sc(HSO_4)SO_4 \cdot 2L$ | H_2SO_4 | heptane | [45] |
| 11 | $UO_2SO_4 \cdot 2L$ | H_2SO_4 | heptane | [56] |
| 12 | $Ce(IV)(HSO_4)_2SO_4 \cdot 2L$ | H_2SO_4 | heptane | [41] |
| 13 | ML_3 (M=La, Gd, Y, Lu) | HCl | heptane | [42] |
| 13 + D2EHPA | $LuCl_2H_4A_3B_2$ (A=13) | HCl | heptane | [46] |
| 14 | MH_2ClL_4 (M=Tm, Yb, Lu) | HCl | heptane | [43] |
| 14 + HEHEHP | MA_2B_4 (A=14, M=Lu, Yb, Tm, Er, Y, Ho) | HCl | heptane | [47] |

Table 3. Cont.

| | Complex | Acid | Diluent | Ref. |
|----|--|--------------------------------|---------|------|
| 15 | LuL(NO ₃) ₂ | HNO ₃ | water | [9] |
| 15 | LaL ₂ (NO ₃) | HNO ₃ | water | [9] |
| 15 | YL ₃ | HNO ₃ | water | [9] |
| 21 | MHL ₃ NO ₃ (M=La, Nd, Gd, Lu) | HNO ₃ | heptane | [50] |
| 22 | ScL ₂ X ₃ | HClO ₄ | toluene | [11] |
| 32 | Ce(IV)(HSO ₄) ₂ SO ₄ · L | H ₂ SO ₄ | heptane | [51] |

* Compositions for LnX₃ with the two different NaPic ratios: 1:250 for former and 10:1 for latter.

The investigations on the complexation of **1** and **2** were continued using the two α -aminophosphonates in several organic solvents to extract Ce(III) and Pr(III) [33]. While the exact composition of the RE complexes of **1** varied, as the number of ligands on the second coordination sphere was found to be dependent on the solvent used, they always had a tri-ligand ML₃ unit at their core as the earlier extraction studies suggested. Complex composition studies with **2** in chloroform came to the same conclusion: both Ce(III) and Pr(III) preferred a tri-ligand system, with the Ce(III) complex including two extractant ligands on the second coordination sphere while the Pr(III) complex had none (Table 3). In both cases, the phosphonic acid group of extractant is deprotonated instead of the carboxyl group that likely participates in the formation of hydrogen bonding interactions supporting the extraction process.

Almost three decades later, the focus of the extraction studies moved to macrocyclic calix[4]resorcinarenes **5** and **6**, which were functionalized with aminophosphonate groups [34]. While poor solubility prevented proper analysis of the La complex obtained with extractant **5**, compound **6** was found to form a LaL₂Pic₃ complex, with the three picrate anions balancing the charge of the cationic RE metal. These anions also played an important role in making the metal complex sufficiently large to be able to effectively coordinate to the cavity of macrocyclic extractant. The calix[4]resorcinarene studies were continued by using compounds **3–5** in the extraction of La(III) and Lu(III) while also comparing the results to **7** to investigate the role of the macrocyclic structure [35]. The lanthanoid–ligand ratio of the complexes was found to be dependent on the relative amount of sodium picrate used: an excess of picrate anions led to the formation of LnL₂X₃ complexes in most cases, whereas a lesser amount of picrate (i.e., excess of metal ions) always gave LnLX₃ complexes (Table 3). Additionally, by comparing the extraction constants of La(III) complexes of **3** and **7**, it was concluded that the La(III) complex of **3** was stabilized by the macrocycle.

Structurally similar extractants **9**, **11**, and **12** were used for the separation of the tetravalent Ce(IV) and Th(IV) from trivalent RE metals. The Ce(IV) and Th(IV) complexes of **9** were found to have the structures of Ce(SO₄)₂ · 2L and Th(HSO₄)₂SO₄ · L, respectively, both containing sulfate anions from the acidic medium [40]. Unsurprisingly, the extracted complexes of **11**—Ce(HSO₄)₂SO₄ · 2L and Th(HSO₄)₂SO₄ · L—were similar, with their only difference from **9** being the anions included in the Ce(IV) complex [39]. Further studies with **11** revealed that the extracted complexes of Sc(III) and U(VI)O₂ also contain two ligands, Sc(HSO₄)SO₄ · 2L and UO₂SO₄ · 2L, respectively, while the number of HSO₄[−] ions decreased due to the lower charge of the extracted cations [45,56]. The Ce(IV) complex of **12** was also found to have the same Ce(HSO₄)₂SO₄ · 2L composition as the complex of **11**, while the Th(IV) complex was not investigated [41].

Studies on congeneric monoacidic α -aminophosphonates **10**, **13**, and **14**, in turn, have concentrated on the extraction of trivalent lanthanoids. The complex formation of acidic α -aminophosphonate **10** was investigated with Yb(III) and Lu(III), and the RE complexes of the metals were found to have the composition of MClH₂L₄ [44]. The N-(2-ethylhexyl) congener **14** of **10** was found to form complexes with the same MClH₂L₄ composition with the trivalent Yb(III), Lu(III), and Tm(III) [43]. In both cases, two dimerized extractants were

partially deprotonated before coordinating to the extracted metal. In contrast, compound **13** with di-ethylated α -carbon was found to form a simple ML_3 complex with the trivalent La(III), Gd(III), Y(III), and Lu(III) [42]. In this case, the deprotonation of the extractant was complete and broke apart the dimerization of **13**. Based on the results obtained with the aforementioned REs, all three studies generalized the observed compositions to concern all trivalent RE complexes of **10**, **13**, and **14**.

An interesting addition to the complex composition studies has been the research on synergistic extraction, where α -aminophosphonates are paired with another organophosphorus extractant. The Lu(III) complex of **13**+D2EHPA was found to have the structure of $LuCl_2H_4A_3B_2$, where A depicts the amount of α -aminophosphonate and B the amount of D2EHPA [46]. The composition had the same amount of **13** as the ML_3 complex of the pure α -aminophosphonate extractant, while also including two D2EHPA units, bringing the total number of extractants from three to five. Furthermore, only one of the three α -aminophosphonates is deprotonated in the synergistic extraction process while the other two, as well as the two D2EHPA units, stay in a neutral dimerized form. A similar trend was observed with the **14**+HEHEHP pairing, as the synergistic system complex MA_2B_4 requires two units of **14** and four HEHEHPs to extract a single RE cation, whereas the RE complex of pure **14**, MH_2ClL_4 , only included four extractants in total. Both extractants of the synergistic system remain in a singly deprotonated dimer form [47]. In contrast, the **10**+Cyanex272 complex $MH_2Cl_2A_2B$ contained one neutral dimer of **10** and one deprotonated Cyanex272, which means that the synergistic system leads to a lower total amount of extractant ligands when compared with the $MClH_2L_4$ complex of pure **10** (Table 3) [48].

A study on α -aminobis(phosphonates) determined the compositions of the complexes via ^{31}P NMR titrations in D_2O [9]. This method was successfully employed for **15** with Y(III), La(III), and Lu(III), and the results revealed the complex compositions of YL_3 , $LaL_2(NO_3)$, and $LuL(NO_3)_2$, respectively. In each case, the extractant was in a zwitterionic form and coordinated in a bidentate manner to the extracted metal cation while NO_3^- ions and/or H_2O most likely complemented the coordination sphere of the RE. In addition, each phosphonate group was only singly deprotonated due to the pH range of the experiments. Further attempts at determining the complexes for Sc(III) and Th(IV) were unsuccessful due to heavy precipitation of the formed complexes at low pH values.

While the research towards new α -aminophosphonates seems ever-expanding, the RE extraction properties of α -aminophosphinates remain largely uncharted. The sole reported study so far used acidic α -aminophosphinate reagent **21** for the extraction of trivalent REs from nitric acid media [50]. The complex formation was studied for La(III), Nd(III), Gd(III), and Lu(III), and all their complexes were found to have the same MHL_3NO_3 composition, consisting of one individual deprotonated ligand and one singly deprotonated dimer for every RE cation.

The extraction studies were expanded to α -aminophosphine oxides when compounds **22–28** were investigated for the extraction of Sc(III) and other selected RE metals. The composition of the Sc(III) complex of **22** in toluene was found to be ScL_2X_3 , with X denoting acidic anions included to balance out the charge of the metal [11]. Attempts to use the bilogarithmic plots to investigate the Sm(III) complex of **22**, as well as the complexes formed by **23**, were unsuccessful, as the former resulted in a nonlinear graph and the latter to ambiguous conclusions. The other synthesized extractants were not researched further [11,36]. Phosphine oxide **32**, in turn, was investigated for the extraction of Ce(IV). Unlike the $Ce(HSO_4)_2SO_4 \cdot 2L$ complexes of its α -aminophosphonate congeners **11** and **9**, the composition of **32** was found to be $Ce(HSO_4)_2SO_4 \cdot L$, including only a single unit of the extractant [51].

In general, the studies have shown that the (mono)acidic α -aminophosphonate and α -aminophosphinate extractants favor three to four coordinated ligands around each metal cation, form complexes through deprotonation of the acid or its dimer and act as the counterions for the cationic metal centers (Table 3). The neutral di-alkoxy α -aminophosphonates and α -aminophosphine oxides, on the other hand, are more likely to stay in the range of one

to two ligands per metal. Moreover, the anions of the acidic solution are often involved in the extraction process, as the extracted complexes transferred to an organic phase must be charge-neutral. This, in turn, means that the complex compositions in different acidic media are inherently varied, and the importance of the counter anion is further underlined by the findings from the extraction experiments with sodium picrate and 3–5. The studies have also confirmed that the solvent of the organic phase can have an impact on the composition as well, despite not being a part of the complex itself. In short, the complex formation can be described as a complicated process with multiple experimental factors affecting the outcome of the extraction.

6. Extraction Ability of α -Aminophosphonates, -Phosphinates, and -Phosphine Oxides towards REs and Actinoids

To compare the recovery and separation properties of extractants and precipitation agents, several parameters have been developed to quantify their performance. The key parameters are the distribution ratio D , separation factor SF , and synergistic enhancement coefficient R , the last of which only applies to synergistic systems containing two extractants [81].

The distribution ratio describes the extraction ability of a compound towards certain elements. In solvent extraction, it can be determined as the concentration of extracted metal in the organic phase $[M]_{org}$ divided by the concentration of the unextracted metal remaining in the aqueous phase $[M]_{aq}$. In the case of precipitation processes, the organic phase concentration is replaced by the amount of precipitated metal $[M]_p$ and calculated as the difference between initial and final concentrations of the aqueous phase, as shown by Equation (1):

$$D = \frac{[M]_{org}}{[M]_{aq}} \text{ or } D = \frac{[M]_p}{[M]_{aq}} = \frac{[M]_{init} - [M]_{aq}}{[M]_{aq}}. \quad (1)$$

High values of distribution ratios indicate a strong transfer of metal ions from the water phase to the organic phase or strong precipitation, whereas values close to zero are a sign of poor transfer of metal ions [81].

The separation factor is calculated with Equation (2) as the quotient of the distribution ratios D of the two metals A and B :

$$SF = \frac{D_A}{D_B}. \quad (2)$$

The parameter describes the ability of the extractant or precipitation agent to separate two metals from each other. Separation factor values close to unity are a sign of poor separation, while significantly higher or lower values indicate that the extractant or precipitation agent can be used to efficiently separate the two metals in question [81].

The second important parameter derived from the distribution ratios is the synergistic enhancement coefficient, which aims to quantify the potential improvement of a system using two extractants simultaneously [82]. This is done by comparing the extraction performance (i.e., distribution ratio) of the combinatory system D_{AB} to the sum of the distribution ratios of the individual components ($D_A + D_B$) according to Equation (3):

$$R = \frac{D_{AB}}{D_A + D_B}. \quad (3)$$

Consequently, enhancement coefficient values over 1 indicate a positive synergistic effect, whereas the opposite is a sign of negative competition between the two extractants. It should be noted that the values of D , SF , and R are dependent on several experimental conditions, such as temperature, pH, and concentration, all of which can affect the behavior of both the metal and the extractant itself.

In addition to the distribution ratio D , separation factor SF , and synergistic enhancement coefficient R , another important factor measuring the performance of extractants is

their loading capacity. This parameter is, simply, the maximum amount of metal that can be extracted under certain experimental conditions, and it is commonly reported in g/L or mol/L. It is therefore essential to pay close attention to the reported concentration of the extractant to determine whether the loading capacity values are directly comparable or not.

6.1. α -Aminophosphonates

Octyl α -anilinobenzylphosphonic acid **1** and its ethyl analogue were the first α -aminophosphonates that were investigated for the solvent extraction of REs and actinoids. While the ethyl analogue was too water-soluble for the extraction of metals, **1** was found to be a very good extracting agent for binary and ternary systems containing radioactive nuclei. Studies on U extraction in ligroin found that U(IV) was extracted quantitatively only between sulfuric acid concentrations of 2 M and 4 M, whereas U(VI) could be extracted with a broader range of 0.5–9 M acidity [52]. A follow-up study showed that **1** was able to separate U(VI) selectively from Eu(III) and Tb(III) when ligroin was used as an organic solvent, and the molarity of the aqueous phase was higher than 0.5 M [53]. According to the authors, the determined $SF_{U/Eu}$ and $SF_{U/Tb}$ were $\sim 26,000$ (Table 4). The full separation between Sr(II) (the source of the radioisotope of ^{88}Y) and Y(III), as well as between ^{131}Ba (II) and ^{140}La (III), was also obtained in petroleum ether, keeping the hydrochloric acid molarity between 0.01 M and 0.1 M [54,55].

Table 4. Highest reported SF for the extraction of actinoids Th(IV) and U(VI) with α -amino-functionalized organophosphorus compounds. FP indicates full precipitation of the metal marked in parentheses, because of which the SF could not be determined.

| Extractant | Ce(IV)/Th | U/Eu | Th/RE | U/RE | Th/Lu | U/Th | U/Lu | Ref. |
|------------|-----------|---------------------|-------|-------|---------------------|--------------------|---------------------|-------------------|
| 1 | - | 26,000 [*] | - | - | - | - | - | [53] ^a |
| 11 | 14.7 | - | - | - | - | - | - | [39] ^b |
| 11 | - | - | >1000 | >1000 | - | - | - | [56] ^c |
| 12 | 754.2 | - | - | - | - | - | - | [41] ^d |
| 15 | - | - | - | - | 4.50 ^g | FP(U) ⁱ | FP(U) ⁱ | [9] |
| 16 | - | - | - | - | 6.02 ^{f,^} | 2.01 ^e | 4.03 ^{f,^} | [9] |
| 17 | - | - | - | - | 9.17 ^g | 2.40 ^e | 8.68 ^g | [9] |
| 18 | - | - | - | - | 44.41 ^g | FP(U) ^h | FP(U) ^h | [9] |
| 19 | - | - | - | - | FP(Lu) ^j | FP(U) ^h | FP(U) ^h | [9] |
| 20 | - | - | - | - | FP(Th) ^j | FP(U) ^e | FP(U) ^e | [9] |
| 32 | 100.3 | - | - | - | - | - | - | [51] ^k |

^{*} Separation factor for U/Tb mentioned to be similar; [^] best SF with error smaller than the value; ^a 5 mM extractant **1**, 0.1 mM Eu(III), 4 mM U(VI)O₂²⁺, 1 M H₂SO₄; ^b 0.1 M extractant **11**, 0.01 M M(IV), 3 M H₂SO₄; ^c 0.1 M extractant **11**, 0.01 M metals, 3.23 M H⁺ for Th/RE, 0.22 M or 3.23 M H⁺ for U/RE; ^d 0.048 M extractant **12**, 6 mM Th, 5 mM Ce, 0.2134 M H₂SO₄; ^e 2.5 g/L extractant, 9 mg/L, pH 1; ^f 2.5 g/L extractant, 9 mg/L, pH 2; ^g 2.5 g/L extractant, 9 mg/L, pH 2.5; ^h 2.5 g/L extractant, 9 mg/L, pH 3; ⁱ 2.5 g/L extractant, 9 mg/L, pH 3.5; ^j 2.5 g/L extractant, 9 mg/L, pH 2.5; ^k 0.1 M extractant **32**, 0.01 M M(IV), 0.9353 M H₂SO₄.

The research on the carboxylic derivative (**2**) of **1** not only revealed that it is a better extractant for Eu(III) and Ln(III), but it was also more selective towards divalent transition metals than trivalent REs compared to **1** [30,31]. However, the solubility of **1** was much better in different organic solvents compared to **2**, which was only well-soluble in CHCl₃. Indeed, the studies in various organic solvents revealed distinguishable changes in the Eu(III) extraction behavior of **1**, with increasing HCl concentration of the aqueous phase. The best extraction ability was maintained with petroleum ether and cyclohexane, with the increasing acid concentration compared to CCl₄, benzene, and CHCl₃ [32]. Both acidic α -aminophosphonates were also utilized to extract Ce(III) and Pr(III) from hydrochloric acid medium, but the differences in their extraction behavior were too small to allow efficient separation of the two metals from each other [33].

A study focusing on the extraction of La(III) with two α -aminophosphonates functionalized macrocyclic calix[4]resorcinarenes **5** and **6** reported that La(III) does not coordinate to nonfunctionalized calix[4]resorcinarenes, nor does it form complexes without the suitably sized lipophilic picrate counterions that fill the cavity of the calix[4]resorcinarene, as mentioned above [34]. The studies were continued with the extraction of La(III) and Lu(III) with compounds **3–5**, and the influence of the relative amount of picrate anions on the extraction properties of **3–5** was also investigated [35]. Interestingly, in the presence of the excess of sodium picrate, the extraction efficiency of **3** towards La(III) was found to be higher than the extraction efficiency of **4** and **5** due to the change in the metal–ligand ratio in the complex formation from 1:1 (**3**) to 1:2 (**4** and **5**). Contrary to La(III), **5** was the most efficient extractant for Lu(III). Importantly, all calix[4]resorcinarene–aminophosphonates were more efficient extractants than **7**, indicating the strength of multiple coordinating arms in the extraction process.

Several studies on α -aminophosphonates have concentrated on the extraction of Ce(IV) and Th(IV) from sulfuric acid leach of the bastnäs site ore using heptane as a diluent. Compound **9** effectively separated the aforementioned tetravalent metals and Sc(III) from the rest of the studied trivalent REs. The extraction of Th(IV) and Sc(III) was found to decrease sharply with increasing acidity, while the extraction of Ce(IV) remained practically complete in the sulfuric acid concentration of <4 M [40]. Comparable results were obtained for the structurally similar α -aminophosphonate **11**, as Ce(IV) and Th(IV) were efficiently separated while the extraction of Th(IV) was more prone to changes in acid concentration. The extractant was successfully used to obtain RE products of high purity with high yields in a pilot test. It was subsequently patented and named as Cextrant 230 [39]. The extractant **12** performed similarly to **9** and **11** in the extraction studies because the most efficient metal separation occurred when the sulfuric acid concentration did not exceed 1 M [41]. However, a notable exception to the other two extractants was the low extractability of Th(IV) with **12**, which enabled the efficient separation of Ce(IV) and Th(IV) ($SF_{Ce/Th} = 754.2$, Table 4). The increased selectivity was assigned to the steric effects arising from the larger ionic radius of Th(IV), hindering its effective coordination to **12**.

Compound **11** was further studied for the extraction of Sc(III) and U(VI). The extraction of Sc(III) from red mud was investigated with various acids, and the results showed that dilute sulfuric acid was by far the most efficient medium. Unfortunately, **11** was also found to extract significant amounts of other REs, as well as Ti(IV) and Fe(III), all of which are prevalent in red mud, but after a series of post-extraction treatment procedures, a purity of ~94% was achieved for the Sc_2O_3 product [45]. The results from the extraction studies of U(VI) and Th(IV) suggested that the separation of two actinoids from RE metals, Fe(III) and Al(III), is effective throughout the studied pH range of 0.22–3.23. U(VI) was best extracted and separated from REs at pH 0.22 with high $SF_{U/RE} > 1000$. Moreover, U(VI) had a higher loading capacity (6.16 g/L vs. 4.08 g/L for 5% extractant in heptane) than Th(IV) (Table 5) [56].

The extraction and separation of trivalent REs from each other have also been investigated with monoacidic α -aminophosphonate reagents **10**, **13**, and **14**. The extraction efficiency of **10** and **13** towards Y(III), La(III), Gd(III), Ho(III), Er(III), Tm(III), Yb(III), and Lu(III) decreased with increasing acid concentration [42,44]. A similar trend was observed for **14** when the extracted metals were Sc(III), Y(III), Ho(III), Er(III), Tm(III), Yb(III), and Lu(III), while the extractabilities of La(III) and Gd(III) were not strongly affected by the concentration of acid [43]. The best results were obtained with extractant **13**, which has some of the highest reported separation factors among all the studied α -aminophosphonate compounds listed in Table 6. In general, the investigated α -aminophosphonate compounds have shown a better ability to separate adjacent heavy REs from each other than the commercially used extractants D2EHPA and HEHEHP [84].

Table 5. Loading capacities of the α -amino-functionalized organophosphorus compounds used in RE and actinoid extraction studies, as reported in the original papers.

| Extractant | Dilution | Metal | Acid | Capacity | Ref. |
|-------------|--|--|--------------------------------|--|---------|
| 9 | 0.63 M in heptane | 0.23 M Ce(IV) (Σ Ce 0.24 M) 0.02 M Th(IV) | H ₂ SO ₄ | 30.0 g/L Ce(IV) 24.4 g/L Th(IV) | [40] |
| 10 | 30% (v/v) in heptane | 0.0985 M YbCl ₃ 0.0986 M LuCl ₃ | HCl | 12.76 g/L Yb 15.43 g/L Lu | [44] |
| 11 | 30% (v/v) in heptane | Ce(IV) & Th(IV) | H ₂ SO ₄ | >30 g/L Ce(IV) ~43 g/L Th(IV) | [39,83] |
| 11 | 30% (v/v) in heptane | 0.064 M Sc | H ₂ SO ₄ | 3.85 g/L Sc | [45] |
| 11 | 5% (v/v) in heptane | 8.08 mM Th(IV) 21 mM U(VI) | H ₂ SO ₄ | 4.08 g/L Th(IV) 6.16 g/L U(VI) | [56] |
| 12 | 30% (v/v) in heptane | 0.29 M Ce(IV) | H ₂ SO ₄ | 31.43 g/L CeO ₂ | [41] |
| 13 | 30% (v/v) in heptane | 0.1 M RE | HCl | 0.201 M Ho 0.205 M Er 0.216 M Yb 0.229 M Lu | [42] |
| 14 | 30% (v/v) in heptane | 0.055 M YbCl ₃ * | HCl | 15.17 g/L Lu 14.46 g/L Yb 12.64 g/L Y | [43] |
| 14 + HEHEHP | 30% (v/v) in heptane (1:1 extractant ratio) | 96 mM Lu 92 mM Yb | HCl | 27.25 g/L Lu ₂ O ₃ 26.59 g/L Yb ₂ O ₃ | [47] |
| 21 | 4 mM in heptane | 0.4 mM RE | HNO ₃ | 0.393 mM Ho 0.402 mM Er 0.422 mM Tm 0.435 mM Yb 0.450 mM Lu | [50] |
| 32 | 30% (v/v) in heptane | 0.143 M Ce(IV) | H ₂ SO ₄ | 16.66 g/L CeO ₂ | [51] |

* Used RE concentration only reported for Yb.

While the majority of previous studies carried out for α -aminophosphonates have focused on solvent extraction, these compounds also work as precipitation agents. A series of α -aminobis(phosphonates) **15–20**, with variable hydrocarbon chain lengths, was studied for the recovery of REs, Th(IV), and U(VI) by direct precipitation of the formed complexes from the nitric acid solution [9]. α -Aminobis(phosphonates) **18–20**, with a longer hydrocarbon chain, separated Sc(III) and both actinoids from the rest of the investigated REs well in the pH range of 1–2. In this pH range, Sc(III), Th(IV), and U(VI) completely precipitated out from the nitric acid solution, while REs remained in the solution (Table 4). While similar trends in selectivity were observed for **15–17**, their precipitation percentages did not surpass 60% at pH < 2, where the precipitation of other trivalent REs stayed under 10%.

Table 6. Best reported *SF* for adjacent RE elements (excluding the radioactive promethium). Precipitation studies carried out for 15–20 were done in water, whereas heptane was used as a diluent in all solvent extraction experiments. The detailed experimental conditions are given below.

| Extractant | Ce/La | Pr/Ce | Nd/Pr | Sm/Nd | Eu/Sm | Gd/Eu | Tb/Gd | Dy/Tb | Ho/Dy | Er/Ho | Tm/Er | Yb/Tm | Lu/Yb | Y/Ho | Er/Y | Ref. |
|-------------------|---------------------|-------------------|-------------------|-------------------|---------------------|---------------------|-------------------|-------------------|---------------------|---------------------|-------|---------------------|---------------------|------|--------------------|-------------------|
| 10 | 1.47 | 1.23 | 0.85 | 1.93 | 1.14 | 0.62 | 1.76 | 1.39 | 1.39 | 2.28 | 4.29 | 1.59 | 1.63 | 1.04 | 2.18 | [44] ^a |
| 10 | - | - | - | - | - | - | - | - | 1.27 | 1.23 | 2.36 | 3.18 | 1.59 | 1.41 | 0.88 | [48] ^b |
| 10 + Cyanex272 | - | - | - | - | - | - | - | - | 2.57 | 3.33 | 3.07 | 3.58 | 1.60 | 1.60 | 2.08 | [48] ^c |
| 12 | 135.1 [*] | - | - | - | - | - | - | - | - | - | - | - | - | - | - | [41] ^d |
| 13 | - | - | - | - | - | - | - | - | - | 2.83 | 3.87 | 5.64 | 4.89 | 2.24 | 2.35 | [42] ^e |
| 13 + D2EHPA | 0.72 | 1.31 | 0.93 | 0.92 | 1.03 | 0.97 | 1.01 | 1.13 | 1.03 | 1.45 | 2.58 | 2.77 | 1.77 | 1.35 | 0.93 ^{**} | [46] ^f |
| 14 | - | - | 1.43 | 1.35 | 1.11 | 1.19 | 1.44 | 1.07 | 1.32 | 1.78 | 1.93 | 1.36 | 1.24 | 1.13 | 1.58 | [43] ^g |
| 14 + HEHEHP | - | - | 1.20 | 1.14 | 1.45 | 1.13 | 1.16 | 1.17 | 1.05 | 2.11 | 1.78 | 1.76 | 1.20 | 1.32 | 1.61 | [47] ^h |
| 15 | 2.56 ^m | 2.06 ^l | 1.16 ^l | 1.41 ^m | 1.28 ^m | 1.22 ^m | 1.01 ⁿ | 2.67 ^l | 1.28 ^{m,^} | 2.00 ^{l,^} | - | 2.88 ^l | 2.52 ^k | - | 3.02 ^l | [9] |
| 16 | 1.33 ^{m,^} | 1.23 ⁱ | 1.48 ^j | 1.50 ^k | 1.45 ^{j,^} | 1.52 ^{j,^} | 1.05 ⁱ | 1.23 ^m | 1.41 ^m | 1.09 ⁱ | - | 1.77 ^{m,^} | 1.30 ⁿ | - | 2.75 ⁱ | [9] |
| 17 | 2.92 ^j | 1.36 ^k | 1.75 ^j | 1.44 ^l | 1.76 ^l | 1.41 ^l | 0.84 ^l | 1.51 ^l | 1.44 ^l | 1.18 ^l | - | 2.22 ^{l,^} | 1.18 ^l | - | 3.33 ^m | [9] |
| 18 | 3.81 ^l | 1.26 ^m | 1.11 ⁿ | 1.70 ^l | 1.07 ^{n,^} | 1.21 ^m | 1.49 ^l | 1.50 ^l | 1.47 ^l | 1.53 ^l | - | 3.60 ^k | 2.32 ⁿ | - | 2.21 ^l | [9] |
| 19 | 2.11 ^l | 2.18 ^k | 1.54 ^k | 2.04 ^k | 1.20 ⁿ | 1.42 ^k | 1.14 ^k | 1.06 ^k | 1.12 ^k | 1.57 ⁿ | - | 4.33 ⁿ | FP(Lu) ⁿ | - | 1.87 ⁿ | [9] |
| 20 | 1.88 ^m | 1.50 ⁿ | 1.15 ^m | 1.73 ^m | 1.29 ^l | 1.16 ^l | 1.77 ^l | 1.20 ^l | 1.08 ^l | 1.36 ^l | - | 1.94 ^l | 2.33 ⁿ | - | 2.03 ^l | [9] |
| 21 | 1.54 | 2.57 | 1.09 | 1.43 | 1.62 | 0.92 | 1.83 | 1.56 | 1.35 | 1.71 | 1.97 | 2.37 | 1.63 | 1.68 | 1.00 | [50] ^o |
| 32 | 167.0 [*] | - | - | - | - | - | - | - | - | - | - | - | - | - | - | [51] ^p |
| D2EHPA | 2.14 | 1.07 | 1.06 | 4.86 | 2.23 | 1.69 | 1.60 | 1.42 | 1.24 | 1.70 | 1.50 | 1.30 | 1.03 | - | - | [84] ^q |
| HEHEHP | 1.30 | 1.09 | 1.17 | 2.00 | 1.96 | 1.46 | 2.35 | 1.62 | 2.58 | 1.25 | 1.33 | 1.12 | 1.13 | - | - | [84] ^q |

^{*} Ce(IV) was used instead of Ce(III); ^{**} value for the reverse pairing reported; [^] best *SF* with error smaller than the value; ^a 0.1 M extractant 10, 2 mM RE, pH 4.5; ^b 0.1 M extractant 10, 1 mM RE, pH 2.5; ^c 0.05 M extractant 10 and 0.05 M Cyanex272, 1 mM RE, pH 2.5; ^d 0.048 M extractant 12, 5.1 mM La, 5 mM Ce, 0.2134 M H₂SO₄; ^e 0.05 M extractant 13, 5 mM RE, c(HCl): Tm/Er 2 M, Yb/Tm 4.1 M, Lu/Yb 3.7 M, Y/Ho 1 M, Er/Y 2.5 M, Er/Ho 2 M; ^f 0.05 M extractant (total, 1:1 molar ratio), 1 mM RE, 2.5 M H⁺; ^g 0.1 M extractant 14, 5 mM RE, pH 1.0; ^h 0.1 M extractant (total, $\chi = 0.5$), 0.01 M RE, pH: Y/Ho 1.3, all others 1.0; ⁱ 2.5g/L extractant, 9 mg/L RE, pH 1; ^j 2.5g/L extractant, 9 mg/L RE, pH 2; ^k 2.5g/L extractant, 9 mg/L RE, pH 2.5; ^l 2.5g/L extractant, 9 mg/L RE, pH 3; ^m 2.5g/L extractant, 9 mg/L RE, pH 3.5; ⁿ 2.5g/L extractant, 9 mg/L RE, pH 4; ^o 4 mM extractant 21, 0.2 mM RE, pH 1.0; ^p 0.1 M extractant 32, 0.01 M RE, 0.4353 M H₂SO₄; ^q 0.2 M extractant in kerosene, 1 g/L RE, 0.1 M HCl.

The synergistic extraction of REs by using binary mixtures of an acidic α -aminophosphonate and another acidic organophosphorus extractant has been studied as a potential way to improve either the selectivity of the system or the extractability of the metals of interest. For the **13**+D2EHPA system, the separation factors for studied REs were found to be lower than with pure **13**, but it still outperformed the separation efficiency of pure D2EHPA for heavier lanthanoids (Table 6) [46]. When comparing the separation factors of pure **14** and its synergistic system with HEHEHP under similar experimental conditions, the latter does not seem to bring a major improvement in performance over the former, as indicated by minor changes (less than ± 0.4) in the determined separation factors (Table 6). However, the loading capacity of the synergistic system is almost doubled for Lu(III) and Yb(III) compared to pure **14** (Table 5), although it does not reach the Yb(III) capacity of pure HEHEHP (32.92 g/L) [47]. The separation factors determined for heavy lanthanoid separation with the **10**+Cyanex272 system, on the other hand, showed general improvement over the separation factors obtained for pure **10** and Cyanex272. A closer inspection of data also reveals that out of these three synergistic systems studied, the binary mixture consisting of **10**+Cyanex272 performed the best in heavy RE separation [48].

The highest synergistic enhancement factors reported in the aforementioned α -aminophosphonate studies are listed in Table 7. It should be noted that the best R values describe the enhancement obtained compared to the individual performance of two extractants, so it does not directly correlate to the best extraction capability of the system. Consequently, while the highest R values were obtained with α -aminophosphonate molar fractions of 0.5–0.6, the highest distribution ratios D of the two-component systems of **14** and **10** were found around molar fractions 0.3–0.4. This observation is consistent with the determined 1:2 extractant ratio of the metal complex of the former system but opposite to **10**+Cyanex272's 2:1 ratio [47,48]. Intriguingly, the maximum D of the **13**+D2EHPA system was found at 0.8 and, while not in perfect agreement with the 3:2 complex composition, both ratios indicate that the α -aminophosphonate component played the more important role in the overall performance of the extraction process [46].

Table 7. The highest values of synergistic enhancement factors R reported for each system (and RE). The molar fraction χ of the α -aminophosphonate is included in parentheses.

| Extractant | Ho | Er | Tm | Yb | Lu | Y | Ref. |
|--------------------------|------------|------------|------------|------------|------------|------------|-------------------|
| 13 + D2EHPA | - | - | - | - | 3.96 (0.5) | - | [46] ^a |
| 14 + HEHEHP | 2.18 (0.4) | 2.14 (0.5) | 2.54 (0.5) | 2.76 (0.5) | 2.89 (0.5) | 2.14 (0.5) | [47] ^b |
| 10 + Cyanex272 | 1.95 (0.4) | 2.71 (0.6) | 2.43 (0.6) | 3.67 (0.5) | 3.39 (0.5) | - | [48] ^c |

^a 0.01 M Lu(III), 0.03 M extractant (sum), 0.6 M H⁺; ^b 0.02 M RE, 0.1 M extractant (sum), pH 2; ^c 3 mM RE, 0.03 M extractant (sum), pH 2.5.

6.2. α -Aminophosphinates

Contrary to the better-explored α -aminophosphonates, only one RE extraction study has been reported for α -aminophosphinates so far [50]. The monoacidic α -aminophosphinate **21** extracted REs from nitrate medium similarly to monoacidic phosphonates **10**, **13**, and **14** because the extractabilities of REs increased with increasing pH. Only the light REs—La(III), Ce(III), Pr(III), Nd(III)—could not reach complete extraction, even at pH 4 or higher. Based on the determined separation factors for the adjacent heavy REs, **21** separated them better than the typical commercial extractants D2EHPA and HEHEHP, but it did not outperform its commercial phosphinic acid analogue P227 (Table 6). However, **21** reached the extraction equilibrium much faster, and its Lu(III) loading capacity of 0.45 mM was 1.5 times higher than P227's 0.32 mM under the same experimental conditions.

6.3. α -Aminophosphine Oxides

The research on α -aminophosphine oxides started with investigations on the possibility of using the compounds as extractants for Sc(III). A series of compounds **22–28**, including also one α -aminophosphonate **8**, was synthesized, and while most of them showed some capability for Sc(III) extraction, only the two best-performing reagents **22** and **23** were investigated further [11]. Both compounds were able to separate Sc(III) from a variety of di- and trivalent metal ions; in particular, **22** was effective in 0.3 M nitric acid medium when toluene was used as a diluent. The selectivity of extractants towards Sc(III) was further confirmed in a follow-up study where the extraction of several trivalent lanthanoids was investigated as well [36]. The highest extraction degree (~80%) of REs was obtained from perchloric acid, surpassing the extraction degree (~30%) of two other acids, hydrochloric and nitric, by 50 percentage points when the acid concentration varied from 0.25 to 0.5 M. The extractability of the investigated REs followed the decreasing ionic radii of REs; Nd(III) was extracted the best, followed by Sm(III), Dy(III), Yb(III), and Lu(III).

The synthesized α -aminophosphine oxide–azapodands **29** and **31** showed extraction properties towards Lu(III) similar to **22**, but their more difficult synthetic procedure contradicted their usability in large-scale solvent extraction [36]. A follow-up study with a slightly smaller azapodand **30** in toluene showed that U(VI) and RE(III) ions, except Y(III), are extracted practically quantitatively from a perchloric acid solution at a pH of 4.7, whereas bis(pentadecyl)phosphoric acid extracted U(VI) and Lu(III) from hydrochloric acid more selectively compared to other studied REs at a low pH regime [37]. Synergistic studies in hydrochloric acid showed that, by combining **30** and bis(pentadecyl)phosphoric acid in a 1:2 ratio, the selectivity towards U(VI), Y(III), and Lu(III) can be increased at low (2.9) and high pH (5.0–5.5) regimes, while other RE ions extracted poorly (La(III), Ce(III), and Nd(III)) or moderately (Gd(III) and Sm(III)) from the aqueous phase.

Like its α -aminophosphonate congener **11**, α -aminophosphine oxide **32** was studied for the extraction of Ce(IV) from bastnäsite ore [51]. The extractant was found to have high selectivity towards Ce(IV), with *SF* exceeding 100 for all studied metal pairings, allowing the effective separation of Ce(IV) from Th(IV) and several REs. Although α -aminophosphonate **12** achieved better Ce(IV)/Th(IV) separation in dilute sulfuric acid, **32** was able to keep the separation relatively high despite increasing acidity. Compound **32** also outperformed **12** in the Ce(IV)/RE(III) separation in virtually all studied acid concentrations. However, the Ce(IV) loading capacity of 16.66 g/L was notably lower for **32** than for the three α -aminophosphonate extractants **9**, **11**, and **12**, as all of them reached the loading capacities of 30 g/L or higher (Table 5).

To summarize Section 6, the various α -amino-functionalized organophosphorus extractants have generally demonstrated good selectivity towards REs and actinoids, particularly U(VI), Th(IV), Ce(IV), and Sc(III). The studied systems have proven to outperform commercial extractants such as D2EHPA and HEHEHP in several aspects, with the improved separation of adjacent heavy REs as one of the most important highlights. While the experimental extraction data of α -aminophosphinates and phosphine oxides—*SFs* in particular—are still more scarce compared to the more studied α -aminophosphonates, the results so far indicate similar performance levels and encourage further studies on their extraction chemistry. The utilization of α -amino-functionalized organophosphorus compounds as part of synergistic extraction systems is another rather unexplored area with few but promising results.

7. Conclusions and Future Perspectives

The interest in the α -amino-functionalized organophosphorus-based extractants and precipitation agents has grown rapidly during the last ten years after the slow start initiated in the 1960s [5]. At the heart of this process have been synthetic methods such as Kabachnik–Fields and Pudovik, developed more than half a century ago, that allow the facile synthesis of a myriad of different α -amino-functionalized organophosphorus compounds [57,58,64]. Despite the progress in synthetic chemistry, their utilization in the extraction chemistry

of REs and actinoids has just scratched the surface of this highly evolving and important field for modern society [5]. In particular, the search for greener separation methods for RE elements and actinoids, as well as the improvement of the existing ones, have recently driven the development of the separation chemistry of RE metals and actinoids [19,21,23]. However, there is still progress to be made, and based on the recent results obtained for α -amino-functionalized organophosphorus-based extractant and precipitation agents, it is highly likely that these compounds play an important role in this progress. Illustrative examples are the development of the patented Cextrant 230 functioning as an efficient and selective extractant for Ce(IV) and Th(IV) over other RE metal ions in the solvent extraction [38,39], as well as the selective separation of U(VI) and Th(IV) from RE mixtures by precipitation using only water as the solvent in acidic conditions [9]. Although the selective precipitation of RE metals from the aqueous phase has not yet been achieved with α -amino-functionalized organophosphorus compounds, it has been shown with other compounds that light and heavy REs, such as Nd and Dy, can be selectively separated by precipitation from the aqueous phase [85–89]. If one also considers the development of sorption materials based on the α -amino-functionalized organophosphorus compounds, as well as the tunability of their solubility, coordination affinity, and steric effects, there will certainly be many new and exciting avenues to be taken with the α -amino-functionalized organophosphorus extractants, separation agents, and sorption materials. We believe that the molecular-level knowledge obtained from the studied systems is the main driving force in this progress because, after all, it is the molecular structure of the compound that dictates its coordination affinity towards metal ions.

Author Contributions: Conceptualization, E.K., E.J.V., and J.O.M.; writing—original draft preparation, E.K., E.J.V., and J.O.M.; writing—review and editing, E.K., E.J.V., and J.O.M.; visualization, E.K., E.J.V., and J.O.M.; supervision, J.O.M.; project administration, J.O.M.; funding acquisition, J.O.M. All authors have read and agreed to the published version of the manuscript.

Funding: This research was funded by the Academy of Finland, grant numbers 315829 and 320015.

Institutional Review Board Statement: Not applicable.

Informed Consent Statement: Not applicable.

Data Availability Statement: Not applicable.

Acknowledgments: E.J.V. thanks the Department of Chemistry at the University of Jyväskylä for the financial support.

Conflicts of Interest: The authors declare no conflict of interest.

References

- Xie, F.; Zhang, T.A.; Dreisinger, D.; Doyle, F. A Critical Review on Solvent Extraction of Rare Earths from Aqueous Solutions. *Miner. Eng.* **2014**, *56*, 10–28. [CrossRef]
- Kislik, V.S. *Solvent Extraction: Classical and Novel Approaches*, 1st ed.; Elsevier: Amsterdam, The Netherlands, 2011; ISBN 978-0-444-53778-2.
- Batchu, N.K.; Li, Z.; Verbelen, B.; Binnemans, K. Structural Effects of Neutral Organophosphorus Extractants on Solvent Extraction of Rare-Earth Elements from Aqueous and Non-Aqueous Nitrate Solutions. *Sep. Purif. Technol.* **2021**, *255*, 117711. [CrossRef]
- Yudaev, P.A.; Kolpinskaya, N.A.; Chistyakov, E.M. Organophosphorous Extractants for Metals. *Hydrometallurgy* **2021**, *201*, 105558. [CrossRef]
- Kuang, S.; Liao, W. Progress in the Extraction and Separation of Rare Earths and Related Metals with Novel Extractants: A Review. *Sci. China Technol. Sci.* **2018**, *61*, 1319–1328. [CrossRef]
- Raju, C.S.K.; Subramanian, M.S. DAPPA Grafted Polymer: An Efficient Solid Phase Extractant for U(VI), Th(IV) and La(III) from Acidic Waste Streams and Environmental Samples. *Talanta* **2005**, *67*, 81–89. [CrossRef] [PubMed]
- Veliscek-Carolan, J.; Hanley, T.L.; Luca, V. Zirconium Organophosphonates as High Capacity, Selective Lanthanide Sorbents. *Sep. Purif. Technol.* **2014**, *129*, 150–158. [CrossRef]
- Galhoum, A.A.; Elshehy, E.A.; Tolan, D.A.; El-Nahas, A.M.; Taketsugu, T.; Nishikiori, K.; Akashi, T.; Morshedy, A.S.; Guibal, E. Synthesis of Polyaminophosphonic Acid-Functionalized Poly(Glycidyl Methacrylate) for the Efficient Sorption of La(III) and Y(III). *Chem. Eng. J.* **2019**, *375*, 121932. [CrossRef]

9. Virtanen, E.J.; Perämäki, S.; Helttunen, K.; Väisänen, A.; Moilanen, J.O. Alkyl-Substituted Aminobis(Phosphonates)—Efficient Precipitating Agents for Rare Earth Elements, Thorium, and Uranium in Aqueous Solutions. *ACS Omega* **2021**, *6*, 23977–23987. [CrossRef]
10. Flett, D.S. Solvent Extraction in Hydrometallurgy: The Role of Organophosphorus Extractants. *J. Organomet. Chem.* **2005**, *690*, 2426–2438. [CrossRef]
11. Cherkasov, R.A.; Garifzyanov, A.R.; Leont'ev, S.V.; Davletshin, R.R.; Koshkin, S.A. Extraction of Scandium Ions by New Aminophosphinyl Extractants. *Russ. J. Gen. Chem.* **2009**, *79*, 2599–2605. [CrossRef]
12. Guanming, Q.; Xikum, L.; Tai, Q.; Haitao, Z.; Honghao, Y.; Ruiting, M. Application of Rare Earths in Advanced Ceramic Materials. *J. Rare Earths* **2007**, *25*, 281–286. [CrossRef]
13. Gschneidner, K.A. *Rare Earth Alloys: A Critical Review of the Alloy Systems of the Rare Earth, Scandium, and Yttrium Metals*; Books on Demand: Norderstedt, Germany, 1961; ISBN 9780598747457.
14. Bünzli, J.-C.G. Lanthanide Photonics: Shaping the Nanoworld. *Trends Chem.* **2019**, *1*, 751–762. [CrossRef]
15. Roesky, P.W. (Ed.) *Molecular Catalysis of Rare-Earth Elements*; Structure and Bonding; Springer: Berlin/Heidelberg, Germany, 2010; Volume 137, ISBN 978-3-642-12810-3.
16. McCallum, R.W.; Lewis, L.; Skomski, R.; Kramer, M.J.; Anderson, I.E. Practical Aspects of Modern and Future Permanent Magnets. *Annu. Rev. Mater. Res.* **2014**, *44*, 451–477. [CrossRef]
17. Alves Dias, P.; Bobba, S.; Carrara, S.; Plazzotta, B. *The Role of Rare Earth Elements in Wind Energy and Electric Mobility: An Analysis of Future Supply/Demand Balances*; Publications Office of the European Union: Luxembourg, 2020.
18. Neodymium—2022 Data—2012–2021 Historical—2023 Forecast—Price—Quote—Chart. Available online: <https://tradingeconomics.com/commodity/neodymium> (accessed on 3 May 2022).
19. Pyrzynska, K.; Kubiak, A.; Wysocka, I. Application of Solid Phase Extraction Procedures for Rare Earth Elements Determination in Environmental Samples. *Talanta* **2016**, *154*, 15–22. [CrossRef]
20. Binnemans, K.; Jones, P.T.; Blanpain, B.; Van Gerven, T.; Yang, Y.; Walton, A.; Buchert, M. Recycling of Rare Earths: A Critical Review. *J. Clean. Prod.* **2013**, *51*, 1–22. [CrossRef]
21. Binnemans, K.; Jones, P.T.; Blanpain, B.; Van Gerven, T.; Pontikes, Y. Towards Zero-Waste Valorisation of Rare-Earth-Containing Industrial Process Residues: A Critical Review. *J. Clean. Prod.* **2015**, *99*, 17–38. [CrossRef]
22. Zhang, Z.; Li, H.; Guo, F.; Meng, S.; Li, D. Synergistic Extraction and Recovery of Cerium(IV) and Fluorin from Sulfuric Solutions with Cyanex 923 and Di-2-Ethylhexyl Phosphoric Acid. *Sep. Purif. Technol.* **2008**, *63*, 348–352. [CrossRef]
23. Zhu, Z.; Pranolo, Y.; Cheng, C.Y. Separation of Uranium and Thorium from Rare Earths for Rare Earth Production—A Review. *Miner. Eng.* **2015**, *77*, 185–196. [CrossRef]
24. Humphrey, U.E.; Khandaker, M.U. Viability of Thorium-Based Nuclear Fuel Cycle for the next Generation Nuclear Reactor: Issues and Prospects. *Renew. Sustain. Energy Rev.* **2018**, *97*, 259–275. [CrossRef]
25. Kurniawan, T.A.; Othman, M.H.D.; Singh, D.; Avtar, R.; Hwang, G.H.; Setiadi, T.; Lo, W. Technological Solutions for Long-Term Storage of Partially Used Nuclear Waste: A Critical Review. *Ann. Nucl. Energy* **2022**, *166*, 108736. [CrossRef]
26. Alexandratos, S.D.; Zhu, X. Polymer-Supported Aminomethylphosphinate as a Ligand with a High Affinity for U(VI) from Phosphoric Acid Solutions: Combining Variables to Optimize Ligand–Ion Communication. *Solvent Extr. Ion Exch.* **2016**, *34*, 290–295. [CrossRef]
27. Imam, E.A.; El-Tantawy El-Sayed, I.; Mahfouz, M.G.; Tolba, A.A.; Akashi, T.; Galhoum, A.A.; Guibal, E. Synthesis of α -Aminophosphonate Functionalized Chitosan Sorbents: Effect of Methyl vs Phenyl Group on Uranium Sorption. *Chem. Eng. J.* **2018**, *352*, 1022–1034. [CrossRef]
28. Cheira, M.F. Synthesis of Aminophosphonate-Functionalised ZnO/Polystyrene-Butadiene Nanocomposite and Its Characteristics for Uranium Adsorption from Phosphoric Acid. *Int. J. Environ. Anal. Chem.* **2021**, *101*, 1710–1734. [CrossRef]
29. Galhoum, A.A.; Eisa, W.H.; El-Tantawy El-Sayed, I.; Tolba, A.A.; Shalaby, Z.M.; Mohamady, S.I.; Muhammad, S.S.; Hussien, S.S.; Akashi, T.; Guibal, E. A New Route for Manufacturing Poly(Aminophosphonic)-Functionalized Poly(Glycidyl Methacrylate)-Magnetic Nanocomposite—Application to Uranium Sorption from Ore Leachate. *Environ. Pollut.* **2020**, *264*, 114797. [CrossRef] [PubMed]
30. Jagodić, V.; Herak, M.J. Synthesis and Physical Properties of a Novel Aminophosphonic Acid as an Extracting Agent for Metals. *J. Inorg. Nucl. Chem.* **1970**, *32*, 1323–1332. [CrossRef]
31. Jagodić, V.; Herak, M.J.; Šipalo, B.; Radošević, J. Solvent Extraction Study of Lanthanum and Europium by Acidic Esters of Aminophosphonic Acids. *J. Inorg. Nucl. Chem.* **1971**, *33*, 2651–2659. [CrossRef]
32. Herak, M.J.; Jagodić, V. Distribution and Dimerization of Organophosphorus Extractants and Their Extraction Efficiency in Different Solvents. *J. Inorg. Nucl. Chem.* **1973**, *35*, 995–1001. [CrossRef]
33. Radošević, J.; Jagodić, V.; Herak, M.J. Extraction and Complex Formation of Cerium(III) and Praseodymium(III) with Monoesters of Phosphonic Acids. *J. Inorg. Nucl. Chem.* **1977**, *39*, 2053–2056. [CrossRef]
34. Ziganshina, A.Y.; Kazakova, E.H.; Fedorenko, S.V.; Mustafina, A.R.; Konovalov, A.I. Aminomethylphosphonate Derivatives of Tetramethylcalix[4]Resorcinolarene. Synthesis and Some Extraction Properties in Relation to the Lanthanide Ions. *Russ. J. Gen. Chem.* **2001**, *71*, 1422–1425. [CrossRef]

35. Fedorenko, S.V.; Mustafina, A.R.; Kazakova, E.K.; Pod'yachev, S.N.; Kharitonova, N.I.; Pudovik, M.A.; Konovalov, A.I.; Tananaev, I.G.; Myasoedov, B.F. Sodium Picrate Effect on Extraction of Lanthanum and Lutetium by Aminophosphonate Calix[4]Resorcinarenes. *Russ. Chem. Bull.* **2003**, *52*, 562–566. [CrossRef]
36. Cherkasov, R.A.; Garifzyanov, A.R.; Bazanova, E.B.; Davletshin, R.R.; Leont'eva, S.V. Liquid Extraction of Some Rare Earth Elements with Aminomethylphosphine Oxides. *Russ. J. Gen. Chem.* **2012**, *82*, 33–42. [CrossRef]
37. Garifzyanov, A.R.; Leont'ev, S.V.; Davletshina, N.V.; Voloshin, A.V.; Cherkasov, R.A. Synthesis, Transport, and Ionophore Properties of α,ω -Biphosphorylated Azapodands: VIII. Solvent Extraction of the Metal Ions with N,N'-Bis(Diethylphosphorylmethyl)-1,8-Diamino-3,6-Dioxaoctane. *Russ. J. Gen. Chem.* **2013**, *83*, 1997–2004. [CrossRef]
38. Liao, W.; Zhang, Z.; Li, Y.; Wu, G.; Lu, Y. CN105734286A—Method for Separating Cerium-Fluoride and Thorium. China Patent CN105734286A, 11 December 2014.
39. Lu, Y.; Zhang, Z.; Li, Y.; Liao, W. Extraction and Recovery of Cerium(IV) and Thorium(IV) from Sulphate Medium by an α -Aminophosphonate Extractant. *J. Rare Earths* **2017**, *35*, 34–40. [CrossRef]
40. Wei, H.; Li, Y.; Zhang, Z.; Xue, T.; Kuang, S.; Liao, W. Selective Extraction and Separation of Ce (IV) and Th (IV) from RE(III) in Sulfate Medium Using Di(2-Ethylhexyl)-N-Heptylaminoethylphosphonate. *Solvent Extr. Ion Exch.* **2017**, *35*, 117–129. [CrossRef]
41. Kuang, S.; Zhang, Z.; Li, Y.; Wu, G.; Wei, H.; Liao, W. Selective Extraction and Separation of Ce(IV) from Thorium and Trivalent Rare Earths in Sulfate Medium by an α -Aminophosphonate Extractant. *Hydrometallurgy* **2017**, *167*, 107–114. [CrossRef]
42. Kuang, S.; Zhang, Z.; Li, Y.; Wei, H.; Liao, W. Extraction and Separation of Heavy Rare Earths from Chloride Medium by α -Aminophosphonic Acid HEHAPP. *J. Rare Earths* **2018**, *36*, 304–310. [CrossRef]
43. Zhao, Q.; Zhang, Z.; Li, Y.; Bian, X.; Liao, W. Solvent Extraction and Separation of Rare Earths from Chloride Media Using α -Aminophosphonic Acid Extractant HEHAMP. *Solvent Extr. Ion Exch.* **2018**, *36*, 136–149. [CrossRef]
44. Wei, H.; Li, Y.; Kuang, S.; Zhang, Z.; Liao, W. Separation of Trivalent Rare Earths from Chloride Medium Using Solvent Extraction with Heptylaminoethyl Phosphonic Acid 2-Ethylhexyl Ester (HEHHAP). *Hydrometallurgy* **2019**, *188*, 14–21. [CrossRef]
45. Le, W.; Kuang, S.; Zhang, Z.; Wu, G.; Li, Y.; Liao, C.; Liao, W. Selective Extraction and Recovery of Scandium from Sulfate Medium by Cextrant 230. *Hydrometallurgy* **2018**, *178*, 54–59. [CrossRef]
46. Kuang, S.; Zhang, Z.; Li, Y.; Wei, H.; Liao, W. Synergistic Extraction and Separation of Rare Earths from Chloride Medium by the Mixture of HEHAPP and D2EHPPA. *Hydrometallurgy* **2017**, *174*, 78–83. [CrossRef]
47. Zhao, Q.; Li, Y.; Kuang, S.; Zhang, Z.; Bian, X.; Liao, W. Synergistic Extraction of Heavy Rare Earths by Mixture of α -Aminophosphonic Acid HEHAMP and HEHEHP. *J. Rare Earths* **2019**, *37*, 422–428. [CrossRef]
48. Wei, H.; Li, Y.; Zhang, Z.; Liao, W. Synergistic Solvent Extraction of Heavy Rare Earths from Chloride Media Using Mixture of HEHHAP and Cyanex272. *Hydrometallurgy* **2020**, *191*, 105240. [CrossRef]
49. Wang, X.; Du, M.; Liu, H. Synergistic Extraction Study of Samarium(III) from Chloride Medium by Mixtures of Bis(2,4,4-Trimethylpentyl)Phosphinic Acid and 8-Hydroxyquinoline. *Sep. Purif. Technol.* **2012**, *93*, 48–51. [CrossRef]
50. Fu, Y.; Huang, M.; Zhou, Z.; Li, Z.; Liao, W.; Lu, Y. Separation of Trivalent Rare Earths from Nitrate Medium Using Solvent Extraction with a Novel Extractant 2-Ethylhexyl ((2-Ethylhexylamino)Methyl) Phosphonic Acid. *J. Rare Earths* **2022**, *40*, 491–500. [CrossRef]
51. Huang, M.; Fu, Y.; Lu, Y.; Liao, W.; Li, Z. A Novel Extractant Bis(2-Ethylhexyl) ((2-Ethylhexylamino)Methyl) Phosphine Oxide for Cerium(IV) Extraction and Separation from Sulfate Medium. *J. Rare Earths* **2020**, *38*, 1330–1336. [CrossRef]
52. Jagodić, V.; Grdenić, D. Aminophosphonic Acid Mono-Esters as Reagents for Solvent Extraction of Metals. *J. Inorg. Nucl. Chem.* **1964**, *26*, 1103–1109. [CrossRef]
53. Herak, M.J.; Jagodic, V. Solvent Extraction and Separation of Europium(III) and Terbium(III) from Uranium(VI) by Monoethyl Anilinobenzylphosphonate. *Croat. Chem. Acta* **1964**, *36*, 51–58.
54. Jagodić, V.; Herak, M.J.; Radošević, J. Separation of Lanthanum from Barium by Solvent Extraction with the Monoethyl Ester of Anilinobenzylphosphonic Acid. *J. Less Common Met.* **1968**, *15*, 371–375. [CrossRef]
55. Herak, M.J.; Vujičić, N.; Jagodić, V. Separation of Radioactive Yttrium from Strontium by Means of Mono-Octyl Anilinobenzylphosphonate. *Mikrochim. Acta* **1969**, *57*, 16–20. [CrossRef]
56. Yang, X.; Zhang, Z.; Kuang, S.; Wei, H.; Li, Y.; Wu, G.; Geng, A.; Li, Y.; Liao, W. Removal of Thorium and Uranium from Leach Solutions of Ion-Adsorption Rare Earth Ores by Solvent Extraction with Cextrant 230. *Hydrometallurgy* **2020**, *194*, 105343. [CrossRef]
57. Fields, E.K. The Synthesis of Esters of Substituted Amino Phosphonic Acids. *J. Am. Chem. Soc.* **1952**, *74*, 1528–1531. [CrossRef]
58. Kabachnik, M.I.; Medved, T.Y. New Synthesis of Aminophosphonic Acids. *Dokl. Akad. Nauk SSSR* **1952**, *83*, 689–692.
59. Moedritzer, K.; Irani, R.R. The Direct Synthesis of α -Aminomethylphosphonic Acids. Mannich-Type Reactions with Orthophosphorous Acid. *J. Org. Chem.* **1966**, *31*, 1603–1607. [CrossRef]
60. Cherkasov, R.A.; Talan, A.S.; Tarasov, A.V.; Garifzyanov, A.P. Synthesis of Novel Mono- and Bisaminophosphoryl Compounds and Their Membrane Transport Properties for Acidic Substrates. *Russ. J. Gen. Chem.* **2008**, *78*, 1330–1333. [CrossRef]
61. Cherkasov, R.A.; Garifzyanov, A.R.; Talan, A.S.; Davletshin, R.R.; Kurnosova, N.V. Synthesis of New Liophilic Functionalized Aminomethylphosphine Oxides and Their Acid-Base and Membrane-Transport Properties toward Acidic Substrates. *Russ. J. Gen. Chem.* **2009**, *79*, 1835–1849. [CrossRef]
62. Pudovik, A.N. Addition of Dialkyl Phosphites to Unsaturated Compounds. A New Method of Synthesis of β -Keto Phosphonic and Unsaturated α -Hydroxyphosphonic Esters. *Dokl. Akad. Nauk SSSR* **1950**, *73*, 499–502.

63. Jagodić, V. Darstellung von Monoestern N-Substituierter Aminomethylphosphonsäuren Durch Teilweise Verseifung Entsprechender Diester. *Chem. Ber.* **1960**, *93*, 2308–2313. [CrossRef]
64. Blicke, F.F. The Mannich Reaction. In *Organic Reactions 1*; Wiley: New York, NY, USA, 1942; pp. 303–341.
65. Juribašić, M.; Bellotto, L.; Tušek-Božić, L. N–H···O=P Hydrogen-Bonded Dimers as the Main Structural Motif of Aminophosphate Diesters. *Struct. Chem.* **2012**, *23*, 257–266. [CrossRef]
66. Nakamoto, K. *Infrared and Raman Spectra of Inorganic and Coordination Compounds*; Griffiths, P.R., Ed.; John Wiley & Sons, Inc.: Hoboken, NJ, USA, 2008; ISBN 9780470405840.
67. Larkin, P.J. *Infrared and Raman Spectroscopy: Principles and Spectral Interpretation*, 2nd ed.; Elsevier: Amsterdam, The Netherlands, 2017; ISBN 9780128042090.
68. Lin-Vien, D.; Colthup, N.B.; Fateley, W.G.; Grasselli, J.G. *The Handbook of Infrared and Raman Characteristic Frequencies of Organic Molecules*; Academic Press: San Diego, CA, USA, 1991; ISBN 0-12-451160-0.
69. Groves, J.A.; Wright, P.A.; Lightfoot, P. Two Closely Related Lanthanum Phosphonate Frameworks Formed by Anion-Directed Linking of Inorganic Chains. *Inorg. Chem.* **2005**, *44*, 1736–1739. [CrossRef]
70. Silva, P.; Vieira, F.; Gomes, A.C.; Ananias, D.; Fernandes, J.A.; Bruno, S.M.; Soares, R.; Valente, A.A.; Rocha, J.; Paz, F.A.A. Thermal Transformation of a Layered Multifunctional Network into a Metal–Organic Framework Based on a Polymeric Organic Linker. *J. Am. Chem. Soc.* **2011**, *133*, 15120–15138. [CrossRef]
71. Colodrero, R.M.P.; Olivera-Pastor, P.; Losilla, E.R.; Aranda, M.A.G.; Leon-Reina, L.; Papadaki, M.; McKinlay, A.C.; Morris, R.E.; Demadis, K.D.; Cabeza, A. Multifunctional Lanthanum Tetrakisphosphonates: Flexible, Ultramicroporous and Proton-Conducting Hybrid Frameworks. *Dalt. Trans.* **2012**, *41*, 4045. [CrossRef] [PubMed]
72. Ren, M.; Bao, S.-S.; Ferreira, R.A.S.; Zheng, L.-M.; Carlos, L.D. A Layered Erbium Phosphonate in Pseudo-D5h Symmetry Exhibiting Field-Tunable Magnetic Relaxation and Optical Correlation. *Chem. Commun.* **2014**, *50*, 7621. [CrossRef] [PubMed]
73. Mendes, R.F.; Almeida Paz, F.A. Dynamic Breathing Effect in Metal–Organic Frameworks: Reversible 2D–3D–2D–3D Single-Crystal to Single-Crystal Transformation. *Inorg. Chim. Acta* **2017**, *460*, 99–107. [CrossRef]
74. Bligh, S.W.A.; Choi, N.; Geraldies, C.F.G.C.; Knoke, S.; McPartlin, M.; Sanganee, M.J.; Woodroffe, T.M. A Novel Hexaaza Macrocyclic with Methylene phosphonate Pendant Arms: A Potential Useful Chelate for Biomedical Applications. *J. Chem. Soc. Dalton Trans.* **1997**, *3*, 4119–4126. [CrossRef]
75. Gałeczowska, J.; Janicki, R.; Kozłowski, H.; Mondry, A.; Młynarz, P.; Szyrwił, Ł. Unusual Coordination Behaviour of a Phosphonate- and Pyridine-Containing Ligand in a Stable Lanthanide Complex. *Eur. J. Inorg. Chem.* **2010**, *2010*, 1696–1702. [CrossRef]
76. Le Fur, M.; Beyler, M.; Lepareur, N.; Fougère, O.; Platas-Iglesias, C.; Rousseaux, O.; Tripier, R. Cyclen Tri-*n*-Butylphosphonate Ester as Potential Chelator for Targeted Radiotherapy: From Yttrium(III) Complexation to ⁹⁰Y Radiolabeling. *Inorg. Chem.* **2016**, *55*, 8003–8012. [CrossRef]
77. Tang, S.-F.; Song, J.-L.; Li, X.-L.; Mao, J.-G. Luminescent Lanthanide(III) Carboxylate–Phosphonates with Helical Tunnels. *Cryst. Growth Des.* **2006**, *6*, 2322–2326. [CrossRef]
78. Ayi, A.A.; Kinnibrugh, T.L.; Clearfield, A. Hydrothermal Synthesis and Structural Characterization of Ammonium Ion-Templated Lanthanide(III) Carboxylate-Phosphonates. *Front. Chem.* **2014**, *2*, 94. [CrossRef]
79. Danesi, P.R.; Chiarizia, R.; Scibona, G. The Meaning of Slope Analysis in Solvent Extraction Chemistry: The Case of Zinc Extraction by Trilaurylammonium Chloride. *J. Inorg. Nucl. Chem.* **1970**, *32*, 2349–2355. [CrossRef]
80. Fang, Y.; Yuan, X.; Wu, L.; Peng, Z.; Feng, W.; Liu, N.; Xu, D.; Li, S.; Sengupta, A.; Mohapatra, P.K.; et al. Ditopic CMPO-Pillar[5]Arenes as Unique Receptors for Efficient Separation of Americium(III) and Europium(III). *Chem. Commun.* **2015**, *51*, 4263–4266. [CrossRef]
81. Gupta, C.K.; Krishnamurthy, N. *Extractive Metallurgy of Rare Earths*; CRC Press: Boca Raton, FL, USA, 2005; ISBN 978-0415333405.
82. Xu, G.X.; Wang, W.Q.; Wu, J.G.; Li, B.L.; Wu, G.B.; Shi, N. Chemistry of Nuclear Fuels Extraction. *At. Energy Sci. Technol.* **1963**, *7*, 487–508.
83. Zhang, Z.; Jia, Q.; Liao, W. Progress in the Separation Processes for Rare Earth Resources. In *Handbook on the Physics and Chemistry of Rare Earths*; Elsevier: Amsterdam, The Netherlands, 2015; Volume 48, pp. 287–376.
84. Sato, T. Liquid-Liquid Extraction of Rare-Earth Elements from Aqueous Acid Solutions by Acid Organophosphorus Compounds. *Hydrometallurgy* **1989**, *22*, 121–140. [CrossRef]
85. Tasaki-Handa, Y.; Abe, Y.; Ooi, K.; Narita, H.; Tanaka, M.; Wakisaka, A. Selective Crystallization of Phosphoester Coordination Polymer for the Separation of Neodymium and Dysprosium: A Thermodynamic Approach. *J. Phys. Chem. B* **2016**, *120*, 12730–12735. [CrossRef] [PubMed]
86. Lu, H.; Guo, X.; Wang, Y.; Diefenbach, K.; Chen, L.; Wang, J.-Q.; Lin, J.; Wang, S. Size-Dependent Selective Crystallization Using an Inorganic Mixed-Oxoanion System for Lanthanide Separation. *Dalt. Trans.* **2019**, *48*, 12808–12811. [CrossRef] [PubMed]
87. Yin, X.; Wang, Y.; Bai, X.; Wang, Y.; Chen, L.; Xiao, C.; Diwu, J.; Du, S.; Chai, Z.; Albrecht-Schmitt, T.E.; et al. Rare Earth Separations by Selective Borate Crystallization. *Nat. Commun.* **2017**, *8*, 14438. [CrossRef] [PubMed]
88. Ya Gao, H.; Li Peng, W.; Pan Meng, P.; Feng Feng, X.; Qiang Li, J.; Qiong Wu, H.; Sheng Yan, C.; Yang Xiong, Y.; Luo, F. Lanthanide Separation Using Size-Selective Crystallization of Ln-MOFs. *Chem. Commun.* **2017**, *53*, 5737–5739. [CrossRef]
89. Nelson, J.J.M.; Cheisson, T.; Rugh, H.J.; Gau, M.R.; Carroll, P.J.; Schelter, E.J. High-Throughput Screening for Discovery of Benchtop Separations Systems for Selected Rare Earth Elements. *Commun. Chem.* **2020**, *3*, 7. [CrossRef]

Article

Deamination of 1-Aminoalkylphosphonic Acids: Reaction Intermediates and Selectivity

Anna Brol  and Tomasz K. Olszewski * 

Department of Physical and Quantum Chemistry, Faculty of Chemistry, Wrocław University of Science and Technology, ul. Wybrzeże Wyspiańskiego 27, 50-370 Wrocław, Poland

* Correspondence: tomasz.olszewski@pwr.edu.pl

Abstract: Deamination of 1-aminoalkylphosphonic acids in the reaction with HNO_2 (generated “in situ” from NaNO_2) yields a mixture of substitution products (1-hydroxyalkylphosphonic acids), elimination products (vinylphosphonic acid derivatives), rearrangement and substitution products (2-hydroxyalkylphosphonic acids) as well as H_3PO_4 . The variety of formed reaction products suggests that 1-phosphonoalkylium ions may be intermediates in such deamination reactions.

Keywords: diazotization; carbenium ion; 1-phosphonoalkylium ion; substitution reaction; elimination reaction; rearrangement

1. Introduction

Organophosphorus compounds are a very interesting class of molecules well known to exist in nature, exhibit very intriguing activity, and have already found broad applications in various sectors of industry, such as in agrochemistry [1], pharmacy [2], catalysis [3], materials [4], as flame retardants [5], or chemical reagents [6]. Particular interest is devoted to substituted 1-aminoalkylphosphonic acids that can be considered structural analogs of natural 2-aminoalkanoic acids [7–9]. In that regard, the use of 1-aminoalkylphosphonic acids in drug discovery has proven successful in many cases, with prominent examples being potential drugs for the treatment of diabetes [10,11], asthma [12], inflammation [13], heart failure [14], cancer [15], malaria [16], and HIV [17]. Due to the importance of the 1-aminoalkylphosphonic acids, several synthetic methods for their preparation have been designed over the years [18–26].

Surprisingly, further transformations of 1-aminoalkylphosphonic acids and their reactivity as reaction substrates in organic synthesis are scarcely described in the literature [27–33]. Those described include among others alkaline deacylation of 1-(acylamino)alkylphosphonic acids, ref. [31] oxidative dephosphorylation of 1-aminoalkylphosphonic acids [32], oxidation of 1-(*N,N*-dialkylamino)-alkylphosphonic acids leading to corresponding *N,N*-dialkyl-*N*-oxide derivatives [30], or recently effective preparation of 1-aminoalkylphosphonic acid quaternary ammonium salts from simple 1-aminoalkylphosphonic acid [27]. On the other hand, the use of analogous 2-aminoalkanoic acids as substrates, particularly in diazotization reaction, is a well-known methodology that yields 2-hydroxyalkanoic acids or 2-chloroalkanoic acids (Scheme 1a) [34–37], useful building blocks in medicinal chemistry [38–40], total synthesis of natural products [41–43], and polymer chemistry [44–46]. Inspired by the activity and utility of 2-amino acids in diazotization reactions we decided to study the reactivity of 1-aminoalkylphosphonic acids in deamination by the diazotization reaction (Scheme 1d). It is well known that the amine group reacts with nitrous acid (HNO_2) generated by the acidification of aqueous solutions of sodium nitrite (NaNO_2) with a mineral acid to yield diazonium salts, followed by reaction with various nucleophiles [47]. However, aliphatic diazonium salts are commonly unstable, and the formation of carbenium ion intermediate is inevitable, which causes complications with controlling the selectivity of such reaction [47,48].

Citation: Brol, A.; Olszewski, T.K. Deamination of 1-Aminoalkylphosphonic Acids: Reaction Intermediates and Selectivity. *Molecules* **2022**, *27*, 8849. <https://doi.org/10.3390/molecules27248849>

Academic Editor: Jakub Adamek

Received: 18 November 2022

Accepted: 5 December 2022

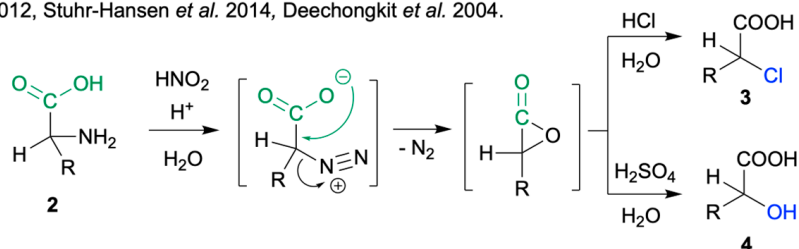
Published: 13 December 2022

Publisher's Note: MDPI stays neutral with regard to jurisdictional claims in published maps and institutional affiliations.

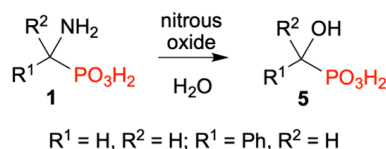


Copyright: © 2022 by the authors. Licensee MDPI, Basel, Switzerland. This article is an open access article distributed under the terms and conditions of the Creative Commons Attribution (CC BY) license (<https://creativecommons.org/licenses/by/4.0/>).

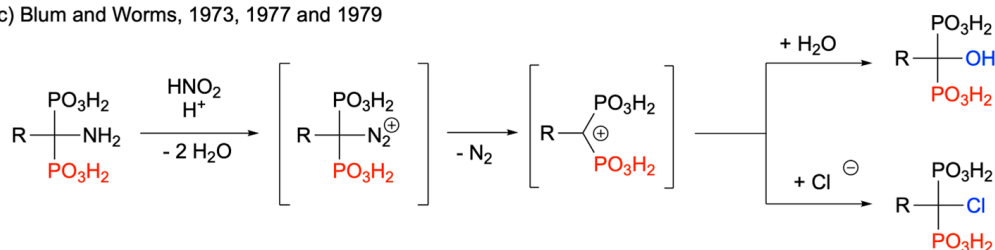
(a) Reaction of 2-aminoalkanoic acids with nitrous acid: Mear *et al.*, 2019, Hu *et al.* 2012, Stuhr-Hansen *et al.* 2014, Deechongkit *et al.* 2004.



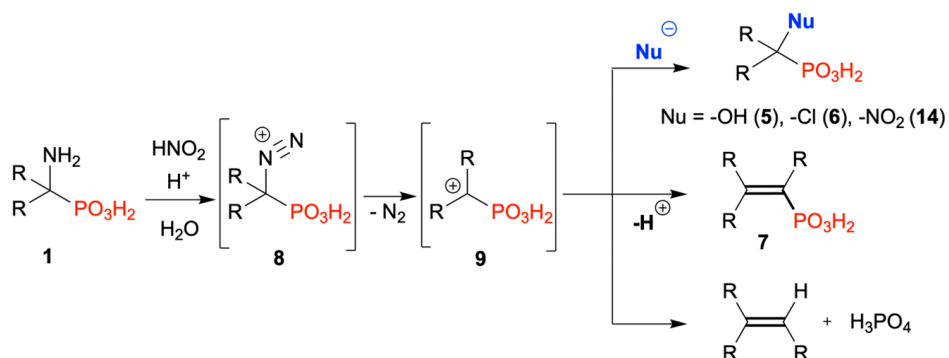
(b) Kabachnik and Medved, 1950 and 1954



(c) Blum and Worms, 1973, 1977 and 1979



(d) This work - the general concept of deamination of 1-aminoalkylphosphonic acids

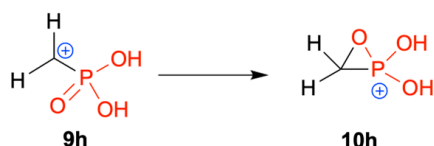


Scheme 1. General presentation of deamination reaction carried out on 2-aminoalkanoic acids and their phosphorus analogs [34–37,49–53].

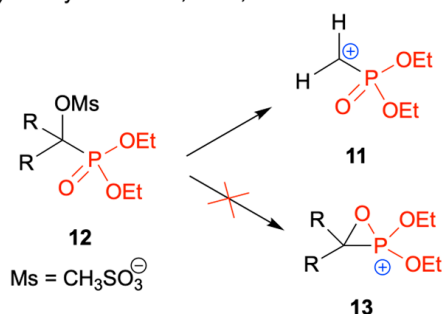
While the deamination of 2-aminoalkanoic acids as substrates has been described in a great number of articles, reactions of structurally similar 1-aminoalkylphosphonic acids are scarcely described in the literature. In 1950 [49] and 1954 [50], Kabachnik and Medved described the analytical applications of the deamination reaction of aminomethylphosphonic acid and 1-amino-1-phenylethylphosphonic acid with nitrous oxides in which hydroxymethylphosphonic acid and 1-hydroxy-1-phenylethylphosphonic acids were formed respectively (Scheme 1b). Much later, reactions of related aminoalkylidene-1,1-diphosphonic acids with nitrous acid were described by Blum and Worms [51–53]. The authors concluded that carbenium ions with two phosphonic groups are formed and the reaction products are hydroxyalkylidene-1,1-diphosphonic acids, chloroalkylidene-1,1-diphosphonic acids, and derivatives of vinylphosphonic acid (Scheme 1c). It is worth mentioning that 1-phosphonoalkylium ions **9**, which may be intermediates in the deamination reaction of 1-aminoalkylphosphonic acids **1**, have also not been extensively studied in the literature. Only theoretical calculations for the simplest phosphonomethylium ion (**9h**) (which exist in the cyclic form **10h**) have been described by Pasto (Scheme 2a) [54]. On the other hand, Creary *et al.* studied the formation of carbenium ions substituted with phosphonic

ester group **11** in the solvolysis reactions of mesylates **12** [55–58]. Experiments on the α -deuterium isotope effect proved that intermediates have an open form **11** and that no cyclic compounds **13** are formed (Scheme 2b). Intrigued by the very scarce literature reports on the deamination of 1-aminoalkylphosphonic acids, and interested in revealing the reactivity of the 1-phosphonoalkylium ions, possible intermediates in deamination of 1-aminoalkylphosphonic acids, we decided to study this interesting reaction in greater detail (Scheme 1d).

(a) Pasto, 1985



(b) Creary *et al.* 1991, 1985, 1983



Scheme 2. Possible structures of the 1-phosphonoalkylium ions known from the literature [54–58].

Herein we present the results of our detailed study on the deamination reaction of structurally diverse 1-aminoalkylphosphonic acids carried out with nitrous acid. The presented results show the potential application of this transformation in organic synthesis and shed light on the possible reaction mechanism and reaction intermediates.

2. Results

For our study, we selected a representative and structurally diverse palette of 1-aminoalkylphosphonic acids (Figure 1, 17 examples). The selected examples include phosphorus analogs of such amino acids as alanine **1a**, valine **1b**, leucine **1d**, glycine **1h**, phenylalanine **1g**, and phenylglycine **1f**.

2.1. Diazotization of 2-Aminoalkanoic Acids vs. 1-Aminoalkylphosphonic Acids—Preliminary Experiments

We started our preliminary experiments using the conditions applied for the diazotization of 2-aminoalkanoic acids (NaNO_2 , 5M HCl) (Scheme 3) [59]. Preliminary experiments clearly showed that 1-aminoalkylphosphonic acids reacted with nitrous acid (HNO_2), generated in situ from sodium nitrite (NaNO_2), differently than the tested amino acids. The degree of conversion in the case of 1-aminoalkylphosphonic was slightly higher than in the case of classical amino acids. No other products than the ones depicted on Scheme 3 were observed and they were additionally accompanied by unreacted starting material. Under the examined conditions, no selectivity towards chloride ions was observed and 1-hydroxyalkylphosphonic acids were the main reaction products.

Moreover, in the case of amino acids **2**, as expected, the main reaction products were 1-hydroxy or 1-chloroalkanoic acids, while in the case of 1-aminoalkylphosphonic **1** a greater number of reaction products, including rearrangement and fragmentation products, were observed (Scheme 3).

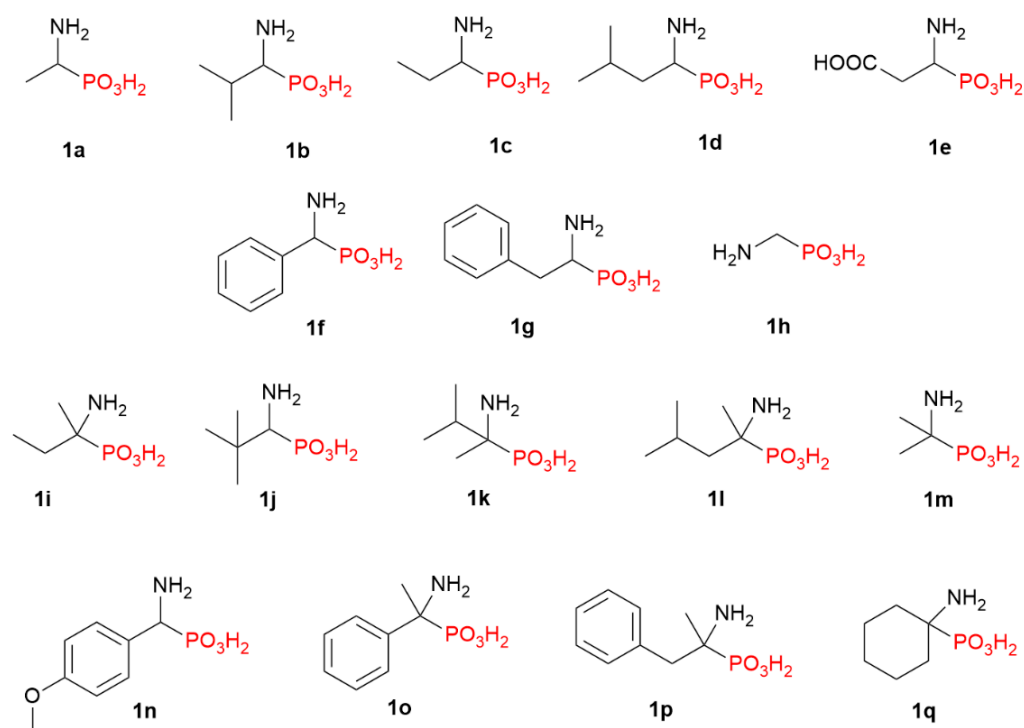
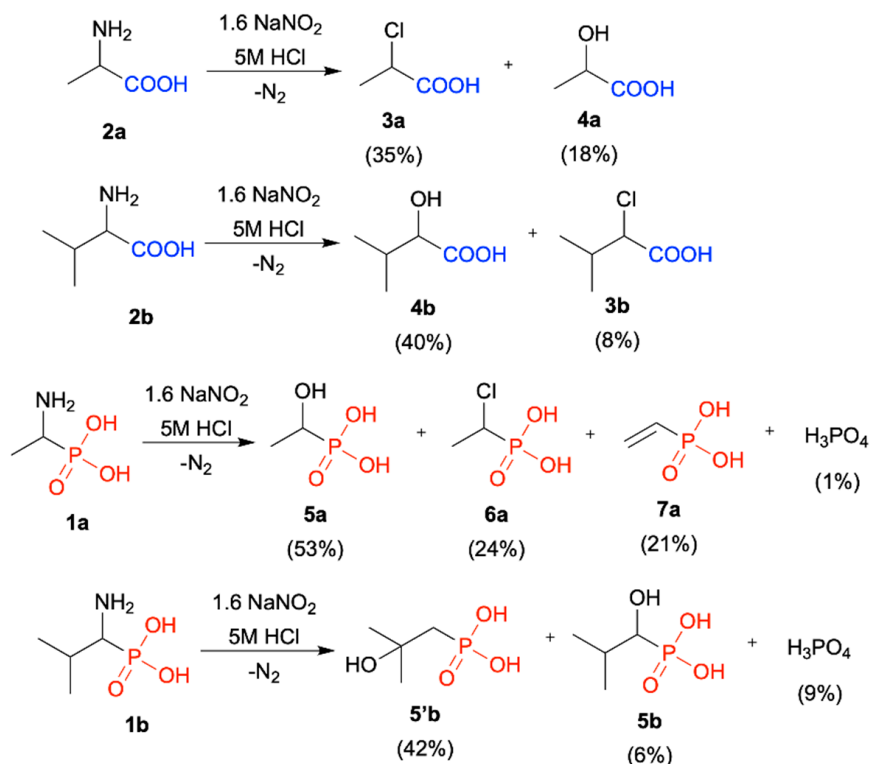


Figure 1. Structures of 1-aminoalkylphosphonic acids used in this study.



Scheme 3. Preliminary experiments on the diazotization of alanine (**2a**) and valine (**2b**) and their corresponding phosphorus analogs **1a** and **1b**.

Due to the complex composition of post-reaction mixtures, we decided to modify the original reaction conditions used for the diazotization of amino acids. Expecting to obtain complex reaction mixtures, we wanted to focus first on generating the carbenium ions and then observe their reactivity with just a limited number of nucleophiles to simplify the

analysis of the results. Based on the literature data describing the diazotization of amino acids, we envisaged that the most important parameter is the initial pH of the reaction mixture [60–63]. Lowering the pH should increase the concentration of the electrophilic nitrosating agent, but at the same time causes the protonation of the amino group in the starting 1-aminoalkylphosphonic acids, which lowers the nucleophile concentration. Additionally, we have assumed that 1-aminoalkylphosphonic acids are strong enough acids to generate the nitrosating agent in situ from sodium nitrite in water, therefore there is no need to use hydrochloric acid in the reaction. After this simplification, the only nucleophiles in the reaction mixture were nitrite ions and water.

2.2. Diazotization of 1-Aminoalkylphosphonic Acids—Optimized Reaction Conditions

When 1-aminoalkylphosphonic acid **1** (1 equiv.) was added to the solution of NaNO_2 (2 equiv.), nitrogen evolution was observed, which proved that diazonium salts **8** were generated. The post-reaction mixtures contained products of substitution reaction (1-hydroxyalkylphosphonic acids **5**), elimination reaction (vinylphosphonic acid derivatives **7**), and additionally 2-hydroxyalkylphosphonic acids **5'** and phosphoric acid (H_3PO_4).

We have observed that the product distribution in these reactions depended strongly on the structure of the starting 1-aminoalkylphosphonic acid **1**, therefore the reaction results are outlined in Tables 1–4, according to the structure of the substrates used.

To avoid the formation of secondary products, the crude post-reaction mixtures were analyzed directly by NMR spectroscopy without isolation of the reaction products, and thus the results are given in the form of conversion. In all cases, the structures of reaction products were confirmed by NMR spectroscopy (especially ^{31}P NMR and ^1H NMR) by the addition of known reference compounds (synthesized separately) or by analysis and comparison of the NMR spectra of the crude reaction mixture with spectra of products known from the literature (see Supplementary Materials for more details).

Substitution was generally the main reaction for most of the investigated 1-aminoalkylphosphonic acids **1** (Tables 1 and 2), especially for those that do not have protons in the β -position (**1f**, **1n**, **1h**). For example, in the reaction of amino(phenyl)methylphosphonic acid (**1f**) the conversion of substrate to hydroxy(phenyl)phosphonic acid (**5f**) was 97% (Table 2, entry 1).

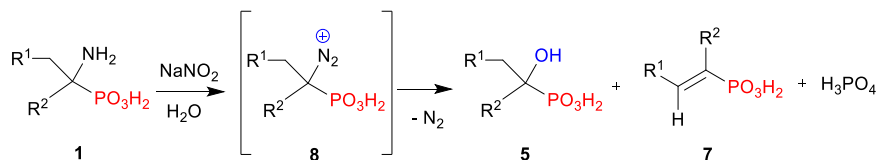
In turn, elimination was the major reaction for 1-aminoalkylphosphonic acids **1q**, **1l**, and **1i** which have bulky substituents (Table 3). For substrates **1l** and **1i**, two isomers of vinylphosphonic acid derivatives were formed: **7l**, **7'l** for **1l** and **7i**, **7'i** for **1i**. We assume that in this case the steric hindrance impedes the access of nucleophiles and, as a result, the elimination reaction is favored.

Furthermore, for substrates **1j**, **1b**, and **1k** that have β -position migrating groups, the major reaction product was phosphoric acid (H_3PO_4), accompanied by various amounts of substitution products **5** and rearrangement products **5'**.

While direct substitution on the diazonium group in 1-phosphonoalkenediazonium salts **8** cannot be excluded (Scheme 4a), the complex composition of the post-reaction mixtures suggests that 1-phosphonoalkylium ions **9** may be intermediates in the diazotization reaction of 1-aminoalkylphosphonic acids **1**. This assumption is supported by the fact that all typical products of carbenium ion reactions, especially rearrangement products **5'**, were observed simultaneously in the crude post-reaction mixtures (Scheme 4b). It has to be mentioned that the accepted mechanism of deamination of analogous aliphatic 2-aminoalkanoic acids assumes the presence of α -lactones as reaction intermediates (Scheme 1a). As postulated, their formation is the reason for the high enantioselectivity of these reactions. By analogy, in the reaction of 1-aminoalkylphosphonic acids similar cyclic intermediates, namely 2-hydroxy-2-oxa-1,2-oxaphosphiranes **10**, could also be postulated (Scheme 4c). However, there is no experimental information about intermediate **10** described thus far in the literature. In addition, our results indicate that the formation of **10** is unlikely. For example, the reaction products of 3-amino-3-phosphonopropanoic acid (**1e**) with nitrous acid may be explained by the assumption that 1-phosphonoalkylium ion **9e** is formed (Scheme 5). The 3-hydroxy-3-phosphonopropanoic acid (**5e**) is formed in the reaction of

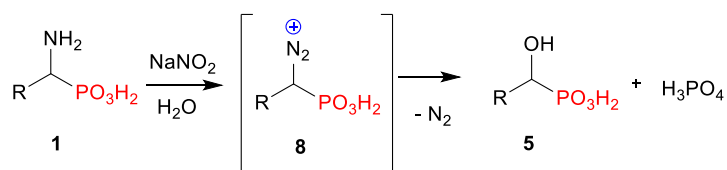
nucleophile (water) addition to 1-phosphonoalkylium ion **9e**, while (*E*)-3-phosphonoacrylic acid (**7e**) is formed as the result of proton elimination from **9e**. Carbenium ion **9e** also undergoes fragmentation and as a result, vinylphosphonic acid (**7a**) and carbon dioxide are formed.

Table 1. Reaction of HNO₂ with 1-aminoalkylphosphonic acids **1** that are stabilized by substituents in 1-position or those that cannot rearrange ^a.



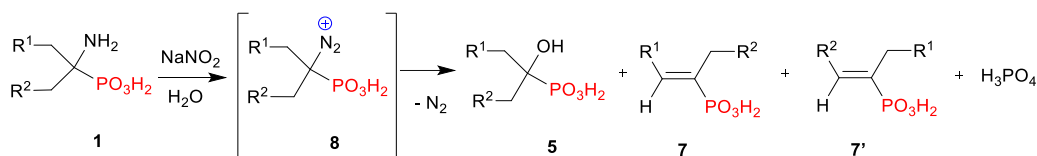
| Entry | Substrate | R1 | R1 | Conversion of 1 to 5 ^b | Conversion of 1 to 7 ^b | Conversion of 1 to H ₃ PO ₄ ^b | |
|-------|-----------|-------------|----|---|---|---|----|
| 1 | | H | Ph | | - | 2% | |
| 2 | | Ph | Me | | | 3% | |
| 3 | | H | Me | | | 2% | |
| 4 | | H | H | | | 10% | |
| 5 | | Me | H | | | 26% | |
| 6 | | <i>i</i> Pr | H | | | 27% | |
| 7 | | COOH | H | | | | 4% |

^a Reaction conditions: 1-aminoalkylphosphonic acid (1.0 mmol), NaNO₂ (2.0 mmol), evolution of N₂ occurs, 21 °C, and NMR analysis of crude reaction mixture; ^b Conversions calculated based on ³¹P NMR (recorded in D₂O) of the crude reaction mixture.

Table 2. Reaction of HNO₂ with 1-aminoalkylphosphonic acids **1** that do not have protons in the β-position ^a.

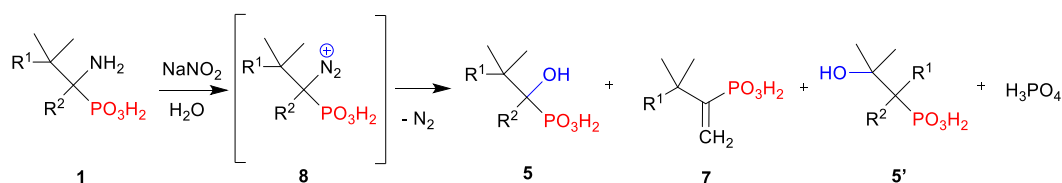
| Entry | Substrate | R | Conversion of 1 to 5 ^b | Conversion of 1 to H ₃ PO ₄ ^b |
|-------|-----------|---------|-----------------------------------|--|
| 1 | | Ph | | 3% |
| 2 | | 4-MeOPh | | 25% |
| 3 | | H | | 9% |

^a Reaction conditions: 1-aminoalkylphosphonic acid (1.0 mmol), NaNO₂ (2.0 mmol), evolution of N₂ occurs, 21 °C, and NMR analysis of crude reaction mixture; ^b Conversions calculated based on ³¹P NMR (recorded in D₂O) of the crude reaction mixture.

Table 3. Reaction of HNO₂ with 1-aminoalkylphosphonic acids **1** having sterically hindered tertiary carbon atom ^a.

| Entry | Substrate | R ¹ | R ² | Conversion of 1 to 5 ^b | Conversion of 1 to 7 ^b | Conversion of 1 to 7' ^b | Conversion of 1 to H ₃ PO ₄ ^b |
|-------|-----------|-------------------------------|----------------|-----------------------------------|-----------------------------------|------------------------------------|--|
| 1 | | C ₃ H ₆ | H | | | | 7% |
| 2 | | <i>i</i> Pr | H | | | | 7% |
| 3 | | Me | H | | | | 8% |

^a Reaction conditions: 1-aminoalkylphosphonic acid (1.0 mmol), NaNO₂ (2.0 mmol), evolution of N₂ occurs, 21 °C, and NMR analysis of crude reaction mixture; ^b Conversions calculated based on ³¹P NMR (recorded in D₂O) of the crude reaction mixture.

Table 4. Reaction of HNO₂ with 1-aminoalkylphosphonic acids **1** that have a migrating group in the β-position^a.

| Entry | Substrate | R ¹ | R ¹ | Conversion of 1 to 5 ^b | Conversion of 1 to 7 ^b | Conversion of 1 to 5' ^b | Conversion of 1 to H ₃ PO ₄ ^b |
|-------|-----------|----------------|----------------|-----------------------------------|-----------------------------------|------------------------------------|--|
| 1 | | Me | H | | - | | 86% |
| 2 | | H | H | | - | | 59% |
| 3 | | H | Me | | | | 40% |

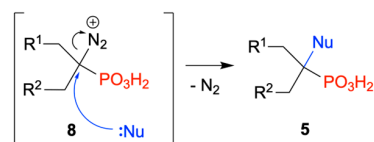
^a Reaction conditions: 1-aminoalkylphosphonic acid (1.0 mmol), NaNO₂ (2.0 mmol), evolution of N₂ occurs, 21 °C, and NMR analysis of crude reaction mixture; ^b Conversions calculated based on ³¹P NMR (recorded in D₂O) of the crude reaction mixture.

An interesting example illustrating the complexity of the deamination reaction of 1-aminoalkylphosphonic acid **1** is the reaction of 1-amino-2-phenylethylphosphonic acid (**1g**) with HNO₂ (Scheme 6). Among the expected products of substitution **5g**, elimination **7g**, and phosphoric acid, in the post-reaction mixture, the rearranged 2-hydroxy-1-phenylethylphosphonic acid (**5''g**) was identified. Considering the formation of carbenium ion **9g** we expected the rearrangement of this carbenium ion to **9'g**, which should be more stable due to the stabilizing effect of the phenyl group. Subsequent addition of nucleophile (H₂O) to both carbenium ions should lead to the corresponding hydroxyalkylphosphonic acids **5g** and **5'g** respectively (Scheme 6). However, analysis of the NMR spectra of the crude reaction mixture revealed that the second product of the reaction is not the **5'g** but **5''g** (see Supplementary Materials for more details).

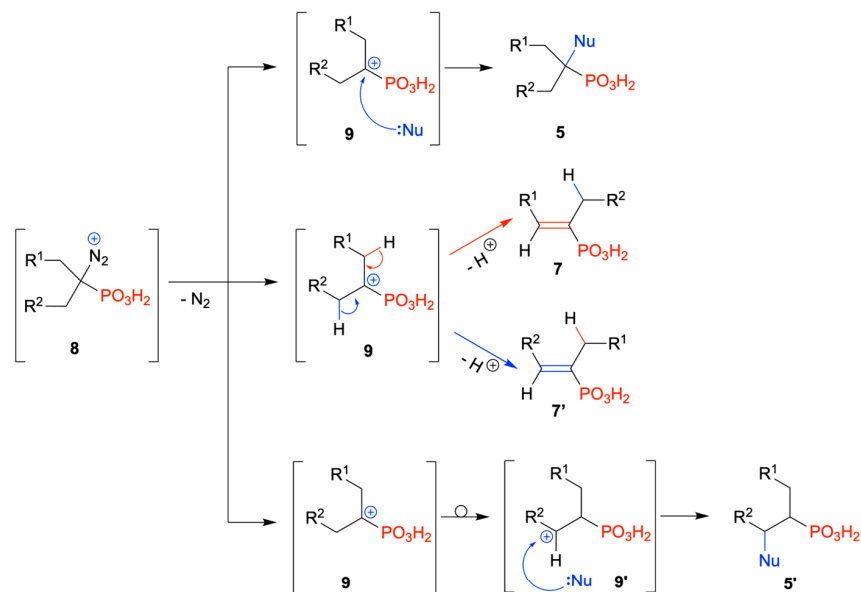
Formation of 2-hydroxy-1-phenylphosphonic acid (**5''g**), as well as unrearranged **5g** and phosphoric acid may be explained by the formation of cyclic intermediate **9''g** (Scheme 6a). The nucleophilic attack of water on the less crowded side (pink arrow on Scheme 6a) of intermediate **9''g** yields rearranged 2-hydroxyalkylphosphonic acid **5''g**, while fragmentation of **9''g** (Scheme 6b) yields styrene and metaphosphoric acid which hydrolyses to phosphoric acid. Finally, when examining the reactivity of 1-aminoalkylphosphonic acids **1** in a deamination reaction with HNO₂, in every reaction we have always observed the presence of various amounts of phosphoric acid (H₃PO₄). We postulate that the formation of H₃PO₄ could be explained by two reaction mechanisms which depend on the structure of the used 1-aminoalkylphosphonic acids **1** (Schemes 7 and 8). According to the first reaction mechanism (Scheme 7a), if the structure of the formed 1-phosphonoalkylium ion **9** enables its rearrangement to the more stable 2-phosphonoalkylium ion **9'** (compounds **1j**, **1b**, **1k**, **1g**), then ion **9'** can further undergo fragmentation with cleavage of the C–P bond resulting in the formation of alkene and metaphosphoric acid (that undergo hydrolysis to phosphoric acid in the presence of water). A similar mechanism was proposed by Mastalerz and Richtarski for the deamination of 2-aminoethylphosphonic acid and

related compounds, where the main reaction products were ethylene and phosphoric acid (Scheme 7b) [64–66].

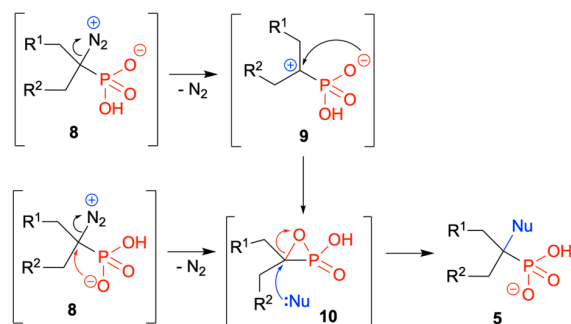
(a) by direct substitution on diazonium salt **8**



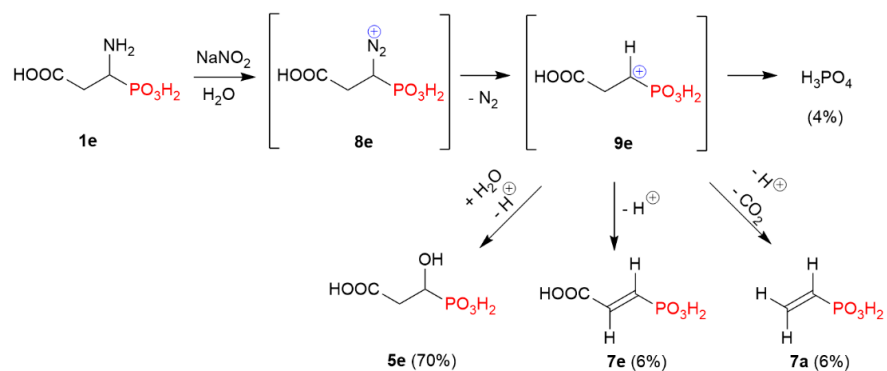
(b) by formation of carbenium ion **9**



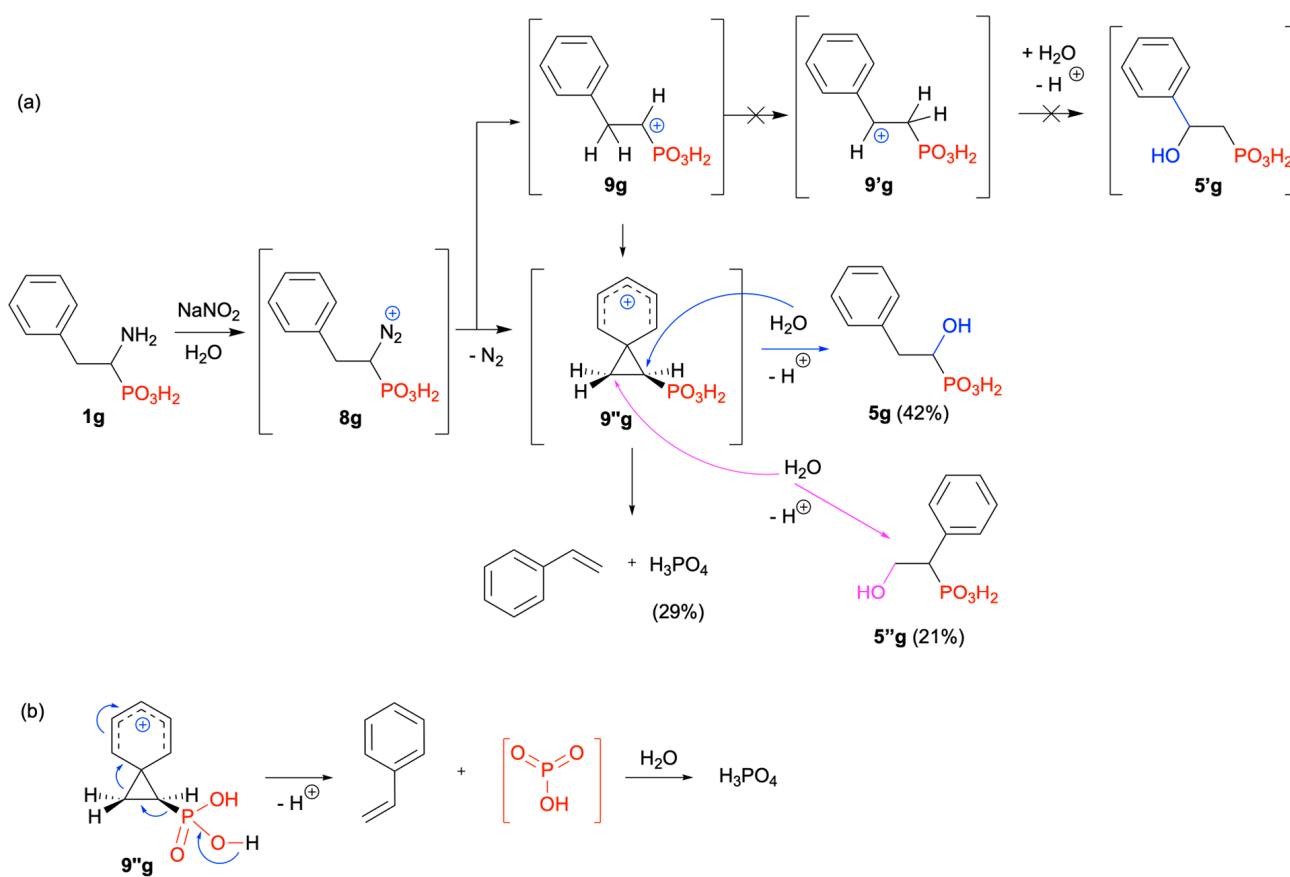
(c) by substitution on cyclic intermediate **10**



Scheme 4. Possible mechanism of the reaction of 1-aminoalkylphosphonic acids **1** with HNO_2 .

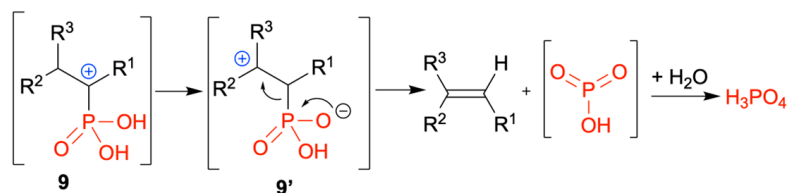


Scheme 5. Deamination reaction of 3-amino-3-phosphonopropanoic acid (**1e**) with HNO_2 .

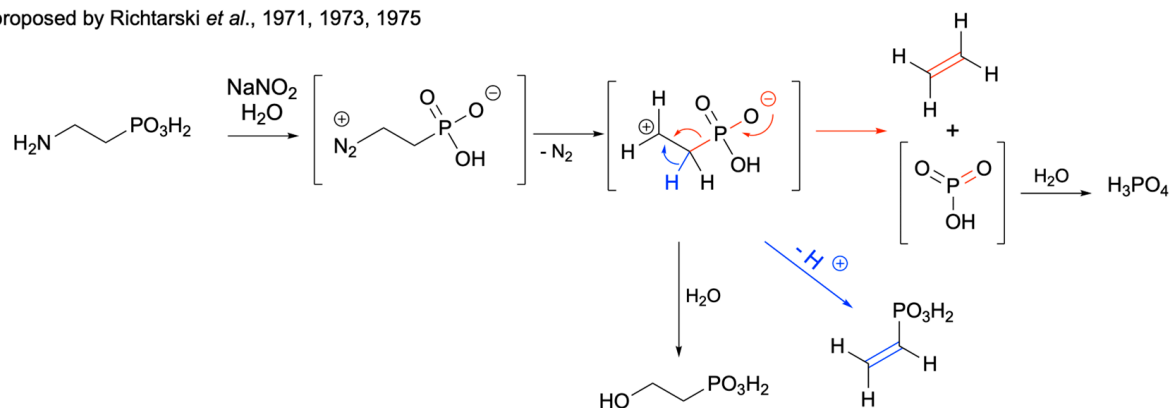


Scheme 6. (a) Deamination of 1-amino-2-phenylethylphosphonic acid (**1g**) with HNO_2 and analysis of the reaction products. (b) Mechanism of phosphoric acid formation from cyclic intermediate **9''g**.

(a) formation of H_3PO_4 - if the structure of the 1-phosphonoalkylium ion **9** enables its rearrangement to the more stable 2-phosphonoalkylium ion **9'** then it can further undergo fragmentation with cleavage of the C–P bond



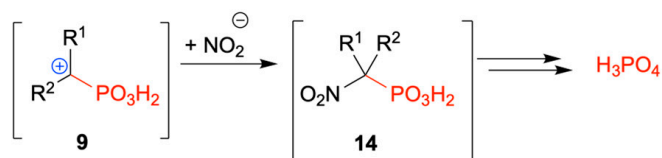
(b) similar mechanism to the one presented in (a) described for the deamination of 2-aminoethylphosphonic acid and proposed by Richtarski *et al.*, 1971, 1973, 1975



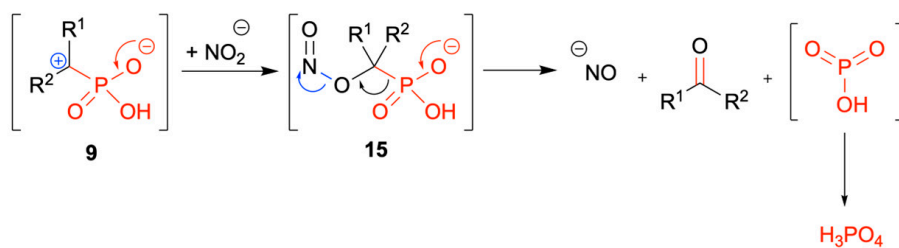
Scheme 7. Mechanism of H_3PO_4 formation in rearrangement and fragmentation reaction [64–66].

The second reaction mechanism should explain the formation of H_3PO_4 in the case where there is no possibility of rearrangement of the formed carbenium ion **9** (Scheme 8), especially for the reaction of substrates **1a**, **1f**, **1n**, and **1h**. By analogy to reactions of 2-aminoalkanoic acids with HNO_2 [67], the reaction of 1-phosphonoalkylium ion **9** with biphilic nitrite ion (NO_2^-) gives 1-nitroalkylphosphonic acid **14** (Scheme 8a) or nitrite ester of 1-hydroxyalkylphosphonic acids **15** (Scheme 8b). Compounds **14** and **15** may undergo secondary reactions which ultimately produce phosphoric acid.

(a) formation of H_3PO_4 via reaction of 1-phosphonoalkylium ion **9** with biphilic nitrite ion (NO_2^-) affording 1-nitroalkylphosphonic acid **14** that may undergo further reactions leading to phosphoric acid



(b) formation of H_3PO_4 via reaction of 1-phosphonoalkylium ion **9** with biphilic nitrite ion (NO_2^-) affording nitrite ester of 1-hydroxyalkylphosphonic acids **15** that may undergo further reactions leading to phosphoric acid



Scheme 8. Proposed mechanisms of H_3PO_4 formation in the reactions of 1-phosphonoalkylium ion with nitrite ion.

3. Materials and Methods

3.1. General Information

The ^1H , $^{13}\text{C}\{^1\text{H}\}$, ^{31}P NMR, and DEPT-135 spectra were collected on a Jeol 400yh instrument (Jeol, Ltd., Tokyo, Japan) (400 MHz for ^1H NMR, 162 MHz for ^{31}P NMR, and 100 MHz for ^{13}C NMR) and were processed with dedicated software (Delta 5.0.5). NMR experiments recorded in D_2O were referenced to the respective residual ^1H signal of the solvent. Multiplicities were reported using the following abbreviations: s (singlet), d (doublet), t (triplet), q (quartet), and m (multiplet). The reported coupling constants (J) values were those observed from the splitting patterns in the spectrum and may not reflect the true coupling constant values. The composition of post-reaction mixtures (as the conversion of substrate to the given product) was calculated based on ^{31}P NMR (recorded in D_2O) of the crude reaction mixture. Structural assignments of **5''g** were made with additional information from gCOSY, gHSQC, and gHMBC experiments.

3.2. Reagents

Aminomethylphosphonic acid (**1h**) was obtained in the reaction of benzamide, formaldehyde, and phosphorous trichloride [68]. 3-Amino-3-phosphonopropanoic acid (**1e**) was synthesized from diethyl acetamidomethylenemalonate [69]. The remaining 1-aminoalkylphosphonic acids **1** were obtained in the reaction of an appropriate carbonyl compound with acetamide, acetyl chloride, and PCl_3 in acetic acid, using Soroka's protocol [70]. 1-Hydroxyalkylphosphonic acids **5**, which were used as reference materials for confirmation of reaction products structures, were synthesized by dealkylation of diethyl 1-hydroxyalkylphosphonates, which were obtained in the reaction of triethyl phosphite with suitable aldehyde or ketone and hydrogen chloride [71].

3.3. Deamination of 1-Aminoalkylphosphonic Acids **1** and 2-Aminoalkanoic Acids **2** in 5M HCl

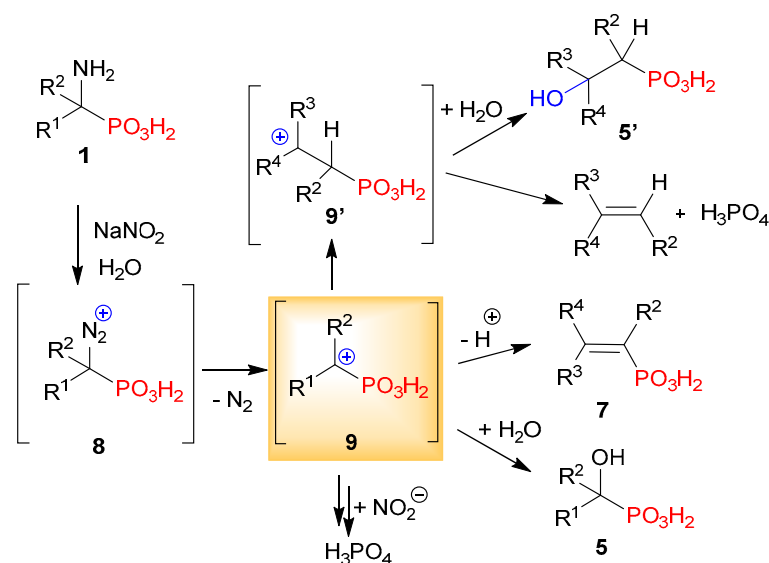
The deamination experiments were conducted in a three-necked flask equipped with a reflux condenser, thermometer, dropping funnel, and magnetic stirrer, as described in the original protocol [40]. The solution of 1-aminoalkylphosphonic acid **1** or 2-aminoalkanoic acid **2** (10 mmol) in 5M HCl (65 mmol, 13 mL) was cooled in an ice/NaCl cooling bath to a temperature of $-12\text{ }^{\circ}\text{C}$. Subsequently, 4 M NaNO₂ solution in water (16 mmol, 4.0 mL) was added dropwise for 2 min. The temperature of the reaction mixture was maintained under $0\text{ }^{\circ}\text{C}$ for 5 h, and then at $25\text{ }^{\circ}\text{C}$ for 12 h. The samples for ¹H and ³¹P NMR spectra were prepared by diluting post-reaction mixtures (0.10 mL) in D₂O (0.40 mL). The samples were re-measured after the addition of reference materials. The composition of the mixture was calculated based on the integration of signals on the ³¹P NMR spectra (for phosphorous substrates) or on the ¹H NMR spectra (for 2-aminoalkanoic acids).

3.4. Deamination of 1-Aminoalkylphosphonic Acids **1** in Water

The deamination reactions of 1-aminoalkylphosphonic acids **1** were conducted in a round-bottom flask equipped with a magnetic stirrer and calibrated gas burette (Figure S11 in Supplementary Materials). The flask was placed in a water bath at a temperature of about $20\text{ }^{\circ}\text{C}$. 1-Aminoalkylphosphonic acid **1** (3.0 mmol) was added to a 0.67 M solution of NaNO₂ (6.0 mmol, 9.0 mL). The solution or suspension was stirred by the means of a magnetic stirrer until the stoichiometric volume of gas was evolved, and additionally for 12 h. The ¹H and ³¹P NMR spectra were recorded after that time and additionally after a few days. The composition of the mixture was calculated based on the integration of signals on the ³¹P NMR spectra.

4. Conclusions

We have studied the deamination of 17 1-aminoalkylphosphonic acids **1** in the reaction with nitrous acid. We have postulated that 1-phosphonoalkylium ions **9** are plausible reactive intermediates in these reactions. Depending on the structure of 1-aminoalkylphosphonic acid **1** used, these ions **9** react with a nucleophile (H₂O or NO₂⁻), undergo elimination of protons, or a rearrangement/fragmentation reaction (Scheme 9). Furthermore, we explained the formation of the phosphoric acid (H₃PO₄), present in every reaction mixture, through two mechanisms (Schemes 6 and 7). We have experimentally demonstrated that the selectivity of the reaction of 1-phosphonoalkylium ions **9** is not easy to control but, in some cases, the addition of nucleophile (H₂O) is the major reaction and the starting 1-aminoalkylphosphonic acids **1** could be transformed into 1-hydroxyphosphonic acids **5** (Scheme 9). In turn, the derivatives of vinylphosphonic acid **7** resulting from proton elimination from 1-phosphonoalkylium ions **9** (Scheme 9) could be major products in the case of 1-aminoalkylphosphonic acids having a positive charge positioned at the tertiary carbon atom and surrounded by bulky substituents, such as compounds **1q**, **1l**, and **1i** (Scheme 9, Table 3). Finally, if the generated 1-phosphonoalkylium ions **9** have migrating groups in the β-position, such as in compounds **9j**, **9b**, **9k**, and **9g**, they can further rearrange to more stable 2-phosphonoalkylium ions **9'** and either react with a nucleophile to form 2-hydroxyalkylphosphonic acid **5'** or undergo fragmentation to alkene and H₃PO₄ (Scheme 9, Table 4). Although the reported procedure of the deamination of 1-aminoalkylphosphonic **1** generally may have limited synthetic application, in specific cases, it may be an irreplaceable synthetic method leading to the desired products.



Scheme 9. Possible transformations of 1-phosphonoalkylium ions **9** discussed in this study.

Supplementary Materials: The following supporting information can be downloaded at: <https://www.mdpi.com/article/10.3390/molecules27248849/s1>, The material includes detailed procedures and NMR spectra for all reactions and compounds [72–88].

Author Contributions: Conceptualization, A.B. and T.K.O.; methodology, A.B.; formal analysis, A.B. and T.K.O.; investigation, A.B.; writing—original draft preparation, A.B. and T.K.O.; writing—review and editing, A.B. and T.K.O.; supervision, T.K.O. All authors have read and agreed to the published version of the manuscript.

Funding: This research received no external funding.

Institutional Review Board Statement: Not applicable.

Informed Consent Statement: Not applicable.

Data Availability Statement: Not applicable.

Conflicts of Interest: The authors declare no conflict of interest.

References

- Zhou, C.; Luo, X.; Chen, N.; Zhang, L.; Gao, J. C–P natural products as next-generation herbicides: Chemistry and biology of glufosinate. *J. Agric. Food Chem.* **2020**, *68*, 3344–3353. [CrossRef] [PubMed]
- Demmer, C.S.; Krogsgaard-Larsen, N.; Bunch, L. Review on modern advances of chemical methods for the introduction of a phosphonic acid group. *Chem. Rev.* **2011**, *111*, 7981–8006. [CrossRef] [PubMed]
- Guo, H.; Fan, Y.C.; Sun, Z.; Wu, Y.; Kwon, O. Phosphine organocatalysis. *Chem. Rev.* **2018**, *118*, 10049–10293. [CrossRef] [PubMed]
- Wehbi, M.; Mehdi, A.; Negrell, C.; David, G.; Alaaeddine, A.; Ameduri, B. Phosphorus-containing fluoropolymers: State of the art and applications. *ACS Appl. Mater. Interfaces* **2020**, *12*, 38–59. [CrossRef] [PubMed]
- Wendels, S.; Chavez, T.; Bonnet, M.; Salmeia, K.A.; Gaan, S. Recent developments in organophosphorus flame retardants containing P–C bond and their applications. *Materials* **2017**, *10*, 784. [CrossRef]
- Cabre, A.; Riera, A.; Verdaguer, X. P-Stereogenic amino-phosphines as chiral ligands: From privileged intermediates to asymmetric catalysis. *Acc. Chem. Res.* **2020**, *53*, 676–689. [CrossRef]
- Abdou, M.M. Synopsis of recent synthetic methods and biological applications of phosphinic acid derivatives. *Tetrahedron* **2020**, *76*, 131251. [CrossRef]
- Rodriguez, J.B.; Gallo-Rodriguez, C. The role of the phosphorus atom in drug design. *ChemMedChem* **2019**, *14*, 190–216. [CrossRef]
- Sevrain, C.M.; Berchel, M.; Couthon, H.; Jaffres, P.-A. Phosphonic acid: Preparation and applications. *Beilstein J. Org. Chem.* **2017**, *13*, 2186–2213. [CrossRef]
- Combs, A.P. Recent advances in the discovery of competitive protein tyrosine phosphatase 1B inhibitors for the treatment of diabetes, obesity, and cancer. *J. Med. Chem.* **2010**, *53*, 2333–2344. [CrossRef]






11. Dang, Q.; Kasibhatla, S.R.; Xiao, W.; Liu, Y.; DaRe, J.; Taplin, F.; Reddy, K.R.; Scarlato, G.R.; Gibson, T.; van Poelje, P.D.; et al. Fructose-1, 6-bisphosphatase inhibitors. 2. Design, synthesis, and structure—Activity relationship of a series of phosphonic acid containing benzimidazoles that function as 5'-adenosinemonophosphate (AMP) mimics. *Med. Chem.* **2010**, *53*, 441–451. [CrossRef] [PubMed]
12. Maryanoff, B.E. Inhibitors of serine proteases as potential therapeutic agents: The road from thrombin to tryptase to cathepsin G. *J. Med. Chem.* **2004**, *47*, 769–787. [CrossRef] [PubMed]
13. Lassaux, P.; Hamel, M.; Gulea, M.; Delbruck, H.; Mercuri, P.S.; Horsfall, L.; Dehareng, D.; Kupper, M.; Frere, J.-M.; Hoffmann, K.; et al. Mercaptophosphonate Compounds as Broad-Spectrum Inhibitors of the Metallo- β -lactamases. *J. Med. Chem.* **2010**, *53*, 4862–4876. [CrossRef] [PubMed]
14. Kumar, T.S.; Zhou, S.-Y.; Joshi, B.V.; Balasubramanian, R.; Yang, T.; Liang, B.T.; Jacobson, K.A. Structure–activity relationship of (N)-methanocarba phosphonate analogues of 5'-AMP as cardioprotective agents acting through a cardiac P2X receptor. *J. Med. Chem.* **2010**, *53*, 2562–2576. [CrossRef]
15. Kang, S.-U.; Shi, Z.-D.; Worthy, K.M.; Bindu, L.K.; Dharmawardana, P.G.; Choyke, S.J.; Bottaro, D.P.; Fisher, R.J.; Burke, T.R., Jr. Examination of Phosphoryl-Mimicking Functionalities within a Macrocyclic Grb2 SH2 Domain-Binding Platform. *J. Med. Chem.* **2005**, *48*, 3945–3948. [CrossRef] [PubMed]
16. Haemers, T.; Wiesner, J.; Van Poecke, S.; Goeman, J.; Henschker, D.; Beck, E.; Jomaa, H.; Van Calenbergh, S. Synthesis of α -substituted fosmidomycin analogues as highly potent *Plasmodium falciparum* growth inhibitors. *Bioorg. Med. Chem. Lett.* **2006**, *16*, 1888–1891. [CrossRef] [PubMed]
17. Robbins, B.L.; Srinivas, R.V.; Kim, C.; Bischofberger, N.; Fridland, A. Anti-human immunodeficiency virus activity and cellular metabolism of a potential prodrug of the acyclic nucleoside phosphonate 9-R-(2-phosphonomethoxypropyl)adenine (PMPA), bis(isopropylloxymethylcarbonyl)PMPA. *Antimicrob. Agents Chemother.* **1998**, *42*, 612–617. [CrossRef]
18. Maestro, A.; del Corte, X.; López-Francés, A.; Martínez de Marigorta, E.; Palacios, F.; Vicario, J. Asymmetric Synthesis of Tetrasubstituted α -Aminophosphonic Acid Derivatives. *Molecules* **2021**, *26*, 3202. [CrossRef]
19. Varga, P.; Keglevich, G. Synthesis of α -Aminophosphonates and Related Derivatives; The Last Decade of the Kabachnik–Fields Reaction. *Molecules* **2021**, *26*, 2511. [CrossRef]
20. Keglevich, G. Microwaves as “Co-Catalysts” or as Substitute for Catalysts in Organophosphorus Chemistry. *Molecules* **2021**, *26*, 1196. [CrossRef]
21. Rádai, Z.; Keglevich, G. Synthesis and Reactions of α -Hydroxyphosphonates. *Molecules* **2018**, *23*, 1493. [CrossRef] [PubMed]
22. Keglevich, G.; Bálint, E. The Kabachnik–Fields Reaction: Mechanism and Synthetic Use. *Molecules* **2012**, *17*, 12821–12835. [CrossRef] [PubMed]
23. Chen, L.; Liu, X.-Y.; Zou, Y.-X. Recent Advances in the Construction of Phosphorus-Substituted Heterocycles, 2009–2019. *Adv. Synth. Catal.* **2020**, *362*, 1724–1818. [CrossRef]
24. Maestro, A.; Martínez de Marigorta, E.; Palacios, F.; Vicario, J. α -Iminophosphonates: Useful Intermediates for Enantioselective Synthesis of α -Aminophosphonates. *Asian J. Org. Chem.* **2020**, *9*, 538–548. [CrossRef]
25. Chen, L. Recent Advances in the Catalytic Asymmetric Construction of Phosphorus-Substituted Quaternary Carbon Stereocenters. *Synthesis* **2018**, *50*, 440–469. [CrossRef]
26. Ordonez, M.; Viveros-Ceballos, J.L.; Cativiela, C.; Sayago, F.J. An update on the stereoselective synthesis of α -aminophosphonic acids and derivatives. *Tetrahedron* **2015**, *71*, 1745–1784. [CrossRef]
27. Brol, A.; Olszewski, T.K. Synthesis and stability of 1-aminoalkylphosphonic acid quaternary ammonium salts. *Org. Biomol. Chem.* **2021**, *19*, 6422–6430. [CrossRef]
28. Acha, A.; Zineb, A.; Hacene, K.; Yasmine, C.; Racha, G.; Rachida, Z.; Nour-Eddine, A. Recent advances in the synthesis of α -aminophosphonates: A review. *Chem. Select* **2021**, *6*, 6137–6149.
29. Kudzin, M.H.; Drabowicz, J.; Jordan, F.; Kudzin, Z.H.; Urbaniak, P. Reactivity of aminophosphonic acids. 2. Stability in solutions of acids and bases. *Phosphorus Sulfur Silicon Relat. Elem.* **2019**, *194*, 326–328. [CrossRef]
30. Kudzin, M.H.; Drabowicz, J.; Jordan, F.; Kudzin, Z.H.; Urbaniak, P. Reactivity of aminophosphonic acids. 3. Reaction with hydrogen peroxide. *Phosphorus Sulfur Silicon Relat. Elem.* **2019**, *194*, 297–299. [CrossRef]
31. Cypryk, M.; Drabowicz, J.; Gostynski, B.; Kudzin, M.H.; Kudzin, Z.H.; Urbaniak, P. 1-(Acylamino)alkylphosphonic acids-alkaline deacylation. *Molecules* **2018**, *23*, 859. [CrossRef] [PubMed]
32. Drabowicz, J.; Jordan, F.; Kudzin, M.H.; Kudzin, Z.H.; Stevens, C.V.; Urbaniak, P. Reactivity of aminophosphonic acids. Oxidative dephosphonylation of 1-aminoalkylphosphonic acids by aqueous halogens. *Dalton Trans.* **2016**, *45*, 2308–2317. [CrossRef] [PubMed]
33. Kudzin, Z.H.; Kudzin, M.H.; Drabowicz, J.; Stevens, C.V. Aminophosphonic acids—phosphorus analogues of natural amino acids. Part 1: Syntheses of α -aminophosphonic acids. *Curr. Org. Chem.* **2011**, *15*, 2015–2071. [CrossRef]
34. Mear, S.J.; Jamison, T.F. Diazotization of S-sulfonyl-cysteines. *J. Org. Chem.* **2019**, *84*, 15001–15007. [CrossRef] [PubMed]
35. Hu, D.X.; O'Brien, M.; Ley, S.V. Continuous multiple liquid-liquid separation: Diazotization of amino acids in flow. *Org. Lett.* **2012**, *14*, 4246–4249. [CrossRef] [PubMed]
36. Stuhr-Hansen, N.; Padrah, S.; Strömgaard, K. Facile synthesis of α -hydroxy carboxylic acids from the corresponding α -amino acids. *Tetrahedron Lett.* **2014**, *55*, 4149–4151. [CrossRef]

37. Deechongkit, S.; You, S.-L.; Kelly, J.W. Synthesis of all nineteen appropriately protected chiral α -hydroxy acid equivalents of the α -amino acids for Boc-Solid-Phase Depsi-peptide Synthesis. *Org. Lett.* **2004**, *6*, 497–500. [CrossRef]
38. Humber, D.C.; Jones, M.F.; Payne, J.J.; Ramsay, M.V.J.; Zacharie, B.; Jin, H.; Siddiqui, A.; Evans, C.A.; Tse, H.L.A.; Mansour, T.S. Expedient preparation of (–)-2'-deoxy-3'-thiacytidine. *Tetrahedron Lett.* **1992**, *33*, 4625–4628. [CrossRef]
39. Biel, M.; Deck, P.; Giannis, A.; Waldmann, H. Synthesis and evaluation of acyl protein thioesterase 1 (APT1) inhibitors. *Chem.-Eur. J.* **2006**, *12*, 4121–4143. [CrossRef]
40. Raza, A.R.; Saddiqa, A.; Çakmak, O. Chiral pool-based synthesis of naphtho-fused isocoumarins. *Chirality* **2015**, *27*, 951–957. [CrossRef]
41. Hu, D.X.; Bielitz, M.; Koos, P.; Ley, S.V.A. Total synthesis of the ammonium ionophore, (–)-enniain B. *Tetrahedron Lett.* **2012**, *53*, 4077–4079. [CrossRef]
42. Lücke, D.; Dalton, T.; Ley, S.V.; Wilson, Z.E. Synthesis of natural and unnatural cyclooligomeric depsipeptides enabled by flow chemistry. *Chem.-Eur. J.* **2016**, *22*, 4206–4217. [CrossRef] [PubMed]
43. Matthes, D.; Richter, L.; Müller, J.; Denisiuk, A.; Feifel, S.C.; Xu, Y.; Espinosa-Artiles, P.; Sussmuth, R.D.; Molnar, I. In vitro chemoenzymatic and in vivo biocatalytic synthesis of new beauvericin analogues. *Chem. Commun.* **2012**, *48*, 5674–5676. [CrossRef]
44. Sokolsky-Papkov, M.; Agashi, K.; Olaye, A.; Shakesheff, K.; Domb, A.J. Polymer carriers for drug delivery in tissue engineering. *Adv. Drug Deliv. Rev.* **2007**, *59*, 187–206. [CrossRef] [PubMed]
45. Rasal, R.M.; Janorkar, A.V.; Hirt, D.E. Poly(lactic acid) modifications. *Prog. Polym. Sci.* **2010**, *35*, 338–356. [CrossRef]
46. Lu, Y.; Yin, L.; Zhang, Y.; Zhang, Z.; Xu, Y.; Tong, R.; Cheng, J. Synthesis of water-soluble poly(α -hydroxy acids) from living ring opening polymerization of O-benzyl-L-serine carboxyanhydrides. *ACS Macro Lett.* **2012**, *1*, 441–444. [CrossRef]
47. Cupido, T.; Spengler, J.; Burger, K.; Albericio, F. NO as temporary guanidino-protecting group provides efficient access to Pbf-protected argininic acid. *Tetrahedron Lett.* **2005**, *46*, 6733–6735. [CrossRef]
48. Shin, I.; Lee, M.-T.; Lee, J.; Jung, M.; Lee, W.; Yoon, J. Synthesis of optically active phthaloyl D-aminooxy acids from L-amino acids or L-hydroxy acids as building blocks for the preparation of aminoxy peptides. *J. Org. Chem.* **2000**, *65*, 7667–7675. [CrossRef]
49. Kabachnik, M.I.; Medved, T.Y. Organophosphorus compounds. XIV. Synthesis of aminophosphonic acids. *Izv. Akad. Nauk. SSSR Seriya Khimicheskaya* **1950**, 635–640.
50. Medved, T.Y.; Kabachnik, M.I. New method of synthesis of aminophosphonic acids. II. Reaction of ketones with dialkyl phosphites and ammonia. *Izv. Akad. Nauk. SSSR* **1954**, 314–322.
51. Blum, H.; Worms, K.H. (1-Hydroxyalkylidene)diphosphonic Acids. Patent DE 2165833, 4 September 1980.
52. Blum, H.; Worms, K.H. Arylchloromethanediphosphonic Acids. Patent DE 2601644, 5 January 1984.
53. Worms, K.H.; Blum, H. Reactions of 1-aminoalkane-1,1-diphosphonic acids with nitrous acid. *Z. Fuer Anorg. Und Allg. Chem.* **1979**, *457*, 209–213. [CrossRef]
54. Pasto, D.J. A theoretical analysis of the interaction of the phosphonate and sulfonyl groups with a carbocationic center. *J. Org. Chem.* **1985**, *50*, 1014–1018. [CrossRef]
55. Creary, X. Electronegatively substituted carbocations. *Chem. Rev.* **1991**, *91*, 1625–1678. [CrossRef]
56. Creary, X. Carbocationic and related processes in reactions of α -keto mesylates and triflates. *Acc. Chem. Res.* **1985**, *18*, 3–8. [CrossRef]
57. Creary, X.; Geiger, C.C.; Hilton, K. Mesylate derivatives of α -hydroxy phosphonates. Formation of carbocations adjacent to the diethyl phosphonate group. *J. Am. Chem. Soc.* **1983**, *105*, 2851–2858. [CrossRef]
58. Creary, X.; Underiner, T.L. Underiner Stabilization demands of diethyl phosphonate substituted carbocations as revealed by substituent effects. *J. Org. Chem.* **1985**, *50*, 2165–2170. [CrossRef]
59. Koppenhoefer, B.; Schuring, V. (S)-2-Chloroalkanoic acids of high enantiomeric purity from (S)-2-amino acids: (S)-2-Chloropropanoic acid. *Org. Synth.* **1988**, *66*, 151. [CrossRef]
60. del Pilar Garcia-Santos, M.; Gonzalez-Mancebo, S.; Hernandez-Benito, J.; Calle, E.; Casado, J. Reactivity of amino acids in nitrosation reactions and its relation to the alkylating potential of their products. *J. Am. Chem. Soc.* **2002**, *124*, 2177–2182. [CrossRef]
61. Weston, T.; Taylor, J. The action of nitrous acid on amino-compounds. Part II. Aliphatic amino-acids. *J. Chem. Soc.* **1928**, 1897–1906. [CrossRef]
62. Erlenmeyer, E.; Lipp, A. Synthesis of tyrosine. *Justus Liebigs Ann. Chem.* **1883**, *219*, 161–178. [CrossRef]
63. Kowalik, J.; Zygmunt, J.; Mastalerz, P. Determination of absolute configuration of optically active 1-aminoalkane phosphonic acids by chemical correlations. *Phosphorus Sulfur Relat. Elem.* **1983**, *18*, 393–396. [CrossRef]
64. Mastalerz, P.; Richtarski, G. Ethylene formation by fragmentation of 2-aminoethylphosphonic and 2-aminoethylphenylphosphonic acid. *Rocz. Chem.* **1971**, *45*, 763–768.
65. Richtarski, G.; Mastalerz, P. Deamination and rearrangement of (1-phenyl-1-hydroxy-2-aminoethyl)phosphonic acid. *Tetrahedron Lett.* **1973**, *5*, 4069–4070. [CrossRef]
66. Richtarski, G.; Soroka, M.; Mastalerz, P.; Starzemska, H. Deamination and rearrangement of 1-hydroxy-1-phenyl-2-aminoethylphosphonic acid. *Rocz. Chem.* **1975**, *49*, 2001–2005. [CrossRef]
67. Austin, A.T. Deamination of amino acids by nitrous acid with particular reference to glycine. The chemistry underlying the Van Slyke determination of α -amino acids. *J. Chem. Soc.* **1950**, 149–157. [CrossRef]
68. Soroka, M. Comments on the synthesis of aminomethylphosphonic acid. *Synthesis* **1989**, *7*, 547–548. [CrossRef]

69. Soroka, M.; Mastalerz, P. The synthesis of phosphonic and phosphinic analogs of aspartic acid and asparagine. *Rocz. Chem.* **1976**, *50*, 661–666.
70. Soroka, M. The synthesis of 1-aminoalkylphosphonic acids. A revised mechanism of the reaction of phosphorus trichloride, amides and aldehydes or ketones in acetic acid (Oleksyszyn reaction). *Liebigs Ann. Chem.* **1990**, *1990*, 331–334. [CrossRef]
71. Goldman, W.; Soroka, M. The preparation of dialkyl 1-hydroxyalkylphosphonates in the reaction of trialkyl phosphites with oxonium salts derived from aldehydes or ketones. *Synthesis* **2006**, *2006*, 3019–3024. [CrossRef]
72. Baltser, A.E.; Zaitsev, D.A.; Ivanova, T.V.; Babenko, T.G.; Barskova, E.N. Addition of morpholine and pyrrolidine to isopropenylphosphonic acid in situ. *Russ. J. Org. Chem.* **2013**, *49*, 627–628. [CrossRef]
73. Blazis, V.J.; Koeller, K.J.; Spilling, C.D. Reactions of Chiral Phosphorous Acid Diamides: The Asymmetric Synthesis of Chiral α -Hydroxy Phosphonamides, Phosphonates, and Phosphonic Acids. *J. Org. Chem.* **1995**, *60*, 931–940. [CrossRef]
74. Zhou, S.; Pan, J.; Davis, K.M.; Schaperdorth, I.; Wang, B.; Boal, A.K.; Krebs, C.; Bollinger, J.M. Steric enforcement of cis-epoxide formation in the radical C–O-coupling reaction by which (S)-2-hydroxypropyl-phosphonate epoxidase (HppE) produces Fosfomycin. *J. Am. Chem. Soc.* **2019**, *141*, 20397–20406. [CrossRef] [PubMed]
75. Hudson, H.R.; Ismail, F.; Pianka, M.; Wan, C.-W. The formation of α -amino- and α -hydroxyalkanephosphonic acids in the reactions of phosphite esters with aldehydes and alkyl carbamates. *Phosphorus Sulfur Silicon Relat. Elem.* **2000**, *164*, 245–257. [CrossRef]
76. Oehler, E.; Kanzler, S. Synthesis of phosphonic acids related to the antibiotic fosmidomycin from allylic α - and γ -hydroxyphosphonates. *Phosphorus Sulfur Silicon Relat. Elem.* **1996**, *112*, 71–90. [CrossRef]
77. Quast, H.; Heuschmann, M. Three-membered heterocycles. 12. Synthesis of a phosphirane oxide. *Liebigs Ann. Der Chem.* **1981**, *5*, 977–992. [CrossRef]
78. Kenyon, G.L.; Westheimer, F.H. Stereochemistry of unsaturated phosphonic acids. *J. Am. Chem. Soc.* **1966**, *88*, 3557–3561. [CrossRef]
79. Prishchenko, A.A.; Livantsov, M.V.; Novikova, O.P.; Livantsova, L.I.; Petrosyan, V.S. Synthesis of new functionalized aryl-substituted methylphosphonic and methylenediphosphonic acids and their derivatives. *Heteroat. Chem.* **2016**, *27*, 381–388. [CrossRef]
80. Rueppel, M.L.; Marvel, J.T. Proton and phosphorus-31P NMR spectra of substituted methylphosphonic acids with indirect determination of phosphorus-31P shifts. *Org. Magn. Reson.* **1976**, *8*, 19–20. [CrossRef]
81. Yan, F.; Moon, S.-J.; Liu, P.; Zhao, Z.; Lipscomb, J.D.; Liu, A.; Liu, H.-W. Determination of the Substrate Binding Mode to the Active Site Iron of (S)-2-Hydroxypropylphosphonic Acid Epoxidase Using 17O-Enriched Substrates and Substrate Analogues. *Biochemistry* **2007**, *46*, 12628–12638. [CrossRef]
82. Chen, R.; Breuer, E. Direct Approach to α -Hydroxyphosphonic and α,ω -Dihydroxyalkane- α,ω -bisphosphonic Acids by the Reduction of (Bis)acylphosphonic Acids. *J. Org. Chem.* **1998**, *63*, 5107–5109. [CrossRef]
83. Saha, U.; Helvig, C.F.; Petkovich, P.M. Phosphate Management with Small Molecules. U.S. Patent US 9198923; (Granted 2015-12.01).
84. De Macedo Puyau, P.; Perie, J.J. Synthesis Of Substrate Analogues And Inhibitors For The Phosphoglycerate Mutase Enzyme. *Phosphorus Sulfur Silicon Relat. Elem.* **1997**, *129*, 13–45. [CrossRef]
85. Sainz-Diaz, C.I.; Galvez-Ruano, E.; Hernandez-Laguna, A.; Bellanato, J. Synthesis, Molecular Structure, and Spectroscopical Properties of Alkenylphosphonic Derivatives. 1. Vinyl-, Propenyl-, (Bromoalkenyl)-, and (Cyanoalkenyl)phosphonic Compounds. *J. Org. Chem.* **1995**, *60*, 74–83. [CrossRef]
86. Fitch, S.J.; Moedritzer, K. Nuclear magnetic resonance study of the P-C(OH)-P to P-CO-P rearrangement: Tetraethyl-1-hydroxyalkylidenediphosphonates. *J. Am. Chem. Soc.* **1962**, *84*, 1876–1879. [CrossRef]
87. Chang, W.-C.; Mansoorabadi, S.O.; Liu, H.-W. Reaction of HppE with Substrate Analogues: Evidence for Carbon-Phosphorus Bond Cleavage by a Carbocation Rearrangement. *J. Am. Chem. Soc.* **2013**, *135*, 8153–8156. [CrossRef]
88. Liu, P.; Murakami, K.; Seki, T.; He, X.; Yeung, S.M.; Kuzuyama, T.; Seto, H.; Liu, H.W. Protein Purification and Function Assignment of the Epoxidase Catalyzing the Formation of Fosfomycin. *J. Am. Chem. Soc.* **2001**, *123*, 4619–4620. [CrossRef] [PubMed]

Article

Synthesis of Tetrasubstituted Phosphorus Analogs of Aspartic Acid as Antiproliferative Agents

Xabier del Corte [†], Aitor Maestro [†], Adrián López-Francés , Francisco Palacios  and Javier Vicario ^{*}

Departamento de Química Orgánica I, Centro de Investigación y Estudios Avanzados "Lucio Lascaray", Facultad de Farmacia, University of the Basque Country, UPV/EHU Paseo de la Universidad 7, 01006 Vitoria-Gasteiz, Spain

* Correspondence: javier.vicario@ehu.eus; Tel.: +34-945013891

† These authors contributed equally to this work.

Abstract: An efficient general method for the synthesis of a wide family of α -aminophosphonate analogs of aspartic acid bearing tetrasubstituted carbons is reported through an aza-Reformatsky reaction of α -iminophosphonates, generated from α -aminophosphonates, in an umpolung process. In addition, the α -aminophosphonate substrates showed in vitro cytotoxicity, inhibiting the growth of carcinoma human tumor cell lines A549 (carcinomic human alveolar basal epithelial cell) and SKOV3 (human ovarian carcinoma). In view of the possibilities in the diversity of the substituents that offer the synthetic methodology, an extensive profile structure–activity is presented, measuring IC₅₀ values up to 0.34 μ M in the A549 and 9.8 μ M in SKOV3 cell lines.

Keywords: Reformatsky reaction; tetrasubstituted α -aminophosphonates; aspartic acid; antiproliferative effect

Citation: del Corte, X.; Maestro, A.; López-Francés, A.; Palacios, F.; Vicario, J. Synthesis of Tetrasubstituted Phosphorus Analogs of Aspartic Acid as Antiproliferative Agents. *Molecules* **2022**, *27*, 8024. <https://doi.org/10.3390/molecules27228024>

Academic Editor: Jakub Adamek

Received: 16 September 2022

Accepted: 15 November 2022

Published: 18 November 2022

Publisher's Note: MDPI stays neutral with regard to jurisdictional claims in published maps and institutional affiliations.



Copyright: © 2022 by the authors. Licensee MDPI, Basel, Switzerland. This article is an open access article distributed under the terms and conditions of the Creative Commons Attribution (CC BY) license (<https://creativecommons.org/licenses/by/4.0/>).

1. Introduction

The increase in life expectancy is one of the greatest achievements of humankind, which is also linked to far-reaching consequences with implications for nearly all socio-economic sectors [1]. According to a study published in *The Lancet* in 2018 [2], by 2040, it is expected that 59 countries will have an average life expectancy of more than 80 years. In particular, the average life expectancy in Spain is predicted to be the highest in the world and will reach 85.8 years. In the past, the main roots of mortality were associated to infectious and parasitic diseases but, due to the phenomenon of population ageing, chronic and degenerative diseases have become the main concern of all healthcare systems worldwide. Accordingly, cancers figure among the leading causes of morbidity and mortality worldwide and have become one of the world's largest health problems [3].

The systemic treatment of cancer implies a combination of surgery, chemotherapy and radiation. Other options include immunotherapy, targeted therapy, laser or hormonal therapy [4]. Chemotherapeutic agents possess the ability to travel throughout the body, and selectively destroy fast-growing malignant cells [5]. Here, in the first front of battle, drug discovery plays a crucial role in this area through the synthesis and characterization of drug candidates and the evaluation of their anticancer properties, prior to the subsequent clinical trials. Despite the strong efforts made in the last decades for the development of efficient chemotherapeutic agents, the continuous search for newer, safer and more potent cytotoxic drugs is an essential task in science, especially due to the known ability of cancer cells to develop resistance to the known therapies [6,7].

Among the innumerable amount of potentially chemotherapeutic molecules, we focused, in this case, on organophosphorus compounds. In particular, phosphonic acids and their esters are a family of compounds, characterized by the presence of a stable C-P bond in their structure, that show interesting and useful biological properties [8], including anticancer activity, such as the case of cyclophosphamide [9] or zoledronate [10,11].

Specifically, α -aminophosphonic acids are bioisosters of α -amino acids, where the flat carboxylic acid group has been replaced by a tetrahedral phosphonic acid group that shows the fully oxidized phosphorus atom at the core [12]. Due to this isosteric substitution, α -aminophosphonic acid scaffold is able to mimic the tetrahedral geometry and negative charge development found in the transition state of peptide cleavage, thus inhibiting enzymes implied in proteolysis processes (Figure 1) [13–15]. Considering this, it is easy to anticipate that a number of α -aminophosphonic acid derivatives show interesting biological activities, such as herbicidal [16,17], antimicrobial [18–21] or antioxidant [22,23], and some of them have been reported as potential drugs, in particular, for the treatment of infectious diseases [24,25]. Remarkably, some α -aminophosphonate derivatives have been described as anticancer [26–29] agents.

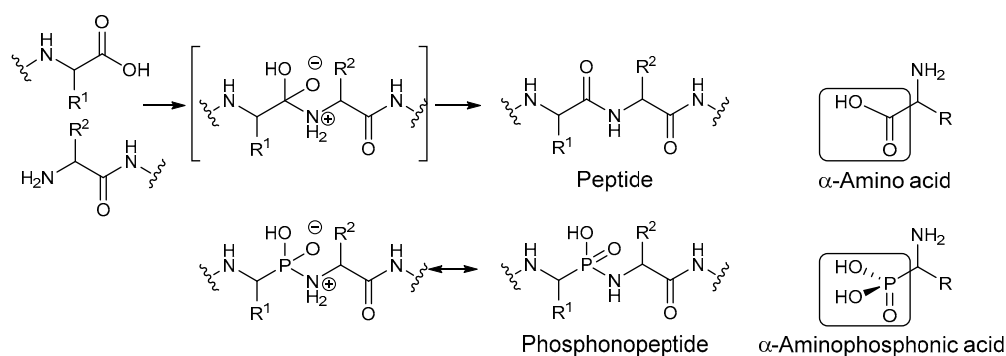
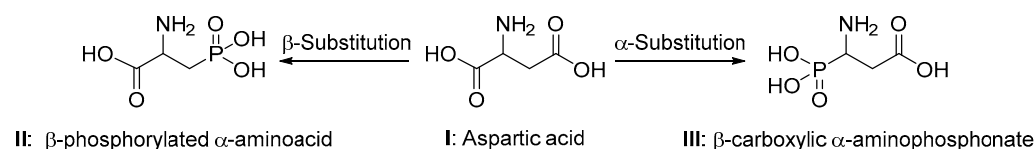


Figure 1. α -Aminophosphonic acid group mimics the transition state of peptide cleavage.

Aspartic acid is one of the 20 building block α -amino acids of proteins that is known to have pharmacological activity at some glutamate receptors [30]. The most interesting feature of the structure of aspartic acid is the presence of a second acidic side chain that may interact with other amino acids, enzymes or proteins in the body. In the context of this research, following the biosisosterism approach, two possible phosphorylated analogs may be designed from aspartic acid scaffold I: β -phosphorylated α -aminoacids II or β -carboxylic α -aminophosphonates III (Scheme 1).



Scheme 1. Two possible isosteric substitutions of the carboxylic moiety by a phosphonic acid group in aspartic acid scaffold.

While the synthesis of phosphonate analogs of aspartic acid by the isosteric substitution of the β -carboxylic group is well documented [31–33], the preparation of the parent α -aminophosphonate analogs III by the substitution of the α -carboxylic moiety has received less attention, and most of the substrates are reported as single examples of general methods leading to α -aminophosphonates or aspartic acid derivatives [32,34,35]. In particular, there are a few examples reported for the synthesis of tetrasubstituted α -aminophosphonates derived from aspartic acid as concrete examples of the scope of reactions that imply C-C or C-P bond formation [36–39]. It is well known that the development of reactions leading to the formation of tetrasubstituted carbons is a challenging task, due to the lack of reactivity of the substrates, derived from the generation of a highly crowded structure.

In this context, the aza-Reformatsky reaction is a widely used method for the synthesis of β -amino acids [40–43], as well as for the synthesis of biologically active molecules [44–46]. During the last years, the use of dialkylzinc reagents has emerged as an alternative to Zn dust [47–50]. In this regard, very recently, we have reported an enantioselective aza-

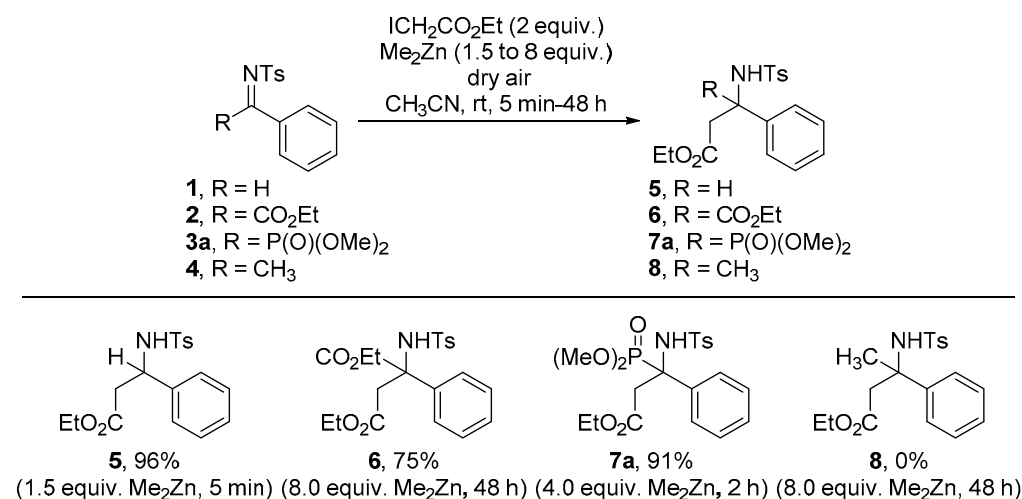
Reformatsky reaction of α -phosphorylated ketimines that leads to the formation of tetra-substituted α -aminophosphonate derivatives [51]. In view of the interesting properties of aspartic acid derivatives and the potential of the isosteric substitution of a carboxylate by a phosphonate group, the corresponding phosphorus analogs of aspartic acid may be very interesting substrates from a biological point of view. According to this, as part of our ongoing research into the identification of new chemotherapeutic agents [52–54], with a special focus on organophosphorus derivatives [55–57], we thought that the preparation of a wide family of phosphorylated analogs of aspartic acid and the study of their anticancer properties would be an interesting contribution to the field of organic and medicinal chemistry. For all the reasons mentioned above, herein, we report a general method for the synthesis of tetrasubstituted phosphorylated analogs of aspartic acid through an aza-Reformatsky reaction of α -ketiminophosphonates and the evaluation of their in vitro cytotoxic activity against several cancer cell lines.

2. Results and Discussion

2.1. Chemistry

During the last years, we have been involved in the synthesis of α -aminophosphonate derivatives through the addition of carbon nucleophiles to imines. The most remarkable feature of our approach is that α -iminophosphonate electrophiles are generated by the oxidation of the parent α -aminophosphonates. Thus, the global reaction can be considered as an umpolung process, where the nucleophilic character of α -aminophosphonate species has been inverted. In particular, following this approach, we have reported the enantioselective synthesis of indolyl phosphoglycines [58] by the addition of indole derivatives to α -phosphorylated aldimines and the nucleophilic addition of cyanide [59], organometallics [60] or nitromethane species [61] to α -phosphorylated ketimines, for the preparation of diverse tetrasubstituted α -aminophosphonate derivatives. More recently, we have extended this strategy to the enantioselective Reformatsky reaction, using α -ketiminophosphonates as the electrophile source [51].

Following this last approach, we tested the aza-Reformatsky reaction of different imines **1–4** with ethyl iodoacetate, under dry air atmosphere, in the presence of dimethylzinc, affording the corresponding β -aminoesters **4–6** very good yields when aldimines or activated ketimines were used (Scheme 2).



Scheme 2. Aza-Reformatsky reaction of imines **1–4**.

Initially, the simple *N*-tosylimine **1** derived from benzaldehyde (R = H) was proved to be an excellent substrate for the reaction, affording β -phenylalanine derivative **5** a very good yield (Scheme 2). Next, we were intrigued whether the reaction could also be applicable to α -iminoesters and, for this reason, we tried the same reaction conditions using *N*-tosyl-protected α -iminoester **2** (R = CO₂Et) as a substrate. In this case, the reaction

also proceeded efficiently to afford quaternary aspartic acid derivative **6** (Scheme 2). In a similar way, using benzaldehyde-derived α -iminophosphonate **3a** ($R = P(O)(OMe)_2$), the tetrasubstituted aspartic acid derivative **7a** was obtained in an excellent yield (Scheme 2). However, the reaction conditions, including the required dimethylzinc and the reaction time, presented high variations depending on the structure of the imine. On the other hand, we also tested a non-activated ketimine **4**, derived from acetophenone. Unfortunately, in this case, the Reformatsky product **8** was not observed, and the starting materials were recovered unaltered.

The substrates obtained from the aza-Reformatsky reaction were fully characterized on the basis of their 1H , ^{31}P , and ^{13}C NMR, IR spectra and HRMS (see Supplementary Materials). The most characteristic pattern for these compounds in the 1H NMR spectrum is the signals corresponding to the two protons of the methylene group next to the tetrasubstituted carbon at $\delta \sim 3.5$ ppm, which, because of the presence of a chiral center in the structure, have a diastereotopic character and appear as two independent signals. In the particular case of phosphorylated aspartic acid derivative **7a**, those signals appear as two double doublets at $\delta = 3.59$ and 3.46 ppm, showing a reciprocal geminal coupling of $^2J_{HH} = 16.4$ Hz and additional vicinal couplings with the phosphorus atom of $^3J_{PH} = 22.7$ and 10.7 Hz, respectively. Accordingly, the dimethyl phosphonate moiety in **7a** is seen as two representative intense doublets at $\delta_H = 3.46$ ppm ($^3J_{PH} = 10.7$ Hz) and $\delta_H = 3.48$ ppm ($^3J_{PH} = 10.5$ Hz), typical for the diastereotopic methoxy groups at the phosphonate moiety. Remarkably, the signal corresponding to the NH group of **6a** appears as a thin doublet at $\delta_H = 6.17$ ppm, that slowly interchanges with D_2O , showing a strong coupling with the phosphorus atom of $^3J_{PH} = 11.2$ Hz, which may be attributable to a weak acidic character of the sulfonamide moiety.

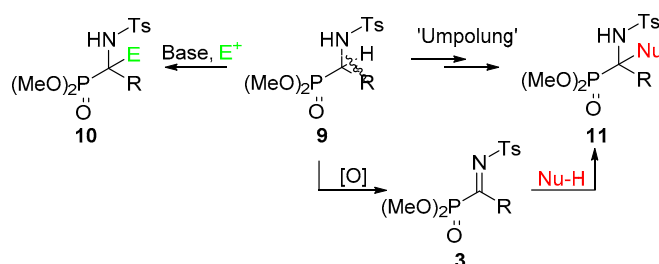
Likewise, in the ^{13}C NMR spectrum of phosphorylated derivative **7a**, undoubtedly, the most characteristic signal is the doublet corresponding to the chiral quaternary carbon (DEPT) at $\delta_C = 62.1$ ppm, which shows a very strong *ipso* coupling with the phosphorus atom of $^1J_{PC} = 153.8$ Hz. The methylene group next to the chiral carbon appears as a doublet at $\delta_C = 54.0$ ppm with a geminal coupling with the phosphorus atom of $^2J_{CP} = 7.0$ Hz, weaker than expected, possibly due to an unfavorable angle in terms of the coupling, which can be related to a distortion at the topology at the sp^3 chiral carbon, attributed to the high steric hindrance present at the quaternary center. The presence of the ester group is evident from the chemical shift at $\delta_C = 170.2$ ppm, typical for carboxylic groups, which appears as a doublet, coupled with the phosphorus atom with a vicinal coupling constant of $^3J_{PC} = 8.0$ Hz. The fact that the vicinal C-P coupling is stronger than the geminal supports the proposed distortion of the bonding angles at the quaternary carbon, as expected from the high steric crowding.

In congruity with the proposed structure, the Heteronuclear Multiple Bond Correlation Spectroscopy (HMBC) spectrum of **7a** presents clear correlations of both diastereotopic methylene protons with the carbonyl group, the chiral tetrasubstituted carbon and the quaternary aromatic carbon of the phenyl substituent.

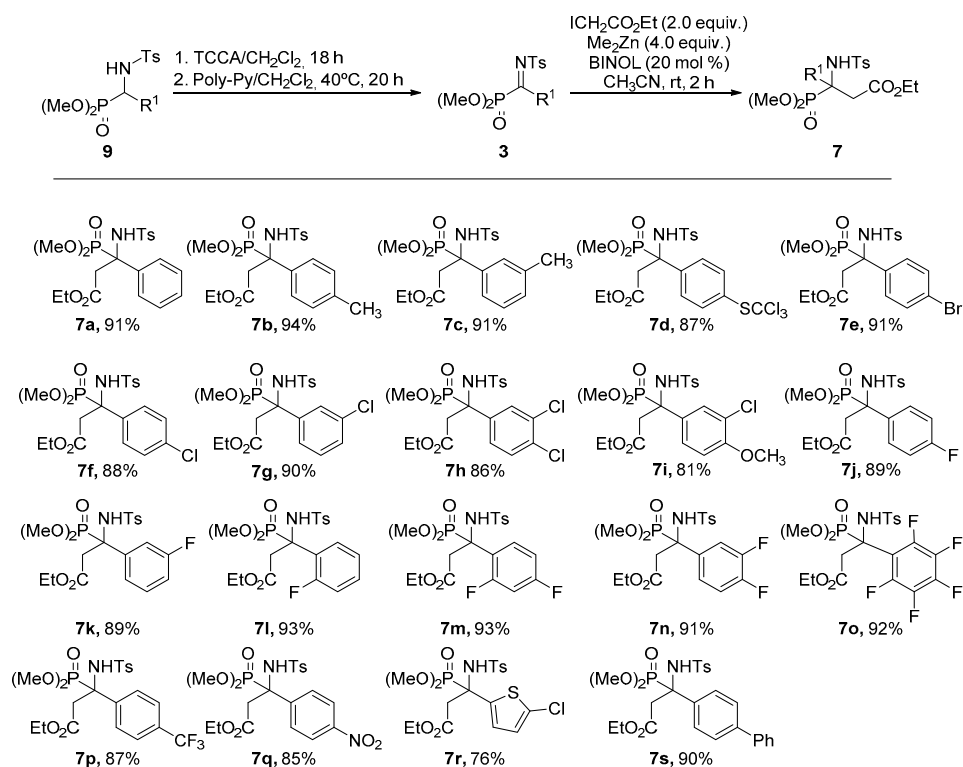
Next, in view of the efficient protocol achieved for the aza-Reformatsky reaction, we focused our efforts on the extension of the reaction to the use of several α -ketiminophosphonate substrates **3**. In this regard, we considered the synthesis of α -iminophosphonate substrates **3** from a formal oxidation of tertiary aminophosphonates **9**. Then, the subsequent addition of a nucleophile species would afford tetrasubstituted aminophosphonates **11**. Therefore, this synthetic approach can be considered globally as a route for the generation of tetrasubstituted α -aminophosphonates by the substitution of hydrogen in a trisubstituted α -aminophosphonate by a nucleophilic reagent and the complementary process ('umpolung reaction') to the typical electrophilic substitution of trisubstituted α -amino-phosphonates **9** leading to functionalized α -aminophosphonates **10** (Scheme 3).

Following this approach, α -ketiminophosphonates **3** were first generated by a formal oxidation of α -aminophosphonates **9**, following the procedure developed by our research group. Then, using dimethylphosphonate-substituted imines and ethyl iodoacetate, 19 tetra-

substituted aspartic acid analogs **7**, bearing different alpha-aromatic substituents, were efficiently synthesized (Scheme 4).



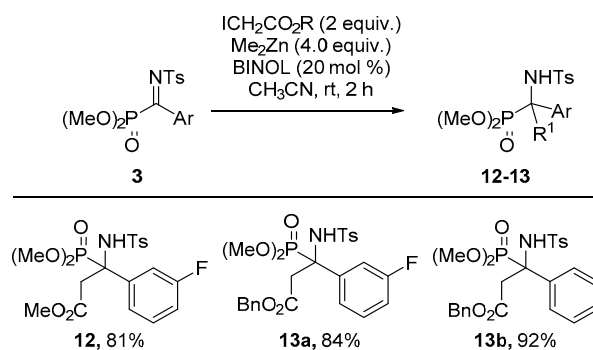
Scheme 3. General strategies for the synthesis of quaternary α -aminophosphonates.



Scheme 4. Phosphorus analogs of aspartic acid **7**, synthesized through an aza-Reformatsky reaction.

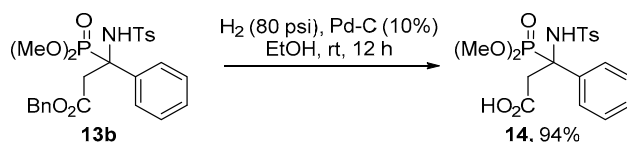
In addition to the model reaction, using an imine with a simple phenyl substituent (Scheme 4, **7a**), the reaction tolerates the presence of *para* and *meta* alkyl substituents at the aromatic ring (Scheme 4, **7b–c**), as well as strong electron donating groups at the *para* position of the aromatic imine (Scheme 4, **7d**). Several halogen-substituted aromatic ketimines were also successfully used in the reaction, including aromatic rings containing bromine (Scheme 4, **7e**), chlorine (Scheme 4, **7f–i**) or fluorine (Scheme 4, **7j–n**) atoms at diverse positions and including a perfluorophenyl substituent (Scheme 4, **7o**). Furthermore, an excellent result was observed using aromatic imines substituted with electron-withdrawing groups such as *p*-trifluoromethyl or *p*-nitro substituents (Scheme 4, **7p–q**). The reaction can even be extended to the use of ketimines holding heteroaromatic or biphenyl substituents (Scheme 4, **7r–s**).

Next, the synthetic procedure was extended to the use of other different alkyl iodoacetates. The reaction using methyl iodoacetate and a *p*-fluorophenyl substituted α -ketiminophosphonate affords the corresponding tetrasubstituted α -aminophosphonate **12** an excellent yield (Scheme 5). Under the same conditions, the reaction using benzyl iodoacetate efficiently yields the benzyl-protected analogs of aspartic acid **13a–b** (Scheme 5).



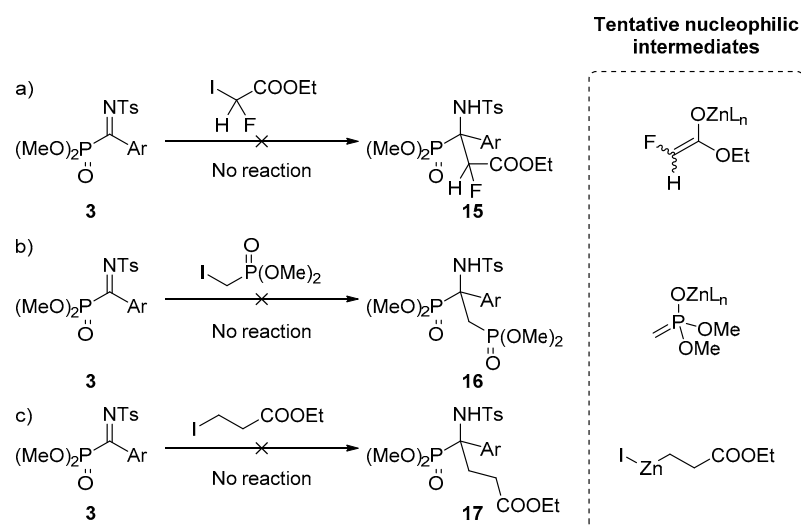
Scheme 5. Extension of the aza-Reformatsky reaction to other alkyl haloacetate derivatives.

In order to obtain the carboxylic acid and/or phosphonic acid derivatives of the aspartate analogs, the hydrolysis of the obtained substrates was attempted. However, under acidic or basic treatment, compounds **7a**, **12** or **13b** led to the formation of complex mixtures. On the contrary, the treatment of benzylester **13b** under hydrogen pressure in the presence of a palladium catalyst afforded the corresponding carboxylic acid **14** an almost quantitative yield (Scheme 6).



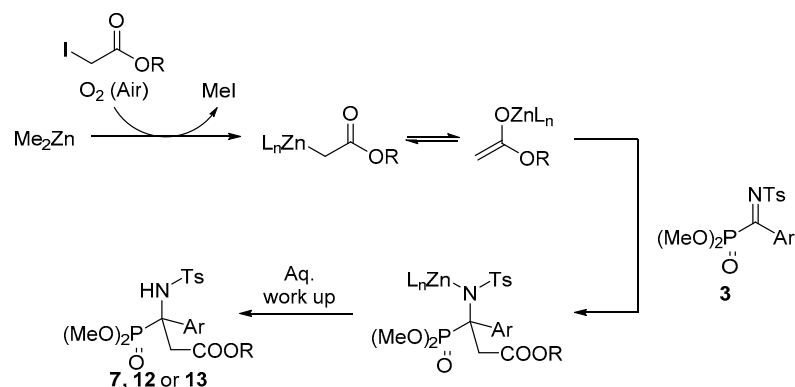
Scheme 6. Hydrogenolysis of benzylester **13b**.

While trying to further understand the nature of the reaction, some control experiments were performed using non-conventional haloacetate derivatives. For instance, the use of α -branched iodoacetate (Scheme 7a) resulted in a complete loss of the reactivity that may be explained due to the electronic effect of the fluorine, which reduces the nucleophilicity of the intermediate species. In contrast, the use of a bulkier phosphonate instead of the ester group increases the steric demand of the nucleophile (Scheme 7b). Finally, when using ethyl 3-iodopropionate, the formation of the enolate intermediate does not occur, and the corresponding organozinc halide species may be formed, which are not usual in nucleophilic additions due to their low reactivity (Scheme 7c).



Scheme 7. Reaction conditions as shown in the Scheme 5. (a) Reaction with α -fluoroiodoacetate. (b) Reaction test with α -iodophosphonate. (c) Remote reformatsky reaction.

Based on these control reactions, as well as on the reaction pathways proposed for similar processes [62,63], we theorize a tentative catalytic cycle in which a combination of electronic and steric effects and the stability of the zinc-enolate intermediate are considered (Scheme 8).



Scheme 8. Proposed reaction mechanism.

As has been addressed above, aspartic acid derivatives have proved to have assorted pharmacological activities [30]. Thus, in view of the described benefits of the isosteric substitution of a carboxylate by a phosphonate group [12], next, we explored the applications of the synthesized phosphorated analogs of aspartic acid as anticancer agents.

2.2. Biological Results

In vitro cytotoxicity of the phosphorated aspartic acid derivatives was evaluated by testing their antiproliferative activities against several human cancer cell lines. Cell counting kit (CCK-8) assay was used for the evaluation of growth inhibition. Moreover, non-malignant MRC5 lung fibroblasts were tested for studying selective toxicity [64] and chemotherapeutic doxorubicin is used as a reference value. In addition, trisubstituted aminophosphonate **9a** (Imine precursor, $R^1 = \text{H}$, $R^2 = \text{P}(\text{O})(\text{OMe})_2$) [59] and tetrasubstituted aminophosphonate **18** ($R^1 = \text{Me}$, $R^2 = \text{P}(\text{O})(\text{OMe})_2$) [60] are used as templates in order to evaluate the effect of the substituents (Table 1).

Table 1. Antiproliferative activity of substrates **5–7**, **9** and **18** against lung and ovarian cancer cell lines.

4-7, 13

| Entry | Comp. | R ¹ | R ² | IC ₅₀ (μM) | | |
|-------|--------------------|------------------------------------|------------------------|-----------------------|--------------|------|
| | | | | SKOV3 | A549 | MRC5 |
| 1 | 5 | CH ₂ CO ₂ Et | H | >50 | 18.68 ± 2.16 | >50 |
| 2 | 6 | CH ₂ CO ₂ Et | CO ₂ Et | >50 | 14.17 ± 0.41 | >50 |
| 3 | 7a | CH ₂ CO ₂ Et | P(O)(OMe) ₂ | >50 | 2.66 ± 0.26 | >50 |
| 4 | 9a | H | P(O)(OMe) ₂ | >50 | 17.56 ± 1.3 | >50 |
| 5 | 18 | CH ₃ | P(O)(OMe) ₂ | >50 | >50 | n.d. |
| 6 | Doxorubicin | | | 0.13 ± 0.098 | <0.1 | >50 |

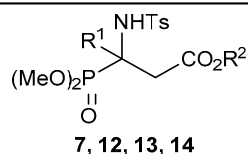
In a preliminary study, the most simple β-alanine substrate **5** showed some cytotoxicity against the A549 cell line, with modest IC₅₀ values of 18.68 ± 2.16 μM but high selectivity if compared with the MCR5 cell line (Table 1, Entry 1). A slightly improved IC₅₀ value of

14.17 ± 0.41 μM was observed for aspartic acid ester **6** in the same cell line and, remarkably, the isosteric substitution of the ester group by a phosphonate group in **7a** resulted in a significantly better IC₅₀ value of 2.66 ± 0.26 μM, still with a high selectivity toward non-malignant cells (Table 1, Entries 2–3).

The presence of the ester group, however, proved to be very relevant to the antiproliferative activity of compound **7a** since tetrasubstituted α-aminophosphonate **18**, lacking such a substituent, showed no cytotoxicity against the A549 cell line and trisubstituted α-aminophosphonate **9a** showed a higher IC₅₀ value of 17.56 ± 1.3 μM (Table 1, Entries 4–5). None of the tested compounds showed in vitro toxicity against the SKOV3 cell line.

This first test of our substrates demonstrated that the best results in activity are obtained when both α-phosphonate and β-carboxylate groups are present in the structure, forming a phosphorus analog of aspartic acid. For this reason, next, we performed a study of the effect of the substitution at the α-aromatic ring of the aspartic acid analogs into the cytotoxicity against the SKOV3 and A549 cell lines (Table 2).

Table 2. Antiproliferative activity of phosphorated analogs of aspartic acid **7**, **12–14** against lung and ovarian cancer cell lines.



| Entry | Comp. | R ¹ | R ² | IC ₅₀ (μM) | | |
|-------|--------------------|--|----------------|-----------------------|--------------|--------------|
| | | | | SKOV3 | A549 | MRC5 |
| 1 | 7a | Ph | Et | >50 | 2.66 ± 0.26 | >50 |
| 2 | 7b | 4-Me-C ₆ H ₄ | Et | >50 | 0.34 ± 0.04 | 29.62 ± 2.98 |
| 3 | 7c | 3-Me-C ₆ H ₄ | Et | >50 | 2.00 ± 0.52 | >50 |
| 4 | 7d | 4-Cl ₃ CS-C ₆ H ₄ | Et | 6.43 ± 0.64 | 4.41 ± 0.29 | 2.47 ± 0.30 |
| 5 | 7e | 4-Br-C ₆ H ₄ | Et | >50 | 1.08 ± 0.09 | >50 |
| 6 | 7f | 4-Cl-C ₆ H ₄ | Et | 24.12 ± 1.45 | 3.09 ± 0.14 | >50 |
| 7 | 7g | 3-Cl-C ₆ H ₄ | Et | >50 | 2.96 ± 0.34 | 38.05 ± 1.61 |
| 8 | 7h | 3,4-Cl ₂ -C ₆ H ₃ | Et | 6.94 ± 0.63 | 1.05 ± 0.42 | 11.29 ± 1.16 |
| 9 | 7i | 3-Cl-4-MeO-C ₆ H ₃ | Et | >50 | 1.44 ± 0.15 | >50 |
| 10 | 7j | 4-F-C ₆ H ₄ | Et | >50 | 7.15 ± 0.24 | >50 |
| 11 | 7k | 3-F-C ₆ H ₄ | Et | >50 | 0.59 ± 0.09 | >50 |
| 12 | 7l | 2-F-C ₆ H ₄ | Et | >50 | 0.90 ± 0.12 | >50 |
| 13 | 7m | 2,4-F ₂ -C ₆ H ₃ | Et | >50 | 2.24 ± 0.31 | >50 |
| 14 | 7n | 3,4-F ₂ -C ₆ H ₃ | Et | >50 | 5.70 ± 0.70 | >50 |
| 15 | 7o | C ₆ F ₅ | Et | 20.46 ± 2.75 | 3.65 ± 0.21 | >50 |
| 16 | 7p | 4-CF ₃ -C ₆ H ₄ | Et | 9.80 ± 0.60 | 20.30 ± 1.14 | >50 |
| 17 | 7q | 4-NO ₂ -C ₆ H ₄ | Et | >50 | 0.67 ± 0.06 | >50 |
| 18 | 7r | 5-Cl-2-thienyl | Et | 11.77 ± 0.60 | 1.04 ± 0.28 | >50 |
| 19 | 7s | 4-Ph-C ₆ H ₄ | Et | 17.01 ± 1.22 | 1.48 ± 0.40 | >50 |
| 20 | 12 | 3-F-C ₆ H ₄ | Me | >50 | 24.11 ± 4.01 | n.d. |
| 21 | 13a | 3-F-C ₆ H ₄ | Bn | >50 | 12.75 ± 2.38 | n.d. |
| 22 | 13b | Ph | Bn | >50 | 5.20 ± 0.16 | >50 |
| 23 | 14 | Ph | H | >50 | 20.61 ± 1.05 | >50 |
| 24 | Doxorubicin | | | 0.13 ± 0.098 | <0.1 | >50 |

The introduction of methyl groups into a bioactive structure results in a more lipophilic character, often resulting in an improved ability of molecules to cross cell membranes [65,66]. Indeed, para and meta tolyl-substituted aminophosphonates **7b** and **7c** presented improved IC₅₀ values of 0.34 ± 0.04 and 2.00 ± 0.52 μM in the A549 cell line if compared with the model structure **7a** (Table 2, Entries 2–3 vs. Entry 1). Although compound **7c** showed a high selectivity if compared with the non-malignant cells, derivative **7b** showed some toxicity toward the MCR5 cell line. Unfortunately, no activity was observed against the SKOV3 cell line for both compounds (Table 2, Entries 2–3). In addition, *p*-trichloromethylthiophenyl derivative **7d** showed good IC₅₀ values of 6.43 ± 0.64 and 4.41 ± 0.29 μM in the SKOV3 and A549 cell lines, respectively, but it presented a very low selectivity toward the MRC5 cell line (Table 2, Entry 4).

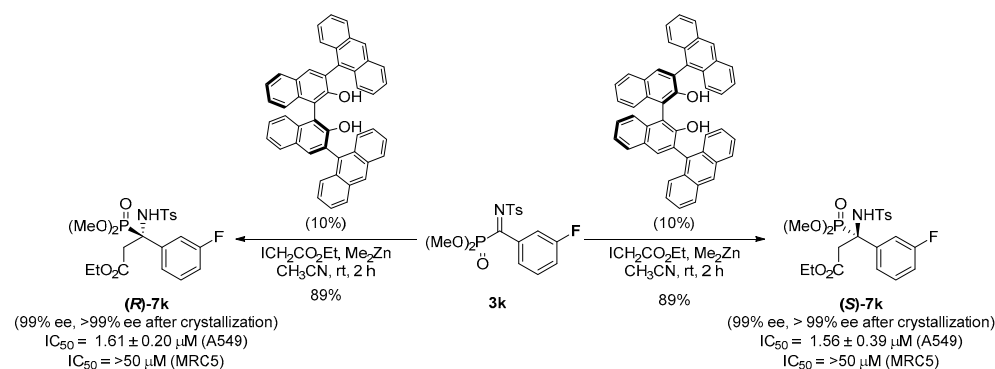
Next, the effect of the substitution of the α -aromatic ring with different halogen atoms was explored. First, *p*-bromo-substituted derivative **7e** proved to be a very good growth inhibitor of the A549 cell line with an IC₅₀ value of 1.08 ± 0.09 μM , and a good selectivity if compared to the SKOV3 or MCR5 cell lines, which showed values over 50 μM (Table 2, Entry 5). *p*-Chlorophenyl derivative **7f** showed very good toxicity against the A549 cell line and some activity in the SKOV3 cell line with IC₅₀ values of 3.09 ± 0.14 and 24.12 ± 1.45 μM , respectively, and a good selectivity against the healthy cells (Table 2, Entry 6). However, the *m*-chlorophenyl isomer **7g** was found to be less effective than the para isomer and toxic against the healthy cells (Table 2, Entry 7). Remarkably, the combination of both substituents in substrate **7h** resulted in a strong cytotoxic effect against all the cell lines and a total lack of selectivity (Table 2, Entry 8). Likewise, the combination of a *meta*-chloro and a *para*-methoxy group in the aromatic ring of **7i** resulted in a very selective activity against the A549 cell line, with an IC₅₀ value of 1.44 ± 0.15 μM (Table 2, Entry 9).

Although, generally, the effect of fluorine substituents on the activity of organic compounds is rather difficult to predict, it is well known that the introduction of fluorine atoms into bioactive molecules very often leads to increased activities [67–69]. With this in mind, we explored the effect of the introduction of different fluorine-containing phosphorylated analogs of aspartic acid **7j–p**. First, the introduction of a *para*-fluorine substituent in **7j** had a negative effect on the cytotoxicity if compared with the model phenyl-substituted compound **7a** (Table 2, Entry 10 vs. Entry 1). On the contrary, the *meta*- and *ortho*-substituted isomers **7k** and **7l**, compared with the model substrate **7a**, showed a very good cytotoxic effect and a high selectivity against the A549 cell line and improved IC₅₀ values of 0.59 ± 0.09 and 0.90 ± 0.12 μM were observed, respectively (Table 2, Entries 11 and 12 vs. Entry 1). Those values could not be improved by the combination of two fluorine substituents at the aromatic ring and, although good IC₅₀ values of 2.24 ± 0.31 and 5.70 ± 0.70 μM were obtained for difluoro-substituted substrates **7m–n** in the A549 cell line, those were significantly higher than the values obtained for mono-substituted substrates **7k–l** (Table 2, Entries 13 and 14 vs. Entries 11 and 12). Moreover, perfluorophenyl derivative **7o** was found to be active against the A549 and SKOV3 cell lines with IC₅₀ values of 3.65 ± 0.21 and 20.46 ± 2.75 μM , respectively, with a good selectivity toward the healthy cells (Table 2, Entry 15).

Surprisingly, the introduction of a *para*-trifluoromethyl electron-withdrawing group at the aromatic ring had a positive effect on the cytotoxicity of substrate **7p** in the SKOV3 cell line, while it had a negative effect for the A549 cell line. In this case, IC₅₀ values of 9.80 ± 0.60 and 20.3 ± 1.14 μM were obtained for each cell line (Table 2, Entry 16 vs. Entry 1) and no toxicity was observed in the MCR5 cells. Aspartic acid analog **7q**, bearing other electron poor aromatic substituents, such as a *p*-nitrophenyl group, showed very good toxicity in the A549 cell line and a high selectivity with an IC₅₀ value of 0.67 ± 0.06 μM (Table 2, Entry 17). Finally, heteroaromatic or biphenyl α -substituted substrates **7r** and **7s** presented very good IC₅₀ values of 1.04 ± 0.28 and 1.48 ± 0.40 μM in the A549 cell line and moderate cytotoxicity against the SKOV3 cell line, with IC₅₀ values of 11.77 ± 0.60 and 17.01 ± 1.22 μM , respectively. Both compounds were found to be selective if compared with the non-malignant cells (Table 2, Entries 18 and 19).

In our next part of this research, we evaluated the influence of the ester group on the antiproliferative activity of our substrates. Considering this, first, we tested the in vitro cytotoxicity of methyl and benzyl ester derivatives **12** and **13a**. Both compounds showed higher IC_{50} values of 24.11 ± 4.01 and 12.75 ± 2.38 μM in the A549 cell line, respectively, if compared with their ethyl ester derivative **7k** and no toxicity against the SKOV3 cell line (Table 2, Entries 20 and 21 vs. Entry 11). The activity of a second benzyl ester derivative **13b** was also tested and that, as in the previous case, presented less toxicity than its ethyl ester derivative **7a** (Table 2, Entry 22 vs. Entry 1). Moreover, carboxylic acid derivative **14** was found also to present less activity than its ethyl ester derivative **7a** (Table 2, Entry 23 vs. Entry 1). Taking into account the results obtained in this experiment, we concluded that ethyl esters are far superior to other esters or carboxylic acid derivatives.

Finally, due to the presence of a stereogenic carbon in the structure of our phosphorylated aspartic acid analogs **7**, one of the final questions to be addressed is which is the real activity of the two individual enantiomers. For that reason, we performed the enantioselective synthesis of α -aminophosphonate **7k**, using both enantiopure isomers of 9-antracenyloxy-substituted BINOL in the aza-Reformatsky reaction. Both enantiomers of **7k** were prepared in 99% ee and, then, two enantiopure samples were obtained by a subsequent crystallization. However, no significant differences were observed for the *R* or *S* enantiomers if compared with the racemic sample with IC_{50} values of 1.61 ± 0.20 and 1.56 ± 0.39 μM in the A549 cell line, respectively (Scheme 9).



Scheme 9. Synthesis and evaluation of each enantiomer of **7k**.

3. Materials and Methods

3.1. Chemistry

3.1.1. General Experimental Information

Solvents for extraction and chromatography were technical grade. All solvents used in reactions were freshly distilled from appropriate drying agents before use. All other reagents were recrystallized or distilled as necessary. All reactions were performed under an atmosphere of dry nitrogen. Analytical TLC was performed with silica gel 60 F₂₅₄ plates. Visualization was accomplished by UV light. ¹H, ¹³C, ³¹P and ¹⁹F-NMR spectra were recorded on a Varian Unity Plus (Varian Inc., NMR Systems, Palo Alto, CA, USA) (at 300 MHz, 75 MHz, 120 MHz and 282 MHz, respectively) and on a Bruker Avance 400 (Bruker BioSpin GmbH, Rheinstetten, Germany) (at 400 MHz for ¹H, and 101 MHz for ¹³C). Chemical shifts (δ) are reported in ppm relative to residual CHCl₃ ($\delta = 7.26$ ppm for ¹H and $\delta = 77.16$ ppm for ¹³C NMR) and using phosphoric acid (50%) or HF as external reference ($\delta = 0.0$ ppm) for ³¹P and ¹⁹F NMR spectra. Coupling constants (*J*) are reported in Hertz. Data for ¹H NMR spectra are reported as follows: chemical shift, multiplicity, coupling constant, integration. Multiplicity abbreviations are as follows: s = singlet, d = doublet, t = triplet, q = quartet, m = multiplet. ¹³C NMR peak assignments were supported by distortionless enhanced polarization transfer (DEPT). High resolution mass spectra (HRMS) were obtained by positive-ion electrospray ionization (ESI). Data are reported in the form *m/z* (intensity relative to base = 100). Infrared spectra (IR) were taken

in a Nicolet iS10 Thermo Scientific spectrometer (Thermo Scientific Inc., Waltham, MA, USA) as neat solids. Peaks are reported in cm^{-1} .

3.1.2. Compounds Purity Analysis

All synthesized compounds were analyzed by HPLC to determine their purity. The analyses were performed on an Agilent 1260 infinity HPLC system (Agilent, Santa Clara, CA, USA) using a CHIRALPAK[®] IA column (5 μm , 0.54 cm ϕ \times 25 cm, Daicel Chiral Technologies, Illkirch Cedex, France) at room temperature. All the tested compounds were dissolved in dichloromethane, and 5 μL of the sample was loaded onto the column. Ethanol and heptane were used as the mobile phase, and the flow rate was set at 1.0 mL/min. The maximal absorbance at the range of 190–400 nm was used as the detection wavelength. The purity of all the derivatives tested in biological essays is >95%, which meets the purity requirement according to the Journal.

3.1.3. Experimental Procedures and Characterization Data for Compounds 3, 5, 6, 7, 12, 13, 14 and 18

General Procedure for Synthesis of α -Ketiminophosphonates 3

Following a modified literature procedure [59], to a solution of the corresponding *N*-tosyl α -aminophosphonate **9** (1 mmol) in CH_2Cl_2 (3 mL) was added trichloroisocyanuric acid (0.7 g, 3 mmol). The obtained suspension was stirred at 0 $^\circ\text{C}$ until the disappearance of the starting *N*-tosyl α -aminophosphonate **9**, as monitored by ^{31}P NMR. The solid residue was eliminated by filtration to afford a clear solution and, then, poly(4-vinylpyridine) (0.3 g), previously dried at 100 $^\circ\text{C}$ overnight, was added. The suspension was stirred under reflux overnight and the reaction was then filtered and concentrated under vacuum. The resulting oily crude was purified by crystallization from diethyl ether to afford pure α -ketiminophosphonates **3**.

Procedure for the Synthesis of Ethyl 3-((4-methylphenyl)sulfonamido)-3-phenylpropanoate 5

A solution of (*E*)-*N*-benzylidene-4-methylbenzenesulfonamide **1** (259.3 mg, 1 mmol) in dry CH_3CN (3 mL) was stirred at room temperature under dry air atmosphere. To this mixture iodoacetate (0.243 mL, 2 mmol) and Et_2Zn (8 mL, 1.0 M in hexane, 8 mmol) were added and the mixture was stirred at room temperature for 2 h. The reaction was quenched by a slow addition of a saturated aqueous solution of NH_4Cl (3 mL), extracted with AcOEt (2 \times 5 mL) and dried with anhydrous MgSO_4 . The organic layer was concentrated under reduced pressure to yield the crude product, which was purified by column chromatography in silica gel (Hexanes/ AcOEt (9:1)) to afford 333 mg (96%) of **5** as a white solid. The spectroscopic data match the data reported in the literature [68].

Procedure for the Synthesis of Diethyl 2-((4-methylphenyl)sulfonamido)-2-phenylsuccinate 6

A solution of ethyl (*Z*)-2-phenyl-2-(tosylimino) acetate **2** (331 mg, 1 mmol) in dry CH_3CN (3 mL) was stirred at room temperature under dry air atmosphere. To this mixture, ethyl iodoacetate (243 μL , 2 mmol) and Me_2Zn (3.3 mL, 1.2 M in toluene, 8 mmol) were added and the mixture was stirred at room temperature until the starting material was completely consumed. The reaction was quenched by a slow addition of a saturated aqueous solution of NH_4Cl (3 mL), extracted with AcOEt (2 \times 5 mL) and dried with anhydrous MgSO_4 . The organic layer was concentrated under reduced pressure to yield the crude product, which was purified by column chromatography in silica gel (AcOEt /Hexanes) to afford 327 mg (78%) of **6** as a white solid. M.p. (Et_2O). 126–127 $^\circ\text{C}$. ^1H NMR (400 MHz, CDCl_3) δ 7.27 (d, $^3J_{\text{HH}} = 8.3$ Hz, 2H), 7.20–7.15 (m, 3H), 7.12–7.06 (m, 2H), 7.02 (d, $^3J_{\text{HH}} = 8.3$ Hz, 2H), 6.3940 (s, 1H), 4.28–4.03 (m, 4H), 3.96 (d, $^3J_{\text{HH}} = 16.4$ Hz, 1H), 3.54 (d, $^3J_{\text{HH}} = 16.4$ Hz, 1H), 2.35 (s, 3H), 1.28 (t, $^3J_{\text{HH}} = 7.0$ Hz, 3H), 1.13 (t, $^3J_{\text{HH}} = 7.0$ Hz, 3H). ^{13}C NMR (101 MHz, CDCl_3) δ 171.4 (C_{quat}), 170.3 (C_{quat}), 142.5 (C_{quat}), 139.2 (C_{quat}), 135.9 (C_{quat}), 129.1 (CH), 128.4 (CH), 126.8 (CH), 126.7 (CH),

64.3 (C_{quat}), 62.9 (CH₂), 61.2 (CH₂), 40.1 (CH₂), 21.5 (CH₃), 14.2 (CH₃), 13.8 (CH₃). HRMS (ESI-TOF) *m/z*: calcd for C₂₁H₂₆NO₆S [M + H]⁺ 420.1481, found 420.1470.

General Procedure for the Aza-Reformatsky Reaction of α -Ketiminophosphonates **3**

A solution of the corresponding α -ketiminophosphonate **3** (1 mmol) in dry CH₃CN (3 mL) was stirred at room temperature under dry air atmosphere. To this mixture, the corresponding iodoacetate (2 mmol) and Me₂Zn (6.6 mL, 1.2 M in toluene, 8 mmol) were added and the mixture was stirred for 2h at room temperature. The reaction was quenched by a slow addition of a saturated aqueous solution of NH₄Cl (3 mL), extracted with AcOEt (2 × 5 mL) and dried with anhydrous MgSO₄. The organic layer was concentrated under reduced pressure to yield the crude product, which was purified by column chromatography in silica gel (AcOEt/Hexanes) [51].

Ethyl 3-(dimethoxyphosphoryl)-3-((4-methylphenyl)sulfonamido)-3-phenylpropanoate (7a). The general procedure was followed, starting from imine **3a** (367 mg, 1 mmol) to afford 414 mg (91%) of **7a** as a white solid. M.p. (CH₂Cl₂-hexanes). 98–99 °C. ¹H NMR (400 MHz, CDCl₃) δ 7.47 (d, ³J_{HH} = 8.3 Hz, 2H), 7.40–7.27 (m, 2H), 7.18 (m, 1H), 7.17–6.93 (m, 4H), 6.17 (d, ³J_{PH} = 11.2 Hz, 1H), 4.14 (q, ³J_{HH} = 7.1 Hz, 2H), 3.59 (dd, ³J_{PH} = 22.7 Hz, ²J_{HH} = 16.4 Hz, 1H), 3.46 (d, ³J_{PH} = 10.7 Hz, 3H), 3.45 (dd, ³J_{PH} = 7.5 Hz, ²J_{HH} = 16.4 Hz, 1H), 3.38 (d, ³J_{PH} = 10.5 Hz, 3H), 2.36 (s, 3H), 1.24 (t, ³J_{HH} = 7.1 Hz, 3H). ¹³C{¹H} NMR (101 MHz, CDCl₃) δ 170.2 (d, ³J_{PC} = 8.0 Hz, C_{quat}), 143.2 (C_{quat}), 139.2 (d, ⁴J_{PC} = 1.5 Hz, C_{quat}), 134.4 (d, ²J_{PC} = 7.3 Hz, C_{quat}), 129.1 (CH), 128.3 (d, ⁵J_{PC} = 2.9 Hz, CH), 128.2 (d, ³J_{PC} = 5.1 Hz, CH), 127.9 (d, ⁴J_{PC} = 2.6 Hz, 2xCH), 127.6 (CH), 62.1 (d, ¹J_{PC} = 153.8 Hz, C_{quat}), 61.0 (CH₂), 54.5 (d, ²J_{PC} = 7.4 Hz, CH₃), 54.0 (d, ²J_{PC} = 7.7 Hz, CH₃), 38.0 (CH₂), 21.6 (CH₃), 14.2 (CH₃). ³¹P NMR (120 MHz, CDCl₃): δ 22.1. FTIR (neat) ν_{\max} 3259 (N-H), 1741 (C=O), 1338 (O=S=O), 1247 (P=O), 1158 (O=S=O). HRMS (ESI-TOF) *m/z*: calcd for C₂₀H₂₇NO₇PS [M + H]⁺ 456.1240, found 456.1245.

Ethyl 3-(dimethoxyphosphoryl)-3-((4-methylphenyl)sulfonamido)-3-(p-tolyl)propanoate (7b). The general procedure was followed, starting from imine **3b** (380 mg, 1 mmol) to afford 403 mg (86%) of **7b** as a white solid. M.p. (CH₂Cl₂-hexanes). 117–118 °C. ¹H NMR (400 MHz, CDCl₃) δ 7.50 (d, ³J_{HH} = 8.3 Hz, 2H), 7.24 (dd, d, ³J_{HH} = 8.6 Hz, ⁴J_{PH} = 2.4 Hz, 2H), 7.15 (d, ³J_{HH} = 7.9 Hz, 2H), 6.94 (d, ³J_{HH} = 8.6 Hz, 2H), 6.13 (d, ³J_{PH} = 11.3 Hz, 1H), 4.16 (qd, ³J_{HH} = 7.1, 1.3 Hz, 2H), 3.63–3.53 (m, 1H), 3.50 (d, ³J_{PH} = 10.7 Hz, 3H), 3.47–3.39 (m, 1H), 3.42 (d, ³J_{PH} = 10.7 Hz, 3H), 2.40 (s, 3H), 2.28 (s, 3H), 1.27 (t, ³J_{HH} = 7.1 Hz, 3H). ¹³C{¹H} NMR (75 MHz, CDCl₃) δ 170.3 (d, ³J_{PC} = 8.1 Hz, C_{quat}), 143.2 (C_{quat}), 139.2 (C_{quat}), 138.2 (d, ⁵J_{PC} = 3.1 Hz, C_{quat}), 131.3 (d, ²J_{PC} = 7.3 Hz, C_{quat}), 129.0 (CH), 128.7 (d, ⁴J_{PC} = 2.7 Hz, CH), 128.1 (d, ³J_{PC} = 5.0 Hz, CH), 127.7 (CH), 61.9 (d, ¹J_{PC} = 154.8 Hz, C_{quat}), 61.0 (CH₂), 54.6 (d, ²J_{PC} = 7.4 Hz, CH₃), 54.0 (d, ²J_{PC} = 7.6 Hz, CH₃), 37.9 (CH₂), 21.6 (CH₃), 21.1 (CH₃), 14.2 (CH₃). ³¹P NMR (120 MHz, CDCl₃): δ 22.3. FTIR (neat) ν_{\max} 3311 (N-H), 1732 (C=O), 1335 (O=S=O), 1244 (P=O), 1160 (O=S=O). HRMS (ESI-TOF) *m/z*: calcd for C₂₁H₂₉NO₇PS [M + H]⁺ 470.1397, found 470.1403.

Ethyl 3-(dimethoxyphosphoryl)-3-((4-methylphenyl)sulfonamido)-3-(m-tolyl)propanoate (7c). The general procedure was followed, starting from imine **3c** (381 mg, 1 mmol) to afford 427 mg (91%) of **7c** as a pale yellow solid. M.p. (CH₂Cl₂-hexanes). 103–104 °C. ¹H NMR (400 MHz, CDCl₃) δ 7.47 (d, ³J_{HH} = 8.2 Hz, 2H), 7.14 (d, ³J_{HH} = 8.2 Hz, 2H), 7.12–6.98 (m, 4H), 6.19 (d, ³J_{PH} = 10.3 Hz, 1H), 4.18 (q, ³J_{HH} = 7.1 Hz, 2H), 3.66 (dd, ³J_{PH} = 24.4 Hz, ²J_{HH} = 16.4 Hz, 1H), 3.49 (d, ³J_{PH} = 10.7 Hz, 3H), 3.45 (m, 1H), 3.42 (d, ³J_{PH} = 10.5 Hz, 3H), 2.38 (s, 3H), 2.09 (s, 3H), 1.28 (t, ³J_{HH} = 7.1 Hz, 3H). ¹³C{¹H} NMR (101 MHz, CDCl₃) δ 170.4 (d, ³J_{PC} = 6.9 Hz, C_{quat}), 143.2 (C_{quat}), 139.4 (d, ⁴J_{PC} = 1.0 Hz, C_{quat}), 137.5 (d, ⁴J_{PC} = 2.9 Hz, C_{quat}), 134.0 (d, ²J_{PC} = 7.5 Hz, C_{quat}), 129.5 (d, ³J_{PC} = 4.8 Hz, CH), 129.2 (d, ⁵J_{PC} = 3.2 Hz, CH), 129.1 (CH), 128.0 (d, ⁴J_{PC} = 2.7 Hz, CH), 127.6 (CH), 125.0 (d, ³J_{PC} = 5.3 Hz, CH), 62.2 (d, ¹J_{PC} = 153.8 Hz, C_{quat}), 61.1 (CH₂), 54.6 (d, ²J_{PC} = 7.4 Hz, CH₃), 54.1 (d, ²J_{PC} = 7.7 Hz, CH₃), 38.3 (CH₂), 21.6 (CH₃), 21.5 (CH₃), 14.3 (CH₃). ³¹P NMR (120 MHz, CDCl₃): δ 22.4. FTIR (neat) ν_{\max} 3276 (N-H), 1735 (C=O), 1338 (O=S=O),

1241 (P=O), 1157 (O=S=O). HRMS (ESI-TOF) m/z : calcd for $C_{21}H_{29}NO_7PS$ $[M + H]^+$ 470.1397, found 470.1398.

Ethyl 3-(dimethoxyphosphoryl)-3-((4-methylphenyl)sulfonamido)-3-(4-(trichloromethyl)thio)phenyl)propanoate (7d). The general procedure was followed, starting from imine **3d** (516 mg, 1 mmol) to afford 525 mg (87%) of **7d** as a pale yellow solid. M.p. (CH_2Cl_2 -hexanes). 123–124 °C. 1H NMR (400 MHz, $CDCl_3$) δ 7.57 (d, $^3J_{HH} = 8.3$ Hz, 2H), 7.53–7.46 (m, 4H), 7.17 (d, $^3J_{HH} = 8.1$ Hz, 2H), 6.26 (d, $^3J_{PH} = 10.5$ Hz, 1H), 4.15 (m, 2H), 3.63 (dd, $^3J_{PH} = 23.5$ Hz, $^2J_{HH} = 16.4$ Hz, 1H), 3.49 (d, $^3J_{PH} = 10.8$ Hz, 3H), 3.46 (m, 1H), 3.49 (d, $^3J_{PH} = 10.6$ Hz, 3H), 2.38 (s, 3H), 1.26 (t, $^3J_{HH} = 7.1$ Hz, 3H). $^{13}C\{^1H\}$ NMR (101 MHz, $CDCl_3$) δ 169.9 (d, $^3J_{PC} = 7.1$ Hz, C_{quat}), 143.7 (C_{quat}), 139.1 (d, $^4J_{PC} = 1.2$ Hz, C_{quat}), 138.8 (d, $^2J_{PC} = 7.3$ Hz, C_{quat}), 136.5 (d, $^4J_{PC} = 2.8$ Hz, CH), 130.8 (d, $^5J_{PC} = 3.6$ Hz, C_{quat}), 129.4 (CH), 129.2 (d, $^3J_{PC} = 4.9$ Hz, CH), 127.5 (CH), 98.5 (d, $^7J_{PC} = 3.2$ Hz, C_{quat}), 62.3 (d, $^1J_{PC} = 152.2$ Hz, C_{quat}), 61.2 (CH_2), 54.8 (d, $^2J_{PC} = 7.4$ Hz, CH_3), 54.4 (d, $^2J_{PC} = 7.6$ Hz, CH_3), 38.3 (CH_2), 21.7 (CH_3), 14.2 (CH_3). ^{31}P NMR (120 MHz, $CDCl_3$): δ 21.5. FTIR (neat) ν_{max} 3291 (N-H), 1733 (C=O), 1331 (O=S=O), 1258 (P=O), 1159 (O=S=O). HRMS (ESI-TOF) m/z : calcd for $C_{21}H_{26}Cl_3NO_7PS_2$ $[M + H]^+$ 605.9919, found 605.9928.

Ethyl 3-(4-bromophenyl)-3-(dimethoxyphosphoryl)-3-((4-methylphenyl)sulfonamido)propanoate (7e). The general procedure was followed, starting from imine **3e** (445 mg, 1 mmol) to afford 485 mg (91%) of **7e** as a white solid. M.p. (CH_2Cl_2 -hexanes). 138–139 °C. 1H NMR (400 MHz, $CDCl_3$) δ 7.38 (d, $^3J_{HH} = 8.3$ Hz, 2H), 7.18–7.12 (m, 4H), 7.07 (d, $^3J_{HH} = 8.3$ Hz, 2H), 6.24 (d, $^3J_{PH} = 10.1$ Hz, 1H), 4.07 (m, 2H), 3.49 (m, 1H), 3.47 (d, $^3J_{PH} = 10.8$ Hz, 3H), 3.39 (d, $^3J_{PH} = 10.6$ Hz, 3H), 3.32 (dd, $^2J_{HH} = 16.4$ Hz, $^3J_{PH} = 8.0$ Hz, 1H), 2.32 (s, 3H), 1.18 (t, $^3J_{HH} = 7.1$ Hz, 3H). $^{13}C\{^1H\}$ NMR (101 MHz, $CDCl_3$) δ 169.6 (d, $^3J_{PC} = 7.7$ Hz, C_{quat}), 143.3 (C_{quat}), 138.8 (m, C_{quat}), 133.4 (d, $^2J_{PC} = 6.7$ Hz, C_{quat}), 130.6 (d, $^4J_{PC} = 2.6$ Hz, CH), 129.8 (d, $^3J_{PC} = 5.1$ Hz, CH), 129.0 (CH), 127.3 (CH), 122.5 (d, $^5J_{PC} = 3.6$ Hz, C_{quat}), 61.6 (d, $^1J_{PC} = 154.3$ Hz, C_{quat}), 60.8 (CH_2), 54.4 (d, $^2J_{PC} = 7.4$ Hz, CH_3), 54.0 (d, $^2J_{PC} = 7.7$ Hz, CH_3), 37.6 (CH_2), 21.36 (CH_3), 14.0 (CH_3). ^{31}P NMR (120 MHz, $CDCl_3$): δ 21.7. FTIR (neat) ν_{max} 3293 (N-H), 1729 (C=O), 1337 (O=S=O), 1245 (P=O), 1154 (O=S=O). HRMS (ESI-TOF) m/z : calcd for $C_{20}H_{26}BrNO_7PS$ $[M + H]^+$ 534.0345, found 534.0311.

Ethyl 3-(4-chlorophenyl)-3-(dimethoxyphosphoryl)-3-((4-methylphenyl)sulfonamido)propanoate (7f). The general procedure was followed, starting from imine **3f** (401 mg, 1 mmol) to afford 430 mg (88%) of **7f** as a pale yellow solid. M.p. (CH_2Cl_2 -hexanes). 133–134 °C. 1H NMR (400 MHz, $CDCl_3$) δ 7.47 (d, $^3J_{HH} = 8.1$ Hz, 2H), 7.29 (dd, $^3J_{HH} = 8.7$ Hz, $^4J_{PH} = 2.4$ Hz, 2H), 7.16 (d, $^3J_{HH} = 8.0$ Hz, 2H), 7.08 (d, $^3J_{HH} = 8.6$ Hz, 2H), 6.18 (d, $^3J_{PH} = 10.3$ Hz, 1H), 4.17 (q, $^3J_{HH} = 7.2$ Hz, 2H), 3.62 (m, 1H), 3.55 (d, $^3J_{PH} = 10.5$ Hz, 3H), 3.47 (d, $^3J_{PH} = 10.5$ Hz, 3H), 3.40 (dd, $^2J_{HH} = 16.1$ Hz, $^3J_{PH} = 7.5$ Hz, 1H), 2.41 (s, 3H), 1.28 (t, $^3J_{HH} = 7.2$ Hz, 3H). $^{13}C\{^1H\}$ NMR (75 MHz, $CDCl_3$) δ 170.0 (d, $^3J_{PC} = 7.2$ Hz, C_{quat}), 143.5 (C_{quat}), 139.0 (C_{quat}), 134.5 (d, $^5J_{PC} = 3.5$ Hz, C_{quat}), 133.0 (d, $^2J_{PC} = 7.0$ Hz, C_{quat}), 129.7 (d, $^3J_{PC} = 5.1$ Hz, CH), 129.2 (CH), 128.0 (d, $^4J_{PC} = 2.7$ Hz, CH), 127.6 (CH), 61.7 (d, $^1J_{PC} = 154.2$ Hz, C_{quat}), 61.1 (CH_2), 54.7 (d, $^2J_{PC} = 7.3$ Hz, CH_3), 54.2 (d, $^2J_{PC} = 7.5$ Hz, CH_3), 38.0 (CH_2), 21.6 (CH_3), 14.2 (CH_3). ^{31}P NMR (120 MHz, $CDCl_3$): δ 21.9. FTIR (neat) ν_{max} 3256 (N-H), 1732 (C=O), 1335 (O=S=O), 1246 (P=O), 1160 (O=S=O). HRMS (ESI-TOF) m/z : calcd for $C_{20}H_{26}ClNO_7PS$ $[M + H]^+$ 490.0851, found 490.0856.

Ethyl 3-(3-chlorophenyl)-3-(dimethoxyphosphoryl)-3-((4-methylphenyl)sulfonamido)propanoate (7g). The general procedure was followed, starting from imine **3g** (401 mg, 1 mmol) to afford 440 mg (90%) of **7g** as a pale yellow solid. M.p. (CH_2Cl_2 -hexanes). 88–89 °C. 1H NMR (400 MHz, $CDCl_3$) δ 7.46 (d, $^3J_{HH} = 8.3$ Hz, 2H), 7.27–7.22 (m, 2H), 7.19–7.09 (m, 4H), 6.20 (d, $^3J_{PH} = 9.4$ Hz, 1H), 4.20 (q, $^3J_{HH} = 7.1$ Hz, 2H), 3.65 (dd, $^3J_{PH} = 24.9$ Hz, $^3J_{HH} = 16.2$ Hz, 1H), 3.54 (d, $^3J_{PH} = 10.7$ Hz, 3H), 3.51 (d, $^3J_{PH} = 10.6$ Hz, 3H), 3.42 (dd, $^3J_{HH} = 16.2$ Hz, $^3J_{PH} = 7.6$ Hz, 1H), 2.40 (s, 3H), 1.29 (t, $^3J_{HH} = 7.1$ Hz, 3H). $^{13}C\{^1H\}$ NMR (101 MHz, $CDCl_3$) δ 170.1 (d, $^3J_{PC} = 6.1$ Hz, C_{quat}), 143.7 (C_{quat}), 139.0 (C_{quat}), 136.5 (d, $^2J_{PC} = 7.7$ Hz, C_{quat}), 134.1 (d, $^4J_{PC} = 3.3$ Hz, C_{quat}), 129.4 (CH), 129.2 (d, $^4J_{PC} = 2.9$ Hz, CH), 129.2 (d, $^3J_{PC} = 4.9$ Hz, CH), 128.6 (d, $^5J_{PC} = 2.9$ Hz, CH), 127.5 (CH), 126.2 (d, $^3J_{PC} = 5.1$ Hz, CH), 62.0 (d, $^1J_{PC} = 153.2$ Hz, C_{quat}), 61.2 (CH_2), 54.7 (d, $^2J_{PC} = 7.3$

Hz, CH₃), 54.4 (d, ²J_{PC} = 7.6 Hz, CH₃), 38.3 (CH₂), 21.7 (CH₃), 14.3 (CH₃). ³¹P NMR (120 MHz, CDCl₃): δ 21.9. FTIR (neat) ν_{max} 3276 (N-H), 1732 (C=O), 1341 (O=S=O), 1238 (P=O), 1161 (O=S=O). HRMS (ESI-TOF) *m/z*: calcd for C₂₀H₂₆ClNO₇PS [M + H]⁺ 490.0851, found 490.0857.

Ethyl 3-(3,4-dichlorophenyl)-3-(dimethoxyphosphoryl)-3-((4-methylphenyl)sulfonamido)propanoate (7h). The general procedure was followed, starting from imine **3h** (435 mg, 1 mmol) to afford 450 mg (86%) of **7h** as a white solid. M.p. (CH₂Cl₂-hexanes). 109–110 °C. ¹H NMR (400 MHz, CDCl₃) δ 7.43 (d, ³J_{HH} = 8.2 Hz, 2H), 7.33 (s, 1H), 7.23–7.18 (m, 2H), 7.15 (d, ³J_{HH} = 8.2 Hz, 2H), 6.24 (d, ³J_{PH} = 9.3 Hz, 1H), 4.17 (q, ³J_{HH} = 7.5 Hz, 2H), 3.59 (m, 1H), 3.58 (d, ³J_{HH} = 10.8 Hz, 3H), 3.54 (d, ³J_{HH} = 10.7 Hz, 3H), 3.36 (dd, ²J_{HH} = 16.2 Hz, ³J_{PH} = 8.3 Hz, 1H), 2.38 (s, 3H), 1.27 (t, ³J_{HH} = 7.5 Hz, 3H). ¹³C{¹H} NMR (101 MHz, CDCl₃) δ 169.7 (d, ³J_{PC} = 6.4 Hz, C_{quat}), 143.9 (C_{quat}), 138.7 (d, ⁴J_{PC} = 1.4 Hz, C_{quat}), 134.7 (d, ²J_{PC} = 6.6 Hz, C_{quat}), 132.7 (d, ⁵J_{PC} = 3.7 Hz, C_{quat}), 132.1 (d, ⁴J_{PC} = 2.9 Hz, C_{quat}), 130.9 (d, ³J_{PC} = 5.1 Hz, CH), 129.7 (d, ⁴J_{PC} = 2.6 Hz, CH), 129.4 (CH), 127.4 (d, ³J_{PC} = 5.1 Hz, CH), 127.3 (CH), 61.4 (d, ¹J_{PC} = 153.7 Hz, C_{quat}), 61.2 (CH₂), 54.7 (d, ²J_{PC} = 7.3 Hz, CH₃), 54.5 (d, ²J_{PC} = 7.6 Hz, CH₃), 38.0 (CH₂), 21.6 (CH₃), 14.2 (CH₃). ³¹P NMR (120 MHz, CDCl₃): δ 21.7. FTIR (neat) ν_{max} 3251 (N-H), 1738 (C=O), 1338 (O=S=O), 1261 (P=O), 1160 (O=S=O). HRMS (ESI-TOF) *m/z*: calcd for C₂₀H₂₅Cl₂NO₇PS [M + H]⁺ 524.0461, found 524.0465.

Ethyl 3-(3-chloro-4-methoxyphenyl)-3-(dimethoxyphosphoryl)-3-((4-methylphenyl)sulfonamido)propanoate (7i). The general procedure was followed, starting from imine **3i** (431 mg, 1 mmol) to afford 420 mg (81%) of **7i** as a white solid. M.p. (CH₂Cl₂-hexanes). 153–154 °C. ¹H NMR (400 MHz, CDCl₃) δ 7.44 (d, ³J_{HH} = 8.3 Hz, 2H), 7.24–7.18 (m, 2H), 7.15 (d, ³J_{HH} = 8.3 Hz, 2H), 6.71 (d, ³J_{HH} = 8.7 Hz, 1H), 6.17 (d, ³J_{PH} = 9.0 Hz, 1H), 4.20 (q, ³J_{HH} = 7.1 Hz, 2H), 3.86 (s, 3H), 3.62 (dd, ³J_{PH} = 25.6 Hz, ²J_{HH} = 16.1 Hz, 1H), 3.55 (d, ³J_{PH} = 10.7 Hz, 3H), 3.52 (d, ³J_{PH} = 10.7 Hz, 3H), 3.36 (dd, ²J_{HH} = 16.1 Hz, ³J_{PH} = 7.6 Hz, 1H), 2.39 (s, 3H), 1.30 (t, ³J_{HH} = 7.1 Hz, 3H). ¹³C{¹H} NMR (101 MHz, CDCl₃) δ 170.1 (d, ³J_{PC} = 5.9 Hz, C_{quat}), 154.9 (d, ⁵J_{PC} = 2.7 Hz, C_{quat}), 143.7 (C_{quat}), 138.9 (d, ⁴J_{PC} = 1.7 Hz, C_{quat}), 130.9 (d, ³J_{PC} = 4.8 Hz, CH), 129.3 (CH), 127.7 (d, ³J_{PC} = 5.5 Hz, CH), 127.5 (CH), 126.8 (d, ²J_{PC} = 7.4 Hz, C_{quat}), 122.0 (d, ⁴J_{PC} = 3.0 Hz, C_{quat}), 111.0 (d, ⁴J_{PC} = 2.6 Hz, CH), 61.3 (d, ¹J_{PC} = 155.4 Hz, C_{quat}), 61.2 (CH₂), 56.2 (CH₃), 54.7 (d, ²J_{PC} = 7.3 Hz, CH₃), 54.3 (d, ²J_{PC} = 7.7 Hz, CH₃), 38.2 (CH₂), 21.7 (CH₃), 14.3 (CH₃). ³¹P NMR (120 MHz, CDCl₃): δ 22.2. FTIR (neat) ν_{max} 3275 (N-H), 1732 (C=O), 1333 (O=S=O), 1263 (P=O), 1158 (O=S=O). HRMS (ESI-TOF) *m/z*: calcd for C₂₁H₂₈ClNO₈PS [M + H]⁺ 520.0956, found 520.0959.

Ethyl 3-(dimethoxyphosphoryl)-3-(4-fluorophenyl)-3-((4-methylphenyl)sulfonamido)propanoate (7j). The general procedure was followed, starting from imine **3j** (417 mg, 1 mmol) to afford 421 mg (89%) of **7j** as a white solid. M.p. (CH₂Cl₂-hexanes). 111–112 °C. ¹H NMR (300 MHz, CDCl₃) δ 7.47 (d, ³J_{HH} = 8.5 Hz, 2H), 7.34 (m, 2H), 7.16 (d, ³J_{HH} = 8.1 Hz, 2H), 6.81 (t, ³J_{HH} = 8.7 Hz, 2H), 6.19 (d, ³J_{PH} = 10.0 Hz, 1H), 4.18 (q, ³J_{HH} = 7.1 Hz, 2H), 3.62 (m, 1H), 3.54 (d, ³J_{PH} = 10.5 Hz, 3H), 3.46 (d, ³J_{PH} = 10.5 Hz, 3H), 3.40 (m, 1H), 2.40 (s, 3H), 1.28 (t, ³J_{HH} = 7.2 Hz, 3H). ¹³C{¹H} NMR (75 MHz, CDCl₃) δ 170.1 (d, ³J_{PC} = 7.0 Hz, C_{quat}), 162.5 (dd, ¹J_{FC} = 248.9 Hz, ⁵J_{PC} = 3.2 Hz, C_{quat}), 143.5 (C_{quat}), 139.1 (C_{quat}), 130.3 (dd, ³J_{FC} = 8.3 Hz, ³J_{PC} = 5.0 Hz, CH), 130.1 (dd, ²J_{PC} = 6.9 Hz, ⁴J_{FC} = 3.3 Hz, C_{quat}), 129.2 (CH), 127.6 (CH), 114.8 (dd, ²J_{FC} = 21.6 Hz, ⁴J_{PC} = 2.7 Hz, CH), 61.7 (d, ¹J_{PC} = 155.0 Hz, C_{quat}), 61.2 (CH₂), 54.7 (d, ²J_{PC} = 7.4 Hz, CH₃), 54.2 (d, ²J_{PC} = 7.7 Hz, CH₃), 38.2 (CH₂), 21.6 (CH₃), 14.2 (CH₃). ³¹P NMR (120 MHz, CDCl₃): δ 22.2. ¹⁹F NMR (282 MHz, CDCl₃) δ −113.8. FTIR (neat) ν_{max} 3264 (N-H), 1735 (C=O), 1335 (O=S=O), 1241 (P=O), 1161 (O=S=O). HRMS (ESI-TOF) *m/z*: calcd for C₂₀H₂₆FNO₇PS [M + H]⁺ 474.1146, found 474.1148.

Ethyl 3-(dimethoxyphosphoryl)-3-(3-fluorophenyl)-3-((4-methylphenyl)sulfonamido)propanoate (7k). The general procedure was followed, starting from imine **3k** (417 mg, 1 mmol) to afford 421 mg (89%) of **7k** as a white solid. M.p. (CH₂Cl₂-hexanes). 111–112 °C. ¹H NMR (400 MHz, CDCl₃) δ 7.48 (d, ³J_{HH} = 8.3 Hz, 2H), 7.17–7.09 (m, 4H), 7.01 (m, 1H), 6.90 (m, 1H), 6.22 (br s, 1H), 4.15 (q, ³J_{HH} = 7.1 Hz, 2H), 3.59 (dd, ³J_{PH} = 23.5 Hz, ²J_{HH} = 16.4 Hz, 1H), 3.51 (d, ³J_{PH} = 10.7 Hz, 3H), 3.47 (d, ³J_{PH} = 10.7 Hz, 3H), 3.40 (dd, ²J_{HH} = 16.4 Hz, ³J_{PH} = 7.5 Hz, 1H), 2.37 (s, 3H), 1.25 (t, ³J_{HH} = 7.1 Hz, 3H). ¹³C{¹H} NMR (101 MHz,

CDCl₃) δ 169.9 (d, $^3J_{PC} = 7.3$ Hz, C_{quat}), 162.2 (dd, $^1J_{FC} = 246.1$ Hz, $^4J_{PC} = 2.9$ Hz, C_{quat}), 143.6 (C_{quat}), 139.0 (d, $^4J_{PC} = 1.4$ Hz, C_{quat}), 137.1 (t, $^2J_{PC} = ^3J_{FC} = 7.1$ Hz, C_{quat}), 129.4 (dd, $^3J_{FC} = 8.1$ Hz, $^4J_{PC} = 2.8$ Hz, CH), 129.2 (CH), 127.5 (CH), 123.7 (dd, $^3J_{PC} = 5.2$ Hz, $^4J_{FC} = 2.9$ Hz, CH), 116.0 (dd, $^2J_{FC} = 24.1$ Hz, $^3J_{PC} = 4.9$ Hz, CH), 115.3 (dd, $^2J_{FC} = 21.0$ Hz, $^5J_{PC} = 3.0$ Hz, CH), 61.9 (dd, $^1J_{PC} = 153.6$ Hz, $^4J_{FC} = 1.9$ Hz, C_{quat}), 61.1 (CH₂), 54.6 (d, $^2J_{PC} = 7.4$ Hz, CH₃), 54.3 (d, $^2J_{PC} = 7.6$ Hz, CH₃), 38.1 (CH₂), 21.6 (CH₃), 14.2 (CH₃). ^{31}P NMR (120 MHz, CDCl₃): δ 21.7. ^{19}F NMR (282 MHz, CDCl₃) δ -113.0. FTIR (neat) ν_{max} 3281 (N-H), 1732 (C=O), 1333 (O=S=O), 1244 (P=O), 1157 (O=S=O). HRMS (ESI-TOF) m/z : calcd for C₂₀H₂₆FNO₇PS [M + H]⁺ 474.1146, found 474.1155.

Ethyl 3-(dimethoxyphosphoryl)-3-(2-fluorophenyl)-3-((4-methylphenyl)sulfonamido)propanoate (7l). The general procedure was followed, starting from imine **3l** (417 mg, 1 mmol) to afford 440 mg (93%) of **7l** as a pale yellow solid. M.p. (CH₂Cl₂-hexanes). 140–141 °C. ^1H NMR (400 MHz, CDCl₃) δ 7.58 (d, $^3J_{\text{HH}} = 8.3$ Hz, 2H), 7.48–7.40 (m, 1H), 7.23–7.19 (m, 1H), 7.16 (d, $^3J_{\text{HH}} = 8.3$ Hz, 2H), 6.99 (m, 1H), 6.80 (dd, $^3J_{\text{FH}} = 12.8$ Hz, $^3J_{\text{HH}} = 8.1$ Hz, 1H), 6.21 (d, $^3J_{\text{PH}} = 13.1$ Hz, 1H), 4.17–4.01 (m, 2H), 3.63 (d, $^3J_{\text{PH}} = 10.8$ Hz, 3H), 3.60 (m, 2H), 3.54 (d, $^3J_{\text{PH}} = 10.7$ Hz, 3H), 2.38 (s, 3H), 1.23 (t, $^3J_{\text{HH}} = 7.1$ Hz, 3H). $^{13}\text{C}\{^1\text{H}\}$ NMR (101 MHz, CDCl₃) δ 170.2 (d, $^3J_{PC} = 10.8$ Hz, C_{quat}), 160.6 (dd, $^1J_{FC} = 249.9$ Hz, $^3J_{PC} = 5.8$ Hz, C_{quat}), 143.3 (C_{quat}), 138.8 (d, $^4J_{PC} = 1.3$ Hz, C_{quat}), 130.4 (dd, $^3J_{FC} = 9.4$, $^3J_{PC} = 2.8$ Hz, CH), 130.3 (dd, $^3J_{FC} = 4.8$ Hz, $^5J_{PC} = 2.9$ Hz, CH), 129.2 (CH), 127.6 (CH), 123.9 (dd, $^4J_{FC} = 3.3$ Hz, $^4J_{PC} = 2.5$ Hz, CH), 123.2 (m, C_{quat}), 116.4 (dd, $^2J_{FC} = 24.6$ Hz, $^4J_{PC} = 2.5$ Hz, CH), 61.4 (dd, $^1J_{PC} = 154.0$, $^3J_{FC} = 3.4$ Hz, C_{quat}), 60.9 (CH₂), 54.7 (d, $^2J_{PC} = 7.6$ Hz, CH₃), 54.5 (d, $^2J_{PC} = 7.4$ Hz, CH₃), 38.6 (d, $^4J_{FC} = 6.8$ Hz, CH₂), 21.6 (CH₃), 14.2 (CH₃). ^{31}P NMR (120 MHz, CDCl₃): δ 22.1. ^{19}F NMR (282 MHz, CDCl₃) δ -107.6. FTIR (neat) ν_{max} 3236 (N-H), 1755 (C=O), 1328 (O=S=O), 1239 (P=O), 1160 (O=S=O). HRMS (ESI-TOF) m/z : calcd for C₂₀H₂₆FNO₇PS [M + H]⁺ 474.1146, found 474.1126. The spectroscopic data match the data reported in the literature [51].

Ethyl 3-(2,4-difluorophenyl)-3-(dimethoxyphosphoryl)-3-((4-methylphenyl)sulfonamido)propanoate (7m). The general procedure was followed, starting from imine **3m** (403 mg, 1 mmol) to afford 457 mg (93%) of **7m** as a white solid. M.p. (CH₂Cl₂-hexanes). 135–136 °C. ^1H NMR (400 MHz, CDCl₃) δ 7.55 (d, $^3J_{\text{HH}} = 8.3$ Hz, 2H), 7.39 (m, 1H), 7.15 (d, $^3J_{\text{HH}} = 8.3$ Hz, 2H), 6.68 (m, 1H), 6.52 (m, 1H), 6.25 (br d, $^3J_{\text{PH}} = 8.9$ Hz, 1H), 4.09 (m, 2H), 3.65 (d, $^3J_{\text{PH}} = 10.8$ Hz, 3H), 3.57 (d, $^3J_{\text{PH}} = 10.7$ Hz, 3H), 3.57–3.47 (m, 2H), 2.37 (s, 3H), 1.22 (t, $^3J_{\text{HH}} = 7.1$ Hz, 3H). $^{13}\text{C}\{^1\text{H}\}$ NMR (101 MHz, CDCl₃) δ 170.0 (d, $^3J_{PC} = 10.9$ Hz, C_{quat}), 162.9 (ddd, $^1J_{FC} = 251.3$ Hz, $^3J_{FC} = 12.7$ Hz, $^5J_{PC} = 2.9$ Hz, C_{quat}), 160.7 (ddd, $^1J_{FC} = 252.9$ Hz, $^3J_{FC} = 11.7$ Hz, $^3J_{PC} = 5.7$ Hz, C_{quat}), 143.5 (C_{quat}), 138.6 (C_{quat}), 131.4 (m, CH), 129.2 (CH), 127.5 (CH), 119.4 (m, C_{quat}), 110.8 (br d, $^2J_{FC} = 21$ Hz, CH), 104.5 (ddd, $^2J_{FC} = 27.9$ Hz, $^2J_{FC} = 25.3$ Hz, $^4J_{PC} = 2.5$ Hz, CH), 60.9 (CH₂), 60.9 (dd, $^1J_{PC} = 154.6$ Hz, $^3J_{FC} = 3.7$ Hz, C_{quat}), 54.6 (br d, $^2J_{PC} = 7.6$ Hz, CH₃), 54.6 (br d, $^2J_{PC} = 7.3$ Hz, CH₃), 38.5 (d, $^4J_{FC} = 6.9$ Hz, CH₂), 21.6 (CH₃), 14.1 (CH₃). ^{31}P NMR (120 MHz, CDCl₃): δ 22.0. ^{19}F NMR (282 MHz, CDCl₃) δ -103.0, -110.3 ppm. FTIR (neat) ν_{max} 3248 (N-H), 1741 (C=O), 1335 (O=S=O), 1247 (P=O), 1155 (O=S=O). HRMS (ESI-TOF) m/z : calcd for C₂₀H₂₅F₂NO₇PS [M + H]⁺ 492.1052, found 492.1058.

Ethyl 3-(3,4-difluorophenyl)-3-(dimethoxyphosphoryl)-3-((4-methylphenyl)sulfonamido)propanoate (7n). The general procedure was followed, starting from imine **3n** (403 mg, 1 mmol) to afford 447 mg (91%) of **7n** as a white solid. M.p. (CH₂Cl₂-hexanes). 98–99 °C. ^1H NMR (400 MHz, CDCl₃) δ 7.48 (d, $^3J_{\text{HH}} = 8.0$ Hz, 2H), 7.19 (d, $^3J_{\text{HH}} = 8.0$ Hz, 2H), 7.17–7.07 (m, 2H), 6.95 (q, $^3J_{\text{HH}} = 9.2$ Hz, 1H), 6.21 (d, $^3J_{\text{PH}} = 9.6$ Hz, 1H), 4.19 (q, $^3J_{\text{HH}} = 7.1$ Hz, 2H), 3.61 (m, 1H), 3.59 (d, $^3J_{\text{PH}} = 11.1$ Hz, 3H), 3.53 (d, $^3J_{\text{PH}} = 10.6$ Hz, 3H), 3.36 (dd, $^2J_{\text{HH}} = 16.1$ Hz, $^3J_{\text{PH}} = 7.9$ Hz, 1H), 2.41 (s, 3H), 1.29 (t, $^3J_{\text{HH}} = 7.2$ Hz, 3H). $^{13}\text{C}\{^1\text{H}\}$ NMR (101 MHz, CDCl₃) δ 169.8 (d, $^3J_{PC} = 6.8$ Hz, C_{quat}), 150.2 (ddd, $^1J_{FC} = 250.6$ Hz, $^2J_{FC} = 11.8$ Hz, $^5J_{PC} = 3.1$ Hz, C_{quat}), 149.5 (ddd, $^1J_{FC} = 246.0$ Hz, $^2J_{FC} = 10.6$ Hz, $^4J_{PC} = 3.0$ Hz, C_{quat}), 143.9 (C_{quat}), 139.0 (d, $^4J_{PC} = 1.3$ Hz, C_{quat}), 131.6 (m, C_{quat}), 129.3 (CH), 127.5 (CH), 124.4 (m, CH), 118.4 (dd, $^2J_{FC} = 19.6$ Hz, $^3J_{PC} = 4.8$ Hz, CH), 116.5 (dd, $^2J_{FC} = 17.4$ Hz, $^4J_{PC} = 2.7$ Hz, CH), 61.5 (d, $^1J_{PC} = 154.6$ Hz, C_{quat}), 61.3 (CH₂), 54.7 (d, $^2J_{PC}$

= 7.3 Hz, CH₃), 54.4 (d, ²J_{PC} = 7.6 Hz, CH₃), 38.2 (CH₂), 21.6 (CH₃), 14.2 (CH₃). ³¹P NMR (120 MHz, CDCl₃): δ 21.7. ¹⁹F NMR (282 MHz, CDCl₃) δ −137.6, −138.0. FTIR (neat) ν_{max} 3262 (N-H), 1738 (C=O), 1338 (O=S=O), 1249 (P=O), 1163 (O=S=O). HRMS (ESI-TOF) *m/z*: calcd for C₂₀H₂₅F₂NO₇PS [M + H]⁺ 492.1052, found 492.1060.

Ethyl 3-(dimethoxyphosphoryl)-3-((4-methylphenyl)sulfonamido)-3-(perfluorophenyl)propanoate (7o). The general procedure was followed, starting from imine **3o** (457 mg, 1 mmol) to afford 501 mg (92%) of **7o** as a colorless oil. ¹H NMR (400 MHz, CDCl₃) δ 7.52 (d, ³J_{HH} = 8.3 Hz, 2H), 7.16 (d, ³J_{HH} = 8.3 Hz, 2H), 6.23 (d, ³J_{PH} = 10.5 Hz, 1H), 4.18–4.07 (m, 2H), 3.98 (m, 1H), 3.80 (d, ³J_{PH} = 10.9 Hz, 3H), 3.75 (d, ³J_{PH} = 10.9 Hz, 3H), 3.45 (m, 1H), 2.36 (s, 3H), 1.24 (t, ³J_{HH} = 7.1 Hz, 3H). ¹³C{¹H} NMR (101 MHz, CDCl₃) δ 170.1 (d, ³J_{PC} = 8.4 Hz, C_{quat}), 145.9 (m, C_{quat}), 144.1 (C_{quat}), 140.8 (m, C_{quat}), 137.7 (d, ⁴J_{PC} = 1.9 Hz, C_{quat}), 137.5 (m, C_{quat}), 129.2 (CH), 127.1 (CH), 111.2 (m, C_{quat}), 61.0 (CH₂), 60.0 (d, ¹J_{PC} = 153.3 Hz, C_{quat}), 55.7 (d, ²J_{PC} = 7.2 Hz, CH₃), 54.9 (d, ²J_{PC} = 7.8 Hz, CH₃), 40.3 (d, ⁴J_{FC} = 5.3 Hz, CH₂), 21.4 (CH₃), 14.1 (CH₃). ³¹P NMR (120 MHz, CDCl₃): δ 21.7. ¹⁹F NMR (282 MHz, CDCl₃) δ −135.0, −154.3, −162.8. FTIR (neat) ν_{max} 3284 (N-H), 1741 (C=O), 1333 (O=S=O), 1254 (P=O), 1166 (O=S=O). HRMS (ESI-TOF) *m/z*: calcd for C₂₀H₂₂F₅NO₇PS [M + H]⁺ 546.0769, found 546.0781.

Ethyl 3-(dimethoxyphosphoryl)-3-((4-methylphenyl)sulfonamido)-3-(4-(trifluoromethyl)phenyl)propanoate (7p). The general procedure was followed, starting from imine **3p** (435 mg, 1 mmol) to afford 455 mg (87%) of **7p** as a white solid. M.p. (CH₂Cl₂-hexanes). 114–115 °C. ¹H NMR (400 MHz, CDCl₃) δ 7.47 (³J_{HH} = 8.8 Hz, ³J_{FH} = 2.3 Hz, 2H), 7.42 (d, ³J_{HH} = 8.4 Hz, 2H), 7.34 (d, ³J_{HH} = 8.4 Hz, 2H), 7.12 (d, ³J_{HH} = 8.2 Hz, 2H), 6.24 (d, ³J_{PH} = 10.1 Hz, 1H), 4.18 (qd, ³J_{HH} = 7.2 Hz, ³J_{FH} = 1.7 Hz, 2H), 3.68 (dd, ³J_{PH} = 23.8 Hz, ²J_{HH} = 16.2 Hz, 1H), 3.58 (d, ³J_{PH} = 10.8 Hz, 3H), 3.49 (d, ³J_{PH} = 10.8 Hz, 3H), 3.44 (dd, ³J_{PH} = 8.2 Hz, ²J_{HH} = 16.2 Hz, 1H), 2.39 (s, 3H), 1.28 (t, ³J_{HH} = 7.1 Hz, 3H). ¹³C{¹H} NMR (75 MHz, CDCl₃) δ 170.0 (d, ³J_{PC} = 6.8 Hz, C_{quat}), 143.7 (C_{quat}), 138.9 (C_{quat}), 138.6 (d, ²J_{PC} = 6.6 Hz, C_{quat}), 130.4 (dq, ²J_{FC} = 32.8 Hz, ⁵J_{PC} = 3.0 Hz, C_{quat}), 129.3 (CH), 128.8 (d, ³J_{PC} = 5.0 Hz, CH), 127.5 (CH), 124.7 (m, CH), 123.9 (q, ¹J_{FC} = 272.4 Hz, C_{quat}), 62.0 (d, ¹J_{PC} = 152.8 Hz, C_{quat}), 61.3 (CH₂), 54.8 (d, ²J_{PC} = 7.4 Hz, CH₃), 54.4 (d, ²J_{PC} = 7.6 Hz, CH₃), 38.1 (CH₂), 21.6 (CH₃), 14.3 (CH₃). ³¹P NMR (120 MHz, CDCl₃): δ 21.9. ¹⁹F NMR (282 MHz, CDCl₃) δ −63.4. FTIR (neat) ν_{max} 3261 (N-H), 1735 (C=O), 1327 (O=S=O), 1263 (P=O), 1163 (O=S=O). HRMS (ESI-TOF) *m/z*: calcd for C₂₁H₂₆F₃NO₇PS [M + H]⁺ 524.1114, found 524.1121.

Ethyl 3-(dimethoxyphosphoryl)-3-((4-methylphenyl)sulfonamido)-3-(4-nitrophenyl)propanoate (7q). The general procedure was followed, starting from imine **3q** (412 mg, 1 mmol) to afford 425 mg (85%) of **7q** as a white solid. M.p. (CH₂Cl₂-hexanes). 129–130 °C. ¹H NMR (400 MHz, CDCl₃) δ 7.96 (d, ³J_{HH} = 9.0 Hz, 2H), 7.56 (dd, ³J_{HH} = 9.0 Hz, ³J_{PH} = 2.3 Hz, 2H), 7.50 (d, ³J_{HH} = 8.2 Hz, 2H), 7.17 (d, ³J_{HH} = 8.2 Hz, 2H), 6.30 (d, ³J_{PH} = 10.3 Hz, 1H), 4.16 (m, 2H), 3.62 (dd, ²J_{HH} = 16.5 Hz, ³J_{PH} = 6.2 Hz, 1H), 3.58 (d, ³J_{PH} = 10.8 Hz, 3H), 3.55 (d, ³J_{PH} = 10.7 Hz, 3H), 3.48 (dd, ²J_{HH} = 16.5 Hz, ³J_{PH} = 8.2 Hz, 1H), 2.41 (s, 3H), 1.27 (t, ³J_{HH} = 7.2 Hz, 3H). ¹³C{¹H} NMR (101 MHz, CDCl₃) δ 169.7 (d, ³J_{PC} = 7.6 Hz, C_{quat}), 147.4 (d, ⁵J_{PC} = 3.4 Hz, C_{quat}), 144.1 (C_{quat}), 142.5 (d, ²J_{PC} = 6.6 Hz, C_{quat}), 138.8 (d, ⁴J_{PC} = 1.4 Hz, C_{quat}), 129.4 (CH), 129.3 (d, ³J_{PC} = 5.0 Hz, CH), 127.5 (CH), 122.8 (d, ⁴J_{PC} = 2.6 Hz, CH), 62.3 (d, ¹J_{PC} = 152.2 Hz, C_{quat}), 61.4 (CH₂), 54.9 (d, ²J_{PC} = 7.3 Hz, CH₃), 54.6 (d, ²J_{PC} = 7.5 Hz, CH₃), 38.3 (CH₂), 21.7 (CH₃), 14.2 (CH₃). ³¹P NMR (120 MHz, CDCl₃): δ 21.2. FTIR (neat) ν_{max} 3272 (N-H), 1743 (C=O), 1349 (O=S=O), 1244 (P=O), 1163 (O=S=O). HRMS (ESI-TOF) *m/z*: calcd for C₂₀H₂₆N₂O₉PS [M + H]⁺ 501.1091, found 501.1098.

Ethyl 3-(5-chlorothiophen-2-yl)-3-(dimethoxyphosphoryl)-3-((4-methylphenyl)sulfonamido)propanoate (7r). The general procedure was followed, starting from imine **3r** (407 mg, 1 mmol) to afford 378 mg (76%) of **7r** as a pale brown solid. M.p. (CH₂Cl₂-hexanes). 93–94 °C. ¹H NMR (400 MHz, CDCl₃) δ 7.48 (d, ³J_{HH} = 8.3 Hz, 2H), 7.17 (d, ³J_{HH} = 8.3 Hz, 2H), 6.79 (dd, ³J_{HH} = 4.0 Hz, ⁴J_{PH} = 3.4 Hz, 1H), 6.61 (d, ³J_{HH} = 4.0 Hz, 1H), 6.23 (d, ³J_{PH} = 7.2 Hz, 1H), 4.20 (q, ³J_{HH} = 7.2 Hz, 2H), 3.68 (d, ³J_{PH} = 10.7 Hz, 3H), 3.66 (d, ³J_{PH} = 10.5 Hz, 3H), 3.61 (m, 1H), 3.21 (dd, ²J_{HH} = 15.5 Hz, ³J_{PH} = 7.1 Hz, 1H), 2.40 (s, 3H), 1.30 (t, ³J_{HH} = 7.2 Hz, 3H). ¹³C{¹H} NMR (101 MHz, CDCl₃) δ 169.5 (d, ³J_{PC} = 5.6 Hz, C_{quat}), 143.6 (C_{quat}),

138.7 (d, $^4J_{PC} = 1.4$ Hz, C_{quat}), 135.9 (d, $^2J_{PC} = 7.7$ Hz, C_{quat}), 132.3 (d, $^5J_{PC} = 3.6$ Hz, C_{quat}), 129.3 (CH), 128.6 (d, $^3J_{PC} = 7.3$ Hz, CH), 127.5 (CH), 125.3 (d, $^4J_{PC} = 2.8$ Hz, CH), 61.4 (CH₂), 60.0 (d, $^1J_{PC} = 161.5$ Hz, C_{quat}), 55.2 (d, $^3J_{PC} = 7.3$ Hz, CH₃), 54.5 (d, $^3J_{PC} = 7.6$ Hz, CH₃), 39.0 (CH₂), 21.7 (CH₃), 14.2 (CH₃). ^{31}P NMR (120 MHz, CDCl₃): δ 20.3. FTIR (neat) ν_{max} 3270 (N-H), 1735 (C=O), 1341 (O=S=O), 1243 (P=O), 1163 (O=S=O). HRMS (ESI-TOF) m/z : calcd for C₁₈H₂₄ClNO₇PS₂ [M + H]⁺ 496.0415, found 496.0444.

Ethyl 3-([1,1'-biphenyl]-4-yl)-3-(dimethoxyphosphoryl)-3-((4-methylphenyl)sulfonamido)propanoate (7s). The general procedure was followed, starting from imine **3s** (443 mg, 1 mmol) to afford 478 mg (90%) of **7s** as a white solid. M.p. (CH₂Cl₂-hexanes). 112–113 °C. 1H NMR (400 MHz, CDCl₃) δ 7.56–7.46 (m, 4H), 7.45–7.40 (m, 5H), 7.39–7.33 (m, 2H), 7.13 (d, $^3J_{HH} = 8.3$ Hz, 2H), 6.21 (d, $^3J_{PH} = 10.5$ Hz, 1H), 4.20 (q, $^3J_{HH} = 7.2$ Hz, 2H), 3.69 (dd, $^3J_{PH} = 23.4$ Hz, $^2J_{HH} = 16.4$ Hz, 1H), 3.56 (d, $^3J_{PH} = 10.7$ Hz, 3H), 3.49 (m, 1H), 3.46 (d, $^3J_{PH} = 10.6$ Hz, 3H), 2.38 (s, 3H), 1.29 (t, $^3J_{HH} = 7.2$ Hz, 3H). $^{13}C\{^1H\}$ NMR (101 MHz, CDCl₃) δ 170.3 (d, $^3J_{PC} = 7.3$ Hz, C_{quat}), 143.3 (C_{quat}), 141.0 (d, $^5J_{PC} = 3.1$ Hz, C_{quat}), 140.1 (d, $^4J_{PC} = 1.4$ Hz, C_{quat}), 139.2 (C_{quat}), 129.2 (CH), 129.0 (CH), 128.8 (d, $^3J_{PC} = 5.1$ Hz, CH), 128.3 (C_{quat}), 127.8 (CH), 127.7 (CH), 127.1 (CH), 126.5 (d, $^4J_{PC} = 2.8$ Hz, CH), 62.1 (d, $^1J_{PC} = 153.9$ Hz, C_{quat}), 61.1 (CH₂), 54.7 (d, $^2J_{PC} = 7.4$ Hz, CH₃), 54.2 (d, $^2J_{PC} = 7.6$ Hz, CH₃), 38.2 (CH₂), 21.7 (CH₃), 14.3 (CH₃). ^{31}P NMR (120 MHz, CDCl₃): δ 22.2. FTIR (neat) ν_{max} 3308 (N-H), 1729 (C=O), 1332 (O=S=O), 1241 (P=O), 1161 (O=S=O). HRMS (ESI-TOF) m/z : calcd for C₂₆H₃₁NO₇PS [M + H]⁺ 532.1553, found 532.1555.

Methyl 3-(dimethoxyphosphoryl)-3-(3-fluorophenyl)-3-((4-methylphenyl)sulfonamido)propanoate (12). The general procedure was followed, starting from imine **3k** (417 mg, 1 mmol) to afford 372 mg (81%) of **12** as a white solid. M.p. (CH₂Cl₂-hexanes). 115–116 °C. 1H NMR (400 MHz, CDCl₃) δ 7.48 (d, $^3J_{HH} = 8.3$ Hz, 2H), 7.20–7.09 (m, 4H), 7.00 (m, 1H), 6.91 (m, 1H), 6.21 (br d, $^3J_{HH} = 7.8$ Hz, 1H), 3.73 (s, 3H), 3.64 (dd, $^3J_{PH} = 24.4$ Hz, $^2J_{HH} = 16.2$ Hz, 1H), 3.56–3.50 (m, 6H), 3.46 (dd, $^2J_{HH} = 16.2$ Hz, $^3J_{PH} = 7.6$ Hz, 1H), 2.39 (s, 3H). $^{13}C\{^1H\}$ NMR (101 MHz, CDCl₃) δ 170.6 (d, $^3J_{PC} = 6.8$ Hz, C_{quat}), 162.3 (dd, $^1J_{FC} = 246.0$ Hz, $^4J_{PC} = 3.0$ Hz, C_{quat}), 143.7 (C_{quat}), 139.0 (C_{quat}), 137.1 (m, C_{quat}), 129.5 (dd, $^3J_{FC} = 8.1$ Hz, $^4J_{PC} = 2.8$ Hz, CH), 129.3 (CH), 127.5 (CH), 123.7 (dd, $^3J_{PC} = 5.1$ Hz, $^4J_{FC} = 3.0$ Hz, CH), 116.1 (dd, $^2J_{FC} = 24.1$ Hz, $^3J_{PC} = 4.8$ Hz, CH), 115.5 (dd, $^2J_{FC} = 21.1$ Hz, $^5J_{PC} = 2.9$ Hz, CH), 62.0 (dd, $^1J_{PC} = 153.7$ Hz, $^4J_{FC} = 1.4$ Hz, C_{quat}), 54.9 (d, $^2J_{PC} = 7.7$ Hz, CH₃), 54.4 (d, $^2J_{PC} = 7.6$ Hz, CH₃), 52.3 (CH₃), 38.2 (CH₂), 21.6 (CH₃). ^{31}P NMR (120 MHz, CDCl₃): δ 21.7. ^{19}F NMR (282 MHz, CDCl₃) δ -112.9. FTIR (neat) ν_{max} 3281 (N-H), 1729 (C=O), 1330 (O=S=O), 1243 (P=O), 1159 (O=S=O). HRMS (ESI-TOF) m/z : calcd for C₁₉H₂₄FNO₇PS [M + H]⁺ 460.0990, found 460.1004.

Benzyl 3-(dimethoxyphosphoryl)-3-(3-fluorophenyl)-3-((4-methylphenyl)sulfonamido)propanoate (13a). The general procedure was followed, starting from imine **3k** (417 mg, 1 mmol) to afford 449 mg (84%) of **13a** as a white solid. M.p. (CH₂Cl₂-hexanes). 78–79 °C. 1H NMR (400 MHz, CDCl₃) δ 7.47 (d, $^3J_{HH} = 8.2$ Hz, 2H), 7.41–7.31 (m, 5H), 7.17–7.08 (m, 4H), 7.03–6.98 (m, 1H), 6.94–6.87 (m, 1H), 6.24 (d, $^3J_{PH} = 10.2$ Hz, 1H), 5.19 (d, $^2J_{HH} = 12.3$ Hz, 1H), 5.13 (d, $^2J_{HH} = 12.3$ Hz, 1H), 3.73–3.63 (m, 1H), 3.57–3.34 (m, 7H), 2.38 (s, 3H). $^{13}C\{^1H\}$ NMR (101 MHz, CDCl₃) δ 169.9 (d, $^3J_{PC} = 6.9$ Hz, C_{quat}), 162.3 (dd, $^1J_{FC} = 246.0$ Hz, $^4J_{PC} = 3.0$ Hz, C_{quat}), 143.6 (C_{quat}), 139.0 (d, $^4J_{PC} = 1.3$ Hz, C_{quat}), 137.1 (C_{quat}), 135.6 (C_{quat}), 129.4 (dd, $^3J_{FC} = 8.2$ Hz, $^4J_{PC} = 2.5$ Hz, CH), 129.3 (CH), 128.7 (CH), 128.7 (CH), 128.5 (CH), 127.5 (CH), 123.7 (dd, $^3J_{PC} = 5.0$, $^4J_{FC} = 2.9$ Hz, CH), 116.0 (dd, $^2J_{FC} = 24.0$ Hz, $^3J_{PC} = 4.7$ Hz, CH), 115.4 (dd, $^2J_{FC} = 21.1$ Hz, $^5J_{PC} = 3.1$ Hz, CH), 67.0 (CH₂), 61.9 (dd, $^1J_{PC} = 153.6$ Hz, $^4J_{FC} = 1.6$ Hz, C_{quat}), 54.8 (d, $^2J_{PC} = 7.5$ Hz, CH₃), 54.3 (d, $^2J_{PC} = 7.7$ Hz, CH₃), 38.2 (CH₂), 21.6 (CH₃). ^{31}P NMR (120 MHz, CDCl₃): δ 21.6. ^{19}F NMR (282 MHz, CDCl₃) δ -112.9. FTIR (neat) ν_{max} 3281 (N-H), 1735 (C=O), 1331 (O=S=O), 1247 (P=O), 1154 (O=S=O). HRMS (ESI-TOF) m/z : calcd for C₂₅H₂₈FNO₇PS [M + H]⁺ 536.1303, found 536.1322.

Benzyl 3-(dimethoxyphosphoryl)-3-((4-methylphenyl)sulfonamido)-3-phenylpropanoate (13b). The general procedure was followed, starting from imine **3a** (367 mg, 1 mmol) to afford 476 mg (92%) of **13b** as a white solid. M.p. (CH₂Cl₂-hexanes). 84–85 °C. 1H NMR (400 MHz, CDCl₃) δ 7.46 (d, $J = 8.3$ Hz, 2H), 7.37–7.29 (m, 7H), 7.20–7.15 (m, 1H), 7.12–7.06 (m, 4H),

6.22 (d, $^3J_{PH} = 11.1$ Hz, 1H), 5.14 (d, $^2J_{HH} = 12.2$ Hz, 1H), 5.09 (d, $^2J_{HH} = 12.2$ Hz, 1H), 3.65 (dd, $^3J_{PH} = 22.3$ Hz, $^2J_{HH} = 16.6$ Hz, 1H), 3.49 (dd, $^2J_{HH} = 16.6$ Hz, $^3J_{PH} = 7.5$ Hz, 1H), 3.37 (d, $^3J_{PH} = 10.7$ Hz, 3H), 3.31 (d, $^3J_{PH} = 10.7$ Hz, 3H), 2.34 (s, 3H). $^{13}\text{C}\{^1\text{H}\}$ NMR (101 MHz, CDCl_3) δ 169.8 (d, $^3J_{PC} = 8.1$ Hz, C_{quat}), 143.1 (C_{quat}), 139.0 (d, $^4J_{PC} = 1.4$ Hz, C_{quat}), 135.5 (C_{quat}), 134.1 (d, $^2J_{PC} = 7.3$ Hz, C_{quat}), 129.0 (CH), 128.4 (CH), 128.4 (CH), 128.2 (CH), 128.2 (CH), 128.0 (d, $^3J_{PC} = 5.0$ Hz, CH), 127.8 (d, $^4J_{PC} = 2.6$ Hz, CH), 127.4 (CH), 66.5 (CH_2), 61.9 (d, $^1J_{PC} = 154.1$ Hz, C_{quat}), 54.4 (d, $^2J_{PC} = 7.4$ Hz, CH_3), 53.8 (d, $^2J_{PC} = 7.7$ Hz, CH_3), 37.7 (CH_2), 21.4 (CH_3). ^{31}P NMR (120 MHz, CDCl_3): δ 22.0. FTIR (neat) ν_{max} 3322 (N-H), 1739 (C=O), 1337 (O=S=O), 1248 (P=O), 1163 (O=S=O). HRMS (ESI-TOF) m/z : calcd for $\text{C}_{25}\text{H}_{29}\text{NO}_7\text{PS}$ $[\text{M} + \text{H}]^+$ 518.1397, found 518.1372.

Procedure for the Obtention of 3-(Dimethoxyphosphoryl)-3-((4-methylphenyl)sulfonamido)-3-phenylpropanoic acid **14**

A mixture of aminophosphonate **13b** (518 mg, 1 mmol) and Pd-C 10% (106 mg, 0.1 mmol) in MeOH (50 mL) were stirred for 12 h under H_2 atmosphere (75 psi). The mixture was then filtered on celite and concentrated under reduced pressure to yield product **14** as a white solid (402 mg, 94%), after crystallization in MeOH. M.p. (MeOH). 145–146 °C. ^1H NMR (400 MHz, CDCl_3) δ 9.91 (br s, 1H), 7.48 (d, $^3J_{HH} = 8.2$ Hz, 2H), 7.33 (d, $^3J_{HH} = 7.6$ Hz, 2H), 7.20 (m, 1H), 7.17–7.09 (m, 4H), 6.60 (d, $^3J_{PH} = 10.6$ Hz, 1H), 3.67 (dd, $^3J_{PH} = 23.9$ Hz, $^2J_{HH} = 16.0$ Hz, 1H), 3.52 (d, $^3J_{PH} = 10.8$ Hz, 3H), 3.49 (m, 1H), 3.47 (d, $^3J_{PH} = 10.6$ Hz, 3H), 2.38 (s, 3H). $^{13}\text{C}\{^1\text{H}\}$ NMR (101 MHz, CDCl_3) δ 173.5 (d, $^3J_{PC} = 7.7$ Hz, C_{quat}), 143.3 (C_{quat}), 139.2 (d, $^4J_{PC} = 1.4$ Hz, C_{quat}), 134.1 (d, $^2J_{PC} = 7.6$ Hz, C_{quat}), 129.2 (CH), 128.4 (d, $^5J_{PC} = 3.0$ Hz, CH), 128.3 (d, $^3J_{PC} = 5.1$ Hz, CH), 128.0 (d, $^4J_{PC} = 2.6$ Hz, CH), 127.6 (CH), 62.1 (d, $^1J_{PC} = 155.6$ Hz, C_{quat}), 55.1 (d, $^2J_{PC} = 7.3$ Hz, CH_3), 54.5 (d, $^2J_{PC} = 7.9$ Hz, CH_3), 38.0 (CH_2), 21.6 (CH_3). ^{31}P NMR (120 MHz, CDCl_3): δ 21.8. FTIR (neat) ν_{max} 3500–2500 (O-H st), 3271 (N-H st), 1714 (C=O st), 1337 (O=S=O st as), 1235 (P=O st), 1163 (O=S=O st sim) cm^{-1} . HRMS (ESI-TOF) m/z : calcd for $\text{C}_{18}\text{H}_{23}\text{NO}_7\text{PS}$ $[\text{M} + \text{H}]^+$ 428.0927, found 428.0901.

Procedure for the Obtention of Dimethyl (1-((4-methylphenyl)sulfonamido)-1-phenylethyl) phosphonate **18**

A solution of **3a** (367 mg, 1 mmol) in dry CH_3CN (3 mL) was stirred at room temperature under N_2 atmosphere. To this mixture, Me_2Zn (1.7 mL, 1.2 M in toluene, 2 mmol) was added and the mixture was stirred for 2h at room temperature. The reaction was quenched by a slow addition of a saturated aqueous solution of NH_4Cl (1 mL) and dried over anhydrous MgSO_4 . The solid was removed by filtration and washed with AcOEt , and the filtrate was concentrated at reduced pressure to yield the crude product, which was purified by column chromatography in silica gel (AcOEt /Hexanes) to give 326 mg (85%) of **18** as a white solid [60]. M.p. (Et_2O /pentane). 163–164 °C. Lit. 161–162 (Et_2O). ^1H NMR (400 MHz, CDCl_3) δ 7.53 (d, $^3J_{HH} = 8.3$ Hz, 2H), 7.40 (m, 2H), 7.22–7.18 (m, 3H), 7.11 (d, $^3J_{HH} = 8.2$ Hz, 2H), 5.78 (d, $^3J_{PH} = 8.1$ Hz, 1H), 3.70 (d, $^3J_{PH} = 10.4$ Hz, 3H), 3.35 (d, $^3J_{PH} = 10.4$ Hz, 3H), 2.36 (s, 3H), 1.97 (d, $^3J_{PH} = 16.8$ Hz, 3H). $^{13}\text{C}\{^1\text{H}\}$ NMR (75 MHz, CDCl_3) δ 142.3 (C_{quat}), 141.8 (d, $^4J_{PC} = 1.7$ Hz, C_{quat}), 133.4 (C_{quat}), 128.6 (CH), 128.4 (d, $^3J_{PC} = 6.0$ Hz, CH), 128.1 (d, $^4J_{PC} = 2.2$ Hz, CH), 128.0 (d, $^5J_{PC} = 2.9$ Hz, CH), 126.7 (CH), 61.1 (d, $^1J_{PC} = 152.2$ Hz, C_{quat}), 54.5 (d, $^2J_{PC} = 7.1$ Hz, CH_3), 53.9 (d, $^2J_{PC} = 7.0$ Hz, CH_3), 21.3 (CH_3), 20.4 (d, $^2J_{PC} = 5.2$ Hz CH_3). ^{31}P NMR (120 MHz, CDCl_3) δ 26.1. FTIR (neat) ν_{max} 3315 (N-H), 1327 (O=S=O), 1242 (P=O), 1166 (O=S=O). HRMS (ESI-TOF) m/z : calcd. for $\text{C}_{17}\text{H}_{22}\text{NO}_5\text{PS}$ $[\text{M} + \text{Na}]^+$ 406.0848, found 406.0856.

3.2. Biology

3.2.1. Materials

Reagents and solvents were used as purchased without further purification. All stock solutions of the investigated compounds were prepared by dissolving the powdered materials in appropriate amounts of dimethylsulfoxide (DMSO). The final concentration

of DMSO never exceeded 5% (*v/v*) in the reactions. The stock solution was stored at 5 °C until it was used.

3.2.2. Cell Culture

Human epithelial lung carcinoma cells (A549) (ATCC[®] CCL-185[™], ATCC, Manassas, VA, USA) were grown in Kaighn's Modification of Ham's F-12 Medium (ATCC[®] 30-2004[™], ATCC, Manassas, VA, USA) and lung fibroblast cells (MRC5) (ATCC[®] CCL-171[™], ATCC, Manassas, VA, USA) were grown in Eagle's Minimum Essential Medium (EMEM, ATCC[®] 30-2003[™], ATCC, Manassas, VA, USA). Epithelial ovary adenocarcinoma cells (SKOV3) (ATCC[®] HTB-77[™], ATCC, Manassas, VA, USA) were grown in McCoy's 5A medium (ATCC[®] 30-2007[™], ATCC, Manassas, VA, USA). All of them were supplemented with 10% of fetal bovine serum (FBS) (Sigma-Aldrich, Madrid, Spain) and with 1% of NORMOCIN solution (Thermo Fisher, Waltham, MA, USA). Cells were incubated at 37 °C and 5% CO₂ atmosphere, and were split every 3–4 days to maintain monolayer coverage. For the cytotoxicity experiments, the A549 and SKOV3 cells were seeded in 96-well plates at a density of $2.5\text{--}3 \times 10^3$ cells per well and incubated overnight to achieve 70% of confluence at the time of exposition to the cytotoxic compound.

3.2.3. Cytotoxicity Assays

Cells were exposed to different concentrations of the cytotoxic compounds and were incubated for 48 h. Then, 10 µL of cell counting kit-8 was added into each well for an additional two hours' incubation at 37 °C. The absorbance of each well was determined by an Automatic Elisa Reader System (Thermo Scientific Multiskan FC Automatic Elisa Reader System, Thermo Scientific, Shanghai, China) at 450 nm wavelength.

4. Conclusions

In conclusion, we report an efficient methodology for the preparation of phosphonate analogs of aspartic acid, holding a variety of substituents at their α -aromatic ring. α -Ketiminophosphonates are generated by the oxidation of their parent tertiary α -aminophosphonates and a subsequent aza-Reformatsky reaction with alkyl iodoacetate derivatives. Moreover, this methodology has been successfully extended to aldimines and activated ketimines, affording the Reformatsky products in high yields. This strategy allows the possibility of assorted structural diversity in the resultant scaffold depending on the starting imine or alkyl iodoacetate. Moreover, the phosphorylated analogues of aspartic acid **6** showed in vitro cytotoxicity inhibiting the growth of human tumor cell lines SKOV3 (human ovarian carcinoma) and A549 (carcinomic human alveolar basal epithelial cell), and a high selectivity toward the MRC5 non-malignant lung fibroblasts. The most active substrates were proved to be ethyl ester derivatives. Although *p*-tolyl derivatives showed the best result against A549, the introduction of a trifluoromethylphenyl moiety in the para position exhibited the most remarkable IC₅₀ value against the SKOV3 cell line. Moreover, the majority of the compounds were selective toward the non-malignant cells. The best IC₅₀ values obtained are 9.80 µM in the SKOV3 cell line for α -aminophosphonate **7p**, with a *p*-trifluorophenyl substituent, and 0.34 µM in the A549 cell line for substrate **7k**, holding a *p*-methylphenyl moiety. Most of the compounds presented in this study show low micromolar activity and a high selectivity toward the non-malignant cells. It has also been proved that the absolute configuration of the tetrasubstituted stereocenter does not have any influence on the biological activity of the phosphorylated aspartic acid derivatives, since both enantiomers of substrate **7k** showed similar IC₅₀ values.

Supplementary Materials: The following supporting information can be downloaded at: <https://www.mdpi.com/article/10.3390/molecules27228024/s1>, ¹H, ¹³C, ³¹P and ¹⁹F copies of compounds **5**, **6**, **7**, **12**, **13**, **14** and **18**. 2D-NMR of compound **7a**.

Author Contributions: Conceptualization, X.d.C., A.M., F.P. and J.V.; methodology: evaluation of the in vitro antiproliferative activity, X.d.C.; methodology: organic synthesis, A.M. and A.L.-F.;

software, X.d.C. and A.M.; validation, J.V.; formal analysis, X.d.C. and A.M.; investigation, X.d.C., A.M. and A.L.-F.; resources, F.P. and J.V.; data curation, X.d.C., A.M. and A.L.-F.; writing—original draft preparation, J.V.; writing—review and editing, X.d.C., A.M., A.L.-F., F.P. and J.V.; visualization, F.P. and J.V.; supervision, J.V.; project administration, F.P. and J.V.; funding acquisition, F.P. and J.V. All authors have read and agreed to the published version of the manuscript.

Funding: Financial support by Ministerio de Economía, Industria y Competividad (PID2021-122558OB-I00) and Gobierno Vasco (GV-IT1701-22) is gratefully acknowledged. X.d.C. and A.L.-F. thank the Basque Country Government for a predoctoral grant.

Institutional Review Board Statement: Not applicable.

Informed Consent Statement: Not applicable.

Data Availability Statement: The data presented in this study are available in the supplementary materials file or on request from the corresponding author (^1H , ^{13}C , ^{19}F and ^{31}P -NMR and HRMS spectra and cytotoxicity essays).

Acknowledgments: The authors thank for the technical and human support provided by SGIker (UPV/EHU/ERDF, EU).

Conflicts of Interest: The authors declare no conflict of interest.

Sample Availability: Samples of the compounds are not available.

References





- Légaré, J. Population Aging: Economic and Social Consequences. In *International Encyclopedia of the Social & Behavioral Sciences*, 2nd ed.; Elsevier: Oxford, UK, 2015; p. 540.
- Foreman, K.J.; Marquez, N.; Dolgert, A.; Fukutaki, K.; Fullman, N.; McGaughey, M.; Pletcher, M.A.; Smith, A.E.; Tang, K.; Yuan, C.-W.; et al. Forecasting life expectancy, years of life lost, and all-cause and cause-specific mortality for 250 causes of death: Reference and alternative scenarios for 2016–40 for 195 countries and territories. *Lancet* **2018**, *392*, 2052. [CrossRef]
- Ferlay, J.; Soerjomataram, I.; Dikshit, R.; Eser, S.; Mathers, C.; Rebelo, M.; Parkin, D.M.; Forman, D.; Bray, F. Cancer incidence and mortality worldwide: Sources, methods and major patterns in GLOBOCAN 2012. *Int. J. Cancer* **2015**, *136*, E359. [CrossRef] [PubMed]
- Bidram, E.; Esmaili, Y.; Ranji-Burachaloo, H.; Al-Zaubai, N.; Zarrabi, A.; Stewart, A. A concise review on cancer treatment methods and delivery systems. *J. Drug Deliv. Sci. Technol.* **2019**, *54*, 101350. [CrossRef]
- Dickens, E.; Ahmed, S. Principles of cancer treatment by chemotherapy. *Surgery* **2018**, *36*, 134–138.
- Cree, I.A.; Charlton, P. Molecular chess? Hallmarks of anti-cancer drug resistance. *BMC Cancer* **2017**, *17*, 10. [CrossRef] [PubMed]
- Housman, G.; Byler, S.; Heerboth, S.; Lapinska, K.; Longacre, M.; Snyder, N.; Sarkar, S. Drug resistance in cancer: An overview. *Cancers* **2014**, *6*, 1769. [CrossRef]
- Horsman, G.P.; Zechel, D.L. Phosponate biochemistry. *Chem. Rev.* **2017**, *117*, 5704–5783. [CrossRef]
- Emadi, A.; Jones, R.J.; Brodsky, R.A. Cyclophosphamide and cancer: Golden anniversary. *Nat. Rev. Clin. Oncol.* **2009**, *6*, 638. [CrossRef]
- Msaouel, P.; Galanis, E.; Koutsilieris, M. Somatostatin and somatostatin receptors: Implications for neoplastic growth and cancer biology. *Expert Op. Investig. Drugs* **2009**, *18*, 1297. [CrossRef]
- Caraglia, M.; D'Alessandro, A.M.; Marra, M.; Giuberti, G.; Vitale, G.; Viscomi, C.; Colao, A.M.; del Prete, S.; Tagliaferri, P.; Tassone, P.; et al. The farnesyl transferase inhibitor R115777 (Zarnestra®) synergistically enhances growth inhibition and apoptosis induced on epidermoid cancer cells by Zoledronic acid (Zometa®) and Pamidronate. *Oncogene* **2004**, *23*, 6900. [CrossRef]
- Kukhar, V.P.; Hudson, H.R. (Eds.) Aminophosphonic and Aminophosphinic Acids. In *Chemistry and Biological Activity*; Wiley: Chichester, UK, 2000.
- Moonen, K.; Laureyn, I.; Stevens, C.V. Synthetic Methods for Azaheterocyclic Phosphonates and Their Biological Activity. *Chem. Rev.* **2004**, *104*, 2177. [CrossRef] [PubMed]
- Berlicki, L.; Kafarski, P. Computer-Aided Analysis and Design of Phosphonic and Phosphinic Enzyme Inhibitors as Potential Drugs and Agrochemicals. *Curr. Org. Chem.* **2005**, *9*, 1829. [CrossRef]
- Kafarski, P.; Lejczak, B. Aminophosphonic Acids of Potential Medical Importance. *Curr. Med. Chem. Anti Cancer Ag.* **2001**, *1*, 301. [CrossRef]
- Reddy, M.V.N.; Balakrishna, A.; Kumar, M.A.; Reddy, G.C.S.; Sankar, A.U.R.; Reddy, C.S.; Krishna, T.M. One-Step Synthesis and Bioassay of *N*-Phosphoramidophosphonates. *Chem. Pharm. Bull.* **2009**, *57*, 1391. [CrossRef]
- Che, J.-Y.; Xu, X.-Y.; Tang, Z.-L.; Gu, Y.-C.; Shi, D.-G. Synthesis and herbicidal activity evaluation of novel α -amino phosphonate derivatives containing a uracil moiety. *Bioorg. Med. Chem. Lett.* **2016**, *26*, 1310. [CrossRef] [PubMed]
- Reddy, M.V.N.; Kumar, B.S.; Balakrishna, A.; Reddy, C.S.; Nayak, S.K.; Reddy, C.D. One-pot synthesis of novel α -amino phosphonates using tetramethylguanidine as a catalyst. *Arkivoc* **2007**, *15*, 246. [CrossRef]

19. Dake, S.A.; Raut, D.S.; Kharat, K.R.; Mhaske, R.S.; Deshmukh, S.U.; Pawar, R.P. Ionic liquid promoted synthesis, antibacterial and in vitro antiproliferative activity of novel α -aminophosphonate derivatives. *Bioorg. Med. Chem. Lett.* **2011**, *21*, 2527. [CrossRef]
20. El-Sayed, N.; Ewies, E.F.; Boulos, L.S.; Moharam, M.E. Synthesis of Novel Alkyl (dialkoxyphosphoryl)-1*H*-indole-3-yl)acetate, Dialkoxyphosphoryl[2,3 *b*]indole-3-carboxylate and Dialkyl methyl phosphonate Derivatives Using Wittig-Horner Reagents and their Antimicrobial Activity. *Res. J. Pharm. Biol. Chem. Sci.* **2014**, *5*, 926.
21. Sivala, M.R.; Devineni, S.R.; Golla, M.; Medarametla, V.; Pothuru, G.K.; Chamarthi, N.R. A heterogeneous catalyst, SiO₂-ZnBr₂: An efficient neat access for α -aminophosphonates and antimicrobial activity evaluation. *J. Chem. Sci.* **2016**, *128*, 1303. [CrossRef]
22. Rao, K.U.M.; Swapna, S.; Manidhar, D.M.; Reddy, K.M.K.; Reddy, C.S. Efficient Synthesis of α -Aminophosphonates and Evaluation of Significance of P=O Group towards Antioxidant Activity. *Phosphorus Sulfur Silicon Relat. Elem.* **2015**, *190*, 232. [CrossRef]
23. Damiche, R.; Chafaa, S. Synthesis of new bioactive aminophosphonates and study of their antioxidant, anti-inflammatory and antibacterial activities as well the assessment of their toxicological activity. *J. Mol. Struct.* **2017**, *1130*, 1009. [CrossRef]
24. Srikant, B.; Parth, S.; Garg, S.K.; Misha, S.; Kaur, P.K.; Singh, S.; Chakrabarti, K.A. α -Aminophosphonates as novel anti-leishmanial chemotypes: Synthesis, biological evaluation, and CoMFA studies. *MedChemCom.* **2014**, *5*, 665.
25. Mulla, S.A.R.; Pathay, M.Y.; Chavan, S.; Gample, S.P.; Sarkar, D. Highly efficient one-pot multi-component synthesis of α -aminophosphonates and bis- α -aminophosphonates catalyzed by heterogeneous reusable silica supported dodecatungstophosphoric acid (DTP/SiO₂) at ambient temperature and their antitubercular evaluation against Mycobacterium Tuberculosis. *RSC Adv.* **2014**, *4*, 7666.
26. Bhattacharya, A.K.; Raunt, D.S.; Rana, K.C.; Polanki, I.K.; Khan, M.S.; Tram, S. Diversity-oriented synthesis of α -aminophosphonates: A new class of potential anticancer agents. *Eur. J. Med. Chem.* **2013**, *66*, 146. [CrossRef]
27. Yao, G.-Y.; Ye, M.-Y.; Huang, R.-Z.; Li, Y.-J.; Pan, Y.-J.; Xu, Q.; Liao, Z.-X.; Wang, H.-S. Synthesis and antitumor activities of novel rhein α -aminophosphonates conjugates. *Bioorg. Med. Chem. Lett.* **2014**, *24*, 501. [CrossRef]
28. Wang, Q.; Yang, L.; Ding, H.; Chen, X.; Wang, H.; Tang, X. Synthesis, X-ray crystal structure, DNA/protein binding and cytotoxicity studies of five α -aminophosphonate *N*-derivatives. *Bioorg. Chem.* **2016**, *69*, 132. [CrossRef]
29. Huang, R.-Z.; Wang, C.-Y.; Li, J.-F.; Yao, G.-Y.; Pang, Y.-M.; Ye, M.-Y.; Wang, H.-S.; Zhang, Y. Synthesis, antiproliferative and apoptosis-inducing effects of novel asiatic acid derivatives containing α -aminophosphonates. *RSC Adv.* **2016**, *6*, 62890. [CrossRef]
30. Johnson, E.C. Aspartic acid. In *Reference Module in Biomedical Sciences*; Elsevier: Amsterdam, The Netherlands, 2017.
31. Qian, R.; Kuliszewska, E.; Macoratti, E.; Hammerschmidt, F. Chemoenzymatic Synthesis of Racemic and Enantiomerically Pure Phosphaaspartic Acid and Phosphaarginine. *Eur. J. Org. Chem.* **2017**, *2017*, 4836. [CrossRef]
32. Łyzwa, P.; Błaszczczyk, J.; Sieroń, L.; Mikołajczyk, M. Asymmetric Synthesis of Structurally Diverse Aminophosphonic Acids by Using Enantiopure *N*-(*p*-Tolylsulfinyl)cinnamaldimines as Reagents. *Eur. J. Org. Chem.* **2013**, *2013*, 2106. [CrossRef]
33. Campbell, M.M.; Carruthers, N.I.; Mickel, S.J. Aminophosphonic and aminophosphinic acid analogues of aspartic acid. *Tetrahedron* **1982**, *38*, 2513. [CrossRef]
34. Vaseila, A.; Voeffray, R. Asymmetric Synthesis of α -Aminophosphonic Acids by Cycloaddition of *N*-Glycosyl-*C*-dialkoxyposphonoylnitrones. *Helv. Chim. Acta* **1982**, *65*, 1953. [CrossRef]
35. Kobayashi, S.; Kiyohara, H.; Nakamura, Y.; Matsubara, R. Catalytic Asymmetric Synthesis of α -Amino Phosphonates Using Enantioselective Carbon–Carbon Bond-Forming Reactions. *J. Am. Chem. Soc.* **2004**, *126*, 6558. [CrossRef] [PubMed]
36. Wang, X.-Q.; Feng, F.-F.; Nie, J.; Zhang, F.-G.; Ma, J.-A. Enantioselective Construction of Amino Carboxylic-Phosphonic Acid Derivatives Enabled by Chiral Amino Thiourea-Catalyzed Decarboxylative Mannich Reaction. *Adv. Synth. Catal.* **2022**, *364*, 1908. [CrossRef]
37. Shao, Q.; Wu, L.; Chen, J.; Gridnev, I.D.; Yang, G.; Xie, F.; Zhang, W. Copper (II)/RuPHOX-Catalyzed Enantioselective Mannich-Type Reaction of Glycine Schiff Bases with Cyclic Ketimines. *Adv. Synth. Catal.* **2018**, *360*, 4625. [CrossRef]
38. Ranu, B.C.; Hajra, A.; Jana, U. General Procedure for the Synthesis of α -Amino Phosphonates from Aldehydes and Ketones Using Indium(III) Chloride as a Catalyst. *Org. Lett.* **1999**, *1*, 1141. [CrossRef]
39. Liu, Y.-J.; Nie, J.-S.L.J.; Ma, J.-A. Organocatalytic Asymmetric Decarboxylative Mannich Reaction of β -Keto Acids with Cyclic α -Ketiminophosphonates: Access to Quaternary α -Aminophosphonates. *Org. Lett.* **2018**, *20*, 3643. [CrossRef]
40. Ross, N.A.; MacGregor, R.R.; Bartsch, R.A. Synthesis of β -lactams and β -aminoesters via high intensity ultrasound-promoted Reformatsky reactions. *Tetrahedron* **2004**, *60*, 2035. [CrossRef]
41. Brinner, K.; Doughan, B.; Poon, D.J. Scalable Synthesis of β -Amino Esters via Reformatsky Reaction with *N*-tert-Butanesulfinyl Imines. *Synlett* **2009**, *2009*, 991. [CrossRef]
42. Su, L.; Xu, M.-H. Asymmetric Reformatsky-Type Reaction of Isatin-Derived *N*-Sulfinyl Ketimines: Efficient and Practical Synthesis of Enantiopure Chiral 2-Oxindoliny- β 3,3-Amino Esters. *Synthesis* **2016**, *48*, 2595.
43. Jing, Z.T.; Huang, Y.G.; Qing, F.L. Synthesis of α -fluoro- β -amino acids via the Reformatsky reaction of chiral *N*-tert-butylsulfinylimines with ethyl bromofluoroacetate. *Chin. Chem. Lett.* **2011**, *22*, 919. [CrossRef]
44. Anan, K.; Iso, Y.; Oguma, T.; Nakahara, K.; Suzuki, S.; Yamamoto, T.; Matsuoka, E.; Ito, H.; Sakaguchi, G.; Ando, S.; et al. Trifluoromethyl Dihydrothiazine-Based β -Secretase (BACE1) Inhibitors with Robust Central β -Amyloid Reduction and Minimal Covalent Binding Burden. *ChemMedChem* **2019**, *14*, 1894. [CrossRef] [PubMed]
45. Woltering, T.J.; Wostl, W.; Hilpert, H.; Rogers-Evans, M.; Pinard, E.; Mayweg, A.; Göbel, M.; Banner, D.W.; Benz, J.; Travagli, M.; et al. BACE1 inhibitors: A head group scan on a series of amides. *Bioorg. Med. Chem. Lett.* **2013**, *23*, 4239. [CrossRef]

46. Hilpert, H.; Guba, W.; Woltering, T.J.; Wostl, W.; Pinard, E.; Mauser, H.; Mayweg, A.V.; Rogers-Evans, M.; Humm, R.; Krummenacher, D.; et al. β -Secretase (BACE1) Inhibitors with High in Vivo Efficacy Suitable for Clinical Evaluation in Alzheimer's Disease. *J. Med. Chem.* **2013**, *56*, 3980. [CrossRef]
47. de Munck, L.; Vila, C.; Muñoz, M.C.; Pedro, J.R. Catalytic Enantioselective Aza-Reformatsky Reaction with Cyclic Imines. *Chem. Eur. J.* **2016**, *22*, 17590. [CrossRef] [PubMed]
48. Ukaji, Y.; Yoshida, Y.; Inomata, K. Asymmetric addition of a Reformatsky-type reagent to 3,4-dihydroisoquinoline *N*-oxides. *Tetrahedron Asymmetry* **2000**, *11*, 733–736. [CrossRef]
49. Cozzi, P.G. A Catalytic Enantioselective Imino-Reformatsky Reaction. *Adv. Synth. Catal.* **2006**, *348*, 2075. [CrossRef]
50. Yutaka, U.; Shoichi, T.; Yoshie, H.; Katsuhiko, I. Asymmetric Addition of Reformatsky-Type Reagent to Imines Utilizing Diisopropyl Tartrate as a Chiral Auxiliary. *Chem. Lett.* **2001**, *30*, 254.
51. Maestro, A.; de Marigorta, E.M.; Palacios, F.; Vicario, J. Enantioselective Aza-Reformatsky Reaction with Ketimines. *Org. Lett.* **2019**, *21*, 9473. [CrossRef]
52. del Corte, X.; López-Francés, A.; Maestro, A.; Villate-Beitia, I.; Sainz-Ramos, M.; de Marigorta, E.M.; Pedraz, J.L.; Vicario, J. A Multicomponent Protocol for the Synthesis of Highly Functionalized γ -Lactam Derivatives and Their Applications as Antiproliferative Agents. *Pharmaceuticals* **2021**, *14*, 782. [CrossRef]
53. del Corte, X.; López-Francés, A.; de Marigorta, E.M.; Palacios, F.; Vicario, J. Stereo- and Regioselective [3 + 3] Annulation Reaction Catalyzed by Ytterbium: Synthesis of Bicyclic 1,4-Dihydropyridines. *Adv. Synth. Catal.* **2021**, *363*, 4761–4771. [CrossRef]
54. del Corte, X.; López-Francés, A.; Maestro, A.; Villate-Beitia, I.; Sainz-Ramos, M.; de Marigorta, E.M.; Palacios, F.; Alonso, C.; de los Santos, J.M.; Pedraz, J.L.; et al. Multicomponent Synthesis of Unsaturated γ -Lactam Derivatives. Applications as Antiproliferative Agents through the Bioisosterism Approach: Carbonyl vs. Phosphoryl Group. *Pharmaceuticals* **2022**, *15*, 511. [CrossRef] [PubMed]
55. Maestro, A.; Martín-Encinas, E.; de Marigorta, E.M.; Alonso, C.; Rubiales, G.; Vicario, J.; Palacios, F. Synthesis of novel antiproliferative hybrid bis-(3-indolyl)methane phosphonate derivatives. *Eur. J. Med. Chem.* **2018**, *158*, 874. [CrossRef] [PubMed]
56. López-Francés, A.; del Corte, X.; de Marigorta, E.M.; Palacios, F.; Vicario, J. Ugi reaction on α -phosphorated ketimines for the synthesis of tetrasubstituted α -aminophosphonates and their applications as antiproliferative agents. *Molecules* **2021**, *26*, 1654. [CrossRef] [PubMed]
57. López-Francés, A.; del Corte, X.; Serna-Burgos, Z.; de Marigorta, E.M.; Palacios, F.; Vicario, J. Exploring the Synthetic Potential of γ -Lactam Derivatives Obtained from a Multicomponent Reaction. Applications as Antiproliferative Agents. *Molecules* **2022**, *27*, 3624. [CrossRef]
58. Maestro, A.; de Marigorta, E.M.; Palacios, F.; Vicario, J. Enantioselective α -aminophosphonate functionalization of indole ring through an organocatalyzed Friedel-Crafts reaction. *J. Org. Chem.* **2019**, *84*, 1094. [CrossRef] [PubMed]
59. Vicario, J.; Ezpeleta, J.M.; Palacios, F. Asymmetric Cyanation of α -Ketiminophosphonates Catalyzed by Cinchona Alkaloids: Enantioselective Synthesis of Tetrasubstituted α -Aminophosphonic Acid Derivatives from Trisubstituted α -Aminophosphonates. *Adv. Synth. Catal.* **2012**, *354*, 2641. [CrossRef]
60. Vicario, J.; Ortiz, P.; Palacios, F. Synthesis of Tetrasubstituted α -Aminophosphonic Acid Derivatives from Trisubstituted α -Aminophosphonates. *Eur. J. Org. Chem.* **2013**, *2013*, 7095. [CrossRef]
61. Vicario, J.; Ortiz, P.; Ezpeleta, J.M.; Palacios, F. Asymmetric Synthesis of Functionalized Tetrasubstituted α -Aminophosphonates through Enantioselective Aza-Henry Reaction of Phosphorylated Ketimines. *J. Org. Chem.* **2015**, *80*, 156. [CrossRef]
62. Pellissier, H. Recent developments in the asymmetric Reformatsky-type reaction. *Beilstein J. Org. Chem.* **2018**, *14*, 325. [CrossRef]
63. Fernández-Ibáñez, M.A.; Maciá, B.; Alonso, D.A.; Pastor, I.M. Recent Advances in the Catalytic Enantioselective Reformatsky Reaction. *Eur. J. Org. Chem.* **2013**, *2013*, 7028. [CrossRef]
64. Recio, R.; Vengut-Climent, E.; Mouillac, B.; Orcel, H.; López-Lázaro, M.; Calderón-Montañó, J.M.; Alvarez, E.; Khiar, N.; Design, I.F. synthesis and biological studies of a library of NK1-Receptor Ligands Based on a 5-arylthiosubstituted 2-amino-4,6-diaryl-3-cyano-4*H*-pyran core: Switch from antagonist to agonist effect by chemical modification. *Eur. J. Med. Chem.* **2017**, *138*, 644. [CrossRef] [PubMed]
65. Barreiro, E.J.; Kümmerle, A.E.; Fraga, C.A.M. The Methylation Effect in Medicinal Chemistry. *Chem. Rev.* **2011**, *111*, 5215. [CrossRef]
66. Schönherr, H.; Cernak, T. Profound methyl effects in drug discovery and a call for new C-H methylation reactions. *Angew. Chem. Int. Ed.* **2013**, *52*, 12256. [CrossRef] [PubMed]
67. Müller, K.; Faeh, C.; Diederich, F. Fluorine in pharmaceuticals: Looking beyond intuition. *Science* **2007**, *317*, 1881. [CrossRef] [PubMed]
68. Shah, P.; Westwell, A.D. The role of fluorine in medicinal chemistry. *J. Enzyme Inhib. Med. Chem.* **2007**, *22*, 527. [CrossRef] [PubMed]
69. Bégué, J.P.; Bonnet-Delpon, D. *Bioorganic and Medicinal Chemistry of Fluorine*; Wiley: Hoboken, NJ, USA, 2007; 365p.

Article

One-Pot Phosphonylation of Heteroaromatic Lithium Reagents: The Scope and Limitations of Its Use for the Synthesis of Heteroaromatic Phosphonates

Ewa Chmielewska ^{1,*} , Natalia Miodowska ¹ , Błażej Dziuk ², Mateusz Psurski ³  and Paweł Kafarski ⁴ 

¹ Department of Bioorganic Chemistry, Faculty of Chemistry, Wrocław University of Science and Technology, Wybrzeże Wyspiańskiego 27, 50-370 Wrocław, Poland

² Department of Inorganic and Structural Chemistry, Faculty of Chemistry, University of Opole, ul. Oleska 48, 45-052 Opole, Poland

³ Laboratory of Experimental Anticancer Therapy, Department of Experimental Oncology, Ludwik Hirszfeld Institute of Immunology and Experimental Therapy, Polish Academy of Sciences, Rudolfa Weigla 12, 53-114 Wrocław, Poland

⁴ Department of Chemistry, Faculty of Agriculture and Forestry, University of Warmia and Mazury, Plac Łódzki 4, 10-721 Olsztyn, Poland

* Correspondence: ewa.chmielewska@pwr.edu.pl; Tel.: +48-71-320-2977

Abstract: A one-pot lithiation–phosphonylation procedure was elaborated as a method to prepare heteroaromatic phosphonic acids. It relied on the direct lithiation of heteroaromatics followed by phosphonylation with diethyl chlorophosphite and then oxidation with hydrogen peroxide. This protocol provided the desired phosphonates with satisfactory yields. This procedure also had some limitations in its dependence on the accessibility and stability of the lithiated heterocyclic compounds. The same procedure could be applied to phosphonylation of aromatic compounds, which do not undergo direct lithiation and thus require the use of their bromides as substrates. The obtained compounds showed weak antiproliferative activity when tested on three cancer cell lines.

Citation: Chmielewska, E.; Miodowska, N.; Dziuk, B.; Psurski, M.; Kafarski, P. One-Pot Phosphonylation of Heteroaromatic Lithium Reagents: The Scope and Limitations of Its Use for the Synthesis of Heteroaromatic Phosphonates. *Molecules* **2023**, *28*, 3135. <https://doi.org/10.3390/molecules28073135>

Academic Editor: Gabriele Micheletti

Received: 7 March 2023

Revised: 24 March 2023

Accepted: 29 March 2023

Published: 31 March 2023



Copyright: © 2023 by the authors. Licensee MDPI, Basel, Switzerland. This article is an open access article distributed under the terms and conditions of the Creative Commons Attribution (CC BY) license (<https://creativecommons.org/licenses/by/4.0/>).

Keywords: aminophosphonates; heteroaromatic; lithiation; phosphonylation; phosphonic acids; organophosphorus chemistry; P-containing drugs

1. Introduction

Useful biological and practical applications of heteroaromatic phosphonates, as well as their utility as intermediates in organic synthesis, have stimulated intensive studies directed toward methods of their preparation [1]. As indicated, this is a challenging research endeavor, and quite frequently, the yields of the applied procedures are moderate or even low [2–5]. Therefore, it is not surprising that the number of papers devoted to the elaboration of methods to prepare these compounds has increased in recent years [6–12]. The most commonly used method for the introduction of a phosphonate moiety to an sp^2 hybridized aromatic carbon atom is a palladium-catalyzed reaction [5–11]. Due to continual improvements in its conditions, catalysts, and procedures, this method provides high yields of products of variable structures. An alternative strategy is to use aryl bromides and the application of copper (I), nickel (II), or manganese (II) catalysts [2,6,13]. Finally, the formation of lithium derivatives or Grignard reagents using aryl halides as substrates may be also employed [2,6,7]. In the past decade, interesting methods of nontypical specific procedures for the synthesis of heteroaromatic phosphonates have been studied and elaborated [12,14–25].

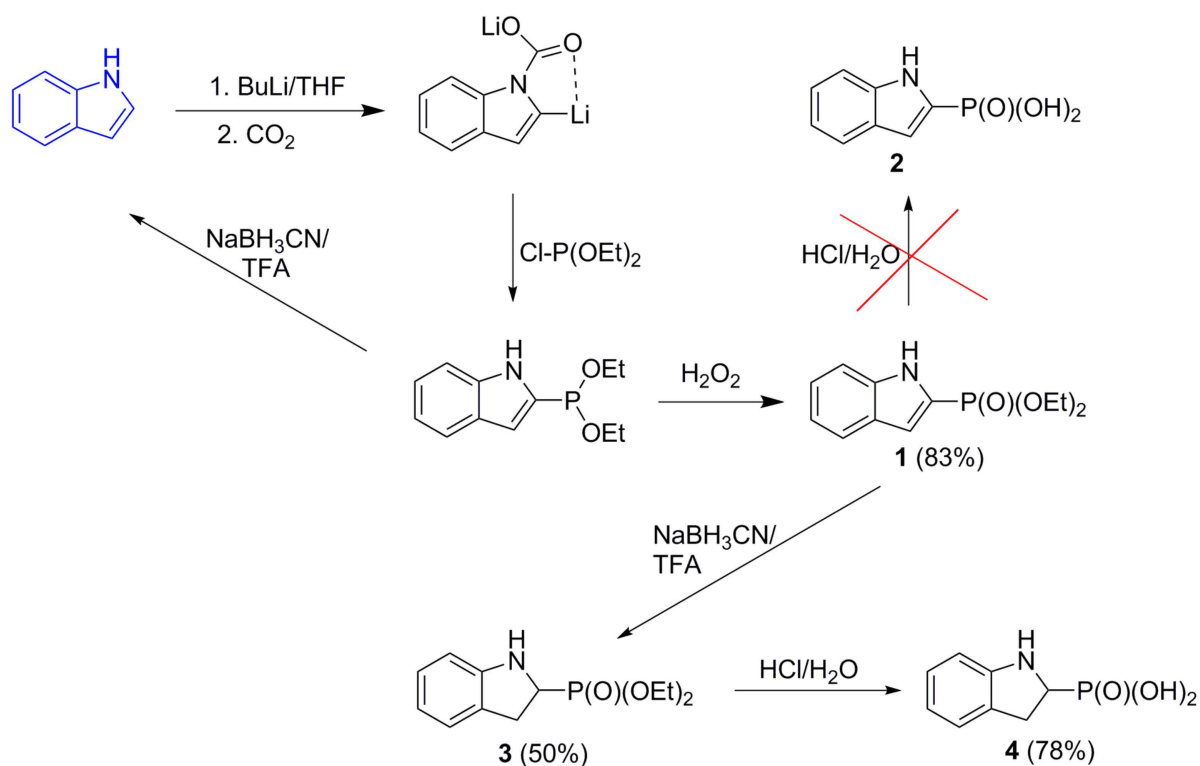
It is well known that electron-rich heterocycles easily undergo direct lithiation at Position 2 when alkyllithium is used. The formed salts are important intermediates in the syntheses of many groups of organic compounds [26–29]. Thus, the objective of this paper is to evaluate the scope and limitations of the direct lithiation of heterocyclic compounds,

followed by a one-pot reaction with chlorophosphates or chlorophosphites, applied as a method to synthesize heteroaromatic phosphonic acids. Additionally, the antiproliferative activity of the obtained phosphonic acids was evaluated using three cell lines, RAW 264.7 (used to screen for possible antiosteoporotic and anti-inflammatory activities), PC-3, and MCF-7 (human prostate cancer and breast cancer cell lines, respectively), showing a practical lack of activity of the obtained compounds.

2. Results

2.1. Chemistry

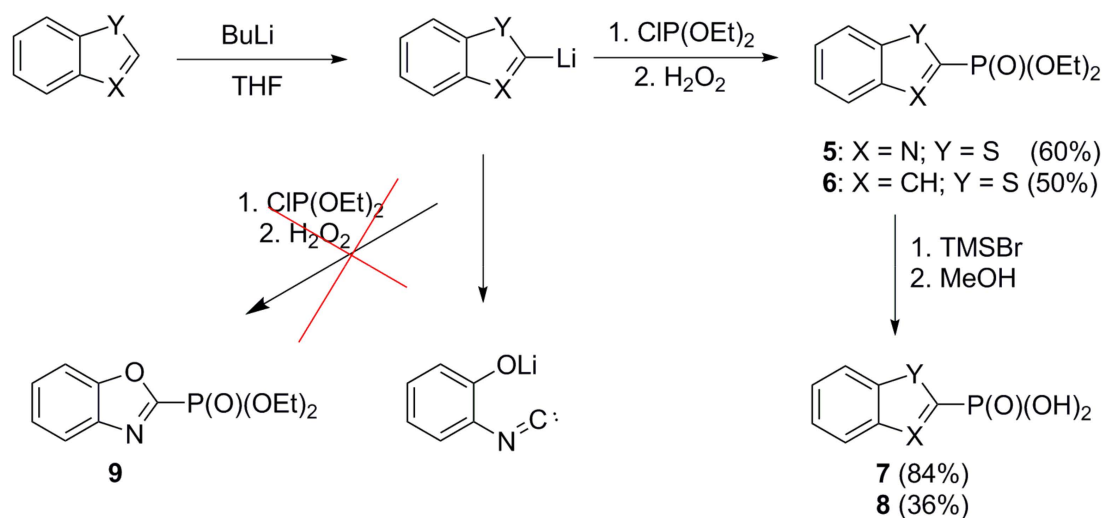
The usefulness of the direct lithiation of indole followed by phosphorylation of the formed lithium salt has been chosen as a model reaction. As shown previously, lithiation of indole with *n*-butyllithium had to be preceded by the suitable protection of the reactive amino group [28]. The use of *t*-butoxycarbonyl- (*Boc*) protection followed by reaction with trivalent phosphoryl chloride, namely, with 1-chloro-*N,N*-diisopropyl-1-methoxyphosphinamine, followed by an aqueous work-up, was described as a method for the synthesis of methyl 2-indolyl phosphinate [30]. Unfortunately, lithiated *Boc*-indole, when reacted with both diethyl chlorophosphate and chlorophosphite, failed to produce the desired product. Thus, the one-pot synthesis of Kartitzky and Akutagawa was adopted [31], which relied on the conversion of indole into 1*H*-indolyl-1-carboxylic acid prior to phosphorylation (Scheme 1). Initially, the utility of diethyl chlorophosphate as an electrophile was planned; however, the literature reports [32] suggested that better results were obtained with the use of diethyl chlorophosphite. Hydrolysis of the resulting diethyl 1*H*-indol-2-ylphosphonate (compound **1a**) in concentrated hydrochloric caused the decomposition of the obtained esters with the simultaneous formation of phosphorous acid (H_3PO_3). Moreover, the application of mild conditions for the removal of ester groups from the phosphonate moiety, by conversion of **1** into its di(trimethylsilyl) ester with trimethylchlorosilane, followed by its cleavage with methanol, also failed to deliver the desired acid **2** [33] and yielded similar products of decomposition.



Scheme 1. Phosphonylation of indole.

The reduction of diethyl 1*H*-indol-2-ylphosphonate **1** provided diethyl indoline-2-phosphonate (compound **3**), which was readily converted into the corresponding acid **4**, albeit with moderate yield. Quite unexpectedly, the hydrolysis of diethyl 1*H*-indol-2-ylphosphinate also failed, and the decomposition of the molecule with production of indole was observed.

The elaborated procedure was then used for the phosphorylation of benzothiazole and benzothiazole (Scheme 2). There was no need to apply the Kartitzky and Akuta-gawa procedure in this case. The only disadvantage of this method was the extreme instability of the lithium derivative of benzothiazole. This problem was solved by slight modifications of the synthetic procedure and reversal of the order of addition of reagents; the heterocyclic compound was added to the solution of *n*-butyllithium. Because the resulting phosphonates esters, diethyl benzo[*d*]thiazol-2-ylphosphonate **5** and diethyl benzo[*b*]thiophen-2-ylphosphonate **6**, could be unstable under harsh acidic conditions, we applied transesterification with bromotrimethylsilane for the preparation of the corresponding acids benzo[*d*]thiazol-2-ylphosphonic acid **7** and benzo[*b*]thiophen-2-ylphosphonic acid **8**.



Scheme 2. Phosphonylation of benzothiazole, benzothiophene and benzoxazole.

The phosphorylation of the lithiated benzoxazole failed, resulting in a complex mixture of products despite the modifications to the synthetic procedure. This may derive from the possible opening of the pentacyclic ring of this compound upon the action of lithium [34]. According to the published data, the opened product is in equilibrium with lithiated benzoxazole (Scheme 2); however, it did not react with diethyl chlorophosphite in the desired manner, and the compound **9** was not obtained.

In turn, the reaction of benzofuran yielded the inseparable mixture of phosphonate **10** and phosphinate **11** in moderate yield accompanied with the equimolar mixture of tri-2-benzofuryl phosphine **12** and its oxide **13**. This mixture was the major reaction product (Scheme 3). The mixture of compounds **12** and **13** readily crystallized out over time from the reaction mixture. The pure compound **13** was obtained in a small quantity only in a single case by crystallization from the spent solvent after the crystallization of the mixture of compounds **12** and **13**. The transesterification of the ester groups of the mixture of **10** and **11** with bromotrimethylsilane followed by methanolysis afforded benzofuran-2-ylphosphonic acid **14**.

hydrogen bonds, arranging the molecules in crystal packing in quite a rare and specific network (Figure 2).

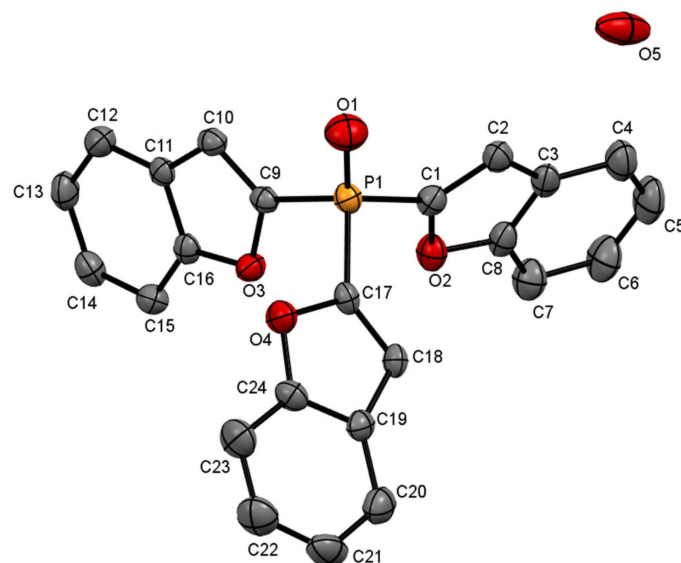


Figure 1. Compound **13** in the asymmetric part of the unit cell. The displacement ellipsoids are drawn at the 50% probability level. Hydrogen atoms are omitted for clarity.

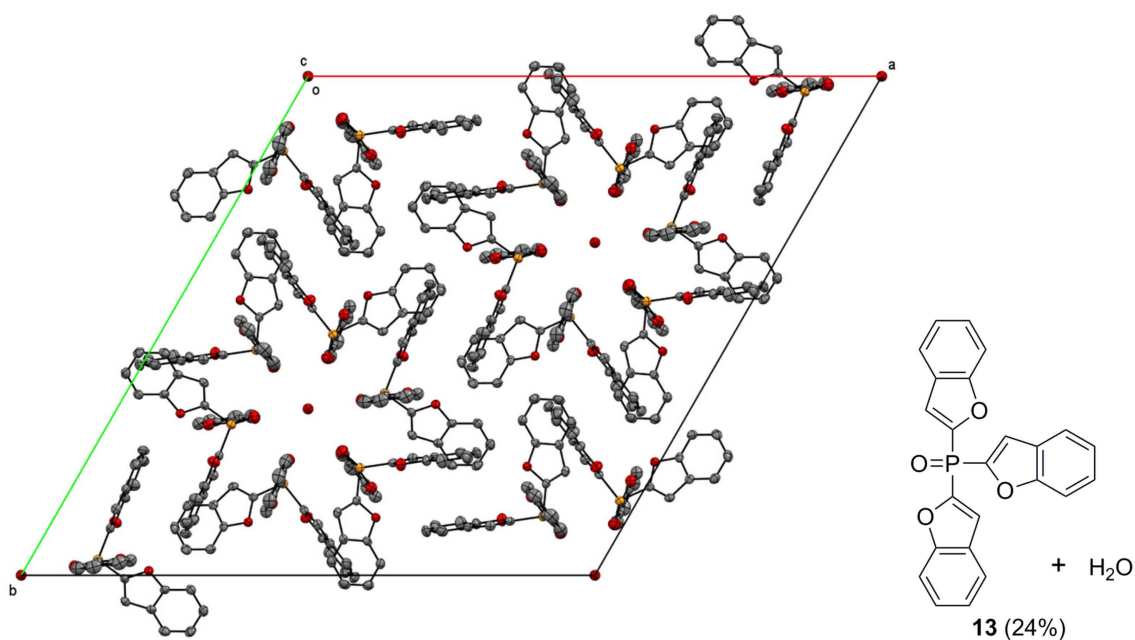
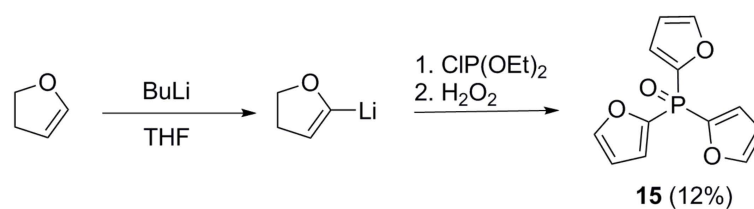


Figure 2. Crystal packing of the complex of tri-2-benzofuryl phosphine oxide **13**. The displacement ellipsoids are drawn at the 50% probability level. Hydrogen atoms are omitted for clarity.

The reaction of furan afforded a complex mixture of products from which only tri-2-furylphosphin oxide **15** was isolated in low yield (Scheme 4). Its structure was also confirmed by X-ray analysis (Figure 3).



Scheme 4. Phosphonylation of furane.

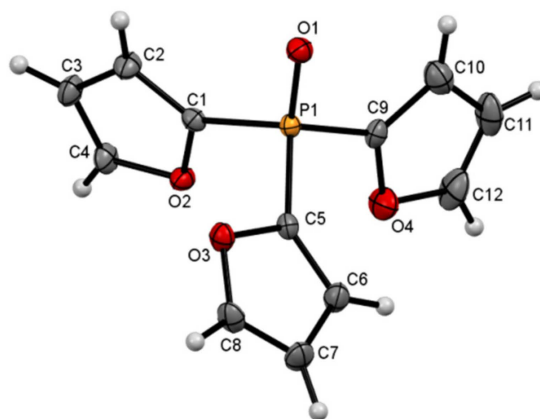


Figure 3. The crystal structure of tri-2-furylphosphinoyl oxide **15**.

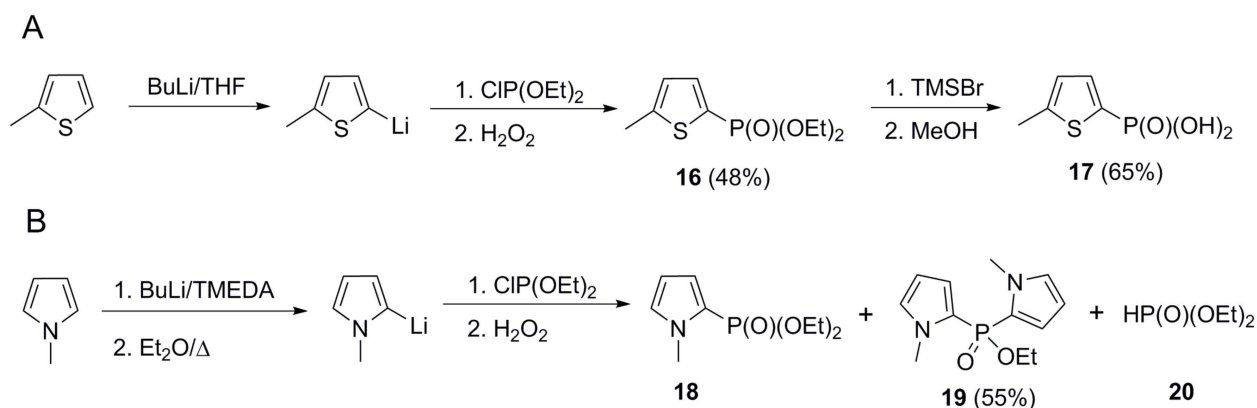
The structure of tri-2-furylphosphinoyl oxide **15** was solved in the orthorhombic crystal system and $P2_12_12_1$ space group, respectively (Figure 3). This structure was measured at room temperature and compared with the one described earlier by Jenkis and coworkers [35]. In our investigation, for the measurement series, the structure was confirmed at 100 K. In the molecular structure, the bond lengths and angles were within normal ranges [36]. The crystal structure involved intermolecular C-H...O hydrogen bonds.

It is well known that *N*-methylbenzimidazole and *N*-methylindoles undergo lithiation quite readily at C2 [27]. However, these compounds, similar to the unprotected benzimidazole, did not provide the desired phosphonates (reaction of butyllithium with trivalent phosphorus compound), and instead the predominant formations of tributyl phosphine or salts of ethyl butyl phosphinous acid were observed. Moreover, the application of the Kartitzky and Akutagawa procedure failed to provide the desired phosphinates in these cases.

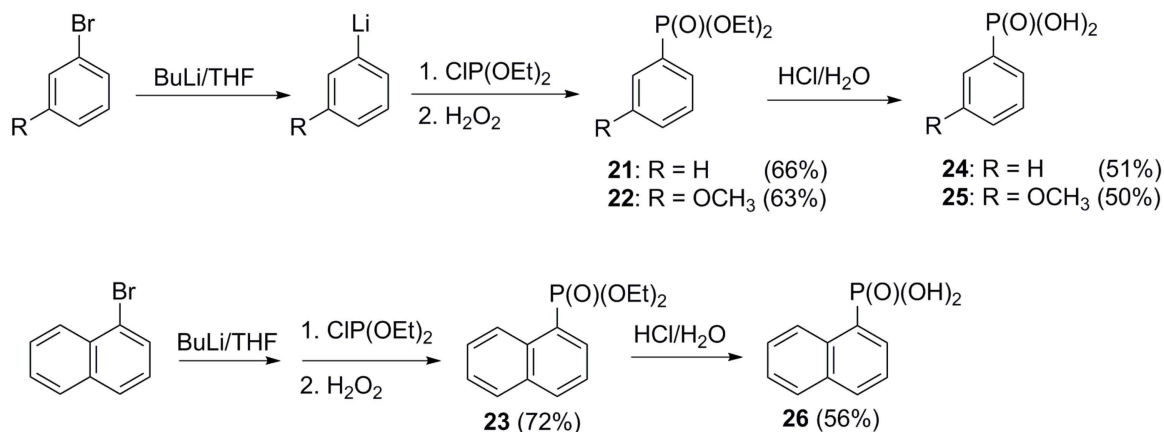
To enlarge the scope of the studied reaction, lithiation–phosphonylation of 2-methylthiophene and *N*-methylpyrrole was carried out. As expected, the 2-methylthiophene reacted readily, providing the desired diethyl 2-methylthiophen-5-yl-phosphonate **16**, which upon sequence of transesterification with trimethylbromosilane and methanolysis readily afforded 2-methylthiophene-5-yl-phosphonic acid **17** in good yield (Scheme 5A). Since *N*-methylpyrrole is not susceptible to direct lithiation [37], addition of a known lithium chelator, tetramethylethylenediamine (TMEDA), and an elevated temperature of the reaction (boiling diethyl ether instead of $-70\text{ }^\circ\text{C}$) were required to promote the reaction. In the reaction carried out in this way, an equimolar amount of chlorophosphite was added dropwise to the solution of the lithiated *N*-methylpyrrole. After oxidation with hydrogen peroxide provided the mixture of two esters, diethyl (1*H*-pyrrol-2-yl)phosphonate **18** and ethyl di(1*H*-pyrrol-2-yl)phosphinate **19** (Scheme 5B) were obtained, with compound **19** being the major. Diethyl phosphite **20** was the third product of this reaction. The reversal of the addition of the reagents (lithium reagent added to chlorophosphite solution) also provided the mixture of esters **18** and **19**, still with the predominance of compound **19**.

The utility of the elaborated procedure of direct phosphonylation was additionally proven using bromobenzene, 1-bromo-3-methoxybenzene, and 1-bromonaphthalene as substrates, since the direct lithiation of benzene, anisole, and naphthalene is impossible. As

seen from Scheme 6, in this case also, the proposed one-pot procedure had satisfactory results providing the desired diethyl phosphonates (diethyl phenylphosphonate **21**, diethyl 3-methoxyphenylphosphonate **22**, and diethyl naphthalen-1-ylphosphonate **23**), which were converted into the corresponding phosphonic acids (compounds **24**, **25**, and **26**) by hydrolysis with 6N concentrated hydrochloric acid.



Scheme 5. Phosphonylation of 2-methylthiophene (**A**) and N-methylpyrrole (**B**).



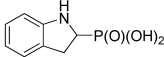
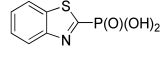
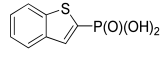
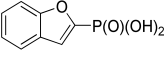
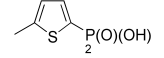
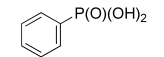
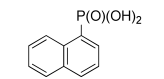
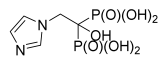
Scheme 6. Phosphonylation of bromobenzene, 1-bromo-3-methoxybenzene, and 1-bromonaphthalene.

2.2. In Vitro Antiproliferative Evaluation

The antiproliferative activities of the obtained phosphonic acids were evaluated towards three cell cultures, namely, RAW 264.7, PC-3, and MCF-7.

The choice of these lines was governed by the fact that the murine macrophage cell line, RAW 264.7, is often used to initially screen the immunomodulating activity of natural compounds [38] and is used as an osteoclast surrogate in preliminary screening for compounds inhibiting osteoclastogenesis [39], thus being promising antiosteoporotic agents. On the other hand, the PC-3 cell is considered as a classic prostate cancer cell line used as a model of androgen-independent prostate cancer [40], while MCF-7 is popular largely due to its exquisite hormone sensitivity through expression of the estrogen receptor, making it an ideal model to study the hormone response [41]. All the studied compounds appeared to be weakly active or lacked activity and could be considered as practically inactive towards these cell lines. The most active compounds are collected in Table 2.

Table 2. Structures and in vitro antiproliferative activities of the phosphonic acids against RAW 264.7 mouse macrophages, PC-3 human prostate cancer cells, and MCF-7 human breast cancer cells.

| Compound | Structure | IC ₅₀ ^a [μM] | | |
|-----------------|--|------------------------------------|--------------|--------------|
| | | RAW 264.7 | PC-3 | MCF-7 |
| 4 |  | 6.49 ± 0.139 | 4.78 ± 3.69 | 1.25 ± 0.47 |
| 7 |  | 16.95 ± 2.11 | 4.942 ± 4.08 | 5.83 ± 2.26 |
| 8 |  | 28.07 ± 17.8 | 16.03 ± 3.40 | 5.40 ± 1.55 |
| 14 |  | 18.21 ± 2.11 | 3.95 ± 4.18 | 15.78 ± 7.55 |
| 17 |  | 15.08 ± 2.47 | 10.00 ± 2.83 | 4.00 ± 2.83 |
| 24 |  | 38.91 ± 0.132 | 6.18 ± 1.02 | 8.55 ± 1.48 |
| 26 |  | 14.05 ± 3.37 | 3.96 ± 1.63 | 6.09 ± 1.73 |
| Zoledronic acid |  | 42.2 ± 8.40 | 146.0 ± 67.4 | 115.3 ± 87.6 |
| Cisplatin | (H ₂ N) ₂ PtCl ₂ | 0.93 ± 0.40 | 9.83 ± 1.70 | 6.37 ± 0.80 |

^a IC₅₀ values were determined at concentrations in the range of 1–1000 μg/mL. Values are the mean ± standard deviation from at least three experiments, performed in triplicate.

As seen in Table 2, all the studied phosphonic acids more effectively inhibited the proliferation of the RAW 264.7 cells than the effective antiosteoporotic drug, zoledronate, simultaneously being significantly less active than the popular anticancer agent cisplatin. This suggests that they could rather be considered as antiosteoporotic than anti-inflammatory agents. However, in order to determine their potential as antiosteoporotics, more detailed studies are required.

All the studied compounds exerted quite substantial antiproliferative activity towards PC-3 and MCF-7 cells, being nearly equipotent or even more active than cisplatin. In this respect, compounds **4**, **7**, **24**, and **26** were found to be the most effective. Thus, they might be considered lead substances for further studies.

3. Conclusions

A one-pot lithiation–phosphonylation procedure starting from the lithiation of a heteroaromatic compound with butyllithium, with the further reaction of an intermediate lithium salt with diethylchlorophospite, followed by the oxidation of the product with hydrogen peroxide, appeared to be an interesting alternative for the synthesis of heteroaromatic phosphonates. This simple reaction, however, had significant limitations, which were dependent on the ease of the lithiation procedure, as well as on the stability and reactivity of the lithium intermediate. The elaborated procedure was also successfully used for the preparation of aromatic phosphonates when starting from simple bromoarenes.

4. Materials and Methods

4.1. General Information

All solvents and reagents, purchased from commercial suppliers were of analytical grade and were used without further purification. Unless otherwise specified, the solvents were removed with a rotary evaporator. The ¹H-, ³¹P-, and ¹³C-NMR spectroscopic experiments were performed on a Bruker Avance II Ultrashield Plus (Bruker, Rheinstetten,

Germany) operating at 600.58 MHz (^1H), 243.12 MHz ($^{31}\text{P}\{^1\text{H}\}$), and 151.016 MHz (^{13}C), a Bruker Avance III 500 MHz (Bruker, Rheinstetten, Germany) operating at 500.14 MHz (^1H), 202.46 MHz ($^{31}\text{P}\{^1\text{H}\}$), and 125.77 MHz (^{13}C), and a JEOL JNM-ECZ 400S Research FT NMR Spectrometer (JEOL Ltd., Tokyo, Japan) operating at 399.78 MHz (^1H), 161.83 MHz ($^{31}\text{P}\{^1\text{H}\}$), and 100.53 (^{13}C). Measurements were made in CDCl_3 , D_2O , and solutions of $\text{D}_2\text{O} + \text{NaOD}$ at 300 K, and all solvents were supplied by Merck Life Science (Darmstadt, Germany). The chemical shifts are reported in ppm relative to TMS and 85% H_3PO_4 , used as external standards, and the coupling constants are reported in Hz. The melting points were determined on an SRS Melting Point Apparatus OptiMelt MPA 100 (Stanford Research Systems, Sunnyvale, CA, USA) and are reported uncorrected. The purity of all test compounds was higher than 95% by ^1H NMR and LC-MS. The mass spectra were recorded at the Faculty of Chemistry, Wrocław University of Science and Technology, using a Waters LCT Premier XE mass spectrometer (method of electrospray ionization, ESI) (Waters, Milford, MA, USA).

4.2. Crystallography

The relevant crystallographic data for the molecules and the full geometrical information are summarized in Table 2 and Supplementary Materials Table S2. The crystals were mounted on a CCD Xcalibur diffractometer (Rigaku Oxford Diffraction, Sevenoaks, Kent, UK), equipped with a CCD detector and a graphite monochromator (Rigaku Oxford Diffraction), with $\text{MoK}\alpha$ radiation, $\lambda = 0.71073 \text{ \AA}$ at 100.0 (1) K. The reciprocal space was explored by ω scans with detector positions at 60 mm distance from the crystal. The diffraction data processing of the studied compounds (Lorentz and polarization corrections were applied) was performed using the CrysAlis CCD software package version 1.171.37.33c; Oxford Diffraction Ltd: Abingdon, Oxfordshire, UK, 2005 [42]. Both crystal structures were solved by direct methods using the SHELXS-2013/1 and SHELXL-2014/7 programs [43,44]. All non-hydrogen atoms were located from difference Fourier synthesis and refined by the least squares method in the full-matrix anisotropic approximation using SHELXL14 software [42,43]. In both structures, the H atoms were located from difference Fourier synthesis. The structure drawings were prepared using the Mercury 2022.3.0 program [45].

The crystallographic data for **13** and **15** have been deposited at the Cambridge Crystallographic Data Centre as supplementary publication nos. CCDC 1904705 for **13** and CCDC 1960286 for **15**. These data can be obtained free of charge via <http://www.ccdc.cam.ac.uk/conts/retrieving.html> (accessed on 5 March 2023) or from the Cambridge Crystallographic Data Centre, 12 Union Road, Cambridge CB2 1EZ, UK; fax: 144-1223-336-033; email: deposit@ccdc.cam.ac.uk.

4.3. General Procedure for the Synthesis

4.3.1. Preparation of Diethyl 1*H*-indol-2-ylphosphonate (**1**)

First, 10 mmol of indole (1.17 g) was dissolved in 20 mL dry THF. The solution was cooled to $-70 \text{ }^\circ\text{C}$ while a slow stream of N_2 was passed through. Subsequently, 10.5 mmol of BuLi (6.6 mL, 1.6 M in hexane) was added to the solution resulting in the appearance of the suspension of the lithium salt. The mixture was left for 30 min at $-70 \text{ }^\circ\text{C}$. Then, dry CO_2 was bubbled through the mixture until the solution became completely clear (ca. 10 min), and it was left for 10 min at $-70 \text{ }^\circ\text{C}$. In the next step, the solvent and excess of CO_2 were evaporated under reduced pressure at the lowest possible temperature. The resulting solid residue was dissolved in 20 mL of dry THF and cooled to $-70 \text{ }^\circ\text{C}$ under a nitrogen atmosphere. Then, 10.5 mmol of BuLi (6.6 mL, 1.6 M in hexane) was added, and the precipitation of the yellow intermediate was observed. The temperature was maintained at $-70 \text{ }^\circ\text{C}$ for 1 h. Afterwards, 10 mmol (1.56 g, 1.42 mL) of $\text{ClP}(\text{OEt})_2$ dissolved in 5 mL dry THF was added dropwise, and the resulting mixture was allowed to warm to $-40 \text{ }^\circ\text{C}$. Subsequently 3 mL of a 30% solution of H_2O_2 was added dropwise, and the solution was left to reach room temperature. The resulting mixture was poured out into 30 mL of saturated solution of NH_4Cl , acidified with sulfuric acid, and slightly warmed.

The product was extracted with diethyl ether and purified by column chromatography (silica gel/ethyl acetate). Compound **1** was obtained as a cream-colored solid (2.10 g, 83%); m.p. 66–67 °C (lit.[46] m.p. 81–82 °C); ^{31}P -NMR (243.12 MHz, CDCl_3): $\delta = 10.54$ ppm; ^1H -NMR (600.58 MHz, CDCl_3): $\delta = 1.36$ (t, 6H, $J = 7.1$ Hz, POCH_2CH_3), 4.12–4.25 (m, 4H, POCH_2CH_3), 7.09 (s, 1H, $\text{CH} = \text{CP}$), 7.19 (t, 1H, $J = 7.4$ Hz, ArH), 7.33 (t, 1H, $J = 8.3$ Hz, ArH), 7.51 (d, 1H, $J = 7.9$ Hz, ArH), 9.67 (s, 1H, NH) ppm; ^{13}C -NMR (151.02 MHz, CDCl_3): $\delta = 16.14$ (d, $J = 7.55$ Hz, POCH_2CH_3), 62.98 (d, $J = 4.53$ Hz, POCH_2), 112.15 (d, $J = 9.06$ Hz, $\text{P}=\text{C}=\text{C}$), 112.26 (d, $J = 9.06$ Hz), 120.48, 121.75, 123.01 (d, $J = 220.49$ Hz, $\text{P}=\text{C}=\text{C}$), 124.60, 127.23 (d, $J = 15.10$ Hz, $\text{P}=\text{C}=\text{C}-\text{C}$), 138.43 (d, $J = 12.08$ Hz, $\text{P}=\text{C}=\text{C}-\text{N}-\text{C}$) ppm; HRMS (ESI + TOF) m/z : $[\text{M} + \text{H}]^+$. Calcd for $\text{C}_{12}\text{H}_{16}\text{NO}_3\text{P}$: 254.0946; found: 254.0954.

4.3.2. Preparation of 1*H*-indolin-2-ylphosphonic Acid (**4**)

To 1 mmol (0.25 g) of ester **1** dissolved in TFA (10 mL) and cooled in an ice bath, 6.3 mmol (0.40 g) of NaBH_3CN was added carefully over a period of 30 min, and the mixture was left stirring for 24 h at room temperature. Then, the flask contents were poured into a solution prepared by dissolving 5 g of NaOH in a 20 mL water/ice mixture. The crude product was extracted with CHCl_3 (4 \times 20 mL) and purified by column chromatography (silica/ethyl acetate). Then, 0.10 g of the resulting diethyl ester of 1*H*-indolin-2-ylphosphonic acid (compound **3**, yield 50%) was refluxed for 4 h with 8 mL of a 1:1 mixture of concentrated HCl and H_2O . Then, the volatile residues were removed by a rotary evaporator, and the solid material was heated with 3 mL of anhydrous EtOH. After cooling, the 1*H*-indolin-2-ylphosphonic acid crystallized from the dry ethanol. The solids were filtered, washed with cooled dry ethanol, and dried.

1*H*-indolin-2-ylphosphonic acid (**4**) was obtained as a white solid (60 mg, 78% of yield; m.p. 217–218 °C; ^{31}P -NMR (202.46 MHz, $\text{D}_2\text{O} + \text{NaOD}$) $\delta = 18.47$ ppm; ^1H -NMR (500.14 MHz, $\text{D}_2\text{O} + \text{NaOD}$) $\delta = 3.17$ – 3.31 (m, 2H, CH_2CHP), 3.69–3.74 (m, 1H, CH_2CHP), 6.85 (t, 1H, $J = 9.35$ Hz, ArH), 6.86 (t, 1H, $J = 7.35$ Hz, ArH), 7.14 (t, 1H, $J = 7.60$ Hz, ArH), 7.24 (d, 1H, $J = 7.25$ Hz, ArH) ppm; ^{13}C -NMR (125.76 MHz, $\text{D}_2\text{O} + \text{NaOD}$) $\delta = 32.11$, 56.87 (d, $J = 137.07$ Hz, CP), 111.15, 119.63, 124.91, 127.23, 131.09, 150.84; HRMS (ESI + TOF) m/z : $[\text{M} - \text{H}]^+$. Calcd. for $\text{C}_8\text{H}_{10}\text{NO}_3\text{P}$: 198.0320; found: 198.0318.

4.3.3. General Procedure for the Preparation of Benzo[*b*]tiophen-2-ylphosphonic Acid (**8**), Tri-2-benzofuryl Phosphine Oxide (**13**), Benzofuran-2-ylphosphonic Acid (**14**), Tri-2-furyl oxide (**15**), 5-Methyltiophen-2-ylphosphonic Acid (**17**), Phenylphosphonic Acid (**24**), 3-Methoxyphenylphosphonic Acid (**25**), and Aaphtha-1-ylphosphonic Acid (**26**)

To the mixture of an appropriate substrate (20 mmol of benzotriophene, benzofuran, furan, 2-methyltiophene, 1-bromo-naphthalene, bromobenzene, or 3-bromoanisole) dissolved in 30 mL anhydrous THF and cooled to -70 °C, BuLi (16.2 mL, 26.0 mmol, 1.6 M in hexane) was added dropwise for 30 min under a stream of N_2 . Then, the resulting solution or suspension was stirred for 30 min at -70 °C followed by the dropwise addition of a solution of 20 mmol of $\text{ClP}(\text{OEt})_2$ (3.13 g, 2.85 mL) in 30 mL of dry THF, maintaining the temperature below -65 °C. After the addition was complete, the reaction was continued for 60 min, and then the cooling bath was removed. When the temperature of the mixture reached -30 °C, 5 mL of 30% aqueous solution of hydrogen peroxide was added very cautiously drop by drop, and the mixture was allowed to warm to room temperature. The resulting solution was poured into 200 mL of water. The crude phosphonic ester was extracted with dichloromethane (3 \times 20 mL). The organic layers were combined, dried over anhydrous MgSO_4 , filtered, and evaporated under reduced pressure. The products were purified by column chromatography (silica/diethyl ether or ethyl acetate) or used directly in the next step. The aryl derivatives were hydrolyzed by refluxing in diluted hydrochloric acid (20%), and the crude products were recrystallized from water. Phosphonate esters of heterocyclic derivatives were deprotected by application of TMSBr. Thus, 10.0 mmol of the ester was mixed with dry CH_2Cl_2 and 40 mmol (6.12 g) of TMSBr and stirred for 72 h. The volatile components were evaporated under reduced pressure to give a solid residue to which 15 mL of MeOH was added, and the mixture was stirred for 1 h at room temperature.

The precipitated product was filtered off, washed with MeOH and Et₂O, and recrystallized from anhydrous ethanol.

Benzo[*b*]tiophen-2-ylphosphonic acid (**8**) was obtained as creamy prisms (36% of yield); m.p. 198–199 °C; ³¹P-NMR (202.46 MHz, D₂O + NaOD) δ = 4.33 ppm; ¹H-NMR (500.14 MHz, D₂O + NaOD) δ = 7.22–7.28 (m, 2H, ArH), 7.44 (d, 1H, *J* = 7.95 Hz, ArH), 7.76 (d, 1H, *J* = 7.45 Hz, ArH), 7.81 (d, 1H, *J* = 7.70 Hz, ArH) ppm; ¹³C-NMR (125.76 MHz, D₂O + NaOD) δ = 122.45 (d, *J* = 1.79 Hz), 123.99, 124.30, 124.60, 126.78 (d, *J* = 9.39 Hz), 140.15 (d, *J* = 14.91 Hz, CS), 141.43 (d, *J* = 6.36 Hz, CHCP), 144.17 (d, *J* = 170.89 Hz, CP); HRMS (ESI + TOF) *m/z*: [M – H]⁺. Calcd. for C₈H₇O₃P: 212.9775; found: 212.9774.

4.3.4. Mixture of Diethyl Benzofuran-2-ylphosphonate (**10**) and Diethyl Benzofuran-2-ylphosphinate (**11**)

After work-up with water, the mixture of products was extracted to dichloromethane (3 × 20 mL), dried over anhydrous MgSO₄, filtered, and evaporated under reduced pressure. This resulted in a mixture of an oily and crystalline product. The first fraction of crystalline product (mixture of compound **12** and **13**) was isolated by treatment of the mixture with methanol and filtration. The remaining oil was purified by column chromatography (silica/diethyl ether), which resulted in the separation of the desired compound **10** from the mixture of **11** and **12**.

The mixture of products **10** (major one) and **11** (minor one) was obtained as a yellow oil (0.90 g, 18%); ³¹P-NMR (151.02 MHz, CDCl₃) δ = 4.57 and –0.79 ppm (respectively); ¹H-NMR (600.58 MHz, CDCl₃) δ = 1.368 and 1.369 (t each, *J*₁ = 7.07 Hz, minor, OCH₂CH₃), 1.40 (t, *J* = 7.07 Hz, major, OCH₂CH₃), 4.05–4.31 (m, both compounds, OCH₂CH₃), 7.330 (t, *J* = 7.51 Hz, minor, ArH), 7.334 (t, *J* = 7.50 Hz, major, ArH), 7.44 (t, *J* = 7.75 Hz, minor, ArH), 7.46 (t, *J* = 7.75 Hz, major, ArH), 7.53 (dd, *J*₁ = 2.67 Hz, *J*₂ = 0.73 Hz, major, ArH), 7.57 (dd, *J*₁ = 3.42 Hz, *J*₂ = 0.72 Hz, minor, ArH), 7.59 (bd, *J* = 8.38 Hz, minor, ArH), 7.60 (bd, *J* = 8.38 Hz, major, ArH), 7.71 (bd, *J* = 7.8 Hz, both compounds, ArH); ¹³C-NMR (151.02 MHz, CDCl₃) δ = 16.16 (d, *J* = 6.63 Hz, minor, POCH₂CH₃), 16.29 (d, *J* = 6.40 Hz, major, POCH₂CH₃), 63.22 (d, *J* = 5.36 Hz, major, POCH₂CH₃), 63.64 (d, *J* = 5.66 Hz, minor, POCH₂CH₃), 112.14 (minor), 112.18 (major), 118.53 (d, *J* = 17.54 Hz, minor); 119.05 (d, *J* = 24.12 Hz, major), 122.48 (major), 122.50 (minor), 123.61 (major), 123.67 (minor), 126.92 (minor), 127.00 (major), 145.97 (d, *J* = 236.47 Hz, major, CP), 148.00 (d, *J* = 214.03 Hz, minor, CP) ppm; HRMS (ESI + TOF) *m/z*: [M + H]⁺. Calcd. for C₁₂H₁₅O₄P (**10**): 255.0786; found: 255.0778; 277.0663 (M + Na); 531.1357 (2M + Na).

The mixture of tri-2-benzofuryl phosphine and its oxide (**12** and **13**) was obtained as white crystals (1.75 g, 62%); m.p. 210–211 °C; ³¹P-NMR (243.12 MHz, CDCl₃) δ = –67.73 and –8.26 ppm; ¹H-NMR (600.58 MHz, CDCl₃) δ = 7.27 (td, 1H, *J*₁ = 7.15 Hz, *J*₂ = 0.70 Hz, ArH), 7.30 (dd, 1H, *J*₁ = 1.83 Hz, *J*₂ = 0.89 Hz, ArH), 7.36 (m, 2H, ArH), 7.48 (t, 1H, *J* = 7.52 Hz, ArH), 7.57 (dd, 1H, *J*₁ = 8.37 Hz, *J*₂ = 0.62 Hz, ArH), 7.61 (dd, 1H, *J*₁ = 1.57 Hz, *J*₂ = 0.61 Hz, ArH), 7.63 (m, 1H, ArH), 7.72 (dd, 1H, *J*₁ = 2.78 Hz, *J*₂ = 0.76 Hz, ArH) 7.74 (d, 1H, *J* = 7.84 Hz, ArH) ppm; ¹³C-NMR (151.02 MHz, CDCl₃) δ = 111.76, 112.43, 118.39 (d, *J* = 22.39 Hz), 120.53 (d, *J* = 20.92 Hz), 121.47, 122.75, 123.04, 123.88, 125.60, 126.50 (d, *J* = 10.02 Hz), 127.53, 127.84 (d, *J* = 6.42 Hz), 147.09 (d, *J* = 152.99 Hz, CP(O)), 150.88 (d, *J* = 4.98 Hz, CP), 158.14 (d, *J* = 5.48 Hz, COCP), 158.09 (d, *J* = 11.61 Hz, COCP(O)) ppm; HRMS (ESI + TOF) *m/z*: [M + H]⁺. Calcd. for C₂₄H₁₅O₄P: 399.0786; found: 399.0792.

Tri-2-benzofuryl phosphine oxide (**13**) was obtained as a white solid (24%) ³¹P-NMR (161.83 MHz, CDCl₃) δ = –7.63 ppm; ¹H-NMR (399.78 MHz, CDCl₃) δ = 7.32 (ddd, 1H, *J*₁ = 0.95 Hz, *J*₂ = 7.20 Hz, *J*₃ = 8.03 Hz, ArH), 7.42–7.46 (m, 1H, ArH), 7.568 (ddd, 1H, *J*₁ = 0.88 Hz, *J*₂ = 1.73 Hz, *J*₃ = 8.44 Hz, ArH), 7.67 (dd, 1H, *J*₁ = 0.98 Hz, *J*₂ = 2.86 Hz, ArH), 7.67–7.71 (m, 1H, ArH) ppm; ¹³C-NMR (100.53 MHz, CDCl₃) δ = 112.50 (d, *J* = 1.16 Hz), 120.62 (d, *J* = 21.01 Hz), 122.84, 123.96 (d, *J* = 1.15 Hz), 126.56 (d, *J* = 10.07 Hz), 127.61, 147.13 (d, *J* = 153.07 Hz, CP), 158.16 (d, *J* = 9.29 Hz) ppm; HRMS (ESI + TOF) *m/z*: [M + H]⁺. Calcd. for C₂₄H₁₅O₄P: 399.0786; found: 399.0854; [M + Na]⁺ 421.0623.

Benzofuran-2-ylphosphonic acid (**14**) was obtained as orange crystals (0.90 g, 46%); decomposed around 400 °C; ^{31}P -NMR (161.83 MHz, D_2O) $\delta = 0.62$ ppm; ^1H -NMR (399.78 MHz, D_2O) $\delta = 7.17$ (dd, $J_1 = 0.95$ Hz, $J_2 = 2.66$ Hz, 1H, ArH), 7.23 (td, $J_1 = 0.97$ Hz, $J_2 = 7.62$ Hz, 1H, ArH), 7.32–7.36 (m, 1H, ArH), 7.52 (dd, $J_1 = 0.84$ Hz, $J_2 = 8.36$ Hz, 1H, ArH), 7.64 (d, $J = 7.72$ Hz, 1H, ArH), ppm; ^{13}C -NMR (100.53 MHz, D_2O) $\delta = 111.82$ (d, $J = 1.27$ Hz), 113.70, 113.92, 122.39, 123.38, 126.13, 127.02 (d, $J = 11.08$ Hz), 152.72 (d, $J = 217.97$ Hz, CP), 156.41 (d, $J = 10.56$ Hz, COCP) ppm; HRMS (ESI + TOF) m/z : $[\text{M} - \text{H}]^-$. Calcd. for $\text{C}_8\text{H}_7\text{O}_4\text{P}$: 197.0004; found: 197.0001; $[\text{2M} - \text{H}]^-$ 395.0263.

Tri-2-furyl oxide (**15**) was obtained as a white solid (0.6 g, 12%); ^{31}P -NMR (161.83 MHz, CDCl_3) $\delta = -11.04$ ppm; ^1H -NMR (399.78 MHz, CDCl_3) $\delta = 6.54$ (dt, 1H, $J_1 = 1.66$ Hz, $J_2 = 3.40$ Hz, ArH), 7.15 (ddd, 1H, $J_1 = 0.72$ Hz, $J_2 = 2.05$ Hz, $J_3 = 3.49$ Hz, ArH), 7.72 (ddd, 1H, $J_1 = 0.72$ Hz, $J_2 = 1.70$ Hz, $J_3 = 2.53$ Hz, ArH) ppm; ^{13}C -NMR (100.53 MHz, CDCl_3) $\delta = 111.15$ (d, $J = 9.41$ Hz), 123.60 (d, $J = 21.05$ Hz), 146.02 (d, $J = 158.84$ Hz, CP), 148.98 (d, $J = 8.81$ Hz) ppm; HRMS (ESI + TOF) m/z : $[\text{M} + \text{H}]^+$. Calcd. for $\text{C}_{12}\text{H}_9\text{O}_4\text{P}$: 249.0317; found: 249.0354; $[\text{M} + \text{Na}]^+$ 271.0129.

Diethyl 2-Methylthiophen-5-yl-phosphonate (**16**) was obtained as a yellow oil (2.22 g, 48%); ^{31}P -NMR (243.12 MHz, CDCl_3) $\delta = 12.10$ ppm; ^1H -NMR (600.58 MHz, CDCl_3) $\delta = 1.35$ (t, 6H, $J = 7.11$ Hz, 6H, OCH_2CH_3), 2.56 (s, 3H, CCH_3), 4.08–4.19 (m, 4H, OCH_2CH_3), 6.85 (q, $J_1 = 2.65$ Hz, 1H ArH), 7.49 (dd, $J_1 = 8.52$ Hz, $J_2 = 3.51$ Hz, 1H ArH) ppm; ^{13}C -NMR (151.03 MHz, CDCl_3) $\delta = 15.26$ (d, $J = 1.38$ Hz, CCH_3), 16.21 (d, $J = 6.87$ Hz, POCH_2CH_3), 62.44 (d, $J = 5.32$ Hz, POCH_2CH_3), 124.91 (d, $J = 211.78$ Hz, CP), 126.59 (d, $J = 17.07$ Hz), 137.28 (d, $J = 11.53$ Hz), 148.90 (d, $J = 7.15$ Hz) ppm; HRMS (ESI + TOF) m/z : $[\text{M} + \text{H}]^+$. Calcd. for $\text{C}_9\text{H}_{15}\text{O}_3\text{PS}$: 235.0558; found: 235.0567; $[\text{M} + \text{Na}]^+$ 257.0345; $[\text{2M} + \text{H}]^+$ 469.0922; $[\text{2M} + \text{Na}]^+$ 491.0674.

5-Methylthiophen-2-ylphosphonic acid (**17**) was obtained as an amorphous solid (65% yield), m.p. 50 °C; ^{31}P -NMR (161.98 Hz, CDCl_3) $\delta = 15.26$ ppm; ^1H -NMR (400.13 MHz, CDCl_3) $\delta = 2.52$ (s, 3H, CCH_3), 6.78–6.80 (m, 1H, ArH), 7.43 (dd, $J_1 = 3.40$ Hz, $J_2 = 9.26$ Hz, 1H, ArH), 7.96–8.21 (m, 2H, PO_3H_2) ppm; ^{13}C -NMR (151.02 MHz, CDCl_3) $\delta = 15.26$ (d, $J = 1.38$ Hz, CCH_3), 124.91 (d, $J = 211.78$ Hz, CCP), 126.59 (d, $J = 17.07$ Hz), 137.28 (d, $J = 11.63$ Hz), 148.90 (d, $J = 7.15$ Hz) ppm; HRMS (ESI + TOF) m/z : $[\text{M} - \text{H}]^-$. Calcd. for $\text{C}_5\text{H}_7\text{SO}_3\text{P}$: 176.9775; found: 176.9773; $[\text{2M} + \text{Na}]^-$ 375.5813.

Diethyl phenylphosphonate (**21**) was obtained as a dense oil (66% yield); ^{31}P -NMR (202.46 MHz, CDCl_3) $\delta = 19.08$ ppm; ^1H -NMR (500.14 MHz, CDCl_3) $\delta = 1.23$ (t, 6H, $J = 7.05$ Hz, OCH_2CH_3), 3.93–4.08 (m, 4H, OCH_2), 7.36–7.41 (m, 2H, ArH), 7.45–7.49 (m, 1H, ArH), 7.67–7.72 (m, 2H, ArH) ppm; ^{13}C -NMR (125.76 MHz, CDCl_3) $\delta = 16.05$ (d, $J = 6.45$ Hz, POCH_2CH_3), 62.25 (d, $J = 5.57$ Hz, POCH_2), 127.69 (d, $J = 198.520$ Hz, PC), 128.46 (d, $J = 15.08$ Hz), 131.53 (d, $J = 9.96$ Hz), 132.51 (d, $J = 3.04$ Hz) ppm; HRMS (ESI + TOF) m/z : $[\text{M} + \text{H}]^+$. Calcd. for $\text{C}_6\text{H}_7\text{O}_3\text{P}$: 159.0211; found: 159.0209.

Phenylphosphonic acid (**24**) was obtained as a white solid (51% yield from bromobenzene); m.p. 161–163 °C (lit.[47] m.p. 166); ^{31}P -NMR (202.46 MHz, $\text{D}_2\text{O} + \text{NaOD}$) $\delta = 11.31$ ppm; ^1H -NMR (500.14 MHz, $\text{D}_2\text{O} + \text{NaOD}$) $\delta = 7.10$ –7.24 (m, 3H, ArH), 7.42–7.55 (m, 2H, ArH) ppm; ^{13}C -NMR (125.76 MHz, $\text{D}_2\text{O} + \text{NaOD}$) $\delta = 127.70$ (d, $J = 12.56$ Hz), 128.71 (d, $J = 2.15$ Hz), 130.07 (d, $J = 8.75$ Hz) ppm; HRMS (ESI + TOF) m/z : $[\text{M} - \text{H}]^+$. Calcd. for $\text{C}_6\text{H}_7\text{O}_3\text{P}$: 157.0055; found: 157.0048.

Diethyl 3-methoxyphenylphosphonate (**22**) was obtained as a dense oil (63%, yield); ^{31}P -NMR (202.46 MHz, CDCl_3) $\delta = 18.64$ ppm; ^1H -NMR (500.14 MHz, CDCl_3) $\delta = 1.32$ and 1.36 (t, 6H, $J_1 = 7.05$ Hz, $J_2 = 7.10$ Hz, OCH_2CH_3), 3.84 (s, 3H, OCH_3), 4.04–4.18 (m, 4H, OCH_2), 7.07–7.09 (m, 1H, ArH), 7.31–7.35 (m, 1H, ArH), 7.36–7.39 (m, 2H, ArH) ppm; ^{13}C -NMR (125.76 MHz, CDCl_3) $\delta = 16.30$ (d, $J = 6.49$ Hz, POCH_2CH_3), 55.40 (OCH_3), 62.16 (d, $J = 5.39$ Hz, POCH_2), 116.37 (d, $J = 11.36$ Hz), 118.72 (d, $J = 3.18$ Hz), 118.72 (d, $J = 3.18$ Hz), 123.93 (d, $J = 9.28$ Hz), 129.55 (d, $J = 186.89$ Hz, CP), 129.73 (d, $J = 17.58$ Hz), 159.43 (d, $J = 18.89$ Hz) ppm; HRMS (ESI + TOF) m/z : $[\text{M} + \text{H}]^+$. Calcd. for $\text{C}_{11}\text{H}_{17}\text{O}_4\text{P}$: 245.0943; found: 245.0940. These data are in good agreement with the literature [48].

3-Methoxyphenylphosphonic acid (**25**) was obtained as a brownish solid (50% yield from bromoanisole) m.p. 124–126 °C (lit.[49] m.p. 139–142 °C); ^{31}P -NMR (202.46 MHz, $\text{D}_2\text{O} + \text{NaOD}$) $\delta = 10.82$ ppm; ^1H -NMR (500.14 MHz, $\text{D}_2\text{O} + \text{NaOD}$) $\delta = 3.75$ (s, 3H, OCH_3), 6.88 (d, 1H, $J = 7.05$ Hz, ArH), 7.19–7.27 (m, 3H, ArH) ppm; ^{13}C -NMR (125.76 MHz, $\text{D}_2\text{O} + \text{NaOD}$) $\delta = 55.38$ (OCH_3), 114.33 (d, $J = 2.64$ Hz), 115.59 (d, $J = 9.85$ Hz), 123.14 (d, $J = 8.23$ Hz), 129.10 (d, $J = 14.46$ Hz), 142.72 (d, $J = 165.84$ Hz, CP), 158.04 (d, $J = 15.82$ Hz) ppm; HRMS (ESI + TOF) m/z : $[\text{M} - \text{H}]^+$. Calcd. for $\text{C}_7\text{H}_9\text{O}_4\text{P}$: 187.0160; found: 187.0169.

Naphth-1-ylphosphonic acid (**26**) was obtained as a white solid (56% yield from 1-bromonaphthalene) m.p. 203–204 °C (lit. [50] m.p. 204–206 °C); ^{31}P -NMR (202.46 MHz, $\text{D}_2\text{O} + \text{NaOD}$) $\delta = 9.09$ ppm; ^1H -NMR (500.14 MHz, $\text{D}_2\text{O} + \text{NaOD}$) $\delta = 7.34$ (t, 2H, $J = 7.40$ Hz, ArH), 7.42 (t, 1H, $J = 7.40$ Hz, ArH), 7.75 (d, $J = 8.10$ Hz, ArH), 7.83 (dd, $J = 6.90$ Hz, $J = 13.85$ Hz, PC = CH), 8.59 (d, 1H, $J = 8.45$ Hz, ArH) ppm; ^{13}C -NMR (125.76 MHz, $\text{D}_2\text{O} + \text{NaOD}$) $\delta = 125.09$ (d, $J = 13.69$ Hz), 125.65 (d, $J = 19.86$ Hz), 128.24, 128.62 (d, $J = 4.55$ Hz), 129.41 (d, $J = 2.64$ Hz), 129.99 (d, $J = 7.58$ Hz), 132.97 (d, $J = 8.79$ Hz), 133.28 (d, $J = 10.16$ Hz), 137.70 (d, $J = 163.22$ Hz, CP) ppm; HRMS (ESI + TOF) m/z : $[\text{M} - \text{H}]^+$. Calcd. for $\text{C}_{10}\text{H}_9\text{O}_3\text{P}$: 207.0211; found 207.0212.

4.3.5. Preparation of Benzo[*b*]thiazol-2-ylphosphonic Acid (**7**)

The mixture of 30 mL anhydrous THF containing 16 mmol of BuLi (16.2 mL, 1.6 M in hexane) was placed in a round-bottom flask and cooled to -70 °C, while 20 mmol of benzothiazole (2.70 g) was added dropwise under a stream of N_2 . The resulting yellow suspension of lithium salt was stirred for an additional 30 min at -70 °C. In the meantime, in a separate flask, 20 mmol of $\text{ClP}(\text{OEt})_2$ (3.13 g) in 30 mL dry THF was prepared and cooled in an ice bath, and the suspension of the lithium salt to the solution of $\text{ClP}(\text{OEt})_2$ in one batch was added to this solution. The resulting orange solution was stirred for the next 30 min, while the temperature was maintained at 0 °C followed by the dropwise addition of 3 mL of 30% aqueous solution of H_2O_2 , which resulted in the appearance of a yellow precipitate. The reaction was continued for an additional 1 h. After that, the flask contents were poured into 200 mL of cold water, and the crude phosphonic ester was extracted with diethyl ether (3×20 mL). The organic phases were combined, dried over anhydrous MgSO_4 , filtered, and evaporated under reduced pressure. The product was purified by column chromatography ($\text{SiO}_2/\text{Et}_2\text{O}$) to yield 3.24 g (60%) of diethyl benzo[*b*]thiazol-2-ylphosphonate, which was used immediately in the next reaction. Thus, 10.0 mmol (2.71 g) of the resulting ester was mixed with dry CH_2Cl_2 and 40 mmol (6.12 g) of TMSBr and stirred for 72 h. The volatile components were evaporated under reduced pressure to give a solid residue to which 15 mL of MeOH was added, and the mixture was stirred for 1 h at room temperature. The precipitated product was filtered off, washed with MeOH and Et_2O , and dried.

Compound **7** was obtained as a yellowish solid (84% yield (total yield 50%) m.p. 231–232 °C (lit.[51] m.p. 161–163 °C); ^{31}P -NMR (202.46 MHz, $\text{D}_2\text{O} + \text{NaOD}$) $\delta = 0.14$ ppm; ^1H -NMR (500.14 MHz, $\text{D}_2\text{O} + \text{NaOD}$) $\delta = 7.34$ (t, 1H, $J = 7.40$ Hz, ArH), 7.42 (t, 1H, $J = 7.10$ Hz, ArH), 7.93 (t, 2H, $J = 7.50$ Hz, ArH) ppm; ^{13}C -NMR (125.76 MHz, $\text{D}_2\text{O} + \text{NaOD}$) $\delta = 122.26$, 122.43, 125.57, 126.23, 135.45, 153.76 (d, $J = 20.00$ Hz), 176.30 (d, $J = 187.65$ Hz, CP) ppm; HRMS (ESI + TOF) m/z : $[\text{M} - \text{H}]^+$. Calcd. for $\text{C}_7\text{H}_6\text{SNO}_3\text{P}$: 213.9728; found: 213.9728.

4.3.6. Preparation of Ethyl Bis(*N*-methylpyrrol-2-yl)phosphinate (**19**)

To the mixture of *N*-methylpyrrole (0.81 g, 10 mmol) and TMEDA (1.42 g, 15 mmol) in 15 mL of dry diethyl ether, a solution of *n*-butyllithium (10.6 mL, 17 mmol, 1.6 M in hexane) was added dropwise, while a slow stream of N_2 was passed through. Then, the resulting solution was refluxed for 1 h, and $\text{ClP}(\text{OEt})_2$ (1.56 g, 10 mmol) in 5 mL of Et_2O was added dropwise with cooling in an ice bath. The reaction was then continued for 8 h at room temperature, and the solution was once again cooled in an ice bath followed by the slow addition of 3 mL of a 30% aqueous solution of H_2O_2 . When the addition

was complete, the flask contents were poured onto 30 mL of water. The crude product containing mostly compound **19** was extracted with CH₂Cl₂ (3 × 20 mL) and purified by column chromatography (silica/AcOEt) to yield 0.66 g (52%) of ethyl bis(1-methylpyrrol-2-yl)phosphinate as a colorless oil. ³¹P-NMR (202.46 MHz, CDCl₃): δ = 14.92 ppm. ¹H-NMR (500.14 MHz, CDCl₃): δ = 1.30 (t, 3H, *J* = 7.05 Hz, POCH₂CH₃), 3.68 (s, 6H, NCH₃), 4.08–4.13 (m, 2H, POCH₂), 6.03–6.06 (m, 2H, ArH); 6.53 (td, 2H, *J* = 3.62 Hz, *J* = 1.70 Hz, ArH), 6.73–6.74 (m, 2H, ArH) ppm; ¹³C-NMR (125.76 MHz, CDCl₃): 16.47 (d, *J* = 6.99 Hz), 36.09, 61.36 (d, *J* = 5.51 Hz), 108.20 (d, *J* = 13.42 Hz), 121.32 (d, *J* = 17.79 Hz), 122.48 (d, *J* = 179.35 Hz, CP), 129.38 (d, *J* = 6.95 Hz) ppm; HRMS (ESI + TOF) *m/z*: [M + H]⁺. Calcd. For C₁₂H₁₇N₂O₂P: 253.1106; found: 253.1112.

For all the spectral data, see the Supplementary Information.

4.4. Antiproliferative Activity

4.4.1. Cell Culture

Mycoplasma-free MCF-7, PC-3, and RAW 264.7 cell lines were purchased from the European Collection of Authenticated Cell Cultures (ECACC) and maintained at the Institute of Immunology and Experimental Therapy (IIET), Wrocław, Poland. The MCF-7 cell line was cultured in an Eagle medium (Life Technologies, Warszawa, Poland), supplemented with 10% (*v/v*) FBS, 2 mM L-glutamine, 1% NEAA, and 0.01 mg/mL insulin (all Sigma-Aldrich, Poznań, Poland). The PC-3 cell line was cultured in RPMI-1640 medium (Life Technologies, Scotland), supplemented with 10% (*v/v*) FBS and 2 mM L-glutamine. The RAW 264.7 cell line was cultured in DMEM (Life Technologies, Scotland), supplemented with 10% (*v/v*) FBS and 2 mM L-glutamine. All culture media were additionally supplemented with 100 µg/mL streptomycin and 100 U/mL penicillin. All cell lines were cultured during all experiments in a humid atmosphere at 37 °C and 5% CO₂ and passaged twice a week using EDTA-Trypsin (pH 8; IIET, Wrocław, Poland) solution as a detachment agent.

4.4.2. SRB Antiproliferative Assay

Twenty-four hours before adding the tested compounds, the cells were seeded on 96-well plates (Sarstedt, Germany) in an appropriate culture medium with 0.75 × 10⁵ cells/mL for MCF-7, 10⁵ cells/mL for PC-3, and 0.1 × 10⁵ cells/mL for RAW 264.7. The cells were treated with each compound in at least four concentrations in the range of 1000 µM⁻¹ µM for 72 h. The 0.2 M NaOH, used as a stock solution solvent, was tested for antiproliferative activity, and it did not affect the cell proliferation at 1 mM, the highest concentration used in the compound solutions.

This was used as previously described [52], with minor modifications for all adherent cells. Briefly, the cells were fixed with 50 µL/well of 50% (*w/v*) trichloroacetic acid (Avantor Performance Materials, Gliwice, Poland). After 1 h incubation, the plates were washed several times with tap water, and 50 µL of a 0.1% (*w/v*) solution of sulforhodamine B (Sigma-Aldrich, Schnellendorf, Germany) in 1% (*v/v*) acetic acid (Avantor Performance Materials, Gliwice, Poland) was added to each well. After 30 min incubation at room temperature, the unbound dye was washed out with 1% (*v/v*) acetic acid, whereas the bound dye was solubilized with 10 mM of unbuffered TRIS (Avantor Performance Materials, Gliwice, Poland) solution. The entire procedure was performed using a Biotek EL-406 washing station (BioTek Instruments, Winooski, VT, USA). The absorbance was then read using a Biotek Hybrid H4 reader (BioTek Instruments, USA) at a 540 nm wavelength.

The compounds at each concentration were tested in triplicate in a single experiment, and each experiment was repeated at least three times independently. The results are presented as the mean IC₅₀ ± standard deviation (SD) calculated using the Prolab-3 system based on Cheburator 0.4 software [53].

Supplementary Materials: The following supporting information can be downloaded at: <https://www.mdpi.com/article/10.3390/molecules28073135/s1>, Figures S1–S77: The ³¹P-NMR, ¹H-NMR, ¹³C-

NMR and HRMS spectra of the representative compounds; Table S1: Relevant crystallographic data for the molecule and the full geometrical information (\AA , $^\circ$); Table S2: Selected hydrogen-bond parameters.

Author Contributions: E.C. performed the synthetic studies, conceived and designed the experiments, wrote the paper and interpreted the NMR spectra; N.M. synthesized compounds; B.D. obtained and analyzed the crystal structure of compounds **13** and **15**; M.P. performed biological studies; P.K. interpreted the obtained results. All authors have read and agreed to the published version of the manuscript.

Funding: Support by subsidy of Ministry of Science and Higher Education No 8211104160.

Institutional Review Board Statement: Not applicable.

Informed Consent Statement: Not applicable.

Data Availability Statement: The data presented in this study and associated additional data are available upon request.

Acknowledgments: We thank K. Ejsmont for the crystallographic analysis.

Conflicts of Interest: The authors declare no conflict of interest. The funding sponsors had no role in the design of the study; in the collection, analyses, or interpretation of data; in the writing of the manuscript; or in the decision to publish the results.

References

- Bałczewski, P.; Skalik, J. Quinquevalent phosphorus acids. In *Organophosphorus Chemistry*; Allen, D.W., Loakes, D., Tebby, J.C., Eds.; Royal Society of Chemistry: Cambridge, UK, 2013; Volume 42, pp. 81–196. [CrossRef]
- Van der Jeught, S.; Stevens, C. Direct phosphorylation of aromatic azaheterocycles. *Chem. Rev.* **2009**, *109*, 2672–2702. [CrossRef] [PubMed]
- Kaur, R.; Mandal, S.; Banerjee, D.; Kumar Yadav, A. Transition metal free α -C–H functionalization of six membered heteroaromatic-N-oxides. *ChemSelect* **2021**, *6*, 2832–2854. [CrossRef]
- Mehwish, H.; Chen, X.-L.; Yu, B.; Qu, L.-B.; Zhao, Y.-F. Applications of H-phosphonates for C element bond formation. *Pure Appl. Chem.* **2019**, *91*, 33–41. [CrossRef]
- Popovics-Tóth, N.; Bálint, E. Multicomponent synthesis of potentially biologically active heterocycles containing a chosphonate or a chosphine oxide moiety. *Acta Chim. Slov.* **2022**, *69*, 735–755. [CrossRef] [PubMed]
- Demmer, C.S.; Krogsgaard-Larsen, N.; Bunch, L. Review on modern advances of chemical methods for the introduction of a phosphonic acid group. *Chem. Rev.* **2011**, *111*, 7981–8001. [CrossRef]
- Bock, T.; Mólwald, H.; Mühlaupt, R. Arylphosphonic acid-functionalized polyelectrolytes as fuel cell membrane material. *Macromol. Chem. Phys.* **2007**, *208*, 1324–1340. [CrossRef]
- Dang, Q.; Kasibhatla, S.R.; Jiang, T.; Fan, K.; Liu, Y.; Taplin, F.; Schulz, W.; Cashion, D.K.; Reddy, K.R.; van Poelje, P.D.; et al. Discovery of phosphonic diamide prodrugs and their use for the oral delivery of a series of fructose 1,6-bisphosphatase inhibitors. *J. Med. Chem.* **2008**, *51*, 4331–4339. [CrossRef]
- Dang, Q.; Liu, Y.; Cashion, D.K.; Kasibhatla, S.R.; Jing, T.; Taplin, F.; Jacintho, J.D.; Li, H.; Sun, Z.; Fan, Y.; et al. Discovery of a series of phosphonic acid-containing thiazoles and orally bioavailable diamide prodrugs that lower glucose in diabetic animals through inhibition of fructose-1,6-bisphosphatase. *J. Med. Chem.* **2011**, *54*, 153–156. [CrossRef]
- Teixeira, F.; Rangel, C.M.; Teixeira, A.P.S. New azaheterocyclic aromatic diphosphonates for hybrid materials for fuel cell applications. *New J. Chem.* **2013**, *37*, 3084–3091. [CrossRef]
- Dziuganowska, Z.A.; Ślepokura, A.; Volle, J.-N.; Virieux, D.; Pirat, J.-L.; Kafarski, P. Structural analogues of Selfotel. *J. Org. Chem.* **2016**, *81*, 4947–4954. [CrossRef]
- Iwanejko, J.; Brol, A.; Szyja, B.; Daszkiewicz, M.; Wojaczyńska, E.; Olszewski, T.K. Hydrophosphonylation of chiral hexahydroquinoxalin-2(1H)-one derivatives as an effective route to new bicyclic compounds: Aminophosphonates, enamines and imines. *Tetrahedron* **2019**, *75*, 1431–1439. [CrossRef]
- Sabat, N.; Poštova Slavětinská, L.; Klepetářová, B.; Hocek, M.C.-H. Phosphonylation of pyrrolopyrimidines: Synthesis of substituted 7- and 9-dezapurine-8-phosphonate derivatives. *J. Org. Chem.* **2016**, *81*, 9507–9514. [CrossRef]
- Chmielewska, E.; Miszczyk, P.; Kozłowska, J.; Prokopowicz, M.; Młynarz, P.; Kafarski, P. Reaction of benzolactams with triethyl phosphite prompted by phosphoryl chloride affords benzoannulated monophosphonates instead of expected bisphosphonates. *J. Organomet. Chem.* **2015**, *785*, 84–91. [CrossRef]
- Cervera-Villanueva, J.M., Jr.; Viveros-Ceballos, J.L.; Ordóñez, M. First practical synthesis of novel 1-phosphonlated pyrrolo[1,2- α]pyrazine derivatives. *Heteroatom Chem.* **2017**, *28*, e21398. [CrossRef]
- Shety, M.; Huang, H.; Kang, J.Y. Regioselective synthesis of α - and γ -amino quinolilyl phosphonamides using N-heterocyclic phosphines (NHPs). *Org. Lett.* **2018**, *20*, 700–703. [CrossRef]

17. Li, Y.; Zhu, Y.; Yang, S.-D. Visible-light-induced tandem phosphorylation cyclization of vinyl azides under mild conditions. *Org. Chem. Front.* **2018**, *5*, 822–826. [CrossRef]
18. Niu, L.; Wang, S.; Liu, J.; Yi, H.; Liang, X.-A.; Liu, T.; Lei, A. Visible-light-mediated oxidative C(sp³)-H phosphonylation of α -aminophosphonates under oxidant-free conditions. *Chem. Commun.* **2018**, *54*, 1659–1662. [CrossRef]
19. Su, X.; Yang, F.; Wu, Y.; Wu, Y. Direct C4-H phosphonylation of 8-hydroxyquinoline derivatives employing photoredox catalysis and silver catalysis. *Org. Biomol. Chem.* **2018**, *16*, 2753–2756. [CrossRef]
20. Wahab, A.; Gao, Z.; Gou, J.; Yu, B. The construction of phosphonate triazolyl by copper(ii)-catalyzed furan dearomatized [3 + 2] cycloaddition. *Org. Biomol. Chem.* **2022**, *20*, 6319–6323. [CrossRef]
21. Ali, T.E.; Assiri, M.A.; Hassanin, N.M. One-pot synthesis, antimicrobial activities, and drug-likeness analysis of some novel 1,2-benzoxaphosphinines, phospholobenzofuran, and chromonyl/coumarinyl/indenonyl phosphonate. *Synth. Commun.* **2022**, *52*, 1967–1980. [CrossRef]
22. Polat-Cakir, S. 1,3-Dipolar cycloaddition reactions of acyl phosphonates with nitrile oxides: Synthesis of phosphonate-containing dioxazole derivatives. *Phosphorus Sulfur Silicon Relat. Elem.* **2020**, *196*, 461–467. [CrossRef]
23. Sreelakshmi, P.; Krishna, B.S.; Sandhisudha, S.; Murali, S.; Reddy, G.R.; Venkataramaiah, C.; Rao, P.V.; Reddy, A.V.K.; Swetha, V.; Zyryanov, G.V.; et al. Synthesis and biological evaluation of novel dialkyl (4-amino-5H-chromeno[2,3-d]pyrimidin-5-yl)phosphonates. *Bioorg. Chem.* **2022**, *129*, 106121. [CrossRef] [PubMed]
24. Bálint, E.; Popovics-Tóth, N.; Tajti, A.; Rávai, B.; Szabó, K.E.; Perdih, F. Microwave-assisted multicomponent syntheses of heterocyclic phosphonates. *Chem. Proc.* **2021**, *3*, 108. [CrossRef]
25. Philippov, I.; Gatilov, Y.; Sonina, A.; Vorob'ev, A. Oxidative [3+2]cycloaddition of alkynylphosphonates with heterocyclic N-imines: Synthesis of pyrazolo[1,5-a]pyridine-3-phosphonates. *Molecules* **2022**, *27*, 7913. [CrossRef] [PubMed]
26. Clayden, J. Organolithiums: Selectivity for Synthesis. In *Tetrahedron Organic Chemistry*; Series 23; Pergamon Press: Oxford, UK, 2002.
27. Nájera, C.; Sansano, J.M.; Yus, M. Recent synthetic uses of functionalised aromatic and heteroaromatic organolithium reagents prepared by non-deprotonating methods. *Tetrahedron* **2003**, *59*, 9255–9303. [CrossRef]
28. Ila, H.; Markiewicz, J.T.; Malakhov, V.; Knochel, P. Metalated indoles, indazoles, benzimidazoles, and azaindoles and their synthetic applications. *Synthesis* **2013**, *45*, 2343–2371. [CrossRef]
29. Power, M.; Alcock, E.; McGlacken, P. Organolithium bases in flow chemistry: A review. *Org. Process Res. Dev.* **2020**, *24*, 1814–1838. [CrossRef]
30. Bissere, P.; Thielges, S.; Bourg, S.; Miethke, M.; Marahiel, M.A.; Eustache, J. Synthesis of a 2-indolylphosphonamide derivative with inhibitory activity against yersiniabactin biosynthesis. *Tetrahedron Lett.* **2007**, *48*, 6080–6083. [CrossRef]
31. Katritzky, A.R.; Akutagawa, K. Carbon dioxide: A reagent for the protection of nucleophilic centres and the simultaneous activation of alternative locations to electrophilic attack: Part I. A new synthetic method for the 2-substitution of 1-unsubstituted indoles. *Tetrahedron Lett.* **1985**, *26*, 5935–5938. [CrossRef]
32. Du, Y.; Wiemer, D.F. Preparation of α -phosphonolactams using electrophilic phosphorus reagents: Application in the synthesis of lactam-based farnesyl transferase inhibitors. *J. Org. Chem.* **2002**, *67*, 5709–5717. [CrossRef]
33. Haelters, J.P.; Corbel, B.; Sturtz, G. Synthèse D'indole phosphonates par cyclisation selon fischer d'arylhydrazones phosphonates. *Phosphorus Sulfur Silicon Relat. Elem.* **1988**, *37*, 41–64. [CrossRef]
34. Iddon, B. Synthesis and reactions of lithiated monocyclic azoles containing two or more heteroatoms. Part II: Oxazoles. *Heterocycles* **1994**, *37*, 1321–1346. [CrossRef]
35. Jenkins, D.; Sykora, R.E.; Assefa, Z. Tri-2-furyl-phosphine oxide: An oxidation product of the weak Lewis base tri-2-furylphosphine. *Acta Cryst.* **2007**, *E63*, 3510–3511. [CrossRef]
36. Allen, F.H. The Cambridge Structural Database: A quarter of a million crystal structures and rising. *Acta Cryst.* **2002**, *B58*, 380–388. [CrossRef]
37. Gjøes, N.; Gronowitz, S. Thienylpyrroles I. Synthesis via Copper intermediates. *Acta Chem. Scand.* **1971**, *25*, 2596–2608. [CrossRef]
38. Merly, I.; Smith, S.L. Murine RAW 264.7 cell line as an immune target: Are we missing something? *Immunopharmacol. Immunotoxicol.* **2017**, *39*, 55–58. [CrossRef]
39. Rogers, T.L.; Holen, I. Tumour macrophages as potential targets of bisphosphonates. *J. Transl. Med.* **2011**, *9*, 177. [CrossRef]
40. Raja Singh, P.; Sugantha Priya, E.; Balakrishnan, S.; Arunkumar, R.; Sharmila, G.; Rajalakshmi, M.; Arunakaran, J. Inhibition of cell survival and proliferation by nimbolide in human androgen-independent prostate cancer (PC-3) cells: Involvement of the PI3K/Akt pathway. *Mol. Cell Biochem.* **2017**, *427*, 69–79. [CrossRef]
41. Holliday, D.L.; Speirs, V. Choosing the right cell line for breast cancer research. *Breast Cancer Res.* **2011**, *13*, 215. [CrossRef]
42. CrysAlis PRO Software System. Version 1 171.37.57. Oxford Diffraction Ltd.: Abingdon, UK, 2005.
43. Sheldrick, G.M. A short history of SHELX. *Acta Crystallogr. Sect. A* **2008**, *64*, 112–122. [CrossRef]
44. Sheldrick, G.M. Crystal structure refinement with SHELXL. *Acta Crystallogr. Sect. C* **2015**, *71*, 3–8. [CrossRef] [PubMed]
45. Macrae, C.F.; Bruno, I.J.; Chisholm, J.A.; Edgington, P.R.; McCabe, P.; Pidcock, E.; Rodriguez-Monge, L.; Taylor, R.; van de Streek, J.; Wood, P.A. Mercury CSD 2.0—New Features for the Visualization and Investigation of Crystal Structures. *J. Appl. Crystallogr.* **2008**, *41*, 466–470. [CrossRef]
46. Chen, C.; Jie, D.; Liying, L.; Yujie, H.; Bolin, Z. Palladium-catalyzed domino cyclization/phosphorylation of gem-dibromoolefins with P(O)H compounds: Synthesis of phosphorylated heteroaromatics. *Adv. Synth. Catal.* **2022**, *364*, 200–205. [CrossRef]

47. Chunya, L.; Yuta, S.; Shun-Ya, O.; Shu, K.; Kazuhiko, S.; Norihisa, F.; Li-Biao, H. Wet and dry processes for the selective transformation of phosphonates to phosphonic acids catalyzed by brønsted acids. *J. Org. Chem.* **2020**, *85*, 14411–14419. [CrossRef]
48. Koohgard, M.; Hosseini-Sarvar, M. Visible-light-mediated phosphorylation reaction: Formation of phosphonates from alkyl/arylhydrazines and trialkylphosphites using zinc phthalocyanine. *Org. Biomol. Chem.* **2021**, *19*, 5905–5911. [CrossRef]
49. Grabiak, R.C.; Miles, J.A.; Schwenzer, G.M. Synthesis of phosphonic dichlorides and correlation of their p-31 chemical shifts. *Phosphorus Sulfur Silicon Relat. Elem.* **1980**, *9*, 197–202. [CrossRef]
50. Kuimov, V.A.; Malysheva, S.F.; Gusarova, N.K.; Vakul'skaya, T.I.; Khutsishvili, S.S.; Trofimov, B.A. The reaction of red phosphorus with 1-bromonaphthalene in the KOH–DMSO system: Synthesis of tri(1-naphthyl)phosphane. *Heteroat. Chem.* **2011**, *22*, 198–203. [CrossRef]
51. Soumyadip, H.; Abhijeet, S.; Singh, R.P. Cu-Catalyzed Direct C–P Bond formation through dehydrogenative cross-coupling reactions between azoles and dialkyl phosphites. *J. Org. Chem.* **2019**, *84*, 6868–6878. [CrossRef]
52. Skehan, P.; Storeng, R.; Scudiero, D.; Monks, A.; McMahon, J.; Vistica, D.; Warren, J.T.; Bokesch, H.; Kenney, S.; Boyd, M.R. New colorimetric cytotoxicity assay for anticancer-drug screening. *J. Natl. Cancer Inst.* **1990**, *82*, 1107–1112. [CrossRef]
53. Nevozhay, D. Cheburator software for automatically calculating drug inhibitory concentrations from in vitro screening assays. *PLoS ONE* **2014**, *9*, e106186. [CrossRef]

Disclaimer/Publisher's Note: The statements, opinions and data contained in all publications are solely those of the individual author(s) and contributor(s) and not of MDPI and/or the editor(s). MDPI and/or the editor(s) disclaim responsibility for any injury to people or property resulting from any ideas, methods, instructions or products referred to in the content.

Article

Highly Z-Selective Horner–Wadsworth–Emmons Olefination Using Modified Still–Gennari-Type Reagents

 Ignacy Janicki *  and Piotr Kielbasiński * 

Division of Organic Chemistry, Centre of Molecular and Macromolecular Studies, Polish Academy of Sciences, Sienkiewicza 112, 90-363 Łódź, Poland

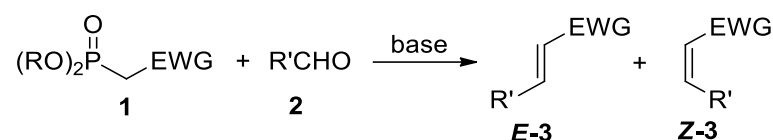
 * Correspondence: ijanicki@cbmm.lodz.pl (I.J.); piokiel@cbmm.lodz.pl (P.K.)

Abstract: In this report, new, easily accessible reagents for highly Z-selective HWE reactions are presented. Alkyl di-(1,1,1,3,3,3-hexafluoroisopropyl)phosphonoacetates, structurally similar to Still–Gennari type reagents, were tested in HWE reactions with a series of various aldehydes. Very good Z-selectivity (up to a 98:2 Z:E ratio) was achieved in most cases along with high yields. Application of the new reagents may be a valuable, practical alternative to the well-established Still–Gennari or Ando Z-selective carbonyl group olefination protocols.

Keywords: HWE reaction; Still–Gennari olefination; Ando olefination; stereoselective synthesis; Z-selectivity; Wittig reaction; phosphonates; alkenes; hexafluoroisopropanol; C=C bond formation

1. Introduction

Stereoselective alkene synthesis is one of the major challenges in organic synthesis [1]. The configuration of carbon–carbon double bonds affects all properties of molecules, therefore, highly selective methods for the synthesis of E or Z olefins are of great value. However, Z-selective reactions are considerably more difficult and less developed, mainly because of thermodynamic factors, which usually favor formation of the more stable E-products [2]. One of the well-established, typically highly E-selective alkene formation methods is the Horner–Wadsworth–Emmons (HWE) reaction, which is based on the olefination of carbonyl groups using dialkyl phosphonate reagents (Scheme 1) [3–7]. Its high E-selectivity results from the thermodynamic stabilization of E-products and intermediates leading to its formation. The selectivity of the HWE reaction is one of its important advantages, but in its classical form, it is restricted to the synthesis of E-alkenes. Nevertheless, the selectivity of the HWE reaction is highly dependent on the structure of the phosphonate reagents and it can be modified [8,9]. Attempts to develop Z-selective HWE reagents were made already in the late 1970s [10–12], but the first reliable and highly Z-selective modification of HWE reaction was reported in 1983 by Still and Gennari (Figure 1) [13]. In the standard HWE reaction, diethyl or dimethyl phosphonate reagents are usually applied. The Still–Gennari modification of the HWE reaction, fairly called “Still–Gennari olefination” due to its broad applicability and inverted selectivity, is based on the application of bis(2,2,2-trifluoroethyl) phosphonate reagents for the olefination of carbonyl compounds, usually in the presence of a strong base system—potassium bis(trimethylsilyl)amide (KHMDs) with 18-crown-6 crown ether. Along with the modification developed in the mid-1990s by Ando [14–18], the Still–Gennari olefination is one of the most widely applied Z-selective modifications of the HWE reaction. Its scope of applications was recently discussed in our review article [19].



Scheme 1. General scheme of the Horner–Wadsworth–Emmons reaction.

Citation: Janicki, I.; Kielbasiński, P. Highly Z-Selective Horner–Wadsworth–Emmons Olefination Using Modified Still–Gennari-Type Reagents. *Molecules* **2022**, *27*, 7138. <https://doi.org/10.3390/molecules27207138>

Academic Editor: Jakub Adamek

Received: 16 September 2022

Accepted: 18 October 2022

Published: 21 October 2022

Publisher’s Note: MDPI stays neutral with regard to jurisdictional claims in published maps and institutional affiliations.



Copyright: © 2022 by the authors. Licensee MDPI, Basel, Switzerland. This article is an open access article distributed under the terms and conditions of the Creative Commons Attribution (CC BY) license (<https://creativecommons.org/licenses/by/4.0/>).

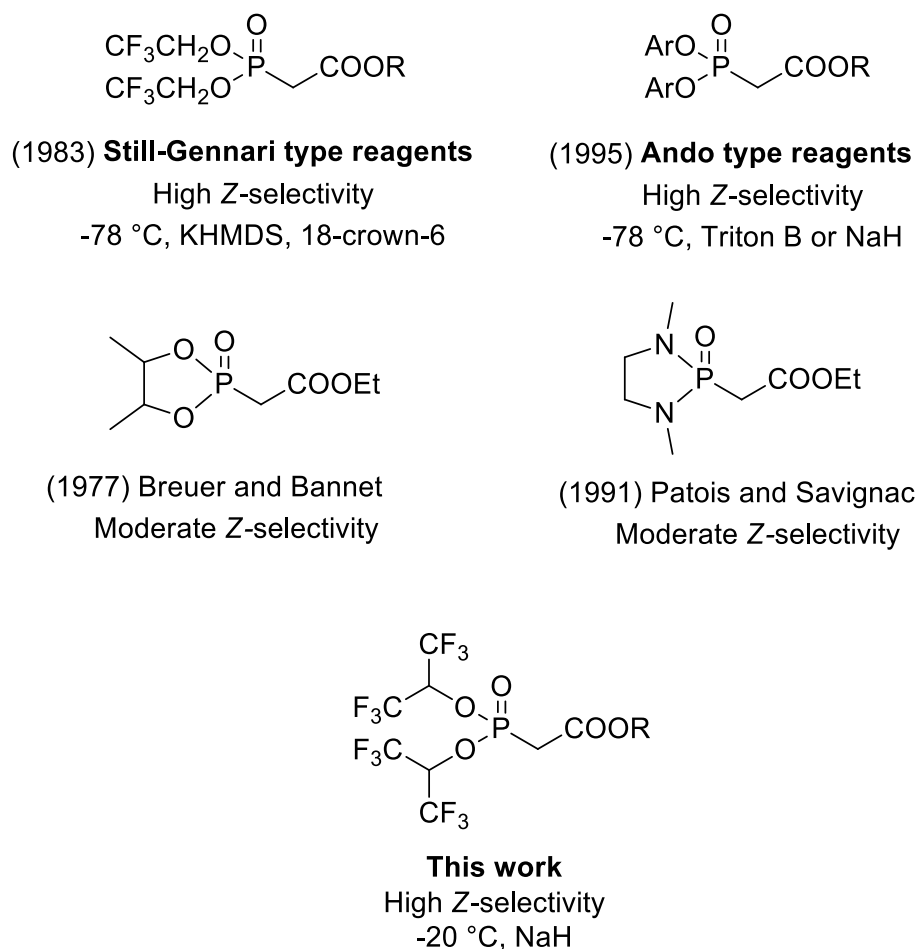


Figure 1. Comparison of Z-selective reagents for the HWE reaction [11–14].

Still–Gennari and Ando-type reagents constitute important tools for the Z-selective alkene formation. However, examples from a total synthesis of biologically active, complex molecules show that achieving high Z-selectivity using these reagents is not always easy and the outcome of the olefination reactions is highly dependent on the reaction conditions and the type of reagent used [19]. Therefore, it would be desirable to broaden the scope of reliable Z-selective carbonyl olefination reagents in order to improve our synthetic toolbox.

The Z-selectivity of Still–Gennari olefination is a result of the kinetic control of the reaction. An electron-withdrawing effect of R groups (Scheme 1), such as 2,2,2-trifluoroethyl or phenyl, favors the Z-selective course of the reaction in contrast to standard E-selective HWE reaction where R is usually the ethyl group (pK_a of 2,2,2-trifluoroethanol is 12.4 and pK_a of phenol is 10, while pK_a of ethanol is 16). The correlation between the electron-withdrawing effect of the R group and the stereoselectivity of the reaction was investigated in more detail by Motoyoshiya and coworkers [9]. Moreover, steric hindrance of R groups may further affect Z-selectivity as in the case of Ando-type reagents bearing aryl substituents.

In our previous study, we reported a very simple protocol for the synthesis of Still–Gennari and Ando-type phosphonates [20]. We also reported the synthesis of new phosphonate reagents bearing 1,1,1,3,3,3-hexafluoroisopropyl R groups. These compounds are expected to be highly Z-selective olefination reagents because of a stronger electron-withdrawing effect of 1,1,1,3,3,3-hexafluoroisopropyl R groups (pK_a of 1,1,1,3,3,3-hexafluoroisopropanol is 9.4). In the present research, we decided to test the performance of our new reagents and evaluate their applicability on the basis of a series of model reactions with various aldehydes.

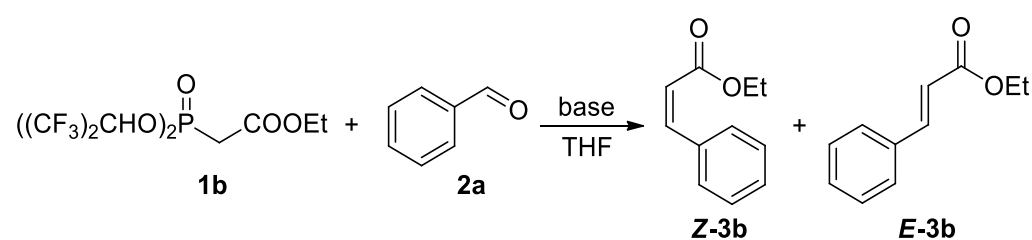
2. Results and Discussion

The reagents being subjects of this study, methyl, and ethyl bis(1,1,1,3,3,3-hexafluoroisopropyl) phosphonates **1a** and **1b**, were synthesized according to our previously reported procedure [20]. Because of a structural resemblance and similar reactivity we may consider **1a** and **1b** as “Still–Gennari-type” reagents. We decided to test these reagents for the synthesis of disubstituted alkenes by Z-selective HWE reaction. In order to maximize the yield and the stereoselectivity of the reaction, optimization of the reaction conditions was necessary (Table 1, Scheme 2).

Table 1. Reaction of **1b** with benzaldehyde **2a**—optimization ^[a].

| Entry | Base | Temperature | Yield ^[b] | Z:E Ratio ^[c] |
|-------|---------------------------------------|-------------|----------------------|--------------------------|
| 1 | NaH | −78 °C | traces | — |
| 2 | NaH | −40 °C | 82% | 97:3 |
| 3 | NaH | −20 °C | 94% | 97:3 |
| 4 | NaH | 0 °C | 85% | 95:5 |
| 5 | NaH (excess) ^[d] | 0 °C | 55% | 95:5 |
| 6 | NaH + NaI ^[e] | −20 °C | 95% | 97:3 |
| 7 | KHMDS | −78 °C | 37% | 91:9 |
| 8 | KHMDS + 18-crown-6 ^[f] | −78 °C | 34% | 84:16 |
| 9 | KHMDS | −40 °C | 52% | 90:10 |
| 10 | KHMDS + 18-crown-6 ^[f] | −40 °C | 61% | 86:14 |
| 11 | <i>t</i> -BuOK | −20 °C | 62% | 81:19 |
| 12 | K ₂ CO ₃ | r.t. | traces | traces of Z |
| 13 | Triton-B | −20 °C | 23% | 14:86 |
| 14 | (CF ₃) ₂ CHONa | −20 °C | 93% | 96:4 |

^[a] All the reactions were conducted in 10 mL of THF for 1 h by analogy with the general procedure (see Section 3.2); ^[b] yield was determined by ¹H-NMR with dimethyl terephthalate as internal standard; ^[c] determined by ¹H-NMR; ^[d] 0.15 equivalent excess of NaH was used; ^[e] 1 equivalent of NaI was used; ^[f] 5 equivalents of 18-crown-6 were used.



Scheme 2. Optimization of conditions based on the reaction of **1b** with benzaldehyde **2a**.

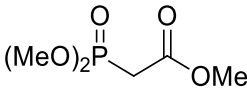
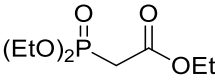
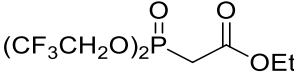
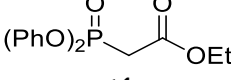
During the optimization study, several base systems were evaluated in the reaction of **1b** with benzaldehyde at various temperatures (Scheme 2). All the reactions were run in THF for 1 h. When using NaH as a base at −78 °C, the reaction was very slow, only traces of Z-product could be detected after 1 h (Table 1, entry 1). This is most probably due to the slow deprotonation of the phosphonate reagent at this low temperature because when the reaction was heated from −78 °C to room temperature, hydrogen gas evolved, and the reaction proceeded. Based on this observation, higher temperatures were evaluated (Table 1, entries 2–4). Quite unexpectedly, the best results regarding yield (94%) and selectivity (97:3 Z:E) were obtained using NaH at −20 °C (Table 1, entry 3), while Still–Gennari olefination is usually conducted at lower temperatures (typically −78 °C). This result is very promising because it shows that by using our new reagents high stereoselectivity may be achieved

at higher temperatures. Only a slight decrease in stereoselectivity was observed at 0 °C (Table 1, entry 4). It is noteworthy that using an excess of a base resulted in a significant decrease in the yield (Table 1, entry 5). The possibility of increasing the stereoselectivity of the reaction by providing additional sodium ions to the reaction mixture according to Pihko et al. was also investigated. However, no influence of the additive on the reaction course was observed (Table 1, entry 6) [21].

In contrast to the classic Still–Gennari olefination protocol, application of KHMDS or KHMDS with 18-crown-6 additive appears to be an inferior option (we made a similar observation in our previous work concerning the synthesis of *Z*- α,β -unsaturated phosphonates) [22]. The yields of the reactions were moderate (34–61%) and the selectivity was lower in comparison to the results obtained with NaH (up to a 91:9 *Z*:*E* ratio—Table 1, entries 7–10). Running the reaction at a lower temperature somewhat favored *Z*-selectivity, however, it decreased the yield (Table 1, entries 8 and 10). The addition of crown ether surprisingly decreased the selectivity of the reaction. Moreover, in our hands, the reaction with KHMDS tends to be a little capricious, sensitive to the reaction conditions, and difficult to reproduce, since we have previously reported better results which we were unable to repeat now.

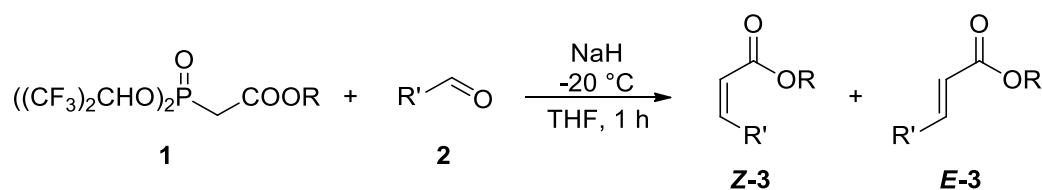
Other bases which were tested include *t*-BuOK, K₂CO₃, triton-B (benzyltrimethylammonium hydroxide), and (CF₃)₂CHONa. Reaction with *t*-BuOK at –20 °C gave 62% yield of the product in only an 81:19 *Z*:*E* ratio (Table 1, entry 11), however, conducting the reaction at a lower temperature may improve the yield and *Z*-selectivity to 80% and 92:8 *Z*:*E*, as presented earlier [20]. Unfortunately, the reaction with a mild base K₂CO₃ was unsuccessful, and only traces of *Z*-product were detected (Table 1, entry 12). Interestingly, the application of triton-B (according to Ando) [14] inverted the stereoselectivity of the reaction (14:86 *Z*:*E* ratio) proving the high influence of the reaction conditions on the observed results (Table 1, entry 13). Unexpectedly, very good results were obtained using (CF₃)₂CHONa—93% yield and 96:4 *Z*:*E* product ratio. Based on this observation we decided to investigate the possibility of using this base with other HWE reagents (Table 2, Scheme 3).

Table 2. HWE reaction of phosphonate reagents **1** and benzaldehyde **2a** with (CF₃)₂CHONa as a base [a].

| Entry | Reagent | Temperature | Yield [b] | <i>Z</i> : <i>E</i> Ratio [c] |
|-------|--|-------------|-----------|-------------------------------|
| 1 |  1c | –20 °C | 87% | 2:98 |
| 2 |  1d | –20 °C | 79% | >99% <i>E</i> |
| 3 |  1e | –20 °C | 99% | 68:32 |
| 4 | | –78 °C | 96% | 75:25 |
| 5 |  1f | –20 °C | 99% | 64:36 |
| 6 | | –78 °C | 97% | 68:32 |

[a] All the reactions were conducted in 10 mL of THF for 1 h according to the general procedure (see Section 3.2).

[b] Yield was determined by ¹H-NMR with dimethyl terephthalate as an internal standard. [c] Determined by ¹H-NMR.



Scheme 3. Reaction of reagents **1** with various aldehydes **2** under optimized conditions.

The application of $(\text{CF}_3)_2\text{CHONa}$ as a base in the standard HWE reaction of methyl dimethylphosphonoacetate **1c** or ethyl diethylphosphonoacetate **1d** with benzaldehyde resulted in excellent *E*-selectivity and very good yields (Table 2, entries 1 and 2). This observation indicates that $(\text{CF}_3)_2\text{CHONa}$ may be successfully used in HWE reactions. Despite excellent results with **1b** and standard HWE reagents **1c** and **1d**, the reaction using $(\text{CF}_3)_2\text{CHONa}$ with Still–Gennari and Ando-type phosphonates (**1e** and **1f**, respectively) was only moderately stereoselective, although very high yielding (Table 2, entries 3–6). It is noteworthy that lowering the temperature to $-78\text{ }^\circ\text{C}$ resulted in little increased *Z*-selectivity compared to the reaction at $-20\text{ }^\circ\text{C}$, without significant loss of yield.

The time course of the reaction of **1b** with benzaldehyde in the presence of NaH at $-20\text{ }^\circ\text{C}$ was also investigated (Figure 2). Measurements were taken after 5, 10, 15, 30, 60, and 120 min. The reaction proceeded very fast, after 5 min the yield reached 72% and the reaction was complete within 1 h (94%).

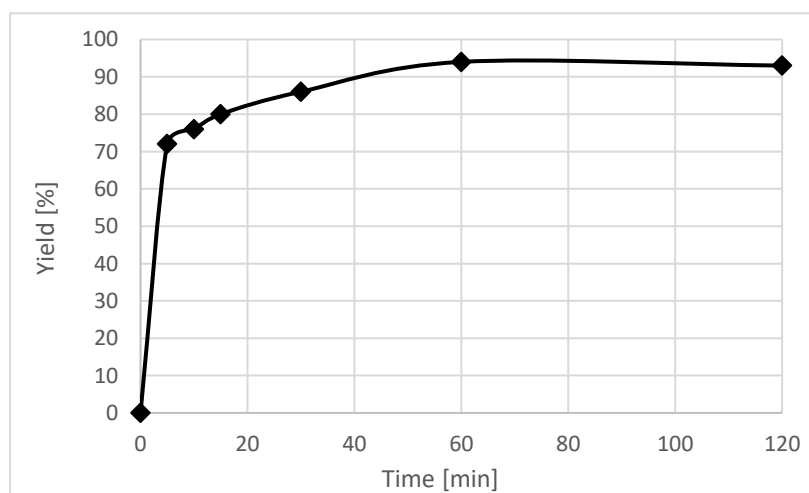


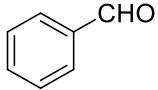
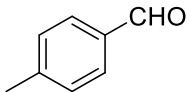
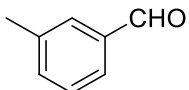
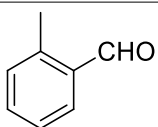
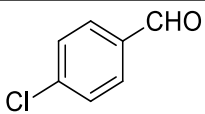
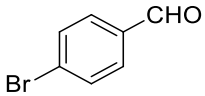
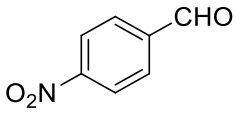
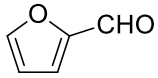
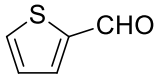
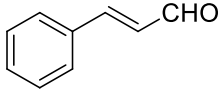
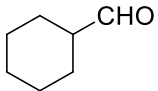
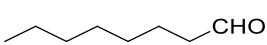
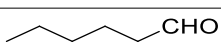
Figure 2. Time course of the reaction of **1b** and benzaldehyde with NaH at $-20\text{ }^\circ\text{C}$.

Based on the above observations, all further reactions of **1a** and **1b** with a series of various aldehydes **2a–2m** were carried out in THF at $-20\text{ }^\circ\text{C}$ for 1 h, using NaH as a base (Scheme 3, Table 3). Generally, similar reaction yields were observed for both reagents **1a** and **1b**; however, slightly better stereoselectivities were observed for ethyl bis-(1,1,1,3,3,3-hexafluoroisopropyl)phosphonoacetate **1b** than for methyl bis-(1,1,1,3,3,3-hexafluoroisopropyl)phosphonoacetate **1a**.

Very good results were obtained with most of the aromatic aldehydes tested (Table 3, entries 1–9). The standard reaction of **1a** or **1b** with benzaldehyde **2a** gave very high yields of products **3aa** and **3ba** respectively along with excellent *Z*-selectivity with a 97:3 *Z*:*E* ratio. Similarly, reactions with *para*, *meta*, and *ortho* tolualdehydes **2b–2d** resulted in high yields of products **3ab–3ad** and **3bb–3bd** (81–87%) and a very high *Z*-selectivity. Besides minimally better stereoselectivity with *o*-tolualdehyde **2d**, no significant differences in reactivity of **2b–2d** with **1a** or **1b** were observed. Olefination of *para* chloro, bromo, and nitro benzaldehydes **2e**, **2f**, and **2g**, respectively, proceeds in a nearly quantitative manner (93–99% yield) with very high *Z*-selectivity as well (94:6–96:4 *Z*:*E* ratio). Olefination of

heterocyclic furfural **2h** and 2-thiophenecarboxaldehyde **2i** resulted in slightly lower yields, however, the reactions were still highly stereoselective.

Table 3. Reactions of **1a** and **1b** with aldehydes **2a–2m** ^[a].

| Entry | Substrate | Aldehyde | Reagent 1a $((CF_3)_2CHO)_2P(=O)CH_2COOMe$ | | | Reagent 1b $((CF_3)_2CHO)_2P(=O)CH_2COOEt$ | | |
|-------|-----------|---|---|----------------------|--------------------|---|-----------------------------|---------------------------------|
| | | | Product | Yield ^[b] | Z:E ^[c] | Product | Yield ^[b] | Z:E ^[c] |
| 1 | 2a |  | 3aa | 91% | 97:3 | 3ba | 95% (99%) ^[d] | 97:3 (74:26) ^[d] |
| 2 | 2b |  | 3ab | 84% | 96:4 | 3bb | 81% | 96:4 |
| 3 | 2c |  | 3ac | 84% | 95:5 | 3bc | 86% | 96:4 |
| 4 | 2d |  | 3ad | 84% | 97:3 | 3bd | 87% | 98:2 |
| 5 | 2e |  | 3ae | 98% | 95:5 | 3be | 99% | 96:4 |
| 6 | 2f |  | 3af | 95% | 95:5 | 3bf | 95% | 94:6 |
| 7 | 2g |  | 3ag | 99% | 94:6 | 3bg | 93% | 95:5 |
| 8 | 2h |  | 3ah | 88% | 92:8 | 3bh | 79% | 95:5 |
| 9 | 2i |  | 3ai | 79% | 94:6 | 3bi | 89% | 95:5 |
| 10 | 2j |  | 3aj | 78% | 89:11 | 3bj | 82% | 91:9 |
| 11 | 2k |  | 3ak | 69% | 86:14 | 3bk | 70% | 87:13 |
| 12 | 2l |  | 3al | 88% | 88:12 | 3bl | 90% (92%) ^[d] | 88:12 (78:22) ^[d] |
| 13 | 2m |  | 3am | 77% | 88:12 | 3bm | 90% | 88:12 |

^[a] All the reactions were conducted according to the general procedure (see Section 3.2). ^[b] Yield was determined by ¹H-NMR with dimethyl terephthalate as the internal standard. ^[c] Determined by ¹H-NMR. ^[d] Reaction with Still-Gennari reagent **1e**.

Olefination of α,β -unsaturated cinnamaldehyde **2j** and aliphatic aldehydes **2k–2m** using reagents **1a** and **1b** gave the corresponding products **3aj–3am** and **3bj–3bm** in good yields (69–90%) with high *Z*-selectivity (86:14–91:9 *Z:E* ratio, Table 3, entries 10–13). Similar to that reported for Ando and Still–Gennari *Z*-selective HWE reaction, olefination of aliphatic aldehydes resulted in a bit inferior selectivity compared to reactions with aromatic aldehydes. Nevertheless, the results obtained with our new reagents **1a** and **1b** are comparable with those previously reported [13–18].

In order to compare the performance of the newly developed reagent **1b** under the reported conditions (using NaH in dry THF at $-20\text{ }^{\circ}\text{C}$) with standard Still–Gennari reagent **1e**, two model reactions with benzaldehyde and octanal were performed (Table 3, entries 1 and 12 in brackets). The *Z:E* selectivity using Still–Gennari reagent **1e** with NaH at $-20\text{ }^{\circ}\text{C}$ was found to be inferior both in the olefination of aromatic and aliphatic aldehydes. The reaction of **1e** with benzaldehyde resulted in a quantitative yield but only moderate *Z:E* selectivity 74:26, while the application of **1b** resulted in an excellent 97:3 *Z:E* ratio. Similarly, the reaction of **1e** with octanal resulted in poorer *Z:E* selectivity (78:22) than the reaction using reagent **1b** (88:12 *Z:E* ratio). These observations (along with data from Table 1—entries 2–4) suggest that a very good stereochemical outcome of the reactions with **1b** may be achieved using an easily accessible base, at higher temperatures than in the case of Still–Gennari reagent **1e**, as typically $-78\text{ }^{\circ}\text{C}$ and KHMDS with 18-crown-6 additive is required in order to achieve high *Z*-selectivity in standard Still–Gennari olefination.

3. Materials and Methods

3.1. General Information

The NMR spectra were recorded using a Bruker Avance Neo 400 spectrometer. Dimethyl terephthalate was used as an internal standard in all NMR experiments [23]. All solvents were dried and distilled prior to use. All the starting materials were purchased from Merck, Sigma-Aldrich, TCI Chemicals, or Fluorochem. Reagents **1a** and **1b** were prepared according to the procedure reported earlier [20]. All the reactions were run in duplicate. The spectra of all the products obtained were in agreement with the data reported in the literature (see Supplementary Materials) [24–38].

3.2. General Procedure for the Reaction of **1a** or **1b** with Aldehydes **2a–2m**

In a round bottom flask with a magnetic stirrer, under an argon atmosphere, 1.2 mmol of base (typically sodium hydride—48 mg of 60% dispersion in mineral oil) was placed and 3 mL of THF was added. The solution was cooled to $-20\text{ }^{\circ}\text{C}$ and 1.3 mmol of reagent **1a** (590 mg) or **1b** (608 mg) in 2 mL of dry THF was added. The reaction mixture was stirred for 15 min and 1 mmol of appropriate aldehyde in 5 mL of THF was added. After 1 h, 0.5 mL samples were collected by a syringe and quenched with saturated NH_4Cl solution. The aqueous layer was extracted two times with 0.5 mL of CH_2Cl_2 . Combined organic fractions were dried using anhydrous Na_2SO_4 , filtered, and next condensed under reduced pressure. To a thus obtained crude product, a specific amount of dimethyl terephthalate was added (as an internal standard for the $^1\text{H-NMR}$ measurements), and the mixture was dissolved in CDCl_3 to take $^1\text{H-NMR}$ spectra. Yields and *Z:E* product ratios of the reactions were calculated based on $^1\text{H-NMR}$ with an internal standard [12].

4. Conclusions

In conclusion, we have developed a successful application of new reagents, methyl, and ethyl bis(1,1,1,3,3,3-hexafluoroisopropyl)phosphonates, **1a** and **1b** in a highly *Z*-selective HWE reaction. The reagents are easily accessible via previously reported synthetic protocol [20]. In contrast to previous *Z*-selective HWE reagents, the application of **1a** or **1b** does not require very low temperatures ($-78\text{ }^{\circ}\text{C}$) to achieve high stereoselectivity. Moreover, readily accessible sodium hydride was found to be a very good base for the presented reaction.

Olefination of aromatic aldehydes using reagents **1a** and **1b** gives excellent results—up to a 98:2 *Z:E* product ratio, and up to quantitative yield. Slightly lower, however, very high *Z*-selectivity can also be achieved in the olefination of aliphatic aldehydes. The presented reagents may constitute a valuable alternative to well-established Ando and Still–Gennari-type reagents for highly *Z*-selective olefination of carbonyl compounds, especially in the total synthesis of complex biologically active products.

Supplementary Materials: The following supporting information can be downloaded at: <https://www.mdpi.com/article/10.3390/molecules27207138/s1>, Section S1: Time study; Section S2: NMR spectra.

Author Contributions: Conceptualization, I.J.; methodology, I.J.; software, I.J.; validation, I.J. and P.K.; formal analysis, I.J.; investigation, I.J.; resources, I.J. and P.K.; data curation, I.J.; writing—original draft preparation, I.J.; writing—review and editing, I.J. and P.K.; visualization, I.J.; supervision, I.J. and P.K.; project administration, I.J.; funding acquisition, P.K. All authors have read and agreed to the published version of the manuscript.

Funding: The research was financed by the Centre of Molecular and Macromolecular Studies, Polish Academy of Sciences (500-02).

Data Availability Statement: Not applicable.

Conflicts of Interest: The authors declare no conflict of interest.

References

- Negishi, E.-I.; Huang, Z.; Wang, G.; Mohan, S.; Wang, C.; Hattori, H. Recent Advances in Efficient and Selective Synthesis of Di-, Tri-, and Tetrasubstituted Alkenes via Pd-Catalyzed Alkenylation–Carbonyl Olefination Synergy. *Acc. Chem. Res.* **2008**, *41*, 1474–1485. [CrossRef]
- Siau, W.-Y.; Zhang, Y.; Zhao, Y. Stereoselective Synthesis of *Z*-Alkenes. *Top. Curr. Chem.* **2012**, *327*, 33–58. [PubMed]
- Maryanoff, B.E.; Reitz, A.B. The Wittig olefination reaction and modifications involving phosphoryl-stabilized carbanions. Stereochemistry, mechanism, and selected synthetic aspects. *Chem. Rev.* **1989**, *89*, 863–927. [CrossRef]
- Bisceglia, J.Á.; Orelli, L.R. Recent applications of the Horner–Wadsworth–Emmons reaction to the synthesis of natural products. *Curr. Org. Chem.* **2012**, *16*, 2206–2230. [CrossRef]
- Bisceglia, J.Á.; Orelli, L.R. Recent progress in the Horner–Wadsworth–Emmons reaction. *Curr. Org. Chem.* **2015**, *19*, 744–775. [CrossRef]
- Kobayashi, K.; Tanaka, K., III; Kogen, H. Recent topics of the natural product synthesis by Horner–Wadsworth–Emmons reaction. *Tetrahedron Lett.* **2018**, *59*, 568–582. [CrossRef]
- Roman, D.; Sauer, M.; Beemelmans, C. Applications of the Horner–Wadsworth–Emmons Olefination in Modern Natural Product Synthesis. *Synthesis* **2021**, *53*, 2713–2739.
- Nagaoka, H.; Kishi, Y. Further synthetic studies on rifamycin S. *Tetrahedron* **1981**, *37*, 3873–3888. [CrossRef]
- Motoyoshiya, J.; Kusaura, T.; Kokin, K.; Yokoya, S.; Takaguchi, Y.; Narita, S.; Aoyama, H. The Horner–Wadsworth–Emmons reaction of mixed phosphonoacetates and aromatic aldehydes: Geometrical selectivity and computational investigation. *Tetrahedron* **2001**, *57*, 1715–1721. [CrossRef]
- Deschamps, B.; Lampin, J.P.; Mathey, F.; Seyden-Penne, J. Stereoselectivity of wittig type olefin synthesis using 5 membered cyclic phosphine oxides or phosphonous acid dimethylamides. *Tetrahedron Lett.* **1977**, *18*, 1137–1140. [CrossRef]
- Breuer, E.; Bannet, D.M. Stereoselectivity of wittig type olefin synthesis using five-membered cyclic phosphonates. preferential formation of *cis* olefins. *Tetrahedron Lett.* **1977**, *18*, 1141–1144. [CrossRef]
- Patois, C.; Savignac, P. 1,3-Dimethyl 2-oxo 1,3,2-diazaphospholidine precursor of (*Z*) α,β -unsaturated esters. *Tetrahedron Lett.* **1991**, *32*, 1317–1320. [CrossRef]
- Still, W.C.; Gennari, C. Direct synthesis of *Z*-unsaturated esters. A useful modification of the horner-emmons olefination. *Tetrahedron Lett.* **1983**, *24*, 4405–4408. [CrossRef]
- Ando, K. Practical synthesis of *Z*-unsaturated esters by using a new Horner–Emmons reagent, ethyl diphenylphosphonoacetate. *Tetrahedron Lett.* **1995**, *36*, 4105–4108. [CrossRef]
- Ando, K. Highly Selective Synthesis of *Z*-Unsaturated Esters by Using New Horner–Emmons Reagents, Ethyl (Diarylphosphono)acetates. *J. Org. Chem.* **1997**, *62*, 1934–1939. [CrossRef]
- Ando, K. *Z*-Selective Horner–Wadsworth–Emmons Reaction of α -Substituted Ethyl (Diarylphosphono)acetates with Aldehydes. *J. Org. Chem.* **1998**, *63*, 8411–8416. [CrossRef]
- Touchard, F.P.; Capelle, N.; Mercier, M. Efficient and Scalable Protocol for the *Z*-Selective Synthesis of Unsaturated Esters by Horner–Wadsworth–Emmons Olefination. *Adv. Synth. Catal.* **2005**, *347*, 707–711. [CrossRef]

18. Touchard, F.P. Phosphonate Modification for a Highly (Z)-Selective Synthesis of Unsaturated Esters by Horner–Wadsworth–Emmons Olefination. *Eur. J. Org. Chem.* **2005**, *2005*, 1790–1794. [CrossRef]
19. Janicki, I.; Kielbasiński, P. Still–Gennari Olefination and its Applications in Organic Synthesis. *Adv. Synth. Catal.* **2020**, *362*, 2552–2596. [CrossRef]
20. Janicki, I.; Kielbasiński, P. A Straightforward, Purification-Free Procedure for the Synthesis of Ando and Still–Gennari Type Phosphonates. *Synthesis* **2022**, *54*, 378–382. [CrossRef]
21. Pihko, P.M.; Salo, T.M. Excess sodium ions improve Z selectivity in Horner–Wadsworth–Emmons olefinations with the Ando phosphonate. *Tetrahedron Lett.* **2003**, *44*, 4361–4364. [CrossRef]
22. Janicki, I.; Kielbasiński, P. Application of the Z-Selective Still–Gennari Olefination Protocol for the Synthesis of Z- α,β -Unsaturated Phosphonates. *Synthesis* **2018**, *50*, 4140–4144. [CrossRef]
23. Mahajan, S.M.; Singh, I.P. Determining and reporting purity of organic molecules: Why qNMR. *Magn. Reson. Chem.* **2013**, *51*, 76–81. [CrossRef] [PubMed]
24. Akkarasamiyo, S.; Chitsomkhan, S.; Buakaew, S.; Samec, J.S.M.; Chuawong, P.; Kuntiyong, P. Synthesis of (Z)-Cinnamate Esters by Nickel-Catalyzed Stereoinvertive Deoxygenation of trans-3-Arylglycidates. *Synlett* **2022**, *33*, 1353–1356. [CrossRef]
25. Shu, P.; Xu, H.; Zhang, L.; Li, J.; Liu, H.; Luo, Y.; Yang, X.; Ju, Z.; Xu, Z. Synthesis of (Z)-Cinnamate Derivatives via Visible-Light-Driven E-to-Z Isomerization. *SynOpen* **2019**, *3*, 103–107. [CrossRef]
26. Gilchrist, T.L.; Rees, C.W.; Tuddenham, D. Generation of 3-methoxy-3a-methyl-3aH-indene and study of its cycloaddition reactions. *J. Chem. Soc. Perkin Trans. I* **1981**, 3214–3220. [CrossRef]
27. Lewis, F.D.; Howard, D.K.; Oxman, J.D.; Uthagrove, A.L.; Quillen, S.L. Lewis-acid catalysis of photochemical reactions. 6. Selective isomerization of .beta.-furylacrylic and urocanic esters. *J. Am. Chem. Soc.* **1986**, *108*, 5964–5968. [CrossRef] [PubMed]
28. Longwitz, L.; Spannenberg, A.; Werner, T. Phosphetane Oxides as Redox Cycling Catalysts in the Catalytic Wittig Reaction at Room Temperature. *ACS Catal.* **2019**, *9*, 9237–9244. [CrossRef]
29. Schabel, T.; Plietker, B. Microwave-Accelerated Ru-Catalyzed Hydrovinylation of Alkynes and Enynes: A Straightforward Approach toward 1,3-Dienes and 1,3,5-Trienes. *Chem. Eur. J.* **2013**, *19*, 6938–6941. [CrossRef]
30. Claridge, T.D.W.; Davies, S.G.; Lee, J.A.; Nicholson, R.L.; Roberts, P.M.; Russell, A.J.; Smith, A.D.; Toms, S.M. Highly (E)-Selective Wadsworth–Emmons Reactions Promoted by Methylmagnesium Bromide. *Org. Lett.* **2008**, *10*, 5437–5440. [CrossRef] [PubMed]
31. Ando, K. Convenient Preparations of (Diphenylphosphono)acetic Acid Esters and the Comparison of the Z-Selectivities of Their Horner–Wadsworth–Emmons Reaction with Aldehydes Depending on the Ester Moiety. *J. Org. Chem.* **1999**, *64*, 8406–8408. [CrossRef] [PubMed]
32. Liang, S.; Hammond, G.B.; Xu, B. Supported gold nanoparticles catalyzed cis-selective semihydrogenation of alkynes using ammonium formate as the reductant. *Chem. Commun.* **2016**, *52*, 6013–6016. [CrossRef] [PubMed]
33. Puri, S.; Babu, M.H.; Reddy, M.S. BF₃·OEt₂-mediated syn-selective Meyer–Schuster rearrangement of phenoxy propargyl alcohols for Z- β -aryl- α,β -unsaturated esters. *Org. Biomol. Chem.* **2016**, *14*, 7001–7009. [CrossRef] [PubMed]
34. Seifert, F.; Drikermann, D.; Steinmetzer, J.; Zi, Y.; Kupfer, S.; Vilotijevic, I. Z-Selective phosphine promoted 1,4-reduction of ynolates and propynoic amides in the presence of water. *Org. Biomol. Chem.* **2021**, *19*, 6092–6097. [CrossRef] [PubMed]
35. Shang, W.; Duan, D.; Liu, Y.; Lv, J. Carbocation Lewis Acid TrBF₄-Catalyzed 1,2-Hydride Migration: Approaches to (Z)- α,β -Unsaturated Esters and α -Branched β -Ketocarboxyls. *Org. Lett.* **2019**, *21*, 8013–8017. [CrossRef] [PubMed]
36. Murai, Y.; Nakagawa, A.; Kojima, S. Highly syn-Selective Elimination of Peterson anti-Adducts to Give Z- α,β -Unsaturated Esters. *Chem. Lett.* **2017**, *46*, 228–231. [CrossRef]
37. Wu, J.; Zhang, D.; Wei, S. Wittig Reactions of Stabilized Phosphorus Ylides with Aldehydes in Water. *Synth. Commun.* **2005**, *35*, 1213–1222. [CrossRef]
38. Yamamoto, Y.; Kawaguchi, S.-I.; Nishimura, M.; Sato, Y.; Shimada, Y.; Tabuchi, A.; Nomoto, A.; Ogawa, A. Phosphorus-Recycling Wittig Reaction: Design and Facile Synthesis of a Fluorous Phosphine and Its Reusable Process in the Wittig Reaction. *J. Org. Chem.* **2020**, *85*, 14684–14696. [CrossRef] [PubMed]

Review

Comprehensive Review on Synthesis, Properties, and Applications of Phosphorus (P^{III}, P^{IV}, P^V) Substituted Acenes with More Than Two Fused Benzene Rings

Marek Koprowski ^{1,*} , Krzysztof Owsianik ¹ , Łucja Knopik ¹ , Vivek Vivek ¹ , Adrian Romaniuk ¹ , Ewa Różycka-Sokołowska ² and Piotr Bałczewski ^{1,2,*} 

¹ Division of Organic Chemistry, Center of Molecular and Macromolecular Studies, Polish Academy of Sciences, Sienkiewicza 112, 90-363 Łódź, Poland

² Institute of Chemistry, Faculty of Science and Technology, Jan Długosz University in Częstochowa, Armii Krajowej 13/15, 42-200 Częstochowa, Poland

* Correspondence: mkopr@cbmm.lodz.pl (M.K.); pbalczew@cbmm.lodz.pl (P.B.)

Abstract: This comprehensive review, covering the years 1968–2022, is not only a retrospective investigation of a certain group of linearly fused aromatics, called acenes, but also a presentation of the current state of the knowledge on the synthesis, reactions, and applications of these compounds. Their characteristic feature is substitution of the aromatic system by one, two, or three organophosphorus groups, which determine their properties and applications. The (P^{III}, P^{IV}, P^V) phosphorus atom in organophosphorus groups is linked to the acene directly by a P-C_{sp2} bond or indirectly through an oxygen atom by a P-O-C_{sp2} bond.

Keywords: acene; anthracene; phosphine; phosphonate; phosphonium salt; phosphorane; phosphate; diphosphene; tri-, tetra-, pentacoordinated phosphorus; properties

Citation: Koprowski, M.; Owsianik, K.; Knopik, Ł.; Vivek, V.; Romaniuk, A.; Różycka-Sokołowska, E.; Bałczewski, P. Comprehensive

Review on Synthesis, Properties, and Applications of Phosphorus (P^{III}, P^{IV}, P^V) Substituted Acenes with More Than Two Fused Benzene Rings. *Molecules* **2022**, *27*, 6611. <https://doi.org/10.3390/molecules27196611>

Academic Editor: Jakub Adamek

Received: 9 September 2022

Accepted: 27 September 2022

Published: 5 October 2022

Publisher's Note: MDPI stays neutral with regard to jurisdictional claims in published maps and institutional affiliations.



Copyright: © 2022 by the authors. Licensee MDPI, Basel, Switzerland. This article is an open access article distributed under the terms and conditions of the Creative Commons Attribution (CC BY) license (<https://creativecommons.org/licenses/by/4.0/>).

1. Introduction

Organophosphorus-substituted acenes are an increasingly important group of aromatic hydrocarbons due to the unique properties of the phosphorus atom, which can form tri-, tetra-, and pentacoordinated compounds. This creates the possibility of tuning the electronic properties of the aromatic system of acenes by substituting with organophosphorus groups with different electron characters, from electron-donating phosphine groups to strongly electron-accepting phosphonium groups. The acenes of this type, especially anthracenes, have usually been synthesized with the intention of applying them to organic light-emitting diodes (OLEDs) [1,2]. Other uses of these acenes include the synthesis of ligands for metal catalysts in the hydroformylation reaction [3] or in the Diels–Alder reaction as dienes [4]. Anthrylphosphonic acids and their derivatives have also been employed in the synthesis of self-assembled monolayers [5,6] and anthrylbisphosphonates were used to synthesize fluorescent organic nanoparticles as apoptosis inducers of cancer cells [7].

Scope: Acenes, as defined, are a group of aromatic compounds containing linearly fused benzene rings. In the literature, compounds with angularly fused benzene rings, such as phenanthrene, and compounds with fused heteroaromatic five- and six-membered rings are sometimes included in this group, and they are specifically called angularly fused acenes and heteroacenes, respectively. Both groups, due to the large number of combinations of ring types and the ring positioning in the fused acene, in addition to derivatives of the simplest linearly fused acene, naphthalene, are not the subject of this review. By virtue of their chemical structure, organophosphorus groups have not been restricted and include all groups containing three-, four-, and five-coordinate phosphorus atoms. In the compounds reviewed, organophosphorus groups contain a phosphorus atom,

which is linked to the acene directly by a P-C_{sp2} bond or indirectly through an oxygen atom by a P-O-C_{sp2} bond, such as in phosphates.

This review of the literature covers the period of 1968–2021 and reveals a lack of aromatics that contain more than three fused benzene rings (tetracenes, pentacenes, etc.). Therefore, the subject of this review is anthracenes substituted with any organophosphorus groups.

In addition to the synthesis, this review discusses the reactions that these compounds undergo, and therefore, due to the difficulty of separating the two categories, “synthesis and reactions” are combined together in sections and subsections. Moreover, this review discusses the properties and applications of the synthesized derivatives as well.

This manuscript is divided into five main sections covering phosphines, P^{III} acids derivatives, diphosphenes, phosphonates and phosphonic acids, phosphates, and the hetero analogs of the mentioned compounds. In the subsections, groups of compounds that can be obtained directly from the precursor included in the main section are identified, e.g., phosphine oxides, phosphonium salts, and phosphoranes can be obtained from phosphines by oxidation, alkylation, and halogenation, respectively, and therefore they are included in the section devoted to the synthesis and reactions of phosphines and derivatives.

Finally, a comment on Section 3 is necessary. Phosphines (λ^3 -phosphanes), by definition, are P^{III} compounds containing a combination of three P-Z bonds (Z = C,H). Halophosphines AnthPX₂ and Anthr₂PX (X = F, Cl), which contain at least one P-C bond and one or two halogen atoms, are here classified as halides of the corresponding lower P^{III} acids [8]. Additionally included in this group are other representatives of the lower P^{III} acids, i.e., phosphonous acid diamides AnthP(NR₂)₂ (diaminophosphines) and phosphorous acid esters (phosphites).

As a consequence of this division, phosphonous acid P^{IV} tautomers (*H*-phosphinic acids) and phosphinous acid P^{IV} tautomers (*H*-phosphine oxides) are also reviewed in this section.

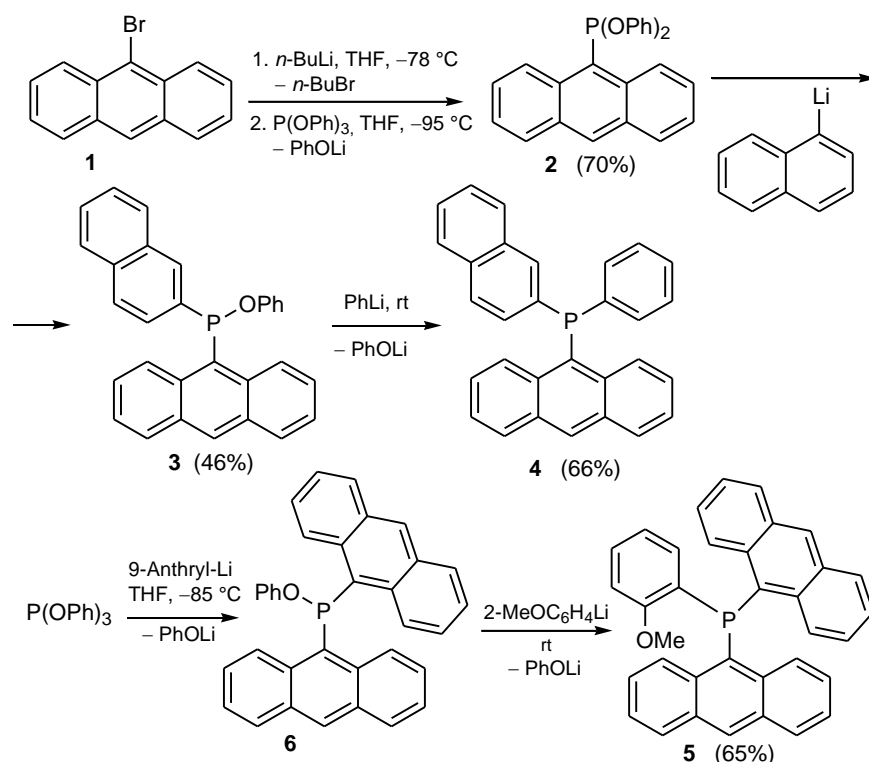
Diphosphenes, as the only compounds with a functional group containing more than one phosphorus atom, are discussed separately in Section 6.

2. Synthesis and Reactions of Phosphines (AnthPR₂) (Anth = Anthryl) and Derivatives

This section discusses phosphines, which contain a three-coordinated phosphorus atom linked to three carbon atoms. The subsections of this chapter include groups of compounds that can easily be obtained from phosphine precursors by direct transformation to give compounds with tetra- and pentacoordinated phosphorus atoms. Phosphine oxides, sulfides, and selenides are placed together in one subsection because most papers simultaneously describe the synthesis and reactions of two or three groups of these derivatives. Secondary phosphine oxides (*H*-phosphine oxides) are discussed in Section 3.5 as phosphinous acid P^{IV} tautomers.

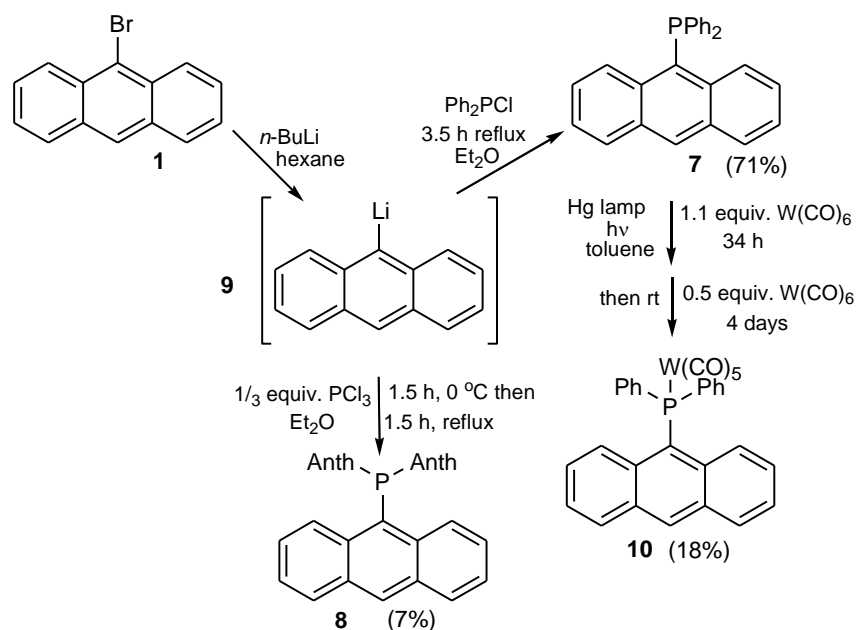
9-Bromoanthracene **1** is the most frequently used starting material for the syntheses of anthryl phosphines and other derivatives (cf. other subsections throughout this review).

A number of sterically shielded phosphorus ligands for metal catalysts were synthesized by Straub and co-workers via a selective stepwise nucleophilic substitution reaction at the phosphorus atom in triphenyl phosphite (Scheme 1). Thus, first, diphenyl 9-anthrylphosphonite **2** was obtained in a 70% yield by substitution of one phenoxy group by anthryllithium, generated from 9-bromoanthracene **1** and *n*-butyllithium. Next, the second phenoxy group in triphenyl phosphite was replaced by 1-naphthyllithium to afford phenyl 9-anthryl(1-naphthyl)phosphinite **3** in an overall yield of 46%. Finally, the third least reactive phenoxy group was replaced by phenyllithium to give (anthryl)(naphthyl)(phenyl)phosphine **4** in a 66% isolated yield over three steps. In another synthetic sequence, [di(9-anthryl)](2-methoxyphenyl)phosphine **5** was obtained from triphenyl phosphite via phenyl phosphinite **6** by reacting triphenyl phosphite first with 9-anthryllithium, followed by 2-methoxyphenyllithium at −85 °C. Since phosphorus ligands, employed in homogeneous catalysis, often contain at least one sterically demanding substituent, this method delivers a strategy for the rapid and cost-efficient synthesis of such ligands [9].



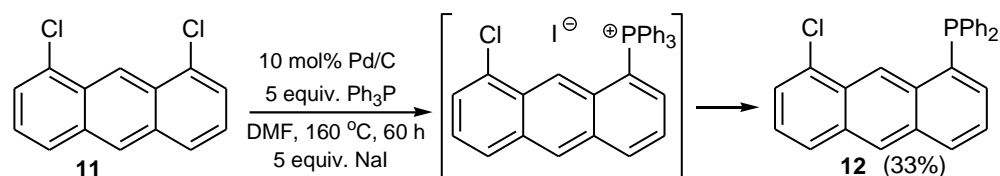
Scheme 1. The synthesis of sterically hindered phosphine ligands 4 and 5.

Schmutzler et al. reported the synthesis of (anthryl)(diphenyl)phosphine 7 and trianthrylphosphine 8 starting from 9-bromoanthracene 1, which was lithiated to give the intermediate 9-lithioanthracene 9. The latter was reacted with 1 equiv. of chlorodiphenylphosphine or 1/3 equiv. of PCl_3 in diethyl ether at reflux to give 7 or 8 in 71% and 7% yields, respectively. The irradiation of 7 in the presence of W(CO)_6 with a mercury lamp for 34 h formed the pentacarbonyltungsten complex 10 in an 18% yield (Scheme 2) [10].



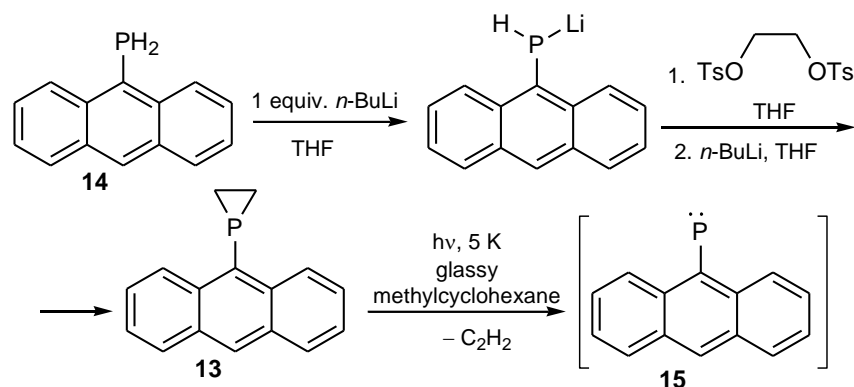
Scheme 2. The synthesis of (anthryl)(diphenyl)phosphine 7 and trianthrylphosphine 8 and the pentacarbonyltungsten complex 10.

Chan and co-workers reported a simple monophosphinylation reaction of 1,8-dichloroanthracene **11**, leading to 8-chloro-1-(diphenylphosphino)anthracenes **12** in a 33% yield (Scheme 3) [11]. This reaction was carried out in DMF at 160 °C for 60 h and catalyzed by 10 mol% of palladium supported on charcoal in the presence of 5 equiv. of triphenylphosphine. The addition of 5 equiv. of sodium iodide improved both the rate and yield of the reaction. The second chlorine atom in **11** was not substituted in this reaction and only the mono-derivative **12** was observed, despite the presence of an excess of triphenylphosphine. The authors claimed that steric hindrance of the diphenylphosphino group in position 1 of anthracene protected against the reaction of the second chlorine atom.



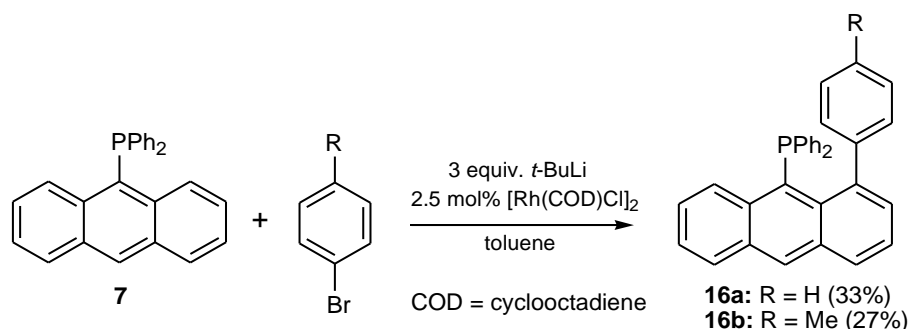
Scheme 3. The synthesis of 8-chloro-1-(diphenylphosphino)anthracenes **12**.

Misochko and co-workers [12] obtained 9-(1-phosphirano)anthracene **13** from 9-phosphinoanthracene **14** and ethylene glycol ditosylate as substrates by adapting the procedure of Robinson et al. [13] (Scheme 4). In the next step, 9-(1-phosphirano)anthracene **13** was subjected to UV photolysis to receive a stable triplet anthrylphosphinidene **15**, which could be characterized by electron paramagnetic resonance (EPR).



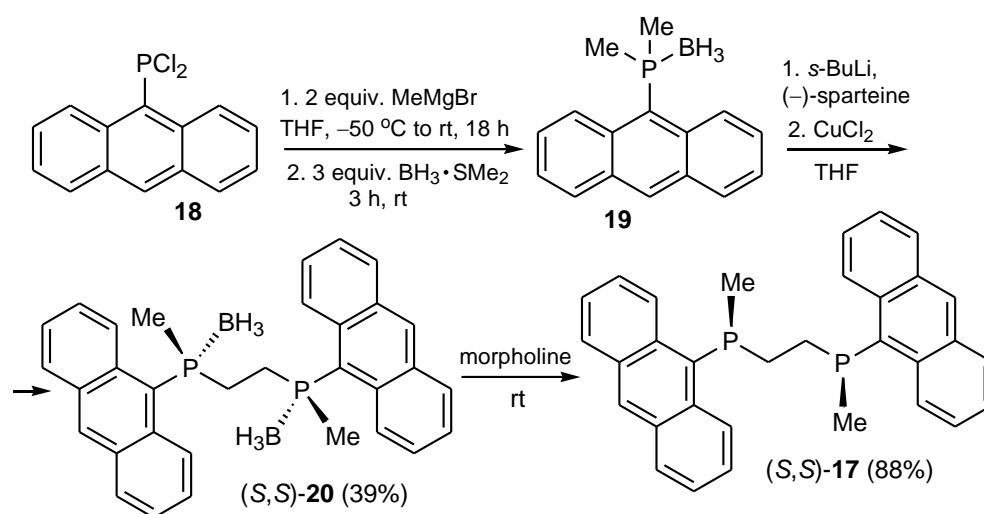
Scheme 4. Synthesis of 9-(1-phosphirano)anthracene **13**, a precursor of the phosphinidene **15**.

Che and co-authors reported the rhodium(I)-catalyzed C–H arylation of 9-(diphenylphosphino)anthracene **7**, as an example of functionalization of phosphines, to give 1-aryl-substituted derivatives **16a** and **16b** (Scheme 5) [14]. The presented strategy provided access to *peri*-substituted (naphth-1-yl)phosphines as well.



Scheme 5. The Rh-catalyzed arylation of 9-(diphenylphosphino)anthracene **7** with different aryl bromides.

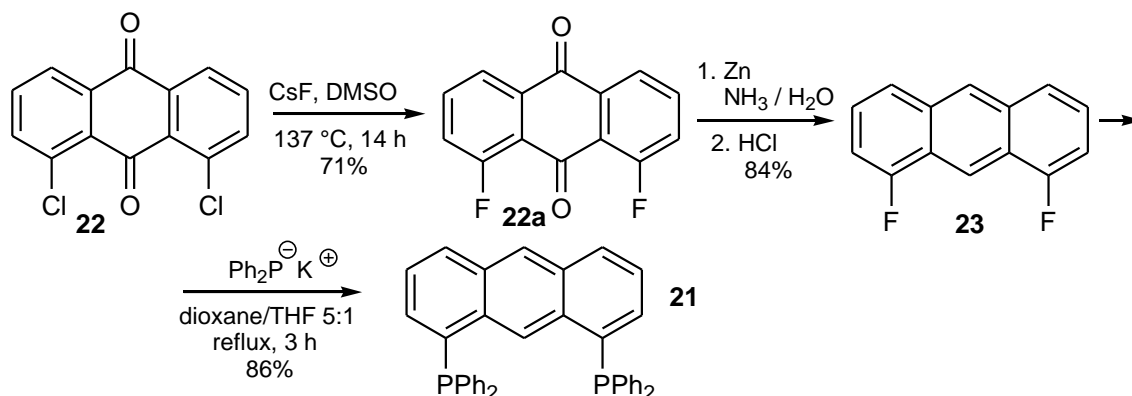
The synthesis of optically active 1,2-ethylene bis(phosphine) (*S,S*)-**17**, presented by Maienza and co-workers, is the only example of a molecule containing two anthrylphosphino moieties linked via an alkyl linker [15]. First, 9-(dichlorophosphino)anthracene **18** was utilized in the reaction with methyl magnesium bromide and $\text{BH}_3 \cdot \text{SMe}_2$ to obtain 9-anthryldimethylphosphine borane **19**. Then, **19** was enantioselectively deprotonated in the presence of (–)-sparteine with *s*-BuLi and then oxidatively coupled with Cu (II) to give a mixture of enantiomers of 1,2-ethylene bis(phosphine) diboranes (*S,S*)-**20** and (*R,S*)-**20** in a 6:1 ratio and 70% total yield (Scheme 6). Diastereomerically pure (*S,S*)-**20** was received by crystallization from a $\text{CH}_2\text{Cl}_2/\text{Et}_2\text{O}$ mixture in a 39% yield and 18% ee. Finally, the diphosphine borane (*S,S*)-**20** was deprotected by stirring in morpholine at room temperature for 12 h. In this reaction, the 1,2-ethylene bis(phosphine) (*S,S*)-**17** was obtained and its enantiomeric excess was determined based on the corresponding phosphine oxide, which was prepared by oxidation of **17** with an excess of H_2O_2 .



Scheme 6. The synthesis of 1,2-ethylene bis(phosphine) **17**.

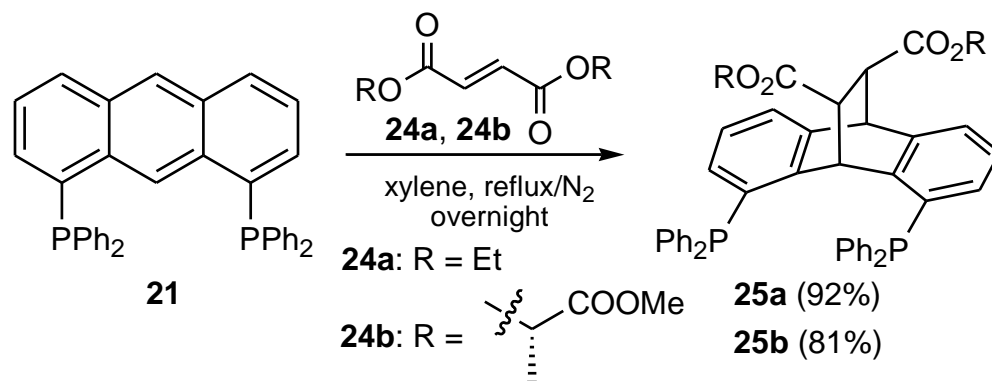
In the reviewed literature, the synthesis, transformations, and utilization of anthracenes with two phosphino groups on the aromatic moiety were found and are presented below.

1,8-Bis(diphenylphosphino)anthracene **21** was synthesized in a three-step reaction in a 51% overall yield starting from 1,8-dichloro-9,10-anthraquinone **22** by Haenel and co-workers (Scheme 7). The anthraquinone **22** was converted to 1,8-difluoroanthracene **23** by chlorine-fluorine exchange to give **22a** followed by reduction with zinc, from which **21** was obtained by reacting it with potassium diphenylphosphide [16].



Scheme 7. The synthesis of 1,8-bis(diphenylphosphino)anthracene **21** from 1,8-dichloro-9,10-anthraquinone **22**.

Gelman and co-workers presented the quantitative Diels–Alder cycloaddition of 1,8-bis-(diphenylphosphino)anthracene **21** to diethyl fumarate **24a**. The adduct **25a** was used for the synthesis of bifunctional PCsp³P pincer catalyst for the acceptorless dehydrogenation (CAD) of the primary and secondary alcohols to give carbonylic and carboxylic compounds (Scheme 8) [17].



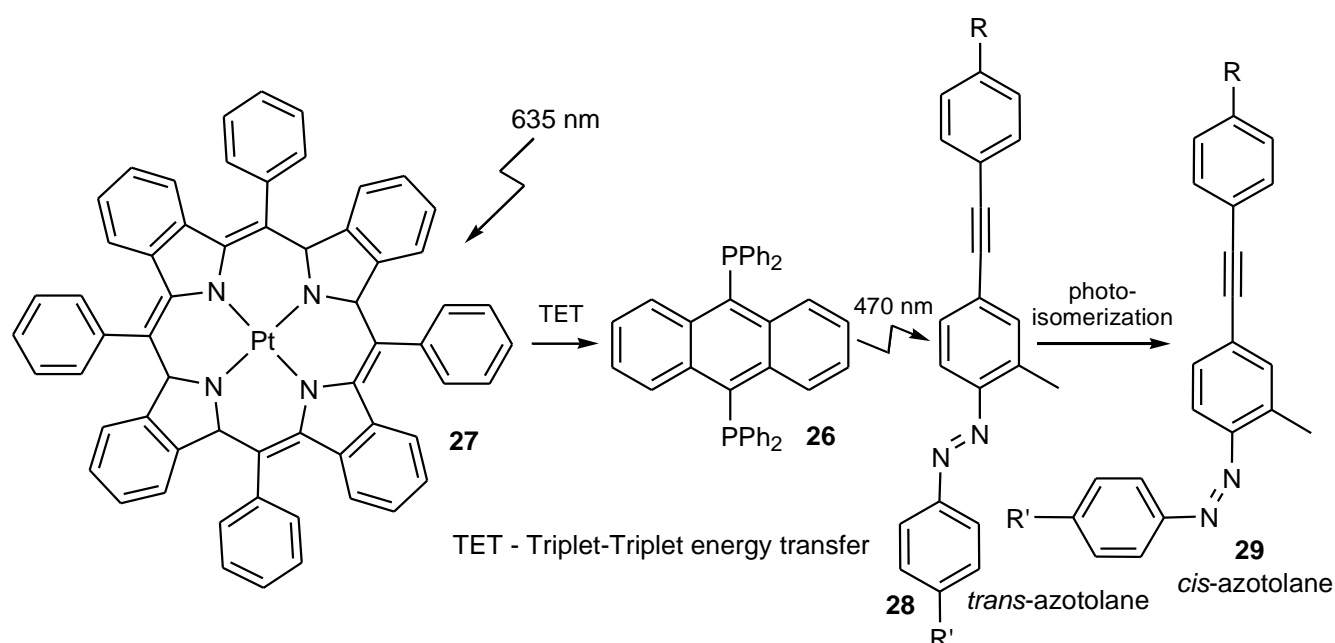
Scheme 8. The Diels–Alder cycloaddition reaction of 1,8-bis-(diphenylphosphino)anthracene **21** with dialkyl fumarates.

The same research group reported a synthetic scheme that relied on the carbo-Diels–Alder reaction cycloaddition of 1,8-bis-(diphenylphosphino)anthracene **21** to enantiomerically pure bis-(methyl-(*S*)-lactyl) fumarate **24b**, leading to the formation of chromatographically resolvable diastereomers **25b** that could be converted into a pair of enantiomerically pure antipodes (Scheme 8) [18].

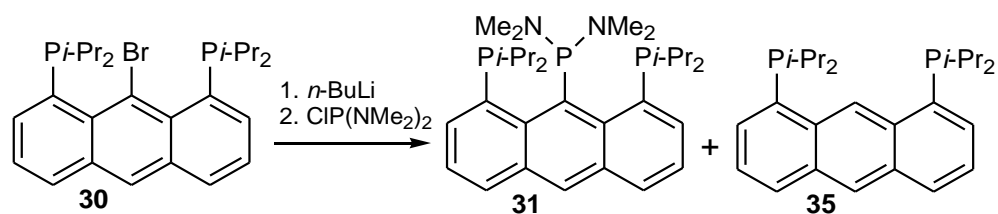
Jiang and co-workers [19] showed a practical utilization of 9,10-bis(diphenylphosphino)anthracene **26**. They obtained a red-light-controllable soft actuator, which was driven by the low-power excited triplet–triplet annihilation-based upconversion luminescence. This system consisted of 9,10-bis(diphenylphosphino)anthracene **26** and the Pt(II) tetraphenyl-tetrabenzoporphyrin complex **27** (Scheme 9). It was then incorporated into a rubbery polyurethane film and assembled with an azotolane-containing film to study its possible utilization as a highly effective phototrigger of photodeformable cross-linked liquid-crystal polymers. In this system, the Pt(II) complex **27** acted as a sensitizer, whereas **26** was an annihilator, which induced *trans-cis* photoisomerization of azotolane **28** and **29**. The authors achieved a highly effective red-to-blue triplet-triplet annihilation-based upconversion layout with a low-energy excitation light source, large anti-Stokes shift (165 nm), and high absolute quantum yield (9.3%).

In the literature reviewed, the chemistry of anthracenes with two or three phosphino groups and their mixed tetracoordinated derivatives was also found and is presented below.

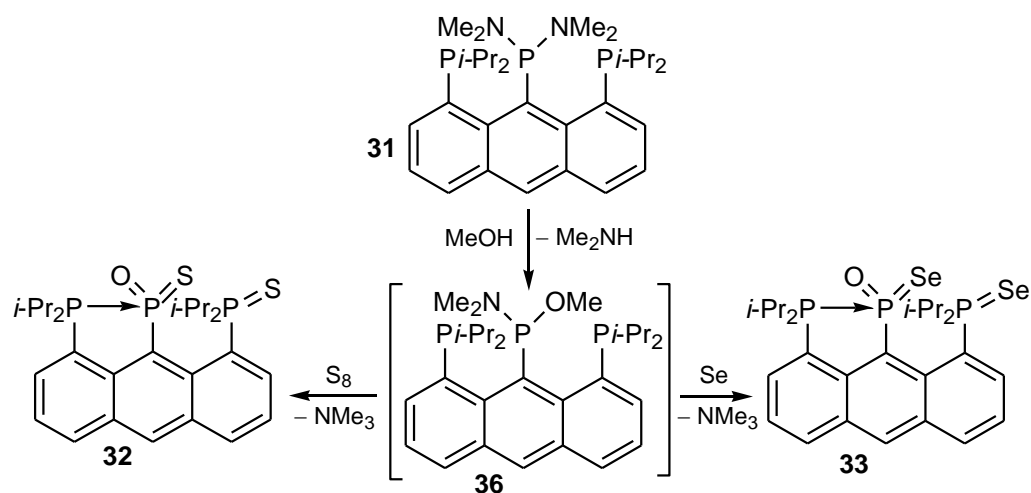
Thus, 9-bromo-1,8-bis(diisopropylphosphino)anthracene **30**, repulsively interacting with 1,8,9-tris(phosphino)anthracene **31** (Scheme 10), single donor stabilized 8-diisopropylphosphino-1-thiophosphinoyl-9-metathio/metasenophosphono)anthracenes **32** and **33** (Scheme 11), and doubly phosphine donor stabilized phosphonium salt **34** (Scheme 12), were synthesized by Kilian and co-workers [20]. The attempted introduction of the third phosphorus atom at the position 9 via Br/Li exchange followed by the reaction with chlorobis(dimethylamino)phosphine resulted in formation of 1,8,9-tris- and 1,8-bis(phosphino)anthracenes **31** and **35**, respectively. The derivative **31** had two relatively inert and bulky diisopropylphosphino groups at positions 1 and 8 whilst the third reactive phosphino group with two P–N bonds on the middle ring opened up the possibility of various transformations on this phosphorus atom, situated in a very crowded surrounding.



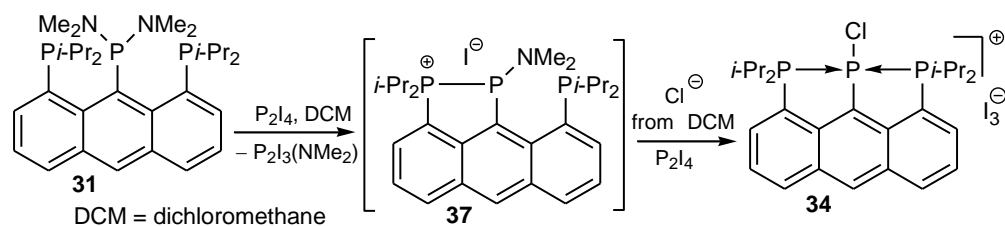
Scheme 9. An example of the application of 26 in a red-light-controllable soft actuator system (photoisomerization of azotolane).



Scheme 10. Synthesis of repulsively interacting 1,8,9-tris(phosphino)anthracene 31 and 1,8-bis(phosphino)anthracene 35.



Scheme 11. The synthesis of single donor stabilized anthracenes 32 and 33 with metathio/selenophosphono groups.



Scheme 12. Synthesis of the doubly phosphine stabilized phosphonium salt **34**.

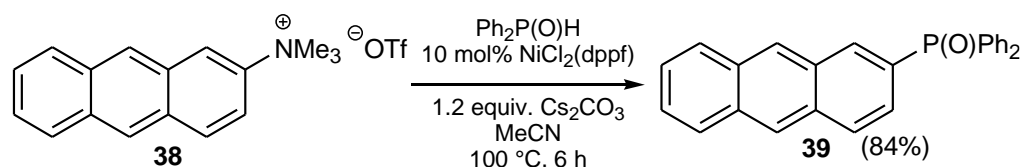
Alcoholysis of **31**, leading to the intermediate **36**, followed by oxidation with sulfur or selenium, afforded phosphine donor stabilized anthracenes **32** or **33** with metaphosphono groups, respectively.

Further reaction of **31** with diphosphorus tetraiodide in 1,2-dichloromethane gave the chlorophosphonium cation **34** stabilized by two phosphino donors at positions 1 and 8, forming a linear P–P–P arrangement. In the first step, the phosphino-phosphonium cation **37** was formed as a transient species. In the next step, the dimethylaminophosphino group was substituted by the chloride anion, which was available from the I/Cl halogen exchange reaction in chlorinated solvent (DCM). Iodide and iodine (I₂) and triiodide originated from disproportionation reaction of P₂I₄.

2.1. Phosphine Oxides (AnthP(=O)R₂), Phosphine Sulfides (AnthP(=S)R₂), Phosphine Selenides (AnthP(=Se)R₂)

Phosphine oxides, sulfides, and selenides are placed together in one subsection because most papers simultaneously describe the synthesis and reactions of two or three groups of these derivatives. All of them were obtained directly from the corresponding phosphines.

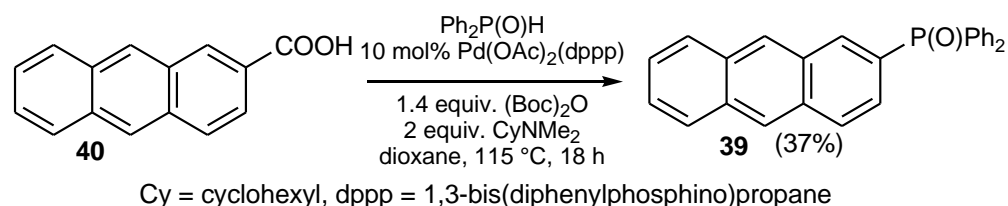
A new method for the synthesis of phosphine oxides was published by Yang et al. [21]. They employed a cross-coupling reaction and showed that aryl, vinyl, and benzyl-ammonium triflates reacted with the corresponding phosphorus-based nucleophiles in the presence of the nickel catalyst NiCl₂/dppf, (dppf = 1,1'-bis(diphenylphosphino)ferrocene) (Scheme 13).



Scheme 13. The synthesis of 2-(diphenylphosphinoyl)anthracene **39** using anthryl ammonium triflate **38**.

The counterion played a minor role in this reaction, so it could be replaced with chloride, bromide, iodide, mesylate, or tosylate anions without a significant loss of yield. A considerable advantage of this synthesis was that ammonium salts are cheap and readily viable.

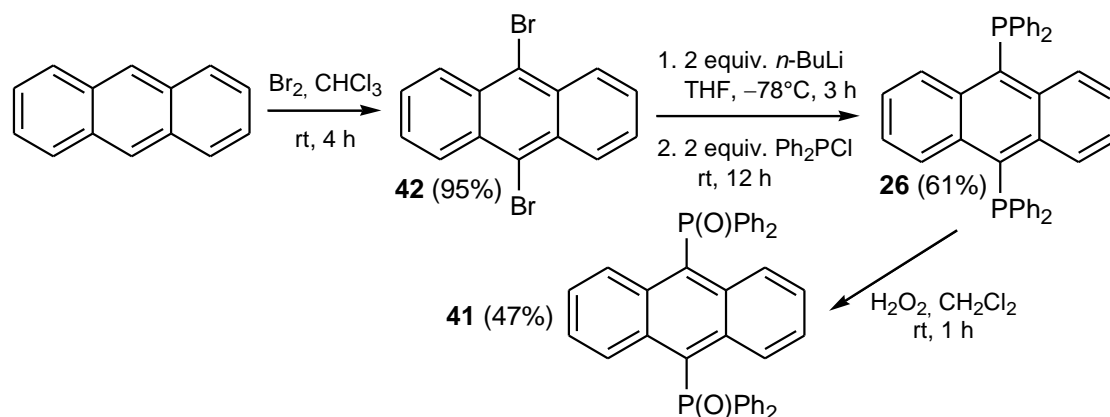
Another method, which was developed by Zhang et al. [22], involved a direct transformation of aromatic acids into the corresponding phosphine oxides in the presence of palladium(II) salts. Several substrates were shown to react in this manner, including 2-anthric acid **40**, which was transformed to 2-(diphenylphosphinoyl)anthracene **39** (Scheme 14), providing an alternative to the synthesis of the latter from anthryl ammonium triflate **38** (Scheme 13), although in significantly lower yields.



Scheme 14. The synthesis of 2-(diphenylphosphinoyl)anthracene **39** using 2-anthric acid **40**.

The optimal temperature for the reaction was 115 °C. Changing the temperature reduced the yield, as did changing the solvent to a highly polar one (DMF, *N,N*-dimethylformamide).

Another study carried out by Zhao and coworkers [1] showed that 9,10-bis(diphenylphosphinoyl)anthracene **41** could readily be synthesized from 9,10-dibromoanthracene **42** by substitution of chlorine in chlorodiphenylphosphine with 9,10-dilithioanthracene obtained from a double Br/Li exchange in **42** followed by oxidation of the resulting bis(diphenylphosphino)anthracene **26** with hydrogen peroxide to yield **41** in a 47% yield. 9,10-Dibromoanthracene **42** was obtained by bromination of anthracene in chloroform (Scheme 15).

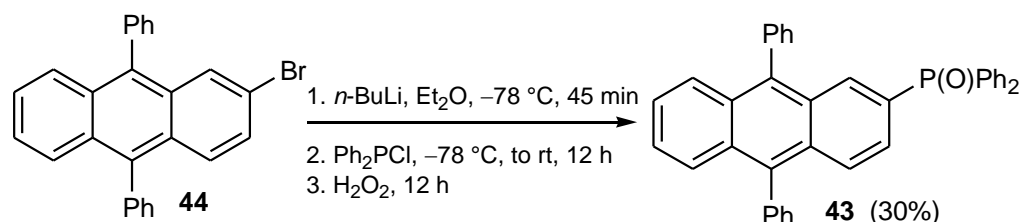


Scheme 15. The synthesis of 9,10-bis(diphenylphosphinoyl)anthracene **41** from 9,10-dibromoanthracene **42**.

The product **41** has been synthesized with the intention of applying it in organic light-emitting diodes (OLEDs). Zhao et al. found that **41** was a yellow-green solid with a melting point that reached 265 °C. A similar study by Tao and co-workers [23] confirmed the fluorescent properties of **41**, which could be used in the construction of OLEDs. The authors also claimed that the conversion from **26** to **41** was the first reported triplet-triplet annihilation system activated by hydrogen peroxide.

Furthermore, Xu and co-workers [24] linked the increase in fluorescence properties within the **26**/ H_2O_2 system to the degree of photooxidation. This system could be used as an indicator of the reaction time, oxygen exposure, and light irradiation or a time-oxygen and light indicator (TOLI). The compound **41** was also the subject of interest in another study by Xu et. al. [25], who used it to investigate the properties of a samarium complex $\text{Sm}(\text{hfac})_3(\mathbf{41})_3$ (hfac = hexafluoroacetylacetonato).

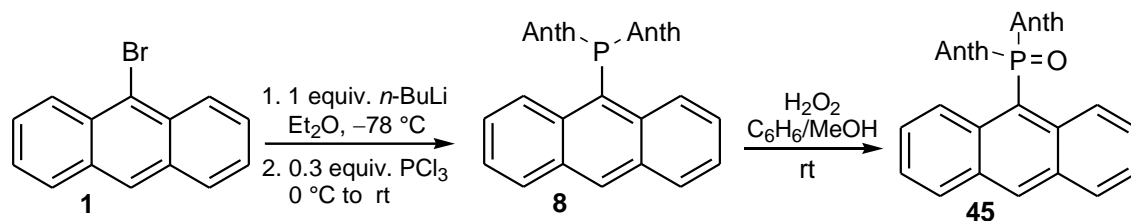
Wu and co-workers [2] showed the synthesis and properties of (9,10-diphenyl-2-phosphinoyl)anthracene **43** with the intention of using it as a true-blue OLED material. The synthesis was similar to the one proposed by Zhao and coworkers [1]: it included treatment of 2-bromo-9,10-diphenylanthracene **44** with *n*-BuLi, followed by the addition of chlorodiphenylphosphine and subsequent oxidation (Scheme 16).



Scheme 16. The synthesis of (9,10-diphenyl-2-phosphinoyl)anthracene **43** from 2-bromo-9,10-diphenylanthracene **44**.

The compound **43**, which readily crystallized as a light-yellow solid, was obtained in a 30% yield. It exhibited red-shift fluorescence compared to 9,10-diphenylanthracene. This study showed that **43** was not suitable for the true-blue OLED material due to the fact that the compound exhibited a red shift.

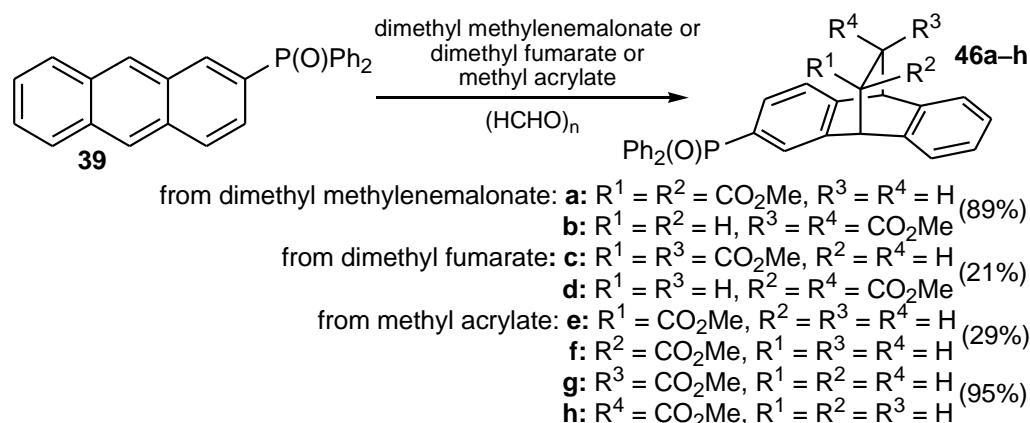
Yamaguchi et al. [26] reported a synthesis and photochemical characterization of tri(9-anthryl)phosphine **8** and tri(9-anthryl)phosphine oxide **45** (Scheme 17).



Scheme 17. The synthesis of trianthryl-substituted derivatives **8** and **45** reported by Yamaguchi and coworkers.

Tri(9-anthryl)phosphine **8** was synthesized from 9-bromoanthracene **1** by treatment with *n*-butyllithium, followed by the addition of phosphorus trichloride. Tri(9-anthryl)phosphine oxide **45** was obtained by oxidation of **8** with hydrogen peroxide (Scheme 17). The tri-coordinated **8** and tetra-coordinated derivative **45** exhibited a weak fluorescence.

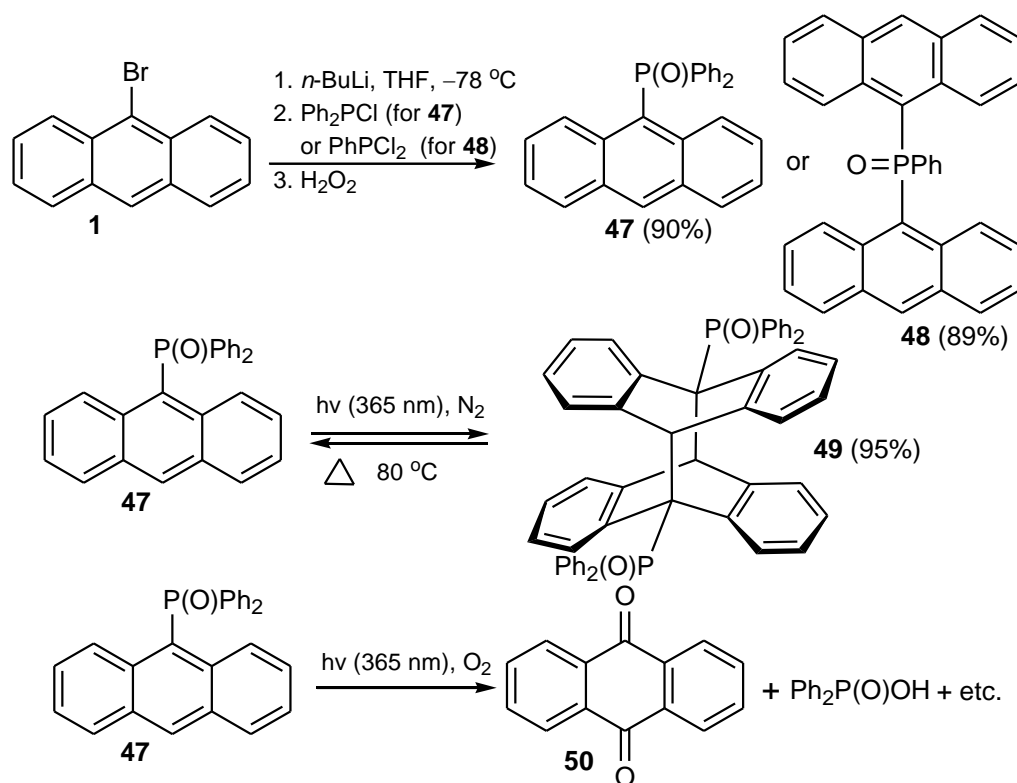
The synthesis of phosphine oxides **46a–h** containing carboxylic acid esters and 9,10-dihydro-9,10-ethanoanthracene moiety, described by Okada and co-workers, is an example of utilization in the synthesis of 2-(diphenylphosphinoyl)anthracene **39**. The bulky compounds **46a–h** were synthesized in the reaction of **39** with dimethyl methylene malonate, dimethyl fumarate, or methyl acrylate and paraformaldehyde in 21–95% yields. (Scheme 18) [27].



Scheme 18. Synthesis of phosphine oxides **46a–h** moiety containing carboxylic acid esters from 2-(diphenylphosphinoyl)anthracene **39**.

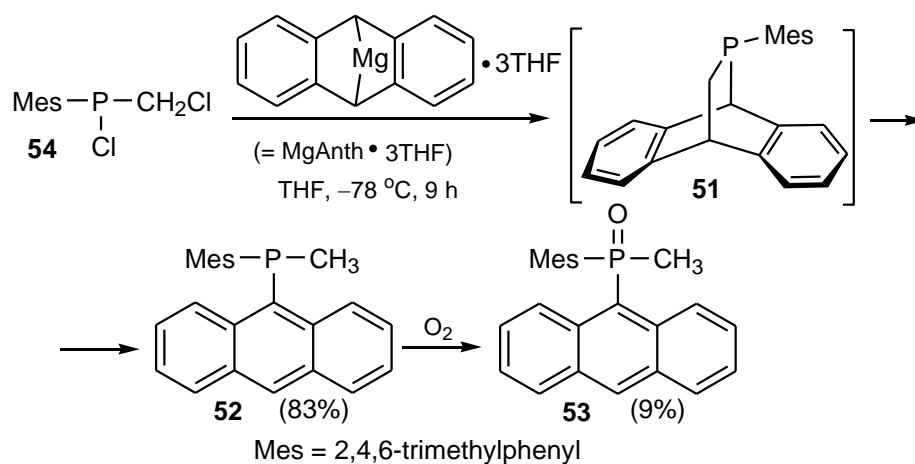
Katagiri et al. [28] synthesized 9-(diphenylphosphinoyl)anthracene **47** and 9-(anthrylphenylphosphinoyl)anthracene **48** from diphenyl chlorophosphine and phenyl dichlorophosphine, respectively (Scheme 19). The synthesis was analogous to the previous method by Schwab and co-workers [29] and first required halogen/lithium exchange and then oxidation with H_2O_2 . The authors revealed that phosphine oxides **47** and **48** did not lead to the formation of a photodimer in the solid state, whereas in chloroform or acetonitrile under an N_2 atmosphere, at the 365-nm-wavelength irradiation, the $[4\pi + 4\pi]$ photodimerization of **47** occurred to give **49**. In addition, the absorption and emission spectra of the compound **47** in acetonitrile showed characteristic absorption and emission bands of anthryl moieties while photodimerization of the anthryl groups led to the disappearance of these bands. The authors reversibly returned **49** to **47** by heating the probe at

80 °C. In contrast, analogous irradiation under an O₂ atmosphere resulted in the formation of anthraquinone **50**.



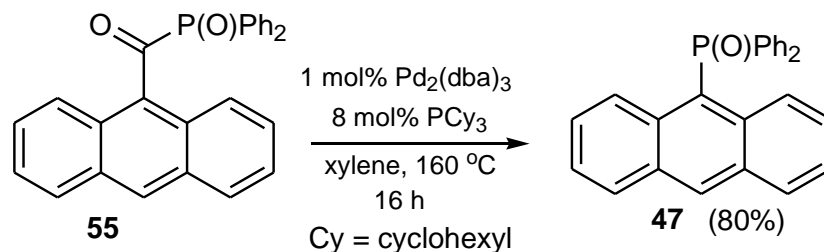
Scheme 19. The synthesis of 9-(diphenylphosphino)anthracene **47**, 9-(anthrylphenylphosphino)anthracene **48**, and the products of irradiation of **47** under N₂ and O₂ conditions, respectively.

During attempts to obtain a “masked” version **51** of the phosphalkene Mes-P=CH₂, Gates and co-workers [30] synthesized 9-[(methyl)(mesityl)phosphino]anthracene **52** and the corresponding 9-[(methyl)(mesityl)phosphinoyl]anthracene **53** in the reaction between (chloro) (chloromethyl) (mesityl) phosphine **54** and the anthracene magnesium (MgAnth•3THF) in THF. The expected adduct **51**, which was initially formed, then decomposed to give the anthracene derivative **52** in an 83% yield. The latter was oxidized to **53** in a 9% yield only (Scheme 20).



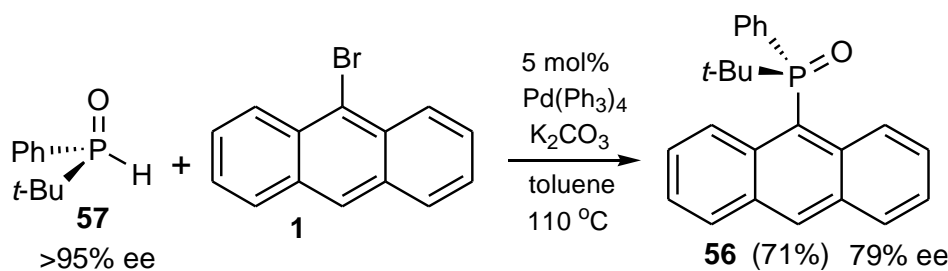
Scheme 20. The synthesis of 9-[(methyl)(mesityl)phosphino]anthracene **52** and the corresponding 9-[(methyl)(mesityl)phosphinoyl]anthracene **53**.

Wang and Zhu reported the palladium-catalyzed decarbonylation of 9-[(1-keto diphenylphosphinoyl)]anthracene **55** in the presence of 1 mol% of $\text{Pd}_2(\text{dba})_3$ and 8 mol% of the phosphine ligand (PCy_3) to give 9-(diphenylphosphinoyl)anthracene **47** in an 80% yield [31] (Scheme 21).



Scheme 21. Decarbonylation of 9-[(1-keto diphenylphosphinoyl)]anthracene **55**.

Drabowicz and co-workers synthesized optically active 9-[(*t*-butyl)(phenyl)phosphinoyl]anthracene **56** in a 71% yield in the Hirao reaction of palladium-catalyzed cross-coupling reaction of 9-bromoanthracene **1** with optically active *t*-butylphenylphosphine oxide **57** (Scheme 22) [32]. The formation of carbon–phosphorus bonds took place with retention of the configuration, and the stereoretention of this reaction was confirmed by X-ray analysis.



Scheme 22. The synthesis of optically active 9-[(*t*-butyl)(phenyl)phosphinoyl]anthracene **56**.

Stalke and co-workers synthesized three positional isomers of 1-, 2-, and 9-(diphenylthiophosphinoyl)anthracenes **58**, **59**, and **60** that revealed a solid-state fluorescence in three different colors with differences in emission wavelengths of over 100 nm. Analysis of the solid-state structure of **59** and photophysical properties allowed the unusual yellow emission to be attributed to the formation of excimer in the solid state. Therefore, substitution at position 1 of the anthracene fluorophore with suitable substituents may be a promising strategy to obtain long wavelength emission in the solid state using structurally easy to modify compounds (Figure 1) [33].

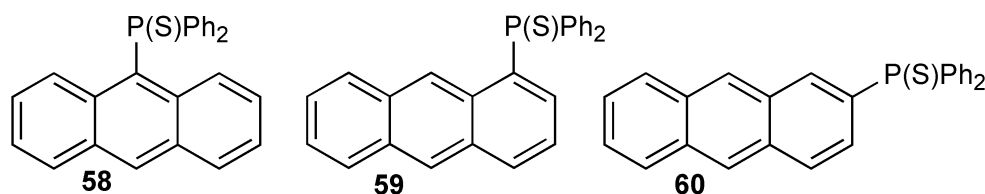
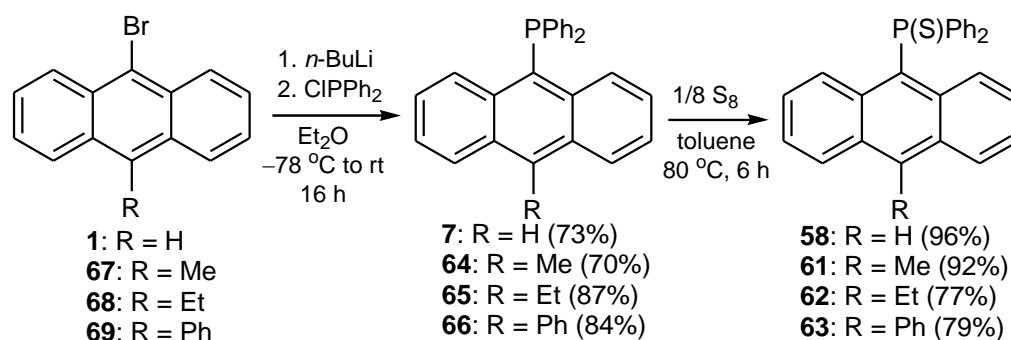


Figure 1. Three positional isomers of 1-, 2- and 9-(diphenylthiophosphinoyl)anthracenes **58**, **59**, and **60**.

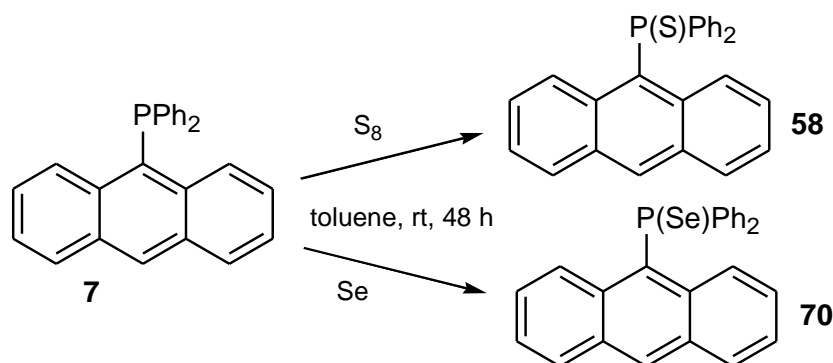
Schillmöller and co-workers [34] synthesized four 9-(diphenylthiophosphinoyl)anthracenes **58** and **61–63** with alkyl and phenyl substituents at the position 10 via sulfuration of 9-(diphenylphosphino)anthracenes **7** and **64–66**. The latter were obtained from the corresponding bromoanthracenes **1** and **67–69** (Scheme 23) [35,36].



Scheme 23. The preparation of 9-(diphenylthiophosphinoyl)anthracenes **58** and **61–63**.

The compounds **58** and **61–63** were crystallized and their X-ray structures were then determined. These studies revealed that oxidation of the phosphorus atom with sulfur significantly changed the molecular structural parameters and the crystal packing. This caused a strong bathochromic shift, which resulted in a green solid-state fluorescence. Moreover, the authors prepared four host-guest complexes, with **62** as a host molecule and benzene, pyridine, toluene, and quinoline as guest molecules. This resulted in enhanced emission and up to a five times higher quantum yield in comparison to the pure compound **62**.

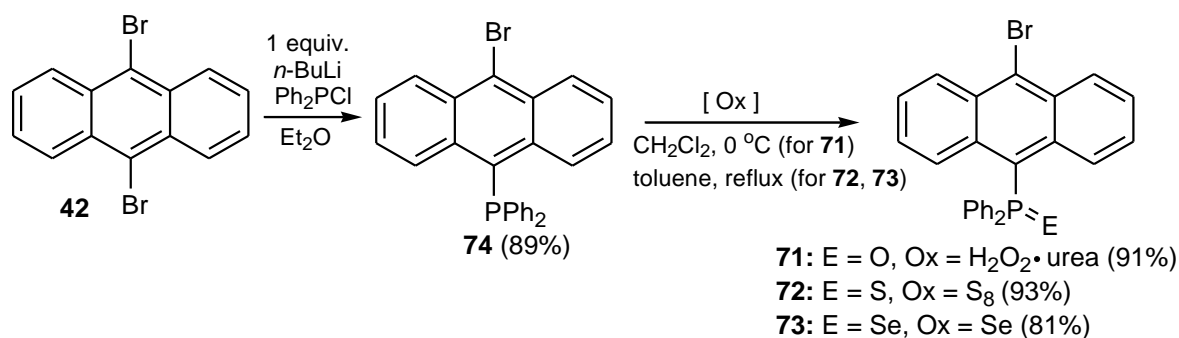
Walensky et al. characterized 9-(diphenylthio- and diphenylselenophosphinoyl)anthracenes **58** and **70**, respectively, by NMR and optical spectroscopy (Scheme 24) [37]. The authors demonstrated that ^{31}P NMR shifts for **58** and **70** were shifted upfield when compared to the unoxidized analog. This was due to the loss of planarity and relatively greater σ - than π -bonding between the phosphorus atom and the anthracene carbon.



Scheme 24. The syntheses of 9-(diphenylthio- and diphenylselenophosphinoyl)anthracenes **58** and **70**.

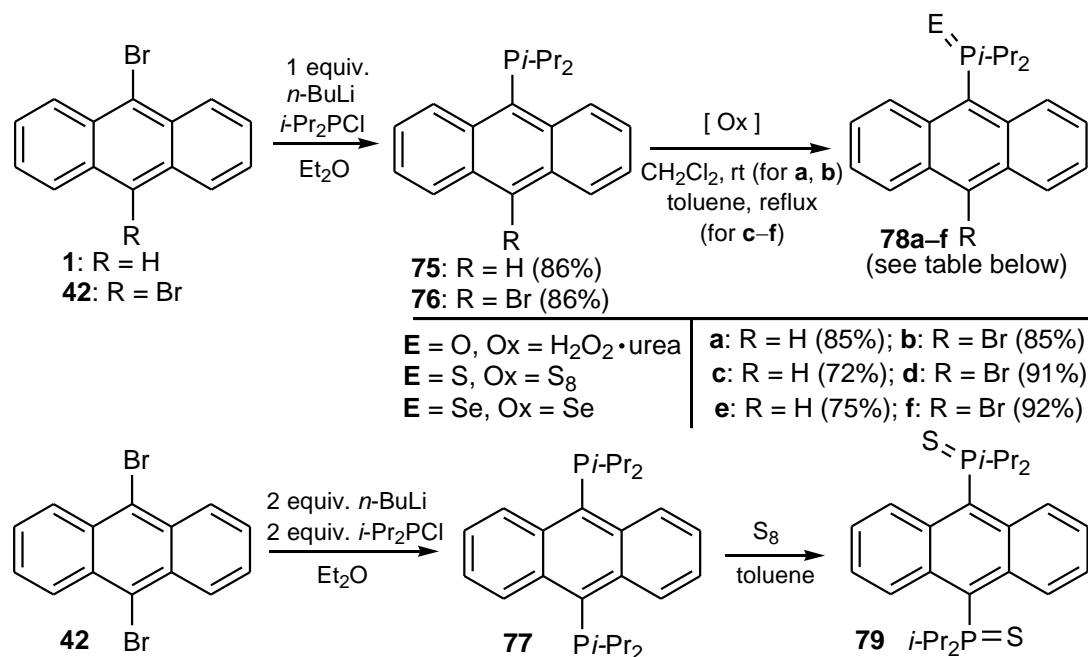
When excited at 310 nm, compounds **58** and **70** showed emission similar to that of unsubstituted anthracene, displaying peaks at 380, 402, 430, and 450 nm. When the excitation wavelength was shifted to 410 nm, the observed emission became structureless and was red-shifted by around 50 nm relative to the typical emission of the unsubstituted anthracene. The authors did not observe excimer formation for these compounds. Moreover, a small deviation from planarity in the anthracene ring was observed for **58** and **70** and the angle of deflection was 3° and 5° , respectively.

Schwab and co-workers [38] obtained 9-bromo-10-(diphenylphosphino)anthracene **71** and its thio- **72** and seleno- **73** derivatives (Scheme 25). In the first stage, 9,10-dibromoanthracene **42** was treated with *n*-BuLi followed by the addition of chlorodiphenylphosphine to give 9-bromo-10-(diphenylphosphino)anthracene **74**. Then, **74** was oxidized to the corresponding oxo-, thio-, and seleno derivatives **71–73** in high yields according to the procedure described by Stalke et al. [39]. Their spectral and structural properties were investigated and shown to be largely consistent with those of the 9,10-diphosphino derivatives **80–82** mentioned below (Scheme 27).



Scheme 25. The synthesis of 9-bromo-10-(diphenylphosphino)anthracene **6** and its oxo-, thio-, and seleno derivatives **71–73**.

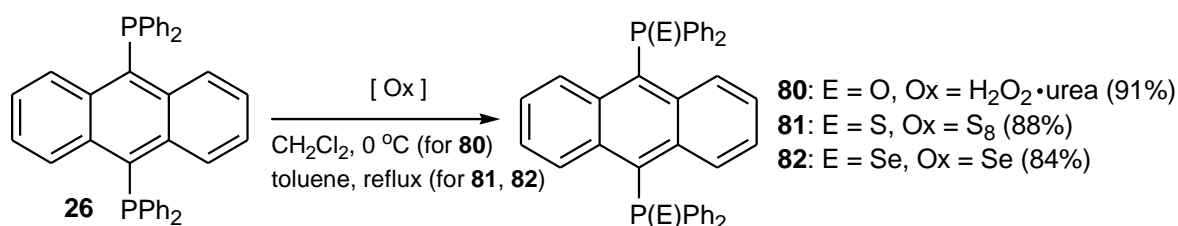
In an analogous manner, the same authors [29] synthesized bulky 9-(diisopropylphosphino)anthracene **75**, 9-bromo-10-(diisopropylphosphino)anthracene **76**, and 9,10-symmetrically-substituted anthracene **77**, which were then oxidized to the corresponding derivatives **78a–f** and **79** (Scheme 26).



Scheme 26. The synthesis of phosphinoanthracenes **75**, **76**, and **77** and their oxo-, thio-, and seleno derivatives **78a–f** and **79**.

9,10-Bis(diphenylphosphinoyl)anthracene **80**, 9,10-bis(diphenylthiophosphinoyl)anthracene **81**, and 9,10-bis(diphenylselenophosphinoyl)anthracene **82** were obtained by oxidation (E = O, S, Se) of 9,10-bis(diphenylphosphino)anthracene **26** again using H₂O₂·(NH₂)₂C=O (urea) (dichloromethane, 0 °C), elemental sulfur (toluene, reflux), and selenium (toluene, reflux), respectively (Scheme 27). The compounds obtained were significantly more soluble in organic solvents than the starting material **26**. The absorption and emission spectra of **80–82** were recorded in solution and in the solid state. In solution, only **80** exhibited a detectable emission whereas **81** did not emit. The latter showed strong fluorescence in the solid state at λ = 508 nm. This molecule formed single crystals possessing a groove suitable for binding toluene reversibly to the anthracene chromophore by means of C-H···π-ring center interactions. Hence, the crystalline **81** was the first solid-state excimer that could serve as a chemosensor to detect toluene selectively. Single crystals of **80** emitted at λ = 482 nm, whereas the selenium derivative **82** did not emit in the solid state. In addition, the crystal structures of compounds **80–82** were analyzed using the single-crystal

X-ray diffraction technique (Scheme 27) [39]. The substrate **26** was obtained based on the procedure described by Prabhavathy and co-workers [40].

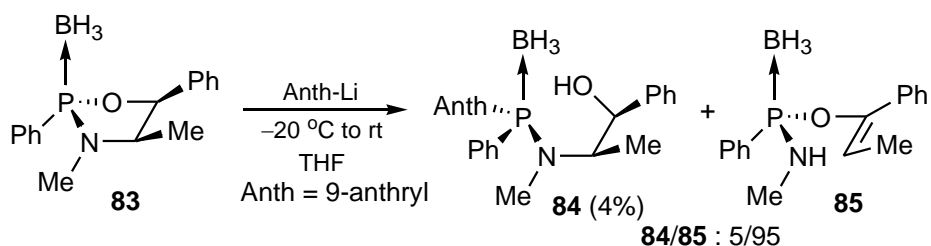


Scheme 27. The synthesis of 9,10-bis(diphenylphosphino)anthracene and thio- and seleno derivatives **80–82**.

2.2. Phosphine Boranes (AnthPR₂•BH₃)

In this subsection, the presented syntheses and reactions of phosphine molecules with P-B coordinate (semipolar, dative) bonds are presented.

The ring opening of enantiomerically pure oxazaphospholidineborane **83** with bulky anthryllithium to give phosphineboranes **84** was studied by Stephan and co-workers. The authors proposed an explanation for the low 4% yield of **84**. They reported that in the case when the attack on the phosphorus atom was hindered, deprotonation of the benzylic proton occurred, yielding *trans*-(*N*-methylamino)(phenyl)(1-phenyl-1-propenyloxy) phosphineborane **85** instead of **84** (**84**/**85** = 5/95) (Scheme 28) [41].



Scheme 28. The reaction of enantiomerically pure oxazaphospholidineborane **83** with anthryllithium.

1,8-Bis-(diisopropylphosphino)-9-methoxyanthracene **86**, as a starting material for the synthesis of 9-boron-substituted 1,8-bis-(diisopropylphosphino)anthracene **87a**/**87b**, was prepared by Akiba and co-workers by treatment of 1,8-dibromo-9-methoxy-anthracene **88**, first with *n*-BuLi and then with diisopropylchlorophosphine. Diphenylchlorophosphine was used as well; however, only the diisopropylphosphine derivative **86** could be successfully transformed into 1,8-bis-(diisopropylphosphino)-9-bromoanthracene **30** with LDBB (lithium di-*tert*-butylbiphenylide) followed by treatment with BrCF₂CF₂Br, as a brominating agent, in a 51% yield. The introduction of a boron substituent at the position 9 in **30** via Br/Li exchange followed by reaction with chloroborane **89** led to the formation of 1,8-bis-(diisopropylphosphino)-9-borylanthracene **87a**/**87b**. The ¹H and ³¹P NMR spectra of **86** showed a symmetrical anthracene pattern at room temperature. This meant that a very rapid bond switching process between **87a** and **87b** occurred in solution (Scheme 29) [42].

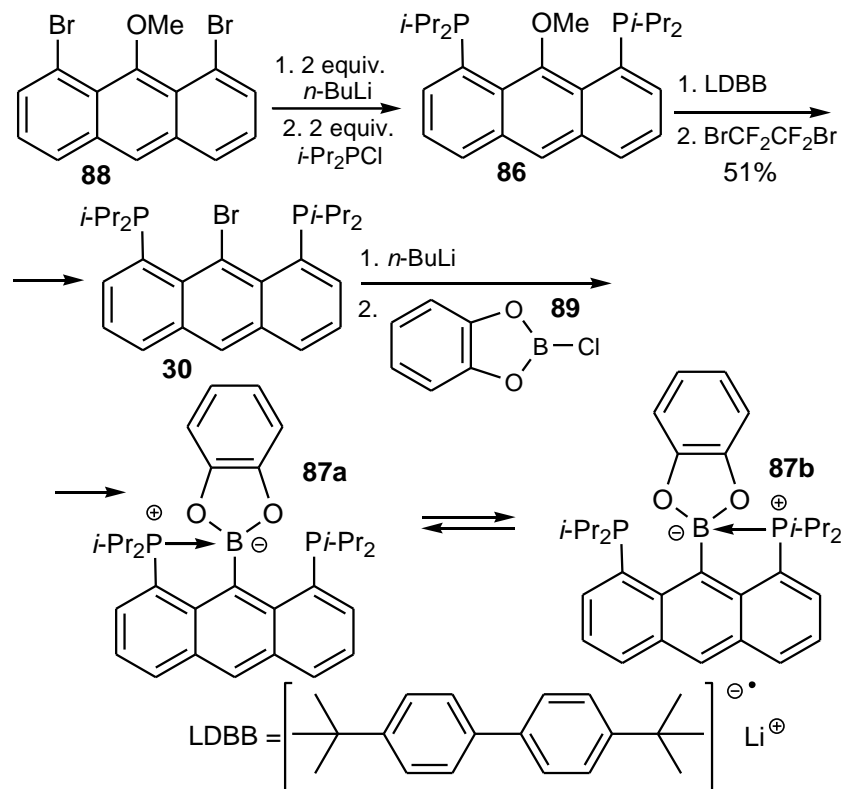
2.3. Phosphine–Metal Complexes (AnthPR₂–Metal)

In this subsection, complexes of phosphines possessing at least one anthryl substituent with metals, such as Au, Ag, Au/Ag/Sb, Fe, Pd, Pt, Ir, Lu, Eu, Ru, and Ni, are reviewed.

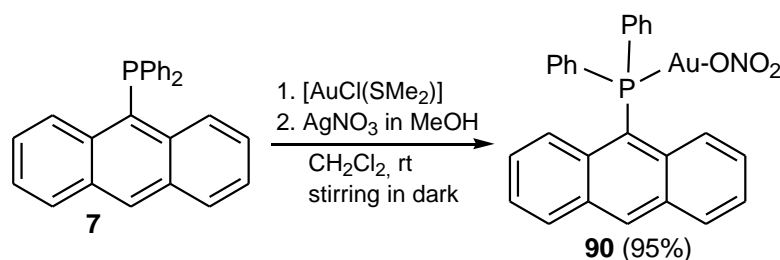
Other metals (W, Os, Co), i.e., the pentacarbonyltungsten complex of 9-diphenylphosphino anthracene, are reported in Section 2 while the triosmiumdodecacarbonyl cluster and dinuclear cobalt complex are discussed in Section 3, respectively.

Gold and platinum(II) complexes of the phosphine ligands PAnth_nPh_{3-n} (Anth = anthryl) were synthesized by Mingos et al. [43]. The authors recorded ³¹P{¹H} NMR chemical shifts for (anthryl)(diphenyl)phosphine, (dianthryl)(phenyl)phosphine and trianthrylphosphine, their

oxo derivatives, and gold (I) halide and gold (I) nitrate complexes. Moreover, a crystal structure of the $[\text{AuCl}(\text{PAnth}_2\text{Ph})]\cdot\text{CH}_3\text{Cl}$ complex was determined by X-ray analysis. An example of the preparation of the gold (I) complex $[\text{Au}(\text{NO}_3)(\text{PAnthPh}_2)]$ **90** obtained from 9-(diphenylphosphino)anthracene **7** is shown in Scheme 30.



Scheme 29. The synthesis of tridentate anthracene ligand **87a/87b**.

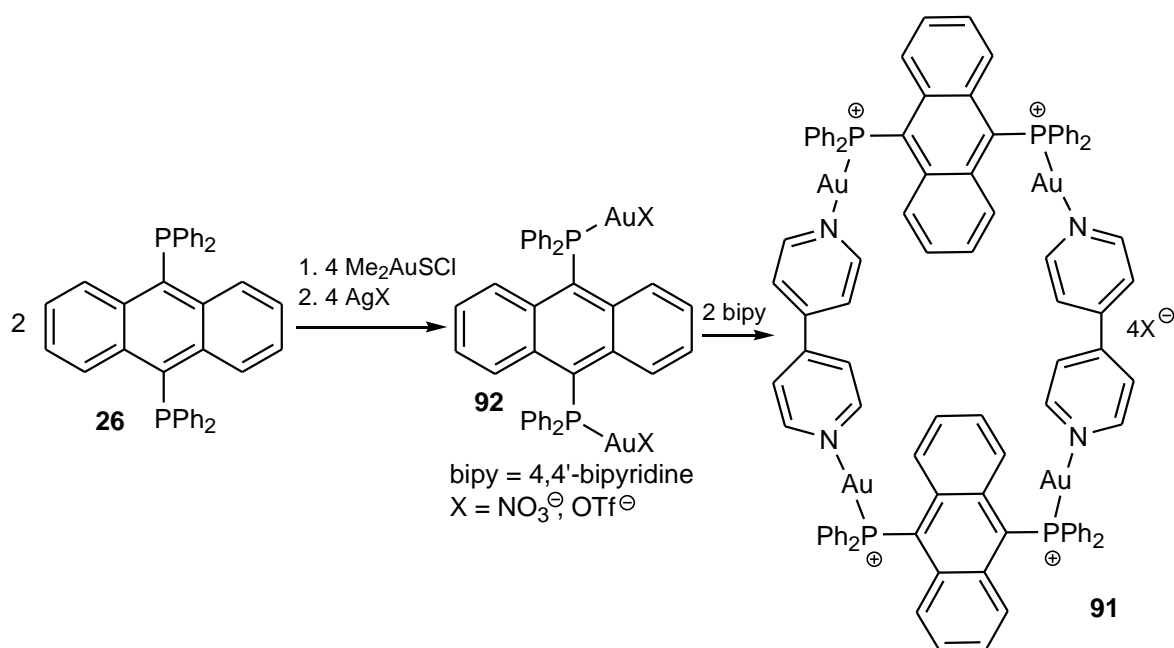


Scheme 30. An example of the preparation of the gold (I) complex $[\text{Au}(\text{NO}_3)(\text{PAnthPh}_2)]$ **90**.

Several other Au and Pt complexes were also synthesized: *trans*- $[\text{PtCl}_2(\text{PAnthPh}_2)_2]$ (64%); *trans*- $[\text{Pt}(\text{CH}_3\text{CN})_2(\text{PAnthPh}_2)_2](\text{BF}_4)_3$ (74%); *trans*- $[\text{Pt}(\text{CH}_3\text{CN})_2(\text{PAnth}_2\text{Ph}_2)](\text{BF}_4)_3$ (68%); $[\text{Au}(\text{NO}_3)(\text{PAnthPh}_2)]$ (95%); $[\text{Au}(\text{NO}_3)(\text{PAnth}_2\text{Ph})]$ (79%); $[\text{Au}(\text{NO}_3)(\text{PAnth}_3)]$ (53%); $[\text{AuCl}(\text{PAnthPh}_2)]$ (91%); $[\text{AuCl}(\text{PAnth}_2\text{Ph})]$ (93%); and $[\text{AuCl}(\text{PAnth}_3)]$ (72%).

A luminescent molecular metalla(Au)cyclophane **91**, which was synthesized from the self-assembly of the molecular “clip” **92** and bipyridine, showed a large rectangular cavity of $7.921(3) \times 16.76(3)$ Å (Scheme 31). The electronic absorption/emission spectroscopy and electrochemistry of **91** were studied. The 2^{4+} ions were self-assembled into a 2D mosaic in the solid state via complementary edge-to-face interactions between phenyl groups. ^1H NMR titrations ratified the 1:1 complexation of the cations **91** and various aromatic molecules. Comparison of the structures of the inclusion complexes indicated an induced-fit mechanism operating in the binding. The luminescence emission of $\mathbf{91}^{4+}$ could be quenched upon the guest binding. The binding constants were determined by both ^1H

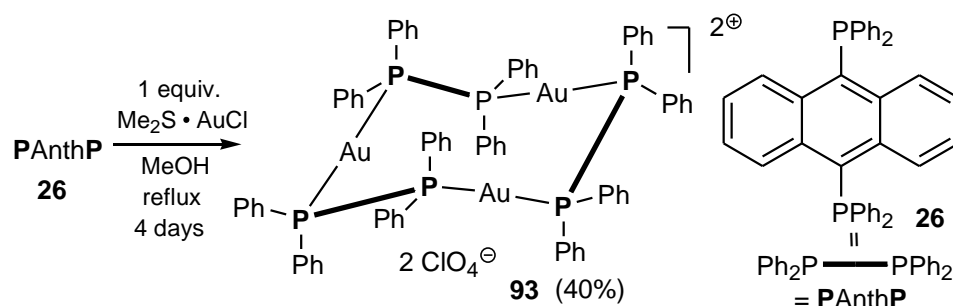
NMR and fluorescence titrations. Solvophobic and ion-dipole effects were shown to be important in stabilizing the inclusion complexes [44].



Scheme 31. Synthesis of metalla(Au)cyclophane **91**.

Complexes **92** (X = OTf[−], ClO₄[−], PF₆[−], BF₄[−]), as discrete binuclear, trinuclear, and tetranuclear metallacycles, were isolated and characterized, showing novel puckered-ring and saddles-like structures in the tri- and tetranuclear metallacycles (Scheme 31) [45].

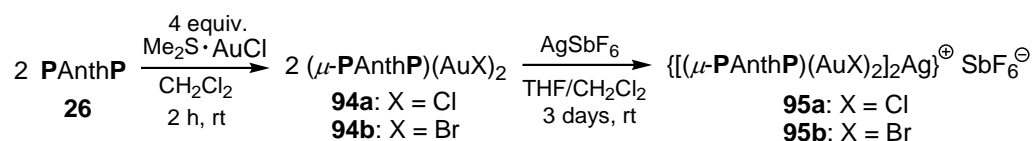
The trinuclear Au(I) complex [Au₃(PAnthP)₃][ClO₄]₃ **93** was synthesized by Yip and co-workers in the reaction of 9,10-bis-(diphenylphino)anthracene (PAnthP) **26** and 1 equiv. of Me₂S AuCl in methanol at reflux. The authors observed a stable gold ring in the solution and no NMR signals arising from the free ligand (Scheme 32) [40].



Scheme 32. The synthesis of the trinuclear Au(I) complex [Au₃(PAnthP)₃][ClO₄]₃ **93**.

The UV/Vis absorption spectra of **26** and its complex **93** showed intense bands at 396 and 424 nm assigned to ¹π-π* transitions in the anthryl ring. Excitation of CH₃CN solution of **93** at 400 nm gave an emission at 475 nm with a quantum yield of $\Theta = 0.05$.

The reaction of **26** (PAnthP) with 2 equiv. of Me₂SAuX in CH₂Cl₂ led to the new binuclear complexes (μ-PAnthP)(AuCl)₂ **94a** and (μ-PAnthP)(AuBr)₂ **94b** with Au(I)-X-Ag(I) halonium cation (Scheme 33) [46]. The reaction of **94a** and **94b** with 2 equiv. of AgSbF₆ led to spontaneous formation of the [(μ-PAnthP)-Au₂]²⁺ ion, and then, after the addition of AgSbF₆ (0.5 equiv.) in a THF solution, gave crystals of {[(μ-PAnthP)(AuCl)₂]₂Ag}⁺SbF₆[−] **95a** and {[(μ-PAnthP)(AuCl)₂]₂Ag}⁺SbF₆[−] **95b** as products.



Scheme 33. The synthesis of Au/Ag/Sb complexes **94a,b** and **95a,b**.

9,10-Bis(diphenylphosphino)anthracene (PAntHP) **26** with two donor phosphorus atoms has been used as a P-ligand unit for metals. Thus, the double-helicate dinuclear silver(I) complex, $[\text{Ag}_2(4'\text{-Ph-terpy})_2](\text{SO}_3\text{CF}_3)_2$, was reacted with **26** to give the corresponding dinuclear complex **96** (4'-Ph-terpy = 4'-phenyl-terpyridine). The latter showed a strong fluorescence in the solid state with an excitation band at 383.5 nm, emission band at 535.5 nm, and lifetime of 4.20 ns, but the derived complexes did not show fluorescent properties (Figure 2) [47].

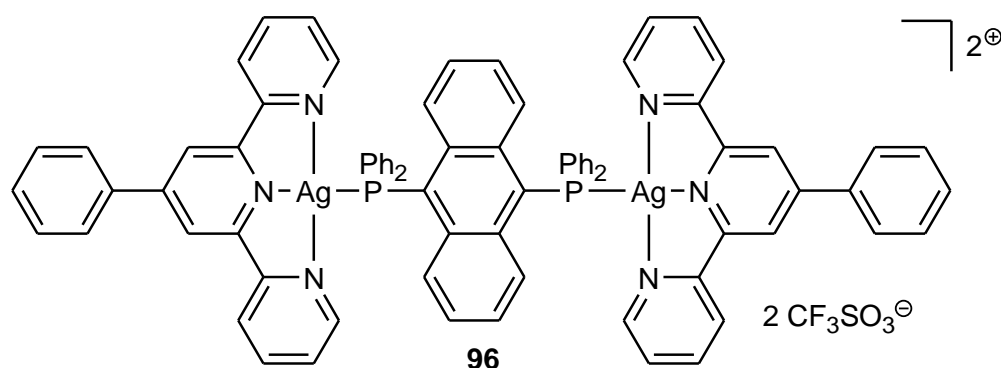
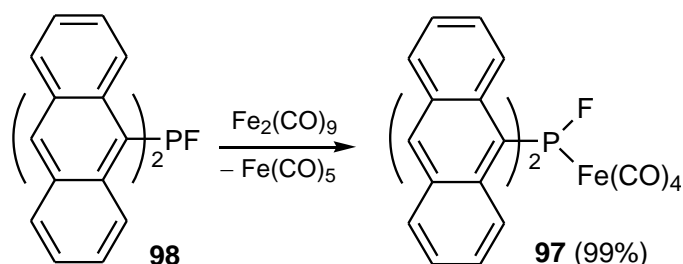


Figure 2. The dinuclear silver complex **96** derived from 9,10-bis(diphenylphosphino)anthracene.

An iron(0)tetracarbonyl complex **97** was synthesized from di(9-anthryl)fluorophosphine **98**, which was stable to redox disproportionation (Scheme 34) [48].



Scheme 34. The synthesis of the iron(0)tetracarbonyl complex **97**.

Pincer iridium complexes **99** derived from 1,8-bis(diphenylphosphino)anthracene **35** turned out to be suitable platforms for the C–H activation of methyl *tert*-butyl ether (MTBE) (Figure 3) [49].

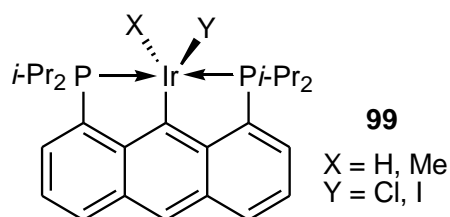
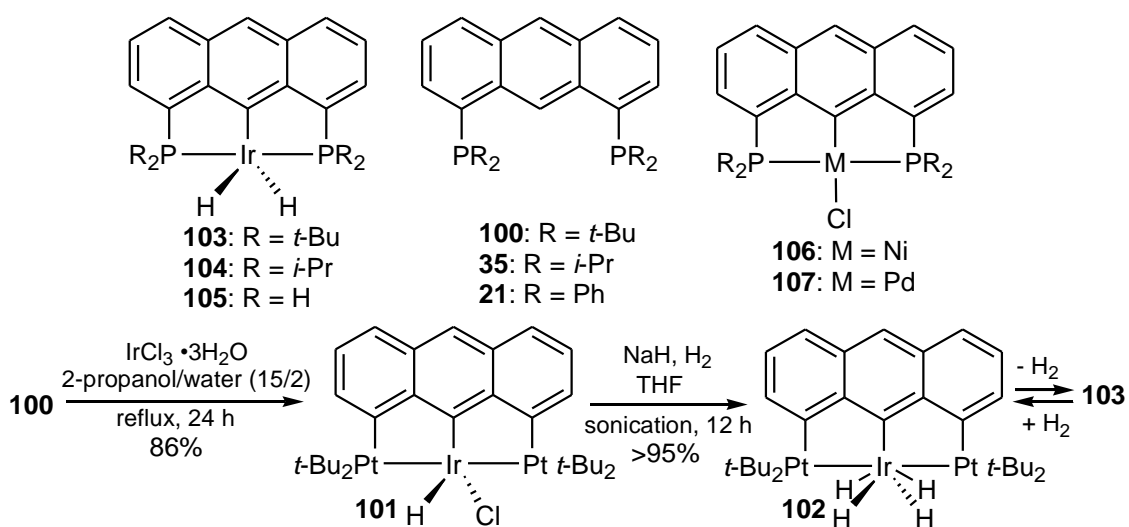


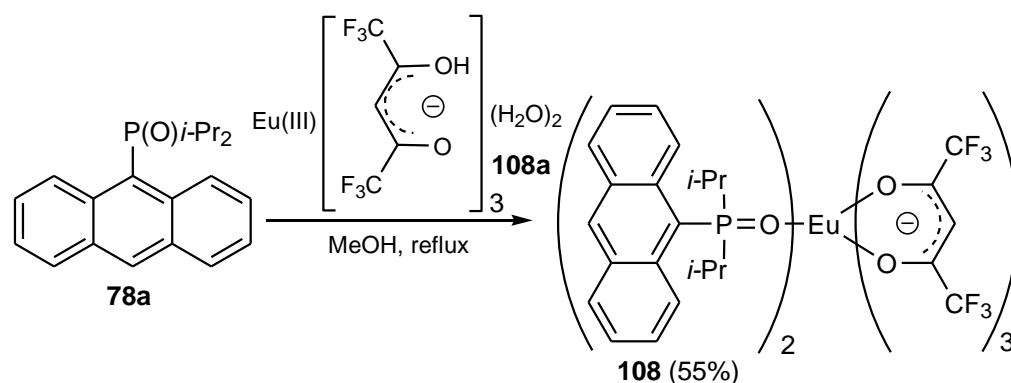
Figure 3. Pincer iridium complexes **99**.

A series of thermally stable Ir, Ni, and Pd complexes were obtained from 1,8-bis(dialkyl and diphenylphosphino)anthracenes **100**, **35**, and **21**. The anthracenes **100** and **35** were prepared similarly to **21** by direct nucleophilic substitution of fluorine atoms in 1,8-difluoroanthracene by potassium di-*tert*-butylphosphide or potassium di-*iso*-propylphosphide. The reaction of **100** with $\text{IrCl}_3 \cdot 3\text{H}_2\text{O}$ in 2-propanol/water afforded the complex **101** as a red crystalline powder in an 86% yield (Scheme 35). The reduction of **101** under a hydrogen atmosphere gave mixtures of the yellow-colored iridium tetrahydride **102** and the red-colored iridium dihydride **103**. By saturating solutions of such mixtures with hydrogen, the equilibrium was shifted towards **102**. Evaporation of the solvent under vacuum resulted in the formation of the analytically pure complex **103** in a >95% yield. The thermally stable complexes **103** and **104** were ideal for homogeneous catalysts in the alkane dehydrogenation above 200 °C. The complex **103** in alkane solution was stable at 250 °C and catalyzed the dehydrogenation reactions at this temperature [50].



Scheme 35. The synthesis of thermally stable iridium complexes **103** and **104**.

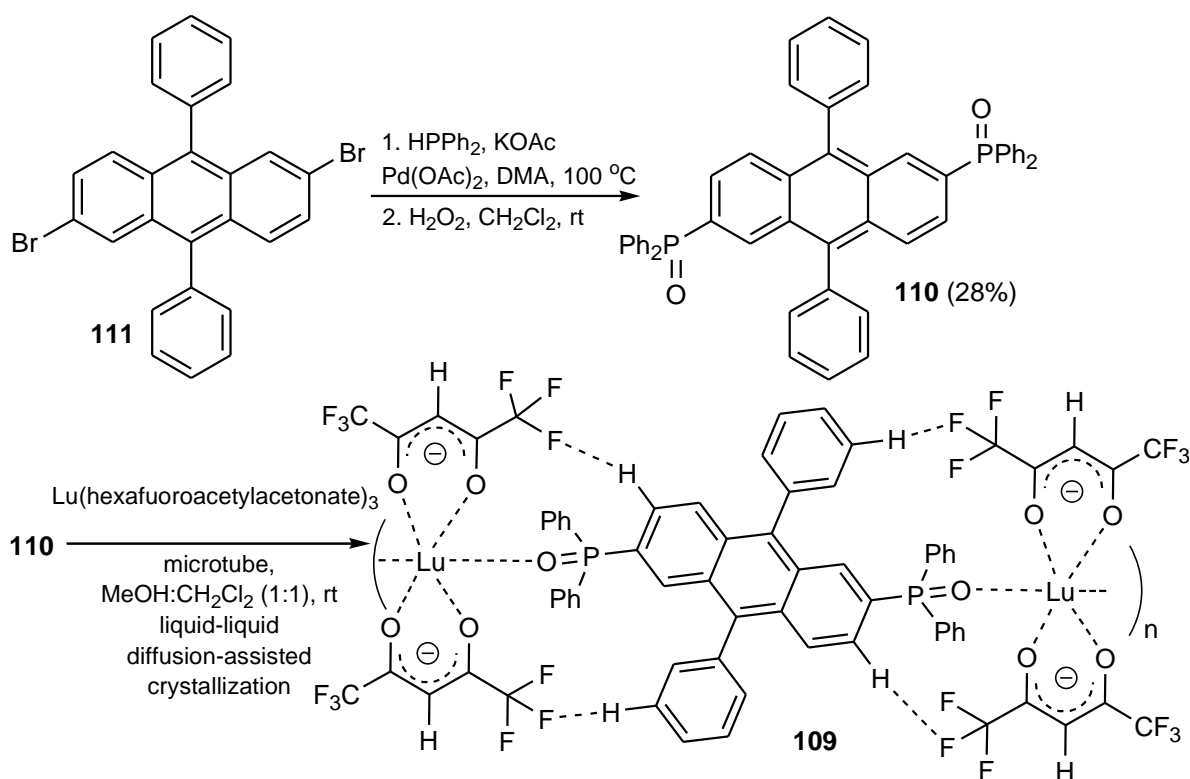
Osawa et al. [51] synthesized bis[(9-diisopropylphosphino)anthracene]-tris(hexafluoroacetylacetonato)europium(III) **108** (Scheme 36). First, the authors prepared 9-(diisopropylphosphino)anthracene **78a** (Scheme 26) according to the Schwab et al. protocol [29], which was next reacted with tris(hexafluoroacetylacetonato)europium(III) **108a** for 8 h in refluxing methanol solution to obtain **108** in a 55% yield after recrystallization.



Scheme 36. The preparation of the europium complex **108**.

Osawa and co-workers determined the crystal structure of the Eu(III) complex **108** and studied its intra-complex energy transfer. The studies revealed that laser irradiation of this compound in *n*-hexane gave blue emission, which was ascribed only to the 9-(diisopropylphosphino)anthracene moiety, not to the central Eu(III) ion (Scheme 36).

Kitagawa and co-workers [52] obtained a novel coordination polymer **109** based on 9,10-diphenyl-2,6-bis(diphenylphosphino)anthracene **110** as a core and two molecules of Lu(hexafluoroacetylacetonate)₃ that interacted with the core (Scheme 37).



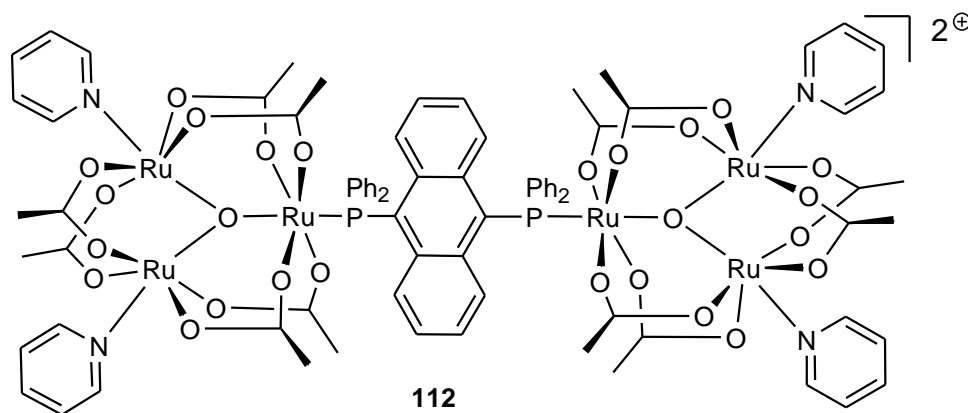
Scheme 37. The preparation of the coordination polymer **109**.

First, the anthracene **110** was synthesized from 2,6-dibromo-9,10-diphenylanthracene **111** and diphenylphosphine. The first step of the synthesis was performed in the presence of potassium acetate and palladium acetate, and next the resulting bisphosphine intermediate was oxidized to **110** in a 28% yield. The polymer **109** was prepared in a microtube by the liquid-liquid diffusion-assisted crystallization method. The authors studied the photophysical properties and thermal stability of **109** and its oxide **110**. The luminescence quantum yield was enhanced from 18% up to 25% ($\lambda_{\text{ex}} = 380 \text{ nm}$) due to the introduction of Lu(hexafluoroacetylacetonate)₃ molecules into the phosphine oxide system, as a result of which bright, pure sky-blue emission was observed. In addition, the compound **109** showed a higher temperature of decomposition (340 °C) than **110**.

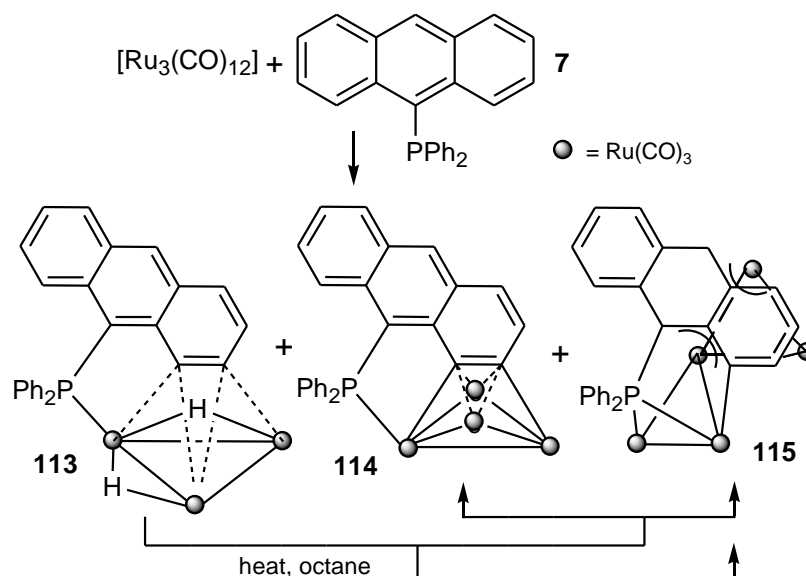
The diphosphine-bridged dimer of the oxo-centered triruthenium–acetate cluster unit $[\{\text{Ru}_3\text{O}(\text{OAc})_6(\text{py})_2\}_2(\text{dppan})](\text{PF}_6)$ **112** was synthesized by Chen and his co-workers (Scheme 38). The reaction of $[\text{Ru}_3\text{O}(\text{OAc})_6(\text{py})_2(\text{CH}_3\text{OH})](\text{PF}_6)$ with 9,10-bis(diphenylphosphino)anthracene (dppan) **26** resulted in the formation of **112** in a 67% yield. The redox studies of the complex **112** revealed the presence of electronic communication between two triruthenium units mediated through bridging dppan [53].

A number of tri-, tetra-, and penta-ruthenium clusters **113–115** were synthesized by Deeming and co-workers. When a suspension of $[\text{Ru}_{13}(\text{CO})_{12}]$ and a slight excess of 9-(diphenylphosphino)anthracene **7** in octane were heated to reflux at 125 °C for 4 h, several products were obtained, including the yellow trinuclear cluster $[\text{Ru}_3(\mu\text{-H})_2(\text{CO})_8(\mu_3\text{-C}_{14}\text{H}_7\text{PPh}_2)]$ **113** and the purple tetra-ruthenium butterfly complex $[\text{Ru}_4(\text{CO})_{11}(\mu_4\text{-C}_{14}\text{H}_7\text{PPh}_2)]$ **114**. Both anthracene complexes and also the dark purple penta-ruthenium bow-tie cluster, $[\text{Ru}_5(\text{CO})_{13}(\mu_5\text{-}\eta^1\text{:}\eta^2\text{:}\eta^3\text{:}\eta^3\text{-C}_{14}\text{H}_8\text{-}\eta^1\text{-PPh}_2)]$ **115** were obtained via the double metallation from one of the unsubstituted rings (Scheme 39). Furthermore, treatment of the trinuclear species **113** with 1 equivalent of $[\text{Ru}_3(\text{CO})_{12}]$ in refluxing octane resulted in a cluster build-up, with the formation

of the tetra- and penta-ruthenium species **114** and **115**. Likewise, the thermolysis reaction of **114** with $[\text{Ru}_3(\text{CO})_{12}]$ also led to **115**. The crystal structure of **3** revealed a unique μ_5 -interaction of the ligand with the ruthenium cluster [54].

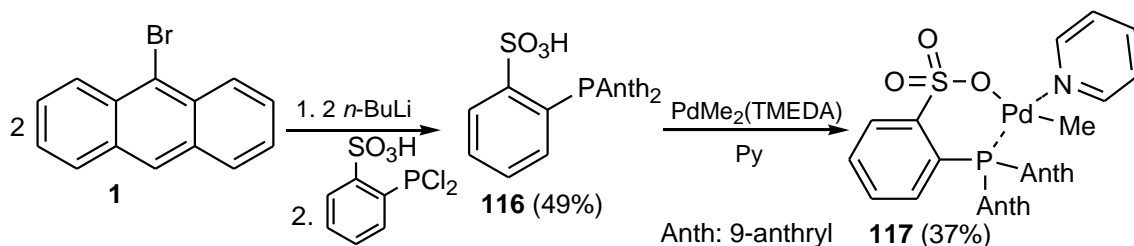


Scheme 38. The synthesis of the Ru-diphosphine-bridged complex **112**.



Scheme 39. The synthesis of tri-, tetra-, and penta-ruthenium clusters **113**, **114**, and **115**.

The bulky phosphine ligand **116** was prepared by Claverie et al. and used to generate the phosphine palladium complex **117**. The complex catalyzed ethene polymerization to yield linear polyethene; however, its catalytic activity was smaller compared to complexes with phenyl, naphthyl or phenanthryl substituents, which corresponded to increasing cone angles and decreasing basicity (Scheme 40) [55].



Scheme 40. The synthesis of the phosphine palladium complex **117**.

Yamamoto and Shimizu synthesized 9-(diphenylphosphino)anthracene-based palladacycles **118a** and **118b** that catalyzed conjugate addition of arylboronic acids to electron-deficient alkenes, such as α,β -unsaturated ketones, esters, nitriles, and nitroalkenes. The monomeric catalysts, which were synthesized from K_2PdCl_4 , 9-(diphenylphosphino)anthracene, and trialkyl phosphites, exhibited turnover numbers of up to 700 (Figure 4) [56].

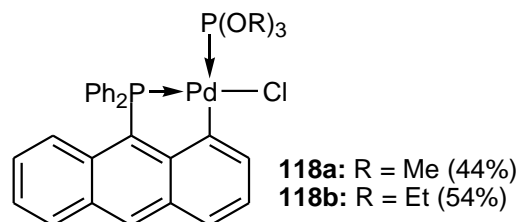
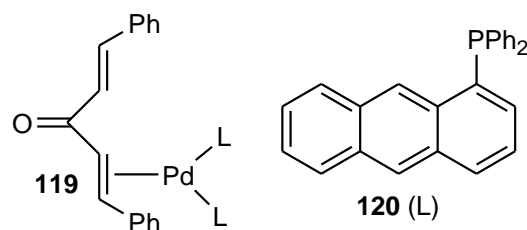


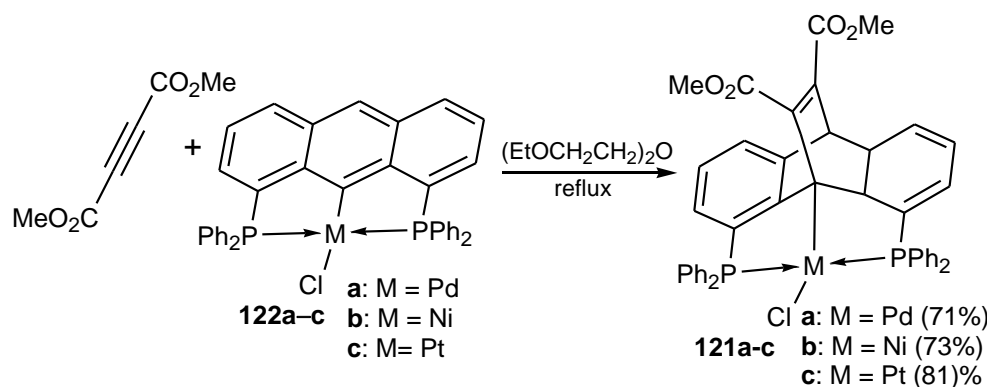
Figure 4. Structures of phosphapalladacycles **118a** and **118b**.

Mingos and co-workers reported the synthesis and structural characterization of the Pd complex $[Pd(dba)_2L_2]$ **119** (where L = **120** and dba = dibenzylideneacetone) obtained from $[Pd_2(dba)_3]$ and the corresponding 1-(diphenylphosphino)anthracene **120** (L) (Scheme 41). The single-crystal X-ray structural analyses confirmed that these complexes adopted a trigonal planar structure, with the dba ligand coordinated by a double bond [57].



Scheme 41. The synthesis of the palladium complex **119** with 1-(diphenylphosphino)anthracene **120** (L) as a ligand.

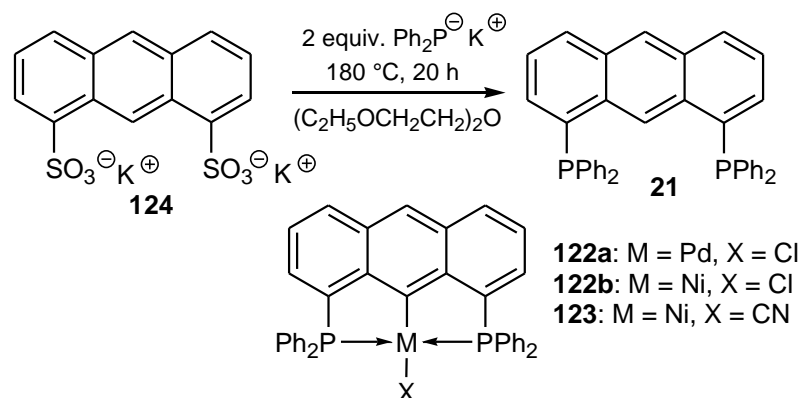
Dibenzobarrelene-based $C(sp^3)$ -metallated pincer complexes **121a**, **121b**, and **121c** were synthesized by the Diels–Alder [4 + 2] cycloaddition reaction of organometallic anthracene dienes **122a**, **122b**, and **122c** with dimethyl alkyne dicarboxylate as a dienophile (Scheme 42). This straightforward approach has an advantage over traditional synthetic routes, such as either C–H activation or oxidative insertion of a coordinated transition metal into the C–X bond of the halogenated spacer [58].



Scheme 42. The synthesis of (Pd, Ni, Pt)-complexes **121a–c** via the Diels–Alder approach.

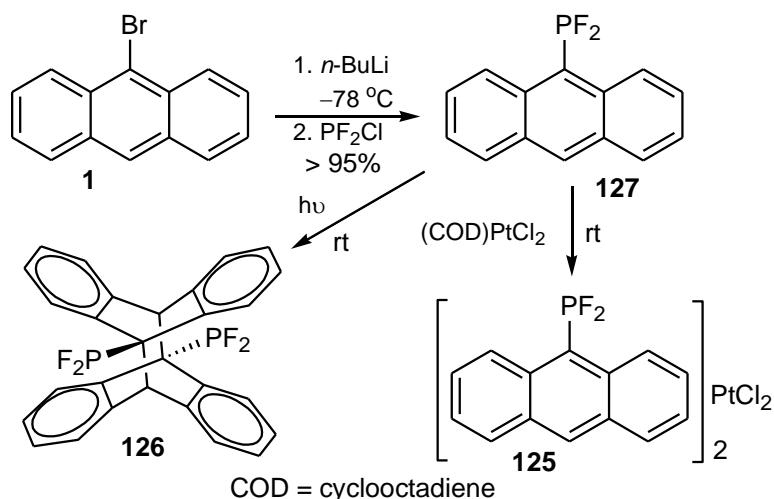
A number of metal complexes **122a**, **122b**, and **123** have been synthesized using 1,8-bis(diphenylphosphino)anthracene **21** as a ligand (Scheme 43). The latter was synthesized from dipotassium 1,8-anthracenedisulfonate **124** and potassium diphenylphosphide

(Ph₂PK). The reaction of **21** with nickel(II) chloride or bis-(benzotriole)palladium(II) chloride led to cyclometallation of the anthracene C-H bond at 9-position and resulted in the formation of square-planar chelate complexes **122b** or **122a**, respectively. Treating the complex **122b** with aqueous potassium cyanide did not remove nickel from **122b** but converted **122b** into **123** by substituting chloride with cyanide, confirming the high stability of these cyclometallated chelate complexes. The strong metal bonding in **122b** made it an ideal ligand for the development of new catalysts. Like the anthracene unit in **21**, other polycyclic acenes or heteroarenes might also be useful as a rigid backbone for bidentate phosphines [59].



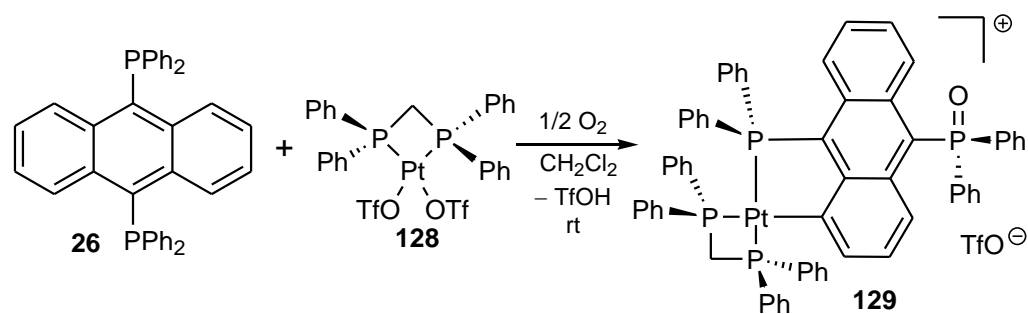
Scheme 43. The synthesis of the 1,8-bis(diphenylphosphino)anthracene ligand **21** and metal complexes **122a**, **122b**, and **123**.

The platinum (II) complex **125** and photochemically dimerized product **126** were synthesized from 9-(difluorophosphino)anthracene **127** (Scheme 44), obtained in the reaction of anthryllithium with chlorodifluorophosphine, with the former being synthesized in the reaction of *n*-butyllithium with 9-bromoanthracene **1**. The dimer **126** constituted one of the six possible rotational isomers. A rotation of the PF₂ group was hindered by strong F-H interactions at temperatures up to at least 105 °C [60].



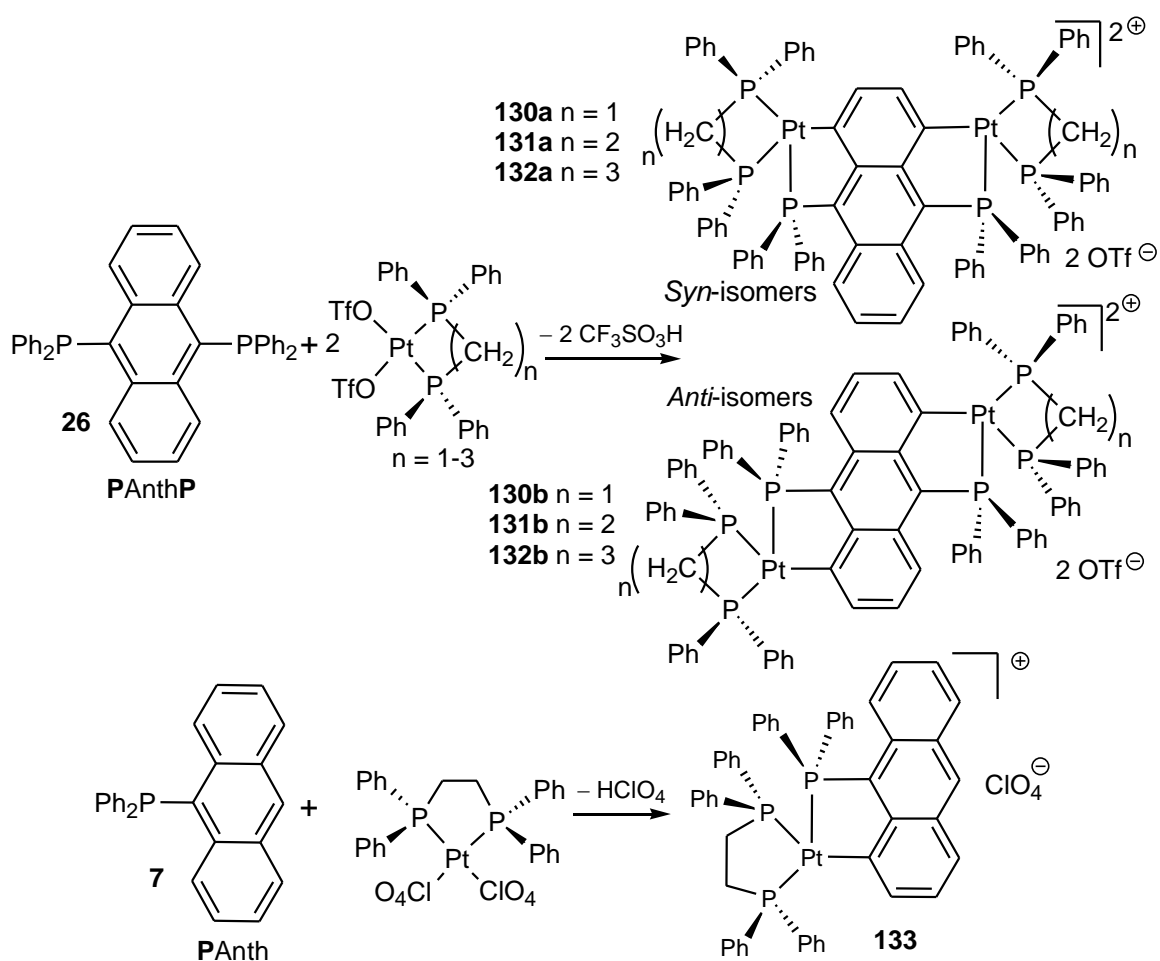
Scheme 44. The synthesis of the Pt(II) complex **125** and the dimer **126**.

Hu et al. [61] described the cycloplatination reaction of 9,10-bis(diphenylphosphino)anthracene **26** with Pt(bis(diphenylphosphino)methane)(OTf)₂ **128** to give [Pt(bis(diphenylphosphino)methane)(9-(diphenylphosphino)anthracene)PO-H)]OTf **129**. The uncoordinated P atom in the complex was oxidized when exposed to air (Scheme 45).



Scheme 45. The preparation of the platinum complex **129**.

The same authors also studied the influence of the reaction conditions on the regioselectivity of the double cyclometallation process (Scheme 46) [62].

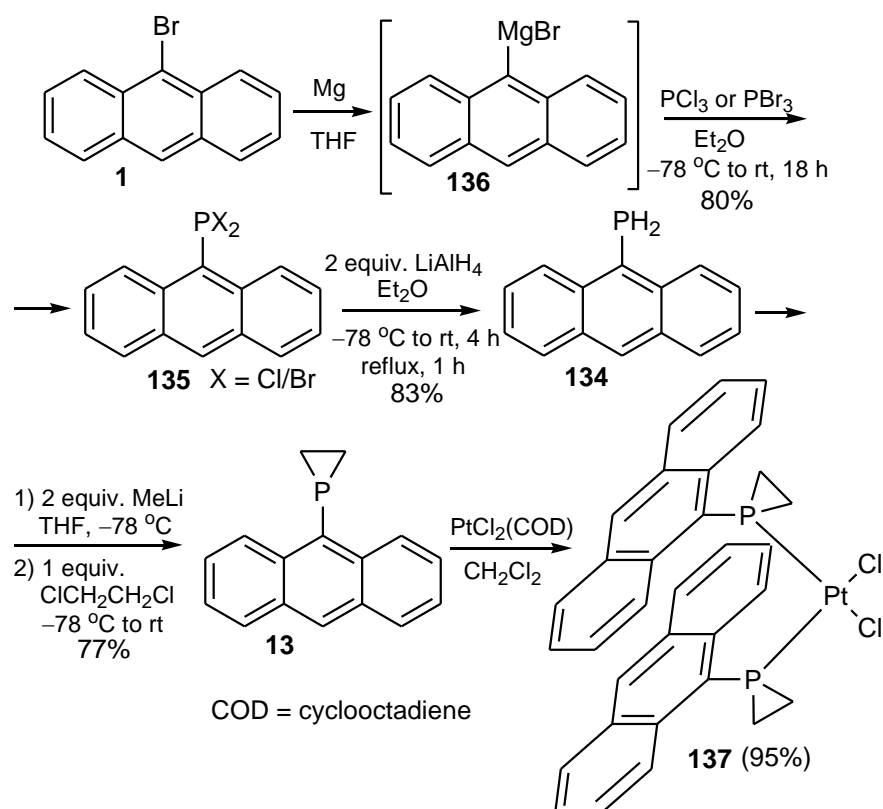


Scheme 46. The synthesis of the dicyclopalladated complexes **130–132** (*syn* and *anti*) and the monocyclopalladated complex **133**.

Other dicyclopalladated complexes *syn*- and *anti*-[Pt₂(L)₂(PAnthP-H₂)](OTf)₂(Pt₂) (Anth = anthrylene) **130–132** have been synthesized in reactions of **26** (PAnthP) with Pt(L)(OTf)₂ (L = diphosphine, OTf) (Scheme 46). To understand the effect of the number of Pt ions on the extent of perturbation, a mononuclear analog **133** was also prepared. The UV–vis absorption spectra of **133** and PAnth displayed moderately intense vibronic bands at around 320–440 nm. The spectra of the binuclear complexes **130–132** were different from that of **133**. The spectra of the *syn*-isomers **130a**, **131a**, and **132a** displayed two intense overlapping absorption bands at 320–520 nm. The *anti*-isomers **130b** and **132b** also displayed two intense

bands in a similar spectral range (300–500 nm). The emission energies in degassed DCM at room temperature followed the order **133** > **131b**, **132b** > **130a**, **131a**, and **132a** [62].

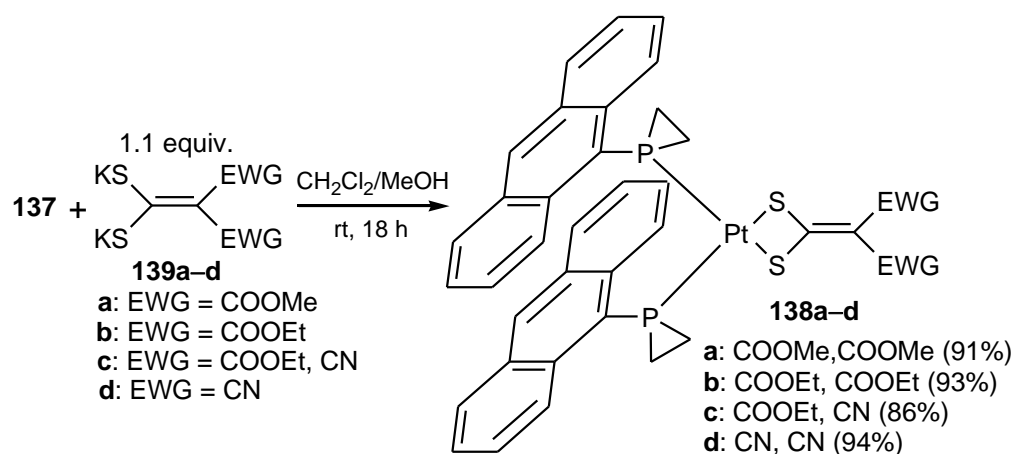
9-(Dihydrophosphino)anthracene **134** was prepared in two steps starting from 9-bromoanthracene **1**, which was next converted to 9-(dihalophosphino)anthracenes **135** (X = Cl, Br) via the Grignard reagent **136**, which reacted with PCl₃ or PBr₃, respectively. Next, reduction of the latter with 2 equiv. of LiAlH₄ in diethyl ether at –78 °C and then reflux for 1 h delivered **134**. In the reaction of the dilithium derivative of **134** with 1,2-dichloroethane, Kubiak and co-workers obtained 9-(1-phosphirano)anthracene **13**. Then, the reaction of **13** with 0.5 equiv. of PtCl₂(1,5-cyclooctadiene) gave the platinum complex, *cis*-dichlorobis[1-(9-anthracene)phosphirano]platinum(II) **137** (Scheme 47) [63]. The complex **137** displayed novel intramolecular π -stacking interactions between the anthracene ring systems.



Scheme 47. The synthesis of 9-(1-phosphirano)anthracene **13** and its platinum complex **137**.

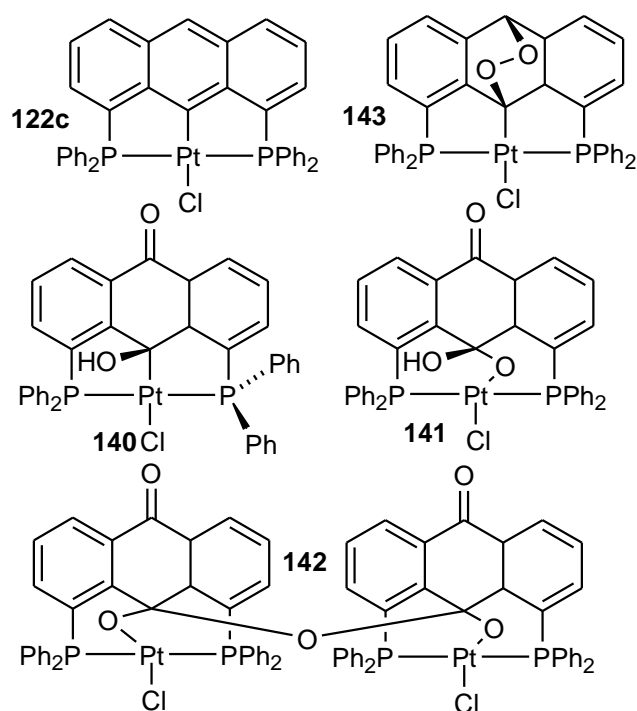
The same research group synthesized other platinum complexes, such as bis[1-(9-anthracene)phosphirano]dithiolateplatinum complexes **138a–d**, in the reaction of **137** with appropriate potassium-ethylene-2,2-dithiolates **139a–d** containing two electron-withdrawing groups (EWGs) in positions 1, such as methoxycarbonyl, ethoxycarbonyl and cyano groups. The final products **138a–d** were obtained in CH₂Cl₂/MeOH mixture after 18 h at room temperature in high yields. X-ray studies of the complexes displayed the intra- or intermolecular anthracene ring of the *cis*-bis{1-(9-anthracene)phosphirane} stacked structures (Scheme 48) [64].

All of the platinum complexes **138a–d** reported emitted light at low temperatures in the solid state. Complexes **138a–d** exhibited a strong green fluorescence at 530 nm at low temperatures in the solid state. Moreover, the complex **138d** strongly emitted blue light in the THF or benzene solution at 450 nm after excitation at 420 nm. The blue emission of the complex **138d** with two cyano groups and a very small Stokes shift was similar to that observed for free 9-(1-phosphirano)anthracene and anthracene rings.



Scheme 48. The synthesis of bis[1-(9-anthracene)phosphirano]dithiolatoplatinum(II) complexes **138a-d**.

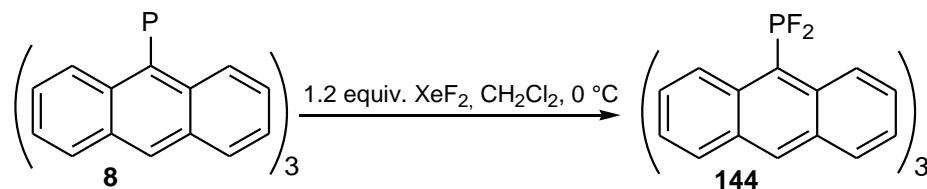
The pincer complexes **140**, **141**, and **142** were synthesized by irradiating the cyclometalated complex **122c** in the presence of O_2 , which led to oxidations of the anthryl ring (Scheme 49). The first photoproduct, a Pt(II)-9,10-endoperoxide complex **143**, was converted photochemically to the Pt(II)-9-hydroxyanthrone complex **140**, which was further oxygenated to the Pt(II)-hemiketal **141**. The oxidation of **140**, which could be accelerated by light irradiation, probably involved a Pt(II)-anthraquinone intermediate. The Pt(II)-hemiketal **141** underwent acid-catalyzed ketalization to form a binuclear Pt(II) 2-diketal **142**. The structures were characterized by NMR and single-crystal X-ray diffraction. All complexes possessed similar absorption spectra, showing a moderately intense vibronic band at 390–480 nm ($\lambda_{\text{max}} = 454 \text{ nm}$, $\epsilon_{\text{max}} = 7.6\text{--}9.2 \times 10^3 \text{ M}^{-1} \text{ cm}^{-1}$) and a very intense band at 280 nm ($\epsilon_{\text{max}} = 5.2\text{--}5.9 \times 10^4 \text{ M}^{-1} \text{ cm}^{-1}$). The Pt complexes were also luminescent in solution and in the solid state at room temperature. Irradiating degassed CH_2Cl_2 solutions of the complexes at 390 nm resulted in an emission band at $\lambda_{\text{max}} = 474 \text{ nm}$ with a vibronic shoulder at 520 nm [65].



Scheme 49. The synthesis of the Pt(II) pincer complex **50** and its sequential oxygenated products **140**, **141**, and **142**.

2.4. Phosphoranes ($\text{AnthPR}_2\text{X}_2$) ($\text{X} = \text{F}$)

Yamaguchi et al. [26] reported the synthesis and photochemical characterization of tri(9-anthryl)difluorophosphorane **144** obtained from the reaction of xenon difluoride with tri(9-anthryl)phosphine **8**. The synthesis of **144** is presented in Scheme 50.

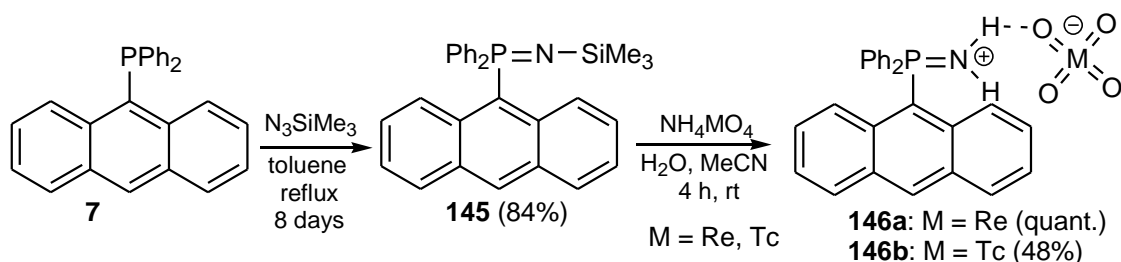


Scheme 50. The synthesis of tri(9-anthryl)difluorophosphorane **144**.

The authors proved that the fluorescence intensity is attributed to the coordination number of phosphorus. The tri-coordinated **8** exhibited a weak fluorescence while pentacoordinated **18** showed a significant fluorescence.

2.5. Phosphinimines ($\text{AnthR}_2\text{P} = \text{N-R}^1$) and Phosphiniminium Derivatives ($\text{AnthR}_2\text{P} = \text{NH}_2^+$)

Jurisson and co-workers synthesized the *N*-protected phosphinimine **145** and its phosphiniminium ion pairs **146a** and **146b** with $[\text{ReO}_4^-]$ and $[\text{TcO}_4^-]$ anions. The phosphinimine **145** was fluorescent but the addition of $[\text{TcO}_4^-]$ or $[\text{ReO}_4^-]$ anions to **145** did not change the original spectrum in terms of the overall spectral features or intensity. In addition, the anthracene molecule scintillated in the presence of $[\text{TcO}_4^-]$, making it a possible reporter group for a scintillation sensor using this molecule (Scheme 51) [66].

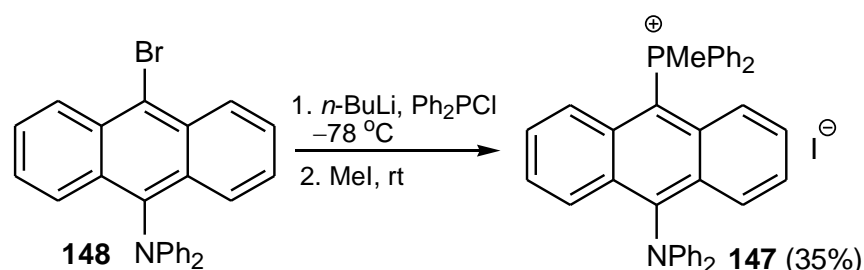


Scheme 51. The synthesis of *N*-trimethylsilyl-protected phosphinimine **1** and phosphiniminium salts **146a** and **146b**.

2.6. Phosphonium Salts (AnthPR_3^+)

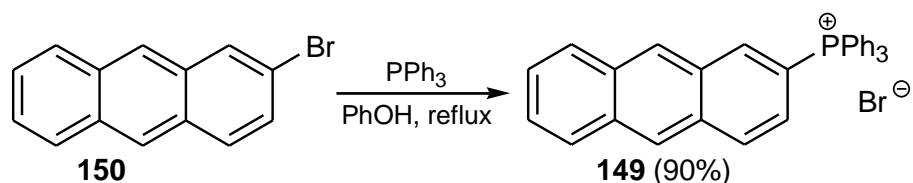
Usually, phosphonium salts are obtained from phosphines by quaternization of a tricoordinated phosphorus atom with a free electron pair.

The D- π -A type of phosphonium salts, in which electron acceptor ($\text{A} = \text{PR}_3^+$) and donor ($\text{D} = \text{NPh}_2$) groups were linked by polarizable π -conjugated spacers, showed an intense fluorescence classically ascribed to the excited state intramolecular charge transfer (ICT). Therefore, a series of such phosphonium salts with different lengths of spacers and counterions were synthesized and characterized. The salt **147** was synthesized by the two-step approach involving the preparation of tertiary aryl phosphine from **158** followed by methylation with methyl iodide. The peak wavelengths (λ_{abs}) were gradually red-shifted along with the extension of the π -spacer: $\pi = \text{phenylene}$ (333 nm) < $\pi = \text{biphenylene}$ (387 nm) < $\pi = \text{naphthylene}$ (407 nm) < $\pi = \text{anthrylene}$ (**147**, 519 nm). The extension of the π -system from phenylene to the polycyclic naphthalene and anthracene motifs in **147** caused a gradual growth of λ_{em} to 560 and 679 nm for **147** in DCM, which was, however, accompanied by a drop in the quantum yield (Scheme 52) [67].



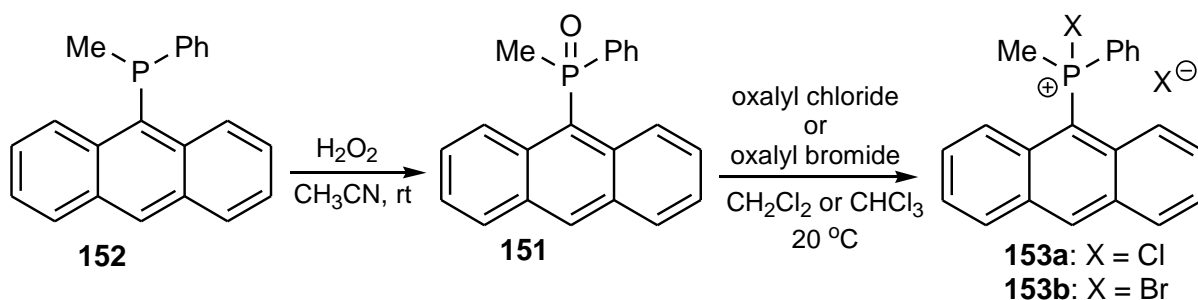
Scheme 52. The synthesis of the phosphonium salt **147**.

A metal-free synthesis of 2-anthryl phosphonium bromide **149** by the reaction of triphenylphosphine with 2-bromoanthracene **150** in refluxing phenol was developed by Huang et al. Examination of other solvents with a boiling point of around 200 °C showed that tetralin, PhCN, ethoxybenzene, or 2-chlorophenol could also produce phosphonium salts, although in lower yields (5–44%). A two-step addition-elimination mechanism was proposed, in which the second step of the bromide elimination was fast, as indicated by the deuterium experiment. The authors suggested that phenol could form a hydrogen bond with bromide, facilitating the addition of triphenylphosphine and elimination of bromide by polarizing the carbon–bromide bond, and making phenol the optimal solvent among the solvents tested (Scheme 53) [68].



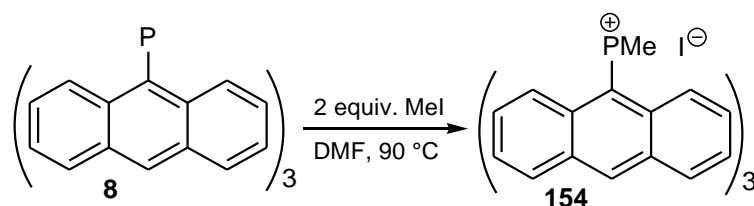
Scheme 53. The synthesis of the phosphonium bromide **149**.

Nikitin and co-workers [69] synthesized 9-(methylphenylphosphinoyl)anthracene **151** by the oxidation of 9-(methylphenylphosphino)anthracene **152** with hydrogen peroxide in acetonitrile solution (Scheme 54). The compound **151** was then converted into the corresponding phosphonium chloride **153a** and bromide **153b** using oxalyl chloride and bromide, respectively. The authors measured the exchange barriers of self- and cross-exchange of halides in phosphonium salts using the 2D EXSY NMR technique to visualize the processes.



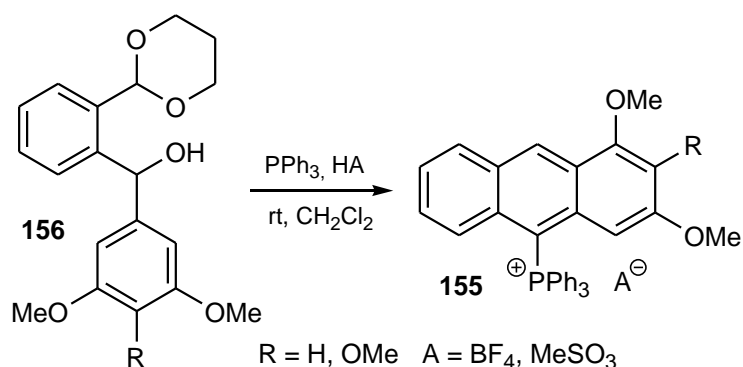
Scheme 54. The synthesis of the phosphonium chloride **153a** and the phosphonium bromide **153b**.

Tri(9-anthryl)(methyl)phosphonium iodide **154** was synthesized by Yamaguchi et al. in the quaternization reaction of the phosphine **8** with methyl iodide. The tri-coordinated **8** and tetra-coordinated derivatives **154** exhibited a weak fluorescence (Scheme 55) [26].



Scheme 55. The synthesis of tri(9-anthryl)methylphosphonium iodide **154**.

Bałczewski et al. [70,71] recently presented a novel, one-pot *phospho*-Friedel–Crafts–Bradsher cyclization, which led to higher-substituted phosphonium salts **155**. In the new reaction, (*o*-diacetoaryl)arylmethanols **156**, as the starting materials, in the presence of triphenylphosphine and acids HA, spontaneously cyclized directly to **155** under very mild reaction conditions (Scheme 56).



Scheme 56. The synthesis of anthryl phosphonium salts **155** from diarylmethanols **156**.

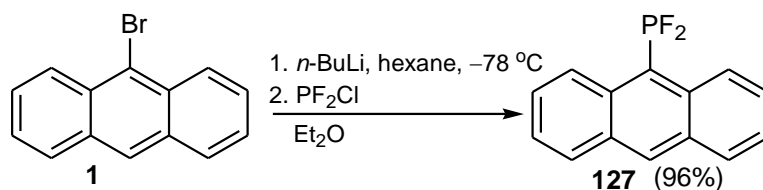
3. Synthesis and Reactions of P^{III} Acids, Their P^{IV} Tautomers, and Derivatives

This section covers P^{III} acids derivatives containing at least one anthracene moiety linked either directly to the phosphorus atom via the P-Csp² (Anth) bond (Sections 3.1 and 3.2) or indirectly via the P-O-Csp² (Anth) bond (Section 3.3). The phosphonous RP(OH)₂, phosphinous R₂POH, and phosphorous P(OH)₃ free acids are the organophosphorus members of the group of substances known as the lower acids of phosphorus. These P^{III} trivalent species exist as minor tautomers in equilibrium with major P^{IV} tetravalent forms, which exhibit one less acidic function than might be expected [8]. Derivatives of P^{III} acids, such as halides, amides, and esters, may exist in stable, trivalent forms and they will be described separately in Sections 3.1–3.3. The P^{IV} tautomers are discussed in Sections 3.4 and 3.5.

3.1. Phosphonous Acid Dihalides and Phosphinous Acid Halides (Halophosphines) (AnthPX₂) and (Anth₂PX) (X = F, Cl, Br)

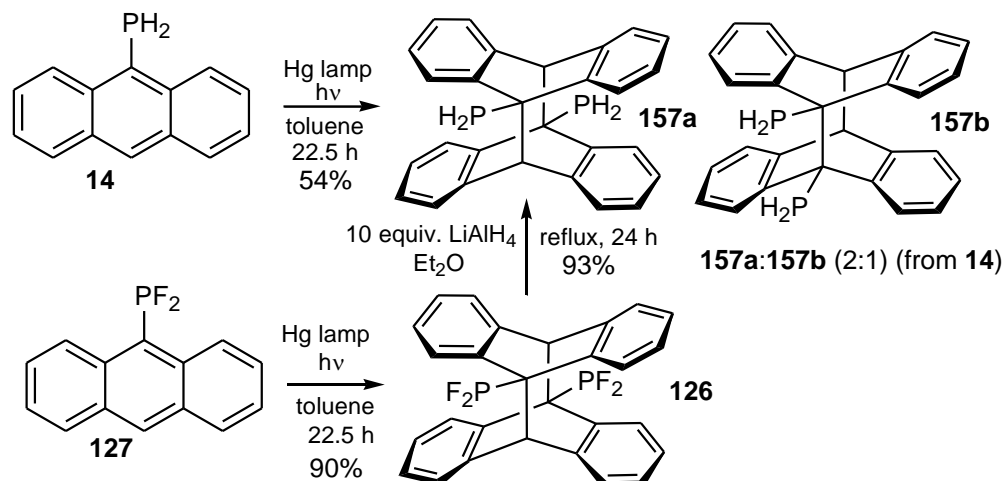
Halo- and dihaloanthracenes of the formula AnthPX₂ and Anth₂PX (X = F, Cl, Br), which contain at least one P-C bond and one or two halogen atoms, are classified as halides of the corresponding lower P^{III} acids. Syntheses of 9-(difluoro, dichloro, dibromo)anthracenes are also described in Section 2.3.

9-Difluoroanthracene **127** was synthesized by Schmutzler et al. starting from 9-bromoanthracene **1** and chlorodifluorophosphine in a 96% yield (Scheme 57) [10].



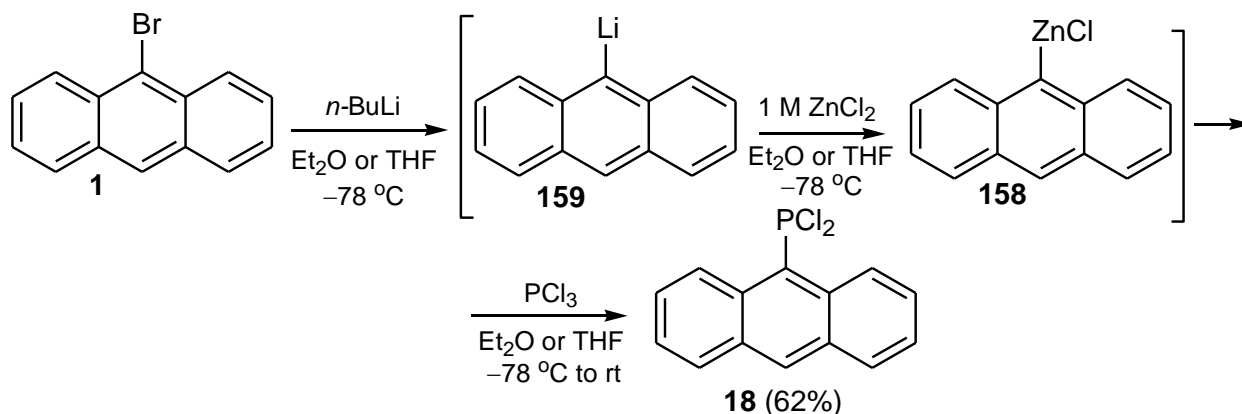
Scheme 57. The synthesis of 9-difluoroanthracene **127**.

9-(Difluorophosphino)anthracene **127** was also employed by the group of Schmutzler in further investigations. They used 9-(dihydrophosphino)anthracene **14** and irradiated it with a mercury lamp in toluene for 22.5 h to obtain two isomeric dimers **157a** and **157b** in a 2:1 ratio, which could be observed in ^{31}P NMR. Irradiation of 9-(difluorophosphino)anthracene **127** under the same conditions gave only one dimeric isomer **126**. Hydrogenation reaction of the latter with 10 equiv. of LiAlH_4 in diethyl ether at reflux for 24 h delivered a single isomer **157a** in a 93% yield (Scheme 58) [10].



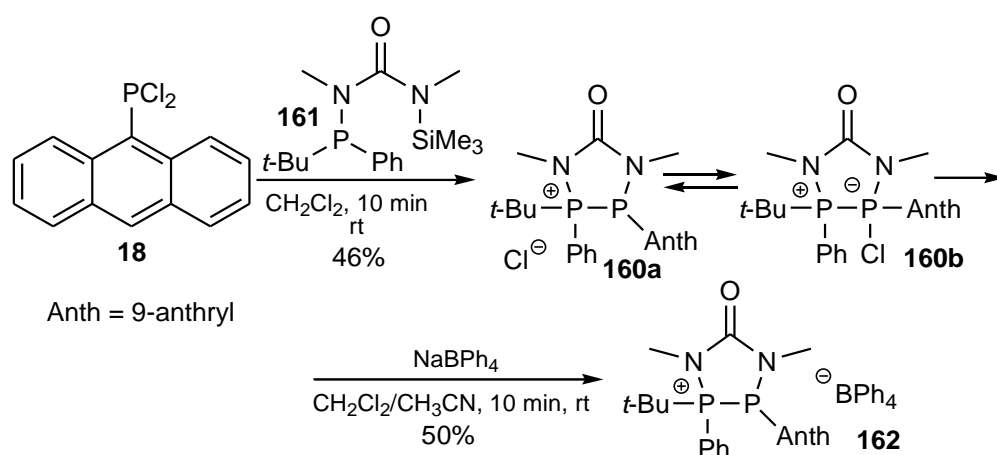
Scheme 58. The photodimerization of **14** and **127** and the reduction reaction of the dimer **126** to **157a**.

Kirst and et al. [72] synthesized 9-(dichlorophosphino)anthracene **18** by the reaction of PCl_3 with the organozinc compound **158**. The latter was obtained from 9-bromoanthracene **1**, which was first lithiated with *n*-butyllithium to obtain **159** and then submitted to the Li/Zn transmetalation with dry ZnCl_2 (Scheme 59).



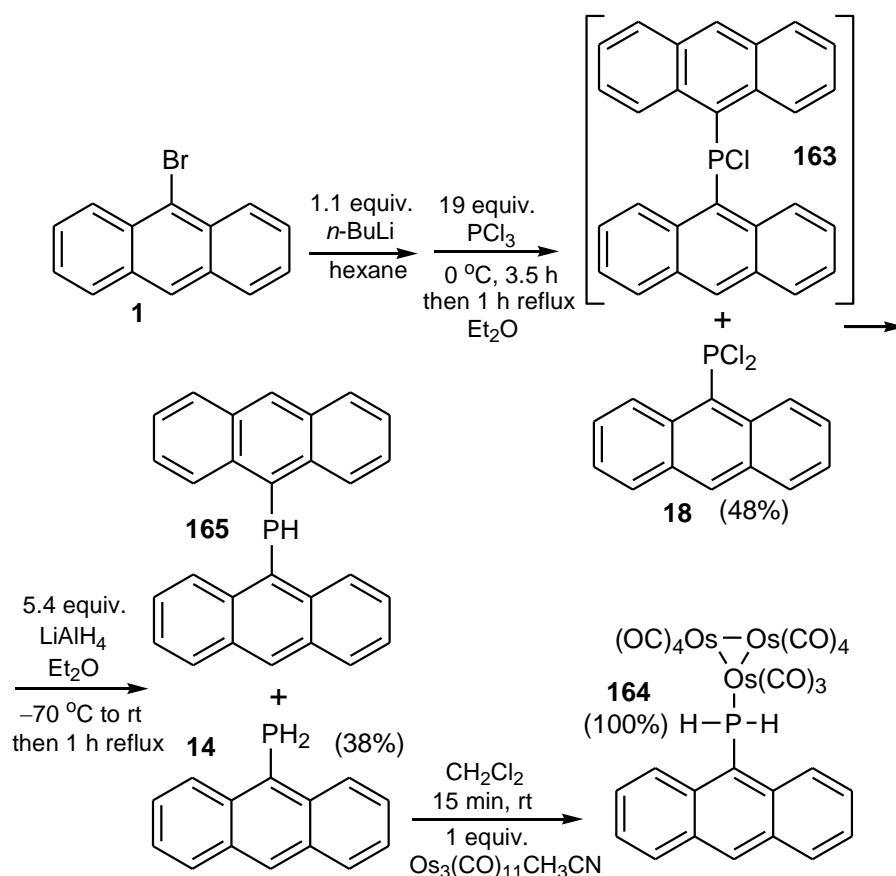
Scheme 59. The synthesis of 9-(dichlorophosphino)anthracene **18**.

9-(Dichlorophosphino)anthracene **18** was further utilized by the group of Schmutzler in the preparation of cyclic (*P*-anthrylphosphino)phosphonium chloride remaining in equilibrium **160a**/**160b** in the reaction of 9-(dichlorophosphino)anthracene **18** and *N*-[*tert*-butyl(phenyl)phosphino]-*N,N*-dimethyl-*N*-(trimethylsilyl)urea **161** in CH_2Cl_2 at room temperature in a 46% yield. The existence in solution of the equilibrium between the ionic structure **160a** and the covalent form **160b** was observed. Next, the chloride **160a**/**160b** was converted into the corresponding phosphonium tetraphenylborate **162** by treatment of NaBPh_4 in $\text{CH}_2\text{Cl}_2/\text{CH}_3\text{CN}$ in a 50% yield (Scheme 60) [73].



Scheme 60. The synthesis of (*P*-anthrylphosphino)phosphonium chloride **160a/160b** and the tetraphenylborate **162**.

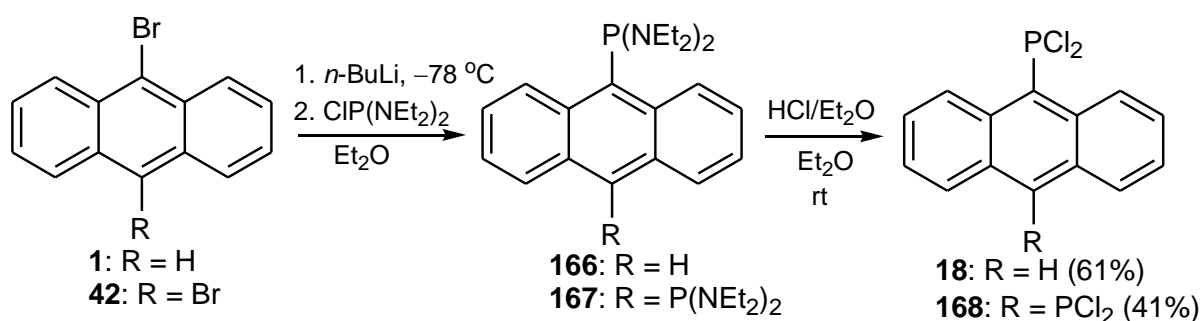
Schmutzler and co-workers presented a synthesis of 9-(dichlorophosphino)anthracene **18** and 9-(anthrylchlorophosphino)anthracene **163** from 9-bromoanthracene **1** using a large excess of PCl_3 (19 equiv.) in a 48% yield. The resulting mixture of **18** and **163** was reduced with 5.4 equiv. of LiAlH_4 in diethyl ether at reflux to obtain 9-(dihydrophosphino)anthracene **14** and (anthrylhydrophosphino)anthracene **165**. Next, pure **14** was reacted with 1 equiv. of $\text{Os}_3(\text{CO})_{11}(\text{CH}_3\text{CN})$ in CH_2Cl_2 at room temperature to give triosmiumdodecacarbonyl cluster **164** quantitatively (Scheme 61) [10].



Scheme 61. The synthesis of 9-(chlorophosphino)anthracenes **18**, **163**, 9-(hydrophosphino)anthracenes **14**, **165**, and the osmium complex **164**.

3.2. Phosphonous Acid Diamides (*AnthP(NR₂)₂*)

9-[Bis(diethylamino)phosphino]anthracene **166** and 9,10-bis[bis(diethylamino)phosphino]anthracene **167** were prepared by Tokitoh and co-workers starting from 9-bromoanthracenes **1** and **42**, which were first lithiated with *n*-butyllithium and then reacted with bis(diethylamino)chlorophosphine. The resulting anthracenes **166** and **167** were transformed to 9-(dichlorophosphino)anthracene **18** and 9,10-bis(dichlorophosphino)anthracene **168** using hydrogen chloride in diethyl ether (Scheme 62) [74].



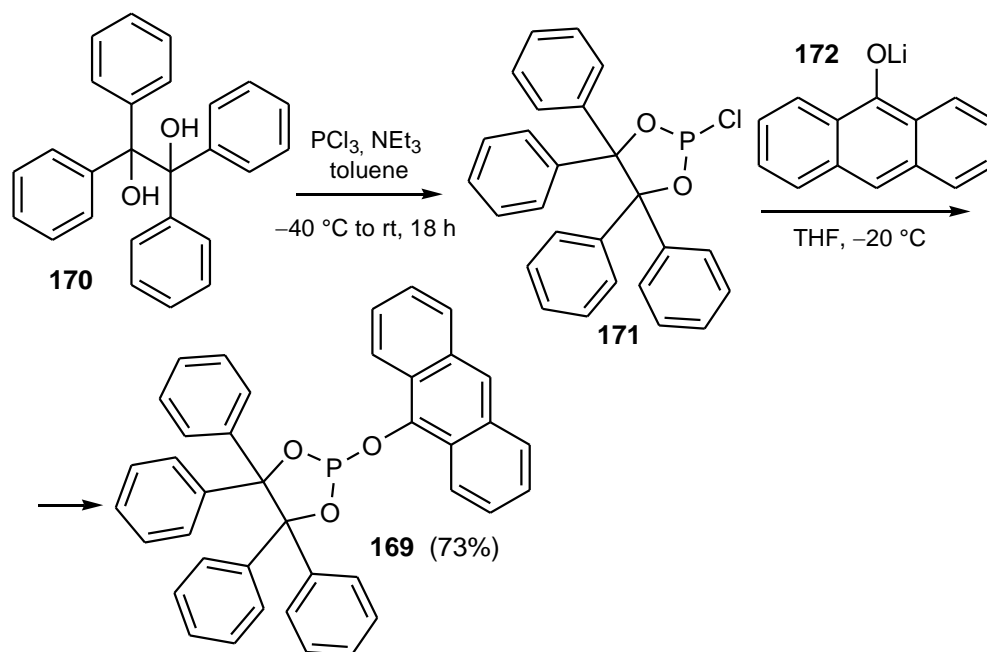
Scheme 62. The synthesis and transformation of bis(diethylamino)phosphinoanthracenes **166** and **167**.

3.3. Phosphorous Acid Esters (Phosphites) (*AnthOP(OR)₂*)

This subsection covers P^{III} acids derivatives containing one anthracene moiety linked indirectly to the phosphorus atom via the P-O-Csp² (Anth) bond.

Kloß et al. conducted a study of numerous phosphite-based ligands for rhodium catalysts, which were used in hydroformylation reactions [3]. The authors revealed that anthryl phosphites were susceptible to hydrolysis, which limits their use for the synthesis of catalysts. Therefore, they synthesized relatively stable phosphites, one of which was the phosphite **169**.

The latter, as a solid, was synthesized by a procedure involving the treatment of benzopinacol **170** with phosphorus trichloride to give chlorophosphite **171**, followed by the addition of lithium anthr-9-olate **172** (Scheme 63).



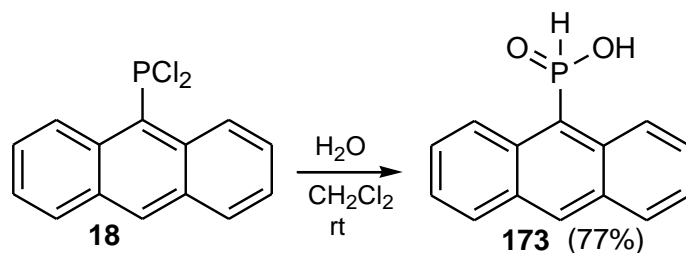
Scheme 63. The synthesis of the phosphite **169** from PCl₃ and the dialcohol **170**.

Implemented in a rhodium catalyst, it exhibited high activity towards hydroformylation. The ligand turned out to be relatively stable under hydrolysis conditions.

3.4. Phosphonous Acid P^{IV} Tautomers (*H*-phosphinic Acids) (*AnthP(O)H(OH)*)

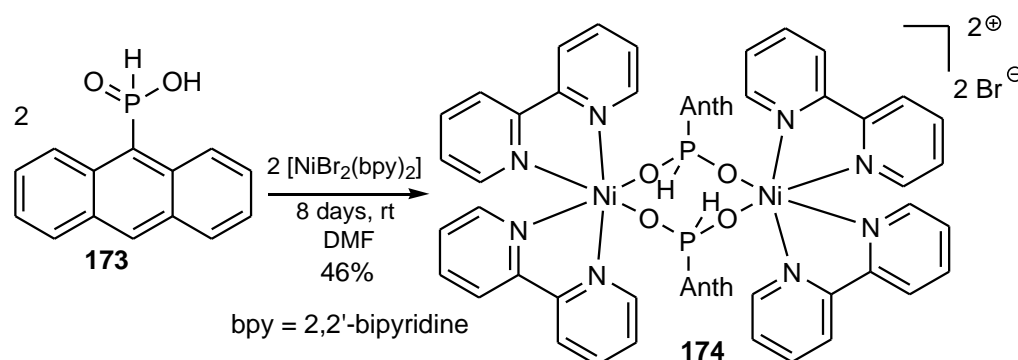
The synthesis of the ester of the P^{III} tautomeric form of phosphonous acid, i.e., diphenyl 9-anthrylphosphonite **2**, is mentioned in Section 2.

Schmutzler and co-workers presented the hydrolysis of 9-(dichlorophosphino)anthracene **18** in CH_2Cl_2 with water at room temperature, which gave anthryl-*H*-phosphinic acid **173** in a 77% yield (Scheme 64) [10].



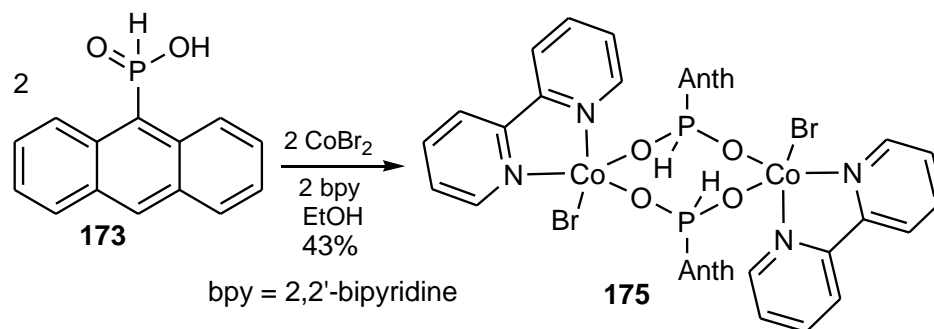
Scheme 64. The synthesis of anthrylphosphinic acid **173**.

Yakhvarov et al. reported the synthesis of the first example of dinuclear nickel complex **20** with the bridging anthr-9-yl- $P(H)O_2$ ligands. Anthr-9-yl-phosphinic acid **173** in the reaction with $NiBr_2(bpy)_2$ in dimethylformamide after 8 days at room temperature gave the nickel complex **174** in a 46% yield (Scheme 65) [75].



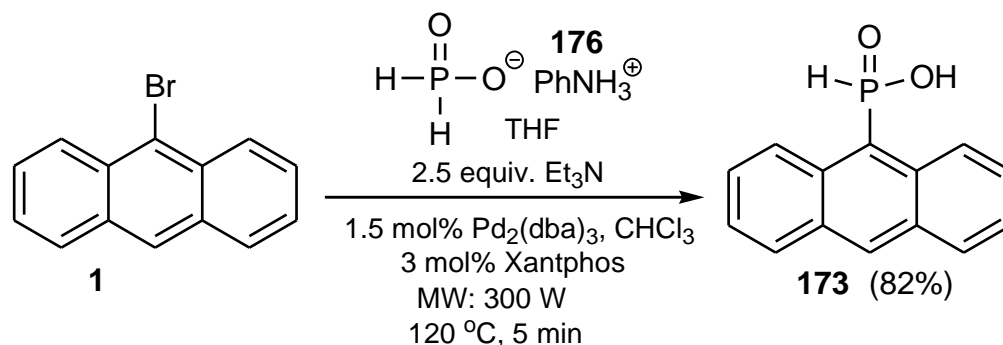
Scheme 65. The synthesis of the binuclear nickel complex **174** with the $AnthP(H)O_2$ ligand.

The same authors reported the formation of the first example of a neutral dinuclear cobalt complex **175** formed in the reaction of cobalt dibromide with 2,2'-bipyridine (bpy) and 9-anthrylphosphinic acid **173** (Scheme 66) [76].



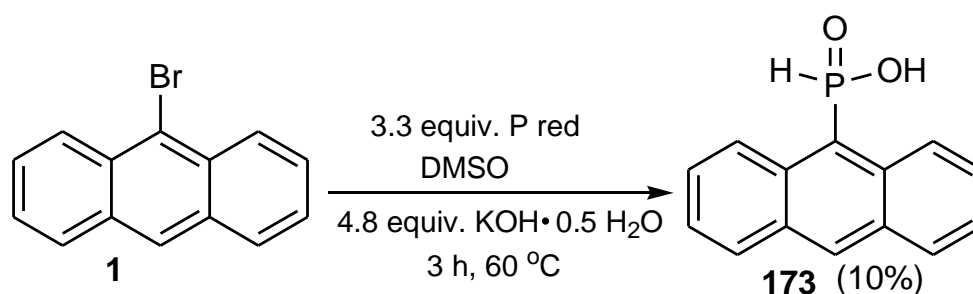
Scheme 66. The synthesis of the dinuclear cobalt complex **175** with the 9-anthrylphosphinic acid ligand.

Stawinski and co-workers reported a microwave-assisted (MW) synthesis of a series monoaryl-*H*-phosphinic acids, including anthr-9-yl-*H*-phosphinic acid **173** [77]. The microwave-assisted cross-coupling of 9-bromoanthracene **1** and anilinium *H*-phosphinate **176** was catalyzed by 3 mol% Pd₂(dba)₃ CHCl₃/Xantphos[®] as a supporting ligand and was carried out in the presence of 2.5 equiv. of triethylamine. Irradiation of the mixture with a microwave (MW) for 5 min at 120 °C produced *H*-phosphinic acid **173** in an 82% yield (Scheme 67).



Scheme 67. The synthesis of anthr-9-yl-*H*-phosphinic acid **173** from 9-bromoanthracene **1**.

Trofimov and co-workers reported another synthesis of anthr-9-yl-phosphinic acid **173** in the reaction of 9-bromoanthracene **1** with elemental phosphorus in a superbasic medium [78]. The authors treated **1** with 3.3 equiv. of phosphorus red in DMSO and the mixture of 4.8 equiv. of KOH and H₂O as a superbase at 60 °C for 3 h (Scheme 68). In this case, the yield of **173** was only 10%.

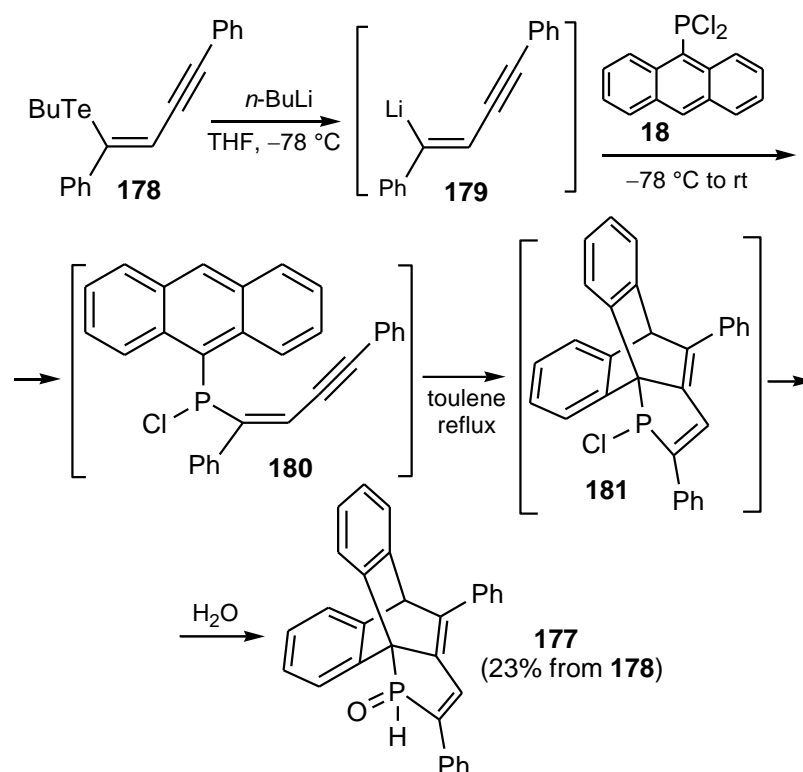


Scheme 68. The reaction of 9-bromoanthracene **1** with red phosphorus.

3.5. Phosphinous Acid P^{IV} Tautomers (*H*-phosphine Oxides) (Anth₂P(O)H)

The synthesis of esters of the P^{III} tautomeric form of phosphinous acid, i.e., phenyl 9-anthryl(1-naphthyl)phosphinite **3** and phenyl dianthrylphosphinite **6**, is mentioned in Section 2.

The 1-(phosphino)-1,4-diphenyl-1,3-butadiene moiety, incorporated with a dibenzobarrelene skeleton in **177**, was synthesized by Ishii and co-workers [79]. They started the synthesis from lithiation of the starting reagent **178** with *n*-butyllithium to obtain the organolithium intermediate **179** followed by treatment of the latter with 9-dichlorophosphinoanthracene **18** to obtain the key precursor (*Z*)-1-(9-anthrylchlorophosphino)butenyne **180**. Then, the dibenzobarrelene structure **181** was obtained by an intramolecular [4+2] cycloaddition reaction of **180** (Scheme 69). Further hydrolysis of **181** gave the secondary phosphine oxide **177**, which exhibited a long-wavelength absorption ($\lambda_{\text{abs}} = 355 \text{ nm}$) and emission ($\lambda_{\text{em}} = 442 \text{ nm}$).

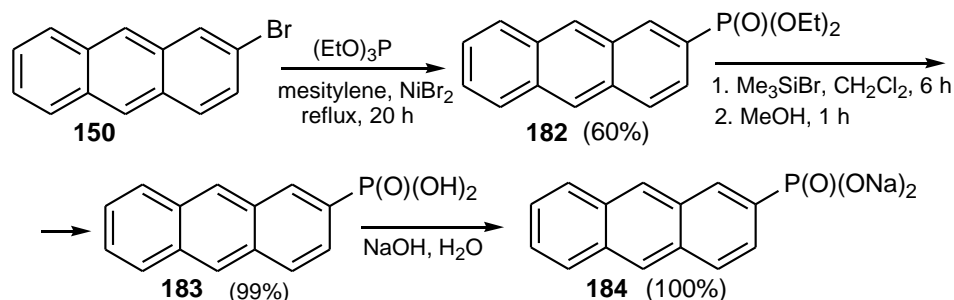


Scheme 69. The synthesis of the secondary phosphine oxide **177** from (*n*-butyltelluro)butenyne **178**.

4. Synthesis and Reactions of Phosphonic Acids (AnthP(O)(OH)₂) and Phosphonates (AnthP(O)(OR)₂) (Anth = Anthryl)

In this section, P^{IV} organophosphorus-substituted acenes with one P-Csp² (Anth) bond, two P-O, and one P=O bonds are reviewed. Hence, this section includes phosphonic acids and their esters. Interestingly, no thio- and seleno phosphonic acids AnthP(X)(YH)₂ and the corresponding hetero-phosphonates AnthP(X)(YR)₂ (Anth = anthryl), (X, Y = S, Se) were reported in the review period.

The synthesis of a series of anthracenes substituted in position 2 with diethoxyphosphoryl groups was described by French and coworkers (Scheme 70) [80]. The Arbuzov reaction of 2-bromo-anthracene **150** with triethylphosphite, catalyzed by nickel bromide, proceeded in refluxing mesitylene for 20 h and led to 2-(diethoxyphosphoryl)anthracene **182**. Then, the latter was transformed into the disilyl diester by treatment with bromotrimethylsilane in dichloromethane and next hydrolyzed to the free acid **183** with methanol. Dissolving **183** in an aqueous solution of a stoichiometric amount of sodium hydroxide gave the sodium salt **184** quantitatively.

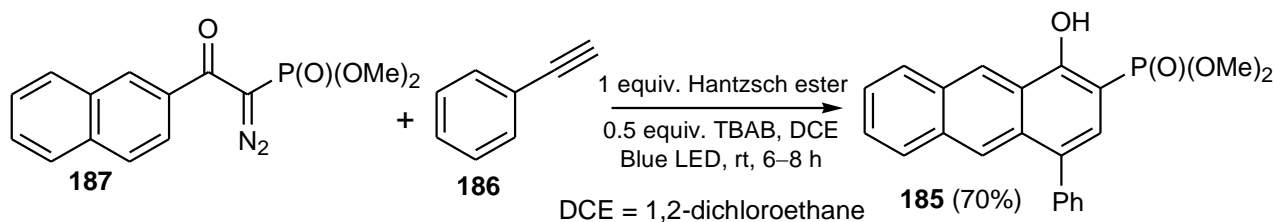


Scheme 70. The synthesis of 2-(dihydroxyphosphoryl)anthracene **183**.

Then, the authors investigated the spectroscopic properties of the obtained compounds, including the absorbance, fluorescence, and quantum yields Φ [80]. A slight blue shift was

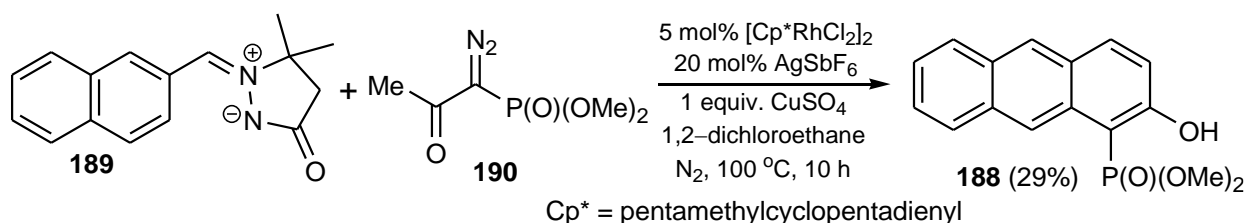
observed after the conversion of phosphonate ester into phosphonic acid and also when the phosphonic acid was converted to the corresponding sodium salt. Shifts of 53, 53, and 49 nm were observed for **182**, **183**, and **184**, respectively. Compounds **182**, **183**, and **184** showed quantum yields of fluorescence $\Phi = 33\%$, 40% , and 0% , respectively. Additionally, compounds **182**, **183**, and **184** formed micelles in water.

Nagode and co-workers [81] synthesized 1-hydroxy-4-phenyl-2-(dimethoxyphosphoryl)anthracene **185** using α -diazophosphonate **186**, phenylacetylene **187**, Hantzsch ester, and tetrabutylammonium bromide (TBAB) in dichloroethane under blue LED irradiation. This reaction was conducted at room temperature for 6–8 h and the product **185** was obtained in a 70% yield (Scheme 71).



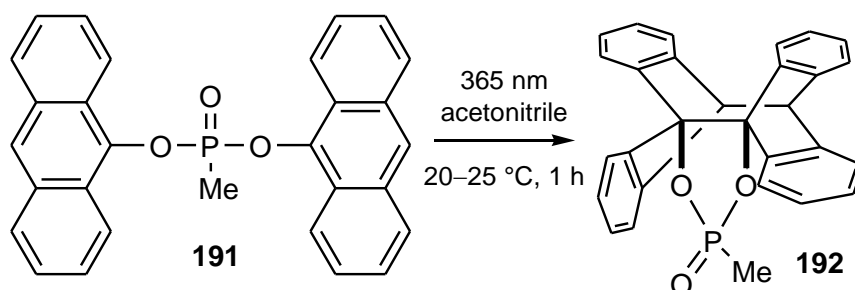
Scheme 71. The synthesis of 1-hydroxy-4-phenyl-2-(dimethoxyphosphoryl)anthracene **185**.

Shu et al. [82] described a new synthetic method for the preparation of 2-hydroxy-1-(dimethoxyphosphoryl)anthracene **188** in the reaction of an imine derivative of azomethine **189** and dimethyl diazophosphonate **190** in the presence of inorganic additives (Scheme 72). The reaction was carried out at $100\text{ }^{\circ}\text{C}$ and the compound **188** was obtained in a 29% yield.



Scheme 72. The synthesis of 2-hydroxy-1-(dimethoxyphosphoryl)anthracene **188**.

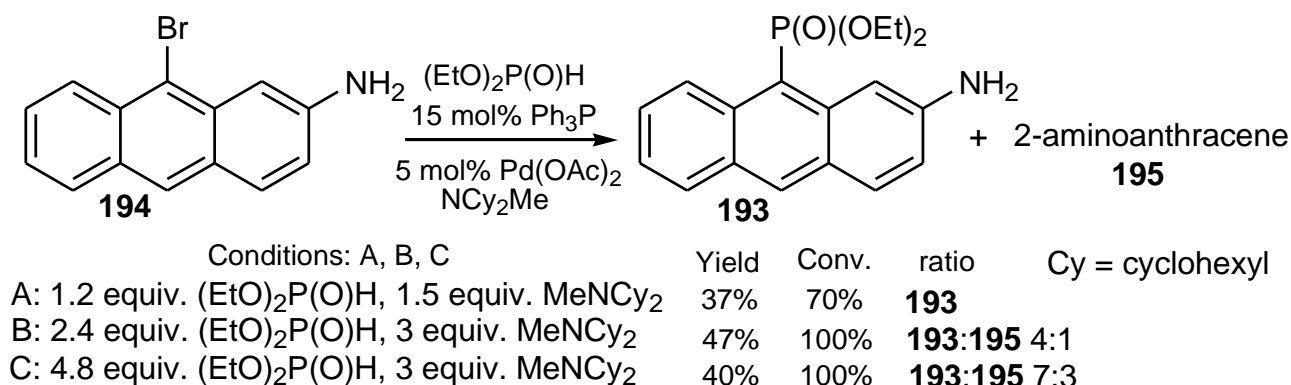
Nakamura and co-workers [83] studied the photolysis reactions of di(anthr-9-yl)methylphosphonate **191**. The authors demonstrated that upon irradiation with monochromatic light at 365 nm, **191** underwent cyclization to **192** (Scheme 73), similarly to the compound **230** (see below Scheme 87).



Scheme 73. The cyclization of **191** to **192** upon irradiation with 365 nm monochromatic light.

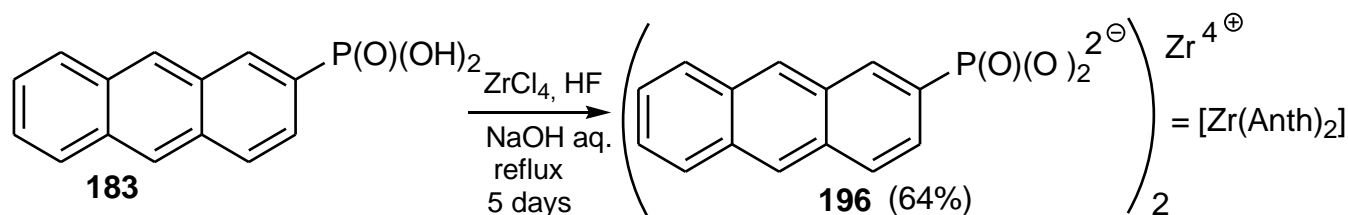
Bessmertnykh and co-authors presented a direct synthesis of 9-(diethoxyphosphoryl)anthracene **193** bearing an amino group on the aromatic ring at the position 2 in a Hirao reaction. The authors carried out a reaction of 2-amino-9-bromoanthracene **194** with diethyl phosphite in the presence of *N,N*-dicyclohexylmethylamine in refluxing ethanol for 48 h and

using catalytic amounts of palladium acetate (5 mol %) and triphenylphosphine (15 mol %). The outcome of this reaction depended on the stoichiometry used (Scheme 74) [84].



Scheme 74. The synthesis of diethyl 2-amino-9-anthrylphosphonate **193**.

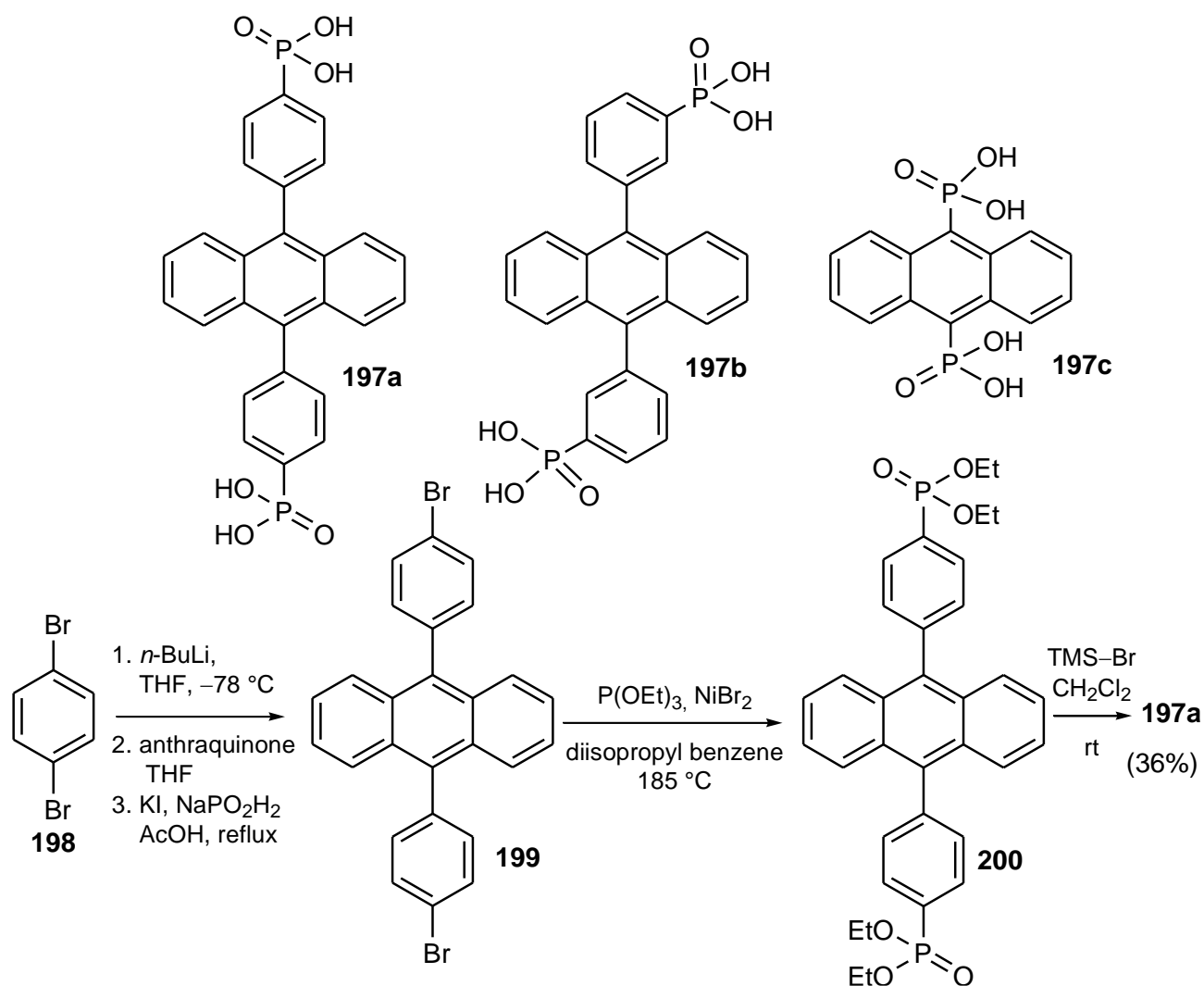
Leenstra and co-workers synthesized zirconium bis-(2-anthrylphosphonate) [Zr(Anth)₂] **196** by mixing zirconyl chloride with hydrofluoric acid, sodium hydroxide, and 2-naphthylphosphonic acid **183** in water for 5 days at reflux (Scheme 75) [85].



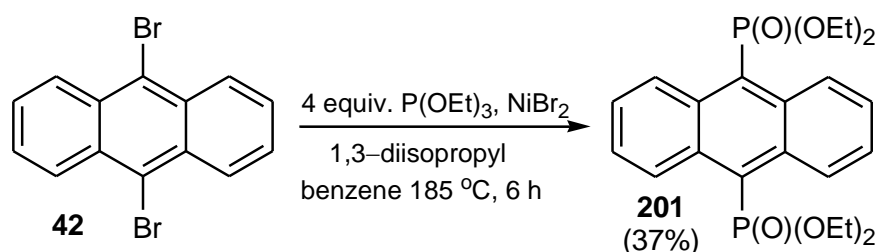
Scheme 75. The synthesis of zirconium bis(2-anthrylphosphonate) **196**.

The same authors showed the readily excimer formation of zirconium bis-(2-anthrylphosphonate) [Zr(Anth)₂] **196** as a powdered solid in glycerol and its precursor, 2-anthrylphosphonic acid **183**, in methanol solution (Scheme 75) [86]. The fluorescence spectrum of **196** [Zr(Anth)₂] had a broad emission band with a maximum at 448 nm in the solid. Additionally, the authors observed that [Zr(Anth)₂] **196** did not display a time-dependent quenching of the fluorescence emission, suggesting that the photodimerization reaction of the anthracene group to bianthryl did not exist in the solid state.

Zhou and coworkers [6] investigated five anthracene-based bis(phosphonic acids), of which three **197a**, **197b**, and **197c** possessed the direct P-C_{sp}² bonding. They were prepared according to the literature procedures cited there (Scheme 76). Thus, 4,4-(anthracene-9,10-diyl)bis(4,1-phenylene) bis(phosphonic acid) **197a** was synthesized by treatment of 1,4-dibromobenzene **198** with *n*-butyllithium, followed by the addition of the resulting 4-bromo-1-lithiobenzene to anthraquinone and subsequent reduction of the resulting anthryl dialcohol to give **199**. Then, the Arbuzov-type reaction followed by hydrolysis with trimethylsilyl bromide (TMS-Br) of the obtained bis(phosphonate) **200** gave the bis(phosphonic acid) **197a** in a 36 % yield (Scheme 76) [87]. Using this procedure and 1,3-dibromobenzene as the starting material, the authors obtained the corresponding regioisomeric 4,4'-(anthracene-9,10-diyl)bis(3,1-phenylene)bis(phosphonic acid) **197b** [88]. Anthracene-9,10-bis(phosphonic acid) **197c** was prepared analogously, based on the procedure by Pramanik et al. of the synthesis of the corresponding tetraethyl ester **201** (Scheme 77) [7], which was next hydrolyzed in this work with TMS-Br to give **197c**. Compounds **197a** and **197c** exhibited red-shift fluorescence. They were deposited on a zirconium dioxide layer as triplet-triplet annihilation acceptors.



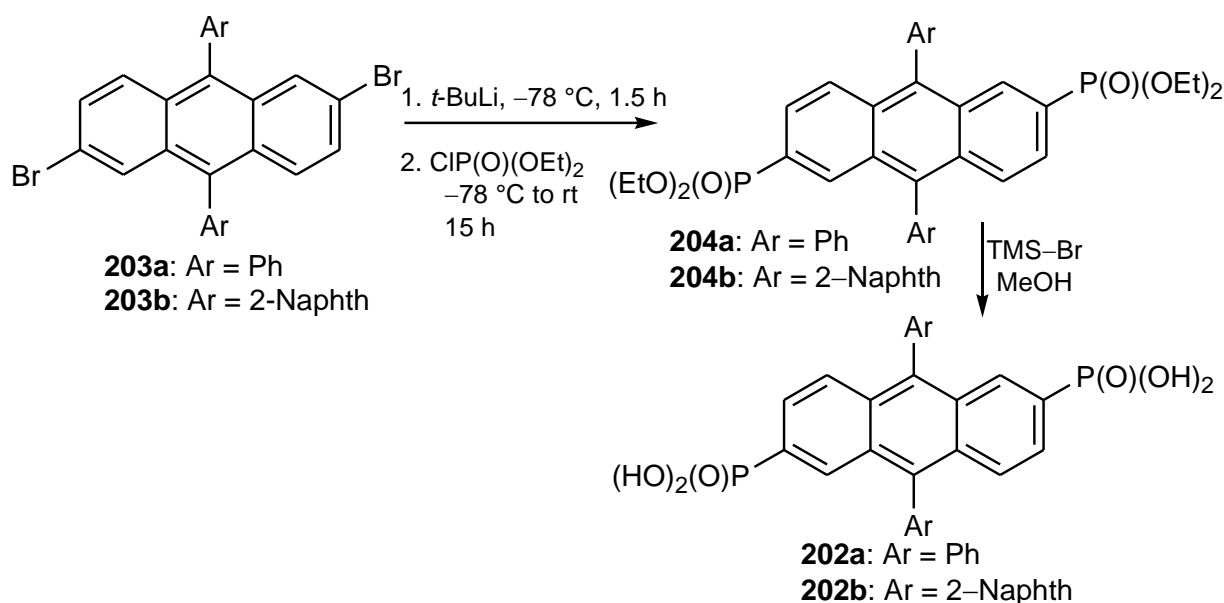
Scheme 76. The synthesis of the bis(phosphonic acid) **197a** from 1,4-dibromobenzene **198**.



Scheme 77. The synthesis of 9,10-bis(diethoxyphosphoryl)anthracene **201**.

M. Pramanik et al. [7] synthesized **201** from 9,10-dibromoanthracene **42** in a 37% yield, at high temperature, using an excess of triethyl phosphite and NiBr₂ in 1,3-diisopropylbenzene (Scheme 77). The compound **201**, in the form of fluorescent organic nanoparticles, was explored as a selective anticancer candidate by apoptosis-mediated cancer therapy towards U937 cells.

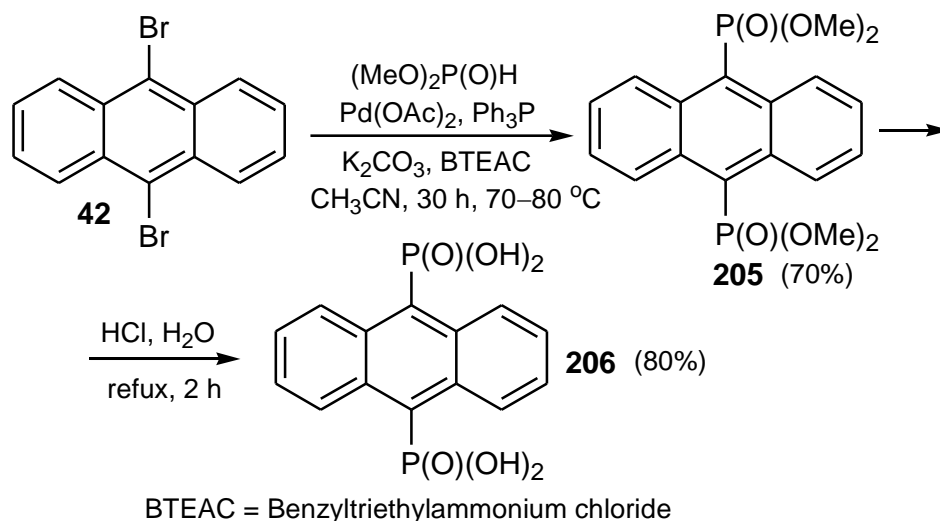
In another study, Yazji et al. [89] obtained 9,10-diphenyl-2,6-bis(phosphonic acids) **202a** and **202b** (Scheme 78) from 9,10-diaryl-2,6-dibromoanthracenes **203a** and **203b** which next were transformed to the corresponding 2,6-dilitio derivatives with *t*-butyllithium, and then reacted with diethyl phosphorochloridate to give bis(phosphonates) **204a** and **204b**, which were finally converted, by the hydrolysis of the diester, to the corresponding bis(phosphonic acids) **202a** and **202b** (Scheme 78).



Scheme 78. The synthesis of bis(phosphonic acids) **202a** and **202b** from 9,10-diaryl-2,6-dibromoanthracenes **203a** and **203b**.

The authors investigated the use of these compounds in thin films deposited on a silicon dioxide surface, acting as nucleation sites for pentacene crystallization. This study suggested that high optical anisotropy of pentacene, crystallized on such films, indicated that compounds **202a** and **202b** changed the silicon dioxide surface into a lattice, which induced the nucleation of pentacene. A similar study involving **202a** and **202b** was also conducted by Cattani-Scholz and co-workers [90], who synthesized these compounds in the same manner as the group of Yazji et al.

Kabachnik and coworkers demonstrated a synthesis of tetramethyl bis(phosphonate) **205** starting from 9,10-dibromo-anthracene **42** and dimethyl phosphite (Scheme 79) [91]. This reaction was catalyzed by palladium acetate/triphenylphosphine and was carried out under bi-phasic conditions for 30 h at 70–80 °C in acetonitrile in the presence of K_2CO_3 as a base and benzyltriethylammonium chloride (BTEAC) as a phase-transfer catalyst (PTC) to give the desired product **205** in a 70% yield.



Scheme 79. The synthesis of 9,10-bis(phosphonic acid) **206** from 9,10-dibromoanthracene **42**.

Next, the authors transformed both phosphonate ester groups in **205** to the corresponding bis(phosphonic acid) **206** by refluxing it in an aqueous solution of hydrochloric acid for 2 h in an 80% yield (Scheme 79) [91].

Organic thin-film transistors based on pentacene as a semiconductor were fabricated on silicon. A self-assembled monolayer derived from the phosphonate (SAMP) **207a** showed an improvement over monolayers using octadecylsilane and other phosphonates (Figure 5). These devices had substantially reduced trap states, on/off ratios of 10^8 , sub-threshold slopes of 0.2 V/decade, and substantially uniform threshold voltages of -4.5 V across a large number of devices [92].

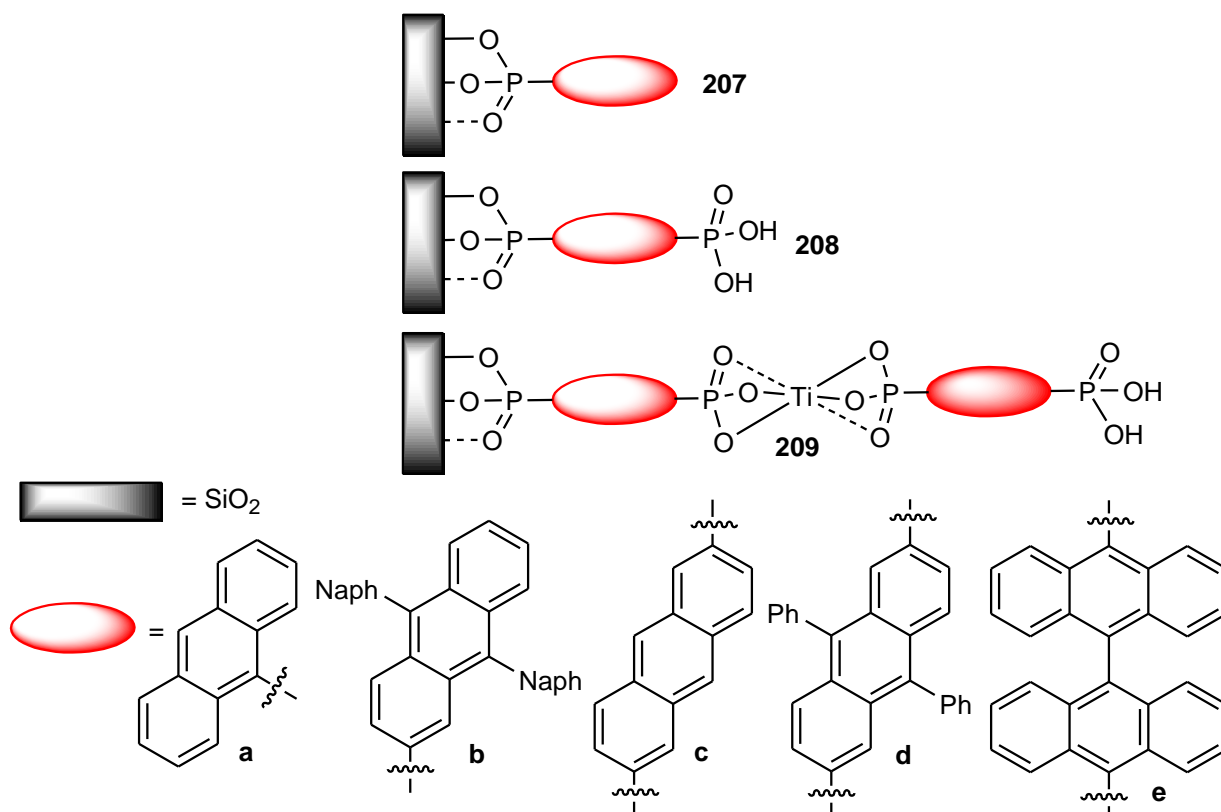
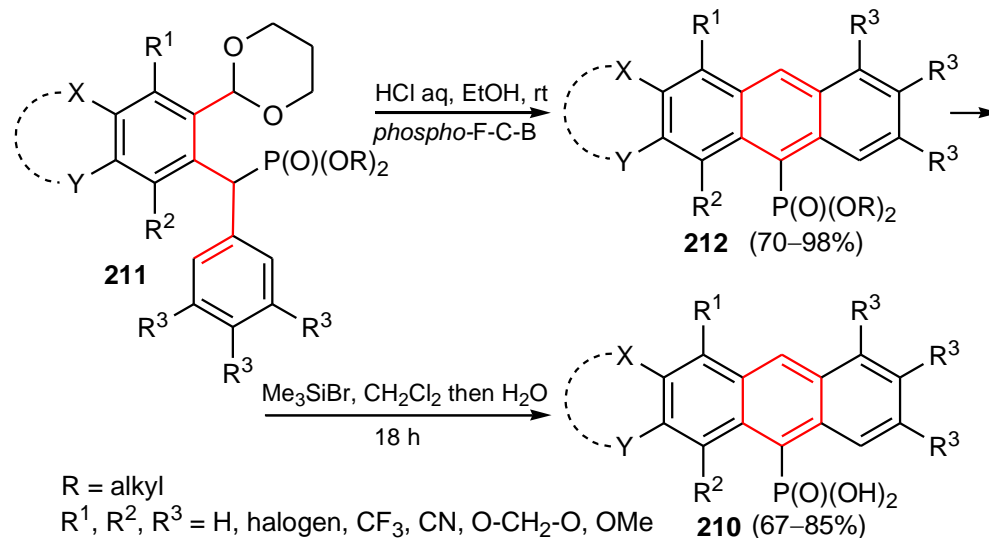


Figure 5. General structures of SAMPs **207**, **208**, and duplexes **209**.

Good device characteristics were also measured for the monolayer **207b**, in which the calculated molecular spacings were about 0.7 nm. This created channels that were on the order of the “thickness” of an aromatic π system, and which could allow intercalation of pentacene units, favoring a π -stacking motif for this first pentacene layer [93].

Tornow and co-workers synthesized SAMPs **208c–e** and self-assembled organophosphonate duplexes **209c,d** ensemble on nanometer-thick SiO_2 -coated, highly doped silicon electrodes (Figure 5) [5].

Most of the reviewed papers in the previous sections discussed organophosphorus-substituted anthracenes that did not contain other substituents or anthracenes with a very low degree of substitution. This problem also concerns a group of phosphonates and phosphonic acids. Bałczewski et al. [70,71] recently presented a new *phospho*-Friedel–Crafts–Bradsher cyclization, which enabled the synthesis of highly substituted anthracenes **210**. In this new reaction, (*o*-diacetoaryl)arylmethylphosphonates **211** were cyclized under very mild conditions at room temperature to give 10-(dialkoxyphosphorylanthracenes **212** in a 70–98% yield. The latter were hydrolyzed to the corresponding phosphonic acids **210** in a 67–85% yield (Scheme 80).

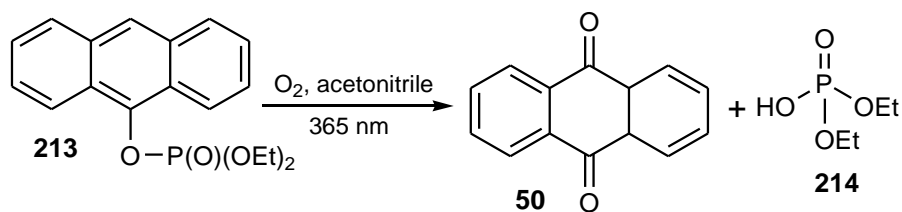


Scheme 80. The *phospho*-Friedel–Crafts–Bradsher cyclization of phosphonates **211** to sterically hindered anthracenes **212**.

5. Synthesis and Reactions of Phosphoric Acids and Phosphates (AnthOP(=O)(OR)₂) (R = H, alkyl, aryl)

Unlike previous sections (except Section 3.3), which reviewed the synthesis and reactions of compounds containing a phosphorus atom linked to the anthracene moiety directly by the P-Csp² (Anth) bond, this section and Section 3.3 cover anthracenes that are bonded to the phosphorus atom indirectly via an oxygen atom by the P-O-Csp² (Anth) bond. Interestingly, no hetero-analogs of phosphates were reported in the reviewed period.

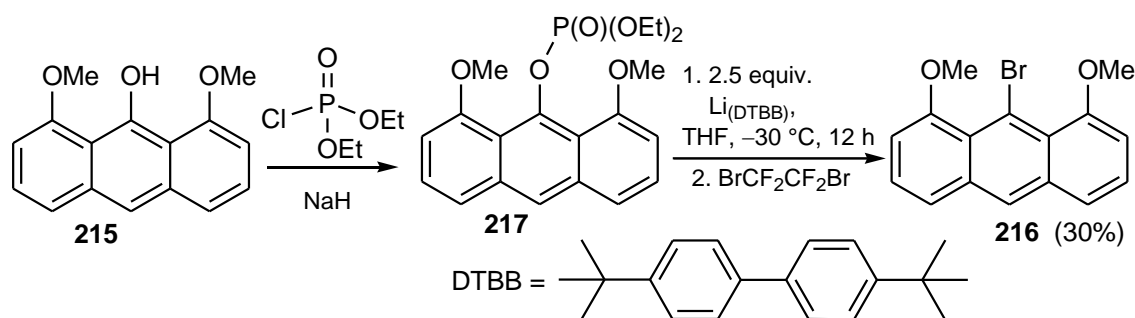
Buckland and Davidson [94] investigated the photo-oxidation of 10-diethoxyphosphoryloxyanthracene **213**, which represents a group of acenyl phosphates. The authors showed that in the presence of oxygen, the photochemically labile phosphate **213**, dissolved in acetonitrile, could be oxidized to anthraquinone **50** and diethyl hydrogen phosphate **214** upon irradiation with a 365 nm monochromatic light (Scheme 81).



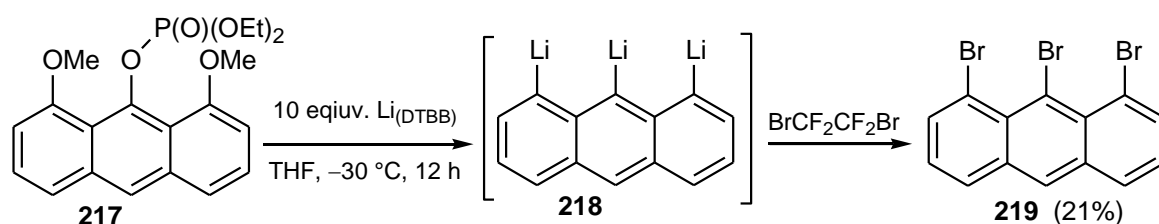
Scheme 81. The aerobic photochemical oxidation of the phosphate **213**.

Yamashita et al. [95] conducted a study in which 1,8-dimethoxyanthr-9-ol **215** was used for the synthesis of 9-bromo-1,8-dimethoxyanthracene **216**. The former was treated with diethyl phosphorochloridate in the presence of sodium hydride, yielding 9-diethoxyphosphoryloxy-1,8-dimethoxy-anthracene **217**. Then, the phosphate/lithium exchange with Li_(DTBB) (DTBB = 4,4'-di-tert-butylbiphenyl) followed by bromination with 1,2-dibromo-1,1,2,2-tetrafluoroethane gave **216** as a pale-yellow solid in a 30 % yield (Scheme 82).

Another study, carried out by the group of Yamashita and co-workers [96], showed further application of the Li_(DTBB) system towards the substrate **217**. When 2.5 equiv. of Li_(DTBB) was used, the reaction followed the path from Scheme 82. However, when an excess (10 equiv.) of the Li_(DTBB) reagent was used, the phosphate **217** was transformed to 1,8,9-trilithioanthracene **218**, which then underwent bromination with 1,2-dibromo-1,1,2,2-tetrafluoroethane to give 1,8,9-tribromoanthracene **219** (Scheme 83).

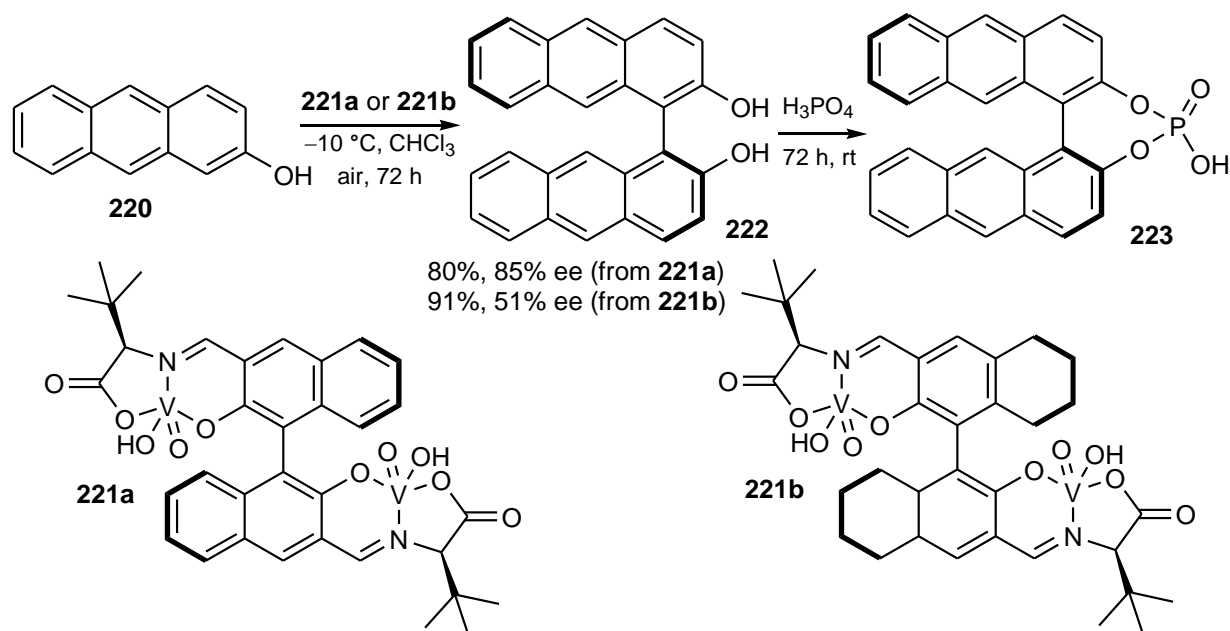


Scheme 82. The synthesis of 9-bromo-1,8-dimethoxyanthracene **216** via 9-diethoxyphosphoryloxy-1,8-dimethoxyanthracene **217** as the intermediate.



Scheme 83. The conversion of the phosphate **217** to 1,8,9-tribromoanthracene **219**.

Takizawa et. al. [4] discovered an enantioselective, oxidative-coupling reaction of anthr-2-ol **220** with the chiral vanadium complexes **221a** and **221b** to deliver bianthrol **222**, which was then esterified with phosphoric acid to give 4,4'-bianthryl phosphoric acid **223** (Scheme 84).

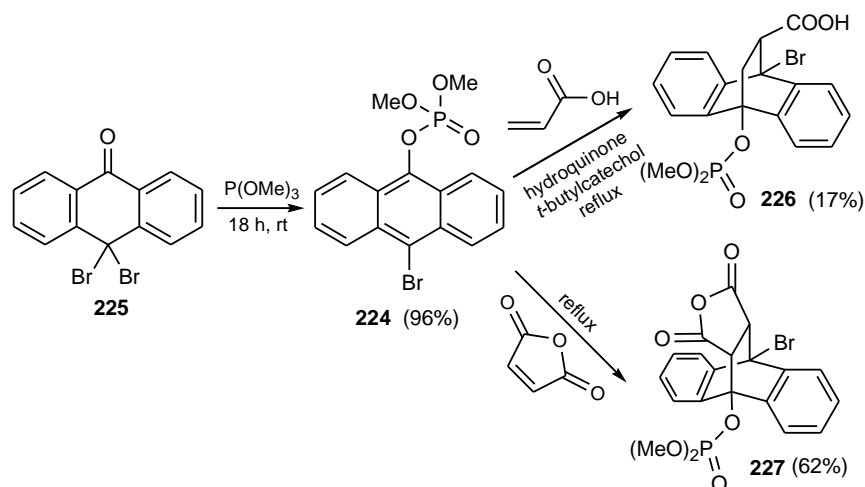


Scheme 84. The synthesis of 4,4'-bianthryl phosphoric acid **223** from anthr-2-ol **220** using the vanadium complexes **221a** and **221b**.

The authors investigated the catalytic properties of **223** in the Diels–Alder reaction of 2-cyclohexenone with aldimines; however, it gave only racemic mixtures.

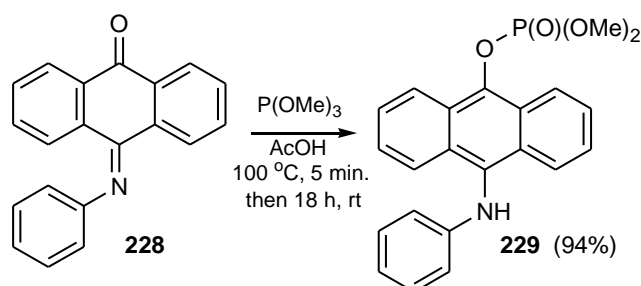
Another application of anthryl phosphates in the Diels–Alder reaction was performed by Meek and Koh [97], who described the synthesis of 10-bromo-9-(dimethoxyphosphoryloxy)

anthracene **224** obtained from 10,10-dibromoanthrone **225** and trimethyl phosphite. Next, they applied **224** as a diene in the Diels–Alder reaction with acrylic acid and maleic anhydride, which delivered adducts **226** and **227**, respectively (Scheme 85).



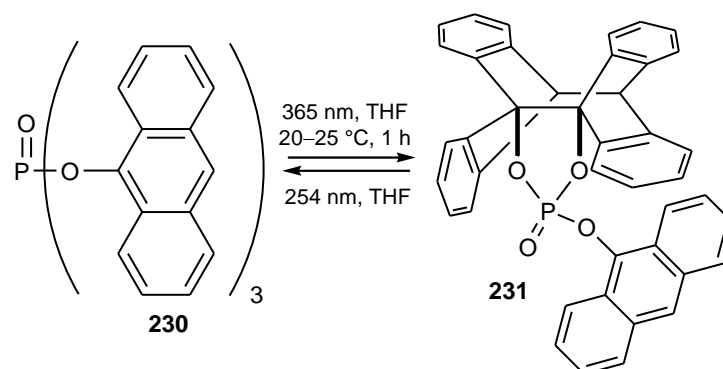
Scheme 85. The synthesis of **224** and its application in the Diels–Alder reaction with maleic anhydride and acrylic acid.

Then, the authors [97] described the reaction of anthraquinone anil **228** with trimethyl phosphite, yielding 9-dimethoxyphosphoryloxy-10-(phenylamino)anthracene **229** as yellow needles (Scheme 86).



Scheme 86. The synthesis of 9-dimethoxyphosphoryloxy-10-(phenylamino)anthracene **229** from anthraquinone anil **228**.

Nakamura and co-workers [83] studied the photolysis reactions of tri(anthr-9-yl)phosphate **230**. The authors demonstrated that upon irradiation with a 365 nm monochromatic light, **230** underwent cyclization to **231** (Scheme 87). Interestingly, the product **231** could be transformed back to **230** upon irradiation with a 254 nm monochromatic light.

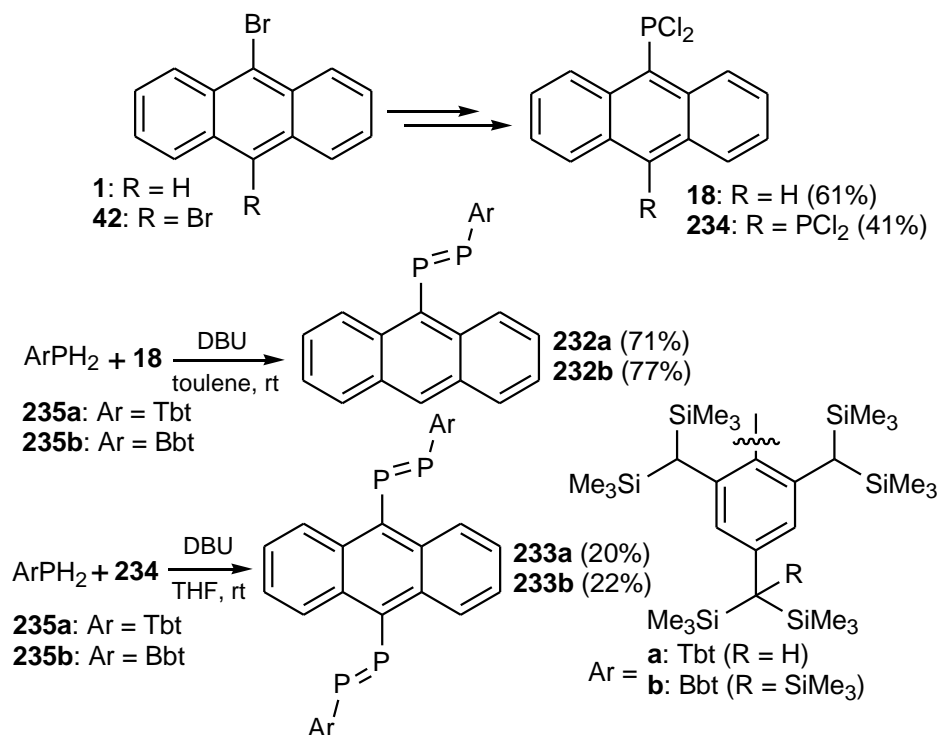


Scheme 87. The cyclization of **230** to **231** upon irradiation with a 365 nm monochromatic light.

6. Synthesis and Reactions of Diphosphenes (Anth(P=PR)) and Derivatives

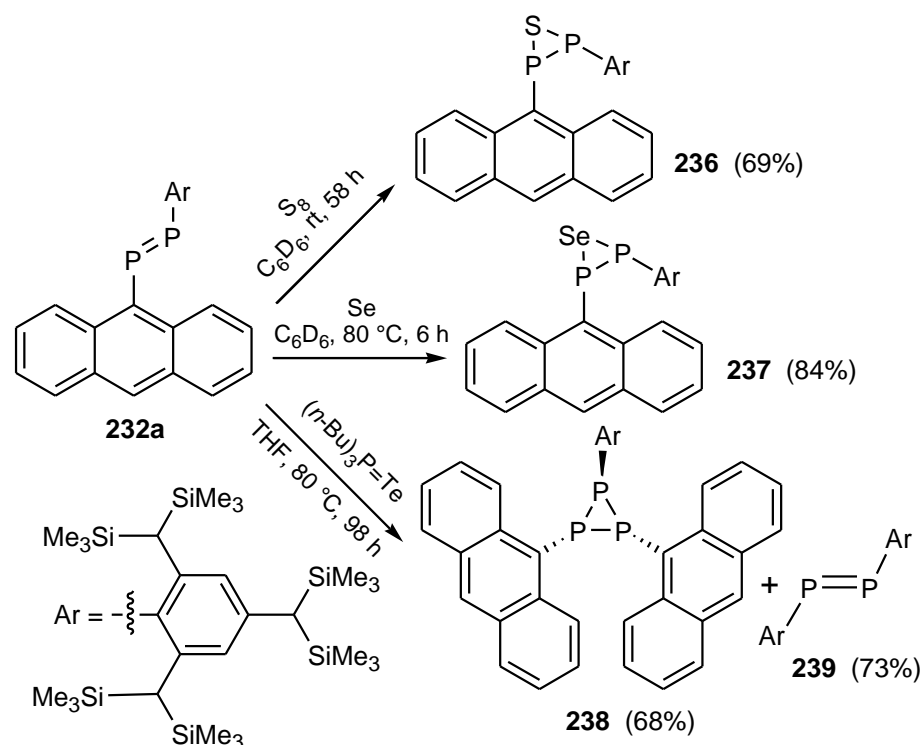
In addition to anthracenes substituted by one, two, or three organophosphorus groups with one phosphorus atom in each group, which have been described in previous sections, this section reviews anthracenes substituted by organophosphorus groups containing two or three phosphorus atoms.

9-(Diphospheno)anthracenes **232** and 9,10-bis(diphospheno)anthracenes **233**, presumably the first stable (diphospheno)anthracenes, were synthesized by Tokitoh and co-workers [74,98]. The 2,4,6-tris[bis(trimethylsilyl)methyl]phenyl (Tbt) and 2,6-bis[bis(trimethylsilyl)methyl]-4-[tris(trimethylsilyl)methyl]phenyl (Bbt) groups, reported by Yoshifuji and co-workers, were employed for stabilization of these molecules [99]. First, 9-dichlorophosphinoanthracene **18** and 9,10-bis(dichlorophosphino)anthracene **234** were readily prepared in moderate yields from 9-bromoanthracenes **1** and **42**. Next, the condensation reaction of TbtPH₂ **235a** and BbtPH₂ **235b** with 9-dichlorophosphinoanthracene **18** in the presence of DBU (DBU = 1,8-diazabicyclo[5.4.0]undec-7-ene) as a base afforded 9-diphosphenoanthracenes **232a** and **232b** as stable red crystals in 71 and 77% yields, respectively (Scheme 88). 9,10-Bis(diphospheno)anthracenes **233a** and **233b** were synthesized in a ca. 20% yield in a manner similar to the synthesis of 9-diphosphenoanthracenes **232a** and **232b** using 9,10-bis(dichlorophosphino)anthracene **234** instead of 9-(dichlorophosphino)anthracene **18**. The UV-vis spectra of **232** and **233** revealed the electronic communication between the anthryl and P=P units, which was also supported by the TD-DFT calculations. The monodiphosphene derivative **232a** exhibited a weak fluorescence in hexane solution, whereas the bis(diphosphene) derivatives **233** displayed no appreciable luminescence under the same conditions. The compounds **232a,b** and **233a,b** showed absorption maxima at 380–400, 380–400, 403–426, and 404–427 nm, accordingly.



Scheme 88. The synthesis of 9-diphospheno- **232** and 9,10-bis(diphospheno)anthracenes **233**.

The same research group also examined the specific reactions of the 9-(diphospheno)anthracene **232a**, including sulfonation, selenation, and attempted telluration with tributylphosphine telluride (Scheme 89) [74,100].



Scheme 89. Sulfonation, selenation, and attempted telluration of **232a**.

Thus, sulfonation of **232a** gave thiadiphosphirane **236** while selenation delivered selenadiphosphirane **237** in good yields.

Surprisingly, treatment of **232a** with tributylphosphine telluride did not result in telluration via the tellurium transfer. Instead, the reaction yielded triphosphirane **238** as yellow crystals and the diphosphene derivative **239** as red crystals.

7. Conclusions

In this review, covering the period 1968–2022, the synthetic methods, reactions, and applications of acenes were discussed. This review revealed that phosphorus-substituted acenes with a number of benzene rings greater than three remain unknown. This opens the way for the development of new syntheses of longer acenes and insights into the properties and novel applications of such materials. Based on the current knowledge of the properties of multi-ring fused aromatics, it can be predicted that such acenes, especially electron-tunable (P^{III} , P^{IV} , P^V) phosphorus-substituted tetracenes and pentacenes, will find more effective applications than lower analogs, mainly in optoelectronics. In particular, solid-anchored phosphonic acids that form monolayers may provide an example of such an application [5,92,93].

The second characteristic of the reviewed compounds was the low degree of substitution of aromatic rings by other substituents than organophosphorus groups and, in particular, most of anthracene moieties were unsubstituted. Apart from our preliminary work [70,71], this review showed, practically, a lack of works devoted to the highly substituted acene systems. It is noteworthy that highly substituted acenes containing thioorganic substituents showed extremely high thermal and photochemical stabilities, properties that would be interesting to verify for acenes with organophosphorus substituents [101,102]. Furthermore, the absence of hetero(S, Se)-analogs of phosphonates and phosphates was recorded during the reviewed period, which additionally opens the way for further research in this area.

Funding: This research was funded by the National Science Center (Poland), grant number 2019/33/B/ST4/02843 (2019–2022).

Acknowledgments: We thank the Bio-Med-Chem Doctoral School at the University of Łódź and Łódź Institutes of the Polish Academy of Sciences (Ł. K. and V. V) as well as the Faculty of Chemistry, University of Łódź (A. R) for the administrative support.

Conflicts of Interest: The authors declare no conflict of interest.

References

- Zhao, Y.; Duan, L.; Zhang, X.; Zhang, D.; Qiao, J.; Dong, G.; Wang, L.; Qiu, Y. White Light Emission from an Exciplex Based on a Phosphine Oxide Type Electron Transport Compound in a Bilayer Device Structure. *RSC Adv.* **2013**, *3*, 21453–21460. [CrossRef]
- Wu, C.L.; Chang, C.H.; Chang, Y.T.; Chen, C.T.; Chen, C.T.; Su, C.J. High Efficiency Non-Dopant Blue Organic Light-Emitting Diodes Based on Anthracene-Based Fluorophores with Molecular Design of Charge Transport and Red-Shifted Emission Proof. *J. Mater. Chem. C* **2014**, *2*, 7188–7200. [CrossRef]
- Kloß, S.; Selent, D.; Spannenberg, A.; Franke, R.; Börner, A.; Sharif, M. Effects of Substitution Pattern in Phosphite Ligands Used in Rhodium-Catalyzed Hydroformylation on Reactivity and Hydrolysis Stability. *Catalysts* **2019**, *9*, 1036. [CrossRef]
- Takizawa, S.; Kodera, J.; Yoshida, Y.; Sako, M.; Breukers, S.; Enders, D.; Sasai, H. Enantioselective Oxidative-Coupling of Polycyclic Phenols. *Tetrahedron* **2014**, *70*, 1786–1793. [CrossRef]
- Cattani-Scholz, A.; Liao, K.-C.; Bora, A.; Pathak, A.; Hundschell, C.; Nickel, B.; Schwartz, J.; Abstreiter, G.; Tornow, M. Molecular Architecture: Construction of Self-Assembled Organophosphonate Duplexes and Their Electrochemical Characterization. *Langmuir* **2012**, *28*, 7889–7896. [CrossRef]
- Zhou, Y.; Ayad, S.; Ruchlin, C.; Posey, V.; Hill, S.P.; Wu, Q.; Hanson, K. Examining the role of acceptor molecule structure in self-assembled bilayers: Surface loading, stability, energy transfer, and upconverted emission. *Phys. Chem. Chem. Phys.* **2018**, *20*, 20513–20524. [CrossRef]
- Pramanik, M.; Chatterjee, N.; Das, S.; Saha, K.D.; Bhaumik, A. Anthracene-bisphosphonate based novel fluorescent organic nanoparticles explored as apoptosis inducers of cancer cells. *Chem. Commun.* **2013**, *49*, 9461–9463. [CrossRef]
- Frank, A.W. The Phosphonous Acids and Their Derivatives. *Chem. Rev.* **1961**, *61*, 389–424. [CrossRef]
- Keller, J.; Schlierf, C.; Nolte, C.; Mayer, P.; Straub, B.F. One-pot syntheses of sterically shielded phosphorus ligands by selective stepwise nucleophilic substitution at triphenyl phosphite. *Synthesis* **2006**, *2*, 354–365. [CrossRef]
- Wesemann, J.; Jones, P.G.; Schomburg, D.; Heuer, L.; Schmutzler, R. Phosphorus derivatives of anthracene and their dimers. *Chem. Ber.* **1992**, *125*, 2187–2197. [CrossRef]
- Wang, Y.; Lai, C.W.; Kwong, F.Y.; Jia, W.; Chan, K.S. Synthesis of aryl phosphines via phosphination with triphenylphosphine by supported palladium catalysts. *Tetrahedron* **2004**, *60*, 9433–9439. [CrossRef]
- Misochko, E.Y.; Akimov, A.V.; Korchagin, D.V.; Ganushevich, Y.S.; Melnikov, E.A.; Miluykov, V.A. Generation and direct EPR spectroscopic observation of triplet arylphosphinidenes: Stabilisation versus internal rearrangements. *Phys. Chem. Chem. Phys.* **2020**, *22*, 27626–27631. [CrossRef]
- Li, X.; Robinson, K.D.; Gaspar, P.P. A New Stereoselective Synthesis of Phosphiranes. *J. Org. Chem.* **1996**, *61*, 7702–7710. [CrossRef]
- Luo, X.; Yuan, J.; Yue, C.-D.; Zhang, Z.-Y.; Chen, J.; Yu, G.-A.; Che, C.-M. Synthesis of peri-Substituted (Naphthalen-1-yl)phosphine Ligands by Rhodium(I)-Catalyzed Phosphine-Directed C–H Arylation. *Org. Lett.* **2018**, *20*, 1810–1814. [CrossRef]
- Maienza, F.; Spindler, F.; Thommen, M.; Pugin, B.; Malan, C.; Mezzetti, A. Exploring Stereogenic Phosphorus: Synthetic Strategies for Diphosphines Containing Bulky, Highly Symmetric Substituents. *J. Org. Chem.* **2002**, *67*, 5239–5249. [CrossRef]
- Haenel, M.W.; Oevers, S.; Bruckmann, J.; Kuhnigk, J.; Krüger, C. Facile Syntheses of 1,8-bis(diphenylphosphino)anthracene and 1,8-bis(dimethylamino)anthracene by nucleophilic substitution of 1,8-difluoroanthracene. *Synlett.* **1998**, *3*, 301–303. [CrossRef]
- Musa, S.; Shaposhnikov, I.; Cohen, S.; Gelman, D. Ligand–Metal Cooperation in PCP Pincer Complexes: Rational Design and Catalytic Activity in Acceptorless Dehydrogenation of Alcohols. *Angew. Chem. Int. Ed.* **2011**, *50*, 3533–3537. [CrossRef]
- Radchenko, Y.; Mujahed, S.; Musa, S.; Gelman, D. Synthesis and characterization of chiral enantiopure PC(sp³)P pincer ligands and their complexes. *Inorg. Chim. Acta* **2021**, *521*, 120350. [CrossRef]
- Jiang, Z.; Xu, M.; Li, F.; Yu, Y. Red-Light-Controllable Liquid-Crystal Soft Actuators via Low-Power Excited Upconversion Based on Triplet–Triplet Annihilation. *J. Am. Chem. Soc.* **2013**, *135*, 16446–16453. [CrossRef]
- Kilian, P.; Slawin, A.M.Z. 1,8,9-Substituted anthracenes, intramolecular phosphine donor stabilized metaphosphonate and phosphonium. *Dalton Trans.* **2007**, 3289–3296. [CrossRef]
- Yang, B.; Wang, Z.X. Ni-Catalyzed C–P Coupling of Aryl, Benzyl, or Allyl Ammonium Salts with P(O)H Compounds. *J. Org. Chem.* **2019**, *84*, 1500–1509. [CrossRef]
- Zhang, J.S.; Chen, T.; Han, L.B. Palladium-Catalyzed Direct Decarbonylative Phosphorylation of Benzoic Acids with P(O)–H Compounds. *Eur. J. Org. Chem.* **2020**, *2020*, 1148–1153. [CrossRef]
- Tao, R.; Zhao, J.; Zhong, F.; Zhang, C.; Yang, W.; Xu, K. H₂O₂-Activated Triplet-Triplet Annihilation Upconversion via Modulation of the Fluorescence Quantum Yields of the Triplet Acceptor and the Triplet-Triplet-Energy-Transfer Efficiency. *Chem. Commun.* **2015**, *51*, 12403–12406. [CrossRef]
- Xu, M.; Han, C.; Yang, Y.; Shen, Z.; Feng, W.; Li, F. Time-Oxygen & Light Indicating: Via Photooxidation Mediated up-Conversion. *J. Mater. Chem. C* **2016**, *4*, 9986–9992. [CrossRef]

25. Xu, H.B.; Wang, J.; Chen, X.L.; Xu, P.; Xiong, K.T.; Guan, D.B.; Deng, J.G.; Deng, Z.H.; Kurmoo, M.; Zeng, M.H. Regulating Structural Dimensionality and Emission Colors by Organic Conjugation between SmIII at a Fixed Distance. *Dalton Trans.* **2018**, *47*, 6908–6916. [CrossRef]
26. Yamaguchi, S.; Akiyama, S.; Tamao, K. The Coordination Number-Photophysical Properties Relationship of Trianthrylphosphorus Compounds: Doubly Locked Fluorescence of Anthryl Groups. *J. Organomet. Chem.* **2002**, *646*, 277–281. [CrossRef]
27. Okada, Y.; Okeya, K.; Murata, Y.; Aoki, N.; Aoki, T.; Sugitani, M.; Yasui, S.; Sawada, Y.; Ogura, F. Synthesis of Phosphine Oxide-Carboxylic Acid Esters Bearing 9,10-Dihydro-9,10-ethanoanthracene Moiety. *Phosphorus Sulfur Silicon Relat. Elem.* **2003**, *178*, 821–829. [CrossRef]
28. Katagiri, K.; Yamamoto, Y.; Takahata, Y.; Kishibe, R.; Fujimoto, N. Photoreaction of anthracenyl phosphine oxides: Usual reversible photo- and heat-induced emission switching, and unusual oxidative PC bond cleavage. *Tetrahedron Lett.* **2019**, *60*, 2026–2029. [CrossRef]
29. Schwab, G.; Stern, D.; Stalke, D. Structural and Variable-Temperature NMR Studies of 9-Diisopropylphosphanyl anthracenes and 9,10-Bis(diisopropylphosphanyl)anthracenes and Their Oxidation Products. *J. Org. Chem.* **2008**, *73*, 5242–5247. [CrossRef]
30. Chen, L.; Wang, S.; Werz, P.; Han, Z.; Gates, D.P. A “masked” source for the phosphalkene $\text{MesP}=\text{CH}_2$: Trapping, rearrangement, and oligomerization. *Heteroat. Chem.* **2018**, *29*, e21474. [CrossRef]
31. Chen, X.; Liu, X.; Zhu, H.; Wang, Z. Palladium-catalyzed C–P bond activation of aroyl phosphine oxides without the adjacent “anchoring atom”. *Tetrahedron* **2021**, *81*, 131912. [CrossRef]
32. Chrzanowski, J.; Krasowska, D.; Urbaniak, M.; Sieroń, L.; Pokora-Sobczak, P.; Demchuk, O.M.; Drabowicz, J. Synthesis of Enantioenriched Aryl-*tert*-Butylphenylphosphine Oxides via Cross-Coupling Reactions of *tert*-Butylphenylphosphine Oxide with Aryl Halides. *Eur. J. Org. Chem.* **2018**, *2018*, 4614–4627. [CrossRef]
33. Schillmöller, T.; Ruth, P.N.; Herbst-Irmer, R.; Stalke, D. Three colour solid-state luminescence from positional isomers of facily modified thiophosphoranyl anthracenes. *Chem. Commun.* **2020**, *56*, 7479–7482. [CrossRef] [PubMed]
34. Schillmöller, T.; Ruth, P.N.; Herbst-Irmer, R.; Stalke, D. Analysis of Solid-State Luminescence Emission Amplification at Substituted Anthracenes by Host–Guest Complex Formation. *Chem. Eur. J.* **2020**, *26*, 17390–17398. [CrossRef]
35. Köhler, C.; Lübber, J.; Krause, L.; Hoffmann, C.; Herbst-Irmer, R.; Stalke, D. Comparison of different strategies for modelling hydrogen atoms in charge density analyses. *Acta Cryst. B* **2019**, *75*, 434–441. [CrossRef]
36. Niepötter, B.; Herbst-Irmer, R.; Stalke, D. Empirical correction for resolution- and temperature-dependent errors caused by factors such as thermal diffuse scattering. *J. Appl. Cryst.* **2015**, *48*, 1485–1497. [CrossRef]
37. Breshears, A.T.; Behrle, A.C.; Barnes, C.L.; Laber, C.H.; Baker, G.A.; Walensky, J.R. Synthesis, spectroscopy, electrochemistry, and coordination chemistry of substituted phosphine sulfides and selenides. *Polyhedron* **2015**, *100*, 333–343. [CrossRef]
38. Schwab, G.; Stern, D.; Leusser, D.; Stalke, D. Syntheses and Structures of 9-Bromo-10-diphenylphosphanyl anthracene and its Oxidation Products. *Z. Naturforsch. B* **2007**, *62*, 711–716. [CrossRef]
39. Fei, Z.; Kocher, N.; Mohrschladt, C.J.; Ihmels, H.; Stalke, D. Single Crystals of the Disubstituted Anthracene 9,10-($\text{Ph}_2\text{P}=\text{S}$) $_2\text{C}_{14}\text{H}_8$ Selectively and Reversibly Detect Toluene by Solid-State Fluorescence Emission. *Angew. Chem. Int. Ed.* **2003**, *42*, 783–787. [CrossRef]
40. Yip, J.H.K.; Prabhavathy, J. A Luminescent Gold Ring That Flips Like Cyclohexane. *Angew. Chem. Int. Ed.* **2001**, *40*, 2159–2162. [CrossRef]
41. Stephan, M.; Šterk, D.; Modéc, B.; Mohar, B. Study of the Reaction of Bulky Aryllithium Reagents with 3,4-Dimethyl-2,5-diphenyl-1,3,2-oxazaphospholidine-2-borane Derived from Ephedrine. *J. Org. Chem.* **2007**, *72*, 8010–8018. [CrossRef]
42. Watanabe, K.; Yamashita, M.; Yamamoto, Y.; Akiba, K.-y. Synthesis and Application of New Tridentate Anthracene Ligands Bearing Donative Phosphorus(III) Atoms at 1,8-Positions. *Phosphorus Sulfur Silicon Relat. Elem.* **2002**, *177*, 2047–2048. [CrossRef]
43. Müller, T.E.; Green, J.C.; Mingos, D.M.P.; McPartlin, C.M.; Whittingham, C.; Williams, D.J.; Woodroffe, T.M. Complexes of gold(I) and platinum(II) with polyaromatic phosphine ligands. *J. Organomet. Chem.* **1998**, *551*, 313–330. [CrossRef]
44. Lin, R.; Yip, J.H.K.; Zhang, K.; Koh, L.L.; Wong, K.-Y.; Ho, K.P. Self-Assembly and Molecular Recognition of a Luminescent Gold Rectangle. *J. Am. Chem. Soc.* **2004**, *126*, 15852–15869. [CrossRef]
45. Lin, R.; Yip, J.H.K. Self-Assembly, Structures, and Solution Dynamics of Emissive Silver Metallacycles and Helices. *Inorg. Chem.* **2006**, *45*, 4423–4430. [CrossRef]
46. Zhang, K.; Prabhavathy, J.; Yip, J.H.K.; Koh, L.L.; Tan, G.K.; Vittal, J.J. First Examples of $\text{AuI}-\text{X}-\text{AgI}$ Halonium Cations ($\text{X} = \text{Cl}$ and Br). *J. Am. Chem. Soc.* **2003**, *125*, 8452–8453. [CrossRef]
47. Ma, Z.; Xing, Y.; Yang, M.; Hu, M.; Liu, B.; Guedes da Silva, M.F.C.; Pompeiro, A.J.L. The double-helicate terpyridine silver(I) compound $[\text{Ag}_2\text{L}_2](\text{SO}_3\text{CF}_3)_2$ ($\text{L} = 4'$ -phenyl-terpyridine) as a building block for di- and mononuclear complexes. *Inorg. Chim. Acta* **2009**, *362*, 2921–2926. [CrossRef]
48. Meyer, T.G.; Jones, P.G.; Schmutzler, R. Darstellung neuer Monofluorosphine und einiger ihrer Übergangsmetallkomplexe; Einkristall-Röntgenstrukturanalyse eines Platin(II)-Komplexes/Preparation of New Monofluorophosphines and Some of their Transition Metal Complexes; Single Crystal X-ray Diffraction Study of a Platinum(II) Complex. *Z. Naturforsch. B* **1993**, *48*, 875–885. [CrossRef]
49. Romero, P.E.; Whited, M.T.; Grubbs, R.H. Multiple C–H Activations of Methyl *tert*-Butyl Ether at Pincer Iridium Complexes: Synthesis and Thermolysis of Ir(I) Fischer Carbenes. *Organometallics* **2008**, *27*, 3422–3429. [CrossRef]

50. Haenel, M.W.; Oevers, S.; Angermund, K.; Kaska, W.C.; Fan, H.; Hall, M.B. Thermally Stable Homogeneous Catalysts for Alkane Dehydrogenation. *Angew. Chem. Int. Ed.* **2001**, *40*, 3596–3600. [CrossRef]
51. Osawa, M.; Hoshino, M.; Wada, T.; Hayashi, F.; Osanai, S. Intra-Complex Energy Transfer of Europium(III) Complexes Containing Anthracene and Phenanthrene Moieties. *J. Phys. Chem. A* **2009**, *113*, 10895–10902. [CrossRef] [PubMed]
52. Kitagawa, Y.; Naito, A.; Fushimi, K.; Hasegawa, Y. Bright sky-blue fluorescence with high colour purity: Assembly of luminescent diphenyl-anthracene lutetium-based coordination polymer. *RSC Adv.* **2021**, *11*, 6604–6606. [CrossRef]
53. Chen, J.; Zhang, L.; Shi, L.; Ye, H.; Chen, Z. Preparation, characterization and redox chemistry of oxo-centered triruthenium dimers linked by bis(diphenylphosphino)anthracene and -ferrocene. *Inorg. Chim. Acta.* **2005**, *358*, 859–864. [CrossRef]
54. Deeming, A.J.; Martin, C.M. Coordination of an anthracene-derived ligand through eight carbon atoms in the pentaruthenium bow-tie clature, $[\text{Ru}_5(\text{CO})_{13}(\mu_5\text{-}\eta^1\text{:}\eta^2\text{:}\eta^3\text{:}\eta^3\text{-C}_{14}\text{H}_8\text{-}\eta^1\text{-PPh})]$. *Chem. Commun.* **1996**, 53–54. [CrossRef]
55. Piche, L.; Daigle, J.-C.; Poli, R.; Claverie, J.P. Investigation of Steric and Electronic Factors of (Arylsulfonyl)phosphane-Palladium Catalysts in Ethene Polymerization. *Eur. J. Inorg. Chem.* **2010**, *2010*, 4595–4601. [CrossRef]
56. Shimizu, M.; Yamamoto, T. 9-(Diphenylphosphino)anthracene-based phosphapalladacycle catalyzed conjugate addition of arylboronic acids to electron-deficient alkenes. *Tetrahedron Lett.* **2020**, *61*, 152257. [CrossRef]
57. Burrows, A.D.; Choi, N.; McPartlin, M.; Mingos, D.M.P.; Tarlton, S.V.; Vilar, R. Syntheses and structural characterisation of the compounds $[\text{Pd}(\text{dba})\text{L}_2]$ (where $\text{L}=\text{PBz}_3$ and PPh_2Np) and the novel dimer $[\text{Pd}_2(\text{m-dba})(\text{m-SO}_2)(\text{PBz}_3)_2]$. *J. Organomet. Chem.* **1999**, *573*, 313–322. [CrossRef]
58. Azerraf, C.; Shpruhman, A.; Gelman, D. Diels–Alder cycloaddition as a new approach toward stable $\text{PC}(\text{sp}^3)\text{P}$ -metalated compounds. *Chem. Commun.* **2009**, 466–468. [CrossRef]
59. Haenel, M.W.; Jakubik, D.; Krüger, C.; Betz, P. 1,8-Bis(diphenylphosphino)anthracene and Metal Complexes. *Chem. Ber.* **1991**, *124*, 333–336. [CrossRef]
60. Heuer, L.; Schomburg, D.; Schmutzler, R. Dimeres 9-(Difluorophosphino)anthracen: Synthese, Eigenschaften und Struktur. *Chem. Ber.* **1989**, *122*, 1473–1476. [CrossRef]
61. Hu, J.; Yip, J.H.K. Regioselective Double Cycloplatination of 9,10-Bis(diphenylphosphino)anthracene. *Organometallics* **2009**, *28*, 1093–1100. [CrossRef]
62. Hu, J.; Lin, R.; Yip, J.H.K.; Wong, K.; Ma, D.; Vittal, J.J. Synthesis and electronic spectroscopy of luminescent cyclometalated platinum-anthracenyl complexes. *Organometallics* **2007**, *26*, 6533–6543. [CrossRef]
63. Yang, F.; Fanwick, P.E.; Kubiak, C.P. Synthesis of 1-(9-Anthracene)phosphirane and Novel Intramolecular π -Stacking of 1-(9-Anthracene)phosphirane Ligands in a cis-Platinum(II) Complex. *Organometallics* **1999**, *18*, 4222–4225. [CrossRef]
64. Yang, F.; Fanwick, P.E.; Kubiak, C.P. Inter- and Intramolecular π -Stacking Interactions in cis-Bis{1-(9-anthracene)}phosphirane Complexes of Platinum(II). *Inorg. Chem.* **2002**, *41*, 4805–4809. [CrossRef]
65. Hu, J.; Xu, H.; Nguyen, M.; Yip, J.H.K. Photooxidation of a platinum-anthracene pincer complex: Formation and structures of Pt(II)-anthrone and -ketal complexes. *Inorg. Chem.* **2009**, *48*, 9684–9692. [CrossRef]
66. Arrigo, L.M.; Galenas, M.; Bassil, D.B.; Tucker, S.A.; Kannan, R.; Katti, K.V.; Barnes, C.L.; Jurisson, S.S. Fluorescent phosphinimine as possible precursor to an anionic and fluorescent sensor for Tc-99. *Radiochim. Acta* **2008**, *96*, 835–844. [CrossRef]
67. Belyaev, A.; Cheng, Y.-H.; Liu, Z.-Y.; Karttunen, A.J.; Chou, P.-T.; Koshevoy, I.O. A Facile Molecular Machine: Optically Triggered Counterion Migration by Charge Transfer of Linear Donor- π -Acceptor Phosphonium Fluorophores. *Angew. Chem. Int. Ed.* **2019**, *58*, 13456–13465. [CrossRef]
68. Huang, W.; Zhong, C.-H. Metal-Free Synthesis of Aryltriphenylphosphonium Bromides by the Reaction of Triphenylphosphine with Aryl Bromides in Refluxing Phenol. *ACS Omega* **2019**, *4*, 6690–6696. [CrossRef]
69. Nikitin, K.; Jennings, E.V.; Al Sulaimi, S.; Ortin, Y.; Gilheany, D.G. Dynamic Cross-Exchange in Halophosphonium Species: Direct Observation of Stereochemical Inversion in the Course of an $\text{S}_{\text{N}}2$ Process. *Angew. Chem. Int. Ed.* **2018**, *57*, 1480–1484. [CrossRef]
70. Bałczewski, P.; Dudziński, B.; Koprowski, M.; Knopik, Ł.; Owsianik, K. Fused aromatic hydrocarbons substituted with organophosphorus groups, method of their production, intermediate compounds, and applications. Patent Appl. PL-438275, 26 June 2021.
71. Bałczewski, P.; Koprowski, M.; Knopik, Ł.; Dudziński, B.; Owsianik, K.; Różycka-Sokołowska, E. IL-15, P-111, P-112, P-116. In Proceedings of the International Conference on Phosphorus Chemistry (23rd ICPC), Częstochowa, Poland, 5–9 July 2021.
72. Kirst, C.; Tietze, J.; Ebeling, M.; Horndasch, L.; Karaghiosoff, K. The Formation of P–C Bonds Utilizing Organozinc Reagents for the Synthesis of Aryl- and Heteroaryl-Dichlorophosphines. *J. Org. Chem.* **2021**, *86*, 17337–17343. [CrossRef]
73. Vogt, R.; Jones, P.G.; Schmutzler, R. Darstellung, Struktur und Eigenschaften von harnstoffverbrückten cyclischen Phosphoniumsalzen mit Phosphor-Phosphor-, Phosphor-Arsen-, Phosphor-Antimon- und Phosphor-Zinn-Bindung. *Chem. Ber.* **1993**, *126*, 1271–1281. [CrossRef]
74. Tsurusaki, A.; Nagahora, N.; Sasamori, T.; Matsuda, K.; Kanemitsu, Y.; Watanabe, Y.; Hosoi, Y.; Furukawa, Y.; Tokitoh, N. Synthesis, structures, and reactivity of kinetically stabilized anthryldiphosphene derivatives. *Bull. Chem. Soc. Jpn.* **2010**, *83*, 456–478. [CrossRef]
75. Yakhvarov, D.; Trofimova, E.; Sinyashin, O.; Kataeva, O.; Budnikova, Y.; Lönnecke, P.; Hey-Hawkins, E.; Petr, A.; Krupskaya, Y.; Kataev, V.; et al. New Dinuclear Nickel(II) Complexes: Synthesis, Structure, Electrochemical, and Magnetic Properties. *Inorg. Chem.* **2011**, *50*, 4553–4558. [CrossRef]

76. Yakhvarov, D.G.; Trofimova, E.A.; Dobrynin, A.B.; Gerasimova, T.P.; Katsyuba, S.A.; Sinyashin, O.G. First neutral dinuclear cobalt complex formed by bridging $[\mu\text{-O}2\text{P}(\text{H})\text{R}]$ -ligands: Synthesis, X-ray crystal structure and quantum-chemical study. *Mendeleev Commun.* **2015**, *25*, 27–28. [CrossRef]
77. Kalek, M.; Stawinski, J. Efficient synthesis of mono- and diarylphosphinic acids: A microwave-assisted palladium-catalyzed cross-coupling of aryl halides with phosphinate. *Tetrahedron* **2009**, *65*, 10406–10412. [CrossRef]
78. Kuimov, V.A.; Matveeva, E.A.; Telezhkin, A.A.; Malysheva, S.F.; Gusarova, N.K.; Trofimov, B.A. Reaction of 9-bromoanthracene with red phosphorus in the system KOH–DMSO. *Russ. J. Org. Chem.* **2016**, *52*, 1059–1061. [CrossRef]
79. Ishii, A.; Kikushima, C.; Hayashi, Y.; Ohtsuka, N.; Nakata, N.; Muranaka, A.; Tanaka, Y.; Uchiyama, M. 1-Phosphino-1,3-butadiene derivatives Incorporated with dibenzobarrelene skeleton: Synthesis and photophysical properties. *Bull. Chem. Soc. Jpn.* **2020**, *93*, 1430–1442. [CrossRef]
80. French, D.; Simmons, J.G.; Everitt, H.; Foulger, S.H.; Gray, G.M. Synthesis and Characterization of Amphiphilic Arenephosphonates as Water-Soluble Micellar Radioluminescent Probes. *ChemRxiv* **2020**. [CrossRef]
81. Nagode, S.B.; Kant, R.; Rastogi, N. Hantzsch Ester-Mediated Benzannulation of Diazo Compounds under Visible Light Irradiation. *Org. Lett.* **2019**, *21*, 6249–6254. [CrossRef]
82. Shu, Z.; Zhou, J.; Li, J.; Cheng, Y.; Liu, H.; Wang, D.; Zhou, Y. Rh(III)-Catalyzed Dual C–H Functionalization/Cyclization Cascade by a Removable Directing Group: A Method for Synthesis of Polycyclic Fused Pyrano[de]Isochromenes. *J. Org. Chem.* **2020**, *85*, 12097–12107. [CrossRef]
83. Nakamura, M.; Sawasaki, K.; Okamoto, Y.; Takamuku, S. Photolyses of Derivatives of Naphthyl and Anthryl Phosphates and Methylphosphonates. *Bull. Chem. Soc. Jpn.* **1995**, *68*, 3189–3197. [CrossRef]
84. Bessmertnykh, A.; Douaihy, C.M.; Guillard, R. Direct Synthesis of Amino-substituted Aromatic Phosphonates via Palladium-catalyzed Coupling of Aromatic Mono- and Dibromides with Diethyl Phosphite. *Chem. Lett.* **2009**, *38*, 738–739. [CrossRef]
85. Amicangelo, J.C.; Leenstra, W.R. Zirconium Arene-Phosphonates: Chemical and Structural Characterization of 2-Naphthyl- and 2-Anthracenylphosphonate Systems. *Inorg. Chem.* **2005**, *44*, 2067–2073. [CrossRef]
86. Amicangelo, J.C.; Leenstra, W.R. Excimer Formation in the Interlayer Region of Arene-Derivatized Zirconium Phosphonates. *J. Am. Chem. Soc.* **2003**, *125*, 14698–14699. [CrossRef]
87. Hill, S.P.; Banerjee, T.; Dilbeck, T.; Hanson, K. Photon Upconversion and Photocurrent Generation via Self-Assembly at Organic–Inorganic Interfaces. *J. Phys. Chem. Lett.* **2015**, *6*, 4510–4517. [CrossRef]
88. Zhou, Y.; Hill, S.P.; Hanson, K. Influence of meta- and para-phosphonated diphenylanthracene on photon upconversion in self-assembled bilayers. *J. Photon. Energy* **2007**, *8*, 022004. [CrossRef]
89. Yazji, S.; Westermeier, C.; Weinbrenner, D.; Sachsenhauser, M.; Liao, K.C.; Noever, S.; Postorino, P.; Schwartz, J.; Abstreiter, G.; Nickel, B.; et al. Surface-Directed Molecular Assembly of Pentacene on Aromatic Organophosphonate Self-Assembled Monolayers Explored by Polarized Raman Spectroscopy. *J. Raman Spectrosc.* **2017**, *48*, 235–242. [CrossRef]
90. Cattani-Scholz, A.; Liao, K.-C.; Bora, A.; Pathak, A.; Krautloher, M.; Nickel, B.; Schwartz, J.; Tornow, M.; Abstreiter, G. A New Molecular Architecture for Molecular Electronics. *Angew. Chem. Int. Ed.* **2011**, *50*, A11–A16. [CrossRef]
91. Kabachnik, M.; Solntseva, M.; Izmer, V.; Novikova, Z.; Beletskaya, I. Palladium-catalyzed phase-transfer arylation of dialkyl phosphonates. *Russ. J. Org. Chem.* **1998**, *34*, 93–97.
92. McDermott, J.E.; McDowell, M.; Hill, I.G.; Hwang, J.; Kahn, A.; Bernasek, S.L.; Schwartz, J. Organophosphonate Self-Assembled Monolayers for Gate Dielectric Surface Modification of Pentacene-Based Organic Thin-Film Transistors: A Comparative Study. *J. Phys. Chem. A* **2007**, *111*, 12333–12338. [CrossRef]
93. Liao, K.C.; Ismail, A.G.; Kreplak, L.; Schwartz, J.; Hill, I.G. Designed Organophosphonate Self-Assembled Monolayers Enhance Device Performance of Pentacene-Based Organic Thin-Film Transistors. *Adv. Mater.* **2010**, *22*, 3081–3085. [CrossRef] [PubMed]
94. Buckland, S.J.; Davidson, R.S. The Photooxidation of Some Anthryl Phosphorus Compounds. *Phosphorus Sulfur Relat. Elem.* **1983**, *18*, 225–228. [CrossRef]
95. Yamashita, M.; Yamamoto, Y.; Akiba, K.-Y.; Nagase, S. Synthesis of a Versatile Tridentate Anthracene Ligand and Its Application for the Synthesis of Hypervalent Pentacoordinate Boron Compounds (10-B-5). *Angew. Chem. Int. Ed.* **2000**, *39*, 4055–4058. [CrossRef]
96. Yamashita, M.; Yamamoto, Y.; Akiba, K.; Hashizume, D.; Iwasaki, F.; Takagi, N.; Nagase, S. Syntheses and Structures of Hypervalent Pentacoordinate Carbon and Boron Compounds Bearing an Anthracene Skeleton – Elucidation of Hypervalent Interaction Based on X-Ray Analysis and DFT Calculation. *J. Am. Chem. Soc.* **2005**, *127*, 4354–4371. [CrossRef]
97. Meek, J.S.; Koh, L. Syntheses and Reactions of Phosphates from Dibromoanthrone. Anthraquinone Anil, and 1,8-Dichloroanthraquinone. *J. Org. Chem.* **1970**, *35*, 153–156. [CrossRef]
98. Sasamori, T.; Tsurusaki, A.; Nagahora, N.; Matsuda, K.; Kanemitsu, Y.; Watanabe, Y.; Furukawa, Y.; Tokitoh, N. Synthesis and Properties of 9-Anthryldiphosphene. *Chem. Lett.* **2006**, *35*, 1382–1383. [CrossRef]
99. Yoshifuji, M.; Shima, I.; Inamoto, N.; Hirotsu, K.; Higuchi, T. Synthesis and structure of bis(2,4,6-tri-tert-butylphenyl)diphosphene: Isolation of a true phosphobenzene. *J. Am. Chem. Soc.* **1981**, *103*, 4587–4589. [CrossRef]
100. Tokitoh, N.; Tsurusaki, A.; Sasamori, T. A Unique Thermal Reaction of 9-Anthryldiphosphene Leading to the Formation of a Triphosphirane Derivative. *Phosphorus Sulfur Silicon Relat. Elem.* **2009**, *184*, 979–986. [CrossRef]

101. Bałczewski, P.; Kowalska, E.; Różycka-Sokołowska, E.; Skalik, J.; Owsianik, K.; Koprowski, M.; Marciniak, B.; Guziejewski, D.; Ciesielski, W. Mono-Aryl/Alkylthio-Substituted (Hetero)acenes of Exceptional Thermal and Photochemical Stability by the Thio-Friedel-Crafts/Bradsher Cyclization Reaction. *Chem. Eur. J.* **2019**, *25*, 14148–14161. [CrossRef]
102. Bałczewski, P.; Kowalska, E.; Różycka-Sokołowska, E.; Uznański, P.; Wilk, J.; Koprowski, M.; Owsianik, K.; Marciniak, B. Organosulfur Materials with High Photo- and Photo-Oxidation Stability: 10-Anthryl Sulfoxides and Sulfones and Their Photo-physical Properties Dependent on the Sulfur Oxidation State. *Materials* **2021**, *14*, 3506. [CrossRef]

MDPI
St. Alban-Anlage 66
4052 Basel
Switzerland
Tel. +41 61 683 77 34
Fax +41 61 302 89 18
www.mdpi.com

Molecules Editorial Office
E-mail: molecules@mdpi.com
www.mdpi.com/journal/molecules





Academic Open
Access Publishing

www.mdpi.com

ISBN 978-3-0365-8036-4